

Quantum algorithms for optimizers

Lecture notes

GIACOMO NANNICINI

Developed for course ISE 612 at the University of Southern California

Last update: July 9, 2025

This set of lecture notes is a self-contained graduate-level course on quantum algorithms, with an emphasis on optimization algorithms. It is written for applied mathematicians and engineers: we do not rely on physics or physical intuition, but rather, we derive all results in a rigorous manner starting from first principles and just three postulates. Thus, knowledge of quantum mechanics or physics is not assumed or required. A solid background in linear algebra, elementary calculus, and some knowledge of mathematical optimization are extremely helpful, if not necessary, to understand the material.

The material contained here started from a set of lecture notes developed over the years, teaching a “special topics” Ph.D.-level class on quantum algorithms in Industrial & Systems Engineering departments: first at Columbia University IEOR in the Fall 2019, then at Lehigh University ISE in the Spring 2020, finally at the University of Southern California ISE, first offered in the Fall 2023. The experience in the classroom had a tremendous impact on the structure and exposition style of this set of lecture notes.

This set of lecture notes is intended to be appropriate for graduate students and researchers who want to learn about quantum algorithms, and who are particularly interested in mathematical optimization. The choice of topics is heavily skewed in favor of optimization: among the many topic areas in quantum computing and quantum algorithms, the material contained here covers those areas that have already proven useful for the development of quantum optimization algorithms, or that seem likely to be useful for that end, because of their strong connections with classical (i.e., non-quantum) optimization theory or practice. It is also worth mentioning that the focus of this set of lecture notes is on the theory of quantum algorithms, i.e., how to design, understand, and analyze quantum algorithms; we sometimes discuss practical considerations, but we still assume access to a fully fault-tolerant quantum computing device, and do not attempt to discuss the (very interesting, and practically useful) intricacies of running quantum algorithms on real devices. Throughout the set of lecture notes, we give references to key results for each of the topics discussed.

The main goal of this set of lecture notes is to equip the reader with the tools necessary to investigate fundamental questions in quantum optimization algorithms: Can quantum algorithms be useful for optimization? And if so, how? What are some of the tasks that quantum computers are good at, and that can be used for optimization? Although we do not give definitive answers to these questions, at the end of this course the reader will be able to form their own informed opinion. Perhaps more importantly, the reader will have the tools and background to jump into the beautiful and constantly evolving literature on quantum algorithms — especially quantum optimization algorithms — where new discoveries are being made at a tremendous rate.

Acknowledgments. The author is grateful to the Office of Naval Research for supporting the research behind several chapters of this set of lecture notes, through award # N000142312585. The author is also grateful to everyone who attended his quantum algorithms classes over the years.

Copyright notice. This is a possibly-outdated preprint, using the author’s lecture notes, of the book “Quantum algorithms for optimizers,” edited by SIAM. All rights to the book’s material belong to SIAM. Please refer to the SIAM version of the book.

Contents

1	Model of computation	7
1.1	Basic definitions and notation	8
1.2	Qubits and quantum states	12
1.2.1	Basis states and superposition	13
1.2.2	Product states and entanglement	14
1.3	Operations on qubits	16
1.3.1	Notation for quantum circuits	17
1.3.2	Input-output, and measurement gates	18
1.3.3	The no-cloning principle	23
1.3.4	Basic operations and universality	23
1.3.5	Can we solve NP-hard problems?	29
1.3.6	Dealing with errors	30
1.3.7	Implicit measurement, reversibility, and uncomputation	32
1.4	Mixed states and purifications	34
1.4.1	Properties of density matrices	36
1.4.2	Reduced density matrix	37
1.4.3	Purifications	40
1.5	Notes and further reading	41
2	Early examples of quantum algorithms	43
2.1	Phase kickback	43
2.2	The first quantum algorithm: Deutsch's algorithm	46
2.3	Quantum interference and period finding: Simon's algorithm	47
2.3.1	Classical algorithm	47
2.3.2	Quantum algorithm	48
2.3.3	Full description and analysis	51
2.4	Notes and further reading	53
3	Quantum Fourier transform and phase estimation	55
3.1	Quantum Fourier transform	55
3.1.1	A useful way of expressing the QFT	56
3.1.2	Implementation of the QFT	58
3.2	Phase estimation	60
3.2.1	Main idea for quantum phase estimation	60
3.2.2	General phase estimation algorithm	62
3.3	Iterative phase estimation	64
3.3.1	Algorithm for constant precision	64
3.3.2	Iterative algorithm	66
3.4	Notes and further reading	67

4	Amplitude amplification and estimation	69
4.1	Grover’s algorithm for black-box search	69
4.1.1	Classical algorithm	70
4.1.2	Grover’s search: algorithm description	70
4.1.3	Determining the number of iterations	74
4.1.4	A geometric interpretation of the algorithm	76
4.2	Amplitude amplification	78
4.2.1	Obtaining all marked states	80
4.2.2	Oblivious amplitude amplification	80
4.3	Amplitude estimation	83
4.3.1	Solution strategy	83
4.3.2	Implementation of the amplitude estimation circuit	85
4.3.3	Summary and resource requirements	86
4.3.4	Amplitude estimation for counting and probability estimation	87
4.3.5	Application to Monte Carlo simulation	88
4.3.6	Searching when the number of marked items is not known	91
4.4	Quantum minimum finding	95
4.4.1	Base algorithm	95
4.4.2	Function evaluations with errors	97
4.5	Notes and further reading	102
5	Quantum gradient algorithm and vector input/output	105
5.1	The quantum gradient algorithm	105
5.1.1	Linear functions with a binary oracle	106
5.1.2	Polynomial functions with other types of oracles	111
5.1.3	The gradient algorithm for quantum state tomography	114
5.1.4	Separation from membership oracles	117
5.2	Encoding an arbitrary vector in a quantum state	124
5.3	Quantum RAM and faster amplitude encoding	127
5.3.1	Definition	128
5.3.2	QRAM for amplitude encoding	129
5.4	Notes and further reading	131
6	Hamiltonian simulation	133
6.1	Problem definition and preliminaries	133
6.1.1	The class BQP and Hamiltonian simulation	134
6.1.2	Basic remarks on Hamiltonian simulation	137
6.2	Overview of simulation algorithms	137
6.2.1	Diagonalizable Hamiltonians	137
6.2.2	Product formulas: Lie-Suzuki-Trotter decomposition	138
6.2.3	Linear combination of unitaries	140
6.2.4	Hamiltonian simulation for sparse matrices with oracle access	143
6.2.5	Signal processing and the block-encoding framework	144
6.3	Notes and further reading	144
7	Matrix manipulation with quantum algorithms	147
7.1	Quantum linear system solvers	147
7.1.1	Algorithm description: simplified exposition	148
7.1.2	Complexity analysis	151
7.1.3	Non-Hermitian matrices	152
7.1.4	Unknown condition number	153
7.1.5	Improvements to the running time	155
7.1.6	Extracting the solution and iterative refinement	157
7.2	Block-encodings	159
7.2.1	Operations on block-encodings	160

7.2.2	Block-encoding from sparse matrices	163
7.2.3	Block-encoding with QRAM access	168
7.2.4	Sampling from Gibbs distributions and trace estimation	170
7.3	Notes and further reading	174
8	Quantum algorithms for SDP using mirror descent	177
8.1	The mirror descent framework	178
8.1.1	Mirror descent as a generalization of steepest descent	178
8.1.2	Online mirror descent and the entropy mirror map	180
8.2	Classical MMWU algorithm for SDP	184
8.2.1	From mirror descent to the MMWU algorithm	184
8.2.2	Turning the MMWU algorithm into an SDP solver	187
8.3	Quantum MMWU algorithm for SDP	191
8.3.1	Dealing with inexact trace values	192
8.3.2	Computing the dual vector	193
8.3.3	Further improvements	196
8.4	Quantum algorithm for the SDP relaxation of MaxCut	198
8.4.1	Obtaining the normalized SDP relaxation	198
8.4.2	Solving the relaxation using inexact mirror descent	200
8.4.3	Complexity of the quantum algorithm	203
8.5	Notes and further reading	205
9	Optimization with the adiabatic theorem	207
9.1	The adiabatic theorem	208
9.1.1	Combinatorial optimization as an eigenvalue problem	208
9.1.2	Theorem statement	210
9.1.3	High-level proof	213
9.1.4	Filling the gaps	217
9.1.5	Spectral gap dependence and estimation	224
9.2	The quantum approximate optimization algorithm	229
9.2.1	Derivation from the adiabatic theorem	229
9.2.2	Algorithm description and properties	231
9.2.3	QAOA for MaxCut with fixed p	234
9.2.4	Implementation	236
9.3	Notes and further reading	237
	List of Definitions	239
	Bibliography	241

Chapter 1

Model of computation

Quantum computing is a relatively new area of computing that has the potential to greatly speed up the solution of certain problems. Quantum computers work in a fundamentally different way than classical computers. This set of lecture notes is a course on quantum algorithms, with a focus on algorithms that may be useful for mathematical optimization. We begin by introducing the model of computation, and then proceed to study several quantum algorithms. In the following, the term “classical” is used to mean “non-quantum”, as is common in the field.

The quantum computing device is, in abstract terms, similar to a classical computing device: it has a state, and the state of the device evolves by applying certain operations. The model of computation that we consider is the quantum circuit model, which works as follows:

1. The quantum computer has a *state* that is contained in a quantum register and is initialized in a predefined way.
2. The state evolves by applying *operations* specified in advance in the form of an algorithm.
3. At the end of the computation, some information on the state of the quantum register is obtained by means of a special operation, called a *measurement*.

All terms in italics are the subject of postulates, on which our exposition builds. Note that this type of computing device is similar to a Turing machine, except for the presence of a tape. It is possible to assume the presence of a tape and be more formal in defining a device that is the quantum equivalent of a Turing machine, but there is no need to do so for the purposes of this set of lecture notes. Fundamental results regarding universal quantum computers (i.e., the quantum equivalent of a universal Turing machine) are presented in [Deutsch, 1985, Yao, 1993, Bernstein and Vazirani, 1997].

We use the quantum circuit model throughout this set of lecture notes. This model of computation closely matches the general-purpose implementation provided by certain quantum hardware technologies used by some of the major players in the field. We should note, however, that the hardware is affected by noise and therefore it does not provide an exact implementation of the theoretical model. To understand the effect of noise, we can give the following simple, but overall quite accurate, intuitive explanation. According to the model of computation, the state evolves by applying operations, and some information on the state can be extracted via a measurement; due to noise, the state may not evolve in the desired way (e.g., applying a certain operation on the state s_1 should yield the state s_2 , but we obtain a different state s_3 instead), or the information extracted by a measurement may not be what it is supposed to be (e.g., a measurement should produce the output 0 with probability p_1 , but it produces 0 with a different probability p_2 instead).

This set of lecture notes is written for applied mathematicians and engineers, and aims to be “physics-free”; for this reason, we do not discuss further the specifics of existing quantum hardware that follows the circuit model. However, we note that a different model for quantum computing exists: the so-called adiabatic model. We provide some notes and references on the adiabatic model of computation in Sect. 9.3, after discussing the adiabatic theorem. We do not

discuss the adiabatic model in detail for at least two reasons: first, because the adiabatic and the circuit model are equivalent in theory [Aharonov et al., 2008]; second, because the circuit model is more commonly used in the literature, likely due to the fact that it is often easier to analyze.

1.1 Basic definitions and notation

A formal treatment of quantum algorithms requires familiarity with the properties of the tensor product. We describe here the necessary concepts and the notation. It also requires working with the decimal and the binary representation of integers, discussed subsequently in this section.

Definition 1.1 (Tensor product). *Given two vector spaces V and W over a field K with bases e_1, \dots, e_m and f_1, \dots, f_n respectively, the tensor product $V \otimes W$ is another vector space (that we call tensor product space) over K of dimension mn . The tensor product space is equipped with a bilinear operation $\otimes : V \times W \rightarrow V \otimes W$. The tensor product space $V \otimes W$ has basis $e_i \otimes f_j \forall i = 1, \dots, m, j = 1, \dots, n$.*

If the origin vector spaces are complex Euclidean spaces of the form \mathbb{C}^n , and we choose the standard basis (consisting of the orthonormal vectors that have a 1 in a single position and 0 elsewhere) in the origin vector spaces, then the bilinear operation of the tensor product is none other than the Kronecker product. This is formalized next.

Definition 1.2 (Kronecker product). *Given $A \in \mathbb{C}^{m \times n}, B \in \mathbb{C}^{p \times q}$, the Kronecker product $A \otimes B$ is the matrix $D \in \mathbb{C}^{mp \times nq}$ defined as:*

$$D := A \otimes B = \begin{pmatrix} a_{11}B & \dots & a_{1n}B \\ a_{21}B & \dots & a_{2n}B \\ \vdots & & \vdots \\ a_{m1}B & \dots & a_{mn}B \end{pmatrix}.$$

If we choose the standard basis over the vector spaces $\mathbb{C}^{m \times n}$ and $\mathbb{C}^{p \times q}$, then the bilinear operation \otimes of the tensor product $\mathbb{C}^{m \times n} \otimes \mathbb{C}^{p \times q}$ corresponds to the Kronecker product. This definition naturally applies to vectors by taking $n = q = 1$.

In this set of lecture notes we always work with complex Euclidean spaces of the form \mathbb{C}^n , using the standard basis. With a slight but common abuse of notation, we therefore use the tensor product to also refer to the Kronecker product. In this way, we can apply \otimes to vector spaces, vectors and matrices, and in all cases we obtain precisely the mathematical object that we want to obtain: the tensor product space, a vector in the tensor product space, or a linear map on the tensor product space.

Example 1.3. *We provide an example of the tensor product for normalized vectors, which links this concept to probability distributions and hopefully provides an intuition for some of the future material. Consider two independent discrete random variables X and Y that describe the probability of extracting numbers from two urns. The first urn contains the numbers 0 and 1, the second urn contains the numbers 00, 01, 10, 11. Assume that the extraction mechanism is biased and therefore the outcomes do not have equal probability. The outcome probabilities are given below, and for convenience we define two vectors containing them:*

$$x = \begin{pmatrix} \Pr(X = 0) \\ \Pr(X = 1) \end{pmatrix} = \begin{pmatrix} 0.25 \\ 0.75 \end{pmatrix} \quad y = \begin{pmatrix} \Pr(Y = 00) \\ \Pr(Y = 01) \\ \Pr(Y = 10) \\ \Pr(Y = 11) \end{pmatrix} = \begin{pmatrix} 0.2 \\ 0.2 \\ 0.2 \\ 0.4 \end{pmatrix}.$$

Notice that because each vector contains probabilities for all possible respective outcomes, the vectors are normalized so that their entries sum up to 1. Then, the joint probabilities for simulta-

neously extracting numbers from the two urns are given by the tensor product $x \otimes y$:

$$x \otimes y = \begin{pmatrix} 0.25 \\ 0.75 \end{pmatrix} \otimes \begin{pmatrix} 0.2 \\ 0.2 \\ 0.4 \end{pmatrix} = \begin{pmatrix} 0.05 \\ 0.05 \\ 0.05 \\ 0.1 \\ 0.15 \\ 0.15 \\ 0.15 \\ 0.3 \end{pmatrix} = \begin{pmatrix} \Pr(X=0)\Pr(Y=00) \\ \Pr(X=0)\Pr(Y=01) \\ \Pr(X=0)\Pr(Y=10) \\ \Pr(X=0)\Pr(Y=11) \\ \Pr(X=1)\Pr(Y=00) \\ \Pr(X=1)\Pr(Y=01) \\ \Pr(X=1)\Pr(Y=10) \\ \Pr(X=1)\Pr(Y=11) \end{pmatrix} = \begin{pmatrix} \Pr(X=0, Y=00) \\ \Pr(X=0, Y=01) \\ \Pr(X=0, Y=10) \\ \Pr(X=0, Y=11) \\ \Pr(X=1, Y=00) \\ \Pr(X=1, Y=01) \\ \Pr(X=1, Y=10) \\ \Pr(X=1, Y=11) \end{pmatrix},$$

where the last equality is due to the fact that X and Y are independent. The vector $x \otimes y$ is also normalized, which is easy to verify algebraically.

The next proposition states some properties of the tensor product that are useful in the rest of this set of lecture notes.

Proposition 1.4. *Let $A, B : \mathbb{C}^{m \times m}, C, D \in \mathbb{C}^{n \times n}$ be linear transformations on \mathbb{C}^m and \mathbb{C}^n respectively, $u, v \in \mathbb{C}^m, w, x \in \mathbb{C}^n$, and $a, b \in \mathbb{C}$. The tensor product satisfies the following properties:*

- (i) $(A \otimes C)(B \otimes D) = AB \otimes CD$.
- (ii) $(A \otimes C)(u \otimes w) = Au \otimes Cw$.
- (iii) $(u + v) \otimes w = u \otimes w + v \otimes w$.
- (iv) $u \otimes (w + x) = u \otimes w + u \otimes x$.
- (v) $(au) \otimes (bw) = ab(u \otimes w)$.
- (vi) $(A \otimes C)^\dagger = A^\dagger \otimes C^\dagger$.

Above and in the following, the notation A^\dagger denotes the conjugate transpose of A , which is the matrix defined as follows: $A^\dagger := \bar{A}^T$ (\bar{A} denotes the complex conjugate). Given a matrix A , the notation $A^{\otimes n}$ indicates the tensor product of A with itself n times, and the same notation is used for vectors as well as vector spaces \mathbb{S} :

$$A^{\otimes n} := \underbrace{A \otimes A \cdots \otimes A}_{n \text{ times}}, \quad \mathbb{S}^{\otimes n} := \underbrace{\mathbb{S} \otimes \mathbb{S} \cdots \otimes \mathbb{S}}_{n \text{ times}}.$$

The quantum computing literature refers to a Hilbert space, typically denoted \mathcal{H} , rather than a complex Euclidean space \mathbb{C}^n . However, the material discussed in this set of lecture notes does not require any property of Hilbert spaces that is not already present in complex Euclidean spaces, hence we stick to the more familiar concept. We reserve the symbol \mathcal{H} to refer to Hamiltonians, introduced in Ch. 6.

We work extensively with binary strings, using the following definitions.

Definition 1.5 (Binary string). *For any integer $q > 0$, we denote by $\vec{j} \in \{0, 1\}^q$ a binary string on q digits, where we use the arrow to emphasize that \vec{j} is a string of binary digits rather than an integer. Given $\vec{j} \in \{0, 1\}^q$, we denote its k -th digit ($k = 1, \dots, q$) by \vec{j}_k . We use the corresponding symbol without the arrow, j , to denote the decimal number that \vec{j} corresponds to, i.e., $j = \sum_{k=1}^q \vec{j}_k 2^{q-k}$.*

We use the symbol $\vec{0}$ to denote the all-zero binary string, and $\vec{1}$ to denote the all-one binary string; the size of these strings should always be clear from the context. Note that according to Def. 1.5, we use a little-endian convention for binary strings, i.e., the first digit is the most significant one (e.g., 110 is the integer $1 \cdot 2^2 + 1 \cdot 2^1 + 0 \cdot 2^0 = 6$). We write $\mathbb{0}, \mathbb{1}$ to denote the all-zero and all-one vectors respectively (to distinguish them from the all-zero and all-one binary strings $\vec{0}, \vec{1}$), with dimension that is clear from the context.

An additional piece of notation that we use extensively is the *bra-ket* notation, used in quantum mechanics. As mentioned earlier, this set of lecture notes does not rely or touch on quantum physics, however there is an undeniable advantage in the quantum mechanics notation in that it puts the most important information in the center of the symbols, rather than relegate it to a marginal role in the subscript or superscript. Furthermore, a goal of this set of lecture notes is to equip readers with the necessary tools to understand quantum computing papers, hence it is important to familiarize with the bra-ket notation.

Definition 1.6 (Bra-ket). *Given a complex Euclidean space \mathbb{S} (such as $\mathbb{S} = \mathbb{C}^n$), $|\psi\rangle \in \mathbb{S}$ denotes a column vector, and $\langle\psi| \in \mathbb{S}^\dagger$ denotes a row vector that is the conjugate transpose of $|\psi\rangle$, i.e., $\langle\psi| := |\psi\rangle^\dagger$. The vector $|\psi\rangle$ is also called a ket, and the vector $\langle\psi|$ is also called a bra.*

Thus, an expression such as $\langle\psi|\phi\rangle$ is an inner product. (For vectors x, y in the “usual”, i.e., non-bra-ket notation, we denote the inner product by $\langle x, y \rangle$.) To remember what is a bra and what is a ket, it may be helpful to remember that a bra-ket is an inner product. The complex Euclidean spaces used in this set of lecture notes are of the form $(\mathbb{C}^2)^{\otimes q}$, where q is a given integer. It is therefore convenient to give a shorthand notation for the basis elements of such spaces.

Definition 1.7 (Standard basis in bra-ket notation). *The standard basis for \mathbb{C}^2 is denoted by $|0\rangle = \begin{pmatrix} 1 \\ 0 \end{pmatrix}$, $|1\rangle = \begin{pmatrix} 0 \\ 1 \end{pmatrix}$. The standard basis for $(\mathbb{C}^2)^{\otimes q}$, which has 2^q elements, is denoted by $|\vec{j}\rangle$, $\vec{j} \in \{0, 1\}^q$.*

Remark 1.8. *By convention, given column vectors $|\psi\rangle, |\phi\rangle$, their juxtaposition indicates their tensor product, i.e.,*

$$|\psi\rangle|\phi\rangle = |\psi\rangle \otimes |\phi\rangle.$$

The same convention is used for row vectors. This convention is used to shorten expressions whenever it does not create ambiguity, and is used extensively in the quantum computing literature.

According to our notation, for any q -digit binary string $\vec{j} \in \{0, 1\}^q$, $|\vec{j}\rangle$ is the 2^q -dimensional basis vector in $(\mathbb{C}^2)^{\otimes q}$ corresponding to the binary string \vec{j} . Because we always use the standard basis and the most natural order for its vectors, it is easy to verify that for $\vec{j} \in \{0, 1\}^q$, $|\vec{j}\rangle$ is the basis vector with a 1 in position j (using zero-based indices, i.e., 0 corresponds to the first position), and 0 elsewhere.

Example 1.9. $|110\rangle$ is the 8-dimensional basis vector $(00000010)^\top$, obtained as the tensor product $|1\rangle \otimes |1\rangle \otimes |0\rangle$, because the binary string 110 corresponds to the number 6, and $|110\rangle$ has a 1 in position 6 (if we start counting from 0).

Whenever useful for clarity, we use a subscript for bras and kets to denote the dimension of the space that the vector belongs to, e.g., we write $|\vec{j}\rangle_q$ to emphasize that we are working in a 2^q dimensional space (or, in other words, that the basis elements of the space are associated with binary strings with q digits). We typically omit the subscript if the dimension of the space is evident from the context, and we omit it more often in later parts of the set of lecture notes where such details are less of a concern, but for now it can be helpful to give rigorous definitions of the quantities involved in each expression. We provide a further example of this notation below.

Example 1.10. *Let us write the basis elements of $(\mathbb{C}^2)^{\otimes 2} = \mathbb{C}^2 \otimes \mathbb{C}^2$:*

$$\begin{aligned} |00\rangle_2 = |00\rangle = |0\rangle|0\rangle = |0\rangle \otimes |0\rangle &= \begin{pmatrix} 1 \\ 0 \\ 0 \\ 0 \end{pmatrix} & |01\rangle_2 = |01\rangle = |0\rangle|1\rangle = |0\rangle \otimes |1\rangle &= \begin{pmatrix} 0 \\ 1 \\ 0 \\ 0 \end{pmatrix} \\ |10\rangle_2 = |10\rangle = |1\rangle|0\rangle = |1\rangle \otimes |0\rangle &= \begin{pmatrix} 0 \\ 0 \\ 1 \\ 0 \end{pmatrix} & |11\rangle_2 = |11\rangle = |1\rangle|1\rangle = |1\rangle \otimes |1\rangle &= \begin{pmatrix} 0 \\ 0 \\ 0 \\ 1 \end{pmatrix}. \end{aligned}$$

In the above example we used the subscript to denote the dimension of the basis vectors, just to emphasize that $|00\rangle_2$ and $|00\rangle$ are exactly the same. In the remainder of this set of lecture notes, we always write $|01\rangle$ rather than $|01\rangle_2$ because it is clear that the basis element $|01\rangle$ has two digits and therefore lives in the space $(\mathbb{C}^2)^{\otimes 2}$.

In the rest of this set of lecture notes, as is frequent in the quantum computing literature, we use $\vec{j} \in \{0, 1\}^q$ or, interchangeably, the corresponding integer j to index the elements of 2^q -dimensional vectors; such an index is well defined because $\{0, 1\}^q$ has 2^q elements. Thus, whenever we are indexing vectors (or matrices) with indices that correspond to basis states, we use zero-based indices, as opposed to the usual one-based indices. For example: if $x \in \mathbb{R}^{2^q}$ we write $\sum_{\vec{j} \in \{0, 1\}^q} x_j$ to take the sum of its elements, so the first element of x is indexed by zero; at the same time, if $x \in \mathbb{R}^q$ (where q is not necessarily a power of 2), we write $\sum_{j=1}^q x_j$ to take the sum of its elements, so the first element of x is indexed by one, in the usual manner. This should always be clear from the context.

To improve clarity when dealing with vectors in $(\mathbb{C}^2)^{\otimes q}$ in bra-ket notation, we always denote basis vectors using spelled-out binary strings or Roman letters, (e.g., $|01\rangle, |\vec{j}\rangle, |\vec{h}\rangle, |\vec{x}\rangle, |\vec{y}\rangle$ all denote basis vectors), whereas we use Greek letters to denote vectors that may not be basis vectors (e.g., $|\psi\rangle, |\phi\rangle$ all denote vectors that may not be basis vectors). In the same spirit, single-digit binary numbers are always denoted with Roman letters (e.g., if we need to label a scalar that is 0 or 1, we denote it by x, y , or z).

We denote by $I_{n \times n}$ the identity matrix of size $n \times n$. We generally omit the subscript to refer to the 2×2 identity matrix, but sometimes we also omit it if the size of I is clear from the context, for example if we are using an identity matrix to “fill” the unspecified part of an operator on a tensor product space (e.g., if we are constructing an $n \times n$ operator A , and B is a 2×2 matrix, then $A = B \otimes I$ implies that the identity is of size $n/2 \times n/2$.) The reader is not required to remember these details: experience suggests that the size of the identity matrix is clear from the context. We use $\text{diag}(a_1, \dots, a_n)$ to denote the $n \times n$ diagonal matrix with elements a_1, \dots, a_n on the diagonal. The ℓ^p -norm of a vector $x \in \mathbb{C}^n$ is denoted $\|x\|_p := \left(\sum_{j=1}^n |x_j|^p\right)^{1/p}$; if p is omitted then it is assumed that $p = 2$, i.e., the Euclidean norm. The logarithm is always base 2, i.e., $\log = \log_2$, unless otherwise specified.

Finally, when discussing efficiency of algorithms we use the traditional computer science notation $\mathcal{O}(\cdot)$, as well as the perhaps lesser-known $\tilde{\mathcal{O}}(\cdot)$. These are defined below.

Definition 1.11 (Big- \mathcal{O} notation). *We write $f(x) = \mathcal{O}(g(x))$ if there exist scalars $\ell, \alpha > 0$, such that $f(x) \leq \alpha g(x) \forall x > \ell$.*

We write $f(x) = \tilde{\mathcal{O}}(g(x))$ if $f(x) = \mathcal{O}(g(x) \text{polylog}(g(x)))$, where $\text{polylog}(\cdot)$ denotes a polylogarithmic function of the argument. When $\tilde{\mathcal{O}}(\cdot)$ is used to express a property (such as the asymptotic running time) of an algorithm on a class of instances, we allow the $\text{polylog}(\cdot)$ term to also depend (still polylogarithmically) on other instance parameters that are not explicitly noted in $g(x)$.

The $\tilde{\mathcal{O}}(\cdot)$ notation is convenient when one does not want to get bogged down by details: at least from a theoretical standpoint, polylogarithmic factors are for the most part uninfluential when determining the asymptotic running time, and keeping track of the exact expressions can be very cumbersome. Note that to be precise one should indicate which instance parameters are suppressed by the $\tilde{\mathcal{O}}(\cdot)$ notation, but we choose not to do it here to avoid additional notation. In the vast majority of cases, the reader can rely on the references given in the sections adopting $\tilde{\mathcal{O}}(\cdot)$ notation to track down more precise running time expressions.

Further remarks on our notation. In this set of lecture notes we use several notational devices that are meant to enhance clarity, but that are not usually employed in the quantum computing literature. We list the most important ones here, with the hope of facilitating the transition from this set of lecture notes to the rest of the literature.

- We occasionally use the subscript for bra-ket vectors to indicate the dimension of the space, e.g., $|\psi\rangle_q$ for 2^q -dimensional vectors. Typically, the dimension of the space is defined else-

where and/or can be understood from the context. Whenever subscripts for kets are used, it is normally to address registers. We use capital letter subscripts to address registers.

- We always use the vector arrow, e.g., \vec{j} , to indicate binary strings. Typically, binary strings are not distinguished from other mathematical symbols and are to be identified from the context.
- We always use Roman letters for basis vectors and Greek letters for general, i.e., possibly not basis, vectors. This convention is relatively common in the literature, although it is adopted with varying degrees of consistency.
- We use $\vec{0}, \vec{1}$ to denote the all-zero, all-one binary strings. In the literature, these are usually denoted by $0^q, 1^q$ respectively for dimension q . (In our notation, the dimension is defined elsewhere or denoted by a subscript in the ket.)

1.2 Qubits and quantum states

According to the computational model specified at the beginning of this chapter, a quantum computing device has a state that is stored in a quantum register. Qubits are the quantum counterpart of the bits found in classical computers: a classical computer has registers that are made up of bits, whereas a quantum computer has quantum registers that are made up of qubits. It is convenient to assume, without loss of generality, that there is a single quantum register: one can think of multiple registers as being placed “side-by-side” to form a single register, and sometimes it is appropriate to address subregisters of the main single register, as we discuss throughout this chapter. The state of the quantum register, and therefore of the quantum computing device, is defined next.

Postulate 1. *The state of a q -qubit quantum register is a unit vector in $(\mathbb{C}^2)^{\otimes q} = \underbrace{\mathbb{C}^2 \otimes \dots \otimes \mathbb{C}^2}_{q \text{ times}}$.*

Remark 1.12. *A vector $|\psi\rangle \in \mathbb{C}^n$ is a unit vector if $\| |\psi\rangle \| = \sqrt{\langle \psi | \psi \rangle} = 1$.*

Remark 1.13. *Choosing the standard basis for \mathbb{C}^2 , the state of a single-qubit register ($q = 1$) can be represented as $\alpha|0\rangle + \beta|1\rangle = \alpha \begin{pmatrix} 1 \\ 0 \end{pmatrix} + \beta \begin{pmatrix} 0 \\ 1 \end{pmatrix} = \begin{pmatrix} \alpha \\ \beta \end{pmatrix}$ where $\alpha, \beta \in \mathbb{C}$ and $|\alpha|^2 + |\beta|^2 = 1$.*

Remark 1.14. *Given the standard basis for \mathbb{C}^2 and the definition of the tensor product (Def. 1.1), a basis for $(\mathbb{C}^2)^{\otimes q}$ is given by the following 2^q vectors:*

$$\begin{aligned}
 \underbrace{|00\dots 00\rangle}_{q \text{ digits}} &= \underbrace{|0\rangle \otimes \dots \otimes |0\rangle \otimes |0\rangle}_{q \text{ times}} = \underbrace{|0\rangle \dots |0\rangle |0\rangle}_{q \text{ times}} \\
 \underbrace{|00\dots 01\rangle}_{q \text{ digits}} &= \underbrace{|0\rangle \otimes \dots \otimes |0\rangle \otimes |1\rangle}_{q \text{ times}} = \underbrace{|0\rangle \dots |0\rangle |1\rangle}_{q \text{ times}} \\
 &\vdots \\
 \underbrace{|11\dots 11\rangle}_{q \text{ digits}} &= \underbrace{|1\rangle \otimes \dots \otimes |1\rangle \otimes |1\rangle}_{q \text{ times}} = \underbrace{|1\rangle \dots |1\rangle |1\rangle}_{q \text{ times}}.
 \end{aligned}$$

In more compact form, the vectors are denoted by $|\vec{j}\rangle, \vec{j} \in \{0, 1\}^q$, see Def. 1.7. The state of a q -qubit quantum register can then be represented as: $|\psi\rangle = \sum_{\vec{j} \in \{0, 1\}^q} \alpha_j |\vec{j}\rangle$, with $\alpha_j \in \mathbb{C}$ and $\sum_{\vec{j} \in \{0, 1\}^q} |\alpha_j|^2 = 1$.

The coefficients of a quantum state (i.e., the elements of the corresponding vector) are often called *amplitudes*. For brevity, we often write “state of q -qubits” or “ q -qubit state” to refer to the state of a q -qubit quantum register. This is common in the literature, where the discussion of qubits is not necessarily limited to the context of quantum registers. By properties of the tensor

product, as is discussed in the following, sometimes it is appropriate to refer to the state of just some of the qubits of a quantum computing device, rather than all of them, and this may still be a well-defined concept; however, this is not always possible (unlike for classical computers). We revisit this topic in Sect. 1.2.2.

It is important to remark that $(\mathbb{C}^2)^{\otimes q}$ is a 2^q -dimensional space. This is in sharp contrast with the state of classical bits: given q classical bits, their state is a binary string in $\{0, 1\}^q$, which is a q -dimensional space.

Remark 1.15. *Here, to think about the dimension of the space it may be helpful to think about how many “numbers” are necessary to specify the state (formally, the numbers would be the coefficients to express the vector in a basis). For a vector in $(\mathbb{C}^2)^{\otimes q}$ we need to specify 2^q coefficients, whereas for a vector in $\{0, 1\}^q$, q coefficients suffice.*

Thus, the dimension of the state space of quantum registers grows *exponentially* in the number of qubits, whereas the dimension of the state space of classical registers grows *linearly* in the number of bits. Furthermore, to represent a quantum state we need complex coefficients: the state of a q -qubit quantum register is described by 2^q complex coefficients, which is an enormous amount of information compared to what is necessary to describe a q -bit classical register. However, a consequence of one of our main postulates (introduced later) is that a quantum state cannot be accessed directly, therefore even if a description of the quantum state requires infinite precision in principle, we cannot access such description as easily as with classical registers. In fact, as it turns out we cannot extract more than q bits of information out of a q -qubit register! This should be intuitively clear after stating the effect of quantum measurements in Sect. 1.3.2; for a formal proof, see [Holevo, 1973].

1.2.1 Basis states and superposition

We continue our study of the space of quantum states by discussing the concept of superposition.

Definition 1.16 (Superposition). *A q -qubit quantum state $|\psi\rangle$ is a basis state if $|\psi\rangle = \alpha_k|\vec{k}\rangle$ for some $\vec{k} \in \{0, 1\}^q$ and $\alpha_k \in \mathbb{C}, |\alpha_k|^2 = 1$. Otherwise, we say that $|\psi\rangle$ is a superposition (of basis states). Similarly, we say that q qubits are in a basis state if the state of the corresponding register is described by a basis state, and it is a superposition otherwise.*

Remark 1.17. *A simpler, more intuitive definition would be to say that a basis state is such that $|\psi\rangle = |\vec{k}\rangle$ for some $\vec{k} \in \{0, 1\}^q$. It is acceptable to use the simpler definition if desired: as it turns out, even if the states $\alpha_k|\vec{k}\rangle$ for some $\vec{k} \in \{0, 1\}^q$ and $|\alpha_k|^2 = 1$ are all different in principle, they are equivalent to $|\vec{k}\rangle$ up to the multiplication factor α_k , which is unimportant because $|\alpha_k|^2 = 1$, as discussed in Sect. 1.3.2.*

Example 1.18. *Consider two single-qubit registers and their states $|\psi\rangle, |\phi\rangle$:*

$$\begin{aligned} |\psi\rangle &= \alpha_0|0\rangle + \alpha_1|1\rangle \\ |\phi\rangle &= \beta_0|0\rangle + \beta_1|1\rangle. \end{aligned}$$

If we put these single-qubit registers side-by-side to form a two-qubit register, then the state of the two-qubit register is (recall Rem. 1.8):

$$|\psi\rangle|\phi\rangle = \alpha_0\beta_0|0\rangle|0\rangle + \alpha_0\beta_1|0\rangle|1\rangle + \alpha_1\beta_0|1\rangle|0\rangle + \alpha_1\beta_1|1\rangle|1\rangle.$$

If both $|\psi\rangle$ and $|\phi\rangle$ are basis states, we have that either α_0 or α_1 is zero, and similarly either β_0 or β_1 is zero, while the nonzero coefficients have modulus one. Thus, only one of the coefficients in the expression of the state of $|\psi\rangle|\phi\rangle$ is nonzero, and in fact its modulus is one. This implies that if both $|\psi\rangle$ and $|\phi\rangle$ are basis states, $|\psi\rangle|\phi\rangle$ is a basis state as well. But now assume that $\alpha_0 = \beta_0 = \alpha_1 = \beta_1 = \frac{1}{\sqrt{2}}$: the qubits $|\psi\rangle$ and $|\phi\rangle$ are in a superposition. Then the state of $|\psi\rangle|\phi\rangle$ is $\frac{1}{2}|00\rangle + \frac{1}{2}|01\rangle + \frac{1}{2}|10\rangle + \frac{1}{2}|11\rangle$, which is a superposition as well. Notice that the normalization of the coefficients works out, as one can easily check with simple algebra: the tensor product of unit vectors is also a unit vector.

The example clearly generalizes to an arbitrary number of qubits. In fact the following proposition is trivially true:

Proposition 1.19. *A q -qubit register, $q > 1$, is in a basis state if and only if its state can be expressed as the tensor product of q single-qubit registers, each of which is in a basis state.*

Notice that superposition does not have a classical equivalent: q classical bits are always in a basis state, i.e., a q -bit classical register always contains exactly one of the 2^q binary strings in $\{0, 1\}^q$. Indeed, superposition is one of the main features that differentiate quantum computers from classical computers. Another important feature is entanglement, discussed next.

1.2.2 Product states and entanglement

We have seen that the state of a q -qubit register is a vector in $(\mathbb{C}^2)^{\otimes q}$, which is a 2^q dimensional space. Because this is a tensor product of copies of \mathbb{C}^2 , i.e., the space in which single-qubit states live, it is natural to ask whether moving from single qubits to multiple qubits gained us anything beyond increasing the dimension of the space: are the quantum states representable on q qubits simply the tensor product of q single-qubit states, or are they a larger set? We can answer this question by using the definitions and concepts introduced so far. A q -qubit state is a unit vector in $(\mathbb{C}^2)^{\otimes q}$, and it can be written as:

$$|\psi\rangle = \sum_{\vec{j} \in \{0,1\}^q} \alpha_j |\vec{j}\rangle, \quad \sum_{\vec{j} \in \{0,1\}^q} |\alpha_j|^2 = 1.$$

Now let us consider the tensor product of q single-qubit states, the k -th of which is given by $\beta_{k,0}|0\rangle + \beta_{k,1}|1\rangle$, for $k = 1, \dots, q$ (the first qubit corresponds to the most significant bit, according to the little-endian convention). Taking the tensor product we obtain the vector:

$$\begin{aligned} |\phi\rangle &= (\beta_{1,0}|0\rangle + \beta_{1,1}|1\rangle) \otimes (\beta_{2,0}|0\rangle + \beta_{2,1}|1\rangle) \otimes \dots \otimes (\beta_{q,0}|0\rangle + \beta_{q,1}|1\rangle) \\ &= \sum_{j_1=0}^1 \sum_{j_2=0}^1 \dots \sum_{j_q=0}^1 \left(\prod_{k=1}^q \beta_{k,j_k} \right) \underbrace{|j_1 j_2 \dots j_q\rangle}_{\text{taken as a binary string}} = \sum_{\vec{j} \in \{0,1\}^q} \left(\prod_{k=1}^q \beta_{k,j_k} \right) |\vec{j}\rangle, \end{aligned}$$

satisfying $|\beta_{k,0}|^2 + |\beta_{k,1}|^2 = 1 \quad \forall k = 1, \dots, q$.

It is straightforward to verify (for example, with a proof by induction on the number of qubits q) that the normalization condition for the coefficients in $|\phi\rangle$ implies the normalization condition for the coefficients in $|\psi\rangle$, but the converse is not true. That is, $|\beta_{k,0}|^2 + |\beta_{k,1}|^2 = 1 \quad \forall k = 1, \dots, q$ implies $\sum_{j_1=0}^1 \sum_{j_2=0}^1 \dots \sum_{j_q=0}^1 \left| \prod_{k=1}^q \beta_{k,j_k} \right|^2 = 1$, but not viceversa. This means that there exist values of the coefficients α_j of $|\psi\rangle$, with $\sum_{\vec{j} \in \{0,1\}^q} |\alpha_j|^2 = 1$, that cannot be obtained as the coefficients of a state $|\phi\rangle$ by choosing appropriate coefficients $\beta_{k,0}, \beta_{k,1}$ (for $k = 1, \dots, q$). This is easily verified with an example.

Example 1.20. *Consider two single-qubit states:*

$$\begin{aligned} |\psi\rangle &= \alpha_0|0\rangle + \alpha_1|1\rangle \\ |\phi\rangle &= \beta_0|0\rangle + \beta_1|1\rangle. \end{aligned}$$

Taking the two qubits together in a two-qubit register, the state of the two-qubit register is:

$$|\psi\rangle|\phi\rangle = \alpha_0\beta_0|00\rangle + \alpha_0\beta_1|01\rangle + \alpha_1\beta_0|10\rangle + \alpha_1\beta_1|11\rangle, \tag{1.1}$$

with the normalization conditions $|\alpha_0|^2 + |\alpha_1|^2 = 1$ and $|\beta_0|^2 + |\beta_1|^2 = 1$. The general state of a two-qubit register $|\xi\rangle$ is:

$$|\xi\rangle = \gamma_{00}|00\rangle + \gamma_{01}|01\rangle + \gamma_{10}|10\rangle + \gamma_{11}|11\rangle, \tag{1.2}$$

with normalization condition $|\gamma_{00}|^2 + |\gamma_{01}|^2 + |\gamma_{10}|^2 + |\gamma_{11}|^2 = 1$. Comparing Eq.s (1.1) and (1.2), we determine that $|\xi\rangle$ is of the form $|\psi\rangle \otimes |\phi\rangle$ (i.e., a tensor product of two single-qubit states) if and only if it satisfies the relationship:

$$\gamma_{00}\gamma_{11} = \gamma_{01}\gamma_{10}. \quad (1.3)$$

Clearly $|\psi\rangle|\phi\rangle$ yields coefficients that satisfy this condition. To see the converse, let $\theta_{00}, \theta_{01}, \theta_{10}, \theta_{11}$ be the phases of $\gamma_{00}, \gamma_{01}, \gamma_{10}, \gamma_{11}$. Notice that Eq. (1.3) implies:

$$\begin{aligned} |\gamma_{00}|^2 |\gamma_{11}|^2 &= |\gamma_{01}|^2 |\gamma_{10}|^2 \\ \theta_{00} + \theta_{11} &= \theta_{01} + \theta_{10}. \end{aligned}$$

Using these relationships, we can determine an explicit expression for $\alpha_0, \alpha_1, \beta_0, \beta_1$ based on $\gamma_{00}, \gamma_{01}, \gamma_{10}, \gamma_{11}$; i.e., we show that if Eq. (1.3) holds, then $|\xi\rangle$ can be written as $|\psi\rangle \otimes |\phi\rangle$. We first define the modulus of the coefficients in $|\psi\rangle, |\phi\rangle$. We have:

$$\begin{aligned} |\gamma_{00}| &= \sqrt{|\gamma_{00}|^2} = \sqrt{|\gamma_{00}|^2(|\gamma_{00}|^2 + |\gamma_{01}|^2 + |\gamma_{10}|^2 + |\gamma_{11}|^2)} \\ &= \sqrt{|\gamma_{00}|^4 + |\gamma_{00}|^2|\gamma_{01}|^2 + |\gamma_{00}|^2|\gamma_{10}|^2 + |\gamma_{01}|^2|\gamma_{10}|^2} \\ &= \underbrace{\sqrt{|\gamma_{00}|^2 + |\gamma_{01}|^2}}_{|\alpha_0|} \underbrace{\sqrt{|\gamma_{00}|^2 + |\gamma_{10}|^2}}_{|\beta_0|}, \end{aligned}$$

and similarly for the other coefficients, we obtain:

$$\begin{aligned} |\gamma_{01}| &= \underbrace{\sqrt{|\gamma_{00}|^2 + |\gamma_{01}|^2}}_{|\alpha_0|} \underbrace{\sqrt{|\gamma_{01}|^2 + |\gamma_{11}|^2}}_{|\beta_1|} \\ |\gamma_{10}| &= \underbrace{\sqrt{|\gamma_{10}|^2 + |\gamma_{11}|^2}}_{|\alpha_1|} \underbrace{\sqrt{|\gamma_{00}|^2 + |\gamma_{10}|^2}}_{|\beta_0|} \\ |\gamma_{11}| &= \underbrace{\sqrt{|\gamma_{10}|^2 + |\gamma_{11}|^2}}_{|\alpha_1|} \underbrace{\sqrt{|\gamma_{01}|^2 + |\gamma_{11}|^2}}_{|\beta_1|}. \end{aligned}$$

To fully define the coefficients $\alpha_0, \alpha_1, \beta_0, \beta_1$ we must determine their phases. We can assign:

$$\alpha_0 = e^{i\theta_{00}}|\alpha_0|, \quad \alpha_1 = e^{i\theta_{10}}|\alpha_1|, \quad \beta_0 = |\beta_0|, \quad \beta_1 = e^{i(\theta_{01}-\theta_{00})}|\beta_1|. \quad (1.4)$$

Using the fact that $\theta_{11} = \theta_{01} + \theta_{10} - \theta_{00}$, it is now easy to verify that the state $|\xi\rangle$ in Eq. (1.2) can be expressed as $|\psi\rangle \otimes |\phi\rangle$ in Eq. (1.1) with coefficients $\alpha_0, \alpha_1, \beta_0, \beta_1$ as given in Eq. (1.4).

The condition in Eq. (1.3), to verify if a two-qubit state $|\xi\rangle$ can be expressed as a tensor product of two single-qubit states, can also be written in matrix form, which makes it easier to remember. If we assign the rows of the matrix to the first qubit, and the columns to the second qubit, we can arrange the coefficients γ as follows (notice how the first qubit has value 0 in the first row and 1 in the second row; similarly for the second qubit and the columns):

$$\begin{pmatrix} \gamma_{00} & \gamma_{01} \\ \gamma_{10} & \gamma_{11} \end{pmatrix}.$$

Then, $|\xi\rangle$ is a tensor product of two single-qubit states if and only if this matrix has rank 1. This is equivalent to Eq. (1.3).

We formalize the concept of expressing a quantum state as a tensor product of lower-dimensional quantum states as follows.

Definition 1.21 (Entangled state). A quantum state $|\psi\rangle \in (\mathbb{C}^2)^{\otimes q}$ is a product state if it can be expressed as a tensor product $|\psi_1\rangle \dots |\psi_q\rangle$ of q single-qubit states. Otherwise, it is entangled.

Notice that a general quantum state $|\psi\rangle$ could be the product of two or more lower-dimensional quantum states, e.g., $|\psi\rangle = |\psi_1\rangle \otimes |\psi_2\rangle$, with $|\psi_1\rangle$ and $|\psi_2\rangle$ being entangled states. In such a situation, $|\psi\rangle$ exhibits some entanglement, but in some sense it can still be “simplified”. Generally, according to the definition above, we call a quantum state entangled as long as it cannot be fully decomposed into a tensor product of single-qubit states. In the case of quantum systems composed of multiple subsystems (rather than just two subsystems as in the example $|\psi\rangle = |\psi_1\rangle \otimes |\psi_2\rangle$), the concept of entanglement as discussed in the literature is not as simple as given in Def. 1.21 (and the rank-1 test discussed at the end of Example 1.20 is not well-defined). However, our simplified definition works in this set of lecture notes and for most of the literature on quantum algorithms, therefore we can leave other considerations aside; we refer to [Coffman et al., 2000] as an entry point for a discussion on multipartite entanglement.

Example 1.22. Consider the following two-qubit state:

$$\frac{1}{2}|00\rangle + \frac{1}{2}|01\rangle + \frac{1}{2}|10\rangle + \frac{1}{2}|11\rangle.$$

This is a product state because it is equal to $\left(\frac{1}{\sqrt{2}}|0\rangle + \frac{1}{\sqrt{2}}|1\rangle\right) \otimes \left(\frac{1}{\sqrt{2}}|0\rangle + \frac{1}{\sqrt{2}}|1\rangle\right)$. By contrast, the following two-qubit state:

$$\frac{1}{\sqrt{2}}|00\rangle + \frac{1}{\sqrt{2}}|11\rangle$$

is an entangled state, because it cannot be expressed as a product of two single-qubit states.

1.3 Operations on qubits

Operations on quantum states must satisfy certain conditions, ensuring that applying an operation does not break the basic properties of a quantum state. The required property of operations on quantum states is stated below, and we treat it as a postulate.

Postulate 2. An operation applied by a quantum computer with q qubits, also called a gate, is a unitary matrix in $\mathbb{C}^{2^q \times 2^q}$.

Remark 1.23. A matrix U is unitary if $U^\dagger U = U U^\dagger = I$.

Remark 1.24. The term “unitary,” used as a noun, is a short form for “unitary matrix.” This usage is common in the quantum computing literature.

A well-known property of unitary matrices is that they are norm-preserving; that is, given a unitary matrix U and a vector v , $\|Uv\| = \|v\|$. Thus, for a q -qubit system, the quantum state is a unit vector $|\psi\rangle \in \mathbb{C}^{2^q}$, a quantum operation is a matrix $U \in \mathbb{C}^{2^q \times 2^q}$, and the application of U onto the state $|\psi\rangle$ is the unit vector $U|\psi\rangle \in \mathbb{C}^{2^q}$. This leads to the following remarks:

- Quantum operations are *linear*.
- Quantum operations are *reversible*.

While these properties may initially seem to be extremely restrictive, it is possible to show that a universal quantum computer is Turing-complete, implying that it can simulate any Turing-computable function, given sufficient time; see the notes in Sect. 1.5 for several references on a universal quantum Turing machine. Out of the two properties indicated above, the most counterintuitive is perhaps reversibility: the classical notion of computation does not appear to be reversible, because memory can be erased and, in the classical Turing machine, symbols can be erased from the tape. However, [Bennett, 1973] shows that all computations (including classical computations) can be made reversible by means of extra space. The general idea to make a function invertible is to have separate input and output registers: any output is stored in a different location than the input, so that the input does not have to be erased. This is a standard trick in quantum computing that is discussed in Sect. 1.3.7, but in order to present it in detail, we first need to introduce some notation for quantum circuits.

1.3.1 Notation for quantum circuits

The sequence of operations applied onto the qubits is usually represented by means of a *quantum circuit*. A quantum circuit indicates which operations are performed on each qubit, or group of qubits. For a quantum computer with q qubits, we represent q qubit lines, where the top line indicates qubit 1 and the rest are given in increasing order from the top. Operations are represented as gates; we use the terms “operation” and “gate” interchangeably. Gates take qubit lines as input, have the same number of qubit lines as output, and apply the unitary matrix indicated on the gate to the quantum state of those qubits. To think about the mathematical representation corresponding to a circuit, one should imagine that there is a tensor product symbol between the qubit lines. Fig. 1.1 is a simple example, with a gate acting on all qubits in the circuit.

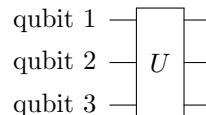


Figure 1.1: A simple quantum circuit.

Note that circuit diagrams are read from left to right, but because each gate corresponds to applying a matrix to the quantum state, the matrices corresponding to the gates should be written from right to left in the mathematical expression describing the action of the circuit. For example, in the circuit in Fig. 1.2, the outcome of the circuit is the state $BA|\psi\rangle$, because we start with

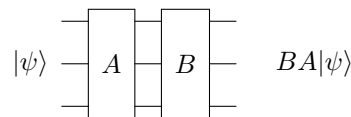


Figure 1.2: Order of the operations in a quantum circuit.

state $|\psi\rangle$, and we first apply the gate with unitary matrix A , and then B .

Gates can also be applied to individual qubits. Because a single qubit is a vector in \mathbb{C}^2 , a single-qubit gate is a unitary matrix in $\mathbb{C}^{2 \times 2}$. Consider the same three-qubit device, and suppose we want to apply the gate only to the third qubit. We would write it as in Fig. 1.3.

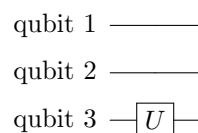


Figure 1.3: A circuit with a single-qubit gate.

From an algebraic point of view, the action of our first example in Fig. 1.1 on the quantum state is clear: the state of the three qubits is mapped onto another three-qubit state, as U acts on all the qubits. To give a proper mathematical characterization of the example in Fig. 1.3, where U is a single-qubit gate that acts on qubit 3 only, we have to imagine that an identity gate is applied to all the empty qubit lines. Therefore, Fig. 1.3 can be thought of as indicated in Fig. 1.4.

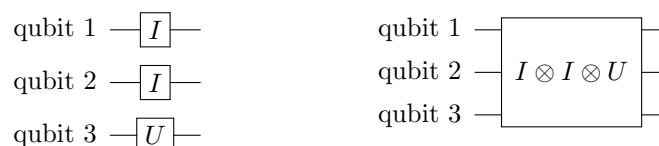


Figure 1.4: Equivalent representation of the circuit with a single-qubit gate in Fig. 1.3.

This circuit can be interpreted as applying the gate $I \otimes I \otimes U$ to the three-qubit state. Notice that by convention the matrix U , which is applied to qubit 3, appears in the rightmost term of

the tensor product. This is because qubit 3 is associated with the least significant digit according to our little-endian convention, see Def. 1.5 and the subsequent discussion. If we have a product state $|\psi\rangle \otimes |\phi\rangle \otimes |\xi\rangle$, the effect of $I \otimes I \otimes U$ is as indicated in Fig. 1.5.

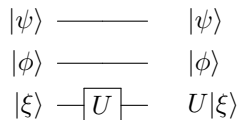


Figure 1.5: Effect of a single-qubit gate on a product state.

Indeed, $(I \otimes I \otimes U)(|\psi\rangle \otimes |\phi\rangle \otimes |\xi\rangle) = |\psi\rangle \otimes |\phi\rangle \otimes U|\xi\rangle$. If the system is in an entangled state, however, the action of $(I \otimes I \otimes U)$ cannot be determined in such a simple way, because the state cannot be factored as a product state. Thus, for a general entangled input state, the effect of the circuit is as indicated in Fig. 1.6. Notice that this fact is essentially the reason why simulation of

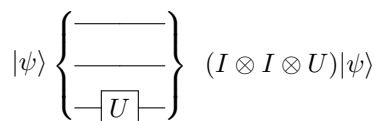


Figure 1.6: Effect of a single-qubit gate on an entangled state.

quantum computations on classical computers may take exponential resources in the worst case: to simulate the effect of even a single-qubit gate on the entangled state $|\psi\rangle$, we have to explicitly compute the effect of the $2^q \times 2^q$ matrix $(I \otimes I \otimes U)$ on the state $|\psi\rangle$. This requires exponential space with a naive approach (if the matrices and vectors are stored explicitly), and even with more parsimonious approaches it may require exponential time (e.g., if we compute elements of the state vector one at a time). As long as the quantum state is not entangled computations can be carried out on each qubit independently, but entanglement requires us to keep track of the full quantum state in 2^q -dimensional complex space, leading to large amounts of memory — or time — required.

1.3.2 Input-output, and measurement gates

We are almost ready to introduce the last postulate that we need to formally define the model of computation. To do so, it is useful to discuss the input-output model for quantum computations. The *input* of a quantum computation consists of an initial quantum state, and the description of a quantum circuit.

Remark 1.25. *The quantum state and the quantum circuit must be described in a suitable compact way: for a circuit on q qubits, a unitary matrix can be of size $2^q \times 2^q$, but for an efficient algorithm we require that the circuit contains polynomially-many gates in q and each gate has a compact representation. This is discussed further in the rest of this chapter.*

By convention, the initial quantum state of the quantum computing device is assumed to be the all-zero binary string $|\vec{0}\rangle$ of appropriate size (i.e., $|\vec{0}\rangle_q$ if we have q qubits in total), unless otherwise specified. Of course, the circuit can act on the state and transform it into a more suitable one. Examples of how this can be done are given in the remainder of this section.

A quantum algorithm consists in the execution of one or more quantum computations. There are also hybrid algorithms involving classical and quantum computations. In such situations, the quantum computations can generally be thought of as subroutines, but this does not change the principle that each of these quantum computations is described by an initial quantum state (typically, $|\vec{0}\rangle$) and a quantum circuit. An important thing to note is that if there is any data that has to be fed to the algorithm, this data has to be embedded in the quantum circuit given as part of the input (which may, sometime, have a significant impact on the number of gates that are necessary to describe the circuit). This summarizes the input model. But what is the *output* of the quantum computer?

So far we characterized properties of quantum states and quantum gates. Remarkably, the state of a q -qubit quantum register is described by a vector of dimension 2^q , exponentially larger than the dimension of the vector required to describe q classical bits. However, there is a catch: in a classical computer we can simply read the state of the bits, whereas in a quantum computer we do not have direct, unrestricted access to the quantum state. Information on the quantum state is only gathered through a *measurement gate*, depicted in the circuit diagram in Fig. 1.7. We now formally define the effect of a single-bit measurement gate.

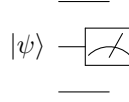


Figure 1.7: Single-qubit measurement.

Postulate 3. *Information on the state of a quantum computing device can only be obtained through a measurement. Given a q -qubit quantum state $|\psi\rangle = \sum_{\vec{j} \in \{0,1\}^q} \alpha_j |\vec{j}\rangle$, a measurement gate on qubit k outputs a sample from a random variable \mathcal{Q}_k with sample space $\{0, 1\}$ and the following distribution:*

$$\Pr(\mathcal{Q}_k = 0) = \sum_{\vec{j} \in \{0,1\}^q: \vec{j}_k=0} |\alpha_j|^2,$$

$$\Pr(\mathcal{Q}_k = 1) = \sum_{\vec{j} \in \{0,1\}^q: \vec{j}_k=1} |\alpha_j|^2.$$

Let $x \in \{0, 1\}$ be the observed value. After the measurement, the quantum state becomes:

$$\sum_{\substack{\vec{j} \in \{0,1\}^q \\ \vec{j}_k=x}} \frac{\alpha_j}{\sqrt{\sum_{\vec{\ell}: \vec{\ell}_k=x} |\alpha_{\ell}|^2}} |\vec{j}\rangle.$$

The original quantum state is no longer recoverable.

Remark 1.26. *The state of the quantum computer after a measurement collapses to a linear combination of only those basis states that are consistent with the outcome of the measurement, i.e., basis states $|\vec{j}\rangle$ with $\vec{j}_k = x$. The coefficients α_j for such basis states are normalized to yield a unit vector.*

The rule for single-qubit measurements leads to a very simple and natural expression for the probability of observing a given binary string when measuring all the qubits.

Proposition 1.27. *Given a q -qubit quantum state $|\psi\rangle = \sum_{\vec{j} \in \{0,1\}^q} \alpha_j |\vec{j}\rangle$, applying a measurement gate to the q qubits in any order yields \vec{j} with probability $|\alpha_j|^2$, for $\vec{j} \in \{0, 1\}^q$.*

Proof. We need to show that the probability of observing \vec{j} after q single-qubit measurements is equal to $|\alpha_j|^2$. We can do this by induction on q . The case $q = 1$ is trivial. We now show how to go from $q - 1$ to q . As in Post. 3, we write $\Pr(\mathcal{Q}_k = x)$ to denote the probability that the measurement of qubit k yields $x \in \{0, 1\}$. If it is important to indicate the quantum state on which the measurement is performed, we use the notation $\Pr_{|\psi\rangle}(\mathcal{Q}_k = x)$ to indicate that the measurement is applied to state $|\psi\rangle$.

Suppose we apply a measurement to all qubits in an arbitrary order, and the qubit in position h is the first to be measured. (The order of the remaining measurements does not matter for the proof, because after the first measurement we rely on the inductive hypothesis). The probability of obtaining the outcome \vec{j} is:

$$\Pr_{|\psi\rangle}(\mathcal{Q}_1 = \vec{j}_1, \dots, \mathcal{Q}_q = \vec{j}_q) =$$

$$\Pr_{|\psi\rangle}(\mathcal{Q}_1 = \vec{j}_1, \dots, \mathcal{Q}_{h-1} = \vec{j}_{h-1}, \mathcal{Q}_{h+1} = \vec{j}_{h+1}, \dots, \mathcal{Q}_q = \vec{j}_q | \mathcal{Q}_h = \vec{j}_h) \Pr_{|\psi\rangle}(\mathcal{Q}_h = \vec{j}_h) =$$

$$\Pr_{|\phi\rangle}(\mathcal{Q}_1 = \vec{j}_1, \dots, \mathcal{Q}_{h-1} = \vec{j}_{h-1}, \mathcal{Q}_{h+1} = \vec{j}_{h+1}, \dots, \mathcal{Q}_q = \vec{j}_q) \Pr_{|\psi\rangle}(\mathcal{Q}_h = \vec{j}_h),$$

where $|\phi\rangle$ is the state obtained from $|\psi\rangle$ after measuring the qubit in position h and observing \vec{j}_h . By Post. 3, we have:

$$|\phi\rangle = \sum_{\substack{\vec{k} \in \{0,1\}^q \\ \vec{k}_h = \vec{j}_h}} \frac{\alpha_{\vec{k}}}{\sqrt{\sum_{\vec{\ell} \in \{0,1\}^q: \vec{\ell}_h = \vec{j}_h} |\alpha_{\vec{\ell}}|^2}} |\vec{k}\rangle =: \sum_{\substack{\vec{k} \in \{0,1\}^q \\ \vec{k}_h = \vec{j}_h}} \beta_{\vec{k}} |\vec{k}\rangle,$$

and the coefficients $\beta_{\vec{k}}$, defined as above, are only defined for $\vec{k} \in \{0,1\}^q : \vec{k}_h = \vec{j}_h$. By Post. 3, applying a single-qubit measurement, we also have:

$$\Pr_{|\psi\rangle}(\mathcal{Q}_h = \vec{j}_h) = \sum_{\vec{k} \in \{0,1\}^q: \vec{k}_h = \vec{j}_h} |\alpha_{\vec{k}}|^2.$$

By the induction hypothesis:

$$\Pr_{|\phi\rangle}(\mathcal{Q}_1 = \vec{j}_1, \dots, \mathcal{Q}_{h-1} = \vec{j}_{h-1}, \mathcal{Q}_{h+1} = \vec{j}_{h+1}, \dots, \mathcal{Q}_q = \vec{j}_q) = |\beta_{\vec{j}}|^2,$$

because: $|\phi\rangle$ is the state after measuring the qubit in position h and obtaining \vec{j}_h as the outcome, therefore it only contains basis states \vec{k} with $\vec{k}_h = \vec{j}_h$; and the induction hypothesis imposes that the probability of observing the entire binary string \vec{j} (for qubits other than qubit h , because qubit h was already measured, i.e., value \vec{j}_ℓ in position ℓ , $\ell \neq h$) is simply $|\beta_{\vec{j}}|^2$. Remembering that $\beta_{\vec{k}} = \alpha_{\vec{k}} / \left(\sqrt{\sum_{\vec{\ell} \in \{0,1\}^q: \vec{\ell}_h = \vec{j}_h} |\alpha_{\vec{\ell}}|^2} \right)$, we finally obtain:

$$\Pr_{|\psi\rangle}(\mathcal{Q}_1 = \vec{j}_1, \dots, \mathcal{Q}_q = \vec{j}_q) = \frac{|\alpha_{\vec{j}}|^2}{\sum_{\vec{\ell} \in \{0,1\}^q: \vec{\ell}_h = \vec{j}_h} |\alpha_{\vec{\ell}}|^2} \left(\sum_{\substack{\vec{k} \in \{0,1\}^q \\ \vec{k}_h = \vec{j}_h}} |\alpha_{\vec{k}}|^2 \right) = |\alpha_{\vec{j}}|^2.$$

□

Proposition 1.27 above shows that the two circuits in Fig. 1.8 are equivalent. In other words,



Figure 1.8: Multiple-qubit measurement.

the single-qubit measurement gate as defined in Post. 3 is sufficient to measure any number of qubits in the most natural way, i.e., the measurement outcome \vec{j} on the q qubits occurs with probability that is exactly equal to $|\alpha_{\vec{j}}|^2$. Notice that with this simple rule, it is easy to compute the probability of obtaining a given string on a given subset of the qubits: we just need to add up the modulus squared of the coefficients for all those basis states that contain the desired string in the desired position.

Example 1.28. Consider again the following two-qubit state:

$$\alpha_{00}|00\rangle + \alpha_{01}|01\rangle + \alpha_{10}|10\rangle + \alpha_{11}|11\rangle = \frac{1}{2}|00\rangle + \frac{1}{2}|01\rangle + \frac{1}{2}|10\rangle + \frac{1}{2}|11\rangle.$$

We noted in Ex. 1.22 that this is a product state. As usual, let qubit 1 the first qubit (i.e., the one corresponding to the first digit in the two-digit binary strings), and let qubit 2 be the second qubit

(i.e., the one corresponding to the second digit in the two-digit binary strings). Then:

$$\begin{aligned}\Pr(\mathcal{Q}_1 = 0) &= |\alpha_{00}|^2 + |\alpha_{01}|^2 = \left(\frac{1}{2}\right)^2 + \left(\frac{1}{2}\right)^2 = \frac{1}{2} \\ \Pr(\mathcal{Q}_1 = 1) &= |\alpha_{10}|^2 + |\alpha_{11}|^2 = \left(\frac{1}{2}\right)^2 + \left(\frac{1}{2}\right)^2 = \frac{1}{2} \\ \Pr(\mathcal{Q}_2 = 0) &= |\alpha_{00}|^2 + |\alpha_{10}|^2 = \left(\frac{1}{2}\right)^2 + \left(\frac{1}{2}\right)^2 = \frac{1}{2} \\ \Pr(\mathcal{Q}_2 = 1) &= |\alpha_{01}|^2 + |\alpha_{11}|^2 = \left(\frac{1}{2}\right)^2 + \left(\frac{1}{2}\right)^2 = \frac{1}{2}.\end{aligned}$$

Suppose we measure qubit 2 and we obtain 1 as the outcome of the measurement. Then the state of the two-qubit system collapses to:

$$\frac{1}{\sqrt{2}}|01\rangle + \frac{1}{\sqrt{2}}|11\rangle.$$

The measurement outcome distribution for qubit 1 for this new state is:

$$\Pr(\mathcal{Q}_1 = 0) = \frac{1}{2} \quad \Pr(\mathcal{Q}_1 = 1) = \frac{1}{2}.$$

Hence, the probability of observing 0 or 1 when measuring qubit 1 did not change after the measurement.

Consider now the following entangled two-qubit state:

$$\beta_{00}|00\rangle + \beta_{11}|11\rangle = \frac{1}{\sqrt{2}}|00\rangle + \frac{1}{\sqrt{2}}|11\rangle.$$

Doing the calculations, we still have:

$$\begin{aligned}\Pr(\mathcal{Q}_1 = 0) &= |\beta_{00}|^2 = \frac{1}{2} & \Pr(\mathcal{Q}_1 = 1) &= |\beta_{11}|^2 = \frac{1}{2} \\ \Pr(\mathcal{Q}_2 = 0) &= |\beta_{00}|^2 = \frac{1}{2} & \Pr(\mathcal{Q}_2 = 1) &= |\beta_{11}|^2 = \frac{1}{2}.\end{aligned}$$

As before, suppose we measure qubit 2 and we obtain 1 as the outcome of the measurement. Then the state of the two-qubit system collapses to:

$$|11\rangle.$$

If we measure qubit 1 from this state, we obtain:

$$\Pr(\mathcal{Q}_1 = 0) = 0 \quad \Pr(\mathcal{Q}_1 = 1) = 1.$$

The situation is now very different: the probability distribution of \mathcal{Q}_1 has changed after measuring qubit 2 (obtaining a sample from \mathcal{Q}_2). This is exactly the concept of entanglement: when two or more qubits are entangled, they affect each other, and measuring one qubit changes the probability distribution characterizing the measurement outcomes for the other qubits.

The example above can be seen in terms of conditional probabilities: if, for all $x, y \in \{0, 1\}$, we have $\Pr(\mathcal{Q}_1 = x) = \Pr(\mathcal{Q}_1 = x | \mathcal{Q}_2 = y)$ (i.e., the random variables $\mathcal{Q}_1, \mathcal{Q}_2$ are independent), then the two qubits are not entangled (product state), whereas if $\Pr(\mathcal{Q}_1 = x) \neq \Pr(\mathcal{Q}_1 = x | \mathcal{Q}_2 = y)$ for some x, y , there is entanglement. Indeed, recall that taking the tensor product of two vectors containing outcome probabilities for independent random variables yields the joint probability distribution. Quantum state vectors do not contain outcome probabilities, but the modulus squared of the components of the state vector corresponds to a probability. Furthermore, for any two complex numbers $\alpha, \beta \in \mathbb{C}$ we have $|\alpha\beta|^2 = |\alpha|^2|\beta|^2$, so the operation to compute probabilities from

state coefficients is distributive with respect to multiplication. A product state is a tensor product of smaller-dimensional state vectors, hence it leads to outcome probabilities that are simply the product of the outcome probabilities corresponding to measuring each of the qubits independently. Conversely, an entangled state is not a product state, and the random variables associated with measuring each of the qubits are no longer independent.

Remark 1.29. *Despite the above discussion, it would be wrong to think of the quantum state as a probability distribution: the quantum state induces a probability distribution by taking the modulus squared of its entries, but it is not a probability distribution! Indeed, the coefficients in a quantum state are complex numbers unrestricted in sign, while probabilities are nonnegative real numbers. Furthermore, just as there is an infinite set of complex numbers that have the same modulus (i.e., the set $\{a \in \mathbb{C} : |a| = v\}$ for some real number $v > 0$ is infinite), there is an infinite number of quantum state vectors in $(\mathbb{C}^2)^{\otimes q}$ that yield the same distribution. After applying the same sequence of operations to two states that induce the same probability distribution, we may or may not obtain quantum states that induce the same outcome distribution: this is shown in the next two examples.*

Example 1.30. *Suppose we have two q -qubit quantum states $|\psi\rangle, |\phi\rangle$ satisfying $|\psi\rangle = e^{i\theta}|\phi\rangle$ for some $\theta \in \mathbb{R}$. Now consider the application of some unitary matrix U onto $|\psi\rangle$ and $|\phi\rangle$, followed by a measurement of all the qubits. Define:*

$$U|\phi\rangle := \sum_{\vec{j} \in \{0,1\}^q} \alpha_j |\vec{j}\rangle$$

for some (normalized) coefficients α_j , which implies:

$$U|\psi\rangle = Ue^{i\theta}|\phi\rangle = \sum_{\vec{j} \in \{0,1\}^q} e^{i\theta} \alpha_j |\vec{j}\rangle.$$

This means that for a given \vec{k} :

$$\Pr_{U|\phi}(\mathcal{Q}_1 = \vec{k}_1, \dots, \mathcal{Q}_q = \vec{k}_q) = |\alpha_k|^2, \quad \Pr_{U|\psi}(\mathcal{Q}_1 = \vec{k}_1, \dots, \mathcal{Q}_q = \vec{k}_q) = |e^{i\theta} \alpha_k|^2 = |\alpha_k|^2,$$

so the probability of obtaining \vec{k} as the outcome of a measurement is the same for both $U|\psi\rangle$ and $U|\phi\rangle$. Because this is true after applying an arbitrary unitary U , it is also true after applying a whole circuit, which is just a sequence of unitaries. Hence, if the vectors $|\psi\rangle, |\phi\rangle$ satisfy the relationship $|\psi\rangle = e^{i\theta}|\phi\rangle$, they induce the same outcome distribution, no matter what (unitary) operations we apply to them. The factor $e^{i\theta}$ is usually called global phase and can safely be ignored in the calculations.

Example 1.31. *Consider the following two single-qubit states:*

$$|\psi\rangle = \frac{1}{\sqrt{2}}|0\rangle + \frac{1}{\sqrt{2}}|1\rangle \quad |\phi\rangle = \frac{1}{\sqrt{2}}|0\rangle - \frac{1}{\sqrt{2}}|1\rangle.$$

Both induce the same probability distribution on the measurement outcomes:

$$\begin{aligned} \Pr_{|\psi\rangle}(\mathcal{Q}_1 = 0) &= \frac{1}{2} & \Pr_{|\psi\rangle}(\mathcal{Q}_1 = 1) &= \frac{1}{2} \\ \Pr_{|\phi\rangle}(\mathcal{Q}_1 = 0) &= \frac{1}{2} & \Pr_{|\phi\rangle}(\mathcal{Q}_1 = 1) &= \frac{1}{2}. \end{aligned}$$

But $|\psi\rangle$ and $|\phi\rangle$ are very different states! If we apply a certain unitary matrix to both (this gate is called Hadamard gate, see Sect. 1.3.4), we obtain very different results – orthogonal vectors, in fact:

$$\begin{aligned} \frac{1}{\sqrt{2}} \begin{pmatrix} 1 & 1 \\ 1 & -1 \end{pmatrix} |\psi\rangle &= \frac{1}{2} \begin{pmatrix} 1 & 1 \\ 1 & -1 \end{pmatrix} \begin{pmatrix} 1 \\ 1 \end{pmatrix} = \frac{1}{2} \begin{pmatrix} 2 \\ 0 \end{pmatrix} = |0\rangle \\ \frac{1}{\sqrt{2}} \begin{pmatrix} 1 & 1 \\ 1 & -1 \end{pmatrix} |\phi\rangle &= \frac{1}{2} \begin{pmatrix} 1 & 1 \\ 1 & -1 \end{pmatrix} \begin{pmatrix} 1 \\ -1 \end{pmatrix} = \frac{1}{2} \begin{pmatrix} 0 \\ 2 \end{pmatrix} = |1\rangle. \end{aligned}$$

This illustrates the dangers of thinking about the quantum state as a probability distribution, rather than a set of complex coefficients that induce a probability distribution.

1.3.3 The no-cloning principle

Because measurement destroys the quantum state, it is natural to look for a way to create a copy of a quantum state. If a clone could be created, it would be possible to perform measurements on the clone, so that the original state would not be destroyed. Furthermore, cloning would allow us to take several measurements of the same set of qubits without having to repeat the circuit that creates the quantum state. However, it turns out that cloning is impossible: this is a direct consequence of the properties of quantum gates, in particular the fact that gates are unitary matrices.

Theorem 1.32 (No-cloning principle). *There does not exist a unitary matrix that maps $|\psi\rangle_q|\vec{0}\rangle_q$ to $|\psi\rangle_q|\psi\rangle_q$ for an arbitrary quantum state on q qubits $|\psi\rangle$.*

Proof. Suppose there exists such a unitary U . Then for any two quantum states $|\psi\rangle, |\phi\rangle$ on q qubits, we have (all registers in this proof are q qubits each):

$$\begin{aligned} U(|\psi\rangle|\vec{0}\rangle) &= |\psi\rangle|\psi\rangle \\ U(|\phi\rangle|\vec{0}\rangle) &= |\phi\rangle|\phi\rangle. \end{aligned}$$

Using these equalities, and remembering that $U^\dagger U = I$, we can write:

$$\begin{aligned} \langle\phi|\psi\rangle &= \langle\phi|\psi\rangle \underbrace{\langle\vec{0}|\vec{0}\rangle}_{=1} = \langle\phi|\psi\rangle \otimes (\langle\vec{0}|\vec{0}\rangle) = (\langle\phi| \otimes \langle\vec{0}|)(|\psi\rangle \otimes |\vec{0}\rangle) \\ &= (\langle\phi| \otimes \langle\vec{0}|)U^\dagger U(|\psi\rangle \otimes |\vec{0}\rangle) = (\langle\phi| \otimes \langle\phi|)(|\psi\rangle \otimes |\psi\rangle) = \langle\phi|\psi\rangle^2. \end{aligned}$$

But $\langle\phi|\psi\rangle = \langle\phi|\psi\rangle^2$ is only true if $\langle\phi|\psi\rangle$ is equal to 0 or to 1, contradicting the fact that $|\phi\rangle, |\psi\rangle$ are arbitrary quantum states. \square

The above theorem shows that we cannot copy an arbitrary quantum state. We remark that the proof does not rule out the possibility of constructing a unitary matrix that copies a specific quantum state. In other words, if we know what quantum state we want to copy, one could construct a unitary matrix to do that; but it is impossible to construct a single unitary matrix to copy all possible states. This establishes that we cannot “cheat” the destructive effect of a measurement by simply cloning the state before the measurement. Hence, whenever we run a circuit that produces an output quantum state, in general we can reproduce the output quantum state only by repeating all the steps of the circuit. So if we think of the circuit as implementing an algorithm, followed by a measurement to get a sample from a certain probability distribution, in general we need to run the algorithm again from scratch to get another sample.

1.3.4 Basic operations and universality

Quantum computation does not allow the user to apply every possible unitary matrix in the circuit that they want to run (i.e., their code), just as classical computations do not allow the user to apply every possible classical function. Rather, the user is limited to gates (unitary matrices) that are efficiently specifiable and implementable, just as classically one can only write efficient programs by specifying a polynomial-size sequence of basic operations on bits. The specification of a unitary matrix must be done by combining gates out of a basic set, which can be thought of as the instruction set of the quantum computer. We now discuss what these basic gates are, and how they can be combined to form other operations.

We use the following two definitions of operations on binary strings; these are frequently used in this and subsequent chapters.

Definition 1.33 (Bitwise XOR). For any integer $q > 0$ and binary strings $\vec{j}, \vec{k} \in \{0, 1\}^q$, we denote by $\vec{j} \oplus \vec{k}$ the bitwise modulo-2 addition of q -digit strings (bitwise XOR), defined as:

$$\vec{j} \oplus \vec{k} := \vec{h}, \text{ with } \vec{h} \in \{0, 1\}^q \text{ and } h_p = \begin{cases} 0 & \text{if } j_p = k_p \\ 1 & \text{otherwise} \end{cases} \text{ for all } p = 1, \dots, q.$$

Definition 1.34 (Bitwise dot product). For any integer $q > 0$ and binary strings $\vec{j}, \vec{k} \in \{0, 1\}^q$, we denote by $\vec{j} \bullet \vec{k}$ the bitwise dot product of q -digit strings, defined as:

$$\vec{j} \bullet \vec{k} := \sum_{h=1}^q j_h k_h.$$

We also use this (common) definition of matrix norm, which we state for completeness. It is usually referred to as the operator norm induced by the Euclidean norm.

Definition 1.35 (Matrix norm). For a given matrix A , we denote $\|A\| = \sup_{x: \|x\|=1} \|Ax\|$.

Single-qubit gates. The first operations that we discuss are the *Pauli gates*.

Definition 1.36 (Pauli gates). The four Pauli gates are the following single-qubit gates:

$$\begin{aligned} I &= \begin{pmatrix} 1 & 0 \\ 0 & 1 \end{pmatrix} & X &= \begin{pmatrix} 0 & 1 \\ 1 & 0 \end{pmatrix} \\ Y &= \begin{pmatrix} 0 & -i \\ i & 0 \end{pmatrix} & Z &= \begin{pmatrix} 1 & 0 \\ 0 & -1 \end{pmatrix}. \end{aligned}$$

Proposition 1.37. The Pauli gates form a basis for $\mathbb{C}^{2 \times 2}$, they are Hermitian, and they satisfy the relationship $XYZ = iI$.

The proof is left as an exercise. The X gate is the equivalent of the NOT gate in classical computers, as it implements a bit (rather, qubit) flip, changing from $|0\rangle$ to $|1\rangle$ and vice versa:

$$X|0\rangle = |1\rangle \quad X|1\rangle = |0\rangle.$$

The Z gate is also called a phase flip gate: it leaves $|0\rangle$ unchanged, and maps $|1\rangle$ to $-|1\rangle$.

$$Z|0\rangle = |0\rangle \quad Z|1\rangle = -|1\rangle.$$

A single-qubit gate that is used in many quantum algorithms is the so-called Hadamard gate:

$$H = \frac{1}{\sqrt{2}} \begin{pmatrix} 1 & 1 \\ 1 & -1 \end{pmatrix}.$$

The action of H is as follows:

$$H|0\rangle = \frac{1}{\sqrt{2}} (|0\rangle + |1\rangle) \quad H|1\rangle = \frac{1}{\sqrt{2}} (|0\rangle - |1\rangle).$$

In the rest of this set of lecture notes we sometimes need an algebraic expression for the action of Hadamard gates on basis states. The effect of H on a single-qubit basis state $|x\rangle$, $x \in \{0, 1\}$, can be summarized as follows:

$$H|x\rangle = \frac{1}{\sqrt{2}} (|0\rangle + (-1)^x |1\rangle) = \frac{1}{\sqrt{2}} \sum_{k=0}^1 (-1)^{kx} |k\rangle.$$

This is consistent with the previous expression for H . Using our notation, we can define the effect of $H^{\otimes q}$ on a q -qubit basis state $|\vec{x}\rangle_q$ as:

$$\begin{aligned} H^{\otimes q}|\vec{x}\rangle_q &= \frac{1}{\sqrt{2^q}} \sum_{k_1=0}^1 \cdots \sum_{k_q=0}^1 (-1)^{\sum_{h=1}^q k_h \bar{x}_h} |k_1\rangle \otimes \cdots \otimes |k_q\rangle \\ &= \frac{1}{\sqrt{2^q}} \sum_{\vec{k} \in \{0,1\}^q} (-1)^{\vec{k} \bullet \vec{x}} |\vec{k}\rangle, \end{aligned} \tag{1.5}$$

where \bullet is the bitwise dot product, see Def. 1.34. When considering multiple Hadamard gates in parallel, it is sometimes useful to rely on the following relationship, that can be easily verified using the definition:

$$H^{\otimes q} = \frac{1}{\sqrt{2}} \begin{pmatrix} H^{\otimes q-1} & H^{\otimes q-1} \\ H^{\otimes q-1} & -H^{\otimes q-1} \end{pmatrix}.$$

The next proposition shows one of the reasons why the Hadamard gate is frequently employed in many quantum algorithms.

Proposition 1.38. *Given a q -qubit quantum register initially in the state $|\vec{0}\rangle_q$, applying the Hadamard gate to all qubits, or equivalently the matrix $H^{\otimes q}$, yields the uniform superposition of basis states $\frac{1}{\sqrt{2^q}} \sum_{\vec{j} \in \{0,1\}^q} |\vec{j}\rangle$.*

Proof. We have:

$$H^{\otimes q}|\vec{0}\rangle_q = H^{\otimes q}|0\rangle^{\otimes q} = (H|0\rangle)^{\otimes q} = \left(\frac{1}{\sqrt{2}}|0\rangle + \frac{1}{\sqrt{2}}|1\rangle \right)^{\otimes q} = \frac{1}{\sqrt{2^q}} \sum_{\vec{j} \in \{0,1\}^q} |\vec{j}\rangle.$$

□

Remark 1.39. *The uniform superposition of the 2^q basis states on q qubits can be obtained from the initial state $|\vec{0}\rangle_q$ by applying q gates only.*

The multiple Hadamard can be represented by one of the equivalent circuits given in Fig. 1.9. Several quantum algorithms start by setting the state of the quantum device to a uniform super-



Figure 1.9: Two representations for multiple Hadamard gates.

position, and then apply further operations which, by linearity, are simultaneously applied to all the possible binary strings. This is a remarkable advantage of quantum computing over classical computing.

Readers with advanced knowledge of theoretical computer science might be wondering how this compares to classical probabilistic computation, i.e., probabilistic Turing machines, a well-known concept in computational complexity theory. A probabilistic Turing machine is initialized with a set of random bits that take an unknown value and influence the state transition. The state is described by a probability distribution over all the possible states, because we do not know the value of the random bits with which the machine is initialized. When a state transition occurs, to update the description of the state we need to apply the transition to all states that appear with positive probability. In this sense, operations in a probabilistic Turing machine can be thought of as being simultaneously applied to many (possibly all) binary strings. However, a probabilistic Turing machine admits a more compact description of the state: if we know the random bits with which the machine is initialized, then the state becomes deterministically known. Hence, for a

given value of the random bits, the state of the probabilistic Turing machine can be described in linear space, and operations map one state into another state. On the other hand, it is not known how to obtain such a compact description for a quantum computer: there is no equivalent for the random bits, and a characterization of the state truly requires an exponential number of complex coefficients. In fact, it is believed that quantum computers are more powerful than probabilistic Turing machines, although there is no formal proof.

To conclude our discussion on single-qubit gates, we note that all single-qubit can be represented by the following parameterized matrix that describes all unitary matrices (up to a global phase factor):

$$U(\theta, \phi, \lambda) = \begin{pmatrix} e^{-i(\phi+\lambda)/2} \cos(\theta/2) & -e^{-i(\phi-\lambda)/2} \sin(\theta/2) \\ e^{i(\phi-\lambda)/2} \sin(\theta/2) & e^{i(\phi+\lambda)/2} \cos(\theta/2) \end{pmatrix}$$

All single-qubit gates can be obtained by an appropriate choice of parameters θ, ϕ, λ . This parameterized expression is used in some of the existing programming languages for quantum circuits.

Two-qubit gates. Another fundamental gate is the CX gate, also called “controlled NOT” or “CNOT” (because the X gate acts as a NOT). The CX gate is a two-qubit gate that has a control bit and a target bit, and acts as follows: if the control bit is $|0\rangle$, nothing happens, whereas if the control bit is $|1\rangle$, the target bit is bit-flipped (i.e., the same effect as the X gate). The corresponding circuit diagram is given in Fig. 1.10.



Figure 1.10: The CX_{12} , or controlled NOT, gate with control qubit 1 and target qubit 2.

The matrix description of the gate with control qubit 1 and target qubit 2 is as follows:

$$CX_{12} = \begin{pmatrix} 1 & 0 & 0 & 0 \\ 0 & 1 & 0 & 0 \\ 0 & 0 & 0 & 1 \\ 0 & 0 & 1 & 0 \end{pmatrix}.$$

Thus, the effect of CX is:

$$\begin{aligned} CX_{12}|00\rangle &= |00\rangle & CX_{12}|01\rangle &= |01\rangle \\ CX_{12}|10\rangle &= |11\rangle & CX_{12}|11\rangle &= |10\rangle. \end{aligned}$$

This leads to the following formula for the effect of CX:

$$CX_{12}|x\rangle|y\rangle = |x\rangle|y \oplus x\rangle, \quad \forall x, y \in \{0, 1\}.$$

The CX gate can create and destroy entanglement, as shown in the next example.

Example 1.40. Consider the circuit in Fig. 1.11.

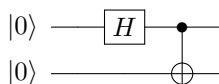


Figure 1.11: A circuit that produces an entangled state.

The circuit yields the following state:

$$CX_{12}(H \otimes I)|00\rangle = CX_{12} \left(\frac{1}{\sqrt{2}}(|0\rangle + |1\rangle)|0\rangle \right) = \frac{1}{\sqrt{2}}(|00\rangle + |11\rangle).$$

As we have seen in Ex. 1.28, this is an entangled state. In this case it is also easy to break entanglement: just apply CX one more time, which reverses the last operation and brings us back to the state $\frac{1}{\sqrt{2}}(|0\rangle + |1\rangle)|0\rangle$.

An interesting feature of the CX gate is that it can be used to swap two qubits. A swap between two qubits j and k is defined as the operation that maps a quantum state to a new quantum state in which every basis state has its j -th and k -th digit permuted; this corresponds to the following matrix:

$$\text{SWAP} = \begin{pmatrix} 1 & 0 & 0 & 0 \\ 0 & 0 & 1 & 0 \\ 0 & 1 & 0 & 0 \\ 0 & 0 & 0 & 1 \end{pmatrix}.$$

If two qubits are in a product state $|\psi\rangle_1 \otimes |\phi\rangle_1$, then $\text{SWAP}(|\psi\rangle_1 \otimes |\phi\rangle_1) = |\phi\rangle \otimes |\psi\rangle$. The circuit diagram for the SWAP gate is given in Fig. 1.12. Considering that CX , like all quantum gates,



Figure 1.12: The SWAP gate.

is a linear map, it may sound surprising that it can implement a swap. However, the SWAP gate can indeed be constructed out of CX gates using the circuit depicted in Fig. 1.13.

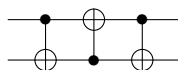


Figure 1.13: Implementation of SWAP using CX gates.

Proposition 1.41. *The circuit in Fig. 1.13, constructed with three CX gates, swaps qubits 1 and 2.*

Proof. By linearity, it suffices to show that the circuit above maps $|00\rangle \rightarrow |00\rangle$, $|01\rangle \rightarrow |10\rangle$, $|10\rangle \rightarrow |01\rangle$, and $|11\rangle \rightarrow |11\rangle$. We have:

$$\begin{aligned} CX_{12}CX_{21}CX_{12}|00\rangle &= CX_{12}CX_{21}|00\rangle = CX_{12}|00\rangle = |00\rangle. \\ CX_{12}CX_{21}CX_{12}|01\rangle &= CX_{21}CX_{12}|01\rangle = CX_{12}|11\rangle = |10\rangle. \\ CX_{12}CX_{21}CX_{12}|10\rangle &= CX_{12}CX_{21}|11\rangle = CX_{12}|01\rangle = |01\rangle. \\ CX_{12}CX_{21}CX_{12}|11\rangle &= CX_{12}CX_{21}|10\rangle = CX_{12}|10\rangle = |11\rangle. \end{aligned}$$

Therefore, the SWAP circuit maps:

$$\alpha_{00}|00\rangle + \alpha_{01}|01\rangle + \alpha_{10}|10\rangle + \alpha_{11}|11\rangle \rightarrow \alpha_{00}|00\rangle + \alpha_{01}|10\rangle + \alpha_{10}|01\rangle + \alpha_{11}|11\rangle.$$

□

The SWAP circuit is particularly important for practical reasons: sometimes, in the current generation of quantum computing hardware, two-qubit gates can only be applied among certain pairs of qubits. For example, when employing one of the most prevalent quantum hardware technologies (superconducting qubits, see e.g. [Devoret and Schoelkopf, 2013, Castelveccchi, 2017]), two-qubit gates can only be applied to qubits that are physically adjacent on a chip. Thanks to the SWAP, as long as the graph representing the qubit adjacency in the hardware device is a connected graph, two-qubit gates can be applied to any pair of qubits: if the qubits are not directly connected by an edge on the graph (e.g., physically located next to each other on the chip), we just need to SWAP one of them as many times as is necessary to bring it to a location adjacent to the other qubit. In this way, we can assume that each qubit can interact with all other qubits from a theoretical point of view, even if from a practical perspective this may require extra SWAP gates.

Multiple-qubit gates. Defining and constructing every possible unitary matrix of every size seems like an impossible endeavor: clearly there must be some methodology by which general multiple-qubit gate can be implemented in a finite way without requiring a brand-new physical construction, otherwise implementing all possible gates would be a never-ending engineering task. Indeed, it can be shown that a set of gates consisting of (some) single-qubit gates plus CX is sufficient to construct any unitary matrix with arbitrary precision. This is the concept of *universality*.

Definition 1.42 (Universal set of gates). *A unitary matrix V is an ϵ -approximation of a unitary matrix U if $\|U - V\| = \sup_{x: \|x\|=1} \|(U - V)x\| \leq \epsilon$. A finite set of gates that can be used to construct an ϵ -approximation of any unitary matrix, for any $\epsilon > 0$ and on any given number of qubits, is called a universal set of gates.*

To build a universal set of gates, the first step is to show how to construct arbitrary single-qubit gates from a finite set of basic gates, then we use arbitrary single-qubit gates (together with some entangling gate) to build multiple-qubit gates. A possible universal set of gates is described in the next result.

Theorem 1.43 (Solovay-Kitaev theorem; [Kitaev, 1997, Nielsen and Chuang, 2002]). *Let $U \in \mathbb{C}^{2 \times 2}$ be an arbitrary unitary matrix. Then there exists a sequence of gates of length $\mathcal{O}(\log^c \frac{1}{\epsilon})$, where c is a constant, that yields an ϵ -approximation of U and consists only of H , $T = \begin{pmatrix} 1 & 0 \\ 0 & e^{i\frac{\pi}{4}} \end{pmatrix}$ and CX gates.*

The theorem implies that just two single-qubit gates together with CX allow us to build any single-qubit gate with arbitrary precision. We discuss the value of the constant c in the notes in Sect. 1.5. The crucial observation is that the length of the sequence is polylogarithmic in the precision, so we can obtain high-precision approximations with a relatively small gate count. To go from single-qubit gates to general q -qubit gates, one needs at most $\mathcal{O}(q^2 4^q)$ basic gates (i.e., the gates of Theorem 1.43); intuitively, this is because each gate on q qubits has $2^q \times 2^q = 4^q$ elements, and it takes q^2 basic gates to “fill” an arbitrary element of a large matrix — for a detailed discussion of how this can be done, see [Nielsen and Chuang, 2002, Ch. 4]. This implies that the set of gates consisting of just H , T and CX is universal: with a very small set of basic gates, we can construct any unitary matrix in any dimension to high precision, although this may require many operations. As mentioned above, this fact is extremely important for practical reasons: when constructing a quantum computer, it is sufficient to focus on a small number of gates (e.g., some single-qubit gates and CX), and all other gates can be constructed from these. Although many existing hardware platforms offer the possibility of applying arbitrary single-qubit gates (i.e., parameterized with continuous parameters) in a seemingly native way, the sufficiency of a small, finite set of gates assumes tremendous practical importance when considering the necessity of fault tolerance. Without going into details (consistent with the stated goal of this set of lecture notes to be “physics-free”, and ignore the specifics of quantum hardware), fault tolerance refers to the ability to correct physical errors that occur in the course of a quantum computation; such errors are bound to happen in practice. Thanks to the above discussion, it is sufficient to provide a fault-tolerant implementation only for gates forming a universal set: all remaining gates can be constructed from those. On the other hand, and still remaining at a high level, implementing a family of gates with continuous parameters in a fault-tolerant manner would be impossible.

From now on, we ignore any issue related to physical errors, and assume that the gates in the chosen universal set can be implemented exactly, i.e., in a fault-tolerant manner. Still, with Thm. 1.43 (and its generalization to unitaries of arbitrary dimension) we only construct an approximation of the target unitary, so one may wonder how the errors due to this approximation accumulate throughout the computation. Note that such errors are different from physical errors in the universal set of gates: even if the basic gates are implemented exactly, which is what we assume, we have errors arising from the finite approximation of arbitrary unitaries. We study this aspect in Sect. 1.3.6.

We conclude our discussion on basic operations with a quantum circuit for the logic AND gate. We already know that the X gate performs the logic NOT: having access to the AND gate

guarantees that we can construct any Boolean circuit — because we already stated that quantum computers are Turing-complete, being able to perform Boolean logic is of course implied.

Remark 1.44. *With quantum gates that perform the logic AND and NOT operations, we can simulate any classical Boolean circuit with a quantum circuit, possibly using a polynomial amount of additional resources (space, i.e., qubits, or time, i.e., gates). In fact, we are about to see that the quantum equivalent of the AND gate has separate input and output registers, so it requires one extra qubit to store the output of the computation. This implies that any function $f : \{0, 1\}^m \rightarrow \{0, 1\}^n$ that can be classically computed using T logic gates (i.e., in time T) can be computed by a quantum circuit using $\mathcal{O}(T)$ quantum gates and additional qubits. See also Sec. 1.3.7 for a discussion on how to make computations reversible.*

The quantum version of the AND gate is the CCX (doubly-controlled NOT) gate, that acts on three qubits: it has two control qubits, and it flips (bit flip, i.e., as the X gate) the third qubit if and only if both control qubits are $|1\rangle$. The gate is depicted in Fig. 1.14. The action of CCX

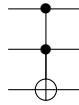


Figure 1.14: The CCX, or doubly-controlled NOT, gate.

can be described as: $|x\rangle \otimes |y\rangle \otimes |z\rangle \rightarrow |x\rangle \otimes |y\rangle \otimes |z \oplus (x \cdot y)\rangle$, where $x, y, z \in \{0, 1\}$. Notice that if $z = 0$, CCX indeed outputs the logical AND between x and y because $0 \oplus (x \cdot y) = x \wedge y$.

Following our earlier discussion, CCX can be constructed using only the basic gates indicated in Theorem 1.43. For this, we can use the circuit in Fig. 1.15, see [Nielsen and Chuang, 2002]. In this circuit we also use the conjugate transpose T^\dagger of the T gate, but it is easy to see that if we really want to stick to the gates H, T, CX only, T^\dagger can be constructed from T because $e^{-i\frac{\pi}{4}} = e^{i\frac{7\pi}{4}}$. Verifying correctness of the construction in Fig. 1.15 requires a few calculations, that we leave as an exercise. One way is to carry out the matrix multiplications; another way, probably more manageable if doing calculations by hand, is to use linearity and look at the effect of the circuit on each of the 2^3 possible basis states. We show only part of the calculations here. Suppose the circuit is applied to the basis state $|11x\rangle$ with $x \in \{0, 1\}$. After performing several simplifications (T and T^\dagger cancel out, the T gate has no effect on a qubit in state $|0\rangle$), and we can transform the CX s on the third qubit line into X gates because we already know that the first and second qubit are in state $|1\rangle$), we find out that the circuit maps:

$$|1\rangle \otimes |1\rangle \otimes |x\rangle \rightarrow (T|1\rangle) \otimes (T|1\rangle) \otimes (HTXT^\dagger XTX T^\dagger XH|x\rangle).$$

Doing the calculations, we see that:

$$HTXT^\dagger XTX T^\dagger XH = \begin{pmatrix} 0 & -i \\ -i & 0 \end{pmatrix},$$

so that the mapping reads:

$$\begin{aligned} |1\rangle \otimes |1\rangle \otimes |1\rangle &\rightarrow (T|1\rangle) \otimes (T|1\rangle) \otimes (HTXT^\dagger XTX T^\dagger XH|1\rangle) = \\ & (e^{i\frac{\pi}{4}}|1\rangle) \otimes (e^{i\frac{\pi}{4}}|1\rangle) \otimes (-i|0\rangle) = |1\rangle \otimes |1\rangle \otimes |0\rangle \\ |1\rangle \otimes |1\rangle \otimes |0\rangle &\rightarrow (e^{i\frac{\pi}{4}}|1\rangle) \otimes (e^{i\frac{\pi}{4}}|1\rangle) \otimes (-i|1\rangle) = |1\rangle \otimes |1\rangle \otimes |1\rangle. \end{aligned}$$

In general, coming up with these constructions requires a good deal of experience, or a piece of code implementing the algorithms referenced in Sect. 1.5 to approximate any unitary with a universal set of gates.

1.3.5 Can we solve NP-hard problems?

It is important to remark that even if we can easily create a uniform superposition of all basis states, the rules of measurement imply that using this easily-obtained superposition does not allow

up to precision ϵ , it suffices to approximate each gate to precision ϵ/m . In light of the logarithmic error scaling of Thm. 1.43, from a theoretical perspective this is a fully satisfactory answer: if we have a quantum circuit that solves a problem in a polynomial number of “ideal” gates, m is a polynomial of the input size, therefore compiling these ideal gates to a universal set with error scaling $\mathcal{O}(\log \frac{m}{\epsilon})$ only adds a small (i.e., polylogarithmic) number of gates. Even if m is not polynomial in the input size, e.g., if we are implementing an exponential-time algorithm, the number of extra gates remains very small compared to the total complexity of the circuit.

Proposition 1.46. *Let $U_1 U_2 \dots U_T, U'_1 U'_2 \dots U'_T$ be two sequences of unitaries of the same length. Then*

$$\|U_1 U_2 \dots U_T - U'_1 U'_2 \dots U'_T\| \leq \sum_{j=1}^T \|U_j - U'_j\|.$$

Proof. By induction on the length T . When $T = 1$ it is obvious. For larger T , we have:

$$\begin{aligned} & \|U_1 U_2 \dots U_T - U'_1 U'_2 \dots U'_T\| \\ &= \|U_1 U_2 \dots U_{T-1} U_T - U'_1 U'_2 \dots U'_{T-1} U_T + U'_1 U'_2 \dots U'_{T-1} U_T - U'_1 U'_2 \dots U'_{T-1} U'_T\| \\ &= \|(U_1 U_2 \dots U_{T-1} - U'_1 U'_2 \dots U'_{T-1}) U_T + U'_1 U'_2 \dots U'_{T-1} (U_T - U'_T)\| \\ &\leq \|U_1 U_2 \dots U_{T-1} - U'_1 U'_2 \dots U'_{T-1}\| \|U_T\| + \|U'_1 U'_2 \dots U'_{T-1}\| \|U_T - U'_T\| \\ &\leq \sum_{j=1}^{T-1} \|U_j - U'_j\| + \|U_T - U'_T\|, \end{aligned}$$

where we used the induction hypothesis for the terms with $j = 1, \dots, T-1$, the triangle inequality, Cauchy-Schwarz and the fact that unitary matrices (and their products) have unit operator norm. \square

Throughout this discussion there is an implicit assumption that the approximation metric of Def. 1.42, i.e., the operator norm of the difference between a target unitary and its approximation, is the right metric to use. We now show that this is indeed the case, in the sense that a circuit V that approximates a target circuit U up to some operator norm distance ϵ yields almost the same output. To do so, we show that two quantum states with Euclidean distance at most ϵ yield measurement outcome distributions with total variation distance at most ϵ .

Definition 1.47 (Total variation distance). *Given two discrete probability distributions P and Q with the same sample space $\Omega = \{1, \dots, n\}$, let p, q be the n -dimensional vectors with entries corresponding to the probability of $j = 1, \dots, n$ according to P, Q respectively. The total variation distance between P and Q is*

$$d_{TV}(P, Q) := \frac{1}{2} \sum_{j=1}^n |p_j - q_j|.$$

Remark 1.48. *It is not difficult to show that the total variation distance between two probability distributions, as defined in Def. 1.47, is also the maximum difference of the probability that these two distributions can assign to any event. In other words, $d_{TV}(P, Q) = \sup_{S \subseteq \{1, \dots, n\}} |\Pr_P(S) - \Pr_Q(S)|$.*

Proposition 1.49. *Let $|\psi\rangle = \sum_{\vec{j} \in \{0,1\}^q} \alpha_j |\vec{j}\rangle, |\phi\rangle = \sum_{\vec{j} \in \{0,1\}^q} \beta_j |\vec{j}\rangle$ be two quantum states on q qubits. Let P, Q be the discrete probability distributions over $\{0, 1\}^q$ induced, respectively, by $|\psi\rangle, |\phi\rangle$ when performing a measurement of all qubits. Suppose $\| |\psi\rangle - |\phi\rangle \| \leq \epsilon$. Then $d_{TV}(P, Q) \leq \epsilon$.*

Proof. Let us define vectors $a, b \in \mathbb{R}^{2^q}$ with entries $|\alpha_j|, |\beta_j|$ respectively. Furthermore, define the vectors $u, v \in \mathbb{R}^{2^q}$ with entries $u_j = |a_j + b_j|, v_j = |a_j - b_j|$. By Def. 1.47 we can write:

$$\begin{aligned} d_{TV}(P, Q) &= \frac{1}{2} \sum_j |a_j^2 - b_j^2| = \frac{1}{2} \sum_j |(a_j + b_j)(a_j - b_j)| \leq \frac{1}{2} \sum_j |a_j + b_j| |a_j - b_j| \\ &= \frac{1}{2} u^\top v \leq \frac{1}{2} \|u\| \|v\|. \end{aligned}$$

Let us analyze $\|u\|, \|v\|$. For $\|u\|$, recalling that $\|a\| = \|b\| = 1$, we have:

$$\begin{aligned} \|u\|^2 &= \sum_j |a_j + b_j|^2 = \sum_j (a_j^2 + b_j^2 + 2a_j b_j) = \|a\|^2 + \|b\|^2 + 2a^\top b \\ &\leq \|a\|^2 + \|b\|^2 + 2\|a\|\|b\| \leq 4. \end{aligned}$$

For $\|v\|$, we have:

$$\begin{aligned} \|v\|^2 &= \sum_j |a_j - b_j|^2 = \sum_j (a_j^2 + b_j^2 - 2a_j b_j) = \sum_j (|\alpha_j|^2 + |\beta_j|^2 - 2|\alpha_j||\beta_j|) \\ &\leq \sum_j (|\alpha_j|^2 + |\beta_j|^2 - 2\Re(\alpha_j^\dagger \beta_j)) = \|\psi\rangle - |\phi\rangle\|^2 \leq \epsilon^2, \end{aligned}$$

where we used the fact that $|\alpha_j||\beta_j| \geq |\alpha_j^\dagger \beta_j| \geq \Re(\alpha_j^\dagger \beta_j)$. Putting everything together, we find:

$$d_{\text{TV}}(P, Q) \leq \frac{1}{2} \|u\| \|v\| \leq \epsilon.$$

□

Prop. 1.49 tells us that if two quantum states are close to each other in Euclidean norm, then any measurement on the two states yields similarly-distributed outcomes. Thus, suppose our goal is to prepare some state $|\psi\rangle$, encoding the answer to some problem using an algorithm that is successful with probability $1 - \delta$. Suppose also that we can only prepare $|\phi\rangle$ instead, with the property that $\|\psi\rangle - |\phi\rangle\| \leq \epsilon$; for example, this may happen because we do not know how to implement the unitary that prepares $|\psi\rangle$ exactly, but we can find an ϵ -approximation of it. Eventually, to obtain the answer to the problem from $|\psi\rangle$ we have to perform a measurement; thanks to Prop. 1.49, we can perform the measurement on $|\phi\rangle$ instead, knowing that we get the correct answer with probability at least $1 - \delta - \epsilon$.

1.3.7 Implicit measurement, reversibility, and uncomputation

As a direct consequence of the laws of measurement (Post. 3), we can introduce the following general principle of quantum computing that is often helpful when thinking about what happens to a quantum state after measurement, see [Nielsen and Chuang, 2002] for further discussion.

Proposition 1.50 (Principle of implicit measurement). *Any qubits that are not measured at the end of a quantum circuit may be assumed to be measured, and the corresponding information is discarded.*

The principle is quite intuitive if one thinks about the necessity of quantum states to be consistent with the observations after a measurement. Indeed, suppose we have a multiple-qubit state, and we plan to apply a measurement on one specific qubit. For consistency, the distribution of the measurement outcomes on that qubit before we perform any measurement is the same as if we were instead planning to measure all qubits at the same time, rather than just one. Thus, if we apply a measurement to only some of the qubits, and there remain some other qubits on which we never perform a measurement, we could also assume that those other qubits have been measured as well, but the corresponding measurement outcomes were discarded. (Assuming that some qubits have been measured, and the corresponding outcomes are discarded without looking at them, does not give us any additional information and therefore does not modify the distribution of measurement outcomes.)

This raises an issue concerning any information that might be stored into working registers: if we have a register that is used as working space for some computation, and is subsequently discarded (i.e., ignored), we can assume that, at the end of the circuit, a measurement is applied onto the working register as well. Moreover, the contents of the working register may very well be entangled with other registers, so we cannot reuse the working register: due to entanglement, any additional operation on the working register risks affecting the “main” (other) registers. This is easily clarified with an example.

Example 1.51. Suppose we have a function f that takes as input a binary string, and outputs a binary string, i.e., $f : \{0, 1\}^m \rightarrow \{0, 1\}^n$, where m is not necessarily equal to n . Every operation on a quantum computer has to be reversible, so we must find an appropriate form of this function that can be represented as a valid operation for a quantum computer. The conventional way of constructing such a function is with a unitary that implements the following map:

$$U_f |\vec{x}\rangle_m |\vec{y}\rangle_n = |\vec{x}\rangle_m |\vec{y} \oplus f(\vec{x})\rangle_n.$$

This map is defined for all input states (because it is defined for all input basis states), it allows us to read the value of $f(\vec{x})$ (if we apply it when the second register contains $\vec{0}$: $U_f |\vec{x}\rangle |\vec{0}\rangle = |\vec{x}\rangle |\vec{0} \oplus f(\vec{x})\rangle = |\vec{x}\rangle |f(\vec{x})\rangle$), and it is reversible:

$$U_f U_f (|\vec{x}\rangle |\vec{y}\rangle) = U_f (|\vec{x}\rangle |\vec{y} \oplus f(\vec{x})\rangle) = |\vec{x}\rangle |\vec{y} \oplus f(\vec{x}) \oplus f(\vec{x})\rangle = |\vec{x}\rangle |\vec{y}\rangle,$$

i.e., applying the circuit U_f twice goes back to the initial state. (This way of specifying the function, whereby we apply \oplus in the second register to write the output in a reversible way, lets us clarify the confusion regarding the unspecified action of U_f in Rem. 1.45.)

Now assume that the computation carried out by U_f requires some additional working space, as is often the case for all but the simplest functions (e.g., recall that the quantum version of the logic AND gate already requires a separate output qubit, see Sect. 1.3.4; so if we construct a circuit that contains many AND gates, we may use several auxiliary qubits to store intermediate results of AND operations). W.l.o.g. we can assume that there is a third register, containing q bits and typically initialized in the all-zero basis state, used as working space. The mapping then becomes:

$$U_f |\vec{x}\rangle_m |\vec{y}\rangle_n |\vec{0}\rangle_q = |\vec{x}\rangle_m |\vec{y} \oplus f(\vec{x})\rangle_n |g(\vec{x})\rangle_q,$$

where $g(\vec{x})$ is some function of the input \vec{x} that outputs a binary string representing the final state of the working space. (We only define the output of this function when the working register contains $\vec{0}$; if it does not, the circuit computes some function of the input registers, but we do not need to characterize it because we plan to apply U_f only if the working register contains $\vec{0}$.) If we apply this map with $\vec{y} = \vec{0}$, we compute $f(\vec{x})$:

$$U_f |\vec{x}\rangle |\vec{0}\rangle |\vec{0}\rangle = |\vec{x}\rangle |f(\vec{x})\rangle |g(\vec{x})\rangle.$$

The last register still contains $g(\vec{x})$, which is uninfluential, but it is still there, and it depends on \vec{x} . Therefore, if we had a superposition over different values of \vec{x} , all three registers — including the last one — would be entangled. If we apply a measurement onto the second register, and observe $f(\vec{x})$, the implicit measurement principle tells us that the last register also collapses to $g(\vec{x})$. Worse, we cannot reuse the last register as working register for additional function evaluations, because it still contains $g(\vec{x})$.

The fact that we cannot reuse the working register would seem to imply that every function application needs its own working register, so that a large number of qubits is needed even for relatively simple calculations. In fact, we can avoid this issue, as well as the issue of a working register entangled with the other registers, by using a technique called *uncomputation*.

Definition 1.52 (Uncomputation). Let U_f be a unitary that implements some Boolean function f using a working register, relying on the assumption that the working register is initialized to the all-zero binary string. To uncompute the function means to apply a sequence of operations to reset the state of the working register to the all-zero binary string.

To uncompute a function, we introduce an auxiliary register with the same size as the output register. Thus, in total, we have four registers, which we order as follows: input, auxiliary, working, and output register. The auxiliary and working registers are initialized with the all-zero basis state. We first apply U_f onto the input, auxiliary, and working register; this writes the output of U_f , say, $f(\vec{x})$, onto the auxiliary register. We then perform bitwise CX from the auxiliary register onto the output register, to “copy” $f(\vec{x})$ into the output register using bitwise modulo-2

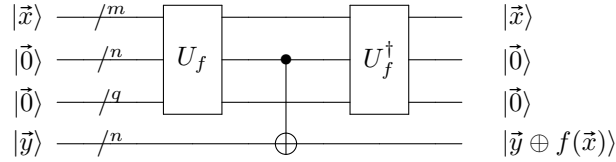


Figure 1.16: A circuit implementing U_f with an uncomputation step.

addition. Finally, we apply U_f^\dagger onto the input, auxiliary, and working register, erasing the last two registers and resetting them to the all-zero binary string (because $U_f|\bar{x}\rangle|\bar{0}\rangle|\bar{0}\rangle = |\bar{x}\rangle|f(\bar{x})\rangle|g(\bar{x})\rangle$, we have $U_f^\dagger|\bar{x}\rangle|f(\bar{x})\rangle|g(\bar{x})\rangle = |\bar{x}\rangle|\bar{0}\rangle|\bar{0}\rangle$). The corresponding circuit is shown in Fig. 1.16. Because the working and auxiliary registers are reset to $\bar{0}$ at the end of the circuit, they are no longer entangled with the rest and can be reused for other purposes, thereby saving working space. We could also SWAP the auxiliary and output register if we want the output in the second register, obtaining the same order of the registers as discussed in Ex. 1.51.

1.4 Mixed states and purifications

Our discussion so far has been based on Post. 1: the state of a q -qubit quantum computer is a unit vector in $(\mathbb{C}^2)^{\otimes q}$. This is correct, but there are situations where such a formalism is not the best approach to describe the state of a quantum register, or to determine its evolution. For example, consider the situation of a system with several qubits, but starting from a certain point of the computation we only apply operations onto some of the qubits, and discard (i.e., ignore) the rest. How should we characterize the state of a system when some of the qubits have been discarded?

Example 1.53. *Suppose we are in the state:*

$$\frac{1}{2}|00\rangle + \frac{1}{2}|01\rangle + \frac{1}{\sqrt{2}}|11\rangle,$$

but we only have access to the first qubit; this might be the case if the second qubit is physically distant (i.e., the above state was constructed over a quantum network), or simply because from now on we only want to perform computation on the first qubit line. The principle of implicit measurement tells us that ignoring the second qubit is equivalent to performing a measurement and discarding the information that we obtained. The measurement outcomes for both qubits are:

$$\Pr(00) = \frac{1}{4} \quad \Pr(01) = \frac{1}{4} \quad \Pr(11) = \frac{1}{2}.$$

If the outcome of the measurement on the second qubit is 0, the first qubit is in state $|0\rangle$ with certainty. If the outcome of the measurement on the second qubit is 1, the first qubit might be in state $|0\rangle$ or $|1\rangle$. Because the outcome of the measurement on the second qubit is assumed to be discarded (by principle of implicit measurement), we do not know how to characterize the state of the first qubit within the formalism for quantum states used so far: there is no single-qubit state (i.e., a unit vector in \mathbb{C}^2) that would accurately describe the state of the first qubit. We could find a quantum state that matches the probability distribution of the measurement outcomes, but we know from Ex. 1.31 that this is not sufficient to correctly characterize a quantum state.

As seen in the above example, our formalism to represent the state of a quantum register does not work very well when we want to consider only a subset of the qubits of a larger system. There is another formalism to express the state of a quantum computer: it is the language of *mixed states*, as opposed to the *pure states* that we have studied so far. Mixed states generalize pure states, and they are better able to deal with situations such as the one in Ex. 1.53, at the price of more cumbersome notation and calculations.

Definition 1.54 (Pure state). *A pure state $|\psi\rangle$ on q qubits is a unit vector in $(\mathbb{C}^2)^{\otimes q}$, i.e., the state of a q -qubit quantum register.*

Definition 1.55 (Mixed state). *An ensemble of pure states on q qubits is a collection $\{p_j, |\psi_j\rangle\}_{j=1,\dots,m}$ of pure states $|\psi_j\rangle$ and corresponding probabilities p_j . A q -qubit quantum register that is in state $|\psi_j\rangle$ with probability p_j for $j = 1, \dots, m$ is said to be in a mixed state, described by the density matrix corresponding to the ensemble, defined as the matrix $\rho := \sum_{j=1}^m p_j |\psi_j\rangle\langle\psi_j|$.*

Remark 1.56. *Recall our notation: $|\psi_j\rangle$ is a column vector, $\langle\psi_j|$ is a row vector, so $|\psi_j\rangle\langle\psi_j|$ is the matrix that performs the orthogonal projection onto $|\psi_j\rangle$.*

Remark 1.57. *Density matrices are also called density operators. Technically the matrix is the representation of the operator once we choose a basis, but because we always use the standard orthonormal basis, in the context of this set of lecture notes these terms are fully interchangeable. We use density matrix in the following.*

It is relatively straightforward to rewrite Post.s 2 and 3 to work with mixed states. It is sufficient to write the expression for the application of an operation to each state $|\psi_j\rangle$ in the ensemble, and define the resulting collection of states as the new ensemble, with the same probability distribution as before. This yields the following.

- The application of a q -qubit gate U to the register in state $\rho = \sum_{j=1}^m p_j |\psi_j\rangle\langle\psi_j|$ evolves the system to the state: $U\rho U^\dagger = \sum_{j=1}^m p_j U|\psi_j\rangle\langle\psi_j|U^\dagger$.
- Define the matrices:

$$M_k^{(0)} = \underbrace{I_{2 \times 2} \otimes I_{2 \times 2} \otimes \cdots \otimes \overbrace{[|0\rangle\langle 0|]}^{k\text{-th position}} \otimes \cdots \otimes I_{2 \times 2} \otimes I_{2 \times 2}}_{q \text{ times}}$$

$$M_k^{(1)} = \underbrace{I_{2 \times 2} \otimes I_{2 \times 2} \otimes \cdots \otimes \overbrace{[|1\rangle\langle 1|]}^{k\text{-th position}} \otimes \cdots \otimes I_{2 \times 2} \otimes I_{2 \times 2}}_{q \text{ times}}.$$

A measurement gate on qubit k yields a sample from a random variable \mathcal{Q}_k with sample space $\{0, 1\}$, $\Pr(\mathcal{Q}_k = x) = \text{Tr}(M_k^{(x)}\rho)$ for $x \in \{0, 1\}$, and the state after the measurement becomes:

$$\frac{M_k^{(x)}\rho(M_k^{(x)})^\dagger}{\text{Tr}(M_k^{(x)}\rho)} = \frac{M_k^{(x)}\rho M_k^{(x)}}{\text{Tr}(M_k^{(x)}\rho)}.$$

Remark 1.58. *The derivation of the expression for the state after a measurement highlights the fact that the effect of this type of measurement is captured by a projection matrix: $M_k^{(x)}$ projects a pure state onto the components that are consistent with the measurement. Indeed, this is called a projective measurement.*

Remark 1.59. *If we apply measurements to all qubits, by repeating the procedure described above for single-qubit measurements we see that the probability of obtaining outcome $|\vec{k}\rangle$, $\vec{k} \in \{0, 1\}^q$, is $\text{Tr}(|\vec{k}\rangle\langle\vec{k}|\rho) = \langle\vec{k}|\rho|\vec{k}\rangle$ (due to the cyclic property of the trace), and if we observe $|\vec{k}\rangle$, the state after measurement becomes $|\vec{k}\rangle\langle\vec{k}|$. This is consistent with the pure state formalism, because each state in the ensemble collapses to $|\vec{k}\rangle$, therefore now the quantum register is in the state $|\vec{k}\rangle$ with certainty.*

There are more general types of measurements than the projective measurements described above. The most general expression for a measurement operator M_k is that we observe the corresponding outcome with probability $\text{Tr}(M_k\rho M_k^\dagger)$, and the state after the measurement becomes:

$$\frac{M_k\rho M_k^\dagger}{\text{Tr}(M_k\rho M_k^\dagger)},$$

see [Nielsen and Chuang, 2002, Sect. 2.4.1]. However, we never use the general case in this set of lecture notes: the projective measurement onto the states $|0\rangle$ or $|1\rangle$ (usually called *measurement in the computational basis*) suffices. It is easy to see that for measurements in the computational basis, the general formulas for the outcome probabilities and for the state after the measurement reduce to the simplified ones given before Rem. 1.58, due to the fact that the matrices $M_k^{(x)}$ are Hermitian projections, and using the cyclic property of the trace.

1.4.1 Properties of density matrices

Density matrices are precisely characterized by two properties: they have unit trace, and they are positive semidefinite. We use the standard notation for positive (semi)definite matrices: $\rho \succeq 0$ indicates that ρ is positive semidefinite, $\rho \succeq \rho'$ indicates that $\rho - \rho'$ is positive semidefinite, and similar notation with \succ instead of \succeq to indicate positive definiteness.

Theorem 1.60 (Characterization of density matrices). *The matrix ρ is a density matrix associated with some ensemble of pure states $\{p_j, |\psi_j\rangle\}_{j=1,\dots,m}$ (for some unknown m) if and only if it satisfies the following two properties: (i) it has unit trace, and (ii) it is positive semidefinite.*

Proof. First let us suppose ρ is a density matrix associated with the ensemble of pure states $\{p_j, |\psi_j\rangle\}_{j=1,\dots,m}$. Then, using the cyclic property of the trace:

$$\mathrm{Tr}(\rho) = \mathrm{Tr}\left(\sum_{j=1}^m p_j |\psi_j\rangle\langle\psi_j|\right) = \sum_{j=1}^m p_j \mathrm{Tr}(|\psi_j\rangle\langle\psi_j|) = \sum_{j=1}^m p_j = 1,$$

and

$$\langle\phi|\rho|\phi\rangle = \sum_{j=1}^m p_j \langle\phi|\psi_j\rangle\langle\psi_j|\phi\rangle = \sum_{j=1}^m p_j |\langle\phi|\psi_j\rangle|^2 \geq 0$$

for every vector $|\phi\rangle$ (even unnormalized ones).

Then, let us suppose ρ has unit trace and $\rho \succeq 0$. We want to show it corresponds to some ensemble of pure states. Because ρ is a Hermitian positive semidefinite matrix, it admits a spectral decomposition with an orthonormal eigenbasis, and its eigenvalues are real and nonnegative. So

$$\rho = \sum_{j=1}^m p_j |\psi_j\rangle\langle\psi_j|$$

for some $m \leq$ number of columns of ρ , values p_j , and vectors $|\psi_j\rangle$. Because $\mathrm{Tr}(\rho) = 1$ we also have $\sum_{j=1}^m p_j = 1$, therefore ρ describes an ensemble of pure states. \square

Remark 1.61. *There could be multiple ensembles that correspond to the same density matrix, i.e., the spectral decomposition may not be unique. For example, suppose we have a unitary transformation U , and we define $\sqrt{q_i}|\phi_i\rangle = \sum_j U_{ij} \sqrt{p_j}|\psi_j\rangle$. Then:*

$$\begin{aligned} \sum_i q_i |\phi_i\rangle\langle\phi_i| &= \sum_i \left(\sum_j U_{ij} \sqrt{p_j}|\psi_j\rangle\right) \left(\sum_j \langle\psi_j|\sqrt{p_j}(U_{ij})^\dagger\right) = \sum_{i,j,k} U_{ij} (U_{ik})^\dagger \sqrt{p_j p_k} |\psi_j\rangle\langle\psi_k| \\ &= \sum_{j,k} \sum_i (U_{ij} (U_{ik})^\dagger) \sqrt{p_j p_k} |\psi_j\rangle\langle\psi_k| = \sum_{j,k} \sum_i (U_{ij} U_{ki}^\dagger) \sqrt{p_j p_k} |\psi_j\rangle\langle\psi_k| \\ &= \sum_j p_j |\psi_j\rangle\langle\psi_j|, \end{aligned}$$

where the fourth equality follows by definition of conjugate transpose of a matrix (notice that the indices i, k get swapped), and the last equality is due to the fact that U is unitary matrix so the term in parentheses is 1 if $j = k$, and 0 otherwise. This shows that the ensembles $\{p_j, |\psi_j\rangle\}_j$ and $\{q_i, |\phi_i\rangle\}_i$ are represented by the same density matrix. In fact, it is possible to show that this type of transformation between two ensembles is not only a sufficient condition to have the same density matrix, but also necessary, see [Nielsen and Chuang, 2002, Thm. 2.6].

1.4.2 Reduced density matrix

Arguably one of the greatest advantages of the density matrix formalism is the fact that it allows a rigorous treatment of the situation discussed in Ex. 1.53: we have a quantum register of a certain size, but we want to study the state of only a subset of the qubits, and continue the computation on those qubits while disregarding the rest. Naturally we could look at the evolution of the pure state of the entire register, but sometimes this is not feasible, or it is mathematically cumbersome; even when it is possible, it still faces the issue that in the pure state formalism, we can no longer describe the state of only the qubits that we are interested in. However, by implicit measurement it is easy to see that the state of a subset of qubits in the register is described by an ensemble of pure states, where the probability distribution is obtained by looking at the distribution of the measurement outcomes of the other qubits (i.e., the ones that are disregarded). The density matrix formalism provides an abstraction and computational rules for this concept.

Formally, suppose we have a quantum register AB whose state is described by the density matrix $\rho^{(AB)}$, and we split the register into two distinct quantum registers A and B . We now define the *reduced density matrix* obtained by tracing out one of the registers, and we claim that this describes the state of only one of the registers, in some sense that is formally specified in Prop. 1.67.

Definition 1.62 (Partial trace). *Let AB be a quantum register composed of two registers A, B with m_a, m_b qubits respectively. The partial trace over register B is the operation Tr_B defined as follows:*

(i) for any $\vec{j}, \vec{k} \in \{0, 1\}^{m_a}, \vec{h}, \vec{\ell} \in \{0, 1\}^{m_b}$, we have:

$$\text{Tr}_B \left(|\vec{j}\rangle\langle\vec{k}| \otimes |\vec{h}\rangle\langle\vec{\ell}| \right) := |\vec{j}\rangle\langle\vec{k}| \text{Tr} \left(|\vec{h}\rangle\langle\vec{\ell}| \right) = |\vec{j}\rangle\langle\vec{k}| \langle\vec{\ell}|\vec{h}\rangle;$$

(ii) Tr_B is linear.

This is a proper definition, because Tr_B is linear, and we are defining its effect on every basis element for the space of density matrices over AB . Computing the partial trace over register B is often called *tracing out* register B . In the setting of Def. 1.62, let $\rho^{(AB)}$ be the density matrix describing the state of register AB . An alternative definition of the partial trace, that might appear more intuitive to some readers, is given by the following expression:

$$\text{Tr}_B \left(\rho^{(AB)} \right) := \sum_{\vec{j} \in \{0,1\}^{m_b}} (I^{\otimes m_a} \otimes \langle\vec{j}|) \rho^{(AB)} (I^{\otimes m_a} \otimes |\vec{j}\rangle),$$

where $I^{\otimes m_a}$ is the identity matrix of size $2^{m_a} \times 2^{m_a}$, i.e., the appropriate size for register A . We can of course give similar definitions swapping the role of registers A and B , and obtain the partial trace over register A , which is the following operation:

$$\text{Tr}_A \left(\rho^{(AB)} \right) := \sum_{\vec{j} \in \{0,1\}^{m_a}} (\langle\vec{j}| \otimes I^{\otimes m_b}) \rho^{(AB)} (|\vec{j}\rangle \otimes I^{\otimes m_b}),$$

or, in the style of Def. 1.62, it is a linear operation with $\text{Tr}_A \left(|\vec{j}\rangle\langle\vec{k}| \otimes |\vec{h}\rangle\langle\vec{\ell}| \right) := \text{Tr} \left(|\vec{j}\rangle\langle\vec{k}| \right) |\vec{h}\rangle\langle\vec{\ell}|$.

Remark 1.63. *The original and alternative definitions are equivalent because the elements $|\vec{j}\rangle\langle\vec{k}| \otimes |\vec{h}\rangle\langle\vec{\ell}|$ constitute a basis for the space of density matrices $\rho^{(AB)}$, and if we express $\rho^{(AB)}$ in this basis and apply the linear operator Tr_B , we obtain:*

$$\sum_{\vec{j}, \vec{k}, \vec{h}, \vec{\ell}} \text{Tr}_B \left(\rho_{|\vec{j}\rangle\langle\vec{k}| \otimes |\vec{h}\rangle\langle\vec{\ell}|}^{(AB)} |\vec{j}\rangle\langle\vec{k}| \otimes |\vec{h}\rangle\langle\vec{\ell}| \right) = \sum_{\vec{j}, \vec{k}, \vec{h}} \rho_{|\vec{j}\rangle\langle\vec{k}| \otimes |\vec{h}\rangle\langle\vec{h}|}^{(AB)} |\vec{j}\rangle\langle\vec{k}| \langle\vec{h}|\vec{h}\rangle = \sum_{\vec{j}, \vec{k}, \vec{h}} \rho_{|\vec{j}\rangle\langle\vec{k}| \otimes |\vec{h}\rangle\langle\vec{h}|}^{(AB)} |\vec{j}\rangle\langle\vec{k}|,$$

where we denoted by $\rho_{|\vec{j}\rangle\langle\vec{k}| \otimes |\vec{h}\rangle\langle\vec{\ell}|}^{(AB)}$ the element of $\rho^{(AB)}$ in the position corresponding to the nonzero element of the subscript matrix (one can think of the subscript as a “mask” to identify the correct

element). Because $|\vec{j}\rangle|\vec{k}\rangle$ is a basis for register A and we keep all the corresponding elements for register A , we are effectively “acting as the identity” on the first register, but we only consider the elements of $\rho^{(AB)}$ that characterize the quantum state if we were to perform a measurement on the second register, collapsing to some basis state $|\vec{h}\rangle$; then, we sum over all $|\vec{h}\rangle$, by principle of implicit measurement.

Definition 1.64 (Reduced density matrix). *In the setting of Def. 1.62, let $\rho^{(AB)}$ be the density matrix describing the state of register AB . The reduced density matrix for register A is $\rho^{(A)} := \text{Tr}_B(\rho^{(AB)})$, and similarly, the reduced density matrix for register B is $\rho^{(B)} := \text{Tr}_A(\rho^{(AB)})$.*

A reduced density matrix characterizes the state of a subsystem (i.e., subregister) of the entire register, as can be seen in the following examples.

Example 1.65. *Consider the state:*

$$\frac{1}{\sqrt{2}}(|00\rangle + |11\rangle).$$

The corresponding density matrix is:

$$\frac{1}{2}(|00\rangle + |11\rangle)(\langle 00| + \langle 11|) = \frac{1}{2}(|00\rangle\langle 00| + |00\rangle\langle 11| + |11\rangle\langle 00| + |11\rangle\langle 11|) = \begin{pmatrix} \frac{1}{2} & 0 & 0 & \frac{1}{2} \\ 0 & 0 & 0 & 0 \\ 0 & 0 & 0 & 0 \\ \frac{1}{2} & 0 & 0 & \frac{1}{2} \end{pmatrix} = \rho^{(AB)}.$$

Let us denote the first qubit as register A and the second qubit as register B . If we now want to drop the second qubit and consider only the first, its state is represented by the following reduced density matrix:

$$\begin{aligned} \text{Tr}_B \left(\frac{1}{2}(|00\rangle\langle 00| + |00\rangle\langle 11| + |11\rangle\langle 00| + |11\rangle\langle 11|) \right) &= \frac{1}{2}(|0\rangle\langle 0| \langle 0|0\rangle + |0\rangle\langle 1| \langle 0|1\rangle + |1\rangle\langle 0| \langle 1|0\rangle + |1\rangle\langle 1| \langle 1|1\rangle) \\ &= \frac{1}{2}(|0\rangle\langle 0| + |1\rangle\langle 1|). \end{aligned}$$

Using the alternative definition, we equivalently obtain:

$$\begin{aligned} \rho^{(A)} &= \text{Tr}_B(\rho^{(AB)}) = \sum_{j=0,1} (I \otimes \langle j|) \rho^{(AB)} (I \otimes |j\rangle) \\ &= \begin{pmatrix} 1 & 0 & 0 & 0 \\ 0 & 0 & 1 & 0 \end{pmatrix} \begin{pmatrix} \frac{1}{2} & 0 & 0 & \frac{1}{2} \\ 0 & 0 & 0 & 0 \\ 0 & 0 & 0 & 0 \\ \frac{1}{2} & 0 & 0 & \frac{1}{2} \end{pmatrix} \begin{pmatrix} 1 & 0 \\ 0 & 0 \\ 0 & 1 \\ 0 & 0 \end{pmatrix} + \begin{pmatrix} 0 & 1 & 0 & 0 \\ 0 & 0 & 0 & 1 \end{pmatrix} \begin{pmatrix} \frac{1}{2} & 0 & 0 & \frac{1}{2} \\ 0 & 0 & 0 & 0 \\ 0 & 0 & 0 & 0 \\ \frac{1}{2} & 0 & 0 & \frac{1}{2} \end{pmatrix} \begin{pmatrix} 0 & 0 \\ 1 & 0 \\ 0 & 0 \\ 0 & 1 \end{pmatrix} \\ &= \begin{pmatrix} \frac{1}{2} & 0 \\ 0 & 0 \end{pmatrix} + \begin{pmatrix} 0 & 0 \\ 0 & \frac{1}{2} \end{pmatrix} = \begin{pmatrix} \frac{1}{2} & 0 \\ 0 & \frac{1}{2} \end{pmatrix} = \frac{1}{2}(|0\rangle\langle 0| + |1\rangle\langle 1|). \end{aligned}$$

Intuitively this makes sense: from the initial state, if we ignore the second qubit we still have a system that is $|0\rangle$ or $|1\rangle$ with probability 0.5 each, which is what we see from the reduced density matrix. We do not have additional information on the first qubit because, even though it is entangled with the second qubit and it might be considered measured by principle of implicit measurement, we discard the outcome of the measurement on the second qubit.

Example 1.66. *Let us study Ex. 1.53 using the formalism of reduced density matrices. Recall that in that example, we are considering the pure state:*

$$\frac{1}{2}|00\rangle + \frac{1}{2}|01\rangle + \frac{1}{\sqrt{2}}|11\rangle,$$

and we want to analyze what happens if we want to describe the state of the first qubit only. The density matrix for the entire system is:

$$\begin{aligned}\rho^{(AB)} &= \left(\frac{1}{2}|00\rangle + \frac{1}{2}|01\rangle + \frac{1}{\sqrt{2}}|11\rangle \right) \left(\frac{1}{2}\langle 00| + \frac{1}{2}\langle 01| + \frac{1}{\sqrt{2}}\langle 11| \right) \\ &= \frac{1}{4}|00\rangle\langle 00| + \frac{1}{4}|00\rangle\langle 01| + \frac{1}{2\sqrt{2}}|00\rangle\langle 11| + \frac{1}{4}|01\rangle\langle 00| + \frac{1}{4}|01\rangle\langle 01| + \\ &\quad \frac{1}{2\sqrt{2}}|01\rangle\langle 11| + \frac{1}{2\sqrt{2}}|11\rangle\langle 00| + \frac{1}{2\sqrt{2}}|11\rangle\langle 01| + \frac{1}{2}|11\rangle\langle 11|.\end{aligned}$$

Calling B the register with the second qubit, and tracing it out, we obtain:

$$\mathrm{Tr}_B \left(\rho^{(AB)} \right) = \frac{1}{2}|0\rangle\langle 0| + \frac{1}{2\sqrt{2}}|0\rangle\langle 1| + \frac{1}{2\sqrt{2}}|1\rangle\langle 0| + \frac{1}{2}|1\rangle\langle 1|.$$

Recalling Ex. 1.53, let us consider the ensemble of pure states where a qubit is in state $|0\rangle$ with probability $1/4$, and is in state $\frac{1}{\sqrt{3}}|0\rangle + \sqrt{\frac{2}{3}}|1\rangle$ with probability $3/4$; this is a natural description of the state of the first qubit, if we apply the principle of implicit measurement and look at what happens if we observe the second qubit to be $|0\rangle$ or $|1\rangle$. (The probabilities $1/4$, $3/4$ are the eigenvalues obtained from an eigendecomposition of $\mathrm{Tr}_B(\rho^{(AB)})$, and the pure states in the ensemble are the corresponding eigenvectors; here we constructed them from intuition, looking for probabilities and pure states that yield the probability distribution that we expect to see.) The density matrix corresponding to this ensemble is:

$$\frac{1}{4}|0\rangle\langle 0| + \frac{3}{4} \left(\frac{1}{\sqrt{3}}|0\rangle + \sqrt{\frac{2}{3}}|1\rangle \right) \left(\frac{1}{\sqrt{3}}\langle 0| + \sqrt{\frac{2}{3}}\langle 1| \right) = \frac{1}{2}|0\rangle\langle 0| + \frac{1}{2\sqrt{2}}|0\rangle\langle 1| + \frac{1}{2\sqrt{2}}|1\rangle\langle 0| + \frac{1}{2}|1\rangle\langle 1|,$$

which is precisely $\mathrm{Tr}_B(\rho^{(AB)})$. Thus, the chosen ensemble yields the reduced density matrix obtained above after tracing out register B , and is, in fact, a natural expression for the state of the first qubit. In general, the eigendecomposition of a reduced density matrix is not unique: not only there could be eigenvalues with algebraic multiplicity greater than one, but when we consider global phases, there are infinite eigenvectors that are indistinguishable in the sense that they yield the same probability distribution of measurement outcomes. So, there are multiple ensembles of pure states that equivalently describe the state of the same system.

We can now precisely state in what sense density matrices correctly characterize the state of a register after discarding (or ignoring) some other registers: they lead to the correct probability distribution of the measurement outcomes. We state this result using the reduced density matrix for register A , but clearly we can obtain a symmetric result for register B .

Proposition 1.67. *Let register AB be in a state characterized by the density matrix $\rho^{(AB)}$, and let $\rho^{(A)} = \mathrm{Tr}_B(\rho^{(AB)})$. Then $\rho^{(A)}$ correctly characterizes the probabilities of the measurement outcomes for register A , when discarding register B .*

Proof. We need to show that the probability of observing outcome \vec{j} from a measurement on register A is the same whether we compute it from $\rho^{(A)}$ or starting from the original mixed state $\rho^{(AB)}$.

Using the entire system, the probability of observing outcome \vec{j} is (recall Rem. 1.59):

$$\sum_{\vec{k} \in \{0,1\}^{m_b}} \langle \vec{j} | \langle \vec{k} | \rho^{(AB)} | \vec{j} \rangle | \vec{k} \rangle,$$

because it is equal to the probability of observing any string starting with \vec{j} if we apply a measurement on all qubits. Using the reduced density matrix, the probability of observing outcome \vec{j} in the first register is:

$$\langle \vec{j} | \rho^{(A)} | \vec{j} \rangle = \langle \vec{j} | \left(\sum_{\vec{k} \in \{0,1\}^{m_b}} (I^{\otimes m_a} \otimes \langle \vec{k} |) \rho^{(AB)} (I^{\otimes m_a} \otimes | \vec{k} \rangle) \right) | \vec{j} \rangle = \sum_{\vec{k} \in \{0,1\}^{m_b}} \langle \vec{j} | \langle \vec{k} | \rho^{(AB)} | \vec{j} \rangle | \vec{k} \rangle,$$

so we obtain the same probability as above. \square

1.4.3 Purifications

An important concept in the study of density matrices is the idea of a purification; this is also crucial in several quantum algorithms for semidefinite optimization, and in particular in Ch. 8 we exploit purifications to construct mixed states corresponding to candidate solutions for semidefinite optimization problems. Our previous discussion shows that a mixed state is described by a density matrix. We show next that given a density matrix ρ , we can construct a *pure state* on two registers such that tracing out one of the registers yields a mixed state corresponding to ρ .

Theorem 1.68 (Every density matrix admits a purification). *Let $d = 2^q$. Let $\rho \in \mathbb{C}^{d \times d}$ be a given density matrix. Then, there exists a pure state $|\phi\rangle$ over two registers A, B such that A has q qubits and tracing out B yields a mixed state described by ρ in register A . Moreover, it is possible to choose register B so that it has at most q qubits.*

Proof. Let $\rho = \sum_{j=0}^{d-1} \lambda_j |\psi_j\rangle\langle\psi_j|$ be an eigendecomposition of ρ , which always exists because ρ is a Hermitian positive semidefinite matrix. Note that $\lambda_j \in \mathbb{R}$ and they are nonnegative. Furthermore, we can assume that there are d eigenvalues without loss of generality: if there are fewer we can simply add some zero eigenvalues, and clearly there cannot be more because the rank of ρ is at most d . Let $|\psi_j\rangle := \sum_{\vec{k}} \alpha_k^{(j)} |\vec{k}\rangle$ for some vector of coefficients $\alpha^{(j)}$. Consider the pure state

$$|\phi\rangle = \sum_{\vec{j} \in \{0,1\}^q} \sqrt{\lambda_j} |\psi_j\rangle |\vec{j}\rangle$$

over $2q$ qubits (each register has q qubits). Tracing out the second register, which we call register B , yields:

$$\begin{aligned} \text{Tr}_B(|\phi\rangle\langle\phi|) &= \text{Tr}_B \left(\sum_{\vec{j}, \vec{k}} \sqrt{\lambda_j \lambda_k} |\psi_j\rangle |\vec{j}\rangle \langle\psi_k| \langle\vec{k}| \right) \\ &= \text{Tr}_B \left(\sum_{\vec{j}, \vec{k}} \sqrt{\lambda_j \lambda_k} \left(\sum_{\vec{h}} \alpha_h^{(j)} |\vec{h}\rangle \right) |\vec{j}\rangle \left(\sum_{\vec{\ell}} (\alpha_\ell^{(k)})^\dagger \langle\vec{\ell}| \right) \langle\vec{k}| \right) \\ &= \sum_{\vec{j}, \vec{k}} \sqrt{\lambda_j \lambda_k} \left(\sum_{\vec{h}} \alpha_h^{(j)} |\vec{h}\rangle \right) \left(\sum_{\vec{\ell}} (\alpha_\ell^{(k)})^\dagger \langle\vec{\ell}| \right) \text{Tr}(|\vec{j}\rangle\langle\vec{k}|) \\ &= \sum_{\vec{j}, \vec{k}} \sqrt{\lambda_j \lambda_k} |\psi_j\rangle\langle\psi_k| \langle\vec{k}|\vec{j}\rangle = \sum_{j=0}^{d-1} \lambda_j |\psi_j\rangle\langle\psi_j| = \rho, \end{aligned}$$

concluding the proof. (In the third equality, we applied the definition of Tr_B .) \square

Essentially, the second register is used to construct the ensemble of pure states on the first register by assigning the correct probability to each state of the ensemble. This leads to the concept of a *purification*. We use purifications in Ch.s 7 and 8.

Definition 1.69 (Purification). *Given a density matrix ρ describing the state of register A , a purification of ρ is a pure state over two registers A, B such that tracing out register B yields ρ .*

The register B that is traced out is typically called *purifying register*.

We conclude this section with another result that is often useful in the study of composite systems (i.e., registers with subregisters), and that plays a crucial role in some classical simulation algorithms for quantum circuits, e.g., [Markov et al., 2018, Pednault et al., 2019]. The result can be seen as a restatement of the singular value decomposition, but in quantum information theory it is referred to as *Schmidt decomposition*.

Theorem 1.70 (Schmidt decomposition). *Let $|\psi\rangle$ be a pure state for a composite register AB . Then, there exist orthonormal states $|\phi_j^A\rangle$ for register A , and $|\phi_j^B\rangle$ for register B , such that $|\psi\rangle = \sum_j \lambda_j |\phi_j^A\rangle |\phi_j^B\rangle$, where λ_j are nonnegative reals such that $\sum_j \lambda_j^2 = 1$.*

Proof. Let $|\psi\rangle = \sum_{\vec{j}, \vec{k}} \alpha_{jk} |\vec{j}\rangle |\vec{k}\rangle$. Arrange the coefficients α_{jk} into a matrix M where j indexes the rows and k indexes the columns, i.e., $M_{jk} = \alpha_{jk}$. The matrix M admits a singular value decomposition: $M = U\Sigma V^\dagger$, and in particular $M_{jk} = \sum_h U_{jh} \sigma_h V_{hk}^\dagger$ where σ_h is the h -th diagonal element of Σ . Then:

$$\begin{aligned} |\psi\rangle &= \sum_{\vec{j}, \vec{k}} M_{jk} |\vec{j}\rangle |\vec{k}\rangle = \sum_{\vec{j}, \vec{k}} \left(\sum_h U_{jh} \sigma_h V_{hk}^\dagger \right) |\vec{j}\rangle |\vec{k}\rangle \\ &= \sum_h \sigma_h \left(\sum_{\vec{j}} U_{jh} |\vec{j}\rangle \right) \left(\sum_{\vec{k}} V_{hk}^\dagger |\vec{k}\rangle \right) = \sum_h \sigma_h |\phi_h^A\rangle |\phi_h^B\rangle, \end{aligned}$$

where we defined $|\phi_h^A\rangle := \sum_{\vec{j}} U_{jh} |\vec{j}\rangle$ and $|\phi_h^B\rangle := \sum_{\vec{k}} V_{hk}^\dagger |\vec{k}\rangle$. Note that these are indeed orthonormal vectors, because U, V are unitary and the vectors $|\phi_h^A\rangle, |\phi_h^B\rangle$ are simply the columns of U, V . This yields the desired decomposition up to relabeling. Finally, note that the σ_h are real because they are the singular values, and $1 = \|\psi\|^2 = \sum_h \sigma_h^2$, because all the cross terms in the expression for $\|\psi\|^2$ cancel out due to orthonormality of the vectors $|\phi_h^A\rangle, |\phi_h^B\rangle$. \square

1.5 Notes and further reading

On the topic of Turing machines, quantum Turing machines, and their equivalence, fundamental references are [Deutsch, 1985, Bennett, 1973, Bernstein and Vazirani, 1997]. [Deutsch, 1985] shows the existence of a universal quantum Turing machine, that can simulate any quantum Turing machine; the simulation overhead is only polynomial, as shown in [Bernstein and Vazirani, 1997]. Results from [Bennett, 1973] imply that polynomial-time quantum Turing machines can simulate polynomial-time deterministic and probabilistic Turing machines.

Regarding upper bounds on the length of the sequence of gates from a universal set that is necessary to construct an arbitrary single-qubit gate, which we discussed in Sect. 1.3.4 and more specifically in Thm. 1.43, [Dawson and Nielsen, 2005] gives a detailed proof with $c \approx 3.98$, and in general, Solovay-Kitaev-type algorithms yield $c = 3 + \delta$ for $\delta > 0$ [Kitaev et al., 2002]. Lower values are possible: for general gate sets, [Kuperberg, 2023] reduces c to $1.44 + \delta$, and for special sets of gates, even $c = 1$ is possible [Selinger, 2012, Kliuchnikov et al., 2016]. The exact values do not matter much for the high-level exposition in this set of lecture notes: it is sufficient to know that a polylogarithmic number of gates suffices. It can, however, be very important for practical implementations.

We conclude these notes by giving references to additional reading material that discusses the fundamentals of quantum computing and quantum algorithms. The most celebrated reference is [Nielsen and Chuang, 2002], a comprehensive treatment of quantum computing, including error correction and quantum algorithms. Due to its sheer size and scope, the book is often used as a reference, and may not be the most suitable instrument (or the fastest way) for an applied mathematician who wants to learn about quantum algorithms from scratch. It does, however, contain a rigorous treatment of many important topics, and is especially valuable for readers with a background in physics. [Rieffel and Polak, 2011] is another extensive treatment of quantum computing, with a sizeable discussion of quantum algorithms, and it uses a language that may be more familiar for applied mathematicians. [Kaye et al., 2007] is a concise but rigorous introduction to quantum computing, quantum algorithms and quantum error correction. Being more recent than [Nielsen and Chuang, 2002], it has the added benefit of covering certain topics in quantum algorithms using a modern, and possibly clearer, approach.

In addition to the three well-known books above, there are excellent sets of lecture notes by prominent scientists available on the arXiv or directly on their author's website. We mention three in particular. [Childs, 2017] is an advanced treatment of multiple topics in quantum algorithms, including quantum algorithms for algebraic problems (e.g., the hidden subgroup problem, see Sect. 3.4) and quantum walks. This set of lecture notes is written with a computer science perspective. Another set of lectures notes with a computer science perspective is [de Wolf, 2019];

the style in [de Wolf, 2019] is more informal (although it is precise), and as a result, it may be a more accessible starting point for some readers. [de Wolf, 2019] covers a vast number of topics, including some that have gained steam quite recently. Finally, [Lin, 2022] is a set of lecture notes on quantum algorithms for scientific computation, and it includes an in-depth discussion of quantum phase estimation and operations on matrices (which is also the subject of our Ch. 7) via block-encodings and the quantum singular value transformation.

Chapter 2

Early examples of quantum algorithms

In this chapter we explore some of the principles of quantum algorithm design, together with a discussion of some of the (chronologically) first algorithms providing evidence of a quantum speedup of some type. These algorithms are not directly useful for optimization, but they serve the purpose of familiarizing the reader with, and building intuition on, the analysis of quantum algorithms; for this purpose, it is generally helpful to start from simple algorithms.

2.1 Phase kickback

As discussed in Sect. 1.3.4, the CX gate may create entangled states. Recall that the CX gate takes a control qubit and a target qubit. However, one should not make the mistake of thinking of CX as acting on the target qubit only. When CX is applied onto a basis state it is natural to think of the control qubit as being left alone while acting on the target qubit, but overall, the effect of CX (like any other two-qubit gate) is dependent on the state on which it is applied, and one cannot think of each qubit in isolation. To see this, we show an example of a controlled gate sandwiched between some single-qubit gates, and overall this makes it look like the target qubit is acting on the control (instead of the converse), if we follow the same intuitive interpretation.

Example 2.1. Consider this operation on a two-qubit state:

$$H^{\otimes 2} CX_{12} H^{\otimes 2}.$$

We claim that this is the same as CX_{21} (note the swapped role of control and target qubit). Indeed:

$$\frac{1}{2} \begin{pmatrix} 1 & 1 & 1 & 1 \\ 1 & -1 & 1 & -1 \\ 1 & 1 & -1 & -1 \\ 1 & -1 & -1 & 1 \end{pmatrix} \begin{pmatrix} 1 & 0 & 0 & 0 \\ 0 & 1 & 0 & 0 \\ 0 & 0 & 0 & 1 \\ 0 & 0 & 1 & 0 \end{pmatrix} \frac{1}{2} \begin{pmatrix} 1 & 1 & 1 & 1 \\ 1 & -1 & 1 & -1 \\ 1 & 1 & -1 & -1 \\ 1 & -1 & -1 & 1 \end{pmatrix} = \begin{pmatrix} 1 & 0 & 0 & 0 \\ 0 & 0 & 0 & 1 \\ 0 & 0 & 1 & 0 \\ 0 & 1 & 0 & 0 \end{pmatrix},$$

and the last matrix swaps the second and third row, i.e., it maps $|01\rangle \rightarrow |11\rangle$ and $|11\rangle \rightarrow |01\rangle$.

In circuit form, Ex. 2.1 implies that the circuits in Fig. 2.1 are equivalent. The left part of Fig. 2.1



Figure 2.1: Interchanging the control and target qubit of CX .

is essentially an indication of a basis change: instead of expressing each qubit in the standard

orthonormal basis, via Hadamard gates, we are expressing it in a different basis (with basis elements $H|0\rangle$ and $H|1\rangle$). We know from linear algebra that we can express a linear transformation in a different basis by premultiplying and postmultiplying by a matrix containing the new basis as its columns, or its inverse, depending on the direction of the transformation. So if A is expressed in the basis \mathcal{B} , and U maps each element of \mathcal{B} to some other basis \mathcal{B}' , we have that UAU^{-1} is the expression of the linear transformation associated with A in terms of the basis \mathcal{B}' . Going back to Ex. 2.1, this means that the operation CX_{21} is the same as the operation CX_{12} in a different basis.

Example 2.2. *Instead of the standard orthonormal basis, consider the basis $H|0\rangle = \frac{1}{\sqrt{2}}(|0\rangle + |1\rangle)$, $H|1\rangle = \frac{1}{\sqrt{2}}(|0\rangle - |1\rangle)$ for each qubit. (This is often called the Hadamard basis, for obvious reasons.) Given a vector in the Hadamard basis, we can express it in the standard orthonormal basis by multiplying by $H^{-1} = H^\dagger = H$. In a tensor product space, the basis change operation is applied identically on each vector space taking part in the tensor product. So, for example, given the two-qubit state $|01\rangle$ in the Hadamard basis (for each qubit), its expression in the standard orthonormal basis is:*

$$(H^\dagger \otimes H^\dagger)|01\rangle = \frac{1}{\sqrt{2}}(|0\rangle + |1\rangle) \otimes \frac{1}{\sqrt{2}}(|0\rangle - |1\rangle) = \frac{1}{2}(|00\rangle - |01\rangle + |10\rangle - |11\rangle).$$

If we apply CX_{12} in the standard orthonormal basis, we obtain:

$$\frac{1}{2}(|00\rangle - |01\rangle - |10\rangle + |11\rangle) = \frac{1}{\sqrt{2}}(|0\rangle - |1\rangle) \otimes \frac{1}{\sqrt{2}}(|0\rangle - |1\rangle)$$

Transforming from the standard orthonormal basis back to the Hadamard basis, the expression for this state is:

$$(H \otimes H) \frac{1}{\sqrt{2}}(|0\rangle - |1\rangle) \otimes \frac{1}{\sqrt{2}}(|0\rangle - |1\rangle) = |11\rangle = CX_{21}|01\rangle.$$

We have recovered the equivalence shown in Fig. 2.1.

As stated in Ch. 1, we always work with the standard orthonormal basis, so we do not explicitly use the Hadamard basis in the rest of this set of lecture notes. But the concept exemplified in Ex. 2.2 stands: a controlled gate in a certain basis may look like a completely different operation in another basis, even one with control and target qubit exchanged. Unitary matrices encode a basis change between orthonormal bases, so for general quantum states, we can never assume that the control qubit of a controlled operation does not get affected by it. Indeed, depending on the state on which a gate is applied, a CX gate can be interpreted as having an effect on the control qubit, rather than the target qubit. We can generalize this idea further, and exploit it for computation, so that applying a CX has some quantifiable effect on the control qubit. In this section we develop a technique that encodes information on the value of certain types of functions as the phase of the control qubit (or, in general, of some basis states). The technique relies on properties of the *eigenstate* $\frac{1}{\sqrt{2}}(|0\rangle - |1\rangle)$ of the X gate.

Definition 2.3 (Eigenstate). *Given a unitary $U \in \mathbb{C}^{2^q \times 2^q}$, we say that the q -qubit state $|\psi\rangle$ is an eigenstate of U if the 2^q -dimensional vector corresponding to $|\psi\rangle$ is an eigenvector of U , i.e., $U|\psi\rangle = e^{i\theta}|\psi\rangle$ for some θ .*

In other words, “eigenstate” simply means that the quantum state is an eigenvector of a given operator.

Remark 2.4. *All eigenvalues of a unitary matrix have modulus 1, so they can be written as $e^{i\theta}$ for some $\theta \in [0, 2\pi)$.*

Notice that:

$$\begin{pmatrix} 0 & 1 \\ 1 & 0 \end{pmatrix} \frac{1}{\sqrt{2}}(|0\rangle - |1\rangle) = \frac{1}{\sqrt{2}}(|1\rangle - |0\rangle) = -\frac{1}{\sqrt{2}}(|0\rangle - |1\rangle)$$

and:

$$\begin{pmatrix} 1 & 0 \\ 0 & 1 \end{pmatrix} \frac{1}{\sqrt{2}}(|0\rangle - |1\rangle) = \frac{1}{\sqrt{2}}(|0\rangle - |1\rangle),$$

i.e., $\frac{1}{\sqrt{2}}(|0\rangle - |1\rangle)$ is an eigenstate with eigenvalue -1 of X , and (trivially) it is an eigenstate with eigenvalue $+1$ of the identity gate I . The CX gate applies X to target qubit if the control is 1, and applies I to the target qubit if the control is 0. Thus, if the target qubit is in the state $\frac{1}{\sqrt{2}}(|0\rangle - |1\rangle)$, depending on the value of the control qubit we “obtain” a different eigenvalue, i.e., multiply the quantum state by a different scalar. It is easy to check that we can write:

$$CX \left(|x\rangle \otimes \frac{1}{\sqrt{2}}(|0\rangle - |1\rangle) \right) = (-1)^x \left(|x\rangle \otimes \frac{1}{\sqrt{2}}(|0\rangle - |1\rangle) \right).$$

With this operation, some information on x becomes encoded in the coefficient of the quantum state: if $x = 0$ nothing happens, but if $x = 1$ the entire quantum state gets sign-flipped.

This effect can be applied even more in general. Let us study a two-qubit operation U_f that implements the map $|x\rangle|y\rangle \rightarrow |x\rangle|y \oplus f(x)\rangle$, where, as usual, $x, y \in \{0, 1\}$ and we also assume that $f(x) \in \{0, 1\}$. (Recall the definition of \oplus given in Def. 1.33.) As we discussed in Sect. 1.3.7, this particular form of the function, with a second register used to contain the output by means of \oplus , is typical of the quantum computing world. Let us apply the two-qubit operation U_f on a target qubit that is prepared in the state $\frac{1}{\sqrt{2}}(|0\rangle - |1\rangle) = H|1\rangle$. We have:

$$U_f \left(|x\rangle \otimes \frac{1}{\sqrt{2}}(|0\rangle - |1\rangle) \right) = |x\rangle \otimes \frac{1}{\sqrt{2}}(|0 \oplus f(x)\rangle - |1 \oplus f(x)\rangle).$$

If $f(x) = 0$, this has no effect on the second qubit. If $f(x) = 1$, this bit-flips the second qubit (i.e., $|0\rangle$ becomes $|1\rangle$ and $|1\rangle$ becomes $|0\rangle$), which has the overall effect of changing the sign of the second qubit. Thus, we can write the effect of U_f as:

$$U_f \left(|x\rangle \otimes \frac{1}{\sqrt{2}}(|0\rangle - |1\rangle) \right) = (-1)^{f(x)} \left(|x\rangle \otimes \frac{1}{\sqrt{2}}(|0\rangle - |1\rangle) \right). \quad (2.1)$$

The CX gate can be obtained from Eq. 2.1 with $f(x) = x$. If the control qubit is in a general state $\alpha_0|0\rangle + \alpha_1|1\rangle$ rather than a basis state $|x\rangle$, we have:

$$U_f \left((\alpha_0|0\rangle + \alpha_1|1\rangle) \otimes \frac{1}{\sqrt{2}}(|0\rangle - |1\rangle) \right) = \left((-1)^{f(0)}\alpha_0|0\rangle + (-1)^{f(1)}\alpha_1|1\rangle \right) \otimes \frac{1}{\sqrt{2}}(|0\rangle - |1\rangle).$$

If the second qubit is prepared in the state $\frac{1}{\sqrt{2}}(|0\rangle - |1\rangle)$, applying U_f yields the situation that is depicted in Fig. 2.2. By properties of the tensor product, we can interpret the multiplicative

$$\begin{array}{ccc} |x\rangle & \text{---} & \boxed{U_f} & \text{---} & |x\rangle \\ \frac{1}{\sqrt{2}}(|0\rangle - |1\rangle) & \text{---} & & \text{---} & \frac{(-1)^{f(x)}}{\sqrt{2}}(|0\rangle - |1\rangle) \end{array}$$

Figure 2.2: Application of U_f when the second qubit is prepared with an eigenstate of X .

factor $(-1)^{f(x)}$ as being applied to the first qubit, rather than the second one, writing the mapping as

$$|x\rangle \otimes \frac{1}{\sqrt{2}}(|0\rangle - |1\rangle) \rightarrow (-1)^{f(x)}|x\rangle \otimes \frac{1}{\sqrt{2}}(|0\rangle - |1\rangle).$$

The relative phase that is — in principle — applied to the second qubit is now “kicked back” to the first qubit, by virtue of the fact that $\frac{1}{\sqrt{2}}(|0\rangle - |1\rangle)$ is an eigenstate of the addition $\oplus f(x)$ that U_f applies to the second qubit. The net effect is to flip the sign of a basis state $|x\rangle$ such that $f(x) = 1$. This technique, called *phase kickback*, is at the heart of several quantum algorithms discussed in this set of lecture notes.

2.2 The first quantum algorithm: Deutsch's algorithm

We discuss Deutsch's algorithm [Deutsch, 1985] as a direct application of phase kickback, and as a way to introduce the idea of quantum interference that is exploited in Simon's algorithm as well, in Sect. 2.3. Historically, Deutsch's algorithm was the first to show a quantum speedup over classical algorithms for the same problem; it also has the tremendous benefit of being simple to understand.

For Deutsch's algorithm, we are given access to a function $f : \{0, 1\} \rightarrow \{0, 1\}$, and the goal is to find $f(0) \oplus f(1)$ by querying the function the smallest number of times.

Remark 2.5. *For the first two algorithms discussed in this set of lecture notes (i.e., Deutsch's and Simon's), as well as some of the subsequent algorithms, the complexity of the algorithm is determined only in terms of the number of calls to a function f given as part of the input. Considerations on what the function f actually implements, and how many operations are performed inside of f , or between the calls to f , are not part of how we determine this type of complexity. This model is known as query complexity, because — as the name implies — it defines the complexity of an algorithm as the number of queries to a given function (in this case, f). Query complexity is used as a model to answer important theoretical questions. There are many quantum algorithms that yield speedups under the query complexity model; some others, e.g., Shor's algorithm, are faster than (known) classical algorithms under the more traditional computational complexity model, according to which complexity is measured by the number of basic operations — usually called gate complexity because it counts the number of (elementary) gates. In fact, even for cases where we are interested in the query complexity, we may separately discuss the number of gates applied between calls to f to give a more precise characterization of the gate complexity as well. The gate complexity is equivalently called time complexity.*

Classically, solving the problem described above requires two queries to f : if we query both $f(0)$ and $f(1)$ we can easily compute $f(0) \oplus f(1)$, and if we query only one of the two we cannot determine the correct answer with certainty. Surprisingly, we can solve the problem with only one quantum query using an appropriate quantum circuit. We assume that f is given in the form of a quantum oracle $U_f : |x\rangle|y\rangle \rightarrow |x\rangle|y \oplus f(x)\rangle$, as we have seen before.

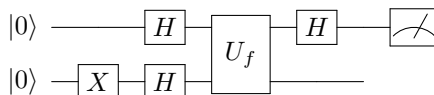


Figure 2.3: Circuit to solve Deutsch's algorithm.

Deutsch's algorithm works by applying the circuit depicted in Fig. 2.3. Let us study the evolution of the quantum state. The final quantum state before the measurement is:

$$(H \otimes I)U_f(H \otimes H)(I \otimes X)(|0\rangle \otimes |0\rangle).$$

We have:

$$\begin{aligned} (I \otimes X)(|0\rangle|0\rangle) &= |0\rangle|1\rangle \\ (H \otimes H)(|0\rangle|1\rangle) &= \frac{|0\rangle + |1\rangle}{\sqrt{2}} \otimes \frac{|0\rangle - |1\rangle}{\sqrt{2}} \\ U_f \left(\frac{|0\rangle + |1\rangle}{\sqrt{2}} \otimes \frac{|0\rangle - |1\rangle}{\sqrt{2}} \right) &= \frac{(-1)^{f(0)}}{\sqrt{2}} |0\rangle \otimes \frac{|0\rangle - |1\rangle}{\sqrt{2}} + \frac{(-1)^{f(1)}}{\sqrt{2}} |1\rangle \otimes \frac{|0\rangle - |1\rangle}{\sqrt{2}} \\ &= (-1)^{f(0)} \left(\frac{|0\rangle + (-1)^{f(0) \oplus f(1)} |1\rangle}{\sqrt{2}} \right) \otimes \frac{|0\rangle - |1\rangle}{\sqrt{2}}. \end{aligned}$$

In the third equation above we applied phase kickback, Eq. (2.1), and in the last line we simply collected the term $(-1)^{f(0)}$. Finally, we apply $(H \otimes I)$ to this state, and doing the calculations we obtain:

$$(-1)^{f(0)} \left(\frac{(1 + (-1)^{f(0) \oplus f(1)})|0\rangle + (1 - (-1)^{f(0) \oplus f(1)})|1\rangle}{2} \right) \otimes \frac{|0\rangle - |1\rangle}{\sqrt{2}}.$$

The outcome of the measurement operation then depends on the value of $f(0) \oplus f(1)$. We can ignore the global phase factor $(-1)^{f(0)}$: it is irrelevant when we take the modulus squared to look at the measurement outcome probabilities, see Ex. 1.30. We are measuring the first qubit, and the state is in a product state, so we only need to look at the first qubit. If $f(0) \oplus f(1) = 0$, then the coefficient for $|0\rangle$ is $(1 + (-1)^0)/2 = 1$, implying that we have probability 1 of observing 0 as the measurement outcome. If, on the other hand, $f(0) \oplus f(1) = 1$, the coefficient for $|0\rangle$ is $(1 + (-1)^1)/2 = 0$ and the coefficient for $|1\rangle = 1$, implying that we have probability 1 of obtaining 1 as the measurement outcome. Thus, with this measurement we can determine with probability 1 the value of $f(0) \oplus f(1)$. Notice that Fig. 2.3 contains a single application of U_f , as opposed to the two function evaluations required classically: a quantum speedup, in the query complexity model!

2.3 Quantum interference and period finding: Simon’s algorithm

In the final part of this chapter we describe a quantum algorithm, known as Simon’s algorithm [Simon, 1997], that gives an expected exponential speedup with respect to classical algorithms. Although Simon’s algorithm has not been directly helpful for quantum optimization algorithms (at least so far), we discuss it because it has many interesting features from an educational perspective: namely, it uses both classical and quantum computation, and it yields an exponential speedup.

Admittedly, the problem that Simon’s algorithm solves is not very useful (just as Deutsch’s algorithm), but the ideas shown here give us further intuition of what quantum computing can do. In fact, this algorithm was an inspiration for the well-known and groundbreaking work of Shor on integer factorization [Shor, 1997]: a large part of Shor’s algorithm relies on the solution of a period finding problem, and Simon’s algorithm solves a simplified problem of the same flavor. Shor’s algorithm is, however, much more involved than Simon’s algorithm, and a full treatment requires several number-theoretical results that are beyond the scope of this set of lecture notes. Thus, we focus on Simon’s algorithm; some notes on Shor’s algorithm are given in Sect. 2.4.

For Simon’s algorithm, we are given access to a function $f : \{0, 1\}^n \rightarrow \{0, 1\}^n$ with the property that $f(\vec{x}) = f(\vec{z})$ if and only if $\vec{x} = \vec{z} \oplus \vec{a}$, for some unknown $\vec{a} \in \{0, 1\}^n$. We do not know anything else about the function, and the goal is to find \vec{a} by querying the function the smallest number of times, again using a query complexity model. Notice that if $\vec{a} = \vec{0}$ then the function is one-to-one, whereas if $\vec{a} \neq \vec{0}$ the function is two-to-one, because for every \vec{x} , there is exactly another number in domain for which the function has the same value. The function f is assumed to be given as a quantum circuit on $q = 2n$ qubits, via the unitary U_f depicted in Fig. 2.4, therefore we are allowed to query the function in superposition (this gives us an advantage over classical computation, but remember that a classical circuit to compute f can be turned into a quantum circuit to compute U_f , see Rem. 1.44). Recall that by linearity, to describe the effect of U_f it is enough to describe its behavior on all basis states, so Fig. 2.4 fully specifies the unitary.

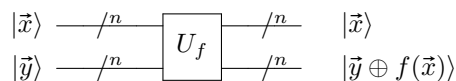


Figure 2.4: The circuit implementing U_f for Simon’s problem, with basis states $\vec{x}, \vec{y} \in \{0, 1\}^n$.

2.3.1 Classical algorithm

Because we do not know anything about the binary string \vec{a} , the best we can do to recover its value is to feed inputs to the function f , and try to extract information from the output. The string \vec{a} is determined once we find two distinct inputs \vec{x}, \vec{z} such that $f(\vec{x}) = f(\vec{z})$, because then $\vec{x} = \vec{z} \oplus \vec{a}$ which implies $\vec{x} \oplus \vec{z} = \vec{a}$. So we are successful once \vec{a} belongs to the set $\{\vec{x} \oplus \vec{z} \text{ for all pairs of distinct tested inputs } \vec{x}, \vec{z}\}$.

Suppose we have evaluated m distinct input values and we did not find a match. Then $\vec{a} \neq \vec{x} \oplus \vec{z}$ for all \vec{x}, \vec{z} previously evaluated, therefore we have eliminated at most $m(m-1)/2$ possible values of \vec{a} from the search space. (Fewer values may have been eliminated if we test inputs equal to $\vec{x} \oplus \vec{y} \oplus \vec{z}$ for any three input values $\vec{x}, \vec{y}, \vec{z}$ already tested. In fact, if we test \vec{w} such that $\vec{w} = \vec{x} \oplus \vec{y} \oplus \vec{z}$, we have that $\vec{w} \oplus \vec{z} = \vec{x} \oplus \vec{y}$, therefore the value $\vec{w} \oplus \vec{z}$ had already been eliminated from the list of possible values of \vec{a} .) In the worst case all possible values for \vec{a} have equal probability, so this approach is successful with probability $\frac{m(m-1)}{2^{n+1}}$, i.e., the number of values of \vec{a} that have already been tested divided by the probability that any one of them is the correct answer. Because $m(m-1)/2$ is small compared to 2^n , the probability of success of this algorithm (i.e., $\frac{m(m-1)}{2^{n+1}}$) is very small until we have evaluated a number of inputs that is in the order of 2^n . In particular, to guarantee a probability of success of at least δ , we need $m(m-1) \geq \delta 2^{n+1}$, which implies that $m = \mathcal{O}(\sqrt{\delta 2^n})$. Hence, for any positive constant δ , the number of required iterations is exponential: $\mathcal{O}(2^{n/2})$. After evaluating $\frac{1+\sqrt{2^{n+3}+1}}{2} = \mathcal{O}(2^{n/2})$ distinct input values satisfying the condition outlined above for non-matching triplets (to obtain this number, we found the smallest value of m such that $m(m-1) \geq 2^{n+1}$), we are guaranteed that a matching pair has been found, or we can safely determine that $\vec{a} = \vec{0}$.

2.3.2 Quantum algorithm

Using a quantum computer, we can determine \vec{a} much faster. The idea, first described in [Simon, 1997], is to apply the circuit in Fig. 2.5.

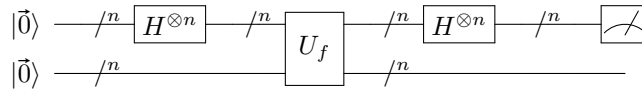


Figure 2.5: Quantum circuit used in Simon's algorithm.

From an algebraic point of view, the state produced by this circuit just before the measurement is described by the following expression

$$(H^{\otimes n} \otimes I^{\otimes n})U_f(H^{\otimes n} \otimes I^{\otimes n})(|\vec{0}\rangle_n \otimes |\vec{0}\rangle_n).$$

We now analyze the output of the quantum circuit, by looking at the quantum states at intermediate steps of the circuit. Define the following three states, used to track the evolution of the quantum state through the end of the circuit:

$$\begin{aligned} |\psi\rangle &= (H^{\otimes n} \otimes I^{\otimes n})(|\vec{0}\rangle|\vec{0}\rangle) \\ |\phi\rangle &= U_f(H^{\otimes n} \otimes I^{\otimes n})(|\vec{0}\rangle|\vec{0}\rangle) \\ |\chi\rangle &= (H^{\otimes n} \otimes I^{\otimes n})U_f(H^{\otimes n} \otimes I^{\otimes n})(|\vec{0}\rangle|\vec{0}\rangle). \end{aligned}$$

For $|\psi\rangle$, we know that $H^{\otimes n}$ applied onto $|\vec{0}\rangle_n$ creates a uniform superposition of $|\vec{j}\rangle, \vec{j} \in \{0, 1\}^n$. Therefore we have:

$$|\psi\rangle = (H^{\otimes n} \otimes I^{\otimes n})(|\vec{0}\rangle|\vec{0}\rangle) = \frac{1}{\sqrt{2^n}} \sum_{\vec{j} \in \{0, 1\}^n} |\vec{j}\rangle|\vec{0}\rangle.$$

By linearity, applying U_f onto this state yields:

$$|\phi\rangle = U_f|\psi\rangle = \frac{1}{\sqrt{2^n}} \sum_{\vec{j} \in \{0, 1\}^n} |\vec{j}\rangle|\vec{0} \oplus f(\vec{j})\rangle = \frac{1}{\sqrt{2^n}} \sum_{\vec{j} \in \{0, 1\}^n} |\vec{j}\rangle|f(\vec{j})\rangle.$$

We now need to analyze the effect of applying further Hadamard gates on the top lines of the circuit, i.e., the first register. Using the algebraic expression for the Hadamard gate found in

Eq. (1.5), the next step in the circuit yields the state:

$$\begin{aligned} |\chi\rangle &= (H^{\otimes n} \otimes I^{\otimes n})|\phi\rangle = (H^{\otimes n} \otimes I^{\otimes n}) \frac{1}{\sqrt{2^n}} \sum_{\vec{j} \in \{0,1\}^n} |\vec{j}\rangle |f(\vec{j})\rangle \\ &= \frac{1}{2^n} \sum_{\vec{j} \in \{0,1\}^n} \sum_{\vec{k} \in \{0,1\}^n} (-1)^{\vec{k} \bullet \vec{j}} |\vec{k}\rangle |f(\vec{j})\rangle. \end{aligned} \quad (2.2)$$

When we make a measurement on the top n qubit lines of $|\chi\rangle$ (i.e., the first n -qubit register, containing qubits 1 through n), we obtain any given binary string \vec{k} with probability equal to the sum of the modulus squared of the coefficient of the states $|\vec{k}\rangle |f(\vec{j})\rangle$, for all \vec{j} . This is a direct consequence of the principle of implicit measurement (Prop. 1.50): if we only measure the first register, and discard the second, we can assume that the measurement is applied to the second register as well; thus, we observe \vec{k} in the first register if measurement of the entire state yields any string that starts with \vec{k} , hence the sum over all the possibilities in the second register.

It is easy to verify that for fixed \vec{k} , the probability of observing \vec{k} in the first measurement (i.e., the sum of the modulus squared of the coefficient of the states $|\vec{k}\rangle |f(\vec{j})\rangle$, for all \vec{j}) is equal to:

$$\left\| \frac{1}{2^n} \sum_{\vec{j} \in \{0,1\}^n} (-1)^{\vec{k} \bullet \vec{j}} |f(\vec{j})\rangle \right\|^2.$$

A simple formal argument for why this is the case can be derived by using the density matrix formalism. The density matrix corresponding to the pure state in Eq. (2.2) is:

$$\rho = \left(\frac{1}{2^n} \sum_{\vec{j} \in \{0,1\}^n} \sum_{\vec{x} \in \{0,1\}^n} (-1)^{\vec{x} \bullet \vec{j}} |\vec{x}\rangle |f(\vec{j})\rangle \right) \left(\frac{1}{2^n} \sum_{\vec{h} \in \{0,1\}^n} \sum_{\vec{y} \in \{0,1\}^n} (-1)^{\vec{y} \bullet \vec{h}} \langle \vec{y} | \langle f(\vec{h}) | \right).$$

Computing the reduced density matrix by tracing out the second register (see Sect. 1.4.2), and then applying a measurement on all qubits in the first register (recall Rem. 1.59), the probability of observing \vec{k} in the first register is:

$$\begin{aligned} \text{Tr} \left(\left(|\vec{k}\rangle \langle \vec{k}| \otimes I^{\otimes n} \right) \rho \right) &= \text{Tr} \left(\left(|\vec{k}\rangle \langle \vec{k}| \otimes I^{\otimes n} \right) \rho \left(|\vec{k}\rangle \langle \vec{k}| \otimes I^{\otimes n} \right) \right) \\ &= \text{Tr} \left(\left(\frac{1}{2^n} \sum_{\vec{j} \in \{0,1\}^n} (-1)^{\vec{k} \bullet \vec{j}} |f(\vec{j})\rangle \right) \left(\frac{1}{2^n} \sum_{\vec{h} \in \{0,1\}^n} (-1)^{\vec{k} \bullet \vec{h}} \langle f(\vec{h}) | \right) \right) \\ &= \left\| \frac{1}{2^n} \sum_{\vec{j} \in \{0,1\}^n} (-1)^{\vec{k} \bullet \vec{j}} |f(\vec{j})\rangle \right\|^2, \end{aligned}$$

so we have the following relationship:

$$\text{Pr}(\vec{k}) = \left\| \frac{1}{2^n} \sum_{\vec{j} \in \{0,1\}^n} (-1)^{\vec{k} \bullet \vec{j}} |f(\vec{j})\rangle \right\|^2,$$

where we denote by $\text{Pr}(\vec{k})$ the probability of observing string \vec{k} after applying a measurement to the first register. Now we analyze the expression for $\text{Pr}(\vec{k})$. First, we deal with the case $\vec{a} = \vec{0}$, which is easier to analyze. In this case the function f is one-to-one, so the summation $\sum_{\vec{j} \in \{0,1\}^n} (-1)^{\vec{k} \bullet \vec{j}} |f(\vec{j})\rangle$ is over every basis vector, and:

$$\left\| \frac{1}{2^n} \sum_{\vec{j} \in \{0,1\}^n} (-1)^{\vec{k} \bullet \vec{j}} |f(\vec{j})\rangle \right\|^2 = \frac{1}{2^n}.$$

This means that we have probability $\frac{1}{2^n}$ to observe a given binary string \vec{k} , i.e., each measurement gives an n -digit binary string uniformly at random. Let us now analyze the case $\vec{a} \neq \vec{0}$, which is a bit more involved but also more interesting. Assuming $\vec{a} \neq \vec{0}$, the function f is two-to-one: $f(\vec{j}) = f(\vec{j} \oplus \vec{a})$. So $|\vec{k}\rangle|f(\vec{j})\rangle = |\vec{k}\rangle|f(\vec{j} \oplus \vec{a})\rangle$, which means that there are only $2^n/2 = 2^{n-1}$ nonzero entries in the vector $\frac{1}{2^n} \sum_{\vec{j} \in \{0,1\}^n} (-1)^{\vec{k} \bullet \vec{j}} |f(\vec{j})\rangle$. Let R be a set of cardinality 2^{n-1} with the following property: $R \cup \{\vec{j} \oplus \vec{a} : \vec{j} \in R\} = \{0,1\}^n$. In other words, for every $\vec{j} \in \{0,1\}^n$, R contains either \vec{j} or $\vec{j} \oplus \vec{a}$, but not both — it does not matter which one of these two we choose, as long as we pick only one. (For readers familiar with the concept of quotient sets, R picks a representative from the quotient set $\{0,1\}^n / \sim$ where \sim is the equivalence relationship defined as: $\vec{x} \sim \vec{y}$ if and only if $\vec{x} = \vec{y} \oplus \vec{a}$.)

Example 2.6. Suppose $n = 3$ and $\vec{a} = 101$. Then the following holds:

$$\begin{aligned} f(000) &= f(101) \\ f(001) &= f(100) \\ f(010) &= f(111) \\ f(011) &= f(110). \end{aligned}$$

In this example, the set R contains four ($= 2^{n-1}$) elements, chosen as follows: for every row of the above set of equations, we either pick the binary string on the l.h.s., or the one on the r.h.s. It does not matter which ones we choose.

For each \vec{k} , the string \vec{k} appears in the first register precisely in the 2^{n-1} basis states $|\vec{k}\rangle|f(\vec{j})\rangle$ for $\vec{j} \in R$. For each $\vec{j} \in R$, the coefficient of the basis state $|\vec{k}\rangle|f(\vec{j})\rangle$ is the sum of the coefficients in Eq. (2.2) for $|\vec{k}\rangle|f(\vec{j})\rangle$ and $|\vec{k}\rangle|f(\vec{j} \oplus \vec{a})\rangle$ (because the content of the second register is the same, so these basis states coincide and the corresponding coefficients must be added together); that is, it is equal to:

$$\begin{aligned} \frac{(-1)^{\vec{k} \bullet \vec{j}} + (-1)^{\vec{k} \bullet (\vec{j} \oplus \vec{a})}}{2^n} &= \frac{(-1)^{\vec{k} \bullet \vec{j}} + (-1)^{\vec{k} \bullet \vec{j}} (-1)^{\vec{k} \bullet \vec{a}}}{2^n} \\ &= \frac{(-1)^{\vec{k} \bullet \vec{j}} (1 + (-1)^{\vec{k} \bullet \vec{a}})}{2^n}. \end{aligned}$$

Therefore the probability of obtaining the binary string \vec{k} after applying a measurement to all qubits in the first register is:

$$\sum_{\vec{j} \in R} \left(\frac{(-1)^{\vec{k} \bullet \vec{j}} (1 + (-1)^{\vec{k} \bullet \vec{a}})}{2^n} \right)^2 = 2^{n-1} \left(\frac{(1 + (-1)^{\vec{k} \bullet \vec{a}})}{2^n} \right)^2 = \begin{cases} \frac{1}{2^{n-1}} & \text{if } \vec{k} \bullet \vec{a} \equiv 0 \pmod{2} \\ 0 & \text{if } \vec{k} \bullet \vec{a} \equiv 1 \pmod{2}, \end{cases}$$

where the multiplication factor 2^{n-1} comes from the fact that $|R| = 2^{n-1}$. Thus, the only binary strings that have positive probability to be observed are those strings \vec{k} for which $\vec{k} \bullet \vec{a} \equiv 0 \pmod{2}$. The remaining strings are never observed: by carefully applying quantum operations we have reduced their state coefficients to zero, a phenomenon known as *destructive interference*. Notice that unless $\vec{k} = \vec{0}$, then there is a nonempty set of bits for which the modulo-2 sum of the corresponding coefficients of \vec{a} must vanish. Thus, excluding “unlucky” or edge cases (see Sect. 2.3.3), we can express one of the bits of \vec{a} as a modulo-2 sum of the others, and we eliminate approximately half of the possible values from the search space for \vec{a} .

Our discussion shows that with a single quantum query to U_f , in the case $\vec{a} \neq \vec{0}$ with high probability we learn very valuable information about \vec{a} , and we can approximately halve the search space for \vec{a} . In the case $\vec{a} = \vec{0}$, we instead obtain a binary string uniformly at random. It now remains to fully specify, in a more precise manner, how this information can be used.

2.3.3 Full description and analysis

The quantum algorithm described in the previous section yields information on \vec{a} , but it does not output \vec{a} directly. To recover \vec{a} , further calculations have to be performed. This is a situation that can be fairly common in quantum algorithms: a quantum computation measures some properties of the desired answer; then, classical computations are used to analyze these properties and obtain the desired answer. Thus, even if the quantum algorithm does not explicitly output the desired answer, it allows us to get closer to our goal.

In the specific case of the problem discussed here in Sect. 2.3, the quantum computation allows us to learn \vec{k} such that $\vec{k} \bullet \vec{a} \equiv 0 \pmod 2$: we already discussed why this is the case when $\vec{a} \neq \vec{0}$, and this is also the case when $\vec{a} = \vec{0}$ because then trivially $\vec{k} \bullet \vec{a} = 0$. Because all \vec{k} with this property have the same probability of being output by the measurement, we obtain a uniformly random sample from the set $\{\vec{k} \in \{0, 1\}^n : \vec{k} \bullet \vec{a} \equiv 0 \pmod 2\}$. We embed the equation $\vec{k} \bullet \vec{a} \equiv 0 \pmod 2$ into a solution algorithm as follows: we initialize the set of equations E to the empty set; then, while the system of equations E has multiple nonzero solutions, we apply the circuit described in Sect. 2.3.2 (Fig. 2.5) to obtain \vec{k} , and add the equation $\vec{k} \bullet \vec{a} \equiv 0 \pmod 2$ to E . Notice that $\vec{a} = \vec{0}$ is always a solution of the homogeneous system E , but we are interested in determining if there are some nonzero solutions as well. In other words, we want to determine if the null space of the matrix of the linear system contains any nonzero vector. The termination condition for the algorithm (i.e., the system of equations E does not have multiple nonzero solutions) triggers in one of two possible situations: either the system has a uniquely determined nonzero solution $\vec{a} \neq \vec{0}$, or the only possible solution is $\vec{a} = \vec{0}$; in both cases, the solution must be the hidden string \vec{a} . Because there are n unknowns and we are dealing with a homogeneous system, to identify which of the two situations happens we need E to contain $n - 1$ linearly independent vectors \vec{k} , where independence is intended in the set \mathbb{F}_2^n .

Remark 2.7. \mathbb{F}_2 , also denoted $GF(2)$, is the finite field with two elements: 0 and 1, where addition and multiplication are performed modulo 2. \mathbb{F}_2^n is essentially the set of n -digit binary strings, combined using XOR and AND.

In total, $n - 1$ linearly independent vectors are sufficient because the space of all vectors perpendicular to \vec{a} modulo 2 has dimension $n - 1$. At every iteration we obtain a random \vec{k} for which $\vec{k} \bullet \vec{a} \equiv 0 \pmod 2$; thus, we need to analyze how many iterations are needed to obtain $n - 1$ linearly independent such vectors with high probability.

In continuous space, uniform random sampling of vectors yields linearly independent vectors with probability 1. In this case we are considering linear independence among vectors that have coefficients 0 or 1, and independence is in terms of the modulo-2 sum, so the argument is less clear; however, we show that even in \mathbb{F}_2^n , the probability of obtaining $n - 1$ linearly independent vectors after sampling $n + t$ times is very large, and in particular it is bounded below by $1 - \frac{1}{2^{t+1}}$. The proof technique is taken from [Mermin, 2007, Apx. G].

Proposition 2.8. Let $\vec{k}^{(1)}, \dots, \vec{k}^{(n+t)}$ be vectors in \mathbb{F}_2^n , i.e., n -dimensional vectors with coefficients $\{0, 1\}$ and addition and multiplication modulo 2. Suppose all vectors are drawn uniformly at random from the subspace of dimension $n - 1$ of all vectors orthogonal to some vector \vec{a} . Then, the probability that the set $\{\vec{k}^{(1)}, \dots, \vec{k}^{(n+t)}\}$ contains $n - 1$ linearly independent vectors (where independence is in \mathbb{F}_2^n) is at least $1 - \frac{1}{2^{t+1}}$.

Proof. Consider the $(n + t) \times n$ matrix obtained by stacking the vectors as rows:

$$M = \begin{pmatrix} \text{-----} \vec{k}^{(1)} \text{-----} \\ \text{-----} \vec{k}^{(2)} \text{-----} \\ \vdots \\ \text{-----} \vec{k}^{(n+t)} \text{-----} \end{pmatrix}.$$

If this matrix has rank $n - 1$, there are $n - 1$ linearly independent vectors among $\vec{k}^{(1)}, \dots, \vec{k}^{(n+t)}$. By assumption, the vectors are drawn uniformly at random from the subspace of vectors orthogonal

to \vec{a} . Therefore, in a basis of this $(n-1)$ -dimensional subspace, the vectors have coefficients that are drawn uniformly at random from $\{0, 1\}$. Thus, if we express each row of M in such a basis, we obtain a matrix M' of size $(n+t) \times (n-1)$, with coefficients that are drawn uniformly at random from $\{0, 1\}$, and with the property that if its rank is $(n-1)$, there are $n-1$ linearly independent vectors among $\vec{k}^{(1)}, \dots, \vec{k}^{(n+t)}$.

Let B be a set of linearly independent columns of M' , to be constructed, and initialized to be the empty set. Pick a column of M' uniformly at random. This column is an $(n+t)$ -dimensional vector, therefore it is nonzero with probability $1 - \frac{1}{2^{n+t}}$. If so, add it to B . Now for $h = 2, \dots, n-1$, repeat the following steps as long as each step successfully adds a column to B . Pick a random column of M' that was not picked in previous iterations. If this column is linearly independent of the columns in B , add it to B . The probability of this happening is at least $1 - \frac{1}{2^{n+t+1-h}}$: at iteration h , $|B| = h-1$, so the subspace of vectors spanned by B contains at most 2^{h-1} vectors (only the coefficients $\{0, 1\}$ are allowed in each linear combination), implying that the probability of sampling a random vector and obtaining a vector in the subspace spanned by B is at most $\frac{2^{h-1}}{2^{n+t}} = \frac{1}{2^{n+t+1-h}}$. The probability that this algorithm terminates at $h = n-1$ with $|B| = n-1$ (i.e., after finding $n-1$ linearly independent columns) is therefore at least:

$$p = \prod_{j=1}^{n-1} \left(1 - \frac{1}{2^{n+t+1-j}} \right).$$

We show below that $\prod_{j=1}^{n-1} \left(1 - \frac{1}{2^{n+t+1-j}} \right) \geq 1 - \sum_{j=1}^{n-1} \frac{1}{2^{n+t+1-j}}$, which allows us to lower bound p and prove the main result:

$$p = \prod_{j=1}^{n-1} \left(1 - \frac{1}{2^{n+t+1-j}} \right) \geq 1 - \sum_{j=1}^{n-1} \frac{1}{2^{n+t+1-j}} = 1 - \sum_{j=0}^{n-2} \frac{1}{2^{t+2+j}} \geq 1 - \frac{1}{2^{t+1}}.$$

It remains to show that $\prod_{j=1}^{n-1} \left(1 - \frac{1}{2^{n+t+1-j}} \right) \geq 1 - \sum_{j=1}^{n-1} \frac{1}{2^{n+t+1-j}}$. We prove a more general statement: given scalars $0 \leq c_1, \dots, c_n \leq 1$, $\prod_{j=1}^n (1 - c_j) \geq 1 - \sum_{j=1}^n c_j$. The proof is by induction on n . For $n = 1$ the inequality is trivially satisfied at equality. For the induction step (from $n-1$ to n), we have:

$$\begin{aligned} \prod_{j=1}^n (1 - c_j) &= (1 - c_n) \prod_{j=1}^{n-1} (1 - c_j) \geq (1 - c_n) \left(1 - \sum_{j=1}^{n-1} c_j \right) \\ &= \left(1 - \sum_{j=1}^n c_j \right) + c_n \sum_{j=1}^{n-1} c_j \geq 1 - \sum_{j=1}^n c_j, \end{aligned}$$

where the first inequality used the induction hypothesis and the fact that $1 - c_n \geq 0$, and the last inequality used the fact that all c_j are nonnegative. \square

The lower bound of Prop. 2.8 does not depend on n : if we pick, e.g., $t = 9$, the probability of success is at least 99.9%. Hence, with overwhelming probability after slightly more than n executions of the quantum circuit, and therefore $\mathcal{O}(n)$ queries to the function f , we determine the solution to the problem with a classical computation that can be performed in polynomial time (i.e., $\mathcal{O}(n^2)$ to determine a solution to the system of linear equations modulo 2). We remark that once the unique nonzero \vec{a} is determined, we can easily verify that it is the sought binary string by querying the function f . On the other hand, if $\vec{a} = \vec{0}$, the algorithm detects that this is the case because at some point the system of linear equations E has $\vec{a} = \vec{0}$ as the only possible solution. Compare the $\mathcal{O}(n)$ queries of this approach with the $\mathcal{O}(2^{n/2})$ queries that are required by a classical algorithm, and we have shown an exponential speedup in the query complexity.

This algorithm shows a typical feature of many quantum algorithms: oftentimes, there is a classical computation to complement the quantum computation. For example, the classical computation could be used to verify, with certainty, that the correct solution to the problem

has indeed been found. In this case, the verification is carried out by checking whether the system of equations has a unique nonzero solution. Indeed, quantum algorithms are probabilistic algorithm, and we can only try to increase the probability that the correct answer is returned; only in rare cases the solution can be obtained with probability 1, see e.g. [Brassard et al., 2002]. For this reason, it is desirable to have a way to deterministically verify correctness. This may require a classical computation. In other words, sometimes the quantum algorithm is applied to a problem for which it is difficult to classically compute the solution, but once the solution (or some information about it) is obtained, it is easy to classically verify that we have the right answer. Note that this may not be possible in general, because the complexity class BQP (Def. 6.7) is not known or believed to be contained in NP (recall that NP is the class of problems that admit efficient classical verification). Some of the quantum algorithms presented in this set of lecture notes admit simple classical verification.

2.4 Notes and further reading

The Deutsch-Jozsa algorithm [Deutsch and Jozsa, 1992] generalizes Deutsch’s algorithm. The Bernstein-Vazirani algorithm is another quantum algorithm developed in the early days of the field [Bernstein and Vazirani, 1997], and it is based on a modified version of the Deutsch-Jozsa construction. [Bernstein and Vazirani, 1997] additionally lays the mathematical foundations for computational complexity theory of quantum algorithms. Two other notable and groundbreaking examples of early work on quantum algorithms are Shor’s prime factorization algorithm [Shor, 1997] and Grover’s search algorithm [Grover, 1996]. An ample discussion of Grover’s algorithm is given in Ch. 4. We do not discuss Shor’s algorithm, although one of its most important building blocks, the quantum Fourier transform, is the subject of Ch. 3. Some notes on the relationship between the quantum Fourier transform and Shor’s algorithm are given therein, Sect. 3.4. In fact, Simon’s algorithm is a specific instance of the hidden subgroup problem, discussed in the notes for Ch. 3.

On the topic of classical verification of quantum computation, we mention that it is an active topic of research to design verification protocols for generic quantum computations, see, e.g., [Broadbent et al., 2009, Aharonov et al., 2017, Reichardt et al., 2013, Mahadev, 2018]. In particular [Mahadev, 2018] proposes a scheme that allows a classical computer to verify the output of a quantum computation, with an interactive protocol in which the classical computer uses the quantum computer to run some quantum computations and report the results of measurements.

Chapter 3

Quantum Fourier transform and phase estimation

In this chapter we present two fundamental building blocks for quantum algorithms: the quantum Fourier transform, and one of its direct applications known as phase estimation. Both building blocks are used extensively in the rest of this set of lecture notes.

3.1 Quantum Fourier transform

The definition of the quantum Fourier transform originates directly from the classical discrete Fourier transform (DFT). The DFT finds numerous applications in science and engineering, and it is so crucial in many areas that the fast Fourier transform algorithm — a classical algorithm to compute the DFT — is considered one of the most important algorithms of the 20th century. Given $x \in \mathbb{C}^{2^n}$, its DFT is defined as the vector $y \in \mathbb{C}^{2^n}$ with components:

$$y_j = \sum_{k=0}^{2^n-1} x_k e^{2\pi i j k / 2^n} \quad \forall j = 0, \dots, 2^n - 1. \quad (3.1)$$

Our goal in this section is to discuss a quantum algorithm to compute the DFT, or at least something similar to it. To do so, it is convenient to look at the value of the DFT when applied onto the k -th standard orthonormal basis vector; i.e., suppose the input vector x coincides with $|\vec{k}\rangle$. Then the output vector y has components:

$$y_j = e^{2\pi i j k / 2^n} \quad \forall j = 0, \dots, 2^n - 1,$$

which in the bra-ket notation can be written as $y = \sum_{\vec{j} \in \{0,1\}^n} e^{2\pi i j k / 2^n} |\vec{j}\rangle$. The vector y , as written, is not normalized, so it is not a quantum state. In a very natural way, we then define the quantum Fourier transform as follows.

Definition 3.1 (Quantum Fourier transform). *The quantum Fourier transform (QFT) on n qubits is the operation Q_n that implements the following map:*

$$Q_n |\vec{k}\rangle = \frac{1}{\sqrt{2^n}} \sum_{\vec{j} \in \{0,1\}^n} e^{2\pi i j k / 2^n} |\vec{j}\rangle \quad \forall \vec{k} \in \{0,1\}^n. \quad (3.2)$$

With this definition, given a quantum state of the form $\sum_{\vec{k} \in \{0,1\}^n} x_k |\vec{k}\rangle$, the j -th component of the quantum state $|\psi\rangle$ obtained by applying the QFT to $\sum_{\vec{k} \in \{0,1\}^n} x_k |\vec{k}\rangle$, i.e., the coefficient of the j -th basis state in $|\psi\rangle$, is given by:

$$\langle \vec{j} | \psi \rangle = \langle \vec{j} | \left(\frac{1}{\sqrt{2^n}} \sum_{\vec{k} \in \{0,1\}^n} x_k \sum_{\vec{h} \in \{0,1\}^n} e^{2\pi i h k / 2^n} |\vec{h}\rangle \right) = \frac{1}{\sqrt{2^n}} \sum_{\vec{k} \in \{0,1\}^n} x_k e^{2\pi i j k / 2^n}.$$

This is consistent with the classical definition in Eq. (3.1): the only difference is the normalization factor, which is necessary to ensure that the QFT can be implemented as a unitary (because it has to output a unit vector when applied onto a unit vector).

Define $\omega_n = e^{2\pi i/2^n}$. Then the matrix Q_n that implements the n -qubit QFT has elements:

$$(Q_n)_{jk} = \frac{1}{\sqrt{2^n}} \omega_n^{jk} \quad \forall \vec{j}, \vec{k} \in \{0, 1\}^n.$$

In matrix form, this yields:

$$Q_n = \frac{1}{\sqrt{2^n}} \begin{pmatrix} 1 & 1 & 1 & \dots & 1 \\ 1 & \omega_n & \omega_n^2 & \dots & \omega_n^{2^n-1} \\ 1 & \omega_n^2 & \omega_n^4 & \dots & \omega_n^{2(2^n-1)} \\ \vdots & & & \ddots & \vdots \\ 1 & \omega_n^{(2^n-1)} & \omega_n^{2(2^n-1)} & \dots & \omega_n^{(2^n-1)(2^n-1)} \end{pmatrix} = \frac{1}{\sqrt{2^n}} \begin{pmatrix} 1 & 1 & 1 & \dots & 1 \\ 1 & \omega_n & \omega_n^2 & \dots & \omega_n^{-1} \\ 1 & \omega_n^2 & \omega_n^4 & \dots & \omega_n^{-2} \\ \vdots & & & \ddots & \vdots \\ 1 & \omega_n^{-1} & \omega_n^{-2} & \dots & \omega_n \end{pmatrix},$$

using the fact that $\omega_n^{2^n} = 1$. The conjugate transpose of this matrix is:

$$Q_n^\dagger = \frac{1}{\sqrt{2^n}} \begin{pmatrix} 1 & 1 & 1 & \dots & 1 \\ 1 & \omega_n^{-1} & \omega_n^{-2} & \dots & \omega_n \\ 1 & \omega_n^{-2} & \omega_n^{-4} & \dots & \omega_n^2 \\ \vdots & & & \ddots & \vdots \\ 1 & \omega_n & \omega_n^2 & \dots & \omega_n^{-1} \end{pmatrix}.$$

If Q_n is to be implemented as a quantum algorithm, it has to be a unitary matrix. We can verify that it is by showing $Q_n^\dagger Q_n = I^{\otimes n}$. We have:

$$(Q_n^\dagger Q_n)_{jk} = \sum_{\vec{\ell} \in \{0,1\}^n} (Q_n^\dagger)_{j\ell} (Q_n)_{\ell k} = \frac{1}{2^n} \sum_{\vec{\ell} \in \{0,1\}^n} \omega_n^{-j\ell} \omega_n^{\ell k} = \frac{1}{2^n} \sum_{\vec{\ell} \in \{0,1\}^n} \omega_n^{\ell(k-j)}.$$

This last expression is 1 if $j = k$ (because all terms in the summation are equal to 1, and there are 2^n of them), and it is equal to 0 otherwise, because of the formula for a geometric series and using again the fact that $\omega_n^{2^n} = 1$:

$$\frac{1}{2^n} \sum_{\vec{\ell} \in \{0,1\}^n} (\omega_n^{k-j})^\ell = \frac{1}{2^n} \sum_{\ell=0}^{2^n-1} (\omega_n^{k-j})^\ell = \frac{1}{2^n} \frac{1 - \omega_n^{2^n(k-j)}}{1 - \omega_n^{k-j}} = 0.$$

Thus, $(Q_n^\dagger Q_n)_{jk} = 1$ if $j = k$ and 0 otherwise, implying that $(Q_n^\dagger Q_n)_{jk} = I^{\otimes n}$, i.e., it is the identity matrix of size $2^n \times 2^n$. This confirms that Q_n is unitary, so there may exist an efficient quantum circuit that implements it. We describe such a circuit in the next section.

3.1.1 A useful way of expressing the QFT

To construct a circuit that implements the QFT and therefore the matrix Q_n , we first show that the image of a basis state after applying the QFT is a product state, implying that it can be decomposed as a tensor product of smaller-dimensional quantum states. The expression for the decomposition leads to a circuit construction. We make use of the following fact.

Remark 3.2. *The exponential $e^{2\pi i j/2^n}$ can always be expressed in terms of $j \bmod 2^n$: $e^{2\pi i}$ is equal to 1, therefore any integer multiple of $2\pi i$ in the exponent can be neglected.*

To express the QFT as a tensor product, we write the definition of $Q_n|\vec{k}\rangle$, and then split the

corresponding sum into basis states ending with 0 and basis states ending with 1:

$$\begin{aligned}
 Q_n|\vec{k}\rangle &= \frac{1}{\sqrt{2^n}} \sum_{\vec{j} \in \{0,1\}^n} e^{2\pi i j k / 2^n} |\vec{j}\rangle \\
 &= \frac{1}{\sqrt{2^n}} \sum_{\vec{j} \in \{0,1\}^{n-1}} e^{2\pi i (2j) k / 2^n} |\vec{j}0\rangle + \frac{1}{\sqrt{2^n}} \sum_{\vec{j} \in \{0,1\}^{n-1}} e^{2\pi i (2j+1) k / 2^n} |\vec{j}1\rangle \\
 &= \frac{1}{\sqrt{2^n}} \sum_{\vec{j} \in \{0,1\}^{n-1}} e^{2\pi i j k / 2^{n-1}} |\vec{j}\rangle \otimes |0\rangle + \frac{e^{2\pi i k / 2^n}}{\sqrt{2^n}} \sum_{\vec{j} \in \{0,1\}^{n-1}} e^{2\pi i j k / 2^{n-1}} |\vec{j}\rangle \otimes |1\rangle \\
 &= \left(\frac{1}{\sqrt{2^{n-1}}} \sum_{\vec{j} \in \{0,1\}^{n-1}} e^{2\pi i j k / 2^{n-1}} |\vec{j}\rangle \right) \otimes \frac{1}{\sqrt{2}} (|0\rangle + e^{2\pi i k / 2^n} |1\rangle) \\
 &= \left(Q_{n-1} |\vec{k}_2 \vec{k}_3 \dots \vec{k}_n\rangle \right) \otimes \frac{1}{\sqrt{2}} (|0\rangle + e^{2\pi i k / 2^n} |1\rangle).
 \end{aligned}$$

In the expression above, Q_{n-1} is the $2^{n-1} \times 2^{n-1}$ unitary representing the QFT on $n-1$ qubits (consistent with Def. 3.1), and $|\vec{k}_2 \vec{k}_3 \dots \vec{k}_n\rangle$ is the basis state corresponding to dropping the first (most significant) digit of \vec{k} . For the last equality, we used the fact that:

$$\frac{1}{\sqrt{2^{n-1}}} \sum_{\vec{j} \in \{0,1\}^{n-1}} e^{2\pi i j k / 2^{n-1}} |\vec{j}\rangle = Q_{n-1} |\vec{k}_2 \vec{k}_3 \dots \vec{k}_n\rangle$$

because the value of the summation does not depend on \vec{k}_1 , the first digit of \vec{k} (if $\vec{k}_1 = 0$ we obtain $Q_{n-1} |\vec{k}_2 \vec{k}_3 \dots \vec{k}_n\rangle$ directly, if $\vec{k}_1 = 1$ — corresponding to adding 2^{n-1} to the value of the integer k — we would simply add $2\pi i j$ to the exponent, which has no effect on the entire expression because $e^{2\pi i j} = 1$ for integer j). Thus, we have expressed the n -qubit transformation $Q_n|\vec{k}\rangle$ recursively in terms of the $(n-1)$ -qubit transformation Q_{n-1} acting on the last $n-1$ bits of $|\vec{k}\rangle$. We can further simplify and better understand this expression using a little additional notation, which is the natural extension of the notation for decimal fractions to binary strings.

Definition 3.3 (Binary fraction). *For any integer $q > 0$ and binary string $\vec{j} \in \{0,1\}^q$, we denote by $0.\vec{j}$ the fractional number defined as:*

$$0.\vec{j} := \sum_{k=1}^q \frac{\vec{j}_k}{2^k} = \frac{j}{2^q}.$$

Example 3.4. *With this notation, $0.011 = 0 \cdot \frac{1}{2} + 1 \cdot \frac{1}{4} + 1 \cdot \frac{1}{8} = \frac{3}{8}$.*

Substituting all terms of the recursion from n down to 1, and simplifying integer powers of $e^{2\pi i}$, we then obtain the following equation, that uses different “shifts” of the binary point (separating the integer from the fractional part) or the notation for binary fractions introduced in Def. 3.3:

$$\begin{aligned}
 Q|\vec{k}\rangle &= \frac{1}{\sqrt{2}} (|0\rangle + e^{2\pi i k / 2} |1\rangle) \otimes \frac{1}{\sqrt{2}} (|0\rangle + e^{2\pi i k / 4} |1\rangle) \otimes \\
 &\quad \frac{1}{\sqrt{2}} (|0\rangle + e^{2\pi i k / 8} |1\rangle) \otimes \dots \otimes \frac{1}{\sqrt{2}} (|0\rangle + e^{2\pi i k / 2^n} |1\rangle) \\
 &= \frac{1}{\sqrt{2}} (|0\rangle + e^{2\pi i 0.\vec{k}_n} |1\rangle) \otimes \frac{1}{\sqrt{2}} (|0\rangle + e^{2\pi i 0.\vec{k}_{n-1} \vec{k}_n} |1\rangle) \otimes \\
 &\quad \frac{1}{\sqrt{2}} (|0\rangle + e^{2\pi i 0.\vec{k}_{n-2} \vec{k}_{n-1} \vec{k}_n} |1\rangle) \otimes \dots \otimes \frac{1}{\sqrt{2}} (|0\rangle + e^{2\pi i 0.\vec{k}} |1\rangle).
 \end{aligned} \tag{3.3}$$

Eq. (3.3) shows that the QFT maps $|\vec{k}\rangle$ to a product state, enabling the recursive definition, and gives a precise description of the state of each qubit in the product state.

3.1.2 Implementation of the QFT

We have established that the QFT of a basis state is a product state, and this helps in the construction of a circuit that implements it. We now describe this circuit, one qubit at a time. We first discuss the construction of the least-significant qubit $\frac{1}{\sqrt{2}}(|0\rangle + e^{2\pi i 0.\vec{k}}|1\rangle)$; the others follow similarly. Note that the expression for the least-significant qubit can be rewritten in the following way, by definition of $0.\vec{k}$:

$$\frac{1}{\sqrt{2}}(|0\rangle + e^{2\pi i 0.\vec{k}}|1\rangle) = \frac{1}{\sqrt{2}}(|0\rangle + e^{2\pi i 0.\vec{k}_1} e^{2\pi i 0.0\vec{k}_2} \dots e^{2\pi i 0.00\dots\vec{k}_n}|1\rangle)$$

Each exponential $e^{2\pi i 0.\vec{k}_1}, e^{2\pi i 0.0\vec{k}_2}, \dots$ applies a phase shift of a certain magnitude to $|1\rangle$ if the qubit corresponding to $\vec{k}_1, \vec{k}_2, \dots$ is $|1\rangle$, and acts as the identity otherwise. Therefore, these operations can be implemented as controlled phase shifts. Let us define the following gate.

Definition 3.5 (Phase shift gate). *The phase shift gate $P(\theta)$ is defined as the matrix:*

$$P(\theta) := \begin{pmatrix} 1 & 0 \\ 0 & e^{i\theta} \end{pmatrix}.$$

Notice that the Z gate is a particular case of the phase shift gate, setting $\theta = \pi$; see also Def. 9.37 and the surrounding discussion. The effect of the phase shift gate is to apply a phase to $|1\rangle$, while $|0\rangle$ is untouched. Because we need to apply the phase shift only if certain values of \vec{k} are 1, we use a controlled version of the $P(\theta)$ gate, easy to obtain from a basic set of operations, see Sect. 1.3.4; thus, we can efficiently implement the unitary that constructs $\frac{1}{\sqrt{2}}(|0\rangle + e^{2\pi i 0.\vec{k}}|1\rangle)$. The corresponding circuit is given in Fig. 3.1. The desired qubit state is found in the first (topmost) qubit.

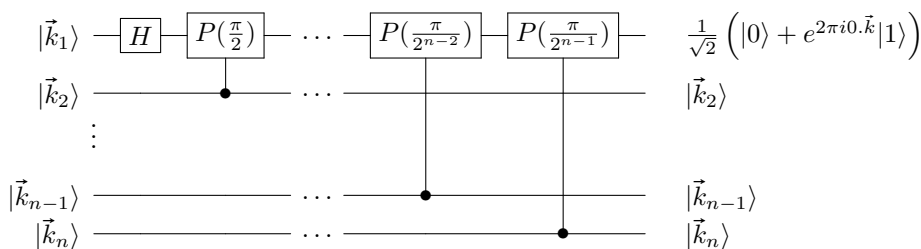


Figure 3.1: Implementation of one qubit of the QFT.

The circuit first applies the Hadamard gate H on the top qubit; we claim that this is equivalent to the transformation:

$$|\vec{k}_1\rangle \rightarrow \frac{1}{\sqrt{2}}(|0\rangle + e^{2\pi i 0.\vec{k}_1}|1\rangle).$$

Indeed, this is exactly what the Hadamard does, because $e^{2\pi i 0.\vec{k}_1} = (-1)^{\vec{k}_1}$, see Eq. (1.5). Next, it is obvious that each of the subsequent controlled gates applies one of the phase factors $e^{2\pi i 0.0\vec{k}_2}, \dots, e^{2\pi i 0.00\dots\vec{k}_n}$ to the $|1\rangle$ state in the first qubit, because these are given by the $P(\theta)$ gates controlled by qubits $2, \dots, n$. Hence, the circuit in Fig. 3.1 constructs the rightmost qubit of the QFT applied to $|\vec{k}\rangle$, i.e., the single-qubit state $\frac{1}{\sqrt{2}}(|0\rangle + e^{2\pi i 0.\vec{k}}|1\rangle)$, mapping the first qubit of the input (the one containing \vec{k}_1) to the last qubit of the expression of the QFT. We can now proceed by induction, because this qubit is in a product state with the remaining qubits, see Eq. (3.3). Thus, we recursively apply the same circuit, with its size reduced by one each time, to the qubit lines containing $\vec{k}_2 \dots \vec{k}_n$, yielding the full QFT implementation. Note that we no longer have access to \vec{k}_1 after applying Fig. 3.1, but this is not an issue: from Eq. (3.3), we can see that \vec{k}_1 only appears in the rightmost qubit on the r.h.s. of the equation. Hence, we do not need \vec{k}_1 after the the rightmost qubit of the QFT (top qubit in Fig. 3.1) is computed.

Remark 3.6. Because each application of the circuit in Fig. 3.1 outputs the last qubit of the desired output in the first position of the output lines, at the end of the computation we should swap all qubits to restore the initial order. Alternatively, we do not need to swap as long as we keep track of the position of each qubit and consequently adjust all subsequent operations in the circuit, including measurements. (If the QFT is the last operation of a circuit, followed by a measurement of all qubits, we can simply rearrange the classical bits after measurement.)

Putting it all together, we obtain the circuit depicted in Fig. 3.2. This circuit contains $\mathcal{O}(n^2)$ one and two-qubit gates. Rather than use oracle complexity to determine the runtime of an algorithm — which is useful for information-theoretical purposes — for this algorithm there is no natural query concept (i.e., no function is being queried), and it makes more sense to use gate complexity, in which we assess the performance of an algorithm by looking at how many elementary gates it uses, see Rem. 2.5. We consider all single-qubit and two-qubit gates as elementary, because they can all be constructed with a constant number of basic gates (if the precision is fixed), i.e., gates from a minimal, universal set of gates. (Technically, to keep the same accuracy of the entire implementation as n grows, we need to increase the precision with which each gate is approximated with basic gates, but remember that the cost for doing so is only polylogarithmically-large in the precision, see Thm. 1.43.) Thus, the QFT uses a number of basic gates polynomial (in fact, quadratic) in n ; this is an exponential improvement over the classical fast Fourier transform, which uses $\mathcal{O}(n^{2^n})$ basic operations and therefore time.

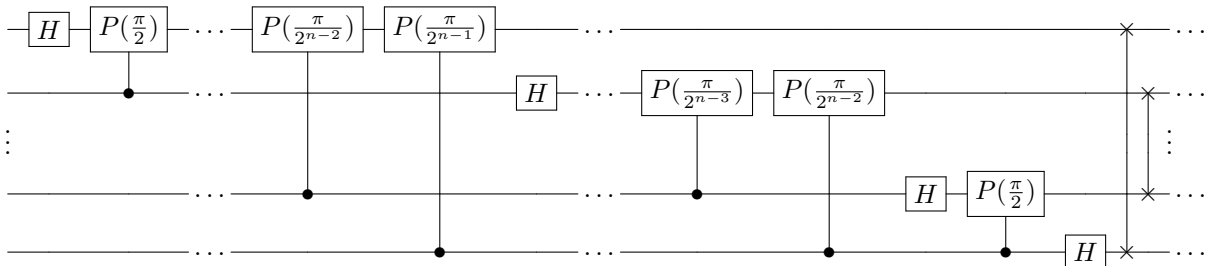


Figure 3.2: Implementation of the QFT.

Example 3.7. We show a full example of the QFT circuit on three qubits. It is given in Fig. 3.3. The gates $P(\frac{\pi}{2})$ and $P(\frac{\pi}{4})$ are commonly called S and T , respectively. We have seen the T gate

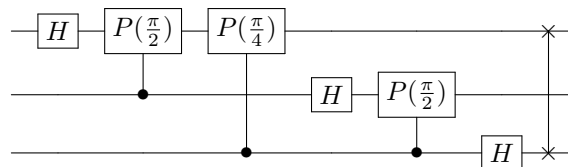


Figure 3.3: Example of the QFT on three qubits.

in Thm. 1.43. Using these new names and substituting the SWAP in terms of CX, we obtain the circuit in Fig. 3.4. As an exercise, perhaps aided by computer code, we could carry out

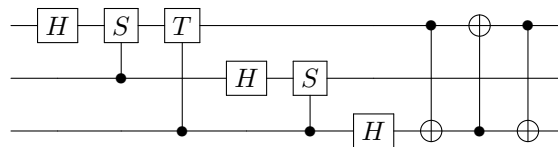


Figure 3.4: Example of the QFT on three qubits, with the SWAP gate decomposed into basic operations.

the calculations to compute the unitary matrix corresponding to this circuit, and verify that it implements the matrix Q_3 .

3.2 Phase estimation

The QFT is a crucial building block of many useful quantum subroutines, and its application leads almost directly to another crucial building block for quantum algorithms, called *phase estimation* (quantum phase estimation, QPE). Under an appropriate input model, phase estimation gives an exponential speedup with respect to classical algorithms for the same problem.

The purpose of phase estimation is to determine the eigenvalue of a given eigenstate of a given unitary. Let U be a unitary on n qubits that we can efficiently implement. Let $|\psi\rangle$ be an eigenstate (Def. 2.3) of U . Because U is unitary, its eigenvalues have modulus one. Hence, we can write:

$$U|\psi\rangle = e^{2\pi i\varphi}|\psi\rangle,$$

where $\varphi \in [0, 1)$. Phase estimation solves the following problem: given $\epsilon > 0$, quantum circuits for a controlled version of U^{2^k} for any $k \leq \lceil \log \frac{1}{\epsilon} \rceil$, and a circuit to construct the state $|\psi\rangle$ such that $U|\psi\rangle = e^{2\pi i\varphi}|\psi\rangle$, determine $\tilde{\varphi}$ such that $\min\{|\varphi - \tilde{\varphi}|, 1 - |\varphi - \tilde{\varphi}|\} \leq \epsilon$.

Remark 3.8. *The distance between φ and $\tilde{\varphi}$ is intended with period 1, i.e., 0.99 is close to 0.01: all angles in the exponential can be interpreted modulo 2π , and the angle $2\pi(0.99)$ is close to the angle $2\pi(0.01)$. This is why we take $\min\{|\varphi - \tilde{\varphi}|, 1 - |\varphi - \tilde{\varphi}|\}$: if $\varphi = 0.99$ and $\tilde{\varphi} = 0.01$, the expression $\min\{|\varphi - \tilde{\varphi}|, 1 - |\varphi - \tilde{\varphi}|\}$ evaluates to 0.02.*

Note that classically, φ can be computed by carrying out the multiplication $U|\psi\rangle$, but this takes time $\mathcal{O}(4^n)$ in general because U is a $2^n \times 2^n$ matrix.

3.2.1 Main idea for quantum phase estimation

Let $m = \lceil \log \frac{1}{\epsilon} \rceil$: if we obtain a representation $\tilde{\varphi}$ of φ with m correct binary digits, then $\tilde{\varphi}$ is no more than ϵ away from φ . For now, we make the simplifying assumption that φ is exactly representable on m bits. More formally, we assume that there exists $\vec{p} \in \{0, 1\}^m$ such that $\varphi = p/2^m = 0.\vec{p}$. Thus, to obtain a representation of φ with m correct digits we need to output \vec{p} . (If the assumption is not verified, i.e., φ requires more than m digits to be written in binary, then we would like to output the closest representation of φ on m bits; we discuss this case more precisely in Sect. 3.2.2.)

We exploit the fact that quantum computation is reversible: we would like to produce the state $|\vec{p}\rangle$, because it encodes the desired answer, so we study how to obtain a state that can be transformed into $|\vec{p}\rangle$. In particular, we study the Fourier state obtained from $|\vec{p}\rangle$. The image of the basis state $|\vec{p}\rangle$ under the QFT on m qubits is:

$$Q_m|\vec{p}\rangle = \frac{1}{\sqrt{2^m}} \sum_{\vec{j} \in \{0,1\}^m} e^{2\pi i j p / 2^m} |\vec{j}\rangle = \frac{1}{\sqrt{2^m}} \sum_{\vec{j} \in \{0,1\}^m} e^{2\pi i j 0.\vec{p}} |\vec{j}\rangle.$$

Using the definition of $0.\vec{p}$, relying on the same argument that we used in Eq. (3.3), this expression can be rewritten as:

$$\begin{aligned} Q_m|\vec{p}\rangle &= \frac{1}{\sqrt{2}} (|0\rangle + e^{2\pi i 0.\vec{p}_m} |1\rangle) \otimes \frac{1}{\sqrt{2}} (|0\rangle + e^{2\pi i 0.\vec{p}_{m-1}\vec{p}_m} |1\rangle) \otimes \cdots \otimes \frac{1}{\sqrt{2}} (|0\rangle + e^{2\pi i 0.\vec{p}} |1\rangle) \\ &= \frac{1}{\sqrt{2}} (|0\rangle + e^{2\pi i p/2} |1\rangle) \otimes \frac{1}{\sqrt{2}} (|0\rangle + e^{2\pi i p/4} |1\rangle) \otimes \cdots \otimes \frac{1}{\sqrt{2}} (|0\rangle + e^{2\pi i p/2^m} |1\rangle). \end{aligned} \quad (3.4)$$

Note that $e^{2\pi i 0.\vec{p}_m} = e^{2\pi i p/2} = e^{2\pi i 2^{m-1}\varphi}$, because any integer multiple of $2\pi i$ in the exponent cancels out, and similarly, each qubit can be expressed using $e^{2\pi i\varphi}$ with φ multiplied by some power of 2. This gives the following equivalent expression for the QFT applied to $|\vec{p}\rangle$:

$$Q_m|\vec{p}\rangle = \frac{1}{\sqrt{2}} (|0\rangle + e^{2\pi i 2^{m-1}\varphi} |1\rangle) \otimes \frac{1}{\sqrt{2}} (|0\rangle + e^{2\pi i 2^{m-2}\varphi} |1\rangle) \otimes \cdots \otimes \frac{1}{\sqrt{2}} (|0\rangle + e^{2\pi i 2^0\varphi} |1\rangle). \quad (3.5)$$

Then, if we could construct this state, the inverse QFT Q_m^\dagger would recover \vec{p} , allowing us to determine φ . To prepare the state in Eq. (3.5), we must be able to construct a quantum state

that has several phase factors of the form $e^{2\pi i 2^k \varphi}$. We can obtain any such phase factor with phase kickback and repeated applications of U , exploiting the fact that $|\psi\rangle$ is an eigenstate with eigenvalue $e^{2\pi i \varphi}$. Indeed, we have:

$$U^{2^k} |\psi\rangle = (e^{2\pi i \varphi})^{2^k} |\psi\rangle = e^{2\pi i 2^k \varphi} |\psi\rangle.$$

Thus, we start with the state $\frac{1}{\sqrt{2^m}} (|0\rangle + |1\rangle)^{\otimes m} \otimes |\psi\rangle$, that can be constructed using m Hadamard gates applied to $|\vec{0}\rangle$ and the circuit to prepare $|\psi\rangle$, which is given as input by assumption. Next, we apply a controlled version of U to the qubit lines corresponding to $|\psi\rangle$, controlled by the m -th qubit; we follow up with an application of U^{2^1} to the qubit lines corresponding to $|\psi\rangle$, controlled by the $(m-1)$ -th qubit; and so on, applying the unitary U^{2^j} controlled by qubit $m-j$ for $j = 0, \dots, m-1$. This leads to the circuit given in Fig. 3.5.

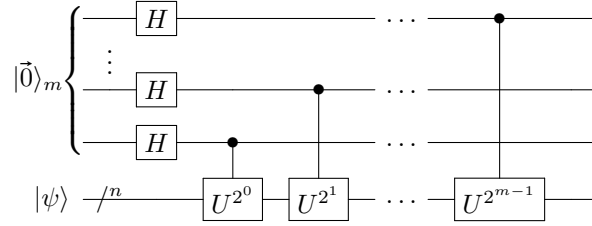


Figure 3.5: State preparation for the quantum phase estimation.

To understand Fig. 3.5, we examine the effect of applying a Hadamard on qubit $m-j$, followed by controlled- U^{2^j} , where qubit $m-j$ is the control, and U^{2^j} acts on $|\psi\rangle$ when the control is active (i.e., $|1\rangle$). We have:

$$CU^{2^j}(H \otimes I)|0\rangle \otimes |\psi\rangle = CU^{2^j} \left(\frac{1}{\sqrt{2}} (|0\rangle + |1\rangle) \otimes |\psi\rangle \right) = \frac{1}{\sqrt{2}} (|0\rangle \otimes |\psi\rangle + |1\rangle \otimes e^{2\pi i 2^j \varphi} |\psi\rangle).$$

This is exactly the state that we want to construct for qubit $m-j$ in Eq. (3.5). It is also a product state, because it can be expressed as the tensor product:

$$\frac{1}{\sqrt{2}} (|0\rangle + e^{2\pi i 2^j \varphi} |1\rangle) \otimes |\psi\rangle$$

By induction, starting from qubit m down to 1, it is easy to prove that the circuit in Fig. 3.5 leaves the first m qubit lines in a product state, and produces Eq. (3.5). Thus, we can construct the full quantum phase estimation circuit as given in Fig. 3.6. The correctness of this construction

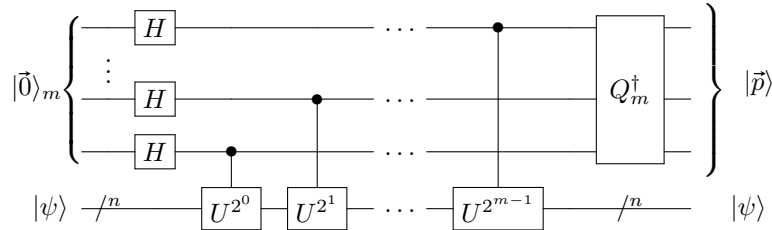


Figure 3.6: Quantum phase estimation circuit on m qubits.

is ensured by the above discussion: the first part of the circuit, i.e., the circuit in Fig. 3.5, outputs the state $\frac{1}{\sqrt{2}} (|0\rangle + e^{2\pi i 2^{m-1} \varphi} |1\rangle) \otimes \frac{1}{\sqrt{2}} (|0\rangle + e^{2\pi i 2^{m-2} \varphi} |1\rangle) \otimes \dots \otimes \frac{1}{\sqrt{2}} (|0\rangle + e^{2\pi i 2^0 \varphi} |1\rangle) \otimes |\psi\rangle$ as in Eq. (3.5). Then the inverse QFT, which is exactly the inverse of the transformation in Eq. (3.4), produces the state $|\vec{p}\rangle$ in the top m output lines.

3.2.2 General phase estimation algorithm

The previous section shows an implementation of the QPE under the assumption that φ is exactly representable on m bits, but this is a restrictive assumption that may not hold in practice. More importantly, a priori we have no way of verifying whether the assumption holds unless we know φ in the first place, which would defeat the purpose of the algorithm. Fortunately it is easy to relax this assumption. Recall that the QFT is a continuous transformation, because it is a linear map on a finite-dimensional vector space. The forward transformation of the QFT is given in Eq. (3.4), mapping $|\vec{p}\rangle$ to its image state. By continuity, if we apply the inverse QFT to a state that is close to $Q_m|\vec{p}\rangle = \frac{1}{\sqrt{2}}(|0\rangle + e^{2\pi i 0 \cdot \vec{p}_m}|1\rangle) \otimes \frac{1}{\sqrt{2}}(|0\rangle + e^{2\pi i 0 \cdot \vec{p}_{m-1}}|1\rangle) \otimes \dots \otimes \frac{1}{\sqrt{2}}(|0\rangle + e^{2\pi i 0 \cdot \vec{p}_1}|1\rangle)$, we obtain a state that is close to $|\vec{p}\rangle$. In particular, while $2^m\varphi$ may not be an integer, it is close to some m -bit-representable integer, hence applying the inverse QFT yields the binary string corresponding to that integer with high probability. This result is formalized next, by stating that if we want to obtain an accurate q -digit representation of the phase φ , we need to run the quantum phase estimation using slightly more than q qubits; this suffices to ensure that the first q digits of the output are correct with good probability.

Theorem 3.9 (Phase estimation; based on Sect. 5.2 in [Nielsen and Chuang, 2002]). *When applying phase estimation, let \vec{p} be the output of the procedure (corresponding to estimating the eigenvalue as $e^{2\pi i 0 \cdot \vec{p}}$) when applied to an eigenstate with eigenvalue $e^{2\pi i \varphi}$, i.e., with phase $2\pi i \varphi$. If we use $q + \lceil \log(2 + \frac{1}{2\delta}) \rceil$ qubits of precision, i.e., execute the circuit in Fig. 3.6 setting $m = q + \lceil \log(2 + \frac{1}{2\delta}) \rceil$, then the first q bits of \vec{p} are accurate with probability at least $1 - \delta$, i.e., $\Pr(\min\{|\varphi - 0.\vec{p}|, 1 - |\varphi - \vec{p}|\} < 2^{-q}) > 1 - \delta$.*

The proof is technical, so we skip it; a detailed proof for the above statement can be found in [Nielsen and Chuang, 2002]. However, there is a precise characterization of the probability distribution of phase estimation that is sometimes very useful in the analysis of certain quantum algorithms, and it is worth mentioning. For the most intuitive version of this result (including the edge case where the phase is representable exactly with the number of qubits used), it is helpful to rely on the sinc function, used in signal processing and defined below.

Definition 3.10 (Normalized sinc function). *The normalized sinc function is defined as $\text{sinc}(x) := \frac{\sin(\pi x)}{\pi x}$ for $x \neq 0$, and $\text{sinc}(x) := 1 = \lim_{y \rightarrow 0} \frac{\sin(\pi y)}{\pi y}$ for $x = 0$.*

Proposition 3.11 (Lem. 7.1.2 in [Kaye et al., 2007]). *Suppose the phase estimation circuit (Fig. 3.6) is applied to an eigenstate $|\psi\rangle$ with phase φ . Let X be the random variable describing the measurement outcomes of the output register (top m qubit lines). Then X satisfies:*

$$\Pr(X = \vec{k}) = \frac{\text{sinc}^2\left(2^m(\varphi - 0.\vec{k})\right)}{\text{sinc}^2(\varphi - 0.\vec{k})}.$$

For a proof of this result, see [Kaye et al., 2007, Sect. 7.1.1], [Brassard et al., 2002, Lem. 10]. Using Prop. 3.11, one can prove a somewhat simpler (and easier to remember) version of Thm. 3.9 to characterize the probability of success of phase estimation.

Theorem 3.12 (Phase estimation, alternative version; Thm. 7.1.5 in [Kaye et al., 2007]). *Let m be fixed, and suppose we apply quantum phase estimation to an eigenstate $|\psi\rangle$ with eigenvalue $e^{2\pi i \varphi}$. Suppose further that φ satisfies $\frac{k}{2^m} \leq \varphi \leq \frac{k+1}{2^m}$ for $k \in \{0, \dots, 2^m - 1\}$. Then the phase estimation circuit (Fig. 3.6) outputs k or $k+1$ (expressed in binary) as measurement outcomes with probability at least $\frac{8}{\pi^2} \approx 0.81$, corresponding to estimating the eigenvalue as $e^{2\pi i k/2^m}$ or $e^{2\pi i (k+1)/2^m}$.*

Note that in Thm. 3.12, the integers k and $k+1$ are the two closest representations of the exact phase φ using m digits of precision (the denominator 2^m is fixed, we are aiming to determine a fraction), and they both lead to error $\leq 2^{-m}$. The result states that we obtain one of these two integers with high probability, ≈ 0.81 . The bound for the probability of obtaining the closest integer, rather than one of the two closest integers, is $\frac{4}{\pi^2} \approx 0.41$, see [Kaye et al., 2007] for details.

Gate complexity. The gate complexity of the QPE algorithm is $\mathcal{O}(m^2)$, which is the gate complexity of the inverse QFT, plus the cost of applying all the controlled unitaries U^{2^j} for $j = 0, \dots, m-1$. If each gate is compiled down to basic gates from a universal set, the total gate complexity increases slightly to $\tilde{\mathcal{O}}(n^2)$ for arbitrarily high (but constant) precision.

Remark 3.13. *Constructing U^{2^j} may not be easy: a trivial construction that applies U repeatedly a total of 2^j times incurs an exponential cost in m , in general. Sometimes this is acceptable: usually we want to estimate the phase with error at most ϵ , and we choose $m = \mathcal{O}(\log \frac{1}{\epsilon})$, so $2^m = \mathcal{O}(\frac{1}{\epsilon})$. In other words, even if the number of calls to U (query complexity) depends exponentially on the number of qubits, the number of qubits is usually polylogarithmic in one of the input parameters, i.e., the desired precision. This yields a number of applications of U that is polynomial in ϵ : $\mathcal{O}(\frac{1}{\epsilon} \log \frac{1}{\delta})$ for probability of failure at most δ . Other times the exponential cost in m may not be acceptable. Unfortunately, in general we cannot “fast forward” the implementation of U^{2^j} using a polynomial number operations. However, for some specific matrices U it may be possible to construct U^{2^j} more efficiently, avoiding exponential costs. One situation where this is known to be the case is the modular exponentiation function used in Shor’s algorithm [Shor, 1997], in which U applies the function $f(x) = a^x \pmod{2^n}$. Because this is the power function, it can be implemented efficiently using the repeated squaring algorithm, i.e., computing a^2, a^4, a^8, \dots simply by squaring the result each time. This implies that constructing U^{2^j} is much less expensive than expected. Another situation where this occurs is discussed in Sect. 5.1.1, in the context of the gradient algorithm; there, we exploit a binary representation of a certain function and phase kickback to efficiently construct U^{2^j} .*

Inexact eigenstates. We conclude our study of the QPE by analyzing the effect of applying QPE to a state that is not an eigenstate of U . Let $|\psi_j\rangle, j = 0, \dots, 2^n-1$ be an orthonormal eigenbasis for U with corresponding eigenvalues $e^{2\pi i \varphi_j}$. Then there exist coefficients α_j such that:

$$|\psi\rangle = \sum_{j=0}^{2^n-1} \alpha_j |\psi_j\rangle,$$

with $\sum_{j=0}^{2^n-1} |\alpha_j|^2 = 1$ due to the normalization condition. Because QPE maps $|\vec{0}\rangle_m |\psi_j\rangle \rightarrow |\vec{p}^{(j)}\rangle |\psi_j\rangle$ with probability at least $1 - \delta$, where $\vec{p}^{(j)}$ is some integer representation of the (potentially fractional) phase φ_j , by linearity it maps:

$$|\vec{0}\rangle_m \otimes \left(\sum_{j=0}^{2^n-1} \alpha_j |\psi_j\rangle \right) \longrightarrow \sum_{j=0}^{2^n-1} \alpha_j \left(|\vec{p}^{(j)}\rangle \otimes |\psi_j\rangle \right)$$

with probability at least $1 - \delta$. Hence, if we perform a measurement of the first register, with probability $1 - \delta$ we are able to obtain the phase of one of the eigenvalues as the output of the circuit; which eigenvalue is produced depends on the overlap $|\langle \psi_j | \psi \rangle| = |\alpha_j|$. If we want to obtain the phase of a specific eigenvalue φ_j , we must be able to produce a state with large $|\alpha_j|^2$. We formalize this as follows.

Proposition 3.14. *Suppose we want to estimate the eigenvalue $e^{2\pi i \varphi^*}$ of the eigenstate $|\psi^*\rangle$ of a unitary U , but we only have the ability to prepare a state $|\xi\rangle$ that may not coincide with $|\psi^*\rangle$. Then, applying phase estimation with precision ϵ and probability of success $\geq 1 - \delta$, gives us a binary description \vec{p}^* of φ^* with precision ϵ with probability at least $(1 - \delta)|\langle \xi | \psi^* \rangle|^2$.*

Proof. Using an eigenbasis of U to express $|\xi\rangle$, just as in the discussion before the proposition statement, we have:

$$|\xi\rangle = \sum_{j=0}^{2^n-1} \alpha_j |\psi_j\rangle.$$

Suppose the desired eigenstate is $|\psi^*\rangle = |\psi_h\rangle$. By linearity, the action of the QPE is:

$$\text{QPE}(|\vec{0}\rangle \otimes |\xi\rangle) = \text{QPE}\left(|\vec{0}\rangle \otimes \sum_{j=0}^{2^n-1} \alpha_j |\psi_j\rangle\right) = \sum_{j=0}^{2^n-1} \alpha_j (|\vec{p}^{(j)}\rangle \otimes |\psi_j\rangle),$$

and this operation is successful with probability at least $1 - \delta$. It follows that the probability of obtaining $\vec{p}^{(h)} = \vec{p}^*$ is at least $|\alpha_h|^2(1 - \delta)$. Then, note that $\alpha_h = \langle \xi | \psi^* \rangle$. This concludes the proof. \square

3.3 Iterative phase estimation

Rather than performing phase estimation in a single pass, i.e., obtaining at the same time the entire bit description of the phase with a given accuracy, it is possible to break the procedure down to simpler steps, obtaining one bit of the phase at a time. This line of work was initially developed by Kitaev, and a detailed description can be found in [Kitaev et al., 2002]. Iterative phase estimation allows splitting the phase estimation circuit into several smaller circuits, which are more likely to be executable by a quantum computing device with limited capabilities. Although the query complexity (i.e., number of calls to the unitary whose eigenvalue is being estimated) for the iterative phase estimation algorithm is not better than the standard algorithm described in Sect. 3.2, its analysis is instructive for at least two reasons. First, it gives an avenue to obtain a different tradeoff regarding the requirement of computational resources, i.e., number of qubits and number of gates. Second, it uses an idea that we have not seen so far in this set of lecture notes, and that has proven very successful in a variety of situations: start by obtaining a coarse approximation of the answer, and then, based on that approximation, define a new problem that iteratively improves over the current estimate. In a different context and with different benefits and costs, this idea can be powerful also for linear algebra and optimization; we discuss some approaches based on a related scheme in Sect.s 7.1.6 and 7.3.

Let us formally state the goal of the algorithm described in this section. It is exactly the same as in Sect. 3.2: given $\epsilon > 0$, quantum circuits for a controlled version of U^{2^k} for any $k \leq \lceil \log \frac{1}{\epsilon} \rceil$, and a circuit to construct the state $|\psi\rangle$ such that $U|\psi\rangle = e^{2\pi i \varphi} |\psi\rangle$, determine a binary string \vec{p} with the property that $\Pr(\min\{|\varphi - 0.\vec{p}|, 1 - |\varphi - 0.\vec{p}|\} \leq \epsilon) > 1 - \delta$ for a given probability δ . Let q be the number of correct binary digits of \vec{p} that we aim to obtain, similarly to the notation used in the statement of Thm. 3.9. By choosing $q = \lceil \log \frac{1}{\epsilon} \rceil$, we ensure that obtaining q accurate digits yields error $< 2^{-q} \leq \epsilon$. Thus, we aim to obtain an estimate of φ with q correct digits. (Note that in Sect. 3.2 we run QPE using an m -qubit register, but not all of those bits may be accurate in the output, see Thm.s 3.9 and 3.12.)

3.3.1 Algorithm for constant precision

The basic circuit executed by the algorithm is the one indicated in Fig. 3.7, which has two parameters: the integer k , and the angle θ .

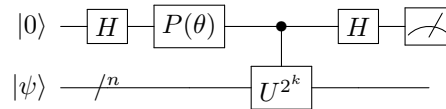


Figure 3.7: Iterative phase estimation circuit.

The state at the end of this circuit is given by:

$$\left(\frac{1 + e^{2\pi i 2^k \varphi + \theta}}{2} |0\rangle + \frac{1 - e^{2\pi i 2^k \varphi + \theta}}{2} |1\rangle \right) \otimes |\psi\rangle,$$

as can be easily verified by noticing that the controlled- U^k gate introduces a phase kickback of $e^{2\pi i 2^k \varphi}$, and the $P(\theta)$ gate adds an extra phase θ (see Def. 3.5). With a slight abuse of notation, in

in this section we use the notation of conditional probabilities to indicate the value of the parameter θ , e.g., we write $\Pr(\mathcal{Q}_1 = 0|\theta = 0)$ to denote the probability of measuring 0 on the first qubit given that the value of θ is 0 (θ is an algorithmic parameter, not a random variable). With relatively straightforward calculations, it can be verified that the measurement in the circuit in Fig. 3.7 yields the following outcome probabilities:

$$\begin{aligned}\Pr(\mathcal{Q}_1 = 0|\theta = 0) &= \left| \frac{1 + e^{2\pi i 2^k \varphi}}{2} \right|^2 = \left| \frac{1 + \cos 2\pi 2^k \varphi + i \sin 2\pi 2^k \varphi}{2} \right|^2 \\ &= \frac{1 + \cos^2 2\pi 2^k \varphi + 2 \cos 2\pi 2^k \varphi + \sin^2 2\pi 2^k \varphi}{4} \\ &= \frac{2 + 2 \cos 2\pi 2^k \varphi}{4} = \frac{1 + \cos 2\pi 2^k \varphi}{2}, \\ \Pr(\mathcal{Q}_1 = 1|\theta = \frac{\pi}{2}) &= \left| \frac{1 - e^{2\pi i (2^k \varphi + \frac{1}{4})}}{2} \right|^2 = \left| \frac{1 - i \cos 2\pi 2^k \varphi + \sin 2\pi 2^k \varphi}{2} \right|^2 \\ &= \frac{1 + \cos^2 2\pi 2^k \varphi + 2 \sin 2\pi 2^k \varphi + \sin^2 2\pi 2^k \varphi}{4} \\ &= \frac{2 + 2 \sin 2\pi 2^k \varphi}{4} = \frac{1 + \sin 2\pi 2^k \varphi}{2}.\end{aligned}$$

Using $\theta = 0$ and performing the observation multiple times, we can obtain an estimate of $\cos 2\pi(2^k \varphi) = 2\Pr(\mathcal{Q}_1 = 0|\theta = 0) - 1$ with a prescribed level of confidence; the number of samples is discussed subsequently in this section. Notice that estimating $\cos 2\pi(2^k \varphi)$ does not give us full knowledge of $2^k \varphi$, due to the symmetry of the cosine. To fully estimate $2^k \varphi$ we should also determine information on the sine of the angle. This is straightforward to do, because using $\theta = \frac{\pi}{2}$, as indicated above, allows us to determine $\sin 2\pi(2^k \varphi) = 2\Pr(\mathcal{Q}_1 = 1|\theta = \frac{\pi}{2}) - 1$.

Because we can estimate $\cos 2\pi(2^k \varphi), \sin 2\pi(2^k \varphi)$ with the circuit in Fig. 3.7, we can estimate $2^k \varphi$, thereby solving the goal of phase estimation at least partially. We now examine the question of how many samples from the circuit are necessary to estimate $\cos 2\pi(2^k \varphi), \sin 2\pi(2^k \varphi)$ up to a certain precision: this tells us how many calls to U^{2^k} are necessary, which we want to know to assess the query complexity of this phase estimation algorithm. Recall that the values are estimated by observing frequencies of a certain outcome, i.e., the cosine is estimated from $\Pr(\mathcal{Q}_1 = 0|\theta = 0)$, while the sine is estimated from $\Pr(\mathcal{Q}_1 = 1|\theta = \frac{\pi}{2})$. Let us discuss the estimation of the cosine, as the analysis for the sine is essentially the same. Given t samples from measuring qubit 1, the observed frequency of $\mathcal{Q}_1 = 0$ can be expressed as $\frac{1}{t} \sum_{j=1}^t X_j$, where X_j are independent Bernoulli trials with probability of success equal to $p^* = \frac{1 + \cos 2\pi 2^k \varphi}{2}$ (success is defined as the outcome that we are interested in; in this case, $\mathcal{Q}_1 = 0$). An error estimate on $\left| \frac{1}{t} \sum_{j=1}^t X_j - p^* \right|$ translates into an error estimate on $\cos 2\pi 2^k \varphi$ using the formula $p^* = \frac{1 + \cos 2\pi 2^k \varphi}{2}$. The Chernoff bound tells us that:

$$\Pr \left(\left| \frac{1}{t} \sum_{j=1}^t X_j - p^* \right| \geq \Delta \right) \leq 2e^{-2\Delta^2 t}.$$

This implies that for any fixed Δ , in order to reduce the probability of error below a certain threshold δ_c we need a number of trials $t = \mathcal{O} \left(\log \frac{1}{\delta_c} \right)$.

Remark 3.15. *For additional clarity, it may be worth emphasizing the role of the different error parameters here. We have the maximum difference Δ between the true value p^* and its estimate $\frac{1}{t} \sum_{j=1}^t X_j$, and we have the maximum probability δ_c that the estimate fails to satisfy the difference upper bound Δ . We discovered that, to ensure that $\Pr \left(\left| \frac{1}{t} \sum_{j=1}^t X_j - p^* \right| \geq \Delta \right) \leq \delta_c$, it suffices to choose the number of samples t in the order of $\log \frac{1}{\delta_c}$. Thus, if the precision Δ for the cosine estimation is fixed (as is the case in the iterative phase estimation algorithm, described below), the number of samples scales logarithmically in the reciprocal of the error probability.*

The final piece needed to determine the accuracy of the estimate for φ is to combine estimates for $\cos 2\pi 2^k \varphi$ and $\sin 2\pi 2^k \varphi$ into a single estimate for $2^k \varphi$, and assess its distance from the true value. There are many possible ways to do so; the next result gives an error bound on one of the most straightforward ways, combining sine and cosine estimates to form a “box” around the correct angle.

Proposition 3.16. *For any $0 \leq \eta \leq \frac{\pi}{2}$ and $\varphi \in [0, 2\pi]$, estimates \tilde{c}, \tilde{s} for cosine and sine of φ with errors $|\tilde{c} - \cos \varphi| \leq \frac{\sin \eta}{\sqrt{2}}$, $|\tilde{s} - \sin \varphi| \leq \frac{\sin \eta}{\sqrt{2}}$ yield a value $\tilde{\varphi}$ such that $|\tilde{\varphi} - \varphi| \leq \eta$.*

A proof is given in [van den Berg, 2020]. The result tells us that if we want an error of η for the angle estimate $\tilde{\varphi}$, we need to choose $\Delta \leq \sin \eta / \sqrt{2}$ as the maximum error for the sine and cosine estimates. So if η is fixed, Δ is also fixed. In summary, as long as we want to estimate $2^k \varphi$ up to constant precision, it is sufficient to take $\mathcal{O}\left(\log \frac{1}{\delta_c}\right)$ samples from the circuit in Fig. 3.7, where δ_c is the maximum probability of failure of the algorithm.

3.3.2 Iterative algorithm

We can now describe an iterative phase estimation algorithm that uses the single-qubit constant-precision phase estimation of Sect. 3.3.1 as a subroutine.

Recall that we aim to obtain \vec{p} such that $\Pr(\min\{|\varphi - 0.\vec{p}|, 1 - |\varphi - 0.\vec{p}|\} \leq 2^{-q}) > 1 - \delta$. Let $h = q - 2$ and let $0.\vec{p} = 0.\vec{p}_1\vec{p}_2 \dots \vec{p}_{h+2}$. The algorithm estimates the digits of \vec{p} starting from the least significant digit, \vec{p}_{h+2} , and down to \vec{p}_1 . It can be described as follows.

- Initialization: use the single-qubit estimation procedure of Sect. 3.3.1 with $k = h - 1$, maximum error probability $\delta_c = \delta/h$, and estimation error at most $\Delta = \frac{1}{16}$; round the result to the closest multiple of $\frac{1}{8}$. Because we use $k = h - 1$, we are estimating the phase of the eigenvalue $e^{2\pi i 2^{h-1} \varphi}$, and because integer multiples of 2π can be ignored, this yields the estimate $0.\vec{p}_h\vec{p}_{h+1}\vec{p}_{h+2}$ of the last three digits of \vec{p} . The maximum approximation error at this step is $< \frac{1}{8}$: an error of at most $\frac{1}{16}$ comes from the estimation of $2^{h-1} \varphi$ (because $\Delta = \frac{1}{16}$), and an additional error of at most $\frac{1}{16}$ comes from rounding the estimate to the closest multiple of $\frac{1}{8}$ (because we are using three digits after the binary point).
- Iteration step, for $j = h - 1, \dots, 1$:
 - Use the single-qubit estimation procedure of Sect. 3.3.1 with $k = j - 1$, maximum error probability $\delta_c = \delta/h$, and estimation error at most $\Delta = \frac{1}{16}$, obtaining an estimate ω_j of the angle $2^j \varphi$.
 - Set:

$$\vec{p}_j = \begin{cases} 0 & \text{if } |0.0\vec{p}_{j+1}\vec{p}_{j+2} - \omega_j| < \frac{1}{4} \\ 1 & \text{if } |0.1\vec{p}_{j+1}\vec{p}_{j+2} - \omega_j| < \frac{1}{4}. \end{cases}$$

One of these two conditions is always satisfied because otherwise the digits $\vec{p}_{j+1}, \vec{p}_{j+2}$ would have to be incorrect, but we show in Prop. 3.17 below that both are correct.

This iterative procedure yields an approximation with precision $2^{-q} = 2^{-(h+2)}$, as shown below.

Proposition 3.17. *At each step $j = h, \dots, 1$, if the angle ω_j is an approximation of $2^{j-1} \varphi$ with error at most $\frac{1}{16}$, then the approximation computed by the above algorithm satisfies:*

$$|0.\vec{p}_j \dots \vec{p}_{h+2} - 2^{j-1} \varphi| < 2^{-(h+3-j)}.$$

Proof. We show it by induction for $j = h, \dots, 1$. The base step $j = h$ is obvious from the Initialization step of the algorithm. Now suppose we are at step j . By the induction hypothesis the digits $\vec{p}_{j+1}, \vec{p}_{j+2}$ are correct (i.e., they correspond to the closest binary representation of φ), because:

$$|0.\vec{p}_{j+1}\vec{p}_{j+2} \dots \vec{p}_{h+2} - 2^j \varphi| < 2^{-(h+2-j)},$$

and there are only $h + 2 - j$ digits in total in the string, so all of them have to be correct. Because $\vec{p}_{j+1}, \vec{p}_{j+2}$ are correct, and ω_j is an approximation of $2^{j-1}\varphi$ with error at most $\frac{1}{16}$, the estimate for \vec{p}_j must be correct as well, otherwise $|0.\vec{p}_j\vec{p}_{j+1}\vec{p}_{j+2} - \omega_j| \geq \frac{1}{4}$. This implies that the total error is less than $2^{-\ell}$ where ℓ is the number of digits, i.e.,

$$|0.\vec{p}_j \dots \vec{p}_{h+2} - 2^{j-1}\varphi| < 2^{-(h+3-j)}.$$

□

Prop. 3.17 shows that the algorithm returns the desired binary string under the assumption that each intermediate angle ω_j is estimated correctly. Because each of these estimations has probability at most δ/h to fail, and there are h such estimations in total (equal to the number of steps of the algorithm), by the union bound the probability that at least one estimation fails is at most $h \frac{\delta}{h} = \delta$, so the entire algorithm is successful (i.e., no estimation fails) with probability at least $1 - \delta$. The total number of samples required by the algorithm is $\mathcal{O}(q \log \frac{q}{\delta}) = \mathcal{O}(\frac{1}{\epsilon} \log \frac{1}{\epsilon\delta})$, and the gate complexity for each step is that of implementing controlled- U^k (where the largest k is at most $q - 3 = \mathcal{O}(\log \frac{1}{\epsilon})$) plus three basic gates. A different tradeoff as compared to the full phase estimation is thus realized: we execute several smaller circuits, rather than a large circuit, at the cost of performing significantly more measurements.

3.4 Notes and further reading

The QFT is one of the main components of Shor's celebrated quantum algorithm for prime factorization [Shor, 1997]. Shor's prime factorization algorithm uses several results from number theory, combined with a quantum algorithm for the solution of the discrete logarithm problem: given a prime number p , the multiplicative group of integers modulo p consisting of the numbers $\{1, \dots, p - 1\}$, and a generator g of the group, the *discrete logarithm* of x in the group, denoted $\log_g x$ is the smallest nonnegative integer a such that $x^a = g$. Here, multiplication is the group operation, i.e., it is intended modulo p . So, for example, for $p = 7$ and the group $G = \{1, \dots, 6\}$, the number 3 is a generator of the group, and $\log_3 6 = 3$ because $3^3 \bmod 7 = 6$. Shor's work showed that quantum computers can be used to solve the discrete logarithm problem faster than classical computers. In fact, the discrete logarithm is a special case of the hidden subgroup problem [Jozsa, 2001], which can be solved efficiently by quantum computers for certain types of groups. Abelian groups are discussed in [Simon, 1997, Shor, 1997] and admit efficient quantum algorithms for the hidden subgroup problem. Non-Abelian groups do not enjoy the same positive results in general [Grigni et al., 2001]. A subexponential-time algorithm for the case of the dihedral group is discussed in [Kuperberg, 2005, Kuperberg, 2011]. See also [van Dam et al., 2006] for a generalization to the hidden coset problem.

Several papers discuss efficient methods to implement the QFT, and how to improve the gate count or depth of the corresponding circuit; see, e.g., [Cleve and Watrous, 2000] for a low-depth implementation, or [Nam et al., 2020] for an approximate QFT implementation on n qubits with only $\mathcal{O}(n \log n)$ gates of a certain important class.

The phase estimation algorithm of Sect. 3.2 is a fundamental subroutine in many quantum algorithms, and is used multiple times throughout this set of lecture notes. One of the limitations of quantum phase estimation is the fact that the estimate produced by the algorithm after measurement can be biased (recall that the possible outcomes are discrete and not necessarily symmetric around the exact real value, see the distribution in Prop. 3.11): this can sometimes interfere with desirable statistical properties. For discussions on how to remove the bias from the estimator, see [Cornelissen and Hamoudi, 2023, Linden and de Wolf, 2022, Lu and Lin, 2022, van Apeldoorn et al., 2023]. One of the simplest techniques to control the bias, discussed in [van Apeldoorn et al., 2023], is to apply — before estimation — a random phase shift to the eigenvalue being estimated, and subtract the same shift after the estimation procedure. If the phase shift is chosen uniformly at random, this reduces the bias. Some care needs to be taken because the phase shift eventually needs to be discretized to obtain a physically-realizable implementation, and the discretization may introduce a bias, but such bias can be shown to be exponentially small.

Chapter 4

Amplitude amplification and estimation

In Ch.s 2 and 3 we described several quantum algorithms that are exponentially faster than classical algorithms for the same problem, under some measure of complexity. Unfortunately, the algorithms of Ch. 2 apply to rather contrived problems that do not have known direct applications. We now describe a quantum algorithm that gives only a polynomial — more specifically, quadratic — speedup with respect to classical algorithms, but it applies to a large class of problems and finds many useful applications, both directly and as an algorithmic design tool. The algorithm is known as Grover’s search [Grover, 1996], and its generalization is known as amplitude amplification [Brassard et al., 2002]. Amplitude amplification is widely used as part of many quantum algorithms. It also serves as the basis for amplitude estimation, a way of estimating probabilities quadratically faster than with classical Monte Carlo, and for quantum minimum finding. All these topics are discussed in this chapter.

4.1 Grover’s algorithm for black-box search

The problem solved by Grover’s algorithm is usually described as *black-box* (or *unstructured*) search: we are given a circuit that computes an unknown function of a binary string, and we want to determine for which value of the input the function gives output 1. In other words, we are trying to find a binary string that satisfies a given property; the property is tested by a circuit that outputs 1 to “mark” any string that satisfies the property. For now, we assume that there is a single binary string that satisfies the property. The original paper [Grover, 1996] describes this as looking for a certain element in a database. The algorithm can be applied whenever we are searching for a specific element in a set, we have a way of testing if an element is the desired element (in fact, this test must be implementable as a quantum subroutine — see below), and we do not have enough information to do anything smarter than a brute force search, i.e., testing all elements in the set.

The basic idea of the algorithm is to start with the uniform superposition of all basis states, and iteratively increase the magnitude of the coefficients of basis states that correspond to binary strings for which the unknown function gives output 1. Crucially, this can be done even without knowing in advance which basis states have their coefficients increased, using phase kickback: we discuss this in Sect. 4.1.2.

We need to introduce some notation to formally state the problem solved by Grover’s algorithm. Let $f : \{0, 1\}^n \rightarrow \{0, 1\}$, and assume that there exists a unique $\vec{\ell} \in \{0, 1\}^n : f(\vec{\ell}) = 1$, i.e., there is a unique element in the domain of the function that yields output 1. We call this the *marked element*. We want to determine $\vec{\ell}$. The function f is assumed to be encoded by a unitary as follows:

$$U_f : |\vec{j}\rangle|y\rangle \rightarrow |\vec{j}\rangle|y \oplus f(\vec{j})\rangle.$$

Note that this is an $(n + 1)$ -qubit unitary. As usual, we are allowed to query the function in superposition.

Remark 4.1. *Grover's search can also be applied to the case in which there are multiple input values that yield output 1, and we want to retrieve any of them: we discuss this in Sect. 4.2.1.*

4.1.1 Classical algorithm

Given the problem definition, classical search has query complexity $\mathcal{O}(2^n)$. Indeed, any deterministic classical algorithm may need to explore all 2^n possible input values before finding $\vec{\ell}$: given any deterministic classical algorithm, there exists a permutation π of $\{0, 1\}^n$ that represents the longest execution path (i.e., sequence of values at which f is queried) of such algorithm. Then, if $\vec{\ell} = \pi(\vec{1})$ (i.e., it is the last element queried by the algorithm in its longest execution path) the algorithm takes 2^n queries to determine the answer.

At the same time, a randomized algorithm with a constant positive probability to determine $\vec{\ell}$ uses $\mathcal{O}(2^n)$ function calls. This can be verified as follows. Suppose we apply a randomized algorithm that tries one untested binary string uniformly at random at each iteration. The expected number of function calls that this algorithm performs until we determine $\vec{\ell}$ is given by:

$$\sum_{k=1}^{2^n} k \Pr(\vec{\ell} \text{ is found at the } k\text{-th function evaluation}).$$

We can expand this by noticing that the probability that $\vec{\ell}$ is found at the k -th evaluation is the product of the probability that $\vec{\ell}$ is selected at the k -th iteration, and the probability that $\vec{\ell}$ is not found for the first $k - 1$ evaluations. This is equal to:

$$\begin{aligned} \sum_{k=1}^{2^n} k \frac{1}{2^n - (k - 1)} \prod_{j=1}^{k-1} \frac{2^n - j}{2^n - (j - 1)} &= \sum_{k=1}^{2^n} k \frac{1}{2^n - (k - 1)} \frac{2^n - (k - 1)}{2^n} \\ &= \sum_{k=1}^{2^n} \frac{k}{2^n} = \frac{2^n(2^n + 1)}{2} \frac{1}{2^n} = \frac{2^n + 1}{2}. \end{aligned}$$

Hence, such an algorithm needs approximately 2^{n-1} function calls. By Yao's principle (the worst case expected cost of a randomized algorithm is no better than the cost of the best deterministic algorithm against the worst probability distribution), no randomized algorithm can do better than the above. Thus, the query complexity of classical algorithms for this problem is $\mathcal{O}(2^n)$, and it cannot be significantly improved.

4.1.2 Grover's search: algorithm description

The query complexity can be improved with Grover's quantum algorithm. The algorithm uses $q = n + 1$ qubits, which is equal to the number of qubits of the unitary U_f .

The outline of the algorithm is as follows. The algorithm starts with the uniform superposition of all basis states on n qubits. The last qubit (i.e., the one in position $n + 1$) is used as an auxiliary qubit, and it is initialized to $H|1\rangle$; this specific state is helpful for phase kickback, see Sect. 2.1. Then, these operations are repeated several times:

- (i) Flip the sign of the vectors for which U_f gives output 1.
- (ii) Invert all the coefficients of the quantum state around the average coefficient; we explain the precise mapping implemented by this operation in Sect. 4.1.2.

A full cycle of the two operations above increases the coefficient of $|\vec{\ell}\rangle \otimes \frac{1}{\sqrt{2}}(|0\rangle - |1\rangle)$, and after a certain number of cycles (to be specified later), the coefficient of the state $|\vec{\ell}\rangle \otimes \frac{1}{\sqrt{2}}(|0\rangle - |1\rangle)$ is large enough that it can be obtained from a measurement with probability close to 1. This phenomenon is known as *amplitude amplification*, see Sect. 4.2.

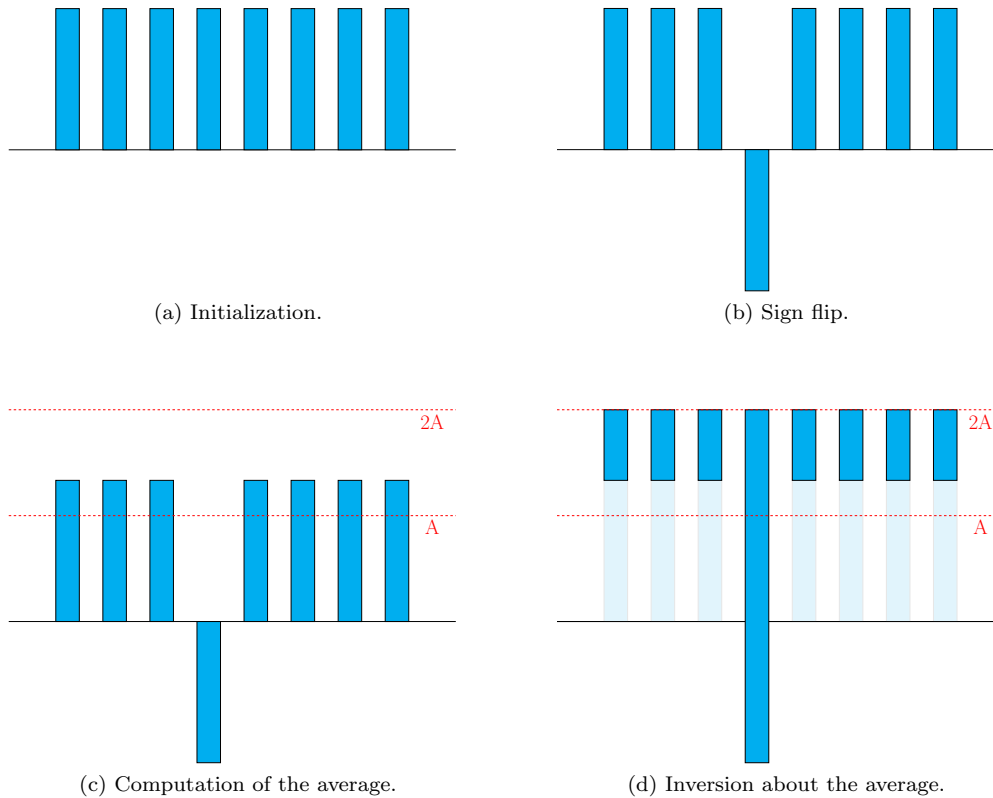


Figure 4.1: Sketch of Grover’s algorithm. The bars represent the coefficients of the basis states.

A sketch of the ideas for the algorithm is depicted in Fig. 4.1: we have eight basis states, and suppose the fourth basis state is the target basis state $|\vec{\ell}\rangle$. The representation is purely meant to convey intuition on the behavior of the coefficients in the quantum state, and does not geometrically represent the vectors encoding the quantum state. In Fig. 4.1a, all basis states have the same coefficient. In Fig. 4.1b, the coefficient of the target basis state has its sign flipped. In Fig. 4.1c, we can see that the average value of the coefficients is slightly below the coefficient for the undesired states. Taking twice the average and subtracting each coefficient now yields the new bars in Fig. 4.1d, where the target basis state $|\vec{\ell}\rangle$ has a coefficient with much larger value than the rest, leading to a higher probability of being output as the outcome of a measurement. Of course, we need to show that these steps can be implemented with unitary matrices that can be constructed with a polynomial number of basic gates.

Next, we describe each step in more detail.

Initialization. The algorithm is initialized by applying the operation $H^{\otimes(n+1)}(I^{\otimes n} \otimes X)$ onto the state $|\vec{0}\rangle_{n+1}$. We can express the quantum state as follows:

$$\begin{aligned} (I^{\otimes n} \otimes X)|\vec{0}\rangle_{n+1} &= |\vec{0}\rangle_n |1\rangle \\ H^{\otimes(n+1)}(I^{\otimes n} \otimes X)|\vec{0}\rangle_{n+1} &= \sum_{\vec{j} \in \{0,1\}^n} \frac{1}{\sqrt{2^n}} |\vec{j}\rangle \otimes \frac{(|0\rangle - |1\rangle)}{\sqrt{2}} = \sum_{\vec{j} \in \{0,1\}^n} \alpha_j |\vec{j}\rangle \otimes \frac{(|0\rangle - |1\rangle)}{\sqrt{2}} = |\psi\rangle, \end{aligned}$$

where $\alpha_j = \frac{1}{\sqrt{2^n}}$ and we labeled the quantum state after the initialization phase as $|\psi\rangle$. We evolve $|\psi\rangle$ through the rest of the algorithm. Note that the initial coefficients α_j of the state $|\psi\rangle$ are real

numbers. Because all the other steps of the algorithm map real numbers to real numbers (as is discussed later), we only need to consider real numbers through the course of the algorithm.

Sign flip: step (i). To flip the sign of the target state $|\vec{\ell}\rangle \otimes \frac{1}{\sqrt{2}}(|0\rangle - |1\rangle)$, we apply U_f to $|\psi\rangle$. This is just an application of phase kickback, because we are applying a function of the form $|\vec{j}\rangle|y\rangle \rightarrow |\vec{j}\rangle|y \oplus f(\vec{j})\rangle$ after preparing the last qubit in the eigenstate $\frac{1}{\sqrt{2}}(|0\rangle - |1\rangle)$ of modulo-2 addition $y \oplus f(\vec{j})$. Indeed, using the expressions derived in Sect. 2.1, we have:

$$\begin{aligned} U_f|\psi\rangle &= U_f \left(\sum_{\vec{j} \in \{0,1\}^n} \alpha_j |\vec{j}\rangle \otimes \frac{1}{\sqrt{2}}(|0\rangle - |1\rangle) \right) \\ &= \sum_{\vec{j} \in \{0,1\}^n} (-1)^{f(\vec{j})} \alpha_j |\vec{j}\rangle \otimes \frac{1}{\sqrt{2}}(|0\rangle - |1\rangle) \\ &= \left(-\alpha_{\vec{\ell}} |\vec{\ell}\rangle + \sum_{\substack{\vec{j} \in \{0,1\}^n \\ \vec{j} \neq \vec{\ell}}} \alpha_j |\vec{j}\rangle \right) \otimes \frac{1}{\sqrt{2}}(|0\rangle - |1\rangle). \end{aligned}$$

As the expression above suggests, we can always think of the last qubit as being in the state $\frac{1}{\sqrt{2}}(|0\rangle - |1\rangle)$ and unentangled from the rest of the qubits, with the sign flip affecting only the first n qubits. Therefore, the state that we obtain by applying U_f to $|\psi\rangle$ is the same as $|\psi\rangle$ except that the sign of $|\vec{\ell}\rangle \otimes \frac{1}{\sqrt{2}}(|0\rangle - |1\rangle)$ has been flipped.

Inversion about the average: step (ii). To perform the inversion about the average, we apply the following operation:

$$\sum_{\vec{j} \in \{0,1\}^n} \alpha_j |\vec{j}\rangle \rightarrow \sum_{\vec{j} \in \{0,1\}^n} \left(2 \left(\sum_{\vec{k} \in \{0,1\}^n} \frac{\alpha_k}{2^n} \right) - \alpha_j \right) |\vec{j}\rangle,$$

where $\sum_{\vec{k} \in \{0,1\}^n} \frac{\alpha_k}{2^n}$ is the average, and therefore we are taking twice the average and subtracting each coefficient from it. It is not clear yet that this is a unitary operation, but it follows from our discussion below. This mapping is realized by the following matrix:

$$W := \begin{pmatrix} \frac{2}{2^n} - 1 & \frac{2}{2^n} & \cdots & \frac{2}{2^n} \\ \frac{2}{2^n} & \frac{2}{2^n} - 1 & \cdots & \frac{2}{2^n} \\ \vdots & \vdots & \ddots & \vdots \\ \frac{2}{2^n} & \frac{2}{2^n} & \cdots & \frac{2}{2^n} - 1 \end{pmatrix} = \begin{pmatrix} \frac{2}{2^n} & \frac{2}{2^n} & \cdots & \frac{2}{2^n} \\ \frac{2}{2^n} & \frac{2}{2^n} & \cdots & \frac{2}{2^n} \\ \vdots & \vdots & \ddots & \vdots \\ \frac{2}{2^n} & \frac{2}{2^n} & \cdots & \frac{2}{2^n} \end{pmatrix} - I^{\otimes n},$$

where in each element of the matrix, the denominator $\frac{1}{2^n}$ computes the average coefficient, the numerator 2 of the fraction takes twice the average, and finally we subtract the identity to subtract each individual coefficient from twice the average. From the definition of the Hadamard gate in Eq. (1.5), we can see that the entry of $H^{\otimes n}$ in position j, k is $(H^{\otimes n})_{jk} = \frac{1}{\sqrt{2^n}}(-1)^{\vec{j} \cdot \vec{k}}$. If we let:

$$M := \begin{pmatrix} 2 & 0 & \cdots & 0 \\ 0 & 0 & \cdots & 0 \\ \vdots & \vdots & \ddots & \vdots \\ 0 & 0 & \cdots & 0 \end{pmatrix} = 2|\vec{0}\rangle\langle\vec{0}| \in \mathbb{R}^{2^n \times 2^n},$$

then we can write $(H^{\otimes n} M H^{\otimes n})_{jk} = (H^{\otimes n})_{j0} M_{00} (H^{\otimes n})_{0k} = \frac{2}{2^n}$, because $M_{jk} = 0$ for $j \neq 0$ or $k \neq 0$. Therefore, using the fact that $H^{\otimes n} H^{\otimes n} = I^{\otimes n}$, we have:

$$\begin{aligned} W &= H^{\otimes n} M H^{\otimes n} - I^{\otimes n} = H^{\otimes n} (M - I^{\otimes n}) H^{\otimes n} \\ &= H^{\otimes n} \underbrace{\text{diag}(1, -1, \dots, -1)}_{\substack{2^n \text{ elements} \\ =: F}} H^{\otimes n} = H^{\otimes n} F H^{\otimes n}. \end{aligned} \tag{4.1}$$

The expression in Eq. (4.1), besides providing a decomposition for W , also shows that W is unitary, because it is a product of unitary matrices ($H^{\otimes n}$ is a tensor product of unitary matrices, F is diagonal with ones on the diagonal hence it is unitary). We must find a way to construct the matrix $F = \text{diag}(1, -1, \dots, -1)$. This is discussed below. For now, we summarize our analysis of the inversion about the average by concluding that it can be performed by applying $W = H^{\otimes n} F H^{\otimes n}$ to the n qubits of interest (i.e., the input lines of U_f — all qubits except the output qubit of U_f , which we use for the sign flip of step (i) via phase kickback).

Constructing the matrix F . We give a sketch of the idea of how to construct $F = \text{diag}(1, -1, \dots, -1)$. Notice that the effect of this quantum operation is to flip the sign of the coefficient of every basis state except $|\vec{0}\rangle_n$. We are going to implement $-F$ rather than F .

Remark 4.2. *As discussed in Ex. 1.30, a global phase factor in a gate has no effect on the outcome of the computation, as it gets canceled out during measurement. The matrices F and $-F$ are equal up to a global phase factor of -1 , hence they implement the same operation.*

The matrix $-F$ flips the sign of $|\vec{0}\rangle$ and leaves other basis state untouched. Instead of flipping the sign of $|\vec{0}\rangle$, let us start by seeing how to flip the sign of $|\vec{1}\rangle$ while leaving all other coefficients untouched. Let $C^{n-1}Z$ be the gate that applies Z to qubit n if qubits $1, \dots, n-1$ are $|1\rangle$, and does nothing otherwise. This is similar to the CX gate, except that it has multiple controls, and it applies a Z gate rather than an X (i.e., X) gate when the control qubits are $|1\rangle$. It is called a “multiply-controlled Z ”. $C^{n-1}Z$ in the case of two qubits ($n = 2$) is given by the following matrix:

$$CZ = \begin{pmatrix} 1 & 0 & 0 & 0 \\ 0 & 1 & 0 & 0 \\ 0 & 0 & 1 & 0 \\ 0 & 0 & 0 & -1 \end{pmatrix}.$$

Notice that in the two-qubit case ($n = 2$), the two circuits depicted in Fig. 4.2 are equivalent: carrying out the matrix multiplications confirms that the circuit on the right in Fig. 4.2 implements exactly the CZ matrix as defined above. Thus, the controlled Z gate can be easily realized with a CX and two Hadamard gates.



Figure 4.2: Controlled Z gate on two qubits: two possible representations.

If we have access to the $C^{n-1}Z$ gate, we can write:

$$-F = X^{\otimes n} (C^{n-1}Z) X^{\otimes n},$$

because, as can be easily verified, this sequence of operations flips the sign of the coefficient of a basis state if and only if all qubits have value $|0\rangle$ in the basis state. In circuit form, these operations can be represented as depicted in Fig. 4.3.

Of course, one has to construct the operation $C^{n-1}Z$. There are several ways to do so. The construction that is simplest to understand is perhaps the one suggested in [Barenco et al., 1995], according to which we use a $C^{n-2}X$ gate and a controlled Z gate. The $C^{n-2}X$ is actually easy to

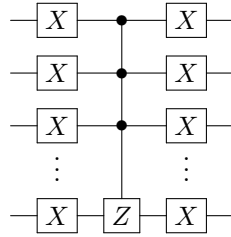


Figure 4.3: Quantum circuit implementing the F operation (up to a global phase factor) used in Grover's algorithm.

implement with some auxiliary qubits. We show this scheme in Fig. 4.4 with an example for $n = 4$ qubits, but clearly it can be generalized to an arbitrary number of qubits. We first implement a $C^{n-2}X$ gate, with an auxiliary qubit (which is initialized to $|0\rangle$, as one can see from the bottom qubit in Fig. 4.4) as the target of the $C^{n-2}X$. We then implement a CCZ gate using a CCX and two Hadamard gates on the target qubit; the reader can easily verify that this implements a doubly-controlled Z , using the identity $HXH = Z$ and carrying out the calculations (in the large unitary matrix for CCZ , the gate being controlled appears in the bottom right, just as in CX). Summarizing, this yields a decomposition of $C^{n-1}Z$ with a number of gates and auxiliary qubits that is linear in n . It is possible to forsake the initialization of the auxiliary qubit, see [Barenco et al., 1995] for details. To conclude, the construction of F (more precisely, $-F$), and therefore of the whole circuit implementing step (ii) of Grover's search, can be done using $\mathcal{O}(n)$ gates and auxiliary qubits.

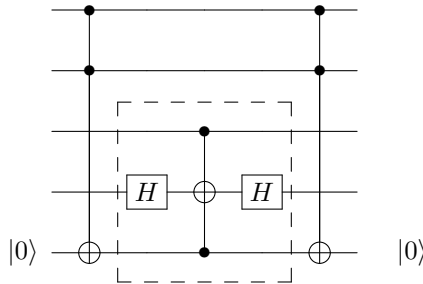


Figure 4.4: Decomposition of $C^{n-1}Z$ for $n = 4$. The fifth (bottom) qubit is initialized to $|0\rangle$ and is used as working space. This implements C^3Z for the top four qubits.

4.1.3 Determining the number of iterations

A single iteration of Grover's search consists of steps (i) and (ii) described in Sect. 4.1.2. It is paramount to determine how many iterations should be performed, so that the coefficient of the desired basis state $|\vec{\ell}\rangle \otimes (|0\rangle - |1\rangle)$ is as large as possible (in modulus), and the binary string $\vec{\ell}$ is the outcome of a measurement with high probability. In this section we study how the amplitude of the target basis state changes through the iterations, and determine the optimal number of iterations.

Because the last, auxiliary qubit is always in the state $\frac{1}{\sqrt{2}}(|0\rangle - |1\rangle)$ and unentangled with the rest, we can ignore it in this section. Let

$$|\psi_G\rangle := |\vec{\ell}\rangle, \quad |\psi_B\rangle := \left(\sum_{\substack{\vec{j} \in \{0,1\}^n \\ \vec{j} \neq \vec{\ell}}} \frac{1}{\sqrt{2^n - 1}} |\vec{j}\rangle \right)$$

be the “good” and “bad” quantum states, respectively. These are valid quantum states, as they have unit norm. (One should think of them as a desirable and undesirable part of the state, i.e.,

some part that we wish to have as the outcome of a computation, and one that we do not wish to have. The quantum computing literature usually labels these states “good” and “bad”.) We claim that after iteration k of the algorithm, the quantum state can be expressed as:

$$|\psi_k\rangle = d_k|\psi_G\rangle + u_k|\psi_B\rangle,$$

with $|d_k|^2 + |u_k|^2 = 1$. We show this by induction. Initially, we pick $d_0 = \frac{1}{\sqrt{2^n}}$ and $u_0 = \sqrt{\frac{2^n-1}{2^n}}$; this yields the initial state $|\psi\rangle$ with uniform coefficients equal to $\frac{1}{\sqrt{2^n}}$. Thus, the claim is true for $k = 0$. Notice that to obtain u_0 from the value of an individual coefficient in $|\psi\rangle$ we multiplied by $\sqrt{2^n - 1}$ for normalization, because there are $2^n - 1$ basis states in $|\psi_B\rangle$. We now need to show the induction step: assuming $|\psi_k\rangle = d_k|\psi_G\rangle + u_k|\psi_B\rangle$ with coefficients d_k, u_k satisfying $|d_k|^2 + |u_k|^2 = 1$, we must show $|\psi_{k+1}\rangle = d_{k+1}|\psi_G\rangle + u_{k+1}|\psi_B\rangle$ with $|d_{k+1}|^2 + |u_{k+1}|^2 = 1$.

At step (i) of the algorithm, the algorithm flips the sign of the coefficient in front of $|\psi_G\rangle$; formally, it applies the mapping $d_k|\psi_G\rangle + u_k|\psi_B\rangle \rightarrow -d_k|\psi_G\rangle + u_k|\psi_B\rangle$.

At step (ii), the algorithm maps $\alpha_h \rightarrow 2A_k - \alpha_h$ for each coefficient α_h , where A_k is the average coefficient at iteration k . Therefore:

$$\begin{aligned} -\alpha_\ell &\rightarrow 2A_k + \alpha_\ell \\ \alpha_h &\rightarrow 2A_k - \alpha_h \quad \forall h \neq \ell. \end{aligned}$$

To compute A_k , we need to determine the value of each individual coefficient. The coefficient for $|\vec{\ell}\rangle$ is clearly d_k , as there is only one such state. On the other hand, there are $2^n - 1$ states with coefficient u_k , so the value of the coefficient for each of the states $|\vec{j}\rangle, \vec{j} \neq \vec{\ell}$ is $\frac{u_k}{\sqrt{2^n-1}}$ (the square root is due to normalization, see above). The average coefficient at iteration k is therefore:

$$A_k = \frac{(2^n - 1) \frac{1}{\sqrt{2^n-1}} u_k - d_k}{2^n} = \frac{\sqrt{2^n-1} u_k - d_k}{2^n}.$$

Again, to obtain u_k from one of the coefficients α_h we multiply by $\sqrt{2^n - 1}$, so the mapping of steps (i) and (ii) can be summarized as:

$$\begin{aligned} d_k|\psi_G\rangle + u_k|\psi_B\rangle &\rightarrow -d_k|\psi_G\rangle + u_k|\psi_B\rangle && \text{(step (i))} \\ -d_k|\psi_G\rangle + u_k|\psi_B\rangle &\rightarrow (2A_k + d_k)|\psi_G\rangle + \sqrt{2^n-1} \left(2A_k - \frac{u_k}{\sqrt{2^n-1}}\right) |\psi_B\rangle && \text{(step (ii))} \\ &= d_{k+1}|\psi_G\rangle + u_{k+1}|\psi_B\rangle, \end{aligned}$$

where we defined:

$$\begin{aligned} d_{k+1} &:= 2A_k + d_k \\ u_{k+1} &:= 2A_k \sqrt{2^n-1} - u_k. \end{aligned}$$

With simple algebraic calculations we can verify that $|d_{k+1}|^2 + |u_{k+1}|^2 = 1$. This finishes the proof of the induction step, and therefore of the entire claim.

Now we analyze the coefficients d_{k+1}, u_{k+1} more closely. Performing the substitution of A_k , we obtain:

$$\begin{aligned} d_{k+1} &= 2 \frac{\sqrt{2^n-1} u_k - d_k}{2^n} + d_k = \left(1 - \frac{1}{2^{n-1}}\right) d_k + \frac{2\sqrt{2^n-1}}{2^n} u_k \\ u_{k+1} &= 2 \frac{\sqrt{2^n-1} u_k - d_k}{2^n} \sqrt{2^n-1} - u_k = -\frac{2\sqrt{2^n-1}}{2^n} d_k + \left(1 - \frac{1}{2^{n-1}}\right) u_k. \end{aligned}$$

This transformation is exactly a clockwise rotation of the vector $\begin{pmatrix} d_k \\ u_k \end{pmatrix}$ by a certain angle 2θ , because it has the form:

$$\begin{pmatrix} \cos 2\theta & \sin 2\theta \\ -\sin 2\theta & \cos 2\theta \end{pmatrix} \begin{pmatrix} d_k \\ u_k \end{pmatrix}$$

and it satisfies the relationship $\sin^2 2\theta + \cos^2 2\theta = 1$. (The reason why we call this angle 2θ , rather than simply θ , is discussed in Sect. 4.1.4; this choice also makes our exposition more consistent with the literature.) The angle θ must satisfy:

$$\sin 2\theta = \frac{2\sqrt{2^n - 1}}{2^n}. \quad (4.2)$$

Note that because this value of the sine is very small for large n , we can use the approximation $\sin x \approx x$ (when x is close to 0) to write:

$$\theta \approx \frac{\sqrt{2^n - 1}}{2^n} \approx \frac{1}{\sqrt{2^n}}. \quad (4.3)$$

Summarizing, the above analysis shows that $|\psi_k\rangle$ belongs to the plane spanned by $|\psi_G\rangle$ and $|\psi_B\rangle$, and at each iteration we perform a rotation of $|\psi_k\rangle$ in that plane by an angle 2θ . Thus, after k iterations the coefficients d_k, u_k satisfy the following equation:

$$\begin{pmatrix} d_k \\ u_k \end{pmatrix} = \begin{pmatrix} \cos 2\theta & \sin 2\theta \\ -\sin 2\theta & \cos 2\theta \end{pmatrix}^k \begin{pmatrix} d_0 \\ u_0 \end{pmatrix},$$

and because this is an application of a rotation k times, the above equation can be rewritten as:

$$\begin{aligned} d_k &= \cos 2k\theta d_0 + \sin 2k\theta u_0 \\ u_k &= -\sin 2k\theta d_0 + \cos 2k\theta u_0. \end{aligned}$$

In order to maximize the probability of obtaining $|\psi_G\rangle$ after a measurement, we recall that $|u_0| \gg |d_0|$ and $|u_0|$ is close to 1 for large n , so we need to set $\sin 2k\theta$ as large as possible. Thus, the best choice is to pick $2k\theta = \frac{\pi}{2}$, which yields the largest value of $|d_k|$. Using Eq. (4.3), and noting that the number of iterations has to be integer, the optimal number of iterations of Grover's search algorithm is:

$$k = \left\lfloor \frac{\pi}{4\theta} \right\rfloor \approx \left\lfloor \frac{2^n \pi}{4\sqrt{2^n - 1}} \right\rfloor \approx \frac{\pi}{4} \sqrt{2^n} = \mathcal{O}(\sqrt{2^n}), \quad (4.4)$$

where we write $\lfloor \cdot \rfloor$ to denote the rounding to the nearest integer. After this many iterations, we have a probability close to 1 of measuring $|\psi_G\rangle$ and obtaining the sought state $|\vec{\ell}\rangle$. In each iteration we apply U_f once (for the sign flip step). Comparing this with a classical algorithm, that performs $\mathcal{O}(2^n)$ queries to the oracle f , we obtained a quadratic speedup.

Remark 4.3. *If we perform more iterations of Grover's algorithm than the optimal number, the probability of measuring the desired state actually goes down, and reduces our chances of success. Therefore, it is important to choose the right number of iterations, see the discussion in Sect. 4.2 for ways to avoid this issue.*

Of course, the approximation for θ given in Eq. (4.3) is only valid for large n : for smaller n , it is better to compute the optimal number of iterations deriving θ from Eq. (4.2). We conclude this section by noting that in case there are multiple input values on which f has value 1, we should amend the above analysis adjusting the values for d_0 and u_0 , but the main steps remain the same: we discuss this in Sect. 4.2. Another situation that can be analyzed is that in which it is not known in advance for how many input strings the function f outputs 1, i.e., we do not know the number of marked elements; this is discussed in Sect. 4.3.6.

4.1.4 A geometric interpretation of the algorithm

To continue our study of Grover's algorithm, and help us transition to a more general version of it, it is helpful to provide a geometric view of the algorithm's effect. We are also going to restate the algorithm's input and objective in a slightly more general form.

Suppose that we want to approximately construct a certain n -qubit state $|\psi_G\rangle$, having access to the following two circuits:

- (i) A circuit S acting on n qubits that has the following action:

$$S|\vec{0}\rangle_n := |\psi_0\rangle = \sin\theta|\psi_G\rangle + \cos\theta|\psi_B\rangle,$$

where $\langle\psi_G|\psi_B\rangle = 0$ (i.e., the states are orthogonal) and $\theta \in (0, \frac{\pi}{2})$.

- (ii) A circuit R acting on n qubits that has the following action:

$$R(\alpha_G|\psi_G\rangle + \alpha_B|\psi_B\rangle) = -\alpha_G|\psi_G\rangle + \alpha_B|\psi_B\rangle$$

for any $\alpha_G, \alpha_B \in [-1, 1] : |\alpha_G|^2 + |\alpha_B|^2 = 1$.

This is a generalization of our previous discussion of Grover's algorithm: if we take $S = H^{\otimes n}$, and we let R be the "sign flip" unitary (that can be constructed with U_f and phase kickback), we obtain exactly the statement of Grover's problem with $|\psi_G\rangle, |\psi_B\rangle$ defined as in Sect. 4.1.3. Let us call the operator $G = SFS^\dagger R$ a *Grover iteration*, and let us look at the effect of the Grover iteration on the plane spanned by $|\psi_G\rangle$ and $|\psi_B\rangle$.

Remark 4.4. *The operation SFS^\dagger implements a reflection through $|\psi_0\rangle = S|\vec{0}\rangle$, because:*

$$SFS^\dagger = S(2|\vec{0}\rangle\langle\vec{0}| - I^{\otimes n})S^\dagger = 2S|\vec{0}\rangle\langle\vec{0}|S^\dagger - SS^\dagger = 2|\psi_0\rangle\langle\psi_0| - I^{\otimes n},$$

which is exactly the desired reflection. ($|\psi_0\rangle\langle\psi_0|$ is the orthogonal projection onto $|\psi_0\rangle$; if we take twice the projection and subtract the identity, we reflect through $|\psi_0\rangle$.) We have shown in Sect. 4.1.2 that we know how to construct the matrix $F = \text{diag}(1, -1, \dots, -1) = M - I^{\otimes n} = 2|\vec{0}\rangle\langle\vec{0}| - I^{\otimes n}$. Then, the operation to reflect through $|\psi_0\rangle$ can be efficiently implemented using F and S, S^\dagger .

We can assume that the mutual relationship between the states is as given in Fig. 4.5a. An application of the operator R reflects $|\psi_0\rangle$ through $|\psi_B\rangle$, obtaining the dashed arrow in Fig. 4.5b. Then, an application of SFS^\dagger reflects $R|\psi_0\rangle$ through $|\psi_0\rangle$, see Rem. 4.4; this is depicted in Fig. 4.5c. Thus, because θ is the angle between $|\psi_0\rangle$ and $|\psi_B\rangle$, reflecting $R|\psi_0\rangle$ through $|\psi_0\rangle$ rotates $|\psi_0\rangle$ closer to $|\psi_G\rangle$ by an angle of 2θ ; this is shown in Fig. 4.5c. At this point we have performed one full iteration of Grover's algorithm: the quantum state is denoted $|\psi_1\rangle$ in Fig. 4.5d, and it is closer to $|\psi_G\rangle$ by an angle 2θ , compared to the initial state $|\psi_0\rangle$.

These operations (reflection through $|\psi_B\rangle$, reflection through $|\psi_0\rangle$) can be repeated multiple times until we obtain $|\psi_k\rangle$ that is close to $|\psi_G\rangle$. The initial angle between $|\psi_0\rangle$ and $|\psi_G\rangle$ is $\frac{\pi}{2} - \theta$, hence the number of iterations is:

$$\left\lceil \frac{\frac{\pi}{2} - \theta}{2\theta} \right\rceil = \left\lceil \frac{\pi}{4\theta} - \frac{1}{2} \right\rceil = \left\lfloor \frac{\pi}{4\theta} \right\rfloor,$$

exactly as derived in Eq. (4.4). Using Eq.s (4.2) and (4.3) we obtain once again the optimal number of iterations previously shown.

Remark 4.5. *The angle θ in this section is defined by the action of S , because $S|\vec{0}\rangle = \sin\theta|\psi_G\rangle + \cos\theta|\psi_B\rangle$. For Grover's algorithm, where $S = H^{\otimes n}$, we obtain exactly the same angle as in Eq. (4.2): using the double angle formula, we have*

$$\frac{2\sqrt{2^n - 1}}{2^n} = \sin 2\theta = 2 \sin\theta \cos\theta = 2 \underbrace{\frac{1}{\sqrt{2^n}}}_{\sin\theta} \underbrace{\sqrt{\frac{2^n - 1}{2^n}}}_{\cos\theta}.$$

Knowing that a Grover iteration performs a rotation, we summarize the effect of applying k Grover iterations as:

$$G^k|\psi_0\rangle = \sin((2k + 1)\theta)|\psi_G\rangle + \cos((2k + 1)\theta)|\psi_B\rangle.$$

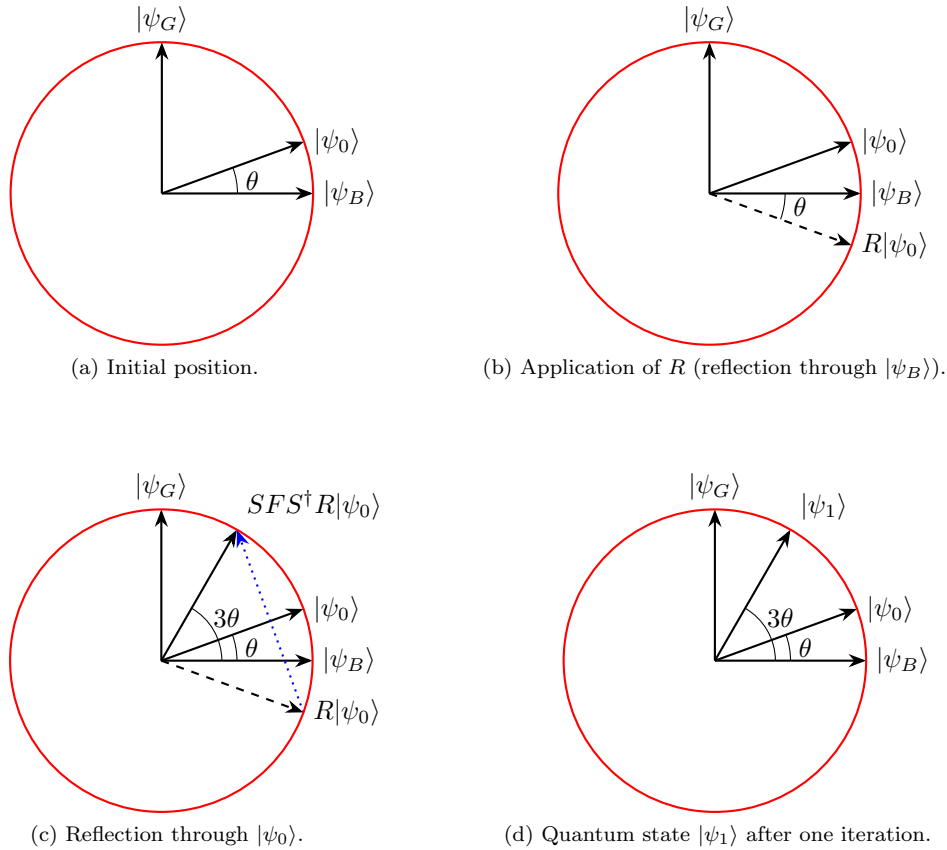


Figure 4.5: Sketch of Grover’s algorithm on the plane spanned by $|\psi_G\rangle$ and $|\psi_B\rangle$.

4.2 Amplitude amplification

The geometric interpretation of Grover’s algorithm given in Sect. 4.1.4, which is more general than the original Grover’s algorithm, leads to a technique known as *amplitude amplification*, first introduced in [Brassard et al., 2002]. The algorithm discussed in Sect. 4.1.4 takes as input a circuit S preparing a superposition of a “good” state $|\psi_G\rangle$ and a “bad” state $|\psi_B\rangle$, and a circuit R that flips the sign of $|\psi_G\rangle$; its goal is to find a state with large overlap with $|\psi_G\rangle$. We have seen that in Grover’s algorithm, R is constructed with phase kickback: the function U_f marks the basis states in $|\psi_G\rangle$ by performing modulo-2 addition on an auxiliary qubit, and if the auxiliary qubit is prepared in the state $H|1\rangle$ (which is an eigenvector of addition modulo 2, with eigenvalue -1) this applies a sign flip. Note that to implement R in this way, the only requirement is that we are able to recognize (“mark”) the basis states in $|\psi_G\rangle$. Amplitude amplification is precisely the algorithm that we described with a geometric interpretation in Sect. 4.1.4, to prepare $|\psi_G\rangle$ given a unitary that marks it.

Using the geometric intuition described in Sect. 4.1.4, we found that the optimal number of iterations is $\frac{\pi}{4\theta}$, where θ is the angle such that $S|\vec{0}\rangle = \sin\theta|\psi_G\rangle + \cos\theta|\psi_B\rangle$. Relying once again on the approximation $\sin\theta \approx \theta$ for small angles, and calling $p = \sin^2\theta$, we obtain the following result, which follows directly from our analysis in Sect. 4.1 and more specifically Sect. 4.1.4.

Theorem 4.6 (Amplitude amplification; [Brassard et al., 2002]). *Let S be an n -qubit unitary such that $S|\vec{0}\rangle = \sqrt{p}|\psi_G\rangle + \sqrt{1-p}|\psi_B\rangle$, where for some $M \subset \{0, 1\}^n$, we have $|\psi_G\rangle = \frac{1}{\sqrt{p}} \sum_{j \in M} \alpha_j |\vec{j}\rangle$, $|\psi_B\rangle = \frac{1}{\sqrt{1-p}} \sum_{j \notin M} \alpha_j |\vec{j}\rangle$ and $p = \sum_{j \in M} |\alpha_j|^2$. Let R be a unitary that maps $|\psi_G\rangle \rightarrow -|\psi_G\rangle$, $|\psi_B\rangle \rightarrow |\psi_B\rangle$. The amplitude amplification algorithm produces a quantum state such that its*

overlap with $|\psi_G\rangle$ is at least $2/3$ using $\mathcal{O}\left(\frac{1}{\sqrt{p}}\right)$ applications of S and R , and additional gates.

This result can potentially be used to boost the probability of success of any randomized algorithm with the property that success can be recognized. The most typical case is the one in which we have some “flag qubits” that indicate success of the algorithm: these can be obtained by running a verification procedure, or sometimes they are obtained as a byproduct of the algorithm itself. Then we define $|\psi_G\rangle$ as the superposition of all basis states in which the flag qubits indicate success, and $|\psi_B\rangle$ as its orthogonal complement. If the original randomized algorithm is successful with probability p , amplitude amplification increases the probability of success to some number very close to one using $\mathcal{O}\left(\frac{1}{\sqrt{p}}\right)$ applications of the circuit that implements the algorithm, whereas classical repetition of the algorithm until success would take $\mathcal{O}\left(\frac{1}{p}\right)$ executions of the circuit in expectation.

Remark 4.7. *The statement of Thm. 4.6 only guarantees probability of success $2/3$, but this can easily be boosted to a number arbitrarily close to one by doing a few repetitions of the algorithm: using standard arguments, with k repetitions the probability that all of them fail is at most $1/3^k$, so for probability $1 - \delta$ of obtaining at least one success, it suffices to pick $k = \mathcal{O}\left(\log \frac{1}{\delta}\right)$.*

Example 4.8. *Let us consider Grover’s problem again: we want to find a value $\vec{\ell} \in \{0, 1\}^n$ such that $f(\vec{\ell}) = 1$. We can determine this using a simple randomized algorithm: sample a binary string \vec{j} uniformly at random, and evaluate f until we find $f(\vec{j}) = 1$. The probability of success of a single sample is $p = 1/2^n$. A quantum circuit implementation of this algorithm can be obtained by applying a layer of Hadamard gates $H^{\otimes n}$ onto the initial state $|\vec{0}\rangle$, applying the unitary U_f that evaluates f on the uniform superposition, and following with a measurement of all qubits. If we obtain a string with $f(\vec{j}) = 1$, the algorithm has succeeded. Repeating this procedure until success results in $\mathcal{O}(1/p) = \mathcal{O}(2^n)$ applications of the quantum circuit in expectation. With amplitude amplification, the probability of success is close to one after only $\mathcal{O}(1/\sqrt{p}) = \mathcal{O}(\sqrt{2^n})$ applications of $H^{\otimes n}$ and U_f , where U_f allows us to implement the reflection circuit R via phase kickback; so we only need that many applications of U_f in expectation.*

Thm. 4.6 can be restated for the (simpler) case of quantum search using a binary marking oracle, just as in Grover’s algorithm, generalizing the argument discussed in Ex. 4.8.

Corollary 4.9. *Let U_f be a quantum (binary) oracle implementing a Boolean function $f : \{0, 1\}^n \rightarrow \{0, 1\}$, and let $M = \{\vec{j} \in \{0, 1\}^n : f(\vec{j}) = 1\}$ be the set of marked elements. Then we can determine an element of M with $\mathcal{O}\left(\sqrt{\frac{2^n}{|M|}}\right)$ applications of U_f , if $|M|$ is known.*

When $|M|$ is unknown we can achieve the same expected running time $\mathcal{O}\left(\sqrt{\frac{2^n}{|M|}}\right)$ with a randomized algorithm discussed in Sect. 4.3.6: we postpone its description because the analysis is simpler after developing a few additional tools.

One potential issue of amplitude amplification (and thus Grover’s algorithm) is that we need to have a reasonable estimate of the value of p before executing the algorithm. Indeed, if we have no such estimate, we cannot compute the right number of iterations k for the algorithm. As a result, the overlap between the target state $|\psi_G\rangle$ and the state produced by the algorithm may be too small. Intuitively, this is easy to see: the overlap is expressed by the function $\sin((2k + 1)\theta)$, and if k is too small or too large we may obtain a small value for the sine.

To overcome this issue, several approaches are possible. A simple one is to use the *amplitude estimation* algorithm to get an estimate of p [Brassard et al., 2002], see Sect. 4.3. This incurs an extra cost, but asymptotically we still obtain a quadratic speedup over classical algorithms. In fact, this algorithm can be executed in a different way that avoids explicit estimation: we discuss a version of it in the context of quantum search, in Sect. 4.3.6. Other approaches are discussed in the notes in Sect. 4.5.

4.2.1 Obtaining all marked states

Suppose we have a known number $t = |M|$ of marked states in total (the set M is defined as in Cor. 4.9), and we want to find them all. Note that this is a direct generalization of the black-box search problem of Sect. 4.1. The most natural approach is to use amplitude amplification to construct a state with a large overlap with $|\psi_G\rangle$, measure in the computational basis, and obtain $\vec{j} \in M$ with high probability. Then we can “unmark” the string \vec{j} , in the following way: construct a lookup-table circuit that for a given \vec{j} , checks whether \vec{j} is a previously observed marked element (i.e., $f(\vec{j}) = 1$), and if so it returns 0, otherwise it returns $f(\vec{j})$. In other words, we implement the following function:

$$f'_E(\vec{j}) = \begin{cases} 0 & \text{if } \vec{j} \in E \\ f(\vec{j}) & \text{otherwise,} \end{cases}$$

where $E \subset M$ is the set of previously observed marked elements. Implementing this function is easy: one call to f'_E can be implemented with at most one call to f and $\mathcal{O}(|E|)$ additional gates.

We then apply the scheme suggested earlier: initialize $E \leftarrow \emptyset$; apply amplitude amplification to the function f'_E with known number of marked elements $t - |E|$ to determine a new element in M ; repeat until all elements in M are found. Using Corollary 4.9, the number of calls to f'_E (and hence f) before we find all elements can be upper bounded as follows (this is an order-of-magnitude upper bound, i.e., we ignore possible constants in front of the expression):

$$\begin{aligned} \sum_{k=0}^{t-1} \sqrt{\frac{2^n}{t-k}} &= \sqrt{2^n} \sum_{k=1}^t \frac{1}{\sqrt{k}} \leq \sqrt{2^n} \int_1^t \frac{1}{\sqrt{x}} dx = \sqrt{2^n} \left(2x^{1/2} \Big|_1^t \right) = \sqrt{2^{n+1}}(\sqrt{t} - 1) \\ &= \mathcal{O}\left(\sqrt{t2^n}\right). \end{aligned}$$

This implies the following.

Corollary 4.10. *Let M be the set of marked elements, and let $|M|$ be known. Then we can determine all elements in M using $\mathcal{O}\left(\sqrt{|M|2^n}\right)$ applications of f .*

4.2.2 Oblivious amplitude amplification

We discussed how to amplify the relative weight of certain quantum states in a superposition, which allows us to increase the probability of success of quantum algorithms in a very general way. To do so, so far we required access to a circuit to prepare an initial state that we can reflect through. In this section we show that amplitude amplification can be applied to select a “useful” part of the state, obtained by applying a unitary to the initial state, even if we do not know the initial state itself and hence cannot reflect through it. This is called *oblivious* amplitude amplification [Berry et al., 2014]. We use this technique in Sect. 6.2.3.

The setup for oblivious amplitude amplification is the following. Suppose we apply some unitary U to an initial state $|\psi\rangle$ on n qubits, and this unitary produces a superposition of a “good state” that we want to obtain with some large probability, and a “bad state”. If we have a way of identifying the good state, for example if we know that all good states are marked by one or more flag qubits, it would seem that we can apply amplitude amplification to increase the probability of observing the good state up to the desired level. Formally, suppose the unitary U has the following action:

$$U|0\rangle|\psi\rangle = \sin\theta|0\rangle V|\psi\rangle + \cos\theta|1\rangle|\phi\rangle,$$

where $V|\psi\rangle$ is the good state, i.e., the state that we are interested in, and $|\phi\rangle$ is the bad state, which is allowed to depend on $|\psi\rangle$ in the above expression. The first qubit serves as a flag qubit to mark the good state. To apply amplitude amplification, as we have seen in Sect. 4.1.4, we need a way of reflecting through $|\psi_G\rangle = |0\rangle V|\psi\rangle$. This is easy to do if we have a circuit to construct $|\psi\rangle$ from $|\vec{0}\rangle$ and we are willing to execute this circuit repeatedly: in this case, we can apply the amplitude amplification algorithm as discussed in the preceding sections (the circuit S of Thm. 4.6 is then given by the circuit that constructs $|\psi\rangle$ from $|\vec{0}\rangle$, followed by U). However, suppose that

we do not have a circuit to construct $|\psi\rangle$, or we have the circuit but we choose not to use it more than once because it requires a large amount of computational resources. Standard amplitude amplification fails because we do not have the circuit S of Thm. 4.6, i.e., a circuit that prepares the initial state starting from $|\bar{0}\rangle$. As it turns out we can still apply amplitude amplification, as we show next.

The first step in studying amplitude amplification in this setting is to identify a two-dimensional subspace in which we can do reflection, and such that the Grover operator never leaves that subspace. In the basic version of Grover search, that was the subspace spanned by $|\psi_G\rangle$ and $|\psi_B\rangle$. Here we define it slightly differently: the two fundamental states are $|0\rangle|\psi\rangle$ and $|1\rangle|\phi\rangle$, where, as mentioned earlier, the first qubit is used to identify the good subspace.

Lemma 4.11 (Based on Lem. 3.7 in [Berry et al., 2014]). *Let U, V be unitaries on $n+1$ and n qubits respectively, and let $\theta \in (0, \pi/2)$. Suppose that for any n -qubit state $|\psi\rangle$, we have*

$$U|0\rangle|\psi\rangle = \sin\theta|0\rangle V|\psi\rangle + \cos\theta|1\rangle|\phi\rangle,$$

where $|\phi\rangle$ may depend on $|\psi\rangle$. Then the state $|\Psi^\perp\rangle$, defined as:

$$|\Psi^\perp\rangle = U^\dagger (\cos\theta|0\rangle V|\psi\rangle - \sin\theta|1\rangle|\phi\rangle),$$

is orthogonal to $|\Psi\rangle = |0\rangle|\psi\rangle$ and has no support on the basis states that have $|0\rangle$ as their first qubit, i.e., $(|0\rangle\langle 0| \otimes I^{\otimes n})|\Psi^\perp\rangle = 0$.

Proof. For the first part, we need to show that $\langle\Psi|\Psi^\perp\rangle = 0$. We have:

$$\begin{aligned} \langle\Psi|\Psi^\perp\rangle &= (\langle 0|\langle\psi|)U^\dagger (\cos\theta|0\rangle V|\psi\rangle - \sin\theta|1\rangle|\phi\rangle) \\ &= (\sin\theta\langle 0|\langle\psi|V^\dagger + \cos\theta\langle 1|\langle\phi|) (\cos\theta|0\rangle V|\psi\rangle - \sin\theta|1\rangle|\phi\rangle) \\ &= \sin\theta\cos\theta - \cos\theta\sin\theta = 0. \end{aligned}$$

For the second part, we want to show that:

$$(|0\rangle\langle 0| \otimes I^{\otimes n})|\Psi^\perp\rangle = (|0\rangle\langle 0| \otimes I^{\otimes n})U^\dagger (\cos\theta|0\rangle V|\psi\rangle - \sin\theta|1\rangle|\phi\rangle) = 0.$$

To show this, we first make a couple of observations. We want to study $(|0\rangle\langle 0| \otimes I^{\otimes n})U^\dagger$, so let us study $(\langle 0| \otimes I^{\otimes n})U^\dagger$ to begin with. From the definition of $U|0\rangle|\psi\rangle$, with algebraic manipulations we see that $|0\rangle V|\psi\rangle = \frac{1}{\sin\theta}(|0\rangle\langle 0| \otimes I^{\otimes n})U|0\rangle|\psi\rangle$. Thus, we have:

$$\begin{aligned} (\langle 0| \otimes I^{\otimes n})U^\dagger|0\rangle V|\psi\rangle &= \frac{1}{\sin\theta}(\langle 0| \otimes I^{\otimes n})U^\dagger(|0\rangle\langle 0| \otimes I^{\otimes n})U|0\rangle|\psi\rangle \\ &= \frac{1}{\sin\theta} \underbrace{(\langle 0| \otimes I^{\otimes n})U^\dagger(|0\rangle\langle 0| \otimes I^{\otimes n})U(|0\rangle \otimes I^{\otimes n})|\psi\rangle}_{=:Q}. \end{aligned} \quad (4.5)$$

The operator Q defined above satisfies:

$$\begin{aligned} \langle\psi|Q|\psi\rangle &= \|(|0\rangle\langle 0| \otimes I^{\otimes n})U|0\rangle|\psi\rangle\|^2 = \|(|0\rangle\langle 0| \otimes I^{\otimes n})(\sin\theta|0\rangle V|\psi\rangle + \cos\theta|1\rangle|\phi\rangle)\|^2 \\ &= \|\sin\theta|0\rangle V|\psi\rangle\|^2 = \sin^2\theta. \end{aligned}$$

Because this holds for any $|\psi\rangle$, it holds for a basis of eigenvectors of Q , so we can assume that $Q = \sin^2\theta I^{\otimes n}$ by working in the corresponding basis. Further, note that:

$$\begin{aligned} U(\sin\theta|0\rangle|\psi\rangle + \cos\theta|\Psi^\perp\rangle) &= U(\sin\theta|0\rangle|\psi\rangle + \cos\theta U^\dagger (\cos\theta|0\rangle V|\psi\rangle - \sin\theta|1\rangle|\phi\rangle)) \\ &= \sin^2\theta|0\rangle V|\psi\rangle + \sin\theta\cos\theta|1\rangle|\phi\rangle + \cos^2\theta|0\rangle V|\psi\rangle - \cos\theta\sin\theta|1\rangle|\phi\rangle \\ &= |0\rangle V|\psi\rangle. \end{aligned}$$

Thus, using Eq. (4.5):

$$\begin{aligned} \sin^2\theta|\psi\rangle &= Q|\psi\rangle = \sin\theta(\langle 0| \otimes I^{\otimes n})U^\dagger|0\rangle V|\psi\rangle = \sin\theta(\langle 0| \otimes I^{\otimes n})(\sin\theta|0\rangle|\psi\rangle + \cos\theta|\Psi^\perp\rangle) \\ &= \sin^2\theta|\psi\rangle + \sin\theta\cos\theta(\langle 0| \otimes I^{\otimes n})|\Psi^\perp\rangle, \end{aligned}$$

which implies $\sin\theta\cos\theta(\langle 0| \otimes I^{\otimes n})|\Psi^\perp\rangle = 0$ and hence $(\langle 0| \otimes I^{\otimes n})|\Psi^\perp\rangle = 0$, because $\sin\theta\cos\theta \neq 0$ due to $\theta \in (0, \pi/2)$. It follows that $(|0\rangle\langle 0| \otimes I)|\Psi^\perp\rangle = 0$. \square

We use Lem. 4.11 to show that the evolution of the state when using the Grover operator remains in a two-dimensional subspace spanned by $|0\rangle|\psi\rangle$ and $|1\rangle|\phi\rangle$.

Theorem 4.12 (Oblivious amplitude amplification; Lem. 3.6 in [Berry et al., 2014]). *Let U, V be unitaries on $n + 1$ and n qubits respectively, and let $\theta \in (0, \pi/2)$. Suppose that for any n -qubit state $|\psi\rangle$, we have*

$$U|0\rangle|\psi\rangle = \sin\theta|0\rangle V|\psi\rangle + \cos\theta|1\rangle|\phi\rangle,$$

where $|\psi\rangle$ may depend on $|\psi\rangle$. Let $R = 2|0\rangle\langle 0| \otimes I^{\otimes n} - I^{\otimes(n+1)}$ and $G = -UR^\dagger U^\dagger R$. Then for any integer $k > 0$ we have:

$$G^k U|0\rangle|\psi\rangle = \sin((2k+1)\theta)|0\rangle V|\psi\rangle + \cos((2k+1)\theta)|1\rangle|\phi\rangle.$$

Proof. Let $|\Phi\rangle = |0\rangle V|\psi\rangle$, $|\Phi^\perp\rangle = |1\rangle|\phi\rangle$ and let $|\Psi\rangle, |\Psi^\perp\rangle$ be defined as in Lem. 4.11. Then:

$$\begin{aligned} U|\Psi\rangle &= \sin\theta|\Phi\rangle + \cos\theta|\Phi^\perp\rangle \\ U|\Psi^\perp\rangle &= \cos\theta|\Phi\rangle - \sin\theta|\Phi^\perp\rangle, \end{aligned} \tag{4.6}$$

where the last equation is by definition of $|\Psi^\perp\rangle$. Adding these two equations with coefficients $(\sin\theta, \cos\theta)$ and $(\cos\theta, -\sin\theta)$, and then multiplying through by U^\dagger , yields:

$$\begin{aligned} U^\dagger|\Phi\rangle &= \sin\theta|\Psi\rangle + \cos\theta|\Psi^\perp\rangle \\ U^\dagger|\Phi^\perp\rangle &= \cos\theta|\Psi\rangle - \sin\theta|\Psi^\perp\rangle. \end{aligned} \tag{4.7}$$

Then, noting that $R|\Phi\rangle = |\Phi\rangle$ (R is a reflection through the states that have $|0\rangle$ as their first qubit, and $|\Phi\rangle$ is a superposition of states satisfying that property), by relying on basic geometry and Lem. 4.11 we can study the effect of G on $|\Phi\rangle$:

$$\begin{aligned} G|\Phi\rangle &= -UR^\dagger U^\dagger R|\Phi\rangle \\ &= -UR^\dagger(\sin\theta|\Psi\rangle + \cos\theta|\Psi^\perp\rangle) \\ &= -U(\sin\theta|\Psi\rangle - \cos\theta|\Psi^\perp\rangle) \\ &= (\cos^2\theta - \sin^2\theta)|\Phi\rangle - 2\cos\theta\sin\theta|\Phi^\perp\rangle \\ &= \cos 2\theta|\Phi\rangle - \sin 2\theta|\Phi^\perp\rangle, \end{aligned}$$

where for the second equality we used Eq. (4.7), and for the fourth equality we used Eq. (4.6). With very similar calculations ($|\Phi^\perp\rangle$ is orthogonal to $|\Phi\rangle$, hence R acts as a sign flip), using Eq.s (4.6) and (4.7) we find:

$$\begin{aligned} G|\Phi^\perp\rangle &= -UR^\dagger U^\dagger R|\Phi^\perp\rangle = UR^\dagger(\cos\theta|\Psi\rangle - \sin\theta|\Psi^\perp\rangle) \\ &= U(\cos\theta|\Psi\rangle + \sin\theta|\Psi^\perp\rangle) \\ &= 2\cos\theta\sin\theta|\Phi\rangle + (\cos^2\theta - \sin^2\theta)|\Phi^\perp\rangle \\ &= \sin 2\theta|\Phi\rangle + \cos 2\theta|\Phi^\perp\rangle, \end{aligned}$$

thereby showing that G acts as a rotation by 2θ in the subspace spanned by $|\Phi\rangle = |0\rangle|\psi\rangle$ and $|\Phi^\perp\rangle = |1\rangle|\phi\rangle$, from which the desired result follows. \square

Thus, we have shown that we can perform amplitude amplification even with just a copy of $|\psi\rangle$, i.e., without repeatedly using a circuit to prepare it: applying Thm. 4.12 we choose k to maximize the probability of obtaining $V|\psi\rangle$, and the asymptotic scaling is the same as with standard amplitude amplification. All that is necessary to apply Thm. 4.12 is the unitary U that performs the desired operation V on $|\psi\rangle$, and a way to recognize (and reflect through) the subspace where the term $V|\psi\rangle$ appears. In particular, note that for simplicity we considered the case of a single flag qubit, but it is straightforward to extend the analysis to the case with multiple flag qubits, i.e.,

$$U|\vec{0}\rangle_q|\psi\rangle_n = \sin\theta|\vec{0}\rangle_q V|\psi\rangle_n + \cos\theta|\phi\rangle_{n+q}$$

where $|\phi\rangle$ is a state that has no support on $|\vec{0}\rangle_q$ (formally, $|\vec{0}\rangle_q\langle\vec{0}\rangle_q \otimes I|\phi\rangle = 0$). For example, one could simply use a unitary that checks whether all the flag qubits are set correctly, and performs a controlled operation to reduce to the case of a single flag qubit. A formal analysis is available in [Berry et al., 2014].

4.3 Amplitude estimation

Amplitude estimation uses the amplitude amplification framework to estimate the magnitude of an amplitude. In the context of Grover's problem, it leads to the following algorithmic building block: rather than identifying a marked binary string $\vec{\ell}$ in $\{0, 1\}^n$, i.e., a string that can be recognized by a function, we can *count* the total number of marked strings. Trivially, counting the number of solutions also answers the question of existence of a solution. Amplitude estimation has many other applications, besides counting the number of solutions; some of them are discussed in subsequent sections. The technique was introduced in [Brassard et al., 2002].

The problem solved by amplitude estimation can be phrased as follows. Similarly to the discussion in Sect. 4.1.4, the input of the algorithm is:

- (i) A circuit S acting on n qubits that prepares the state:

$$S|\vec{0}\rangle_n := |\psi_0\rangle = \sin\theta|\psi_G\rangle + \cos\theta|\psi_B\rangle,$$

with $\langle\psi_G|\psi_B\rangle = 0$ and $\theta \in [0, \frac{\pi}{2}]$.

- (ii) A controlled circuit CR acting on n qubits, plus one control qubit, that has the following action:

$$CR(|x\rangle_1 \otimes (\alpha_G|\psi_G\rangle + \alpha_B|\psi_B\rangle)) = |x\rangle \otimes ((-1)^x \alpha_G|\psi_G\rangle + \alpha_B|\psi_B\rangle),$$

for any $\alpha_G, \alpha_B \in [-1, 1] : |\alpha_G|^2 + |\alpha_B|^2 = 1$ and $x \in \{0, 1\}$. Note that CR is the controlled version of the reflection operator R in Sect. 4.1.4.

- (iii) A precision parameter $\epsilon > 0$.

- (iv) A maximum failure probability $\delta > 0$.

The goal is to determine $\tilde{\theta}$ such that $|\theta - \tilde{\theta}| \leq \epsilon$ with a probability of success at least $1 - \delta$. Note that estimating θ is equivalent to estimating $\langle\psi_0|\psi_G\rangle = \sin\theta$, up to some (constant) conversion factor to translate between the angle θ and its sine.

Remark 4.13. *It is easily established that the problem stated in this form allows counting the number of marked items, e.g., solutions of a satisfiability problem if the function f computes the value of a given Boolean formula for a given truth assignment of the Boolean variables. Indeed, suppose we have access to $f : \{0, 1\}^n \rightarrow \{0, 1\}$ and we want to determine $|M|$ where $M := \{\vec{j} \in \{0, 1\}^n : f(\vec{j}) = 1\}$; the function f identifies the marked binary strings. Using phase kickback, as discussed in Sect. 2.1, the circuit U_f can be used to implement R using an additional qubit set in the state $(|0\rangle - |1\rangle)/\sqrt{2}$; then we can take $S = H^{\otimes n}$ so that $|\psi_G\rangle = \frac{1}{\sqrt{|M|}} \sum_{\vec{j} \in M} |\vec{j}\rangle$, $|\psi_B\rangle = \frac{1}{\sqrt{2^n - |M|}} \sum_{\vec{j} \in \{0, 1\}^n \setminus M} |\vec{j}\rangle$. These two states are orthogonal, and:*

$$S|\vec{0}\rangle = H^{\otimes n}|\vec{0}\rangle = \sqrt{\frac{|M|}{2^n}} |\psi_G\rangle + \sqrt{\frac{2^n - |M|}{2^n}} |\psi_B\rangle.$$

According to our definition, $\sin\theta = \sqrt{\frac{|M|}{2^n}}$, which implies $|M| = 2^n \sin^2\theta$, so that estimating θ (or, equivalently, $\sin\theta$) allows us to recover an estimate on the number of marked items.

4.3.1 Solution strategy

To solve this problem we rely on properties of the Grover iteration operator $G = SFS^\dagger R$.

Remark 4.14. *In Sect. 4.3.2 we clarify why we assume that R , i.e., the reflection through $|\psi_G\rangle$, is given in the form of a controlled operator. Note that Grover search does not require the controlled version of R . Because we have a controlled version of R , we can of course also apply R , so it is legitimate to study the operator G .*

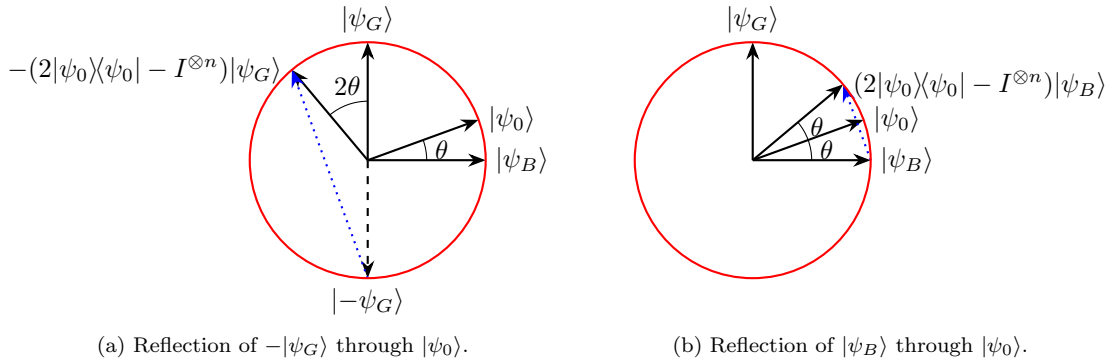


Figure 4.6: Sketch of the two-dimensional plane spanned by $|\psi_G\rangle$ and $|\psi_B\rangle$, to understand the effect of reflections through $|\psi_0\rangle$.

Proposition 4.15. *The states $|\phi_+\rangle = \frac{1}{\sqrt{2}}(|\psi_G\rangle + i|\psi_B\rangle)$, $|\phi_-\rangle = \frac{1}{\sqrt{2}}(|\psi_G\rangle - i|\psi_B\rangle)$ are orthogonal eigenstates of $SFS^\dagger R$ with eigenvalues $e^{2i\theta}$, $e^{-2i\theta}$ respectively.*

Proof. To check that they are eigenstates and find the corresponding eigenvalue, we carry out the matrix-vector multiplication. We use the fact that $(2|\psi_0\rangle\langle\psi_0| - I^{\otimes n})$ is a reflection through $|\psi_0\rangle = \sin\theta|\psi_G\rangle + \cos\theta|\psi_B\rangle$. To see the effect of such a reflection on $-|\psi_G\rangle$ and on $|\psi_B\rangle$, we can rely on Fig. 4.6, together with simple geometry: reflecting $-|\psi_G\rangle$ through $|\psi_0\rangle$ yields $\cos 2\theta|\psi_G\rangle - \sin 2\theta|\psi_B\rangle$ (see Fig. 4.6a), while reflecting $|\psi_B\rangle$ through $|\psi_0\rangle$ yields $\sin 2\theta|\psi_G\rangle + \cos 2\theta|\psi_B\rangle$ (see Fig. 4.6b). Then we have:

$$\begin{aligned} SFS^\dagger R|\phi_+\rangle &= SFS^\dagger \frac{1}{\sqrt{2}}(-|\psi_G\rangle + i|\psi_B\rangle) = (2|\psi_0\rangle\langle\psi_0| - I^{\otimes n}) \frac{1}{\sqrt{2}}(-|\psi_G\rangle + i|\psi_B\rangle) \\ &= \frac{1}{\sqrt{2}}(\cos 2\theta|\psi_G\rangle - \sin 2\theta|\psi_B\rangle + i(\sin 2\theta|\psi_G\rangle + \cos 2\theta|\psi_B\rangle)) \\ &= \frac{1}{\sqrt{2}}(e^{2i\theta}|\psi_G\rangle + ie^{2i\theta}|\psi_B\rangle) = e^{2i\theta}|\phi_+\rangle, \end{aligned}$$

which shows that $|\phi_+\rangle$ is an eigenstate with eigenvalue $e^{2i\theta}$.

The calculations to find the eigenvalue corresponding to $|\phi_-\rangle$ are very similar:

$$\begin{aligned} SFS^\dagger R|\phi_-\rangle &= SFS^\dagger \frac{1}{\sqrt{2}}(-|\psi_G\rangle - i|\psi_B\rangle) = (2|\psi_0\rangle\langle\psi_0| - I^{\otimes n}) \frac{-1}{\sqrt{2}}(|\psi_G\rangle + i|\psi_B\rangle) \\ &= \frac{-1}{\sqrt{2}}(-\cos 2\theta|\psi_G\rangle + \sin 2\theta|\psi_B\rangle + i(\sin 2\theta|\psi_G\rangle + \cos 2\theta|\psi_B\rangle)) \\ &= \frac{1}{\sqrt{2}}(-e^{-2i\theta}|\psi_G\rangle - ie^{-2i\theta}|\psi_B\rangle) = e^{-2i\theta}|\phi_-\rangle. \end{aligned}$$

Finally, orthogonality can be checked by computing the inner product of the two eigenstates, and verifying that it is zero. \square

Given the result in Prop. 4.15, a strategy to compute θ becomes apparent, via the quantum phase estimation algorithm: we can apply phase estimation to the Grover operator G , with the goal of estimating the eigenvalue of one of the two eigenstates $|\phi_+\rangle, |\phi_-\rangle$. However, to apply phase estimation two ingredients are needed: we must be able to prepare one of the two eigenstates $|\phi_+\rangle, |\phi_-\rangle$, and we must be able to implement the controlled operators G^{2^k} for integer k .

Let us turn our attention to the first issue, namely, preparing one of the two eigenstates $|\phi_+\rangle, |\phi_-\rangle$. Recall that by assumption we only know how to prepare $S|\vec{0}\rangle = \sin\theta|\psi_G\rangle + \cos\theta|\psi_B\rangle$.

We show that this state is a linear combination of the two eigenstates above. Indeed, we have:

$$\begin{aligned} S|\vec{0}\rangle &= \sin \theta |\psi_G\rangle + \cos \theta |\psi_B\rangle = \frac{e^{i\theta} - e^{-i\theta}}{2i} |\psi_G\rangle + \frac{e^{i\theta} + e^{-i\theta}}{2} |\psi_B\rangle \\ &= \frac{i}{2} ((-e^{i\theta} + e^{-i\theta}) |\psi_G\rangle - i(e^{i\theta} + e^{-i\theta}) |\psi_B\rangle) \\ &= \frac{i}{2} (-e^{i\theta} (|\psi_G\rangle + i|\psi_B\rangle) + e^{-i\theta} (|\psi_G\rangle - i|\psi_B\rangle)) \\ &= \frac{i}{\sqrt{2}} (-e^{i\theta} |\phi_+\rangle + e^{-i\theta} |\phi_-\rangle). \end{aligned}$$

Thus, $S|\vec{0}\rangle$ is a linear combination (with complex coefficients) of the two eigenstates, and the corresponding coefficients have equal weight in the superposition, i.e., $\left| \frac{-ie^{i\theta}}{\sqrt{2}} \right|^2 = \left| \frac{ie^{-i\theta}}{\sqrt{2}} \right|^2 = \frac{1}{2}$. Because the eigenstates $|\phi_+\rangle, |\phi_-\rangle$ are orthogonal (Prop. 4.15), this decomposition of $S|\vec{0}\rangle$ in terms of eigenstates of the Grover operator is unique (it corresponds to the decomposition of $S|\vec{0}\rangle$ in terms of an eigenbasis of the operator). It follows that if we apply phase estimation to $S|\vec{0}\rangle$, we obtain with equal probability a binary representation of the phase of the eigenvalue corresponding to either of the eigenstates $|\phi_+\rangle, |\phi_-\rangle$, namely, 2θ or -2θ .

Remark 4.16. *More precisely, we obtain a finite-precision representation of $\frac{\theta}{\pi}$ or $-\frac{\theta}{\pi}$, because phase estimation assumes that the phase of the eigenvalue is of the form $2\pi\theta$.*

However, which eigenvalue is obtained does not matter, because by assumption $\theta \in [0, \frac{\pi}{2}]$, hence we can determine with certainty if we obtained $\frac{\theta}{\pi}$ or $-\frac{\theta}{\pi}$ by simply looking at whether we obtained $\theta \leq \frac{1}{2}$ (in which case we must have collapsed onto the eigenstate with eigenvalue 2θ) or $\theta \geq \frac{1}{2}$ (in which case we have collapsed onto the eigenstate with eigenvalue -2θ). Thus, phase estimation leads to an estimate of θ , no matter which of the two eigenvalues we collapse to after measurement. It remains to determine how to construct the controlled operators G^{2^k} for integer k .

4.3.2 Implementation of the amplitude estimation circuit

We now come to the central question of implementing the algorithm described above, so as to estimate its resource requirements. To do so, we first study how to implement the controlled $(SFS^\dagger R)$ operator; then, implementing powers of this operator can be done by simply concatenating multiple copies of the controlled operator.

Remark 4.17. *Implementing a controlled version of G^{2^k} by chaining 2^k copies of controlled- G requires resources (i.e., number of gates) that grow with 2^k , and may therefore be large if k is large. For our purposes, k is as large as m , where m is the number of bits of the phase estimation, which in turn determines the precision of our estimate for θ . In general we cannot do better than this, because we are not assuming much structure on S . However, it is possible that for a specific problem at hand, a more efficient implementation of this operator exists, leading to smaller resource requirements, see also the discussion in Rem. 3.13.*

By assumption we are given access to CR , the controlled version of R . A crucial observation is the fact that to obtain $CG = C(SFS^\dagger R)$, it is sufficient to implement CF . Indeed, consider the circuit in Fig. 4.7. In this circuit, when the control qubit $|x\rangle$ is $|1\rangle$ the full Grover operator

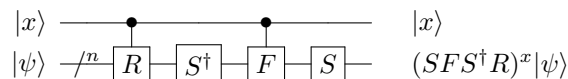


Figure 4.7: Controlled version of the Grover operator, with $x \in \{0, 1\}$.

$(SFS^\dagger R)$ is applied to the second register; if, on the other hand, $|x\rangle = |0\rangle$, the transformation

acts as the identity on the second register, because $SS^\dagger = I^{\otimes n}$. Thus, we only need to determine how to implement CF .

The operator $-F$ is implemented by the circuit in Fig. 4.3, with a global phase factor -1 , see Sect. 4.1.2. Because $-F$ is already a controlled operation with multiple controls, to obtain CF we simply add one more control and one Z gate to get rid of the -1 (otherwise we would implement $C(-F)$, which is not the same as $-CF$, see Rem. 9.38). We obtain the circuit in Fig. 4.8. This can be easily decomposed in terms of CCX gates with some auxiliary qubits.

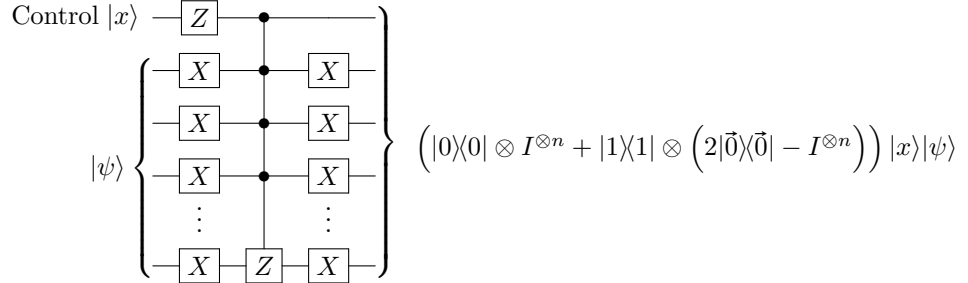


Figure 4.8: Quantum circuit implementing the controlled- F operation (up to a global phase factor) used in the amplitude estimation algorithm.

4.3.3 Summary and resource requirements

We summarize the phase estimation algorithm: the circuits S and CR are given as input (see Sect. 4.3 for a definition), together with parameters $\epsilon, \delta > 0$; the goal is to determine $\tilde{\theta}$ such that $|\theta - \tilde{\theta}| \leq \epsilon$ with a probability of success at least $1 - \delta$.

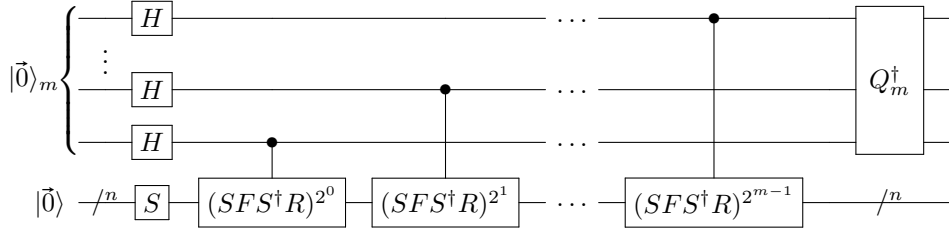
Let $m = \lceil \log \frac{\pi}{\epsilon} \rceil + 2$; by Thm. 3.9, with this number of qubits for phase estimation we obtain θ to precision $\frac{\epsilon}{\pi}$ with probability at least $3/4$. In this setting, it is convenient to pick a constant probability of success for phase estimation, and then repeat the algorithm a few times to boost the probability of obtaining the correct answer.

Remark 4.18. The term $\frac{\pi}{\epsilon}$, rather than $\frac{1}{\epsilon}$, is due to the fact that phase estimation applied to eigenvalues $e^{\pm 2i\theta}$ outputs $\pm \frac{\theta}{\pi}$ rather than $\pm \theta$, so we need to increase the precision slightly.

The algorithm works as follows:

- Initialize the state as $|\vec{0}\rangle_m |\vec{0}\rangle_n$.
- Apply S to the last n qubits (second register) to obtain $|\vec{0}\rangle_m \otimes (\sin \theta |\psi_G\rangle + \cos \theta |\psi_B\rangle)$.
- Run the quantum phase estimation algorithm applied to the operator $G = SFS^\dagger R$, using the first m qubits (first register) to store the phase, and the bottom n qubits to store the “eigenstate” $\sin \theta |\psi_G\rangle + \cos \theta |\psi_B\rangle$. (This is in fact a linear combination of eigenstates.)
- Let \vec{b} be the m -digit binary string obtained as output of phase estimation by measuring the first m qubits. If $b_1 = 1$, i.e., $0.\vec{b} > \frac{1}{2}$, return $\tilde{\theta} = \pi(1 - 0.\vec{b})$; otherwise, return $\tilde{\theta} = \pi 0.\vec{b}$.

This algorithm uses $n + m$ qubits, plus all qubits necessary for auxiliary space, for example for the implementation of the CF operation, as well as the implementation of the black-box circuits S and CR . The gate complexity is $\mathcal{O}(2^m(n + T_S + T_{CR}) + m^2)$, where T_S is the gate complexity of S , and T_{CR} is the gate complexity of CR . This is because phase estimation uses $\mathcal{O}(2^m)$ applications of the Grover operator, and each application involves one call to S , one call to S^\dagger , one call to CR , and one application of CF , which uses $\mathcal{O}(n)$ gates if implemented as in Fig. 4.8. The final $\mathcal{O}(m^2)$ gates are for the inverse quantum Fourier transform. Considering our choice of $m = \lceil \log \frac{\pi}{\epsilon} \rceil + 2$, the complexity amounts to $\mathcal{O}(\frac{1}{\epsilon})$ applications of S and CR , and $\mathcal{O}(\frac{1}{\epsilon} \log^2 \frac{1}{\epsilon})$ additional gates: this yields the correct answer with probability $3/4$. To boost the probability of success to $1 - \delta$ we can repeat the algorithm a few times and output the majority answer, with $\mathcal{O}(\log \frac{1}{\delta})$ repetitions of the algorithm with constant success probability.


 Figure 4.9: Amplitude estimation circuit with m bits of precision.

4.3.4 Amplitude estimation for counting and probability estimation

We discuss an application of amplitude estimation to count marked items, as introduced in Rem. 4.13. In this setting, suppose we have access to $f : \{0, 1\}^n \rightarrow \{0, 1\}$ and we want to determine $|M|$ where $M := \{\vec{j} \in \{0, 1\}^n : f(\vec{j}) = 1\}$; the function f identifies the marked binary strings. We use $S = H^{\otimes n}$ and set $|\psi_G\rangle = \frac{1}{\sqrt{|M|}} \sum_{\vec{j} \in M} |\vec{j}\rangle$, $|\psi_B\rangle = \frac{1}{\sqrt{2^n - |M|}} \sum_{\vec{j} \in \{0, 1\}^n \setminus M} |\vec{j}\rangle$. As remarked in Rem. 4.13, $\sin \theta = \sqrt{\frac{|M|}{2^n}}$, which implies $|M| = 2^n \sin^2 \theta$. We first give a bound on the distance between $\sin^2 \tilde{\theta}$ and $\sin^2 \theta$ based on the distance between the angles.

Proposition 4.19 (Lem. 7 in [Brassard et al., 2002]). *Let $a = \sin^2 \theta$, $\tilde{a} = \sin^2 \tilde{\theta}$ with $0 \leq \theta, \tilde{\theta} \leq 2\pi$. Then*

$$|\theta - \tilde{\theta}| \leq \epsilon \implies |a - \tilde{a}| \leq 2\epsilon \sqrt{a(1-a)} + \epsilon^2.$$

Proof. Using trigonometric identities, we have:

$$\begin{aligned} \sin^2(\theta + \epsilon) - \sin^2 \theta &= (\sin \theta \cos \epsilon + \sin \epsilon \cos \theta)^2 - \sin^2 \theta \\ &= \sin^2 \theta \cos^2 \epsilon + \cos^2 \theta \sin^2 \epsilon + 2 \sin \theta \sin \epsilon \cos \theta \cos \epsilon - \sin^2 \theta. \end{aligned}$$

We rewrite this, using $\cos^2 \epsilon = 1 - \sin^2 \epsilon$, $2 \sin \epsilon \cos \epsilon = \sin 2\epsilon$, $\sin \theta = \sqrt{a}$, $\cos \theta = \sqrt{1-a}$, and obtain:

$$\sin^2(\theta + \epsilon) - \sin^2 \theta = \sqrt{a(1-a)} \sin 2\epsilon + (1-2a) \sin^2 \epsilon.$$

Using similar transformations, we obtain:

$$\sin^2 \theta - \sin^2(\theta - \epsilon) = \sqrt{a(1-a)} \sin 2\epsilon + (2a-1) \sin^2 \epsilon.$$

Finally, using the fact that $\sin x \leq x \forall x \geq 0$, and $|2a-1| \leq 1$, we have:

$$|a - \tilde{a}| \leq \max\{\sin^2(\theta + \epsilon) - \sin^2 \theta, \sin^2 \theta - \sin^2(\theta - \epsilon)\} \leq 2\epsilon \sqrt{a(1-a)} + \epsilon^2.$$

□

Based on this, we can already determine if $\theta = 0$ or not.

Example 4.20. *Suppose our goal is to determine if $|M| = 0$ or not. We choose $\delta = 1/4$ and $\epsilon = 2^{-(n/2+2)}$; this tells us that we should use $m = \lceil \log(\frac{2^{n/2+5}}{\pi}) \rceil = \mathcal{O}(\frac{n}{2})$ qubits of precision for phase estimation. When $|M| = 0$, $\theta = 0$, $a = 0$ and Prop. 4.19 tells us that we have:*

$$|a - \tilde{a}| \leq \frac{1}{2^{2\lceil \frac{n}{2} + 2 \rceil}} = \frac{1}{2^4 \cdot 2^n}.$$

Hence, from our estimate $\tilde{\theta}$ we compute \tilde{a} , and when rounding this value to the closest integer (because the number of solutions has to be an integer) we obtain 0 with probability at least 3/4.

Now assume $|M| = 1$. Then by Prop. 4.19 have:

$$|a - \tilde{a}| \leq 2 \frac{\sqrt{\frac{1}{2^n} (1 - \frac{1}{2^n})}}{2^{2\lceil \frac{n}{2} + 2 \rceil}} + \frac{1}{2^{2\lceil \frac{n}{2} + 2 \rceil}} < \frac{1}{4} \frac{\sqrt{(1 - \frac{1}{2^n})}}{2^n} + \frac{1}{2^4 \cdot 2^n} < \frac{1}{2 \cdot 2^n},$$

so the number of solutions, rounded to the nearest integer, is a value $\neq 0$ with probability at least $3/4$. If $|M| > 1$, the probability to obtain 0 is even lower. It is therefore easy to distinguish the two cases $|M| = 0$ and $|M| \neq 0$. Because $m = \mathcal{O}\left(\frac{n}{2}\right)$, the query complexity of this algorithm (number of applications of the unitary U_f implementing the marking function f) is $\mathcal{O}\left(\sqrt{2^n}\right)$.

Using a similar analysis to the one employed in the derivation of Thm. 3.12 for phase estimation with m qubits, [Brassard et al., 2002] also shows the following (which is the direct analog of Thm. 3.12 in the context of amplitude estimation).

Proposition 4.21 (Thm. 12 in [Brassard et al., 2002]). *Suppose that we apply the amplitude estimation algorithm using m qubits for phase estimation. Define $a = \sin^2 \theta, \tilde{a} = \sin^2 \tilde{\theta}$ with $0 \leq \theta, \tilde{\theta} \leq 2\pi$. Then the algorithm produces an estimate \tilde{a} such that:*

$$|a - \tilde{a}| \leq 2\pi \frac{\sqrt{a(1-a)}}{2^m} + \frac{\pi^2}{2^{2m}} \quad (4.8)$$

with probability at least $\frac{8}{\pi^2}$.

This implies the following simplified statement of the complexity of amplitude estimation.

Corollary 4.22. *Suppose we want to estimate the probability $\sin^2 \theta$ of obtaining $|\psi_G\rangle$ from a measurement of $S|\vec{0}\rangle$. To obtain an estimate with absolute error at most ϵ using amplitude estimation, it is sufficient to use $m = \mathcal{O}\left(\log \frac{1}{\epsilon}\right)$ qubits for phase estimation, leading to $\mathcal{O}\left(\frac{1}{\epsilon}\right)$ queries to the input unitaries S and CR to carry out the algorithm.*

Remark 4.23. *Cor. 4.22 provides a quadratic speedup over classical estimation via the empirical average of a number of samples (see Sect. 4.3.5), but it does not discuss the bias of the estimator for a , which unfortunately can be poor. However, with more advanced techniques amplitude estimation can be made unbiased [Cornelissen and Hamoudi, 2023, Rall and Fuller, 2023], or rather, it can be modified to efficiently reduce the bias (i.e., the cost of the reduction of the bias is merely polylogarithmic in the reduction factor), see the notes in Sect. 4.5.*

4.3.5 Application to Monte Carlo simulation

Amplitude estimation finds a direct application in Monte Carlo simulation. The crucial observation is that the precision of the estimate grows linearly with the number of samples, rather than with the square root of the number of samples. Indeed, this can be observed in Prop. 4.21, by looking at the error estimates: obtaining $a = \sin^2 \theta$ with precision ϵ requires $\mathcal{O}\left(\log \frac{1}{\epsilon}\right)$ qubits to store the outcome of phase estimation, and therefore $\mathcal{O}\left(\frac{1}{\epsilon}\right)$ calls to the unitary S preparing $\sin \theta |\psi_G\rangle + \cos \theta |\psi_B\rangle$. The linear scaling is stated explicitly in Cor. 4.22. This is better scaling than in classical Monte Carlo techniques, where the number of samples that one needs to obtain from a random variable grows quadratically with the precision; i.e., we generally need $\mathcal{O}\left(\frac{1}{\epsilon^2}\right)$ samples, and therefore calls to a function constructing a sample from the desired probability distribution, to obtain an estimate with precision ϵ . We formalize this next, also explaining why the comparison between calls to S (for the quantum case) and classical samples makes sense, at least from some point of view — see Rem. 4.24.

Suppose we are given a discrete random variable X with sample space $\Omega = \{0, 1\}^n$ and $\Pr(X = \vec{j}) = p_j$. Let P be the unitary that maps:

$$P|\vec{0}\rangle_n = \sum_{\vec{j} \in \{0,1\}^n} \sqrt{p_j} |\vec{j}\rangle. \quad (4.9)$$

Such a unitary can be implemented with $\mathcal{O}(2^n)$ basic gates in general, see Sect. 5.2; more efficient implementations, possibly with complexity polynomial in n , exist for distributions with certain properties, see the notes in Sect. 4.5. Suppose further that our goal is to compute the expected value of a function $f : \{0, \frac{1}{2^n}, \dots, \frac{2^n-1}{2^n}\} \rightarrow [0, 1]$, which we assume to be given as the following quantum oracle on $n+1$ qubits:

$$U_f(|\vec{j}\rangle_n \otimes |0\rangle) = |\vec{j}\rangle \otimes \left(\sqrt{1-f(0.\vec{j})} |0\rangle + \sqrt{f(0.\vec{j})} |1\rangle \right).$$

Because f is defined over fractions, the binary string \vec{j} corresponds to the argument $0.\vec{j}$ of the function (i.e., \vec{j} represents the number $j/2^n$): this yields a natural mapping that simplifies subsequent calculations. Note that if we have a binary oracle for f , we can implement the above transformation as a controlled rotation on the last qubit (i.e., we first use the binary oracle to output a binary description of $f(0.\vec{j})$, then we apply rotations controlled on the individual bits of $f(0.\vec{j})$ to rotate the last qubit by the corresponding amount). Thus, we can apply the amplitude estimation algorithm onto the state:

$$U_f(P|\vec{0}\rangle_n \otimes |0\rangle) = \sum_{\vec{j} \in \{0,1\}^n} \sqrt{1-f(0.\vec{j})} \sqrt{p_j} |\vec{j}\rangle |0\rangle + \sum_{\vec{j} \in \{0,1\}^n} \sqrt{f(0.\vec{j})} \sqrt{p_j} |\vec{j}\rangle |1\rangle,$$

aiming to estimate the amplitude of the part of the state that has $|1\rangle$ in the last qubit, i.e., $\sum_{\vec{j} \in \{0,1\}^n} \sqrt{f(0.\vec{j})} \sqrt{p_j} |\vec{j}\rangle |1\rangle$.

Remark 4.24. *In this setting, one application of the unitary P is equivalent to one classical sample in the following sense: if we prepare the state $P|\vec{0}\rangle$ and then apply a measurement to all qubits, we obtain the string \vec{j} with probability p_j . This is exactly what we would obtain from a classical sample from the discrete probability distribution encoded by the vector p . Thus, we can simulate one classical sample by applying the unitary P once on a quantum computer. This implies that an application of P is more powerful than the construction of one classical sample: using P once we can simulate a classical sample, but the converse may not be true. The state produced in Eq. 4.9 is often called a qsample in the literature, because it is the quantum generalization of a classical sample.*

To solve the problem stated above using amplitude estimation, we let:

$$\begin{aligned} |\psi_G\rangle &:= \frac{1}{\sqrt{\sum_{\vec{j} \in \{0,1\}^n} f(0.\vec{j}) p_j}} \sum_{\vec{j} \in \{0,1\}^n} \sqrt{f(0.\vec{j})} \sqrt{p_j} |\vec{j}\rangle |1\rangle \\ |\psi_B\rangle &:= \frac{1}{\sqrt{\sum_{\vec{j} \in \{0,1\}^n} (1-f(0.\vec{j})) p_j}} \sum_{\vec{j} \in \{0,1\}^n} \sqrt{1-f(0.\vec{j})} \sqrt{p_j} |\vec{j}\rangle |0\rangle, \end{aligned}$$

and these are orthogonal states because there is no overlap in the last qubit. The state preparation circuit S is set to be $U_f P$, and we have:

$$S|\vec{0}\rangle_{n+1} = U_f P|\vec{0}\rangle = \sqrt{\sum_{\vec{j} \in \{0,1\}^n} f(0.\vec{j}) p_j} |\psi_G\rangle + \sqrt{\sum_{\vec{j} \in \{0,1\}^n} (1-f(0.\vec{j})) p_j} |\psi_B\rangle. \quad (4.10)$$

With these definitions, we have $\sin^2 \theta = \sum_{\vec{j} \in \{0,1\}^n} f(0.\vec{j}) p_j = \mathbb{E}[f(X)]$. Thus, estimating θ and therefore $\sin^2 \theta$ leads to an estimation of $\mathbb{E}[f(X)]$. If we are interested in the expected value of X , we can, for example, choose $f(0.\vec{j}) = \frac{j}{2^n - 1}$ (recall that $j \in \{0, \dots, 2^n - 1\}$, so this normalizes the output), which leads to estimating $\mathbb{E}[\frac{X}{2^n - 1}]$ and hence $\mathbb{E}[X]$. If we are interested in higher-order moments of X , we could choose $f(0.\vec{j}) = (\frac{j}{2^n - 1})^2$ to estimate $\mathbb{E}[X^2]$, and so on.

Let us discuss the sample complexity of estimating $\mathbb{E}[f(X)]$. Computing $\mathbb{E}[f(X)]$ with classical Monte Carlo yields a standard deviation of the estimator that scales with the square root of the number of samples, by central limit theorem; thus, to obtain an estimate with error $\pm \epsilon$ with high probability, classically we use $\mathcal{O}(\frac{1}{\epsilon^2})$ samples and therefore we perform that many calls to an algorithm that collects the samples (in the quantum setting, the complexity of that algorithm is the same as the gate complexity of circuit P), followed by evaluation of f on each sample. On the other hand, by Prop. 4.21, quantum amplitude estimation has query complexity $\mathcal{O}(\frac{1}{\epsilon})$, i.e., it performs that many calls to U_f and P . Indeed, it is sufficient to use $q = \mathcal{O}(\log \frac{1}{\epsilon})$ qubits to store the output of the phase estimation, leading to $\mathcal{O}(2^q) = \mathcal{O}(\frac{1}{\epsilon})$ applications of U_f and P . The discussion for different choices of the function f is similar.

Remark 4.25. *The statement on the asymptotic behavior in terms of the number of calls to f is accurate, but potentially misleading: in order to apply the quantum algorithm we need access to P*

and to a quantum oracle for f , i.e., to U_f , whereas classically we just need sampling access to f . In other words, classically we only need to be able to draw samples from $f(X)$, whereas in the quantum algorithm described above we must have access to a circuit that prepares the natural quantum encoding of the distribution of X (i.e., the unitary of Eq. (4.9)), and we must be able to implement f as a quantum circuit. In theory this is not an issue, because any function that can be classically computed can also be simulated with a quantum circuit with at most polynomial overhead; however, in practice this requires knowing an explicit algorithm (that can then be translated into a Boolean circuit) to compute f . Certain types of function may not be computable by a Boolean circuit. For example, if we are trying to estimate how many people like the color green more than the color red, a classical sampling algorithm may involve asking people on the street what they prefer and recording the answer, but there is no quantum oracle that can perform the same task.

We end this section with an example, but we first need to define a certain gate.

Definition 4.26 (*Y rotation gate*). The gate $R_Y(\theta)$ is defined as the matrix:

$$R_Y(\theta) := \begin{pmatrix} \cos \theta/2 & -\sin \theta/2 \\ \sin \theta/2 & \cos \theta/2 \end{pmatrix}.$$

The factor $\frac{1}{2}$ in the angles appearing in $R_Y(\theta)$ may look confusing, but this is the convention, and it comes from an interpretation of this gate as a rotation in a certain geometric representation of the space of single-qubit quantum states. We discuss other gates of this form in Ch. 9. (In the language of matrix exponentials, $R_Y(2\theta) = e^{-i\theta Y}$; for readers not familiar with this notation yet, this remark can be ignored until the corresponding discussion in Ch. 9.)

Example 4.27. Let us look at a toy amplitude estimation example, inspired by [Woerner and Egger, 2019]. (For this toy problem, all calculations could be easily done by hand.) Suppose we are trying to determine the expected value of a quantity that takes the value V_h with probability p , and the value V_ℓ with probability $1 - p$. This can correspond to a number of situations, e.g., determining the value of an asset whenever there are two possible outcomes for a random event that determines its value. This example can also be generalized to multiple possible outcomes, but the construction of the circuit becomes considerably more involved and it would complicate this example. The expected value that we want to estimate is thus:

$$V = (1 - p)V_\ell + pV_h.$$

Let us renormalize so that $V_\ell = 0, V_h = 1$. Note that this renormalization does not affect the final outcome: if we can estimate the expected value in the rescaled range $[0, 1]$, we can transform it back to the original range $[V_\ell, V_h]$ with a linear transformation; the absolute error attained by the estimation procedure would have to be rescaled accordingly.

Because there are two possible scenarios, uncertainty can be represented with a single qubit. Furthermore, the amplitude coefficients $\sqrt{f(0)}$, $\sqrt{1 - f(0)}$ in the state in Eq. (4.10), onto which amplitude estimation is applied, are either 0 or 1, because we normalized the value $f(0) = V_\ell = 0, f(1) = V_h = 1$. Hence, the target state is:

$$\begin{aligned} S|00\rangle &= \sqrt{1 - p}|0\rangle \otimes (\sqrt{1 - f(0)}|0\rangle + \sqrt{f(0)}|1\rangle) + \sqrt{p}|1\rangle \otimes (\sqrt{1 - f(1)}|0\rangle + \sqrt{f(1)}|1\rangle) \\ &= \sqrt{1 - p}|00\rangle + \sqrt{p}|11\rangle. \end{aligned}$$

We can prepare this state by applying the circuit given in Fig. 4.10 onto the state $|00\rangle$. In this circuit we use the Y rotation R_Y , as defined in Def. 4.26, with angle γ set to $\gamma = 2 \sin^{-1} \sqrt{p}$ to obtain the correct amplitudes.

We then need to implement the controlled reflection circuits: CR (reflection through $|\psi_B\rangle$) and CF (reflection through $|\vec{0}\rangle$). In this case, we can implement both circuits with a doubly-controlled-Z gate. Indeed, because $|\psi_G\rangle = |11\rangle$, a CZ gate applies a sign-flip to $|11\rangle$ and implements CR; and the reflection through $|\vec{0}\rangle$, given by $2|\vec{0}\rangle\langle\vec{0}| - I^{\otimes 2}$, can be constructed in the way discussed in Sect. 4.1.2, i.e., with multiply-controlled Z and some X gates. Thus, an application of the controlled Grover operator $CG = (I \otimes S)CF(I \otimes S^\dagger)CR$ is given by the circuit in Fig. 4.11.

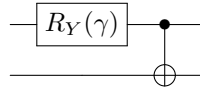


Figure 4.10: State preparation circuit S for the amplitude estimation example.

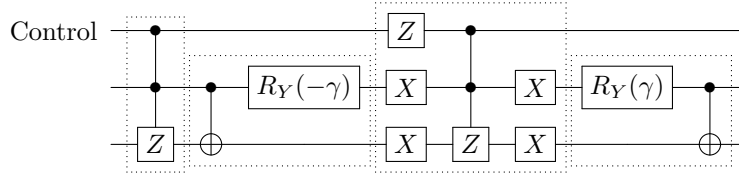


Figure 4.11: Controlled Grover operator $SFS^\dagger R$. The four boxes represent the circuits CR , S^\dagger , CF , S (from the left to the right, in this order).

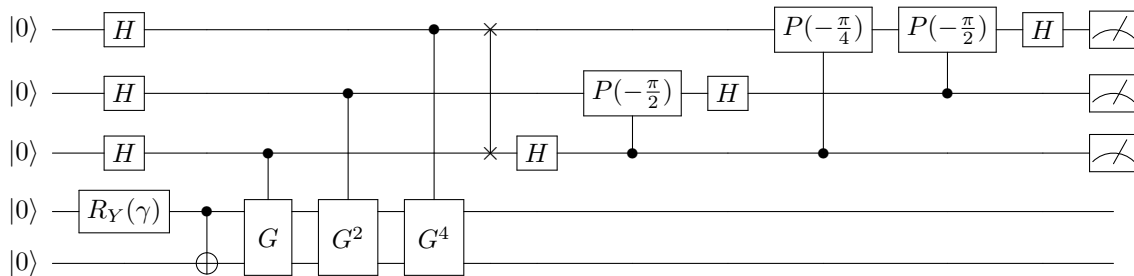


Figure 4.12: Quantum amplitude estimation circuit on two qubits.

We can now construct the full quantum amplitude estimation algorithm. If we use three qubits to store the outcome of the estimation, the full circuit is given in Fig. 4.12. Running some simulations, for $p = 0.75$ with 2048 repetitions, we find that the the distribution of the measurement outcomes is as given in Tab. 4.1. Recall that $\sin^2 \theta$ is the estimate of the probability of observing

\vec{b}	$\sin^2 \tilde{\theta}$	Count
000	0.00000	38
001	0.14645	44
010	0.50000	177
011	0.85355	687
100	1.00000	104
101	0.85355	764
110	0.50000	186
111	0.14645	48

Table 4.1: Measurement outcomes of the amplitude estimation example; we use the notation of Sect. 4.3.3.

$|\psi_G\rangle$, and therefore it should be close to p . We find that the most likely outcome corresponds to ≈ 0.85 , which is fairly close to the original value $p = 0.75$. Notice that with only 3 qubits of precision, the discretization of the possible output values is coarse, and 0.85 is the closest value to the correct answer given this level of granularity.

4.3.6 Searching when the number of marked items is not known

We now revisit Grover’s algorithm and amplitude amplification to show how one can search in time $\mathcal{O}\left(\sqrt{2^n/|M|}\right)$ even when $|M| = |\{\vec{\ell} \in \{0,1\}^n : f(\vec{\ell}) = 1\}|$ is not known. To achieve this result, we rely on amplitude estimation. In the setting of Sect. 4.2, assume $\theta \in (0, \frac{\pi}{2})$. Consider the amplitude estimation circuit in Fig. 4.9; we have seen that the bottom n qubit lines (second

register) are in a superposition of two eigenstates $|\phi_+\rangle, |\phi_-\rangle$ of the Grover operator. Then we can express the output of the amplitude estimation circuit in the following way:

$$\frac{i}{\sqrt{2}} (-e^{i\theta}|\vartheta_+\rangle|\phi_+\rangle + e^{-i\theta}(|\vartheta_-\rangle|\phi_-\rangle)) = \frac{1}{\sqrt{2}} (|\vartheta_+\rangle|\phi_+\rangle - e^{-i2\theta}(|\vartheta_-\rangle|\phi_-\rangle)), \quad (4.11)$$

up to a global phase factor (we can ignore the i in front and multiply everything by $-e^{-i\theta}$ to obtain the expression on the r.h.s.), where $|\vartheta_+\rangle, |\vartheta_-\rangle$ are the m -qubit normalized quantum states produced by the amplitude estimation circuit, and which we analyze in the following. We claim that as the number m of qubits used for the phase estimation increases, the two states $|\vartheta_+\rangle, |\vartheta_-\rangle$ get more and more orthogonal.

Lemma 4.28. *For the quantum state in Eq. (4.11), with m qubits for the first register (containing $|\vartheta_+\rangle, |\vartheta_-\rangle$), it holds that $|\langle\vartheta_-\|\vartheta_+\rangle| = \mathcal{O}(\frac{1}{2^m\theta})$.*

Before giving a formal proof, we provide an intuitive argument. Suppose that the angle θ is exactly representable on m bits: then $|\vartheta_+\rangle, |\vartheta_-\rangle$ are basis states corresponding to the binary representation of $\theta, -\theta$, and they are orthogonal for $\theta \neq 0$ because $\theta \neq -\theta$. However in general θ is not representable on m bits (in fact, in this section we have not specified how we plan to choose m yet). In this case $|\vartheta_+\rangle, |\vartheta_-\rangle$ are superpositions with amplitudes that concentrate on some m -bit representation of the angles $\theta, -\theta$, but their overlap may not be zero. If m is chosen large enough, however, almost all of the weight in the superposition is on the basis states corresponding to the binary representation of $\theta, -\theta$, hence $|\vartheta_+\rangle, |\vartheta_-\rangle$ are almost orthogonal. This is the main idea; we now proceed with the proof.

Proof. Let us write down analytical expressions for $|\vartheta_+\rangle$ and $|\vartheta_-\rangle$. For $|\vartheta_+\rangle$ we can assume that the bottom n qubit lines in Fig. 4.9 contain $|\phi_+\rangle$, and similarly for $|\vartheta_-\rangle$ we can assume that they contain $|\phi_-\rangle$. The circuit in Fig. 4.9 first creates a uniform superposition over m qubits, then applies phase kickback, finally applies the inverse QFT. Carrying out the calculations, and using index \vec{k} to sum over the initial uniform superposition, and index \vec{j} for the superposition created by the inverse QFT, we obtain:

$$\begin{aligned} |\vartheta_+\rangle &= \frac{1}{\sqrt{2^m}} \sum_{\vec{k} \in \{0,1\}^m} e^{2i\theta k} \sum_{\vec{j} \in \{0,1\}^m} \frac{1}{\sqrt{2^m}} e^{-2\pi i j k / 2^m} |\vec{j}\rangle = \frac{1}{2^m} \sum_{\vec{j}, \vec{k} \in \{0,1\}^m} e^{2i(\theta - \pi j / 2^m)k} |\vec{j}\rangle \\ |\vartheta_-\rangle &= \frac{1}{\sqrt{2^m}} \sum_{\vec{k} \in \{0,1\}^m} e^{-2i\theta k} \sum_{\vec{j} \in \{0,1\}^m} \frac{1}{\sqrt{2^m}} e^{-2\pi i j k / 2^m} |\vec{j}\rangle = \frac{1}{2^m} \sum_{\vec{j}, \vec{k} \in \{0,1\}^m} e^{2i(-\theta - \pi j / 2^m)k} |\vec{j}\rangle. \end{aligned}$$

Now we take the inner product of the two states:

$$\begin{aligned} \langle\vartheta_-\|\vartheta_+\rangle &= \frac{1}{4^m} \sum_{\vec{j} \in \{0,1\}^m} \sum_{\vec{k} \in \{0,1\}^m} e^{2i(\theta - \pi j / 2^m)k} \sum_{\vec{\ell} \in \{0,1\}^m} e^{2i(\theta + \pi j / 2^m)\ell} \\ &= \frac{1}{4^m} \sum_{\vec{j} \in \{0,1\}^m} \sum_{\vec{k}, \vec{\ell} \in \{0,1\}^m} e^{2i\theta(k+\ell)} e^{2\pi i j / 2^m (\ell - k)} \\ &= \frac{1}{4^m} \sum_{\vec{k}, \vec{\ell} \in \{0,1\}^m} \left[e^{2i\theta(k+\ell)} \sum_{\vec{j} \in \{0,1\}^m} e^{2\pi i j / 2^m (\ell - k)} \right]. \end{aligned} \quad (4.12)$$

Using the formula for a geometric series, when $\ell \neq k$ we have:

$$\sum_{\vec{j} \in \{0,1\}^m} e^{2\pi i j / 2^m (\ell - k)} = \sum_{j=0}^{2^m-1} e^{2\pi i j / 2^m (\ell - k)} = \frac{1 - e^{2\pi i (\ell - k)}}{1 - e^{2\pi i (\ell - k) / 2^m}} = 0,$$

where the last equality is due to the fact that for $\ell \neq k$, $e^{2\pi i (\ell - k)} = 1$. On the other hand, if $\ell = k$ we have:

$$\sum_{\vec{j} \in \{0,1\}^m} e^{2\pi i j / 2^m (\ell - k)} = 2^m,$$

This is a possibly-outdated preprint, using the author's lecture notes, of the book "Quantum algorithms for optimizers," edited by SIAM. All rights to the book's material belong to SIAM. Please refer to the SIAM version of the book.

because each term of the summation is 1. Back to Eq. 4.12: using what we just discussed, the only nonzero terms in the summation satisfy $\ell = k$, and simplifying using the expression for the case $\ell = k$ we have:

$$\langle \vartheta_- | \vartheta_+ \rangle = \frac{1}{2^m} \sum_{\vec{k} \in \{0,1\}^m} e^{4i\theta k} = \frac{1}{2^m} \frac{1 - e^{4i\theta 2^m}}{1 - e^{4i\theta}}.$$

Now taking the modulus, we obtain:

$$\begin{aligned} |\langle \vartheta_- | \vartheta_+ \rangle| &\leq \frac{1}{2^m} \frac{2}{|1 - e^{4i\theta}|} = \frac{1}{2^m} \frac{2}{\sqrt{(1 - \cos 4\theta)^2 + \sin^2 4\theta}} = \frac{1}{2^m} \sqrt{\frac{2}{1 - \cos 4\theta}} = \frac{1}{2^m \sin 2\theta} \\ &= \mathcal{O}\left(\frac{1}{2^m \theta}\right). \end{aligned}$$

For the third equality, we used the half-angle identity $\sin(\alpha/2) = \pm \sqrt{(1 - \cos \alpha)/2}$. \square

This shows that increasing m makes the $|\vartheta_+\rangle, |\vartheta_-\rangle$ more and more orthogonal. In particular, whenever $2^m \gg \frac{1}{\theta}$, the two states are essentially orthogonal. Suppose, for the sake of analysis, that the states $|\vartheta_+\rangle, |\vartheta_-\rangle$ are indeed orthogonal. To compute the probability of observing $|\psi_G\rangle$ when performing a measurement on the second register, we switch to the density matrix formalism. The density matrix associated with the entire system described in Eq. (4.11) is:

$$\frac{1}{2} (|\vartheta_+\rangle\langle\vartheta_+| \otimes |\phi_+\rangle\langle\phi_+| - e^{i2\theta} |\vartheta_+\rangle\langle\vartheta_-| \otimes |\phi_+\rangle\langle\phi_-| - e^{-i2\theta} |\vartheta_-\rangle\langle\vartheta_+| \otimes |\phi_-\rangle\langle\phi_+| + |\vartheta_-\rangle\langle\vartheta_-| \otimes |\phi_-\rangle\langle\phi_-|),$$

and if we trace out the first register, using $\langle \vartheta_- | \vartheta_+ \rangle = 0$ and then using the definition of $|\phi_+\rangle, |\phi_-\rangle$, we obtain:

$$\frac{1}{2} (|\phi_+\rangle\langle\phi_+| + |\phi_-\rangle\langle\phi_-|) = \frac{1}{2} (|\psi_G\rangle\langle\psi_G| - |\psi_B\rangle\langle\psi_B|).$$

From this equation, we see that the probability of observing $|\psi_G\rangle$ (rather, one of the basis states constituting $|\psi_G\rangle$) when performing a measurement on the second register is $\frac{1}{2}$.

In this analysis, we used the orthogonality of $|\vartheta_+\rangle$ and $|\vartheta_-\rangle$ to simplify the expression of the state when tracing out the first register; otherwise, the expression still contains some cross-terms. If $|\vartheta_+\rangle, |\vartheta_-\rangle$ are not orthogonal, then the probability of observing a basis state from $|\psi_G\rangle$ is at least $\frac{1}{2} - \mathcal{O}\left(\frac{1}{2^m \theta}\right)$, because in the worst case the probability decreases by $|\langle \vartheta_- | \vartheta_+ \rangle|$, and Lem. 4.28 bounds this value. Hence, repeating this circuit twice, we obtain a marked item (i.e., a binary string corresponding to a basis state in $|\psi_G\rangle$), and hence in the set of all solutions M with probability at least $\frac{3}{4} - \mathcal{O}\left(\frac{1}{2^m \theta}\right)$. Relying on this idea, Alg. 1 determines a marked item by increasing m in an iterative fashion. If a marked item is not found before reaching $m = n$, then the algorithm resorts to full enumeration of the binary strings. The intuition is that as soon as $2^m > \theta$, it only takes a few iterations of the “while” loop to have a high probability of success, and each loop execution uses $\mathcal{O}\left(\frac{1}{\theta}\right)$ applications of f , i.e., of the Grover operator.

Theorem 4.29 (Quantum search; [Boyer et al., 1998, Brassard et al., 2002]). *If $\theta > 0$, Alg. 1 returns a value \vec{j} such that $f(\vec{j}) = 1$. The expected number of applications of the circuit U_f implementing f is $\mathcal{O}\left(\frac{1}{\theta}\right)$. If $\theta = 0$, the algorithm returns “no solution” and uses $\mathcal{O}(2^n)$ queries to f .*

Proof. We give a sketch of the proof. Let m_0 be chosen so that $1/(2^{m_0} \sin 2\theta) < 1/10$; hence, $m_0 = \mathcal{O}\left(\log \frac{1}{\theta}\right)$. Let us consider the number of applications of U_f that the algorithm performs when $m \leq m_0$. Because for each value of m we use $\mathcal{O}(2^m)$ applications of U_f , this number is:

$$\mathcal{O}\left(\sum_{k=1}^{m_0} 2^k\right) = \mathcal{O}(2^{m_0}) = \mathcal{O}\left(\frac{1}{\theta}\right).$$

Algorithm 1: Quantum search algorithm (without knowing the number of marked items).

Input: Unitary U_f to evaluate $f : \{0, 1\}^n \rightarrow \{0, 1\}$.

Output: Index $\vec{\ell}$ such that $f(\vec{\ell}) = 1$, or “no solution” if no such $\vec{\ell}$ exists.

```

1 Initialize: As in Rem. 4.13, let  $S = H^{\otimes n}$ , and let  $R$  be the reflection unitary mapping
    $|\vec{j}\rangle \rightarrow (-1)^{f(\vec{j})}|\vec{j}\rangle$  constructed using  $U_f$ .
2 Set  $m \leftarrow 1$ .
3 while  $m < n$  do
4   for  $i = 1, 2$  do
5     Apply the amplitude estimation circuit (Fig. 4.9) with  $m$  qubits of precision.
6     Measure the second register to obtain a string  $\vec{j} \in \{0, 1\}^n$ .
7     if  $f(\vec{j}) = 1$  then
8       return  $\vec{j}$ .
9     end
10  end
11  Set  $m \leftarrow m + 1$ .
12 end
13 for  $\vec{j} \in \{0, 1\}^n$  do
14   if  $f(\vec{j}) = 1$  then
15     return  $\vec{j}$ .
16   end
17 end
18 return “no solution”.

```

Now let us consider the expected number of applications of U_f that the algorithm performs when $m > m_0$. By our choice of m_0 , each iteration is successful with probability at least $3/4 - \mathcal{O}(\frac{1}{2^m \theta}) \geq 3/5$. Following a geometric distribution where each trial has success probability p , the probability that we obtain the first success at iteration k (and not before) is $p(1-p)^{k-1}$. Thus, the expected number of applications is:

$$\begin{aligned} \sum_{k=1}^{n-m_0} \frac{3}{5} \left(1 - \frac{3}{5}\right)^{k-1} 2^{m_0+k} &= \sum_{k=1}^{n-m_0} \frac{3}{5} \left(\frac{2}{5}\right)^{-1} \left(\frac{2}{5}\right)^k 2^{m_0+k} = \frac{3}{2} 2^{m_0} \sum_{k=1}^{n-m_0} \left(\frac{4}{5}\right)^k \\ &= \mathcal{O}(2^{m_0}) = \mathcal{O}\left(\frac{1}{\theta}\right). \end{aligned}$$

By adding the worst-case number of iterations when $m \leq m_0$ and the expected number of iterations when $m > m_0$, we obtain the bound $\mathcal{O}(\frac{1}{\theta})$ on the total expected number of iterations. \square

More details can be found in [Boyer et al., 1998, Brassard et al., 2002].

Corollary 4.30. *Let U_f be a quantum (binary) oracle implementing a Boolean function $f : \{0, 1\}^n \rightarrow \{0, 1\}$, and let $M = \{\vec{j} \in \{0, 1\}^n : f(\vec{j}) = 1\}$ be the set of marked elements. Alg. 1 is a randomized quantum algorithm that does not require knowledge of $|M|$, and that determines an element of M with $\mathcal{O}\left(\sqrt{\frac{2^n}{|M|}}\right)$ applications of U_f in expectation.*

We can simplify this algorithm with the following observation. Note that the circuit used by Alg. 1 is the same as in Fig. 4.9, with a variable qubit count m , and measurement gates added to the second register: we thus obtain the circuit given in Fig. 4.13. An interesting feature of this circuit is the fact that we only measure the second register, which contains \vec{j} with $f(\vec{j}) = 1$ as the answer if the algorithm is successful. Furthermore, recall that the argument for the correctness of Alg. 1 is based on the near-orthogonality of $|\vartheta_+\rangle, |\vartheta_-\rangle$, but the same near-orthogonality relationship also holds before we apply the inverse QFT: trivially, $|\langle \vartheta_- | \vartheta_+ \rangle| = |\langle \vartheta_- | Q_m^\dagger Q_m | \vartheta_+ \rangle|$. So even if we remove the inverse QFT block, the probability of observing a basis state from $|\psi_G\rangle$ is still at least

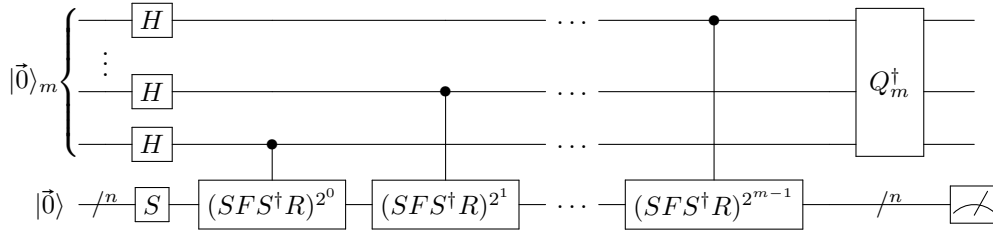


Figure 4.13: Amplitude estimation circuit with m bits of precision, in the context of searching when the number of marked items is unknown.

$\frac{1}{2} - \mathcal{O}\left(\frac{1}{2^{m\theta}}\right)$. Now consider the circuit in Fig. 4.13 without Q_m^\dagger . By the principle of implicit measurement (Prop. 1.50), because the first register is discarded without looking at it, we can assume it is also measured at the end of the circuit. Because the first register contains a uniform superposition of all basis states on m qubits, applying a measurement yields a uniformly random integer in the set $\{0, \dots, 2^m - 1\}$. That integer represents the number of times that the Grover operator was applied to the second register. Thus, we can replicate the effect of the circuit without the inverse QFT (which still yields the correct result) with the following, simpler algorithm.

1. Set $m = 1$.
2. Pick a random $y \in \{0, \dots, 2^m - 1\}$. Repeat twice:
 - Compute $(SFS^\dagger R)^y |\vec{0}\rangle$, and apply a measurement to obtain a string $|\vec{j}\rangle$. If $f(\vec{j}) = 1$, output \vec{j} and stop.
3. If $2^m < 2^n$, increase $m \leftarrow m + 1$ and go back to step (2). If $2^m > 2^n$, then do full enumeration of the 2^n binary strings; if $\vec{j} : f(\vec{j}) = 1$ is found, return \vec{j} , otherwise return “no solution”.

Historically, this simplified version of the algorithm was the first to be proposed in [Brassard et al., 2002], rather than the approach based on the amplitude estimation circuit in Alg. 1. Because the two approaches are equivalent, the query complexity is the same.

4.4 Quantum minimum finding

Grover’s algorithm solves the problem of finding an element satisfying some easy-to-check property in a set, using a subroutine that checks if the property holds for a given element. The generalization of Grover search to the case where the number of marked items is unknown can be turned into an algorithm for finding the minimum of an unstructured function. That algorithm is the subject of this section.

4.4.1 Base algorithm

Let $f : \{0, 1\}^n \rightarrow \mathbb{Z}$, and assume a circuit U_f to evaluate f is given in the usual form:

$$U_f : |\vec{j}\rangle|\vec{k}\rangle \rightarrow |\vec{j}\rangle|\vec{k} \oplus \overline{f(\vec{j})}\rangle.$$

Suppose we want to find the minimum of f , but we do not know anything about the function: it may be completely unstructured. Then, classically we may have to scan all elements in the set $\{0, 1\}^n$. We can do better than that with a quantum computer. The idea is to “guess” the value γ of the minimum, and then perform repeated binary search, searching for some \vec{j} such that $f(\vec{j}) \leq \gamma$ using amplitude amplification. If such \vec{j} exists, we can update γ . If no such \vec{j} exists, then we have found the minimum (provided we know some value $\vec{\ell}$ such that $f(\vec{\ell}) = \gamma$). We can turn this idea into an algorithm, described in Alg. 2. In this algorithm we use the notation $\mathbb{I}(\text{event})$ to denote the indicator function of a certain event; more specifically, we write $\mathbb{I}(f(\vec{j}) < f(\vec{\ell}))$ to denote the function that returns 1 if $f(\vec{j}) < f(\vec{\ell})$, and 0 otherwise.

Algorithm 2: Quantum minimum finding algorithm.

Input: Unitary U_f to evaluate f , total number of evaluations T .

Output: Index $\vec{\ell}$ such that $f(\vec{\ell}) \leq f(\vec{j})$ for all \vec{j} (if T is chosen appropriately).

- 1 **Initialize:** Randomly choose $\vec{\ell} \in \{0, 1\}^n$.
- 2 **while** the number of evaluations of U_f does not exceed T **do**
- 3 Construct marking unitary $U_m : |\vec{j}\rangle|y\rangle \rightarrow |\vec{j}\rangle|y \oplus \mathbb{I}(f(\vec{j}) < f(\vec{\ell}))\rangle$.
- 4 Apply the search algorithm in Alg. 1 using the marking unitary U_m .
- 5 Let \vec{k} be the index returned by the search algorithm. If $\vec{k} : f(\vec{k}) < f(\vec{\ell})$, set $\vec{\ell} \leftarrow \vec{k}$.
- 6 **end**
- 7 **return** $\vec{\ell}$.

Theorem 4.31 (Quantum minimum finding; [Durr and Hoyer, 1996]). *Let $f : \{0, 1\}^n \rightarrow \mathbb{Z}$, let U_f be a circuit that evaluates f in binary, and let $\delta > 0$. Using Alg. 2, we can determine the global minimum of f with probability at least $1 - \delta$ using $\mathcal{O}(\sqrt{2^n} \log \frac{1}{\delta})$ applications of U_f in total, and $\tilde{\mathcal{O}}(\sqrt{2^n})$ additional gates.*

Proof. We call *rank* of an element of $\{0, 1\}^n$, denoted $\text{rank}(\vec{j})$, its position in the set $\{0, 1\}^n$ ordered by nondecreasing value of f ; our goal is to show that we can determine the element of rank 1, i.e., the global minimum.

The proof consists of three steps. We first consider the case where Alg. 2 is executed with $T = \infty$, which we call the *infinite-time* algorithm, and analyze the probability that the index of the rank- r element is returned. Then we use that probability to compute the expected running time of the infinite-time algorithm before it returns the element of rank 1. Finally, we apply Markov's inequality and show the desired result.

The main loop of Alg. 2 consists of running the search algorithm of Cor. 4.30 (Alg. 1) for a fixed $\vec{\ell}$; therefore, the search algorithm is executed to determine an element of the set of marked items $M := \{\vec{j} \in \{0, 1\}^n : f(\vec{j}) < f(\vec{\ell})\}$. Denote $|M| = t$. Let us call $p(r, t)$ the probability that the element of rank r is obtained as \vec{k} on line 5 when running the infinite-time algorithm with a set of marked items of size t . We claim that $p(r, t) = 1/r$ if $r \leq t$, and $p(r, t) = 0$ otherwise. The case $r > t$ is obvious because no element of rank r exists. Then for each fixed r we perform induction on $t = r, r + 1, \dots, 2^n$. If $t = r$, we have $p(r, r) = 1/r$ because the search algorithm returns an element of M chosen uniformly at random, so we have $1/|M| = 1/r$ chance of observing the element of rank r . For any $t > r$, we can express $p(r, t)$ as the sum of two terms: the probability that the index \vec{k} on line 5 is the element of rank r , and the probability that \vec{k} it is not the element of rank r but it becomes so in a subsequent iteration, i.e.,

$$p(r, t) = \Pr(\text{rank}(\vec{k}) = r) + \sum_{\substack{s=1 \\ s \neq r}}^t \Pr(\text{element of rank } r \text{ is chosen subsequently} | \text{rank}(\vec{k}) = s) \Pr(\text{rank}(\vec{k}) = s).$$

Because the index \vec{k} is chosen uniformly at random from M , $\Pr(\text{rank}(\vec{k}) = s) = 1/|M| = 1/t$ for any t . Furthermore, by definition $\Pr(\text{element of rank } r \text{ is chosen subsequently} | \text{rank}(\vec{k}) = s) = p(r, s - 1)$. Using the induction hypothesis, we know $p(r, s - 1) = 0$ if $s \leq r$, and $p(r, s - 1) = 1/r$ if $r < s \leq t - 1$. Thus:

$$p(r, t) = \frac{1}{t} + \sum_{s=r+1}^t p(r, s - 1) \frac{1}{t} = \frac{1}{t} + \frac{1}{t} \sum_{s=r+1}^t \frac{1}{r} = \frac{1}{t} + \frac{1}{t} \frac{t - r}{r} = \frac{1}{r}.$$

We now turn to computing the expected running time (in terms of number of calls to U_f) of the infinite-time algorithm before $\vec{\ell}$ contains the index of the global minimum. Note that once $\text{rank}(\vec{\ell}) = 1$, the index $\vec{\ell}$ no longer changes during the course of the algorithm. By Cor. 4.30, the

number of applications of the marking unitary U_m to find the index of a marked item among 2^n items, where t items are marked, is $\mathcal{O}\left(\sqrt{2^n/t}\right)$ in expectation. Let c be the constant of the $\mathcal{O}(\cdot)$ expression, i.e., Alg. 1 uses $\leq c\sqrt{2^n/t}$ applications of the marking unitary. (To be more concrete, [Boyer et al., 1998] gives a slightly different quantum search algorithm for which $c = \frac{9}{2}\sqrt{2^n/t}$; so we can take $c = \frac{9}{2}$ below.) Then we upper bound the total expected running time in the following way:

$$\sum_{r=1}^{2^n} \Pr(\text{rank}(\vec{\ell}) = r \text{ at some iteration}) (\text{Expected running time to find a better element than rank } r).$$

This is an upper bound because the search at line 4 only looks for better elements, therefore $\text{rank}(\vec{\ell}) = r$ can only occur once in the course of the algorithm. We can expand this expression as follows: when $r = 1$ we are done with a single application of U_m , and otherwise, the formula evaluates to at most:

$$\begin{aligned} \sum_{r=2}^{2^n} p(r, 2^n) c \sqrt{\frac{2^n}{r-1}} &= c\sqrt{2^n} \sum_{r=2}^{2^n} \frac{1}{r} \frac{1}{\sqrt{r-1}} = c\sqrt{2^n} \left(\frac{1}{2} + \sum_{r=2}^{2^n-1} \frac{1}{r+1} \frac{1}{\sqrt{r}} \right) \\ &\leq c\sqrt{2^n} \left(\frac{1}{2} + \sum_{r=2}^{2^n-1} r^{-3/2} \right) \leq c\sqrt{2^n} \left(\frac{1}{2} + \int_{r=1}^{2^n-1} r^{-3/2} \right) \\ &\leq c\sqrt{2^n} \left(\frac{1}{2} + \left(-2r^{-1/2} \Big|_1^{2^n-1} \right) \right) \leq c\sqrt{2^n} \left(\frac{1}{2} + 2 \right) \leq 3c\sqrt{2^n}. \end{aligned} \quad (4.13)$$

Each application of the marking unitary U_m can be implemented with a single call to U_f plus some binary arithmetic operations. Thus, the expected number of calls of the infinite-time algorithm before $\vec{\ell}$ contains the index of the global minimum is $\mathcal{O}(\sqrt{2^n})$. The number of gates also follows from Cor. 4.30 and Sect. 4.3.6.

From this bound on the expected number of iterations of the infinite-time algorithm to obtain the global minimum, we can finish the proof using standard tools. Let X be the random variable corresponding to the number of applications of U_f before Alg. 2 finds the global minimum. Let $\bar{t} = 3c\sqrt{2^n} \geq \mathbb{E}[X]$. By Markov's inequality, if we run Alg. 2 with $T = 3\bar{t}$, the probability that we do not find the minimum is at most:

$$\Pr(X \geq 3\bar{t}) \leq \frac{\mathbb{E}[X]}{3\bar{t}} \leq \frac{1}{3}.$$

We execute Alg. 2 k times in total, setting $T = 3\bar{t}$ each time, and take the index \vec{b} of the best element returned among the k executions as the global minimum. The probability that \vec{b} is not the global minimum is at most $(1/3)^k$. Setting $k = \lceil \log_3 \frac{1}{\delta} \rceil = \mathcal{O}(\log \frac{1}{\delta})$ ensures the success of the algorithm with probability at least $1 - \delta$, and concludes the proof. \square

4.4.2 Function evaluations with errors

We can now address the more general case where we want to find an approximate minimizer of a function that cannot be evaluated exactly. In the previous section f could be evaluated exactly and in binary. But we may not always be so lucky: for example, it may be the case that evaluating f requires acting on quantities obtained from an amplitude/probability estimation procedure, and such an estimation incurs a probability of error. It may be helpful to distinguish the type of errors that are easy to deal with, and those that require a more careful treatment. We proceed in increasing order of difficulty. Here we only discuss cases where positive results are possible; in other settings quantum speedups are negated by noise, see the notes in Sect. 4.5 at the end of this chapter, therefore it is important to pay attention to the details of the error model.

Deterministic noisy evaluation. In this case f is evaluated through a unitary U_f that acts as:

$$U_f : |\vec{j}\rangle|\vec{k}\rangle \rightarrow |\vec{j}\rangle|\vec{k} \oplus \overrightarrow{f(\vec{j}) + \epsilon_j}\rangle,$$

where ϵ_j is some error that may depend on \vec{j} . An example where such a situation may occur is when f is a trigonometric function evaluated on a binary string: the exact value of $f(\vec{j})$ may not be computable in finite precision, so U_f computes a finite-precision approximation whose error depends on \vec{j} . Let ϵ_{\max} be an upper bound for all errors: $|\epsilon_j| \leq \epsilon_{\max} \forall j$. Under this assumption, in each execution of the “while” loop in Alg. 2 the marking unitary U_m is always consistent: each state $|\vec{j}\rangle$ is entangled with a specific binary string $|\overrightarrow{f(\vec{j}) + \epsilon_j}\rangle$, and the state is marked or not marked depending if $f(\vec{j}) + \epsilon_j \leq f(\vec{\ell})$. We might miss the true global minimum of the function because of the error terms ϵ_j , but it is straightforward to conclude that Alg. 2 with high probability determines a value that is at most $2\epsilon_{\max}$ away: the proof of Thm. 4.31 applies directly.

Nondeterministic evaluation with exogenous randomness. In this case f is evaluated through a unitary U_f that acts as:

$$U_f : |\vec{j}\rangle|\vec{k}\rangle \rightarrow |\vec{j}\rangle|\vec{k} \oplus \overrightarrow{f(\vec{j}) + \epsilon_j}\rangle,$$

where ϵ_j is an exogenous random variable. Conceptually, we can think of this situation as having a separate “random seed” register, and the values of ϵ_j are determined once the random seed is fixed, but we do not know the value of the random seed a priori. An example where such a situation may occur is when U_f performs Monte Carlo estimation of a difficult-to-compute function (e.g., a complicated integral): the output of the computation can be different in every execution, and depends on a random seed. We can think of this as “classical randomness.” Applying Alg. 2 directly may not work here: in different executions of the “while” loop the samples from the random variables ϵ_j may be different, so it is theoretically possible that the marking unitary U_m accepts more values \vec{j} than we anticipated (recall that in principle we only want to mark $\vec{j} : f(\vec{j}) < f(\vec{\ell})$). The proof of Thm. 4.31 explicitly relies on the assumption that if the element of rank r is the incumbent, we can find a better element with expected running time $\mathcal{O}\left(\sqrt{\frac{2^n}{r-1}}\right)$; the exogenous randomness model might violate that assumption, because the marking unitary is affected by randomness that is not directly under our control (i.e., it depends on an external random seed) and therefore it may mark (i.e., accept) more than $r - 1$ binary strings.

It is however not difficult to recover the same running time as Thm. 4.31 with some slightly weaker guarantees. There are multiple ways to do so. If we have some information on the distribution of the errors ϵ_j , we can exploit it to our advantage. A weaker but simpler approach can be employed if we know that $|\epsilon_j| \leq \epsilon_{\max} \forall j$. We change the marking unitary on line 3 of the “while” loop of Alg. 2 to:

$$U_m : |\vec{j}\rangle|y\rangle \rightarrow |\vec{j}\rangle|y \oplus \mathbb{I}(f(\vec{j}) < f(\vec{\ell}) - 2\epsilon_{\max})\rangle$$

and the acceptance criterion on line 5 to $f(\vec{k}) < f(\vec{\ell}) - 2\epsilon_{\max}$. Because $|\epsilon_j| \leq \epsilon_{\max}$, these modifications ensure that we only accept elements with a function value guaranteed to be better than the function value of the incumbent $\vec{\ell}$. Thus, in the proof of Thm. 4.31 we can rely on $p(r, t) = 1/r$ being an upper bound on the true probability of selecting the element of rank r . Furthermore, Eq. (4.13) is still a valid upper bound, because the more stringent acceptance criterion $f(\vec{k}) < f(\vec{\ell}) - 2\epsilon_{\max}$ may only result in skipping some of the terms of the summation, thereby decreasing the value of the upper bound. Formally, we can upper bound the expected running time as:

$$\begin{aligned} \sum_{\substack{r: \text{rank}(\vec{\ell})=r \\ \text{at some} \\ \text{iteration}}} \Pr(\text{rank}(\vec{\ell}) = r \text{ at some iteration}) c \sqrt{\frac{2^n}{r-1}} &\leq \sum_{r=2}^{2^n} \Pr(\text{rank}(\vec{\ell}) = r \text{ at some iteration}) c \sqrt{\frac{2^n}{r-1}} \\ &\leq \sum_{r=2}^{2^n} p(r, 2^n) c \sqrt{\frac{2^n}{r-1}}, \end{aligned}$$

and the chain of inequalities continues in Eq. (4.13). This shows that, similarly to Thm. 4.31, with $\mathcal{O}(\sqrt{2^n} \log \frac{1}{\delta})$ we can determine $\vec{\ell}$ such that $f(\vec{\ell}) \leq f_{\min} + 2\epsilon_{\max}$, where f_{\min} is the value of the global minimum of f .

Nondeterministic evaluation with endogenous randomness. In this case f is evaluated through a unitary U_f that acts as:

$$U_f : |\vec{j}\rangle|\vec{0}\rangle \rightarrow |\vec{j}\rangle \left(\sqrt{p_j} |\overrightarrow{f(\vec{j})}\rangle + \sum_{\vec{k} \neq \overrightarrow{f(\vec{j})}} \alpha_{j,k} |\vec{k}\rangle \right)$$

where $\sum_{\vec{k} \neq \overrightarrow{f(\vec{j})}} |\alpha_{j,k}|^2 = 1 - p_j$. The interpretation of this model is the following: the unitary U_f uses a register, initialized in the state $|\vec{0}\rangle$, to output the correct value of f with some probability p_j , and with the complementary probability it outputs some other value. An example where such a situation may occur is mentioned at the beginning of this section, where evaluating f requires some amplitude estimation or phase estimation procedure: in that case the output of the final QFT is a superposition of basis states, one of which leads to the “correct” function value; all other basis states lead to a potentially erroneous computation, and they may also appear with a nonzero but potentially negligible amplitude.

A more detailed example should help clarify the difficulties encountered in this setting.

Example 4.32. Consider the case in which we have a state $\sum_{\vec{j} \in \{0,1\}^n} \alpha_j |\vec{j}\rangle$, we know that all α_j are real and nonnegative up to some global phase, and we want to return the index j such that $|\alpha_j|$ is minimized. One way to do so is to use amplitude estimation followed by quantum minimum finding. For concreteness, let $|\psi\rangle = 0.6|0\rangle + 0.8|1\rangle$. Below we perform several approximations and simplifications for the sake of the example: an actual implementation could yield very different results. The setup is the following: we use three registers, the first one to store the index j over which we search (in this case, $j \in \{0, 1\}$, so it is in fact a single-digit binary string), the second to store $|\psi\rangle$, and the third to contain the output of amplitude estimation.

Suppose we use 4 qubits for the third register. Recall that for an amplitude $\sin \theta$, the phase estimation procedure at the end of amplitude estimation outputs $\pm\theta/\pi$; the “ideal” 4-digit output of amplitude estimation for each of the two amplitudes 0.6, 0.8 is then:

$$\begin{aligned} |0011\rangle &= 0.1875 \text{ in decimal } (\sin 0.1875\pi = 0.5557 \approx 0.6) \\ |0101\rangle &= 0.3125 \text{ in decimal } (\sin 0.3125\pi = 0.8314 \approx 0.8). \end{aligned}$$

We consider these the “correct” function values $f(0), f(1)$. For the sake of this example, assume that amplitude estimation outputs the ideal number with probability $0.81 = (0.9)^2$, and the ideal number $\pm 1/16$ with probability $0.095 \approx (0.308)^2$ each. (In reality the output distribution might have quite a different shape than what we assumed.) Then the amplitude estimation circuit (where, conditioned on some value $|j\rangle$ in the first single-qubit register, we estimate the amplitude of $|j\rangle$ in the second single-qubit register, and write the answer in the third register) would perform the following mapping:

$$\begin{aligned} |0\rangle(0.6|0\rangle + 0.8|1\rangle)|0000\rangle &\rightarrow |0\rangle(0.6|0\rangle + 0.8|1\rangle)(0.308|0010\rangle + 0.9|0011\rangle + 0.308|0100\rangle) \\ |1\rangle(0.6|0\rangle + 0.8|1\rangle)|0000\rangle &\rightarrow |1\rangle(0.6|0\rangle + 0.8|1\rangle)(0.308|0100\rangle + 0.9|0101\rangle + 0.308|0110\rangle). \end{aligned}$$

Let us now apply Alg. 2, where in the initialization phase we randomly choose $\vec{\ell} = 1$. The search on line 4 of the “while” loop tries to determine the index of an element with function value better than $\vec{\ell}$. An issue immediately arises: what is the function value associated with the incumbent? For the incumbent $\vec{\ell} = 1$, the function value is the superposition $(0.308|0100\rangle + 0.9|0101\rangle + 0.308|0110\rangle)$. And how do we compare the function value $f(1)$ with the function value $f(0)$? The output of amplitude estimation for index $j = 0$ is not deterministically strictly smaller than the output of amplitude estimation for index $j = 1$! Assume that we implement the test $f(0) < f(1)$ by using three registers: one to store the output of the procedure that attempts to compute $f(0)$, one for the

procedure that attempts to compute $f(1)$, and one to store the outcome of the comparison. The output of amplitude estimation for the index $j = 0$, is $(0.308|0010\rangle + 0.9|0011\rangle + 0.308|0100\rangle)$. For the index $j = 1$, it is $(0.308|0100\rangle + 0.9|0101\rangle + 0.308|0110\rangle)$. If we compare the binary values stored in the superpositions for the two indices, by doing pairwise comparisons, we see that with probability $(0.308)^2 \cdot (0.308)^2 \approx 0.009$ the comparison yields “ $f(0)$ is larger than or equal to $f(1)$ ”, whereas, for correctness of the algorithm, we wanted “ $f(0)$ is strictly smaller than $f(1)$ ”.

Ex. 4.32 describes a situation where it is not immediately apparent how to execute Alg. 2: to proceed with the algorithm we must be able to compare two function values and determine which one is smaller, but if the function values are produced in a superposition, the comparison is not deterministic. The result of the comparison depends on the outcome of a measurement of the registers involved: this is what we mean by “endogenous randomness” of the evaluation. (Sometimes this setting is called “relational oracles” in the literature, see [van Apeldoorn et al., 2020a].)

Without loss of generality, we can simplify the exposition by considering the following related search problem: given a function $f : \{0, 1\}^n \rightarrow \{0, 1\}$, we want to determine some $\vec{\ell} \in \{0, 1\}^n : f(\vec{\ell}) = 1$, while having access only to a nondeterministic version \tilde{f} of f satisfying the following:

$$\text{if } f(\vec{j}) = 1 \text{ then } \Pr(\tilde{f}(\vec{j}) = 1) \geq 9/10, \quad \text{if } f(\vec{j}) = 0 \text{ then } \Pr(\tilde{f}(\vec{j}) = 0) \geq 9/10.$$

In other words, we cannot access f directly, but we have access to a “noisy” function that outputs the correct function value at least 90% of the time.

Remark 4.33. *The threshold value 9/10 is chosen arbitrarily: as long as it is $> 1/2$, we can always boost it with a few repetitions.*

This setting is a direct generalization of the quantum search problem: now the function f is not correct all the time, but we have a bound on the failure probability; the corresponding problem is usually called *search with bounded error probability* [Høyer et al., 2003]. Clearly, if we can solve search with bounded error probability, then we can generalize Alg. 2 to the same setting, in which function values are computed correctly with bounded error probability: the crucial component of Alg. 2 is precisely the application of quantum search on line 4. In the setting of nondeterministic evaluation with endogenous randomness, the marking unitary can be considered as the noisy function \tilde{f} that outputs the correct value with reasonably large (e.g., $> 9/10$) probability.

The quantum search algorithm in Alg. 1 does not directly work for the bounded error case, because errors could accumulate too quickly. There is a very simple approach to design a search algorithm that works in this setting, at the expense of additional (but polynomial) query complexity. Let m be the number of queries to (exact) f that the quantum search algorithm would have to apply to find a solution $\vec{\ell}$; by Cor. 4.30, $m = \mathcal{O}\left(\sqrt{\frac{2^n}{|M|}}\right)$. Suppose the failure probability of \tilde{f} could be reduced to:

$$\text{if } f(\vec{j}) = 1 \text{ then } \Pr(\tilde{f}(\vec{j}) = 1) \geq 1 - \frac{1}{100m}, \quad \text{if } f(\vec{j}) = 0 \text{ then } \Pr(\tilde{f}(\vec{j}) = 0) \geq 1 - \frac{1}{100m},$$

and apply quantum search (Alg. 1) using \tilde{f} . Because each call to \tilde{f} differs from a call f with probability only $\frac{1}{100m}$, and errors in quantum computation accumulate linearly (see Sect. 1.3.6 and in particular Prop. 1.46), we can bound the difference between the quantum state produced by the search algorithm using \tilde{f} and the quantum state produced by the search algorithm using f as:

$$(\text{number of calls to } \tilde{f})(\text{failure probability of } \tilde{f}) \leq m \frac{1}{100m} \leq \frac{1}{100}$$

in the Euclidean norm. This implies (Prop. 1.49) that the quantum search algorithm using \tilde{f} succeeds with probability at most $\frac{1}{100}$ worse than the success probability of quantum search using f . Thus, if we can reduce the failure probability of \tilde{f} to $\frac{c}{100\sqrt{2^n}}$, where c is the constant in the $\mathcal{O}(\cdot)$ for quantum search, applying quantum search substituting \tilde{f} for f obtains the correct answer with high probability.

To boost the probability of success, using some extra queries to \tilde{f} , we can do the following: we construct a function \tilde{f}_{maj} that makes $k = \mathcal{O}(n)$ queries to \tilde{f} , stores the output in separate working registers, takes the majority vote of the outputs, and finally uncomputes the working registers. More formally, the unitary $U_{\tilde{f}_{\text{maj}}}$, when applied onto the basis state $|\vec{j}\rangle$ and several fresh registers, implements the following steps:

$$\begin{aligned} U_{\tilde{f}_{\text{maj}}} |\vec{j}\rangle \underbrace{|0\rangle \dots |0\rangle}_{k \text{ times}} |0\rangle &\rightarrow |\vec{j}\rangle |\tilde{f}_1(\vec{j})\rangle \dots |\tilde{f}_k(\vec{j})\rangle |0\rangle \\ &\rightarrow |\vec{j}\rangle |\tilde{f}_1(\vec{j})\rangle \dots |\tilde{f}_k(\vec{j})\rangle |\text{MAJ}(\tilde{f}_1(\vec{j}), \dots, \tilde{f}_k(\vec{j}))\rangle \\ &\xrightarrow{\text{uncompute}} |\vec{j}\rangle \underbrace{|0\rangle \dots |0\rangle}_{k \text{ times}} |\text{MAJ}(\tilde{f}_1(\vec{j}), \dots, \tilde{f}_k(\vec{j}))\rangle, \end{aligned}$$

where $\tilde{f}_1(\vec{j}), \dots, \tilde{f}_k(\vec{j})$ denote k different evaluations of \tilde{f} , and the function MAJ takes the majority vote. The uncomputation process cleans up the working registers to a large degree, see Sect. 1.3.7 for a discussion on uncomputation.

Remark 4.34. *In fact, the uncomputation may not be perfect: the issue stems from the fact that after computing $\tilde{f}_1(\vec{j}), \dots, \tilde{f}_k(\vec{j})$ and $\text{MAJ}(\tilde{f}_1(\vec{j}), \dots, \tilde{f}_k(\vec{j}))$, we want to copy $\text{MAJ}(\tilde{f}_1(\vec{j}), \dots, \tilde{f}_k(\vec{j}))$ to a safe register before uncomputation. However, the register containing $\text{MAJ}(\tilde{f}_1(\vec{j}), \dots, \tilde{f}_k(\vec{j}))$ in general could be a superposition of $|0\rangle$ and $|1\rangle$ rather than containing only the correct value. This happens because with a small probability, not enough values among $\tilde{f}_1(\vec{j}), \dots, \tilde{f}_k(\vec{j})$ agree with the correct result. In this case, carefully writing down the effect of uncomputation shows that with small probability we do not uncompute the working registers in a “clean” way. Fortunately, the state that we obtain after the imperfect uncomputation is still very close to the perfect uncomputation state: its overlap with the ideal state is the same as the probability of success for computing $\text{MAJ}(\tilde{f}_1(\vec{j}), \dots, \tilde{f}_k(\vec{j}))$, which is shown in the following to be very large. Thus, we can neglect this issue for ease of exposition, and it only affects the success probability of the algorithm by a very small amount.*

Next, we show that the function \tilde{f}_{maj} implemented in this way has very low failure probability — below the necessary threshold. We analyze the failure probability of \tilde{f}_{maj} using standard arguments: let k be the number of queries to \tilde{f} for the majority vote. \tilde{f}_{maj} outputs the correct answer if at least $k/2$ queries to \tilde{f} give the correct answer. Let X_1, \dots, X_k be Bernoulli random variables that take value 1 if the corresponding query to \tilde{f} gives the correct answer, an event that happens with probability at least $9/10$ by assumption. Let $X = \sum_{j=1}^k X_j$. Using the multiplicative Chernoff bound, the probability that fewer than $k/2$ queries to \tilde{f} give the correct answer can be bounded above as follows:

$$\Pr\left(X \leq \frac{k}{2}\right) = \Pr\left(X \leq \left(1 - \frac{4}{9}\right) \frac{9k}{10}\right) = \Pr\left(X \leq \left(1 - \frac{4}{9}\right) \mathbb{E}[X]\right) \leq e^{-\frac{16}{162} \mathbb{E}[X]}.$$

We want $e^{-\frac{16}{162} \mathbb{E}[X]} \leq e^{-\frac{16}{162} \frac{9}{10} k} \leq \frac{c}{100\sqrt{2^n}}$, and taking the natural logarithm on both sides, we find that $k = \mathcal{O}(n)$ is sufficient to make this inequality hold. Summarizing, if we are willing to perform $\mathcal{O}(n)$ queries to \tilde{f} to simulate one almost-exact query to f , we can employ Alg. 2 using the almost-exact query and no further modifications; this brings the total query complexity of the algorithm to $\mathcal{O}(n\sqrt{2^n} \log \frac{1}{\delta})$.

With some ingenuity it is possible to reduce the query complexity to $\mathcal{O}(\sqrt{2^n} \log \frac{1}{\delta})$, as in Thm. 4.31. We describe an idea introduced in [Høyer et al., 2003] in the context of quantum search: as remarked earlier, if we can perform quantum search the extension to quantum minimum finding is straightforward. We execute quantum search by interleaving iterations of amplitude amplification and error reduction. We start with one iteration of amplitude amplification step to amplify all quantum states $|\vec{j}\rangle$ such that $\tilde{f}(\vec{j}) = 1$: this includes states for which $f(\vec{j}) = 1$, but also “false positives”, i.e., branches of the computation where $f(\vec{j}) = 0$ and \tilde{f} outputs an incorrect value. Then we run an error reduction step: for all \vec{j} : $\tilde{f}(\vec{j}) = 1$ in the previous step we perform

k evaluations of \tilde{f} , take a majority vote, and use the outcome of the majority vote to reduce the probability of observing a false positive to $\mathcal{O}(2^{-k})$. At this point we go back to the amplitude amplification step and iterate. Note that as we do so, we need to add new registers as working registers to store the outcome of the majority votes. The details of this idea can be found in [Høyer et al., 2003], with a detailed proof showing that when f has bounded error probability, the asymptotic complexity of quantum search stays the same, although the algorithm gets more involved and the constants in $\mathcal{O}(\cdot)$ notation get worse.

4.5 Notes and further reading

Even before Grover presented his algorithm for unstructured quantum search with a quadratic speedup over classical algorithms, it was known that at a quadratic speedup is optimal for unstructured search, i.e., relative to an oracle that identifies the optimal solution [Bennett et al., 1997].

Amplitude amplification is a fundamental component of most of the optimization algorithms discussed in subsequent chapters, if only as a way to boost the probability of success of the algorithms. Among the direct applications of Grover’s unstructured search algorithm to optimization, one of the most notable is the acceleration of the solution of certain types of dynamic programming problems, discussed in [Ambainis et al., 2019]. The main feature of these dynamic programs is that they are defined by a recursion across subsets: to determine the optimal decision over a set of given cardinality, one must loop over all of its subsets, potentially with some cardinality constraints. [Ambainis et al., 2019] initializes the dynamic programming recursion with some classical computation, then uses Grover’s algorithm to fill out the rest of the dynamic programming table by looping over all the possible subsets. The classical running time $\tilde{\mathcal{O}}(2^n)$ for doing so gets reduced to an exponential with a smaller base. Notably, for the Bellman-Held-Karp dynamic programming formulation of the traveling salesman problem, [Ambainis et al., 2019] reduces the classical $\tilde{\mathcal{O}}(2^n)$ running time to quantum $\tilde{\mathcal{O}}(1.728^n)$ running time. [Grange et al., 2023] uses this framework to give quantum speedups for (exponential-time) single-machine job scheduling problem solved by dynamic programming across subsets. It is important to remark that this line of work requires QRAM (quantum RAM, see Sect. 5.3) to achieve a quantum speedup, as the values used to initialize the dynamic programming table, on which the recursion is built, are assumed to be available via a constant-time oracle in superposition, and this can be done with QRAM.

As highlighted multiple times throughout the chapter, one of the potential issues of amplitude amplification is that if the number of iterations exceeds the optimal number, the probability of success of the algorithm starts decreasing. In addition to the ideas of estimating the probability of success, or using the quantum search algorithm without knowing the probability of success of Sect. 4.3.6, another possibility is to use fixed-point quantum search: this avoids the problem of choosing too large k altogether [Yoder et al., 2014]. The main idea of fixed-point quantum search is to implement a polynomial function of the amplitudes of the target state $|\psi_G\rangle$ with the property that even when k increases past the optimal value, these amplitudes oscillate between values that are still sufficiently large. Hence, we never go back to amplitudes that are too small: after reaching a large enough probability of observing $|\psi_G\rangle$ when applying a measurement, further iterations may increase this probability slightly, but we have a lower bound ensuring that the probability does not get too small.

There is a version of amplitude amplification that is tailored for algorithms with multiple branches, each of which has different time complexity. This version is called *variable-time* amplitude amplification. We use it in Sect. 7.1.5, but do not give all details as we only need it in that specific section. A general treatment can be found in [Ambainis, 2010].

In Sect. 3.4 we mentioned that phase estimation yields a biased estimator, and that in some contexts this is undesirable. The same considerations apply to amplitude estimation, because in turns it relies on phase estimation (see [Suzuki et al., 2020] for a version of amplitude estimation that employs a maximum likelihood estimator rather than phase estimation). Unbiased amplitude estimation is discussed in [Cornelissen and Hamoudi, 2023, Rall and Fuller, 2023]. It is an important technique in quantum algorithms for the estimation of partition functions, a task that

can be used to approximately count combinatorial objects such as matchings or independent sets in a graph [Cornelissen and Hamoudi, 2023, Harrow and Wei, 2020]. Work on the estimation of partition function has also led to *nondestructive* amplitude estimation, i.e., a technique to apply quantum amplitude estimation on a state while restoring a copy of the state after measurement — as opposed to the standard amplitude estimation described in this chapter, where the final measurement would collapse the quantum state irreversibly.

In general, the preparation of a *qsample* (i.e., a quantum state encoding a probability distribution) such as the one in Eq. (4.9) has gate complexity $\mathcal{O}(2^n)$, i.e., linear in the size of the vector encoding the probability distribution. We can improve on this worst-case complexity with additional assumptions. Two such assumptions are common in the literature. The first assumption is that we have access to QRAM, see Sect. 5.3. Because QRAM implements some operations faster than the standard circuit model, one has to be careful that a potential speedup obtained by encoding probability distributions in quantum states using QRAM is due to some algorithmic quantum advantage, rather than to QRAM only. The second assumption is that the probability distribution being encoded is efficiently integrable, as defined in [Grover and Rudolph, 2002]. Note that this is a strong assumption, as it implies that we can integrate the probability density function between arbitrary endpoints, which usually means we know it analytically and often leads to efficient classical sampling as well.

The topic of quantum search, or quantum minimum finding, in the presence of errors has produced both positive and negative results, and these depend on the error model. We discussed several positive results in Sect. 4.4.2, in particular for those error models that appear to be more directly relevant for fault-tolerant computation (e.g., errors due to oracles that rely on bounded-error subroutines). If the errors are due to hardware noise, results can be markedly more negative. [Regev and Schiff, 2008] shows that if the oracle U_f is faulty, i.e., it applies identity instead with some constant probability, then no quantum speedup can be achieved. An analogous result for continuous-time quantum queries (rather than the discrete-time queries discussed in this chapter) is shown in [Temme, 2014]. Note that if there are no marked elements, then the computation is not affected by noise, because U_f would be the identity map anyways. With a different form of noise (depolarizing noise), that turns the state register of Grover search into a uniform superposition with probability p , at least $\Omega(p2^n)$ queries are necessary [Vrana et al., 2014]. A tight characterization of the complexity of quantum search in the presence of depolarizing noise, as well as additional types of noise, is given in [Rosmanis, 2023]. These noise models are inspired by commonly used models for faulty hardware.

Chapter 5

Quantum gradient algorithm and vector input/output

In this chapter we discuss a quantum algorithm to estimate the gradient of a multivariate function, given access to a quantum circuit to compute the function. The core of the algorithm is a multidimensional version of phase estimation. After introducing the quantum gradient algorithm, we discuss two of its applications: an algorithm to extract the classical description of the vector describing a quantum state, and an algorithm to separate a point from a convex set when we only have an indirect description of the set, via an oracle that determines if a point belongs to it or not. Whereas algorithms discussed in previous chapters always output a scalar, in this chapter they output vectors. We also present an algorithm to create the natural quantum encoding of a given classical vector, which is used as a subroutine in a variety of quantum algorithms, sometimes to encode part of the input data.

5.1 The quantum gradient algorithm

In this section we show how, using phase estimation, we can simultaneously compute multiple components of the gradient of a function using an evaluation circuit for the function. This approach is, in some sense, the quantum analog of numerical computation of the gradient using finite differences in the classical world. The algorithm based on this idea, first introduced in [Jordan, 2005], is often called “Jordan’s gradient algorithm” in the literature.

The problem that this algorithm solves is defined as follows. We are given oracle access to a function $f : \mathbb{R}^d \rightarrow \mathbb{R}$, and we want to output its gradient at the origin. The choice of the origin is w.l.o.g., as one can always translate the function. Furthermore, we only evaluate the function in a certain hyperbox (i.e., $[0, 1]^d$ in the simplest version of the algorithm), rather than over all of \mathbb{R}^d , so we could restrict its domain. We do not have an analytical description of f , so the gradient must be estimated numerically. Without further knowledge on the structure of the function, a classical algorithm that outputs the gradient up to some level of precision takes $\Omega(d)$ function evaluations: otherwise, there is some direction in \mathbb{R}^d on which we do not have enough information to compute the gradient. (The computer science notation $\Omega(d)$ means “at least d asymptotically, up to a multiplicative factor,” similarly to how $\mathcal{O}(d)$ means “at most d asymptotically, up to a multiplicative factor.”) A simple and natural algorithm to perform gradient estimation with a classical computer is to evaluate the objective function along the coordinate axes, with some small step size $\eta > 0$, and output the gradient estimate obtained doing finite differences:

$$\frac{\partial f}{\partial x_j}(\mathbf{0}) \approx \frac{f(\mathbf{0} + \eta e_j) - f(\mathbf{0})}{\eta} \text{ for all } j = 1, \dots, d,$$

where e_j is the j -th orthonormal basis vector. Using this formula, we estimate the gradient with $d + 1$ function evaluations. (A different formula for a finite-difference approximation is given in

Def. 5.26; that formula evaluates f at $2d$ points.) We can do better with a quantum algorithm. We divide our discussion on this topic based on properties of the function f , and how it is specified. Note that in this chapter we generally use d to denote the dimension of the vector space in which a generic vector x lives (e.g., the argument of the function f , or the vector that we want to encode in the amplitudes of a quantum state), because we reserve n to denote the number of qubits in certain sections.

5.1.1 Linear functions with a binary oracle

We first present the quantum algorithm in the setting studied by Jordan [Jordan, 2005]. In this setting, we have access to a binary oracle for the function f , which we define below after introducing some notation.

Definition 5.1 (Addition modulo the largest representable integer). *For any given integer $q > 0$ and integers $j, k \in \{0, \dots, 2^q - 1\}$, we define $j \boxplus k := (j + k \bmod 2^q)$. In other words, \boxplus of two integers representable on q digits is the addition modulo 2^q .*

We extend the definition to binary strings: given $\vec{j}, \vec{k} \in \{0, 1\}^q$, $\vec{j} \boxplus \vec{k} := \vec{h}$ where $h = (j + k \bmod 2^q)$.

The function f is then given to us via the following oracle:

$$U_f |\vec{x}_1\rangle |\vec{x}_2\rangle \cdots |\vec{x}_d\rangle |\vec{y}\rangle = |\vec{x}_1\rangle |\vec{x}_2\rangle \cdots |\vec{x}_d\rangle |\vec{y} \boxplus f(x_1, \dots, x_d)\rangle,$$

where each register is represented on q qubits. We call this a *binary oracle*. We make a further simplifying assumptions in this section: that the function f is linear or approximately linear.

Linear function. The simplest case to analyze is when the function is exactly (as opposed to approximately) linear, i.e., $f(x_1, \dots, x_d) = \langle g, x \rangle + b$ for some vector $g \in \mathbb{R}^d$ and $b \in \mathbb{R}$. (Recall that $\langle g, x \rangle$ denotes an inner product; here, since the vectors lie in real Euclidean space, $\langle g, x \rangle = g^\top x$.)

Remark 5.2. *The precise assumption is that we know that the function is linear, but we do not know what its gradient (i.e., the vector g) is. We could estimate it with a classical algorithm using $d + 1$ function evaluations, and we seek to do better than that.*

Thus, $\nabla f(0) = g$ and the answer that we seek is precisely the vector g . For the sake of building intuition, we also assume that all numbers (i.e., the components of g , as well as $f(x)$ for all x) are representable on q bits. This allows us to ignore many important but cumbersome issues. We discuss how to relax the assumption and give a more precise treatment beginning in the second part of this subsection, and continuing in Sect. 5.1.2.

Assume that $f : [0, 1]^d \rightarrow \mathbb{R}_+$ (one could translate and rescale the function to make this assumption hold, if the function is defined over a compact set and is bounded). Because each argument is represented on q bits, this creates a grid of points with integer numerator, say $0, \frac{1}{2^q}, \frac{2}{2^q}, \dots, \frac{2^q-1}{2^q}$ along each axis. Let us study the following state:

$$|\psi\rangle = \frac{1}{\sqrt{2^{dq}}} \sum_{\vec{x} \in \{0, 1\}^{dq}} e^{2\pi i(\langle g, x \rangle + b)/2^q} |\vec{x}_1\rangle |\vec{x}_2\rangle \cdots |\vec{x}_d\rangle, \tag{5.1}$$

where x is obtained from the dq -dimensional binary string \vec{x} by reshaping it as a d -dimensional vector with q -digit entries (that is: the first q digits indicate the first component of x , the next q indicate the second component, and so on). It is not too difficult to see that the state $|\psi\rangle$ is a tensor product of Fourier states: $e^{2\pi i b/2^q}$ is a constant that can be collected and taken out of the

summation; then we use the fact that $\langle g, x \rangle = g_1 x_1 + \dots + g_d x_d$ to write:

$$\begin{aligned} |\psi\rangle &= \frac{1}{\sqrt{2^{dq}}} \sum_{\vec{x} \in \{0,1\}^{dq}} e^{2\pi i b/2^q} e^{2\pi i(g_1 x_1/2^q)} |\vec{x}_1\rangle e^{2\pi i(g_2 x_2/2^q)} |\vec{x}_2\rangle \dots e^{2\pi i(g_d x_d/2^q)} |\vec{x}_d\rangle \\ &= e^{2\pi i b/2^q} \left(\frac{1}{\sqrt{2^q}} \sum_{\vec{x}_1 \in \{0,1\}^q} e^{2\pi i(g_1 x_1/2^q)} |\vec{x}_1\rangle \right) \otimes \left(\frac{1}{\sqrt{2^q}} \sum_{\vec{x}_2 \in \{0,1\}^q} e^{2\pi i(g_2 x_2/2^q)} |\vec{x}_2\rangle \right) \otimes \dots \\ &\dots \otimes \left(\frac{1}{\sqrt{2^q}} \sum_{\vec{x}_d \in \{0,1\}^q} e^{2\pi i(g_d x_d/2^q)} |\vec{x}_d\rangle \right). \end{aligned}$$

The term $e^{2\pi i b/2^q}$ is a global phase that can be ignored. In the remaining q -qubit registers we have precisely the Fourier states corresponding to the scalars g_1, \dots, g_d . Thus, if each component g_j of g is exactly representable on q bits, applying the inverse QFT to each q -qubit register recovers a binary description of g_1, \dots, g_d :

$$\begin{aligned} Q_q^\dagger \left(\frac{1}{\sqrt{2^q}} \sum_{\vec{x}_1 \in \{0,1\}^q} e^{2\pi i(g_1 x_1/2^q)} |\vec{x}_1\rangle \right) &= |\vec{g}_1\rangle \\ Q_q^\dagger \left(\frac{1}{\sqrt{2^q}} \sum_{\vec{x}_2 \in \{0,1\}^q} e^{2\pi i(g_2 x_2/2^q)} |\vec{x}_2\rangle \right) &= |\vec{g}_2\rangle \\ &\vdots \\ Q_q^\dagger \left(\frac{1}{\sqrt{2^q}} \sum_{\vec{x}_d \in \{0,1\}^q} e^{2\pi i(g_d x_d/2^q)} |\vec{x}_d\rangle \right) &= |\vec{g}_d\rangle. \end{aligned}$$

It follows that if we could create the state $|\psi\rangle$ as in Eq. (5.1), then the application of the q -qubit inverse QFT for d times would output the correct answer to the problem of computing the gradient. As it turns out, creating $|\psi\rangle$ is relatively straightforward given our assumptions, by using phase kickback and exploiting the fact that $Q_q|\vec{1}\rangle$ is an eigenstate of modular addition.

Recall that U_f acts on $d+1$ registers, each of which is on q -qubits: d registers for the input arguments of the function f , one register for the output. We initialize the algorithm with the following state composed of $d+1$ q -qubit registers:

$$|\vec{0}\rangle_q \otimes |\vec{0}\rangle_q \otimes \dots \otimes |\vec{0}\rangle_q \otimes |\vec{1}\rangle_q.$$

Then we apply $H^{\otimes q}$ to each of the first d registers, and the QFT to the last register. We obtain:

$$\begin{aligned} H^{\otimes q}|\vec{0}\rangle \otimes H^{\otimes q}|\vec{0}\rangle \otimes \dots \otimes H^{\otimes q}|\vec{0}\rangle \otimes Q_q|\vec{1}\rangle &= \\ \frac{1}{\sqrt{2^{dq}}} \sum_{\vec{x} \in \{0,1\}^{dq}} |\vec{x}_1\rangle |\vec{x}_2\rangle \dots |\vec{x}_d\rangle \otimes \frac{1}{\sqrt{2^q}} \sum_{\vec{j} \in \{0,1\}^q} e^{-2\pi i \vec{j} / 2^q} |\vec{j}\rangle. \end{aligned}$$

(The expression for the last register can be obtained by noticing that the q -digit all-ones string corresponds to the integer $2^q - 1$, and 2^q can be simplified and eliminated from the expression.) Now we apply U_f to perform modular addition of $f(x_1, \dots, x_d)$ to the last register, obtaining:

$$\begin{aligned} U_f \left(\frac{1}{\sqrt{2^{dq}}} \sum_{\vec{x} \in \{0,1\}^{dq}} |\vec{x}_1\rangle |\vec{x}_2\rangle \dots |\vec{x}_d\rangle \otimes \frac{1}{\sqrt{2^q}} \sum_{\vec{j} \in \{0,1\}^q} e^{-2\pi i \vec{j} / 2^q} |\vec{j}\rangle \right) &= \\ \frac{1}{\sqrt{2^{dq}}} \sum_{\vec{x} \in \{0,1\}^{dq}} \left(|\vec{x}_1\rangle |\vec{x}_2\rangle \dots |\vec{x}_d\rangle \otimes \sum_{\vec{j} \in \{0,1\}^q} \frac{e^{-2\pi i \vec{j} / 2^q}}{\sqrt{2^q}} |\vec{j} \boxplus f(x_1, \dots, x_d)\rangle \right). \end{aligned} \quad (5.2)$$

For every fixed $(\vec{x}_1, \dots, \vec{x}_d) \in \{0, 1\}^{dq}$, relabeling $k = j \boxplus f(x_1, \dots, x_d)$ and looking at the second summation in the last part of Eq. 5.2, we have:

$$\begin{aligned} \frac{1}{\sqrt{2^q}} \sum_{\vec{j} \in \{0,1\}^q} e^{-2\pi i j / 2^q} |\vec{j} \boxplus \overrightarrow{f(x_1, \dots, x_d)}\rangle &= \frac{1}{\sqrt{2^q}} \sum_{\vec{k} \in \{0,1\}^q} e^{-2\pi i (k - f(x_1, \dots, x_d)) / 2^q} |\vec{k}\rangle \\ &= e^{2\pi i f(x_1, \dots, x_d) / 2^q} \underbrace{\frac{1}{\sqrt{2^q}} \sum_{\vec{k} \in \{0,1\}^q} e^{-2\pi i k / 2^q} |\vec{k}\rangle}_{=Q_q|\vec{1}\rangle}. \end{aligned}$$

In the above expression, the first equality is due to the fact that we are still summing over all possible binary strings, because modular addition applies a constant shift to the index of the sum, together with the fact that $j = (k - f(x_1, \dots, x_d) \bmod 2^q)$; the second equality holds because the term $f(x_1, \dots, x_d)$ in the exponent does not depend on the summation index, hence it can be taken out of the sum. Thus, only the phase factor depends on x , whereas the Fourier state $Q_q|\vec{1}\rangle$ is untouched and unentangled with the rest. It follows that Eq. 5.2 can be rewritten as a tensor product of a summation over \vec{x} , and $Q_q|\vec{1}\rangle$:

$$\frac{1}{\sqrt{2^{dq}}} \sum_{\vec{x} \in \{0,1\}^{dq}} e^{2\pi i f(x_1, \dots, x_d) / 2^q} |\vec{x}_1\rangle |\vec{x}_2\rangle \dots |\vec{x}_d\rangle \otimes \frac{1}{\sqrt{2^q}} \sum_{\vec{j} \in \{0,1\}^q} e^{-2\pi i j / 2^q} |\vec{j}\rangle.$$

The first dq qubits in this expression are precisely the state $|\psi\rangle$ in Eq. 5.1, showing that we have constructed the desired state from which the inverse QFT recovers the correct answer. To construct this state via phase kickback, we have used Hadamards everywhere in the first d registers, QFT in the last register, and one application of U_f . The full circuit implementing the algorithm described in this section is given in Fig. 5.1.

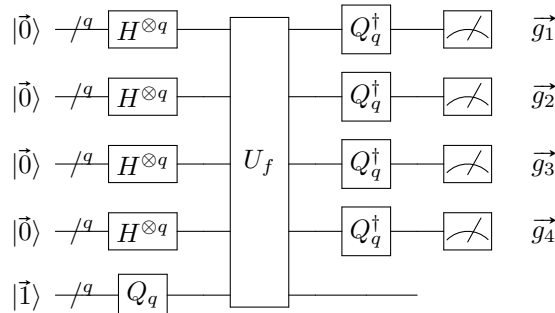


Figure 5.1: Circuit for the quantum gradient algorithm for a four-dimensional function ($d = 4$, the gradient has four components g_1, g_2, g_3, g_4).

We have shown the following.

Proposition 5.3. *Let U_f be given as a binary oracle that performs modular addition in the last register. Assume f is linear, and the value $f(x)$ as well as each component of the gradient of f is exactly representable on q bits. Then the circuit in Fig. 5.1 recovers the gradient of f with a single application of U_f .*

To highlight the connection between the circuit in Fig. 5.1 and phase estimation, consider the case with $d = 1$. Then, we have a single inverse QFT block, similar to the phase estimation circuit in Fig. 3.6. The last register is prepared in an eigenstate of modular addition with phase $2\pi i 0.\vec{g}_1$ (the vector g has a single component with $d = 1$), and the application of U_f prepares the Fourier state. We encourage the reader to verify that the application of U_f has the same effect as applying the controlled- U^{2^k} operations in the phase estimation circuit: if the binary string \vec{x}_1 is the number 2^{q-j} , i.e., the integer whose binary representation has 1 in position j and 0 elsewhere, the product $g_1 x_1 / 2^q$ is equivalent to shifting the binary fractional point of $0.\vec{g}_1$, so we kick back the phase $2\pi i 2^{q-j} 0.\vec{g}_1$, precisely as in the quantum phase estimation circuit.

Remark 5.4. *The gradient algorithm discussed in this section is a multidimensional version of phase estimation. In standard phase estimation, we use phase kickback to construct the Fourier state corresponding to the sought phase — a scalar. In multidimensional phase estimation, we use phase kickback to construct the tensor product of multiple Fourier states, each corresponding to one component of a vector. Rather than a single inverse QFT at the end of the circuit, we apply multiple inverse QFT blocks. Multidimensional phase estimation is a powerful technique to output vectors with a quantum algorithm, when it is applicable.*

Prop. 5.3 has two severe limitations: it assumes that f is linear and calculated exactly, and furthermore, it assumes that $f(x)$ and g are exactly representable on q bits. To broaden the applicability of the gradient algorithm we need to relax these assumptions.

Approximately linear function. If f is exactly linear, it does not matter where it is evaluated: with phase kickback we construct the Fourier states corresponding to the components of the gradient g at the origin, without any error. If f is not exactly linear, it seems more reasonable to evaluate it at a grid centered at the origin, rather than a grid in the hypercube $[0, 1]^d$: Taylor’s theorem tells us that, if we get further away from the origin, there may be a larger discrepancy between the value of the closest linear approximation to f constructed at the origin (i.e., its first-order Taylor approximation) and the true value of f . A grid symmetric around the origin is also helpful to borrow tools from classical numerical analysis to study the error of finite-difference formulas for gradient approximation, e.g., the central difference in the next section (see Def. 5.8). For this discussion we assume $f : [-\frac{1}{2}, \frac{1}{2}]^d \rightarrow \mathbb{R}$, and we consider the following discretization along each axis, also studied in [Jordan, 2005, Gilyén et al., 2019a]:

$$G_q := \left\{ \frac{j}{2^q} - \frac{1}{2} + \frac{1}{2^{q+1}} : j = 0, \dots, 2^q - 1 \right\}.$$

Thus, $G_q^d = G_q \times \dots \times G_q$ denotes a d -dimensional grid where each axis has 2^q grid points.

Example 5.5. *With $q = 3$, $G_3 = \{-\frac{7}{16}, -\frac{5}{16}, -\frac{3}{16}, -\frac{1}{16}, \frac{1}{16}, \frac{3}{16}, \frac{5}{16}, \frac{7}{16}\}$: one can see that the discretization is symmetric around the origin, and the points are equally spaced with distance $\frac{1}{2^q}$.*

There is an obvious bijection between G_q and the discretization $\{\frac{j}{2^q} : j = 0, \dots, 2^q - 1\}$ that we used for the case of (exactly) linear functions. For $\vec{j} \in \{0, 1\}^q$, we write \hat{j} to denote the point $\frac{j}{2^q} - \frac{1}{2} + \frac{1}{2^{q+1}}$ (a more formal treatment should define a function mapping the integer j to the corresponding point in the shifted grid; $\hat{\cdot}$ is a shorthand notation that is sufficient for our exposition). We define the QFT on the transformed domain G_q as the unitary Q_{G_q} that implements the following map:

$$\begin{aligned} Q_{G_q}|\vec{k}\rangle &= \frac{1}{\sqrt{2^q}} \sum_{\vec{j} \in \{0, 1\}^q} e^{2\pi i 2^q \hat{j} \vec{k}} |\vec{j}\rangle \\ &= \frac{1}{\sqrt{2^q}} \sum_{\vec{j} \in \{0, 1\}^q} \exp\left(2\pi i \left(\frac{j k}{2^q} - (j + k) \left(\frac{1}{2} + \frac{1}{2^{q+1}}\right) + \left(2^{q-2} - \frac{1}{2} + \frac{1}{2^{q+2}}\right)\right)\right) |\vec{j}\rangle. \end{aligned}$$

Using the definition, it is easy to verify that $Q_{G_q} = U_q Q_q U_q$, where Q_q is the standard QFT as defined in Def. 3.1, and U_q is the q -qubit unitary:

$$U_q|\vec{j}\rangle = \exp\left(2\pi i - j \left(\frac{1}{2} + \frac{1}{2^{q+1}}\right) + \frac{1}{2} \left(2^{q-2} - \frac{1}{2} + \frac{1}{2^{q+2}}\right)\right) |\vec{j}\rangle \quad \forall \vec{j} \in \{0, 1\}^q.$$

A circuit for U_q can be obtained with q phase shift gates (Def. 3.5), therefore we can implement Q_{G_q} with the same asymptotic gate complexity, in $\mathcal{O}(\cdot)$ notation, as the standard QFT. The quantum gradient algorithm for approximately linear functions then works in the same way as the one for exactly linear functions described earlier, with the difference that we evaluate f at $(\widehat{x}_1, \widehat{x}_2, \dots, \widehat{x}_d)$ instead of (x_1, x_2, \dots, x_d) , and apply the inverse $Q_{G_q}^\dagger$ of the transformed QFT

instead of the standard QFT. We give the pseudocode of the algorithm in Alg. 3. For simplicity, we assume that we have access to a quantum circuit that maps $|\vec{x}\rangle \rightarrow e^{2\pi i 2^q f(\vec{x})} |\vec{x}\rangle$: this type of oracle is formally defined in Def. 5.10 in Sect. 5.1.2. Note that if we have a circuit to evaluate f in binary (i.e., $U_f |\vec{x}\rangle |\vec{y}\rangle = |\vec{x}\rangle |\vec{y} \boxplus f(\vec{x})\rangle$), then the desired circuit can be constructed with phase kickback, as in the circuit in Fig. 5.1, although one has to be careful due to the factor 2^q in the exponent, see Rem. 5.14 as well as [Jordan, 2005, Gilyén et al., 2019a].

Algorithm 3: Quantum gradient algorithm for approximately linear functions.

Input: Dimension d , digits of precision q , unitary U_f to evaluate $f : G_q^d \rightarrow \mathbb{R}$ such that:

$$U_f |\vec{x}_1\rangle |\vec{x}_2\rangle \cdots |\vec{x}_d\rangle = e^{2\pi i 2^q f(\widehat{x}_1, \widehat{x}_2, \dots, \widehat{x}_d)} |\vec{x}_1\rangle |\vec{x}_2\rangle \cdots |\vec{x}_d\rangle.$$

Output: Vector \tilde{g} that is close to a linear approximation of f at the origin.

- 1 **Initialize:** Prepare d q -qubit registers in the state $|\vec{0}\rangle$, and apply $H^{\otimes q}$ to each of them.
 - 2 Apply the (dq) -qubit unitary U_f to all registers.
 - 3 Apply $Q_{G_q}^\dagger$ to each of the d registers.
 - 4 Apply a measurement to all qubits. Calling $\vec{k}_1, \vec{k}_2, \dots, \vec{k}_d \in \{0, 1\}^q$ the measurement outcomes from the d registers, set $\tilde{g} \leftarrow (\widehat{k}_1, \widehat{k}_2, \dots, \widehat{k}_d) \in \mathbb{R}^d$.
 - 5 **return** the vector \tilde{g} .
-

Proposition 5.6 (Based on Lem. 5.1 in [Gilyén et al., 2019a]). *Let $q \in \mathbb{N}, q > 0, b \in \mathbb{R}, g \in \mathbb{R}^d$ with $\|g\|_\infty \leq \frac{1}{3}$. Let $f : [-\frac{1}{2}, \frac{1}{2}]^d \rightarrow \mathbb{R}$. If:*

$$|f(x) - \langle g, x \rangle - b| \leq \frac{1}{20\pi 2^q}$$

for at least 99.9% of the points $x \in G_q^d$, then the output of the gradient algorithm (Alg. 3) satisfies:

$$\Pr(|\tilde{g}_j - g_j| \leq \frac{1}{2q}) > \frac{3}{5} \quad \forall j = 1, \dots, d.$$

Proof. Similarly to our discussion for the exact linear case, we consider the “ideal” quantum state:

$$|\psi\rangle = \frac{1}{\sqrt{2^{dq}}} \sum_{\vec{x} \in \{0,1\}^{dq}} e^{2\pi i 2^q (\langle g, \vec{x} \rangle + b)} |\vec{x}_1\rangle |\vec{x}_2\rangle \cdots |\vec{x}_d\rangle,$$

which is a product state:

$$\begin{aligned} |\psi\rangle &= e^{2\pi i 2^q b} \left(\frac{1}{\sqrt{2^q}} \sum_{\vec{x}_1 \in \{0,1\}^q} e^{2\pi i 2^q g_1 \widehat{x}_1} |\vec{x}_1\rangle \right) \otimes \left(\frac{1}{\sqrt{2^q}} \sum_{\vec{x}_2 \in \{0,1\}^q} e^{2\pi i 2^q g_2 \widehat{x}_2} |\vec{x}_2\rangle \right) \otimes \cdots \\ &\quad \cdots \otimes \left(\frac{1}{\sqrt{2^q}} \sum_{\vec{x}_d \in \{0,1\}^q} e^{2\pi i 2^q g_d \widehat{x}_d} |\vec{x}_d\rangle \right). \end{aligned}$$

The global phase can be ignored. Recalling the relationship between Q_{G_q} and Q_q , by Thm. 3.12, if we apply $Q_{G_q}^\dagger$ to each of the d registers, measure all qubits, and interpret the resulting binary strings as points in the grid G_q , we obtain numbers $\widehat{k}_1 = \tilde{g}_1, \dots, \widehat{k}_d = \tilde{g}_d \in [-\frac{1}{2}, \frac{1}{2}]$ such that:

$$\Pr(|\tilde{g}_j - g_j| \leq \frac{1}{2q}) \geq \frac{8}{\pi^2} > \frac{4}{5} \quad \forall j = 1, \dots, d.$$

(The proof of Thm. 3.12 also applies to the transformed inverse QFT $Q_{G_q}^\dagger$, after accounting for the unitaries U_q in its definition; see the proof of [Gilyén et al., 2019a, Lem. 5.1].) Alg. 3 constructs:

$$|\phi\rangle = \frac{1}{\sqrt{2^{dq}}} \sum_{\vec{x} \in \{0,1\}^{dq}} e^{2\pi i 2^q f(\vec{x})} |\vec{x}_1\rangle |\vec{x}_2\rangle \cdots |\vec{x}_d\rangle,$$

so if we can show that $\|\psi\rangle - |\phi\rangle\| \leq \frac{1}{5}$, by Prop. 1.49 the probabilities of the measurement outcomes cannot change by more than $\frac{1}{5}$, ensuring that each component of \tilde{g} is sufficiently accurate with probability at least $\frac{4}{5} - \frac{1}{5} = \frac{3}{5}$. By assumption, for at least 99.9% of the points $x \in G_q^d$ we have that $|f(x) - \langle g, x \rangle - b| \leq \frac{1}{20\pi 2^q}$; let $S \subseteq G_q^d$ be the set of points that satisfy the inequality. Then we have:

$$\begin{aligned} \|\psi\rangle - |\phi\rangle\|^2 &= \frac{1}{2^{dq}} \sum_{x \in G_q^d} \left| e^{2\pi i 2^q f(x)} - e^{2\pi i 2^q (\langle g, x \rangle + b)} \right|^2 \\ &= \frac{1}{2^{dq}} \sum_{x \in S} \left| e^{2\pi i 2^q f(x)} - e^{2\pi i 2^q (\langle g, x \rangle + b)} \right|^2 + \frac{1}{2^{dq}} \sum_{x \in G_q^d \setminus S} \left| e^{2\pi i 2^q f(x)} - e^{2\pi i 2^q (\langle g, x \rangle + b)} \right|^2 \\ &\leq \frac{1}{2^{dq}} \sum_{x \in S} |2\pi 2^q f(x) - 2\pi 2^q (\langle g, x \rangle + b)|^2 + \frac{1}{2^{dq}} \sum_{x \in G_q^d \setminus S} 4 \\ &= \frac{1}{2^{dq}} \sum_{x \in S} (2\pi 2^q)^2 |f(x) - (\langle g, x \rangle + b)|^2 + \frac{1}{2^{dq}} \sum_{x \in G_q^d \setminus S} 4 \\ &\leq \frac{1}{2^{dq}} \left(\sum_{x \in S} \left(\frac{1}{10} \right)^2 + \sum_{x \in G_q^d \setminus S} 4 \right) \leq \left(\frac{1}{10} \right)^2 + \frac{4}{1000} \leq \left(\frac{1}{5} \right)^2. \end{aligned}$$

In the above chain, for the first inequality we used $|e^{iy} - e^{iz}| \leq |y - z|$, then we used the error bound for the points in S and the assumption on the cardinality of $G_q^d \setminus S$. \square

Prop. 5.6 shows that the output of Alg. 3 is a vector such that each component is close to a linear approximation g of f with probability at least $3/5$. By repeating the algorithm $\mathcal{O}(\log \frac{d}{\delta})$ times and taking the median component-wise, we boost the probability of success so that all components are close to g with probability at least $1 - \delta$ (for a formal proof of this result: suppose that we perform $2m + 1$ repetitions of the algorithm, and we require that for each component j , at least $m + 1$ of the values \tilde{g}_j are within distance $\frac{1}{2^q}$ from g_j ; if this is the case, the median of the values satisfies the desired bound. Then we apply the Chernoff-Hoeffding theorem, choosing m to ensure that the probability that each coordinate does not satisfy the desired condition is at most δ/d ; this gives $m = \mathcal{O}(\log \frac{d}{\delta})$). In this way, we obtain a more robust version of the gradient algorithm, because we allow a small deviation from linearity of the function f .

Remark 5.7. *The choice “99.9% of the points” in Prop. 5.6 is of course arbitrary, and only affects the final probability of success. The main benefit of allowing $f(x)$ to be far from $\langle g, x \rangle + b$ for some x is that we do not need f to be computed exactly at all points. For example, if f is computed via an algorithm that has a small probability of failure (as is often the case with quantum circuits), the gradient algorithm still works because, with high probability, the computation of f fails only at a small fraction of the points.*

5.1.2 Polynomial functions with other types of oracles

In the first part of Sect. 5.1.1 we worked with a linear function, and we had access to some form of a binary oracle for its value, i.e., a unitary that outputs a binary description of the function value. This allowed us to perform phase kickback using the property that the Fourier state corresponding to the all-ones binary string is an eigenvector of addition modulo the largest integer in the register. In the second part of Sect. 5.1.1 we directly assumed access to an oracle that applies the necessary phase, essentially bypassing phase kickback for simplicity: the purpose of the binary oracle in the gradient algorithm is to construct the necessary phases via kickback. In general we may not always have a linear or approximately linear function, and furthermore, we may not have access to a binary oracle for the function value; note that the binary oracle is usually available in situations where we know a (classical) Boolean circuit to compute the function value, but may be difficult to obtain otherwise. We now discuss some other possible computational models for the function f , and also relax the linearity assumption. The different computational models for the function

discussed in this section cover the situations that are most commonly found when implementing quantum circuits to carry out a computation. Results in this section are based on [Gilyén et al., 2019a].

Let us first discuss how to deal with nonlinearity. If we could somehow construct an approximation of the function $\langle \nabla f(0), x \rangle$, starting from an evaluation oracle for the nonlinear function f , then we could apply Alg. 3 to this new function, which is linear in x and such that its gradient is precisely $\nabla f(0)$. We can turn to ideas from calculus and numerical analysis to attain this goal, relying on a central difference approximation of the function f . A central difference approximation is a higher-order version of the simple central difference formula $\frac{\partial f}{\partial x_j}(0) \approx \frac{f(\eta e_j) - f(-\eta e_j)}{2\eta}$. We define it below, where we also state — without proof — that its value approximates $\langle \nabla f(0), x \rangle$. For details on the error bound obtained with this formula, see [Gilyén et al., 2019a].

Definition 5.8 (Central difference approximation). *The degree- $2m$ central difference approximation of a function $f : \mathbb{R}^d \rightarrow \mathbb{R}$ is the function defined as:*

$$f^{(2m)}(x) := \sum_{k=-m}^m a_k^{(2m)} f(kx) \approx \nabla f(0)^\top x,$$

where the coefficients $a_k^{(2m)}$ are defined as:

$$a_k^{(2m)} := \frac{(-1)^{k-1} \binom{m}{|k|}}{k \binom{m+|k|}{|k|}}$$

for $k \neq 0$, and $a_0^{(2m)} := 0$.

By computing $f^{(2m)}$ we obtain an approximation of $\langle \nabla f(0), x \rangle$: the value of m that is necessary for a good approximation depends on the desired error tolerance, and on the degree of nonlinearity of f . Note that evaluating $f^{(2m)}$ at one point requires evaluating f at $2m$ points, thus the value for m determines the cost (query complexity) of implementing an oracle for $f^{(2m)}$. We can then apply the gradient algorithm (Alg. 3) to $f^{(2m)}$, which is linear in x . An example of such a result is given below in Thm. 5.13.

We now move to discussing different input models for the function f . Besides binary oracles, there are two natural way to encode functions that have been used in one way or another in the literature on quantum algorithms. These are probability oracles and phase oracles. We have already used phase oracles without a proper definition, in Alg. 3. Below, x is a vector and \vec{x} is a binary encoding the vector x , e.g., by listing its components in binary in fixed precision.

Definition 5.9 (Probability oracle). *A probability oracle for a function $f : [0, 1] \rightarrow [0, 1]$ is a unitary U_f mapping $|\vec{0}\rangle|\vec{x}\rangle \rightarrow \sqrt{f(x)}|1\rangle|\psi_x^{(1)}\rangle + \sqrt{1-f(x)}|0\rangle|\psi_x^{(0)}\rangle$ for all x , where $|\psi_x^{(0)}\rangle, |\psi_x^{(1)}\rangle$ are some arbitrary quantum states.*

Note that according to the definition of probability oracle, the probability of observing $|1\rangle$ in the first qubit is precisely $f(x)$.

Definition 5.10 (Phase oracle). *A phase oracle for a function $f : [0, 1] \rightarrow [-1, 1]$ is a unitary U_f mapping $|\vec{0}\rangle|\vec{x}\rangle \rightarrow e^{if(x)}|\vec{0}\rangle|\vec{x}\rangle$ for all x .*

Conversion between these oracles is possible, with variable cost. Converting from a probability oracle to a binary oracle can be expensive (it can be done with amplitude estimation). We can efficiently convert a binary oracle to a phase oracle using phase kickback, as shown in Sect. 5.1.1. Converting from a probability oracle to a phase oracle is also efficient: we give a conversion result below.

Theorem 5.11 (Converting probability oracles into phase oracles; Cor. 4.1 in [Gilyén et al., 2019a]). *Let $f : [0, 1] \rightarrow [0, 1]$ and suppose we have access to a probability oracle U_f for f . Then we can implement an ϵ -approximate phase oracle for f using $\mathcal{O}(\log \frac{1}{\epsilon})$ applications of U_f and U_f^\dagger , i.e., a unitary whose output on any valid input state is at most ϵ -away (in Euclidean norm) from the output of an exact phase oracle.*

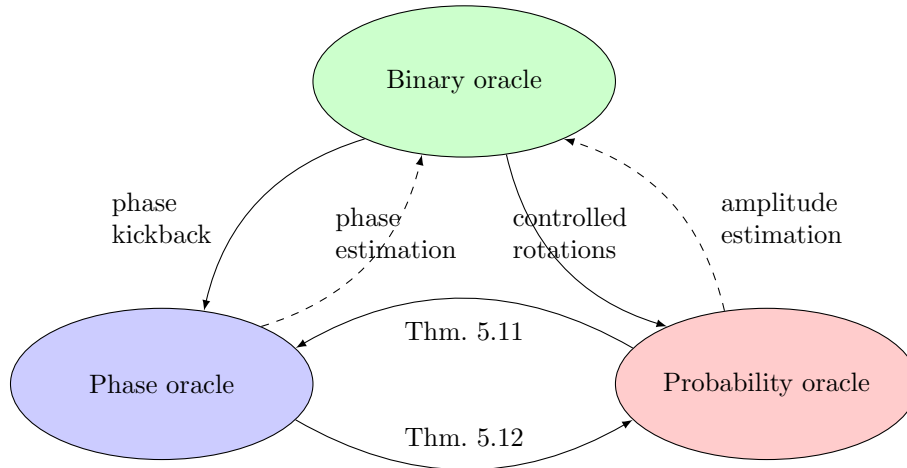


Figure 5.2: Oracle conversion. Solid lines indicate efficient conversions (polylogarithmic cost in $1/\epsilon$), dashed lines indicate inefficient conversions (polynomial cost in $1/\epsilon$).

There are likely many constructive proofs for Thm. 5.11. The approach used in [Gilyén et al., 2019a] approximates the exponential function $e^{if(x)}$ with a Taylor series, then constructs each term in the series (which is a sinusoidal function) relying on an analogy with Grover’s algorithm. Indeed, a probability oracle constructs a superposition of a “good” and a “bad” state, marked by the first qubit, and we can rotate in the plane spanned by these two. The terms are then combined using a linear combination of unitaries, see Sect. 6.2.3. To complement Thm. 5.11, we note that conversion from a phase to a probability oracle is also efficient, provided the probability is bounded away from 0 and 1 by a constant.

Theorem 5.12 (Converting phase oracles into probability oracles; Lem. 16 in the arXiv version of [Gilyén et al., 2019a]). *Let $f : [0, 1] \rightarrow [\delta, 1 - \delta]$ and suppose we have access to a phase oracle U_f for f . Then we can implement an ϵ -approximate probability oracle for f using $\mathcal{O}(\frac{1}{\delta} \log \frac{1}{\epsilon})$ applications of U_f and U_f^\dagger .*

These conversion results are summarized in Fig. 5.2. As indicated in the picture, conversions between oracle types are generally efficient in the inverse precision (i.e., they run in time polylogarithmic in $1/\epsilon$) except when trying to convert a probability or a phase oracle to a binary oracle: such an “analog to digital” transformation can be resource-intensive (i.e., it runs in time polynomial in $1/\epsilon$).

Putting everything together, the cost of gradient computation for nonlinear functions f with an extension of the gradient algorithm of Sect. 5.1.1 is no longer as simple as for the linear case, and it depends on how the function f is specified, i.e., its input model. A detailed analysis is given in [Gilyén et al., 2019a]; we report a version of their results below.

Theorem 5.13 (Gradient estimation for polynomial functions; based on Thm. 5.2 in [Gilyén et al., 2019a]). *Let $f : [-1, 1]^d \rightarrow \mathbb{R}$ be a multivariate polynomial of degree k , and suppose we have access to a phase oracle for f . Then with $\tilde{\mathcal{O}}(\frac{k}{\epsilon})$ calls to the phase oracle, and $\tilde{\mathcal{O}}(\frac{dk}{\epsilon})$ additional gates, we can compute an ϵ -approximation (in ℓ^∞ -norm) of $\nabla f(0)$ with probability at least $1 - \delta$.*

Remark 5.14. *For the case $k = 1$, i.e., linear functions, there is a notable difference between Thm. 5.13 and the approach that we discussed in Sect. 5.1.1 after Prop. 5.6 (i.e., applying Alg. 3, taking $\mathcal{O}(\log \frac{d}{\delta})$ repetitions, and returning the median): Thm. 5.13 has $\frac{1}{\epsilon}$ dependence, whereas $\frac{1}{\epsilon}$ does not show up in Prop. 5.6. This apparent discrepancy is easily explained by the difference in input model: in Alg. 3 we assume access to a phase oracle for $2^q f(x)$, whereas in Thm. 5.13 we assume access to a phase oracle for $f(x)$. Converting a phase oracle for $f(x)$ into one for $2^q f(x)$ leads to $\mathcal{O}(2^q) = \mathcal{O}(\frac{1}{\epsilon})$ applications of the weaker phase oracle, because we need to — in some*

sense — “amplify the signal.” (Recall that if we want error at most ϵ , we need $q = \lceil \log \frac{1}{\epsilon} \rceil$ digits of precision.) On the other hand, suppose we start with a binary oracle for f , under the same assumption of Def. 5.10 that the codomain of f is $[-1, 1]$. Suppose further that the binary oracle outputs a number with h digits of precision, i.e., it writes the value of $f(x)$ as a fraction $0.\vec{\ell}$ with $\vec{\ell} \in \{0, 1\}^h$, where h can be decided. Then, the string $\vec{\ell}$ represents the integer $\ell = 2^h f(x)$, so we can implement the operation $U_f|\vec{x}\rangle|\vec{y}\rangle = |\vec{x}\rangle|\vec{y} \boxplus 2^h f(x)\rangle$: the value of $f(x)$ is initially fractional, we treat it as an integer by shifting the binary point to the right, i.e., multiplying by 2^h , and perform modular addition with the last register over an appropriate number of digits. Thus, given a sufficiently accurate binary oracle for f , we can choose h to implement a phase oracle for $2^q f(x)$ with phase kickback and the construction of Fig. 5.1, using a single call to the binary oracle. In the first part of Sect. 5.1.1 we ignored this detail for simplicity.

Note that for $k > 1$ the performance of the algorithm degrades, due to the cost of computing the central difference approximation. Still, as long as the degree k is small, the dimension d does not appear in the query complexity, except in polylogarithmic factors (but it appears in the gate complexity); this is because the central difference approximation gives a precise gradient approximation for multivariate polynomials. The result of Thm. 5.13 can be extended to more general, nonpolynomial analytic functions by using their Taylor series approximation, and relying on error bounds for the Taylor series. However, we need the higher-order derivatives to be bounded (they are always bounded for polynomial functions over a compact domain), because otherwise the error terms of the Taylor series may make it difficult to accurately determine by how much we are deviating from the “ideal” linear case. We do not pursue the analysis of this more general case.

We also highlight that the quantum gradient algorithm can be made to return an unbiased estimate of the gradient, by modifying the phase estimation part. The reason why bias may occur is the following. In an ideal world, we are able to prepare exactly the state $|\psi\rangle$ in Eq. (5.1), then we apply phase estimation with a sufficient number of digits of precision to store the exact value of the phases. When this happens, the phase estimation algorithm returns a finite-precision representation of the gradient with probability 1. However, errors can occur in either step of the computation: we may not be able to prepare $|\psi\rangle$ exactly (this is especially common whenever the function f is nonlinear, and we rely on the central difference approximations), or we may not have enough digits of precision to store the phase. In this case the output of phase estimation is a random variable, whose expected value is not necessarily the gradient — even if we know that it is close enough to the gradient. By making phase estimation unbiased, for a “sufficiently linear” (in the sense of Prop. 5.6) function we can obtain a gradient algorithm whose output is an unbiased estimate of the gradient. For details, see [van Apeldoorn et al., 2023, Sect. 6.5].

5.1.3 The gradient algorithm for quantum state tomography

A perhaps surprising application of the gradient algorithm is to obtain a classical description of an unknown quantum state that can be prepared with a given unitary; the process of obtaining a description of a quantum state is called *quantum state tomography*. In general we can only obtain information on a quantum state via measurements, as we discussed in Ch. 1, and measuring a q -qubit quantum state only yields q bits of information. But there are algorithms to recover a full description of the quantum state, up to some specified level of precision: obviously, multiple measurements or measurements of a larger number of qubits become necessary. We describe such an algorithm that uses the gradient algorithm as a subroutine. This algorithm, a version of which is described in [van Apeldoorn et al., 2023], is optimal in some settings, but not in all settings: it is targeted at the case in which we have a quantum circuit to prepare the state of interest. In other situations, other algorithms are more efficient. Still, we find the idea to be pedagogical, and the result can be useful as a subroutine in several optimization algorithms.

Remark 5.15. *Quantum state tomography is another possible approach to output a vector with a quantum algorithm. If we have a quantum algorithm that encodes its solution in the amplitudes of a quantum state, and we want a classical description of the solution, we can obtain it with a*

tomography algorithm. For example, quantum linear systems algorithms encode the solution of a linear system in the amplitudes of a quantum state, see Ch. 7 and the notes therein. Note that the cost of a quantum state tomography algorithm to obtain a classical description of the desired state may be large, and therefore it is usually a good idea to try to avoid performing an expensive tomography step, see the discussion in Sect. 7.1.6.

The idea for the algorithm is the following. In Sect. 5.1.1 we have seen that the gradient algorithm (Alg. 3) is efficient for some form of gradient computation: it outputs the gradient of a linear function with a single application of (some implementation of) that function. If we can construct a unitary implementing a function such that its gradient is a description of the quantum state, we can use the gradient algorithm to obtain that description. Let $U|\vec{0}\rangle = |\psi\rangle = \sum_{\vec{j} \in \{0,1\}^n} \alpha_j |\vec{j}\rangle$ be an n -qubit quantum state constructed by the unitary U , and let $d = 2^n$. The function $f(x) := \sum_{\vec{j} \in \{0,1\}^n} \alpha_j^\dagger x_j = \langle \psi | \left(\sum_{\vec{j} \in \{0,1\}^n} x_j |\vec{j}\rangle \right)$ is a linear function such that its gradient is precisely the vector α^\dagger , i.e., a classical description of $|\psi\rangle$. If we can construct a phase oracle for $f(x)$, then we can apply the gradient algorithm to it. (In fact, the algorithm described below obtains a description of the real part of the entries of α^\dagger , so the complex conjugate is irrelevant.)

To construct the phase oracle we use a construction for the inner product of two quantum states, given access to unitaries that prepare them. This can be done in many ways, including via a probability oracle inspired by a construction usually known as *Hadamard test*; we give below such a construction. Readers familiar with the Hadamard test may recognize its basic structure. (We use \Re for the real part and \Im for the imaginary part of a complex number or vector, component-wise.)

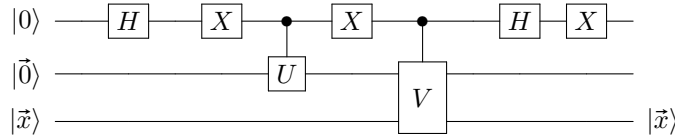


Figure 5.3: Probability oracle for a function encoding a quantity proportional to the inner product of two quantum states.

Proposition 5.16. *Suppose we have two unitaries U, V such that $U|\vec{0}\rangle = |\psi\rangle$ and $V|\vec{0}\rangle|\vec{x}\rangle = |\phi_x\rangle|\vec{x}\rangle$, and controlled version of them. Then the circuit in Fig. 5.3 is a probability oracle for the function $f(x) := \frac{1}{2}(1 + \Re\langle\psi|\phi_x\rangle)$, and it uses a single application of controlled- U and controlled- V , plus a constant number of single-qubit gates.*

Proof. Let us analyze the circuit in Fig. 5.3. After the first Hadamard gate, the state of the system is $\frac{1}{\sqrt{2}}(|0\rangle + |1\rangle)|\vec{0}\rangle|\vec{x}\rangle$. Controlled- U acts on the bottom qubit lines when the top qubit is $|0\rangle$, because it is sandwiched between X gates, whereas controlled- V acts when the top qubit is $|1\rangle$. Thus, after controlled- V , we are in the state $\frac{1}{\sqrt{2}}(|0\rangle|\psi\rangle|\vec{x}\rangle + |1\rangle|\phi_x\rangle|\vec{x}\rangle)$. The final Hadamard gate produces:

$$\frac{1}{2}(|0\rangle(|\psi\rangle|\vec{x}\rangle + |\phi_x\rangle|\vec{x}\rangle) + |1\rangle(|\psi\rangle|\vec{x}\rangle - |\phi_x\rangle|\vec{x}\rangle)).$$

The probability of observing $|0\rangle$ when measuring the first qubit is therefore:

$$\begin{aligned} \left\| \frac{1}{2}(|\psi\rangle|\vec{x}\rangle + |\phi_x\rangle|\vec{x}\rangle) \right\|^2 &= \frac{1}{4}(\langle\psi|\langle\vec{x}| + \langle\phi_x|\langle\vec{x}|)(|\psi\rangle|\vec{x}\rangle + |\phi_x\rangle|\vec{x}\rangle) = \frac{1}{4}(2 + \langle\psi|\phi_x\rangle + \langle\phi_x|\psi\rangle) \\ &= \frac{1}{2}(1 + \Re\langle\psi|\phi_x\rangle). \end{aligned}$$

The final X gate bit-flips the first qubit, ensuring that the probability of observing $|1\rangle$ is the above expression. This concludes the proof. \square

Prop. 5.16 shows how to implement a probability oracle for a function that involves the inner product $\langle \psi | \phi_x \rangle$; using Thm. 5.11, we can then convert it to a phase oracle, which in turn can be employed directly as an input for Alg. 3. However, for Prop. 5.16 to implement exactly the gadget that we need, we still need to specify the precise form of $|\phi_x\rangle$.

Recall that our idea is to implement a tomography algorithm by constructing a phase oracle for the function:

$$f(x) = \langle \psi | \left(\sum_{\vec{j} \in \{0,1\}^n} x_j |\vec{j}\rangle \right),$$

i.e., the inner product of x with $|\psi\rangle$: if we can do this, the gradient algorithm recovers $\nabla_x f(0)$, which is precisely $|\psi\rangle$. In the context of Prop. 5.16, this means that we need $|\phi_x\rangle$ to be the state $\sum_{\vec{j} \in \{0,1\}^n} x_j |\vec{j}\rangle$. Hence, we need a unitary that maps $|\vec{x}\rangle \in \{0,1\}^{dq}$ to an n -qubit state with amplitudes x_0, x_1, \dots, x_{d-1} , where the string \vec{x} is interpreted as a vector with each component encoded on q bits (we use zero-based indices for x , because we index its components with binary strings). We call this operation *amplitude encoding*, as defined in Def. 5.34: we postpone a proper definition to Sect. 5.2 because here we need a slightly different normalization, so to avoid confusion, we do not introduce our shorthand notation for the amplitude encoding until a bit later. The important part, however, is that such a unitary is not difficult to construct, using controlled single-qubit rotations: we give a full description of a circuit to implement it in Sect. 5.2.

An important detail that must be considered is the normalization factor for the state $\sum_{\vec{j} \in \{0,1\}^n} x_j |\vec{j}\rangle$. Unitaries can only construct proper quantum states, i.e., unit vectors, thus we must ensure that the mapping $|\vec{x}\rangle \rightarrow \sum_{\vec{j} \in \{0,1\}^n} x_j |\vec{j}\rangle$ is unitary. In Prop. 5.6 the function f is assumed to have domain $[-\frac{1}{2}, \frac{1}{2}]^d$, and in Thm. 5.13 it has domain $[-1, 1]^d$; indeed, Alg. 3 starts by constructing a superposition of grid points symmetric about the origin. The argument of $f(x)$ therefore lives in $[-1, 1]^d$; the maximum Euclidean norm of such a vector is \sqrt{d} . (The smaller box $[-\frac{1}{2}, \frac{1}{2}]^d$ would be sufficient, but this only makes a constant-factor difference in the norm, so we keep $[-1, 1]^d$ to simplify calculations.) Each vector $x \in [-1, 1]^d$ may have a different norm, so we cannot hope to construct the “quantum state” $\frac{1}{\sqrt{d}} \sum_{\vec{j} \in \{0,1\}^n} x_j |\vec{j}\rangle$ for all $x \in [-1, 1]^d$: it is not always a properly normalized quantum state. On the other hand, we want to keep the same normalization factor regardless of the value of x , otherwise $f(x)$ would not be linear. We resolve this issue by relying on a construction for $\frac{1}{\sqrt{d}} \sum_{\vec{j} \in \{0,1\}^n} x_j |\vec{j}\rangle$ that is not always successful. Specifically, to ensure that some version of the mapping $|\vec{x}\rangle \rightarrow \frac{1}{\sqrt{d}} \sum_{\vec{j} \in \{0,1\}^n} x_j |\vec{j}\rangle$ is well-defined (and unitary) for all input values, we define a unitary that acts as follows:

$$V_{\text{amp}} |0\rangle |\vec{0}\rangle_n |\vec{x}\rangle_{dq} = \left(|0\rangle \left(\frac{1}{\sqrt{d}} \sum_{\vec{j} \in \{0,1\}^n} x_j |\vec{j}\rangle \right) + |1\rangle \left(\frac{1}{\sqrt{d}} \sum_{\vec{j} \in \{0,1\}^n} \sqrt{1 - x_j^2} |\vec{j}\rangle \right) \right) |\vec{x}\rangle.$$

In this way, the output is a normalized quantum state, and the first register acts as a flag register: when its value is $|0\rangle$, we have produced the desired state $\frac{1}{\sqrt{d}} \sum_{\vec{j} \in \{0,1\}^n} x_j |\vec{j}\rangle$, and when its value is $|1\rangle$, the circuit has failed to produce the desired state. This unitary can be constructed with $\tilde{\mathcal{O}}(dq)$ gates, where — as before — q is the number of bits for each component of x , i.e., \vec{x} is a dq -digit bitstring. It can be rigorously proven that it is sufficient to pick q polynomial in the size of the input unitary U , because this already yields the necessary precision for each component of x (intuitively: the precision of each number increases exponentially with the number of binary digits, so with $\mathcal{O}(n) = \mathcal{O}(\log d) = \tilde{\mathcal{O}}(1)$ digits we already achieve exponentially-high precision $\mathcal{O}(2^{-d})$). This simplifies the expression for the number of gates to $\tilde{\mathcal{O}}(d)$.

Putting everything together, we do the following:

- We apply the circuit described in Prop. 5.16, choosing U to be the unitary that prepares the state $|\psi\rangle$ of which we want a description, and choosing V to be the unitary V_{amp} that produces the vector $\frac{1}{\sqrt{d}} \sum_{\vec{j} \in \{0,1\}^n} x_j |\vec{j}\rangle$ with a flag register. This yields a probability oracle

for

$$f(x) = \langle \psi | \left(\frac{1}{\sqrt{d}} \sum_{\vec{j} \in \{0,1\}^n} x_j |\vec{j}\rangle \right). \quad (5.3)$$

- We convert it to a phase oracle using Thm. 5.11.
- We apply the gradient algorithm, Alg. 3. Because the function $f(x)$ is linear, we can set $k = 1$ in Thm. 5.13. To recover the (real part of the) amplitudes α_j of $|\psi\rangle$ to precision ϵ we need to set the precision in Thm. 5.13 to ϵ/\sqrt{d} , because in the definition of the function of Eq. (5.3) each component is scaled down by \sqrt{d} , requiring us to increase precision. This recovers the real part of α_j up to precision ϵ for all j .
- We repeat the same algorithm adding a phase gate in the controlled operation to multiply $|\psi\rangle$ by the imaginary unit i , and recover the imaginary part of α_j .

In this description we have performed a few simplifications. Notably, the fact that V_{amp} has a flag register introduces some difficulty, because repeating the calculations of Prop. 5.16 with the added flag register yields an undesirable extra term in the probability oracle. This should be expected: in some sense, the mapping V_{amp} is not always successful, because it produces $\frac{1}{\sqrt{d}} \sum_j x_j |\vec{j}\rangle$ only with some probability, i.e., when the flag register is $|0\rangle$. Nonetheless, the undesirable extra term can be eliminated when converting from probability to phase oracle: we leave these details as an exercise. We obtain the following.

Theorem 5.17 (Quantum state tomography with element-wise error; Thm. 5.1 in [van Apeldoorn et al., 2023]). *Let $U|\vec{0}\rangle = |\psi\rangle = \sum_{\vec{j} \in \{0,1\}^n} \alpha_j |\vec{j}\rangle$ be a quantum state. Let $d = 2^n$. Using the quantum gradient algorithm in the way described in this section, with probability at least $1 - \delta$ we output $\tilde{\alpha} \in \mathbb{R}^d$ such that $|\Re(\alpha_j) - \tilde{\alpha}_j| \leq \epsilon$ for all j , using $\tilde{O}(\sqrt{d}/\epsilon)$ applications of U and U^\dagger , and $\tilde{O}(d^{1.5}/\epsilon)$ additional gates. A small modification of the same algorithm outputs $\tilde{\alpha} \in \mathbb{R}^d$ such that $|\Im(\alpha_j) - \tilde{\alpha}_j| \leq \epsilon$ for all j with the same running time.*

The gate count can be determined by noticing that we use precision \sqrt{d}/ϵ in Thm. 5.13, and each call to V_{amp} takes $\tilde{O}(d)$ gates.

Due to the relationship between Euclidean distances between quantum states and total variation distance stated in Prop. 1.49, as well as the pervasiveness of the Euclidean distance in many contexts, often one is interested in obtaining a classical description of a quantum state with a bound on the maximum error in Euclidean distance. It is sufficient to set the error in Thm. 5.17 to ϵ/\sqrt{d} : if each amplitude is estimated with that precision, the resulting vector has Euclidean distance at most ϵ from the true vector. Formally, we have the following corollary.

Corollary 5.18. *Let $U|\vec{0}\rangle = |\psi\rangle = \sum_{\vec{j} \in \{0,1\}^n} \alpha_j |\vec{j}\rangle$ be a quantum state. Let $d = 2^n$. Using the quantum gradient algorithm in the way described in this section, with probability at least $1 - \delta$ we output $\tilde{\alpha} \in \mathbb{R}^d$ such that $\|\Re(\alpha) - \tilde{\alpha}\| \leq \epsilon$ using $\tilde{O}(d/\epsilon)$ applications of U and U^\dagger , and $\tilde{O}(d^2/\epsilon)$ additional gates. A small modification of the same algorithm outputs $\tilde{\alpha} \in \mathbb{R}^d$ such that $\|\Im(\alpha) - \tilde{\alpha}\| \leq \epsilon$ with the same running time.*

Additional discussion on quantum state tomography can be found in the notes in Sect. 5.4.

5.1.4 Separation from membership oracles

The seminal work of Grötschel, Lovász and Schrijver [Grötschel et al., 1988] highlighted a powerful connection between membership, separation, optimization, violation, and validity in the context of convex optimization. Each of these five concepts admits a proper mathematical definition, and can be turned into a question such as “does the point x belong to a given set K ” (membership) and “is there a hyperplane separating x from K ” (separation). As [Grötschel et al., 1988] shows, all the resulting questions are equivalent under polynomial-time transformations. In this section we show that a crucial transformation (separation using a membership oracle) can be made more

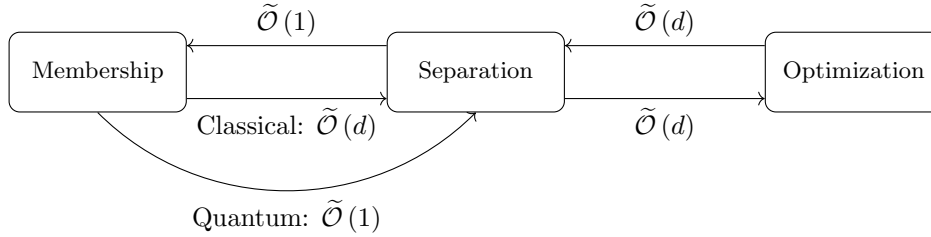


Figure 5.4: Relationship between membership, separation and optimization oracles for a fixed d -dimensional convex set. An arrow from oracle a to oracle b indicates that one can simulate oracle b with a certain number of calls to oracle a ; the number of calls is indicated next to the arrow. These results are based on [Grötschel et al., 1988, Lee et al., 2018, van Apeldoorn et al., 2020a, Chakrabarti et al., 2020].

efficient if one has access to a membership oracle implemented on a quantum computer, by means of the gradient algorithm. We focus our discussion on three of the five oracles: membership, separation, and optimization. For the relationship between the two remaining oracles (violation and validity) and the aforementioned three, we refer to [Grötschel et al., 1988].

Formally, consider the following type of optimization problem:

$$\min_{x \in K} \langle c, x \rangle, \quad (5.4)$$

where $K \subset \mathbb{R}^d$ is a convex set, and $c \in \mathbb{R}^d$. It is well known that algorithms that can solve problem (5.4) can also solve the more general convex optimization problem $\min_{x \in K} f(x)$, with $f: \mathbb{R}^d \rightarrow \mathbb{R}$ convex, via a simple lifting to the $(n+1)$ -dimensional problem:

$$\min_{(x,y) \in K'} y, \quad \text{with } K' := \{(x,y) \in K \times \mathbb{R} : f(x) \leq y \leq F\},$$

where $F \in \mathbb{R}$ is some given upper bound on $f(x)$. Thus, problem (5.4) encompasses a large class of optimization problems. Under fairly general assumptions, if we can separate a point $x \notin K$ from K , then we can optimize $\langle c, x \rangle$ over K ; and conversely, if we can optimize a linear function over K , then we can separate. Similarly, being able to separate from K and being able to determine membership of a point in K are two aspects of the same question, and we can transform between the two. For a fixed set K , the efficiency of the transformation between oracles that determine membership, separation and optimization can vary depending on the algorithm used, and, as discussed in this section, on the model of computation. An application of the quantum gradient algorithm provides an exponential query complexity advantage in constructing a separating hyperplane using a membership oracle for the set K , compared to classical algorithm: the classical separation algorithm uses $\tilde{O}(n)$ calls to a membership oracle, whereas the quantum algorithm uses $\tilde{O}(1)$ (but the membership oracle is implemented by a unitary that can be called in superposition, of course). The relationship between the three oracles, defined formally below, is summarized in Fig. 5.4.

In this section we give an overview of the main idea that leads to this quantum advantage. We sketch some of the proofs, while keeping the discussion at a high-enough level to leave out cumbersome details: although the framework is elegant and most of the ideas admit an intuitive explanation, all rigorous treatments of the subject that we are aware of rely — to some extent — on heavy technical tools, and lead to unwieldy constants that would detract from the pedagogical purpose of this section. A detailed development can be found in our main references for this section: [Grötschel et al., 1988, Lee et al., 2018] for the classical algorithm, [van Apeldoorn et al., 2020a, Chakrabarti et al., 2020] for the quantum algorithm.

Remark 5.19. *An algorithm to solve the convex optimization problem (5.4) using only a membership oracle for the set K is extremely general: typically, even a “basic working description” of a set lets us determine if a given point belongs to it or not. However, it is not the most efficient*

approach for most situations: with some knowledge of the structure of K , it is usually possible to rely on, or construct, more efficient algorithms. Convex optimization with a cutting plane method, i.e., via separation (not necessarily through a membership oracle), can lead to algorithms that are theoretically very efficient, e.g., [Lee et al., 2015] (although to the best of our knowledge, the algorithm of [Lee et al., 2015] has not led to practical implementations of algorithms for the numerical solution of convex optimization problems).

Preliminaries. We need to introduce several concepts to formally characterize our assumptions for problem (5.4), and to define the oracles that constitute the main topic for the section. First, we define the concept of a ball, with distance measured according to the ℓ^p -norm. Then, we define the neighborhood of a set (i.e., the set containing all small balls centered at points in the set) and the interior of a set (i.e., the set of all points such that the ball centered at them is fully contained in the set). Finally, we define the three fundamental oracles: membership, to determine if a point is inside or outside K ; separation, to return a hyperplane separating a point outside K from K ; and optimization, to return a maximizer of a linear function over K (equivalently, we could have defined this oracle to return a minimizer).

Definition 5.20 (Ball in ℓ^p -norm). *Given $r \in \mathbb{R}, r > 0$, and $x \in \mathbb{R}^d$, we define the ball of radius r in the ℓ^p -norm centered at x as:*

$$B_p(x, r) := \{y \in \mathbb{R}^d : \|x - y\|_p \leq r\}.$$

Definition 5.21 (Neighborhood and interior of a convex set). *Given $K \subset \mathbb{R}^d$, K convex, and $r \in \mathbb{R}, r > 0$, we define the r -neighborhood of K as:*

$$B_p(K, r) := \{y \in \mathbb{R}^d : \|x - y\|_p \leq r \text{ for some } x \in K\}.$$

We also define the r -interior of K as:

$$B_p(K, -r) := \{y \in \mathbb{R}^d : B_p(y, r) \subseteq K\}.$$

Definition 5.22 (Membership, separation and optimization oracles). *Fix a convex set $K \subset \mathbb{R}^d$. Let $\epsilon, \delta > 0$ be given. The return values of the oracles defined below are all assumed to be correct with probability at least $1 - \delta$.*

A membership oracle, denoted $MEM_{\epsilon, \delta}(x)$, given $x \in \mathbb{R}^d$ asserts that $x \in B_2(K, \epsilon)$ or that $x \notin B_2(K, -\epsilon)$.

A separation oracle, denoted $SEP_{\epsilon, \delta}(x)$, given $x \in \mathbb{R}^d$ asserts that $x \in B_2(K, \epsilon)$ or it returns a vector $g \in \mathbb{R}^d$ such that $\langle g, y \rangle \leq \langle g, x \rangle + \epsilon$ for all $y \in B_2(K, -\epsilon)$.

An optimization oracle, denoted $OPT_{\epsilon, \delta}(c)$, given $c \in \mathbb{R}^d$ asserts that $B_2(K, -\epsilon)$ is empty, or it returns a vector $x \in B_2(K, \epsilon)$ such that $\langle c, y \rangle \leq \langle c, x \rangle + \epsilon$ for all $y \in B_2(K, -\epsilon)$.

It is clear that an optimization oracle directly solves problem (5.4) up to some desired precision ϵ . It is also known that a separation oracle can be used to construct an optimization oracle with a polynomial number of calls. [Grötschel et al., 1988] already showed how to convert between the three types of oracles in Def. 5.22. The following result characterizes the most efficient known constructive algorithm (at the time of writing this) to build an optimization oracle from a separation oracle.

Theorem 5.23 (From separation to optimization; Thm. 42 in [Lee et al., 2015], Thm. 15 in [Lee et al., 2018]). *Let $K \subset \mathbb{R}^d$ be a convex set satisfying $B_2(0, r) \subset K \subset B_2(0, R)$ for given $r, R \in \mathbb{R}, 0 < r < R$. Let $c \in \mathbb{R}^d$. For any $\epsilon, \delta \in \mathbb{R}, 0 < \epsilon < 1, 0 < \delta < 1$, with probability at least $1 - \delta$, we can compute $x \in B_2(K, \epsilon)$ such that:*

$$\langle c, x \rangle \leq \min_{y \in K} \langle c, y \rangle + \epsilon \|c\|,$$

with $\tilde{\mathcal{O}}(d)$ calls to $SEP_{\delta', \epsilon'}(K)$ and $\tilde{\mathcal{O}}(d^3)$ additional arithmetic operations, in expectation, where δ', ϵ' are polynomially large in the instance parameters.

Thus, construction of a separation oracle is sufficient to perform optimization; this explains the arrow between separation and optimization in Fig. 5.4. Note that in this setting, we know the radius of a ball contained in K , and of a ball containing K , which avoids some degenerate cases and ensures the origin is contained in K . If we only have access to a membership oracle for K , which is weaker than a separation oracle, to perform optimization we can attempt to construct a separation oracle, and then invoke Thm. 5.23. As we discuss in the remainder of this section, one possibility to construct a separation oracle from a membership oracle is to use a subgradient of the so-called height function, measuring the distance of a point from the boundary of K along a given direction. The subgradient can be computed via finite differences (with a classical computer), or with Jordan’s gradient algorithm (with a quantum computer). The concepts of subgradient and approximate subgradient, used repeatedly in this section and in Ch. 8, are formally defined below. The notation V^* refers to the *dual vector space* of the origin vector space V (i.e., the space of all linear forms on V).

Definition 5.24 (Subgradient and ϵ -subgradient). *Let V be a vector space. Given $f : V \rightarrow \mathbb{R}$ convex, $g \in V^*$ is called a subgradient of f at \bar{x} if, for every $x \in V$, we have:*

$$f(x) \geq f(\bar{x}) + \langle g, x - \bar{x} \rangle.$$

$g \in V^*$ is called an ϵ -subgradient of f at \bar{x} if, for every $x \in V$, we have:

$$f(x) \geq f(\bar{x}) + \langle g, x - \bar{x} \rangle - \epsilon.$$

The set of all subgradients at \bar{x} , called the subdifferential, is denoted $\partial f(\bar{x})$. The set of all ϵ -subgradients at \bar{x} , called the ϵ -subdifferential, is denoted $\partial_\epsilon f(\bar{x})$.

Classical separation oracle. We give a rough idea of the approach delineated in [Lee et al., 2018], with some simplifications from [van Apeldoorn et al., 2020a], to construct a separation oracle from a membership oracle. We construct a function, called the *height function*, that measures a notion of distance between a given point z and the boundary of K . Suppose we are trying to separate a point that lies on the “vertical” axis (see below for why this is w.l.o.g.). An $\bar{\epsilon}$ -subgradient of the height function at the origin gives the separating hyperplane, for an appropriate value of $\bar{\epsilon}$. Approximating the subgradient can be difficult because the height function is not necessarily continuous, but it is Lipschitz continuous. Fortunately, it can be shown that the expected value of the subgradient at points randomly sampled from a small ball centered at the origin is a good approximation of the sought subgradient.

We assume that we are trying to separate the point $x = -\tau e_d$ from K with $\tau \in \mathbb{R}, \tau > 0$, i.e., a point where the first $d-1$ coordinates are zero and the last coordinate is negative. This is w.l.o.g., because we can always rotate the coordinate system to verify this condition; the rotation can be determined without much effort, and it would not affect the query complexity of the membership oracle anyway. (Imagining the situation in three dimensions gives a good intuition of how to compute a rotation that zeroes the first $d-1$ coordinates, and makes the last one negative, using a sequence of two-dimensional rotations.) The height function $h : \mathbb{R}^{d-1} \rightarrow \mathbb{R} \cup \{\infty\}$ is defined as:

$$h(y) := \inf_{(y,t) \in K} t,$$

i.e., $h(y)$ is the smallest value such that $(y, h(y)) \in K$ if such a value exists, and it is ∞ if no such value exists. This is the “height” of the $(d-1)$ -dimensional hyperplane where the last coordinate is zero with respect to the boundary of the d -dimensional set K , see Fig. 5.5. This function has several crucial properties, which we state without proof.

Proposition 5.25 (Based on Lem. 19 and Lem. 21 in [van Apeldoorn et al., 2020a]). *Let $K \subset \mathbb{R}^d$ be a convex set satisfying $B_2(0, r) \subset K \subset B_2(0, R)$ for given $r, R \in \mathbb{R}, 0 < r < R$. Let $x = -\tau e_d \notin B(K, -\epsilon)$. The function $h : \mathbb{R}^{d-1} \rightarrow \mathbb{R} \cup \{\infty\}$, $h(y) := \inf_{(y,t) \in K} t$ satisfies the following:*

- (i) *it is convex.*

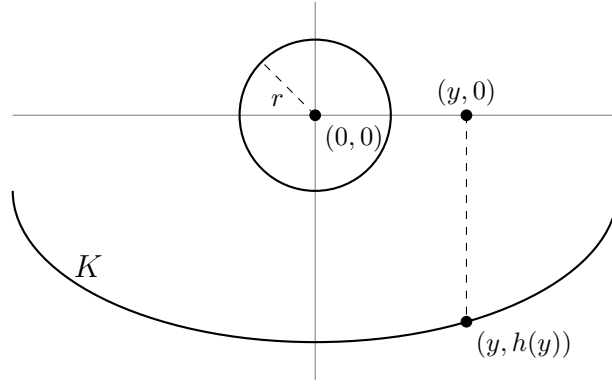


Figure 5.5: Visual representation of the height function $h(y)$ in two dimensions, i.e., with $K \subset \mathbb{R}^2$ and $h : \mathbb{R} \rightarrow \mathbb{R}$.

- (ii) it is Lipschitz continuous with Lipschitz constant $\frac{2R}{r}$ over $B_2(0, r/2)$;
- (iii) if we take $g \in \partial_{\bar{\epsilon}} h(0)$ for an appropriately chosen value of $\bar{\epsilon}$, and let $a = (g, 1) \in \mathbb{R}^d$, the half-space $\langle a, z \rangle \geq \langle a, x \rangle - \bar{b}$ separates x and K for an appropriately chosen $\bar{b} \in \mathbb{R}$, i.e., $\langle a, z \rangle \geq \langle a, x \rangle - \bar{b}$ for all $z \in K$.

We omit a discussion on the values of $\bar{\epsilon}, \bar{b}$ for ease of exposition. It is not difficult to see that the height function can be approximated using binary search exploiting the membership oracle for K : given $y \in \mathbb{R}^{d-1}$, we consider points in \mathbb{R}^d of the form (y, t) , where $t \in \mathbb{R}$, and we perform binary search on t using the membership oracle to determine the smallest value of t such that $(y, t) \in K$. Then we can estimate a subgradient of h at the origin with a finite-difference approximation, and by Prop. 5.25 (in particular property (iii)), this yields the sought separating hyperplane.

Definition 5.26 (Finite-difference gradient approximation). *Let $f : \mathbb{R}^d \rightarrow \mathbb{R}$, and $\eta \in \mathbb{R}, \eta > 0$. The finite-difference gradient approximation of f at $x \in \mathbb{R}^d$ with step η is the vector:*

$$\nabla_{(\eta)} f(x) := \begin{pmatrix} \frac{f(x+\eta e_1) - f(x-\eta e_1)}{2\eta} \\ \frac{f(x+\eta e_2) - f(x-\eta e_2)}{2\eta} \\ \vdots \\ \frac{f(x+\eta e_d) - f(x-\eta e_d)}{2\eta} \end{pmatrix}.$$

Def. 5.26 gives a symmetric formula for a gradient approximation. The error of $\nabla_{(\eta)} f(x)$ can be upper bounded in terms of an approximation of the trace of the Hessian matrix.

Definition 5.27 (Finite-difference Laplace approximation). *Let $f : \mathbb{R}^d \rightarrow \mathbb{R}$, and $\eta \in \mathbb{R}, \eta > 0$. The finite-difference Laplace approximation of f at $x \in \mathbb{R}^d$ with step η is the scalar:*

$$\Delta_{(\eta)} f(x) := \sum_{j=1}^d \frac{f(x + \eta e_j) - 2f(x) + f(x - \eta e_j)}{\eta^2}.$$

Lemma 5.28 (Lem. 10 in [van Apeldoorn et al., 2020a]). *Let $\eta \in \mathbb{R}, \eta > 0, x \in \mathbb{R}^d, f : B_1(x, \eta) \rightarrow \mathbb{R}$ convex. Then:*

$$\sup_{g \in \partial f(x)} \|g - \nabla_{(\eta)} f(x)\|_1 \leq \frac{1}{2} \eta \Delta_{(\eta)} f(x).$$

Thus, if $\Delta_{(\eta)} f(x)$ is small, $\nabla_{(\eta)} f(x)$ is a good approximation of a subgradient. We want to apply this result to obtain a subgradient of the height function $h(y)$ at the origin by computing $\nabla_{(\eta)} h(0)$, but $h(y)$ does not have enough structure to guarantee a straightforward application of Lem. 5.28: we only know that $h(x)$ is convex and Lipschitz continuous, and with just these two properties, $\Delta_{(\eta)} f(x)$ could be unbounded as $\eta \rightarrow 0$.

Example 5.29. Consider $f : \mathbb{R} \rightarrow \mathbb{R}, f(x) = |x|$, which is convex and 1-Lipschitz. We have:

$$\nabla_{(\eta)}f(0) = \frac{f(\eta) - f(-\eta)}{2\eta} = 0,$$

but:

$$\Delta_{(\eta)}f(0) = \frac{f(\eta) - 2f(0) + f(-\eta)}{\eta^2} = \frac{2}{\eta},$$

so $\Delta_{(\eta)}f(0) \rightarrow 0$ as $\eta \rightarrow 0$.

Thus, convexity and Lipschitz continuity alone may not suffice to show that $\nabla_{(\eta)}f(x)$ is a good approximation of a subgradient at x . As a consequence, our task of constructing a sufficiently accurate approximation of a subgradient of the height function at the origin is not complete yet. Fortunately, it can be shown that picking a uniformly random point in a ball around the origin yields small values of the Laplace approximation, in expectation.

Lemma 5.30 (Lem. 11 in [van Apeldoorn et al., 2020a]). Let $\eta, r \in \mathbb{R}, 0 < \eta < r$, and let $f : B_\infty(x, r + \eta) \rightarrow \mathbb{R}$ be convex and L -Lipschitz. Then:

$$\mathbb{E}_{z \in B_\infty(x, r)} \Delta_{(\eta)}f(z) \leq \frac{dL}{r}.$$

This leads to the following strategy: pick a uniform random point in a small ball around the origin, and compute the finite-difference approximation of the subgradient of the height function at that point. In expectation, the Laplace approximation is small, so the finite-difference approximation is an accurate estimate of a subgradient at that point. Because the ball is small, it is also an accurate (but slightly worse) estimate of a subgradient at the origin, i.e., it belongs to $\partial_\epsilon h(0)$ for a larger ϵ (recall Def. 5.24). Additionally, it is not necessary that the finite-difference approximation uses the exact value of h : we can use the estimate obtained with the binary search procedure discussed after Prop. 5.25, taking advantage of the fact that the complexity of binary search scales polylogarithmically with the reciprocal of the error. We obtain the following result.

Proposition 5.31 (Lem. 12 in [van Apeldoorn et al., 2020a]). Let $r, L, \epsilon, \delta \in \mathbb{R}, r > 0, L > 0, 0 < \delta < 1/3, 0 < \epsilon < rL\sqrt{d}/\delta$. Let $f : \mathbb{R}^d \rightarrow \mathbb{R}$ be a convex function that is L -Lipschitz on $B_\infty(0, 2r)$, and let $\tilde{f} : \mathbb{R}^d \rightarrow \mathbb{R}$ be such that $|f(x) - \tilde{f}(x)| \leq \epsilon$ for all $x \in B_\infty(0, 2r)$. Then, for a uniformly random $z \in B_\infty(0, r)$, we can compute parameters $0 < \eta < r, \epsilon' > \epsilon$ such that, with probability at least $1 - \delta$, we have $\nabla_{(\eta)}f(z) \in \partial_{\epsilon'}f(0)$.

Proof. The proof is not difficult, but it would require us to give cumbersome expressions for η and ϵ' . We give a high-level sketch: we use Lem.s 5.28 and 5.30 to show that the finite-difference gradient approximation at a random point z approximates $\partial f(z)$ with error $\frac{\eta dL}{2r}$; since z and 0 are close, and f is L -Lipschitz, it is then straightforward to compute an $\tilde{\epsilon}$ so that $\nabla_{(\eta)}f(z) \in \partial_{\tilde{\epsilon}}f(0)$ in expectation. Using Markov's inequality, with probability $1 - \delta$ a sample from the random variable (i.e., a z picked at random) achieves a gradient error bounded by $\frac{\tilde{\epsilon}}{\delta}$, which gives the final error parameter ϵ' . \square

With Prop. 5.31, the construction of the separation oracle is essentially finished: we compute the finite-difference gradient approximation at a random point in a small ball around the origin, and return the hyperplane specified in Prop. 5.25. By Def. 5.26, the computation of the finite-difference gradient approximation involves $\tilde{O}(d)$ calls to the membership oracle (because we estimate the height function at $\tilde{O}(d)$ points, and each estimation runs in $\tilde{O}(1)$ iterations of binary search). This motivates the ‘‘classical’’ arrow between membership and separation in Fig. 5.4.

Quantum separation oracle. We can construct a separation oracle using a quantum computer in a similar manner. Prop. 5.31 states that in expectation, the finite-difference gradient approximation of h at points picked randomly in a ball around the origin is close to $\partial_\epsilon h(0)$. However, the expression for the finite-difference gradient approximation contains h evaluated at d different

points, leading to the $\tilde{\mathcal{O}}(d)$ query complexity (i.e., number of calls to the membership oracle) of the classical algorithm. We rely on Jordan’s gradient algorithm to take advantage of a quantum computer and reduce the query complexity.

To be able to apply Jordan’s gradient algorithm to estimate $\partial_\epsilon h(0)$, we must first show that the function h is close to linear over an appropriate domain. Lem. 5.28 does not suffice: it bounds the distance of $\nabla_{(\eta)} h(z)$ from to $g \in \partial h(z)$ in terms of $\Delta_{(\eta)} h(z)$, but for Jordan’s algorithm to work we need that h is close to linear almost everywhere in a small ℓ^∞ -ball, not just at a specific point z . Lem. 5.30 still helps: because $\Delta_{(\eta)} h(z)$ is small in expectation, it means that the rate of change of the subgradients is also small (recall that $\Delta_{(\eta)} h(z)$ is a finite-difference approximation of the magnitude of the second-order derivatives). More formally, it can be shown that $\Delta_{(\eta)} h(z)$ bounds by how much h deviates from linearity around z .

Lemma 5.32 (Lem. 17 in [van Apeldoorn et al., 2020a]). *Let $\eta \in \mathbb{R}$, $\eta > 0$, let $z \in \mathbb{R}^d$, and let $f : B_1(z, \eta) \rightarrow \mathbb{R}$ convex. Then:*

$$\sup_{y \in B_1(0, \eta)} |f(z + y) - f(z) - \langle \nabla_{(\eta)} f(z), y \rangle| \leq \frac{1}{2} \eta^2 \Delta_{(\eta)} f(z).$$

Proof. Define $g(y) := f(z + y) - f(z) - \langle \nabla_{(\eta)} f(z), y \rangle$, i.e., $g(y)$ is the difference between $f(z + y)$ and the value at $z + y$ of the linear approximation of f constructed at z . Note that $g(0) = 0$, and for every $j = 1, \dots, d$, using the definition of $\nabla_{(\eta)} f(z)$ we have:

$$\begin{aligned} g(\pm \eta e_j) &= \frac{f(z + \eta e_j) - 2f(z) + f(z - \eta e_j)}{2} \\ &= \frac{\eta^2}{2} (\Delta_{(\eta)} f(z))_j \leq \frac{\eta^2}{2} \Delta_{(\eta)} f(z). \end{aligned}$$

The points $\pm \eta e_j$ for $j = 1, \dots, d$ are the extreme points of the set $B_1(0, \eta)$ over which we are taking the supremum. Using convexity of $g(y)$ and of $B_1(0, \eta)$, it is straightforward to show $\sup_{y \in B_1(0, \eta)} |g(y)| \leq \frac{1}{2} \eta^2 \Delta_{(\eta)} f(z)$. \square

We use Lem. 5.32 to ensure that we satisfy the conditions for Prop. 5.6, when applying the gradient algorithm to the height function. In particular, Prop. 5.6 only requires that a function admits some accurate linear approximation, and if that is the case, it returns such an approximation: it does not require the function to be differentiable. Thus, we can apply it to the height function. There are still a few more obstacles to overcome; in particular, in Alg. 3 and consequently Prop. 5.6, it is assumed that f is computed exactly, but here we apply Alg. 3 to the function h , which is evaluated up to some error. The remaining issues can be addressed using standard tools, leading to the following result.

Theorem 5.33 (Separation oracle via quantum gradient; Thm. 23 in [van Apeldoorn et al., 2020a]). *Let $K \subset \mathbb{R}^d$ be a convex set satisfying $B_2(0, r) \subset K \subset B_2(0, R)$ for given $r, R \in \mathbb{R}$, $0 < r < R$, and let $x \notin B(K, -\epsilon)$. For any $\epsilon, \delta \in \mathbb{R}$, $0 < \epsilon < R$, $0 < \delta < \frac{1}{3}$, we can implement $SEP_{\epsilon, \delta}(x)$ with $\tilde{\mathcal{O}}(1)$ calls to a quantum oracle implementing $MEM_{0, \epsilon'}(K)$, for an appropriately chosen ϵ' .*

Proof. We sketch the proof. By Prop. 5.25, the height function h is $\frac{2R}{r}$ -Lipschitz over $B_2(0, r/2)$. By Lem.s 5.30 and 5.32, if we pick a random point in a small ball around the origin, the function h is close to linear, so we can apply Prop. 5.6 to compute an approximate (sub)gradient. Prop. 5.6 evaluates h only once, and each evaluation of h uses $\tilde{\mathcal{O}}(1)$ evaluations of the membership oracle. \square

Thm. 5.33 motivates the “quantum” arrow between membership and separation in Fig. 5.4, and shows a quantum speedup in terms of query complexity.

5.2 Encoding an arbitrary vector in a quantum state

Given a d -dimensional vector $x \in \mathbb{C}^d$, in many optimization-related contexts we may need access to its encoding as a quantum state, i.e., as a quantum state with amplitudes corresponding to the components of x . Already in Sect. 5.1.3 we needed a way to map a binary description of $x \in \mathbb{R}^d$ to $\frac{1}{\sqrt{d}} \sum_{\vec{j}} x_j |\vec{j}\rangle$, in the context of state tomography (with a slightly different normalization than the canonical $\frac{1}{\|x\|}$ to get a unit vector, but this has little impact on the discussion presented in this section); a similar construction is useful, for example, in our discussion of quantum linear systems algorithms in Ch. 7. We introduce a shorthand notation for this type of encoding of a vector, because it is used multiple times in the rest of this set of lecture notes.

Definition 5.34 (Amplitude encoding). *Given a vector $x \in \mathbb{C}^d$, we denote its amplitude encoding by*

$$|\text{amp}(x)\rangle := \sum_{\vec{j} \in \{0,1\}^n} \frac{x_j}{\|x\|} |\vec{j}\rangle,$$

where $n = \lceil \log d \rceil$.

In this section we describe a classical procedure that, starting from a classical description of the vector x , produces the description of a quantum circuit that maps $|\vec{0}\rangle \rightarrow |\text{amp}(x)\rangle$.

Remark 5.35. *We describe a classical procedure for the amplitude encoding that works as follows: the procedure takes as input a binary description of x , and outputs a quantum circuit that produces $|\text{amp}(x)\rangle$. Because of this, we can also write a quantum circuit for the same task, i.e., a quantum circuit that starts from a basis state encoding x as a binary string, and outputs (in a different register) the state $|\text{amp}(x)\rangle$ (that is, a quantum state with coefficients given by x). To do so, we run a quantum circuit that performs the same steps as the classical procedure, and rather than simply outputting the description of the quantum circuit to construct $|\text{amp}(x)\rangle$, we apply the corresponding operations with controlled gates onto a fresh register initialized as $|\vec{0}\rangle$. Similar considerations apply to any classical procedure that outputs the description of a quantum circuit to perform a given task.*

The construction given in this section is essentially a specialized version of the scheme for creating the quantum encoding of efficiently integrable distributions described in [Grover and Rudolph, 2002]. Assume $d = 2^n$ for simplicity (we can always pad x with zero entries if its dimension is not a power of two), and assume $\|x\| = 1$ because we can only amplitude-encode unit vectors; with this assumption we do not have to keep track of the factor $\frac{1}{\|x\|}$ in Def. 5.34, and of course an algorithm for $x : \|x\| = 1$ can be applied to a general x by normalizing it in a preprocessing step. The construction performs a classical preprocessing and then produces a quantum circuit that maps $|\vec{0}\rangle \rightarrow |\text{amp}(x)\rangle$ for real x , see Rem. 5.35. We discuss the case for complex x subsequently.

Starting from a classical description of $x \in \mathbb{R}^d$ in finite precision, we begin by creating a binary tree, illustrated in Fig. 5.6, that is used to determine the angles of some rotations. The tree has $n + 1$ levels, labeled 0 to n from top to bottom. At the bottom level there are $d = 2^n$ nodes, each node containing a value and its sign; the value contained in the leaf nodes is the square of the corresponding entry of x . For every level $k = n - 1, \dots, 0$, there are 2^k nodes, with each node containing the sum of the values of the nodes below it. Note that the tree has $2^{n+1} - 1$ nodes in total. We index each node with its level and its position in the level, labeled from left to right; for example, node $(0, 0)$ is the root, nodes $(1, 0)$ and $(1, 1)$ are the left and right child of the root respectively, and so on. The value contained in each node is denoted $N(k, j)$, where (k, j) is the index of the node as described above.

The full algorithm to produce a circuit constructing $|\text{amp}(x)\rangle = \sum_{\vec{j} \in \{0,1\}^n} x_j |\vec{j}\rangle$ is described in Alg. 4; the first step of the algorithm is the construction of the binary tree, as the algorithm references the node values throughout. In the “for” loop $k = 1, \dots, n - 1$, we always add a new qubit, and on line 5 of Alg. 4, we apply a controlled operation where the first k qubits — containing $|\psi_k\rangle$ — are the control (where $|\vec{j}\rangle\langle\vec{j}|$ acts), and the last qubit — the fresh qubit — is

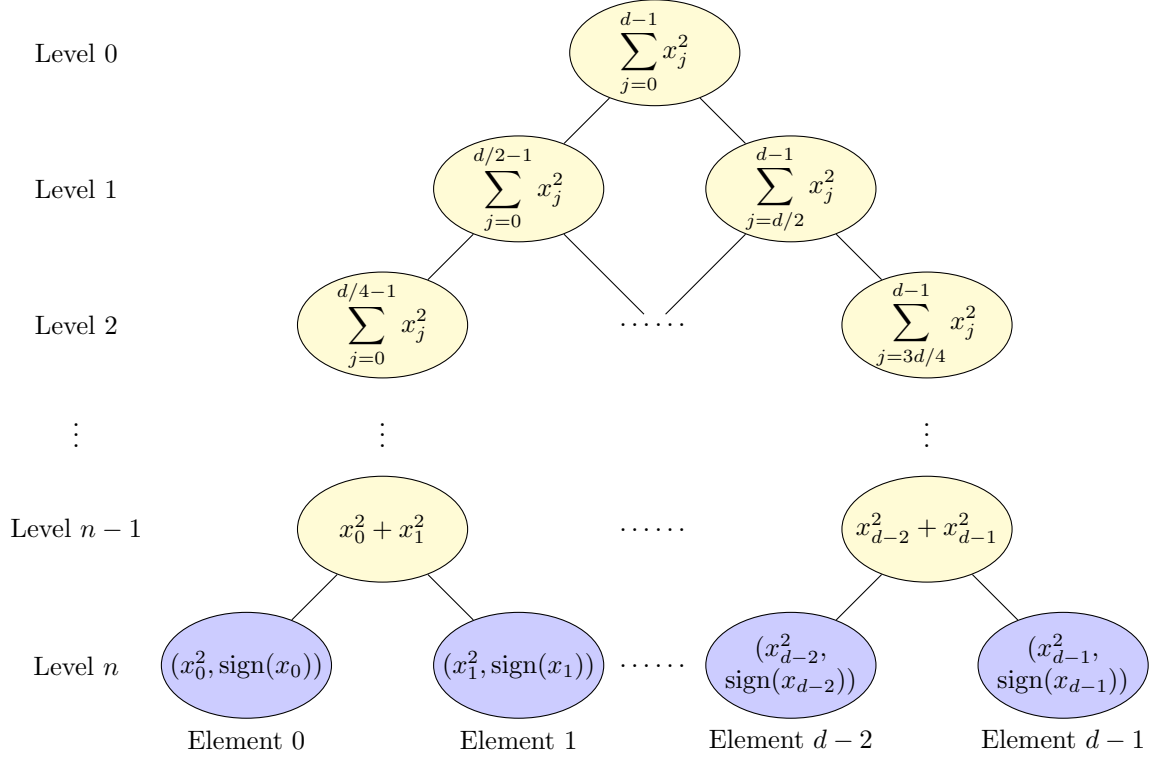


Figure 5.6: Binary tree to prepare the state $\sum_{\vec{j} \in \{0,1\}^n} x_j |\vec{j}\rangle$ (assuming $\|x\| = 1$).

the target, onto which the rotation R_Y acts. (Recall the definition of R_Y in Def. 4.26.) Note that the last operation of the algorithm, on line 7, can be merged with the operation on line 5 into a single unitary, as the last operation simply adjusts the sign of the elements of the rotation matrix R_Y ; we write it separately for ease of exposition. We show that this scheme leads to the desired amplitude encoding.

Proposition 5.36. *Alg. 4 returns a quantum circuit on n qubits mapping $|\vec{0}\rangle$ to $|\text{amp}(x)\rangle$.*

Proof. We first prove by induction that each state $|\psi_k\rangle$ produced by Alg. 4 up until we exit the “for” loop (i.e., before we execute line 7) satisfies the following:

$$|\psi_k\rangle = \sum_{\vec{j} \in \{0,1\}^k} \sqrt{N(k, \vec{j})} |\vec{j}\rangle.$$

The base step $k = 1$ follows directly from the initialization step of the algorithm, remembering that $N(1, 0) + N(1, 1) = \sum_{j=0}^{2^n-1} x_j^2 = 1$.

For the induction step, let $|\psi_{k+1}\rangle = \sum_{\vec{h} \in \{0,1\}^{k+1}} \alpha_h |\vec{h}\rangle$, and consider a specific coefficient α_h . Write $|\vec{h}\rangle_{k+1} = |\vec{j}\rangle_k |z\rangle_1$, i.e., we isolate the last digit z of the binary string \vec{h} . By construction, α_h is equal to the product of $\langle \vec{j} | \psi_k \rangle$ (i.e., the coefficient of $|\vec{j}\rangle$ in $|\psi_k\rangle$) and the coefficient produced by the rotation inside the “for” loop on line 5. Using the induction hypothesis and the definition of R_Y , this is equal to:

$$\begin{aligned} \sqrt{N(k, \vec{j})} & \left(\sqrt{\frac{N(k+1, 2j)}{N(k+1, 2j) + N(k+1, 2j+1)}} \right) & \text{if } z = 0 \\ \sqrt{N(k, \vec{j})} & \left(\sqrt{\frac{N(k+1, 2j+1)}{N(k+1, 2j) + N(k+1, 2j+1)}} \right) & \text{if } z = 1. \end{aligned}$$

Algorithm 4: Algorithm to construct the amplitude encoding of a given vector $x \in \mathbb{R}^d$.

Input: Vector $x \in \mathbb{R}^d$ with $\|x\| = 1$, described in finite precision.

Output: Quantum circuit on n qubits mapping $|\vec{0}\rangle \rightarrow |\text{amp}(x)\rangle$.

1 **Initialize:** Compute the binary tree illustrated in Fig. 5.6.

2 Set $|\psi_1\rangle \leftarrow \sqrt{\frac{N(1,0)}{N(1,0)+N(1,1)}}|0\rangle + \sqrt{\frac{N(1,1)}{N(1,0)+N(1,1)}}|1\rangle$.

3 **for** $k = 1, \dots, n-1$ **do**

4 Prepare a fresh qubit in the state $|0\rangle$, and append it to $|\psi_k\rangle$.

5 Set:

$$|\psi_{k+1}\rangle \leftarrow \left(\sum_{\vec{j} \in \{0,1\}^k} |\vec{j}\rangle\langle\vec{j}| \otimes R_Y \left(2 \arccos \left(\sqrt{\frac{N(k+1,2j)}{\frac{N(k+1,2j)}{N(k+1,2j+1)} + N(k+1,2j+1)}} \right) \right) \right) |\psi_k\rangle|0\rangle.$$

6 **end**

7 Set $|\psi_n\rangle \leftarrow \left(\sum_{\vec{j} \in \{0,1\}^n} \text{sign}(x_j) |\vec{j}\rangle\langle\vec{j}| \right) |\psi_n\rangle$.

8 **return** the circuit that produces the state $|\psi_n\rangle$.

Furthermore, $N(k, j) = N(k+1, 2j) + N(k+1, 2j+1)$ by construction of the binary tree, and $h = 2j$ if $z = 0$, $h = 2j+1$ if $z = 1$. Thus, we can combine and simplify the above expressions, obtaining:

$$\alpha_h = \sqrt{N(k+1, h)}.$$

This concludes the proof of the claim $|\psi_k\rangle = \sum_{\vec{j} \in \{0,1\}^k} \sqrt{N(k, j)} |\vec{j}\rangle$ for all k .

The final operation, applied to $|\psi_n\rangle$ when we exit the “for” loop, i.e., the almost-final n -qubit state produced by the algorithm, adjusts the signs of the coefficients of the quantum state to match those of the vector x , concluding the proof. \square

Because this construction applies one controlled operation for every inner node of the binary tree, and the binary tree has $\mathcal{O}(2^n) = \mathcal{O}(d)$ nodes, it can be implemented with $\mathcal{O}(d)$ multiply-controlled rotations. If we decompose them into basic gates, the total gate complexity becomes $\tilde{\mathcal{O}}(d)$. Note that there are two sources of error in the implementation of the circuit to take into account. The first source is the discretization error, because we assume $x \in \mathbb{R}^d$ and so the values $N(k, j)$ may not be representable exactly in finite precision. However, we assumed that we start from a classical description of x in finite precision, so this error is already accounted for: our goal is to construct the amplitude encoding of the finite-precision representation of x . The second source of error is the implementation of the controlled rotations to the required precision, starting from a binary description of the angles. As usual after our discussion in Thm. 1.43 and Sect. 1.3.6, we simply assume that all operations are performed with high (and sufficient) accuracy, as the cost is merely polylogarithmic in the precision: this gets absorbed in the $\tilde{\mathcal{O}}(\cdot)$ notation.

We described the procedure for $x \in \mathbb{R}^d$ because in this set of lecture notes we only use it for real input, and this simplifies the notation, but it is straightforward to amend the construction for complex input: quantities of the form x_j^2 (i.e., the inner nodes of the binary tree data structure in Fig. 5.6) should be replaced by $|x_j|^2$, and instead of adjusting for $\text{sign}(x_j)$, we also adjust for its complex phase. We obtain the following result.

Corollary 5.37. *Given a classical description of $x \in \mathbb{C}^d$ in finite precision, there is a circuit that implements the mapping $|\vec{0}\rangle \rightarrow |\text{amp}(x)\rangle$ with error at most ϵ with gate complexity $\tilde{\mathcal{O}}(d)$.*

Proof. We follow the construction whose correctness is proven in Prop. 5.36, with the only difference that in the last step, rather than adjusting only $\text{sign}(x_j)$, we apply a general single-qubit

unitary to adjust the phase of each amplitude. As there are $\mathcal{O}(d)$ such operations, this does not affect the running time of $\tilde{\mathcal{O}}(d)$. We emphasize that the parameter ϵ does not appear in the expression for the gate complexity because the dependence is polylogarithmic in $1/\epsilon$. \square

Example 5.38. Let $x = (0.4, 0.4, 0.8, 0.2) \in \mathbb{R}^4$, and note that $\|x\| = 1$. We want to construct $|\text{amp}(x)\rangle$, i.e., the state:

$$|\psi\rangle = 0.4|00\rangle + 0.4|01\rangle + 0.8|10\rangle + 0.2|11\rangle.$$

The binary tree corresponding to this vector is illustrated in Fig. 5.7. Because all coefficients

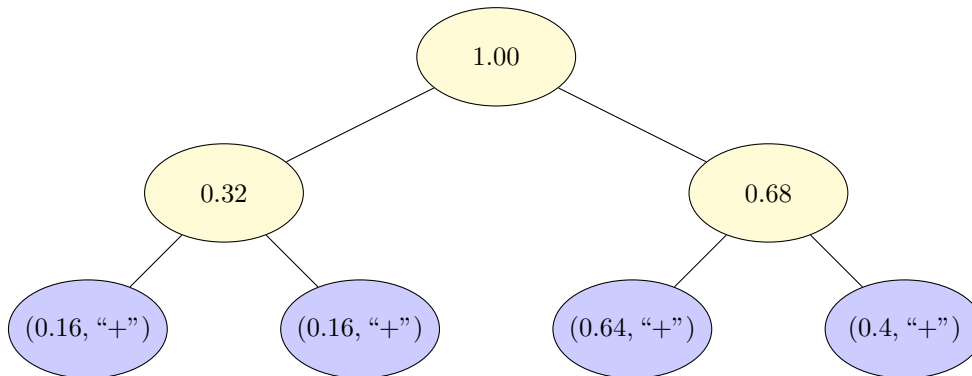


Figure 5.7: Binary tree to prepare the state $|\psi\rangle = 0.4|00\rangle + 0.4|01\rangle + 0.8|10\rangle + 0.2|11\rangle$.

of x are nonnegative, we ignore the sign information at the leaf nodes, i.e., we do not have to implement the corresponding sign-adjusting operations. We can construct the amplitude encoding of x by performing the following mappings, each of which requires a controlled rotation (one per line in the equation below):

$$\begin{aligned} |0\rangle \otimes |0\rangle &\rightarrow (\sqrt{0.32}|0\rangle + \sqrt{0.68}|1\rangle) \otimes |0\rangle \\ (\sqrt{0.32}|0\rangle + \sqrt{0.68}|1\rangle) \otimes |0\rangle &\rightarrow \sqrt{0.16}|00\rangle + \sqrt{0.16}|01\rangle + \sqrt{0.68}|10\rangle \\ \sqrt{0.16}|00\rangle + \sqrt{0.16}|01\rangle + \sqrt{0.68}|10\rangle &\rightarrow \sqrt{0.16}|00\rangle + \sqrt{0.16}|01\rangle + \sqrt{0.64}|10\rangle + \sqrt{0.04}|11\rangle. \end{aligned}$$

In total, this takes three controlled rotations — one for each inner node in the tree.

A modified version of this procedure, described in [Grover and Rudolph, 2002], assumes that the vector x contains the square root of the probabilities of a probability distribution over $\{0, \dots, d-1\}$, and the distribution is efficiently integrable. Indeed, if one takes this view, the values corresponding to inner nodes of the binary tree of Fig. 5.6 are just integrals of the density function with certain lower and upper limits: at level 1 we take the integral between 0 and $d/2 - 1$, and between $d/2$ and $d - 1$; at level 2 we halve these two intervals, and so on. It is not difficult to see that we can then avoid constructing the binary tree a priori, and rather, construct it on the fly invoking an oracle that computes the integrals corresponding to each inner node: details can be found in [Grover and Rudolph, 2002].

5.3 Quantum RAM and faster amplitude encoding

The input model of quantum algorithms usually requires the ability to access data in superposition. This can create slowdowns, because theoretically any piece of the input data can be queried, requiring availability of all the input data in the circuit that implements a query to the input data. For instance, consider the case in which data is accessed via a table containing d pieces of data: a circuit implementing this table has $\tilde{\mathcal{O}}(d)$ gates in general, because it must contain the entire table. The situation is similar to a classical singly-linked list of size d : accessing an element

takes $\mathcal{O}(d)$ time in the worst case. Classically, this issue is solved by using data structures with constant-time access, such as arrays stored in random-access memory (RAM). The fundamental principle of a RAM is that any piece of data contained in it can be accessed in near-constant time. This concept can be translated to the quantum world. We do so in the next subsection, and then discuss a direct application for faster amplitude encoding of vectors.

5.3.1 Definition

Quantum RAM (QRAM) is the quantum equivalent of a classical RAM: it allows constant-time (or in any case, very fast) access to classical data stored in memory. In the literature one can find several possible definitions for QRAM, as there are subtle details that matter depending on the implementation. Here we adopt a straightforward definition. In this section we assume $d = 2^n$.

Definition 5.39 (QRAM). *Let $\vec{M}_1, \dots, \vec{M}_d \in \{0, 1\}^q$. A classical-write, quantum-read quantum RAM (QRAM) of size dq is a device that implements the unitary operation U_{QRAM} satisfying the following property:*

$$U_{\text{QRAM}}|\vec{j}\rangle|\vec{y}\rangle = |\vec{j}\rangle|\vec{y} \oplus \vec{M}_j\rangle \quad \forall \vec{j} \in \{0, 1\}^n, \vec{y} \in \{0, 1\}^q.$$

Remark 5.40. *We call Def. 5.39 a classical-write, quantum-read QRAM because the only operations performed in superposition on the storage device is to read its data: we do not allow writing content in superposition. In fact, all data $\vec{M}_1, \dots, \vec{M}_d$, which is assumed to be classically available in some form, is already stored in the QRAM when we perform the operation U_{QRAM} . In principle we could also define a quantum-read, quantum-write device that allows changing the data $\vec{M}_1, \dots, \vec{M}_d$ stored in the device in superposition, but this would be an even more powerful device than the classical-write, quantum-read QRAM. Generally, in the literature the term QRAM stands for “classical-write, quantum-read QRAM,” unless otherwise specified.*

Remark 5.41. *In principle the operation U_{QRAM} should be parameterized by the data $\vec{M}_1, \dots, \vec{M}_d$, but we do not write this dependence explicitly for the sake of simplicity. In other words, a QRAM of a given size is not just a single unitary, but rather, a family of unitaries, and the specific unitary chosen from the family is determined by the value of the data. This subtlety does not impact our subsequent discussion.*

Given a QRAM containing some data of interest, such as the input data of an algorithm, the running time of an algorithm that needs access to the data can then be given in terms of the number of times that the QRAM is accessed. This is another form of *query* (or oracle) *complexity*, where the query corresponds to accessing the input data. Many (in fact, at the time of this writing, the vast majority of) quantum optimization algorithms assume QRAM, and their running time is usually given in terms of number of QRAM accesses. If the QRAM oracle can be implemented with time complexity $\mathcal{O}(1)$, similar to the time complexity of classical RAM, then the number of QRAM calls immediately translates into a bound on the time complexity. This is not the same as the time complexity in the standard circuit model, where time corresponds to the number of gates (gate complexity).

We emphasize that the operation U_{QRAM} is not possible in $\mathcal{O}(1)$ time in the standard circuit model: something more powerful than the standard quantum gates is necessary. Indeed, in general to construct U_{QRAM} with standard gates we need to implement a lookup table: a circuit that, conditioned on the content \vec{j} of the first register, “writes” (with binary XOR) the corresponding datum \vec{M}_j in the second register. Such a lookup table needs, at the very least, one CX gate for every bit with value 1 among the data $\vec{M}_1, \dots, \vec{M}_d$, i.e., $\Omega(d)$ gates. It is not difficult to give an explicit circuit construction for the lookup table with $\mathcal{O}(dq)$ two-qubit gates. Thus, requiring that U_{QRAM} runs in time $\mathcal{O}(1)$ is a strong assumption, yielding a more powerful input model for quantum algorithms: a quantum algorithm with access to QRAM could run certain operations faster than any quantum algorithm in the standard circuit model; an example of this is discussed in Sect. 5.3.2.

Remark 5.42. *In the quantum algorithms literature that employs QRAM, it is standard to assume that one access to the QRAM (i.e., an application of U_{QRAM}) takes $\mathcal{O}(1)$ time. We make the same assumption in this set of lecture notes, however we additionally report the number of QRAM accesses to allow translation into the standard circuit model, see Rem. 5.44.*

One may wonder why such a powerful input model was initially conceived, and why its use is widespread in the literature: after all, we should be interested in realistic input models only. The simple reason is that, due to the existence of classical RAM, i.e., storage devices that allow access to any piece of data in $\mathcal{O}(1)$ time, QRAM also becomes plausible. For example, we could consider using the same construction of classical RAM, replacing the classical electronics, i.e., gates, with quantum gates. This may be a very poor way of implementing a QRAM, and we are not suggesting that it is practical: we are merely providing an argument as to why the enticing possibility of constructing a QRAM is not easily refuted. Several possible constructions for QRAM are discussed in the literature, and some have even seen some attempts at physical construction and experimental evaluation, but significant skepticism remains on the prospects of successfully implementing a QRAM with good fidelity [Jaques and Rattew, 2023]; see the notes at the end of this chapter (Sect. 5.4) for a list of references and historical notes on QRAM.

5.3.2 QRAM for amplitude encoding

Let us go back to the goal of encoding a given classical vector in the amplitudes of a quantum state; i.e., implementing the mapping $|\vec{0}\rangle \rightarrow |\text{amp}(x)\rangle$ given a description of the classical vector x with $\|x\| = 1$. Suppose the data contained in the nodes of the tree in Fig. 5.6 is stored in QRAM as an ordered list of the nodes $N(0, 0), N(1, 0), N(1, 1), N(2, 0), \dots$, where we use the same notation as in Sect. 5.2. Note that this requires a QRAM of size $\tilde{\mathcal{O}}(d)$. Given the indices that uniquely identify a node, it is easy to determine the position of the node itself in the ordered list: $N(i, j)$ is in position $2^i + j - 1$. Then, on line 5 of Alg. 4, we replace the operation:

$$\sum_{\vec{j} \in \{0,1\}^k} |\vec{j}\rangle\langle\vec{j}| \otimes R_Y \left(2 \arccos \left(\sqrt{\frac{N(k+1, 2j)}{N(k+1, 2j) + N(k+1, 2j+1)}} \right) \right),$$

which is the most expensive operation in the construction, by using QRAM. Denote $|\psi_k\rangle = \sum_{\vec{j} \in \{0,1\}^k} \alpha_j |\vec{j}\rangle$ the state on k qubits at the beginning of the k -th iteration of the “for” loop, as defined in Alg. 4, and recall that $|\psi_k\rangle = \sum_{\vec{j} \in \{0,1\}^k} \sqrt{N(k, j)} |\vec{j}\rangle$ following the proof of Prop. 5.36. Add two fresh registers of size equal to the number of bits necessary to store the data in the nodes of Fig. 5.6, initialized with the all-zero string and positioned between $|\psi_k\rangle$ and the $|0\rangle$ qubit on which the rotation is applied. We can then implement the following mapping:

$$\begin{aligned} & \sum_{\vec{j} \in \{0,1\}^k} \alpha_j |\vec{j}\rangle |\vec{0}\rangle |\vec{0}\rangle |0\rangle \\ & \rightarrow \sum_{\vec{j} \in \{0,1\}^k} \alpha_j |\vec{j}\rangle |\overrightarrow{N(k+1, 2j)}\rangle |\overrightarrow{N(k+1, 2j+1)}\rangle |0\rangle && \text{(QRAM queries)} \\ & \rightarrow \sum_{\vec{j} \in \{0,1\}^k} \alpha_j |\vec{j}\rangle |\overrightarrow{N(k+1, 2j)}\rangle |\overrightarrow{N(k+1, 2j+1)}\rangle && \text{(rotation)} \\ & \left(\sqrt{\frac{N(k+1, 2j)}{N(k+1, 2j) + N(k+1, 2j+1)}} |0\rangle \right. \\ & \quad \left. + \sqrt{\frac{N(k+1, 2j+1)}{N(k+1, 2j) + N(k+1, 2j+1)}} |1\rangle \right) \\ & \rightarrow \sum_{\vec{j} \in \{0,1\}^k} \alpha_j |\vec{j}\rangle |\vec{0}\rangle |\vec{0}\rangle \left(\sqrt{\frac{N(k+1, 2j)}{N(k+1, 2j) + N(k+1, 2j+1)}} |0\rangle \right) && \text{(uncomputation)} \end{aligned}$$

$$\begin{aligned}
 & + \sqrt{\frac{N(k+1, 2j+1)}{N(k+1, 2j) + N(k+1, 2j+1)}} |1\rangle \Big) \\
 = & \sum_{\vec{j} \in \{0,1\}^k} \left(\sqrt{N(k+1, 2j)} |\vec{j}\rangle |0\rangle \right. && \text{(reorder registers)} \\
 & \left. + \sqrt{N(k+1, 2j+1)} |\vec{j}\rangle |1\rangle \right) |\vec{0}\rangle |\vec{0}\rangle \\
 = & |\psi_{k+1}\rangle |\vec{0}\rangle |\vec{0}\rangle.
 \end{aligned}$$

For the sake of brevity we are skipping some minor steps in the chain of operations above, but it is easy to fill in the gaps. We start by performing two QRAM queries to obtain the values of the nodes of interest $N(k+1, 2j)$, $N(k+1, 2j+1)$; to do so, we must first compute the corresponding indices with binary arithmetics (starting from \vec{j}) in some working register that we then uncompute, so we did not show this working register in the sequence of operations above. With these two values we can compute the desired rotation angle $2 \arccos \left(\sqrt{\frac{N(k+1, 2j)}{N(k+1, 2j) + N(k+1, 2j+1)}} \right)$ in a new register, and apply the rotation conditioned on the value of this register, achieving the same effect as line 5 of Alg. 4. Then we simply uncompute the working registers. The crucial difference with Alg. 4 is that, thanks to the QRAM queries, the values $N(k+1, 2j)$, $N(k+1, 2j+1)$ are entangled with the register containing $|\vec{j}\rangle$, therefore we only need a single R_Y rotation to correctly rotate the last qubit in superposition for all \vec{j} ; without QRAM, for each value of $|\vec{j}\rangle$ we had to apply a different rotation controlled on $|\vec{j}\rangle$, greatly increasing the number of gates.

Remark 5.43. *The rotation angle for the operation R_Y is described in binary in a register. It is not difficult to implement the desired operation that, based on the (binary) content of a register, rotates another qubit by a corresponding amount: this can be done with controlled- R_Y gates, one for each qubit in the register that contains the binary description of the angle, see Rem. 7.2.*

As a result, in the QRAM model the construction of $|\text{amp}(x)\rangle$ from $|\vec{0}\rangle$ can be done with a constant number of QRAM queries for each level of the tree in Fig. 5.6, and $\mathcal{O}(q)$ gates per level, where q is the number of bits used to store each of the values $N(k, j)$; we assume $q = \mathcal{O}(\log d)$, as this already gives precision exponential in d . In total, this gives a complexity of $\mathcal{O}(n)$ QRAM queries, and $\mathcal{O}(nq)$ additional gates — an exponential improvement over the $\tilde{\mathcal{O}}(2^n) = \tilde{\mathcal{O}}(d)$ gates for the same construction without QRAM. One should not forget that there is also an initial preparation time of $\tilde{\mathcal{O}}(d)$ to read the classical description of the vector x , prepare the tree data structure, and store it in QRAM: this cost dominates all the other ones, but it only needs to be paid once, after which we can reuse the already-prepared QRAM to construct $|\text{amp}(x)\rangle$ with the stated complexity as many times as we want.

Remark 5.44. *For quantum algorithms in the QRAM model, the recommended (and most accurate) way to describe the running time is to report the number of accesses to the QRAM, the number of additional (two-qubit) gates, and the number of classical operations that need to be performed by the algorithm, e.g., to read and prepare some QRAM data structure. In this way, the cost of each component can be properly assessed. This also immediately translates to an upper bound to the complexity in the standard circuit model without QRAM, because, as we have seen, a QRAM of size dq can be implemented with $\mathcal{O}(dq)$ gates.*

Corollary 5.45. *Given a classical description of $x \in \mathbb{C}^d$ in finite precision and a QRAM of size $\tilde{\mathcal{O}}(d)$, there is a circuit that implements the mapping $|\vec{0}\rangle \rightarrow |\text{amp}(x)\rangle$ with error at most ϵ using $\mathcal{O}(\log d)$ QRAM queries, $\mathcal{O}(\log^2 d)$ additional gates, and $\tilde{\mathcal{O}}(d)$ classical arithmetic operations to initialize the QRAM data structure.*

Proof. Follows from Prop. 5.36 and the discussion preceding the corollary statement. \square

As we discuss in subsequent chapters, QRAM can accelerate many quantum algorithms that require access to data, not just amplitude encoding. It is however important to remember that the QRAM input model is stronger than the standard circuit model, and that there are significant hurdles to the physical construction of QRAM, hence this stronger input model may be an even bigger ask than “just” a fault-tolerant quantum computer.

5.4 Notes and further reading

The two main references for the development of the quantum gradient algorithm presented in this chapter are [Jordan, 2005, Gilyén et al., 2019a]. Some direct applications in optimization, besides the ones already discussed in this chapter, can be found in [Gilyén et al., 2019a]. We also remark that our discussion on convex optimization using quantum membership oracles, akin to the framework of [Grötschel et al., 1988], is mostly based on the approach in [van Apeldoorn et al., 2020a], but a different and equally powerful approach is developed in [Chakrabarti et al., 2020]. The technical tools used in [Chakrabarti et al., 2020] are different: the analysis therein relies on the technique of mollifier functions, which leads to an elegant treatment, but requires additional technical tools that we avoided for the sake of simplicity. We encourage the reader to compare the two approaches for a more comprehensive treatment of the subject.

From a practical point of view, depending on the type of oracle that computes the function f , the quantum gradient algorithm may be less efficient than techniques based on automatic differentiation [Stamatopoulos et al., 2022], which can be applied to quantum circuits that perform arithmetic computation similarly to how they are applied in classical computing. Note, however, that the quantum gradient algorithm can also be applied to functions that are not easily computable on a classical computer, e.g., the quantum state inner product function of Sect. 5.1.3, for which automatic differentiation is not applicable. For a discussion on central difference approximations of functions, an entry point is [Li, 2005].

Quantum state tomography is a fundamental topic in quantum information theory. In the context of optimization, quantum state tomography is useful to recover a classical description of a solution that is encoded in a pure or mixed quantum state. Examples of quantum optimization algorithms that rely on some form of state tomography are [Augustino et al., 2023b, Kerenidis and Prakash, 2020, Wu et al., 2023]; the mirror descent framework, or matrix multiplicative weights update framework (see Ch. 8), would also rely on tomography if a full description of the optimal solution is needed — as opposed to requiring only the objective function value. Quantum state tomography using the gradient algorithm is studied in [van Apeldoorn et al., 2023]; the resulting algorithms are essentially optimal for the case where we have a (controlled, reversible) unitary that prepares the quantum state of interest, which is usually the case in the context of states produced by an algorithm. Thus, Thm. 5.17 gives the best possible complexity (in terms of number of calls to a unitary preparing the state of interest) for obtaining a classical description of a pure quantum state in the stated context; the gate count can be improved with some form of QRAM. The gradient algorithm can also be applied to recover the classical description of a mixed state, but the corresponding derivation is more involved and the complexity increases, see [van Apeldoorn et al., 2023]. Optimal algorithms for mixed states when we do not necessarily have access to a unitary preparing the state are discussed in [Haah et al., 2017, O’Donnell and Wright, 2016]. A simpler algorithm, using compressed sensing, is discussed in [Gross et al., 2010].

Historically, the bucket brigade model of [Giovannetti et al., 2008] was impactful for popularizing the possibility of constructing QRAM. [Giovannetti et al., 2008] proposes an implementation with a tree of gates of depth $\mathcal{O}(\log nd)$, resulting in a $\mathcal{O}(\log nd)$ QRAM access (wall-clock) time. This is a slowdown compared to the ideal $\mathcal{O}(1)$, but it is still exponentially faster than the standard circuit model and its $\mathcal{O}(nd)$ running time. [Blencowe, 2010] points to several papers that attempt to make progress on experimental realization of some form of quantum-accessible memory. However, so far all existing proposals have faced significant hurdles in achieving a successful implementation and experimental demonstration. For example, the bucket brigade model has been labeled impractical due to considerations on how to suppress errors in a device that may have to activate lots of quantum gates at the same time [Arunachalam et al., 2015]. More specifically, [Arunachalam et al., 2015] shows that an application of Grover’s algorithm for unstructured search using QRAM queries to identify the marked element (which is precisely how QRAM is used in the quantum dynamic programming scheme of [Ambainis et al., 2019], see Sect. 4.5) would require exponentially-small gate errors inside the QRAM. The paper also argues that error correction could negate several of the purported advantages of the bucket brigade QRAM. A detailed review of several QRAM models, as well as a discussion of their main drawbacks and limitations that point to difficulties in experimental realizations, can be found in [Jaques and Rattew, 2023]. An-

other model, that exponentially reduces the amount of fault-tolerant quantum resources required to implement a QRAM, is presented in [Dalzell et al., 2025]; however, even the model of [Dalzell et al., 2025] does not answer the question of whether it is possible to create a truly efficient QRAM, because the proposed protocol relies on expensive (i.e., linear in the size of the data) classical update operations in every iteration.

It is worth emphasizing that despite the notorious difficulty of constructing QRAM, the QRAM model is widely used in the literature on quantum algorithms, and it is particularly widespread in quantum optimization and quantum machine learning. Many quantum optimization algorithms are developed in the framework of a query model, where the problem data can be accessed by querying an appropriate oracle. For example, the quantum algorithms for semidefinite optimization discussed Ch. 8 are designed in such a model. Unfortunately, the query model typically loses most of its advantage without QRAM: for a discussion on the impact of QRAM on optimization, or more generally, data-driven problems, see Sect.s 7.2.2 and 7.2.3.

Chapter 6

Hamiltonian simulation

Hamiltonian simulation is the problem for which quantum computers were initially proposed by Richard Feynman [Feynman, 1982], and it is a crucial problem for applications in physics: it corresponds to the simulation of the evolution of a quantum-mechanical system over time. Although this set of lecture notes aims to be physics-free, it is useful to give at least the mathematical foundations of this problem, because Hamiltonian simulation is a central component of many quantum algorithms. We do not discuss the precise physical meaning of these concepts, and aim to provide just enough vocabulary to read the quantum computing literature without too much confusion.

Definition 6.1 (Hamiltonian). *The Hamiltonian of a quantum-mechanical system with n qubits is a Hermitian operator $\mathcal{H} \in \mathbb{C}^{2^n \times 2^n}$ representing the total energy of the system. The corresponding expected energy of the n -qubit system described by the state $|\psi\rangle$ is the value $\langle\psi|\mathcal{H}|\psi\rangle$.*

Remark 6.2. *It is an unfortunate fact that in the quantum computing literature, both Hamiltonians and Hadamard gates are usually indicated with the letter H . Usually it is clear from the context which of these mathematical objects is being referred to. To further avoid ambiguities, we use calligraphic \mathcal{H} for Hamiltonians and H for the Hadamard gate, but this is not always the convention in the literature.*

The evolution of a physical system follows the *Schrödinger equation*:

$$i \frac{d|\psi(t)\rangle}{dt} = \mathcal{H}|\psi(t)\rangle, \quad (6.1)$$

where \mathcal{H} is the Hamiltonian of the system, $|\psi(t)\rangle$ is the state of the system at time t , and the initial condition $|\psi(0)\rangle$ is given; it is implicitly assumed that time starts evolving from $t = 0$. In quantum mechanics Eq. (6.1) is usually stated with the Planck constant \hbar multiplying the l.h.s., but for our purposes the constant is unnecessary: we can think of it as being absorbed into the Hamiltonian, yielding the mathematically-equivalent expression in Eq. (6.1). The solution to the differential equation in Eq. (6.1) is:

$$|\psi(t)\rangle = e^{-i\mathcal{H}t}|\psi(0)\rangle, \quad (6.2)$$

hence if the initial state $|\psi(0)\rangle$ is given (as a quantum state), to determine the state of the system after time t we need to implement the operator $e^{-i\mathcal{H}t}$; this is called *time evolution* of a Hamiltonian, or *Hamiltonian simulation*, see Def. 6.4. In this chapter we limit ourselves to a time-independent Hamiltonian \mathcal{H} ; the situation is considerably more involved when \mathcal{H} is time-dependent, a case that we only address for the very specific case of adiabatic evolution in Ch. 9.

6.1 Problem definition and preliminaries

Before we properly introduce the Hamiltonian simulation problem, it may be helpful to recall some basic facts about the matrix exponential.

Definition 6.3 (Matrix exponential). *The matrix exponential of a square matrix A is defined as:*

$$e^A := \sum_{k=0}^{\infty} \frac{A^k}{k!}.$$

If A is diagonalizable $A = UDU^{-1}$, then it is easy to prove that $\exp(A) = U \exp(D)U^{-1}$, where $\exp(D)$ is a diagonal matrix with elements $(\exp(D))_{jj} = \exp(D_{jj})$. Thus, we are simply applying the exponential function to the eigenvalues of A . Now we can define Hamiltonian simulation.

Definition 6.4 (Hamiltonian simulation). *Given a Hermitian matrix \mathcal{H} , a duration t , and a precision parameter ϵ , the problem Hamiltonian simulation is that of implementing (i.e., providing a quantum circuit for) a unitary U such that $\|U - e^{-i\mathcal{H}t}\| \leq \epsilon$.*

Remark 6.5. $e^{-i\mathcal{H}t}$ is a unitary operation: \mathcal{H} is Hermitian, hence it is diagonalizable and $e^{-i\mathcal{H}t}$ transforms the eigenvalues λ_j of \mathcal{H} into $e^{-i\lambda_j t}$. Thus, all eigenvalues of $e^{-i\mathcal{H}t}$ are complex numbers with unit modulus.

Remark 6.6. *Because the only restriction imposed on \mathcal{H} is that it is Hermitian, we can equivalently consider the problem of simulating $e^{i\mathcal{H}t}$ rather than $e^{-i\mathcal{H}t}$: the negative sign can be absorbed into \mathcal{H} . In the following, we often neglect the minus sign in the exponent for brevity.*

6.1.1 The class BQP and Hamiltonian simulation

The complexity class BQP is the class of decision problems that can be solved efficiently by a quantum computer; it is the quantum analog of the class BPP (bounded-error probabilistic polynomial time), that contains problems that can be solved efficiently by a classical computer.

Definition 6.7 (Bounded-error Quantum Polynomial time (BQP) class). *BQP (Bounded-error Quantum Polynomial time) is the class of decision problems that can be solved by a polynomial-time quantum algorithm with probability at least $\frac{2}{3}$.*

It turns out that Hamiltonian simulation is truly a fundamental problem, as it is BQP-complete; this implies that any problem that can be solved efficiently by a quantum computer can be (efficiently) reduced to a Hamiltonian simulation.

Remark 6.8. *To show that Hamiltonian simulation is in BQP, it suffices to provide a polynomial-time quantum algorithm for the problem. Several such algorithms have been known since the early days of the field, see, e.g., [Lloyd, 1996], or some of the references discussed subsequently in this chapter. To show that Hamiltonian simulation is BQP-complete, we additionally need to prove that any efficient quantum computation can be performed via Hamiltonian simulation.*

Suppose we have a quantum circuit that applies unitaries U_1, \dots, U_{N-1} onto the q -qubit state $|\vec{0}\rangle$, and we want to show that we can simulate the effect of this circuit via Hamiltonian simulation. To do so, we construct a specific Hamiltonian such that $e^{-i\mathcal{H}t}|\vec{0}\rangle = U_{N-1}U_{N-2}\cdots U_1|\vec{0}\rangle$ for some choice of t . If this construction can be done for any choice of unitaries U_1, \dots, U_{N-1} , and the size of the Hamiltonian simulation instance is at most polynomially larger than the size of a description of the quantum circuit (i.e., U_1, \dots, U_{N-1}), this would prove that Hamiltonian simulation is BQP-complete: any problem instance that can be solved by a polynomial-size quantum circuit can also be solved as a polynomial-size Hamiltonian simulation problem instance. It is therefore natural to study Hamiltonian simulation, and many algorithmic advances in quantum computing originated from the study of this problem.

We do not give a full proof of BQP-completeness, but we show most of it, in particular to showcase a possible approach to turn a general circuit into a Hamiltonian simulation instance; the ideas discussed here date back to Feynman's initial vision for quantum computers [Feynman, 1982, Feynman, 2018]. Recall that we are given N unitaries that we want to apply, and for which we assume that we have an efficient description. Let us introduce N auxiliary qubits; for $j = 1, \dots, N$, define binary strings $\vec{u}^{(j)} \in \{0, 1\}^N$, $\vec{u}_h^{(j)} = 1$ if $j = h$, 0 otherwise. Each of these

N -digit strings encodes an integer from 1 to N by having a 1 in the corresponding position, and 0 elsewhere. We use them as the content of a “clock register” to remember the position of the simulation algorithm in the sequence of unitaries, so that each unitary is applied exactly once and in the right order. Construct the following Hamiltonian:

$$\mathcal{H} := \frac{1}{2} \sum_{j=1}^{N-1} \sqrt{j(N-j)} \left(|\vec{u}^{(j+1)}\rangle\langle\vec{u}^{(j)}| \otimes U_j + |\vec{u}^{(j)}\rangle\langle\vec{u}^{(j+1)}| \otimes U_j^\dagger \right). \quad (6.3)$$

We can check that this is Hermitian by construction, as it is a sum of Hermitian terms. Note that this Hamiltonian acts on two registers: the clock register containing the strings $\vec{u}^{(j)}$, and a second register initialized in the state $|\vec{0}\rangle$, onto which we apply the unitaries U_j . Define a set of states:

$$|\psi_k\rangle := |\vec{u}^{(k)}\rangle \otimes \left(U_{k-1} U_{k-2} \cdots U_1 |\vec{0}\rangle \right).$$

If we compute $|\psi_N\rangle$ then we have obtained, in the second register, $U_{N-1} \cdots U_1 |\vec{0}\rangle$, precisely the effect of the circuit that we wish to simulate. First, we show by induction that:

$$\mathcal{H}|\psi_k\rangle = \frac{1}{2} \sqrt{(k-1)(N+1-k)} |\psi_{k-1}\rangle + \frac{1}{2} \sqrt{k(N-k)} |\psi_{k+1}\rangle \text{ for } k = 1, \dots, N-1,$$

where we define $|\psi_0\rangle := 0$ for convenience (i.e., this is not a quantum state, but rather the scalar 0 which simply disappears from the expression). Indeed, for the base step:

$$\begin{aligned} \mathcal{H}|\psi_1\rangle &= \frac{1}{2} \sum_{j=1}^{N-1} \sqrt{j(N-j)} \left(|\vec{u}^{(j+1)}\rangle\langle\vec{u}^{(j)}| \otimes U_j + |\vec{u}^{(j)}\rangle\langle\vec{u}^{(j+1)}| \otimes U_j^\dagger \right) |\vec{u}^{(1)}\rangle \otimes |\vec{0}\rangle \\ &= \frac{1}{2} \sqrt{(N-1)} |\vec{u}^{(2)}\rangle \otimes (U_1 |\vec{0}\rangle) = \frac{1}{2} \sqrt{(N-1)} |\psi_2\rangle, \end{aligned}$$

and for the induction step:

$$\begin{aligned} \mathcal{H}|\psi_k\rangle &= \frac{1}{2} \sum_{j=1}^{N-1} \sqrt{j(N-j)} \left(|\vec{u}^{(j+1)}\rangle\langle\vec{u}^{(j)}| \otimes U_j + |\vec{u}^{(j)}\rangle\langle\vec{u}^{(j+1)}| \otimes U_j^\dagger \right) |\vec{u}^{(k)}\rangle \otimes \left(U_{k-1} \cdots U_1 |\vec{0}\rangle \right) \\ &= \frac{1}{2} \sqrt{k(N-j)} |\vec{u}^{(k+1)}\rangle \otimes (U_k U_{k-1} \cdots U_1 |\vec{0}\rangle) + \\ &\quad \frac{1}{2} \sqrt{(k-1)(N+1-k)} |\vec{u}^{(k-1)}\rangle \otimes U_{k-1}^\dagger (U_{k-1} \cdots U_1 |\vec{0}\rangle) \\ &= \frac{1}{2} \sqrt{k(N-j)} |\psi_{k+1}\rangle + \frac{1}{2} \sqrt{(k-1)(N+1-k)} |\psi_{k-1}\rangle. \end{aligned}$$

This means that \mathcal{H} acts on the subspace spanned by the states $|\psi_k\rangle$, and the effect of $e^{-i\mathcal{H}t}$ can be understood in this subspace. We claim that $e^{-i\mathcal{H}t} |\psi_1\rangle = |\psi_N\rangle$ if we choose $t = \pi$. A full proof of this result can be found in [Kay, 2010]. A high-level sketch of the proof is the following. The effect of \mathcal{H} on the first N qubits (first register), when expressed in the basis $|\vec{u}^{(j)}\rangle$, can be written in this form:

$$\mathcal{H}_B = \frac{1}{2} \begin{pmatrix} 0 & \sqrt{N-1} & 0 & \dots & 0 & 0 \\ \sqrt{N-1} & 0 & \sqrt{2(N-2)} & \dots & 0 & 0 \\ 0 & \sqrt{2(N-2)} & 0 & \dots & 0 & 0 \\ \vdots & \vdots & \vdots & \ddots & \vdots & \vdots \\ 0 & 0 & 0 & \dots & 0 & \sqrt{N-1} \\ 0 & 0 & 0 & \dots & \sqrt{N-1} & 0 \end{pmatrix},$$

which is a symmetric tridiagonal matrix with zeroes on the diagonal. We denote it by \mathcal{H}_B because this is \mathcal{H} expressed in the basis $|\vec{u}^{(j)}\rangle$, and we perform all the analysis in this basis. The eigenvalues

of the matrix \mathcal{H}_B are $-\frac{1}{2}(N-1), -(\frac{1}{2}(N-1)-1), \dots, \frac{1}{2}(N-1)-1, \frac{1}{2}(N-1)$, i.e., they range from $-\frac{1}{2}(N-1)$ to $\frac{1}{2}(N-1)$ spaced by 1. Note that \mathcal{H}_B commutes with the matrix $M_s = \sum_{j=1}^N |\vec{u}^{(j)}\rangle\langle\vec{u}^{(N+1-j)}|$, which sends the j -th element to the $(N+1-j)$ -th and viceversa: this is easy to check. As a consequence of this property, the eigenvectors of \mathcal{H}_B can be divided into symmetric and antisymmetric, based on how M_s acts on them (suppose $|\psi\rangle$ is an eigenvector with eigenvalue λ ; then $\lambda M_s|\psi\rangle = M_s\lambda|\psi\rangle = M_s\mathcal{H}_B|\psi\rangle = \mathcal{H}_B M_s|\psi\rangle$, so $M_s|\psi\rangle$ must be equal to $|\psi\rangle$ or to $-|\psi\rangle$. We call the first type of eigenvalue symmetric, the second antisymmetric). We can then state the following.

Proposition 6.9. *Let $S \subseteq \{1, \dots, N\}$ be the set of indices of symmetric eigenvalues of \mathcal{H}_B . Suppose there exists some time t and angle ϕ such that, for every eigenpair $(\lambda_j, |\psi_j\rangle)$ such that $\langle\psi_j|\vec{u}^{(1)}\rangle \neq 0$, we have $e^{-i\lambda_j t} = e^{i\phi}$ if $j \in S$, and $e^{-i\lambda_j t} = -e^{i\phi}$ if $j \notin S$. Then $e^{-i\mathcal{H}_B t}|\vec{u}^{(1)}\rangle = e^{i\phi}|\vec{u}^{(N)}\rangle$.*

Proof. We consider the decomposition of $|\vec{u}^{(1)}\rangle$ in terms of the eigenvectors $|\psi_j\rangle$ that have nonzero overlap with it. Let $S' := \{j \in S : \langle\psi_j|\vec{u}^{(1)}\rangle \neq 0\}$ be the set of symmetric eigenvalues with nonzero overlap, $A' := \{j \in \{1, \dots, N\} \setminus S : \langle\psi_j|\vec{u}^{(1)}\rangle \neq 0\}$ the set of antisymmetric eigenvalues with nonzero overlap. Let $|\vec{u}^{(1)}\rangle = \sum_{j \in S' \cup A'} \alpha_j |\psi_j\rangle$ for some coefficients α_j , which clearly exist because the eigenvectors $|\psi_j\rangle$ form a basis and we are considering all eigenvectors that are not orthogonal to $|\vec{u}^{(1)}\rangle$. The time evolution according to the Hamiltonian is then:

$$\begin{aligned} e^{-i\mathcal{H}_B t}|\vec{u}^{(1)}\rangle &= e^{-i\mathcal{H}_B t} \left(\sum_{j \in S'} \alpha_j |\psi_j\rangle + \sum_{j \in A'} \alpha_j |\psi_j\rangle \right) = \sum_{j \in S'} e^{-i\lambda_j t} \alpha_j |\psi_j\rangle + \sum_{j \in A'} e^{-i\lambda_j t} \alpha_j |\psi_j\rangle \\ &= e^{i\phi} \left(\sum_{j \in S'} \alpha_j |\psi_j\rangle - \sum_{j \in A'} \alpha_j |\psi_j\rangle \right) = e^{i\phi} M_s \left(\sum_{j \in S'} \alpha_j |\psi_j\rangle + \sum_{j \in A'} \alpha_j |\psi_j\rangle \right) \\ &= e^{i\phi} M_s |\vec{u}^{(1)}\rangle = e^{i\phi} |\vec{u}^{(N)}\rangle. \end{aligned}$$

□

Prop. 6.9 shows that if a certain property is satisfied, then evolving the state $|\vec{u}^{(1)}\rangle$ with the Hamiltonian \mathcal{H} for a specific time t yields the state $|\vec{u}^{(N)}\rangle$ (the global phase factor $e^{i\phi}$ is unimportant, as usual). The property is the following: the length t of the time evolution is such that it yields the same phase for all symmetric eigenvalues, and there is only a sign difference between the symmetric and antisymmetric eigenspaces. As it turns out, for a matrix of the form \mathcal{H}_B (symmetric tridiagonal with positive off-diagonal elements) the symmetry of the eigenvectors alternates, if we examine them in increasing order of the eigenvalues. With this fact in mind, we can see that the following property is sufficient to satisfy the conditions of Prop. 6.9:

$$\lambda_j - \lambda_{j-1} = (2k+1)\pi/t \quad \forall j = 2, \dots, N, \quad (6.4)$$

where $k \in \mathbb{N}$. Indeed, with this property we have:

$$e^{-i\lambda_j t} = e^{-i(\lambda_1 + (j-1)(2k+1)\pi/t)t} = \begin{cases} e^{-i\lambda_1 t} & \text{if } j \text{ odd} \\ -e^{-i\lambda_1 t} & \text{if } j \text{ even,} \end{cases}$$

because the phase $(j-1)(2k+1)\pi$ yields a multiplicative factor 1 or -1 depending on the parity of j . Now recall that by construction, the eigenvalues of \mathcal{H}_B (which alternate between the symmetric and antisymmetric eigenspaces) are spaced by exactly 1. Then, choosing $t = \pi$ satisfies Eq. (6.4) with $k = 0$, thereby showing that evolving the Hamiltonian \mathcal{H}_B for time $t = \pi$ starting from $|\vec{u}^{(1)}\rangle$ yields $|\vec{u}^{(N)}\rangle$. Going back to the original Hamiltonian \mathcal{H} defined in Eq. (6.3), this means that we are evolving $|\psi_1\rangle$ into $|\psi_N\rangle$, which contains the state $U_{N-1}U_{N-2}\dots U_1|\vec{0}\rangle$ in its second register, and therefore the output of the circuit that we wanted to simulate. Thus, we can reduce any problem that can be solved by an efficient (polynomial-time) quantum circuit into an instance of the Hamiltonian simulation problem, showing that Hamiltonian simulation is BQP-complete.

6.1.2 Basic remarks on Hamiltonian simulation

We state here some basic observations on Hamiltonian simulation, helping to set the stage for the simulation algorithms discussed in the remainder of this chapter. First, intuitively it should be clear that the difficulty of simulating a Hamiltonian may depend not only on \mathcal{H} itself, but also on the evolution time t : simulating a quantum-mechanical system for a longer duration cannot be easier than simulating it for a shorter time.

Let \mathcal{H} act on n qubits. For a simulation algorithm to be efficient, we require that the running time of the algorithm is polynomial in n , t , and $\frac{1}{\epsilon}$. In fact, some of the algorithms discussed in the remainder of this chapter even depend polylogarithmically on $\frac{1}{\epsilon}$. Note that \mathcal{H} is a $2^n \times 2^n$ matrix, and the running time of an efficient Hamiltonian simulation algorithm is polynomial in n , which is exponentially faster than classically computing the matrix exponential via its definition. The following remarks follow directly from the requirement, stated above, that we impose on efficient Hamiltonian simulation algorithms.

Remark 6.10. *Hamiltonian simulation algorithms generally assume some upper bound on $\|\mathcal{H}\|$, and the reason for this is easily explained. Suppose we want to compute $e^{i\mathcal{H}t}$: if we define a new Hamiltonian $\mathcal{H}' = \mathcal{H}t$, then $e^{i\mathcal{H}t} = e^{i\mathcal{H}'}$, i.e., the time parameter t can now be set to 1, but note that $\|\mathcal{H}'\| = t\|\mathcal{H}\|$. Thus, we can decrease the time parameter t if we increase the norm of the Hamiltonian. Because the running time of a simulation algorithm generally depends on t , we need to impose some normalization so that different algorithms are comparable under similar conditions. The convention in the literature is to upper bound the norm of \mathcal{H} ($\|\mathcal{H}\| \leq 1$), and analyze the dependence of the running time of a Hamiltonian simulation algorithm on the parameter t .*

Remark 6.11. *If we have an efficient algorithm to simulate $e^{i\mathcal{H}t}$, we can also efficiently simulate $e^{ic\mathcal{H}t}$ for any constant c which is polynomial in n , simply by absorbing it into t .*

6.2 Overview of simulation algorithms

In this section we discuss several methods for Hamiltonian simulation, based on properties of the Hamiltonian or on the input model. In fact, the way in which the Hamiltonian is specified often has an impact on what techniques are suitable. Initially we assume that the Hamiltonian is diagonalizable or expressible as a sum of “local” terms (i.e., tensor products of a few single-qubit operators), and subsequently generalize to Hamiltonians that may not have that structure. For additional resources on Hamiltonian simulation, we refer the reader to the excellent lecture notes [Childs, 2017, de Wolf, 2019], which inspired parts of our presentation.

6.2.1 Diagonalizable Hamiltonians

If we know how to diagonalize \mathcal{H} , then we can simulate $e^{i\mathcal{H}t}$, as we show next. We need the following basic fact about matrix exponentials.

Proposition 6.12. *For any unitary U and Hamiltonian \mathcal{H} , $e^{iU\mathcal{H}U^\dagger t} = Ue^{i\mathcal{H}t}U^\dagger$.*

Proof. We have:

$$e^{iU\mathcal{H}U^\dagger t} = \sum_{k=0}^{\infty} \frac{(iU\mathcal{H}U^\dagger t)^k}{k!} = U \left(\sum_{k=0}^{\infty} \frac{(i\mathcal{H}t)^k}{k!} \right) U^\dagger = Ue^{i\mathcal{H}t}U^\dagger,$$

by definition of the matrix exponential and because $(U\mathcal{H}U^\dagger)^k = U\mathcal{H}^kU^\dagger$, because in the expansion of the product we can simplify $UU^\dagger = U^\dagger U = I$. \square

Then, if we know how to efficiently construct a unitary U that diagonalizes \mathcal{H} , i.e., $\mathcal{H} = UDU^\dagger$ where D is diagonal, and we can compute a binary description of the diagonal elements $D_j =$

$\langle \vec{j} | U^\dagger \mathcal{H} U | \vec{j} \rangle$, we can implement a unitary that performs the following operations:

$$\begin{aligned}
 |\vec{j}\rangle|\vec{0}\rangle &\rightarrow |\vec{j}\rangle|\vec{D}_j\rangle && \text{(because we know how to compute the diagonal elements)} \\
 &\rightarrow e^{iD_j t}|\vec{j}\rangle|\vec{D}_j\rangle && \text{(using controlled phase gates and the bitstring } \vec{D}_j\text{)} \\
 &\rightarrow e^{iD_j t}|\vec{j}\rangle|\vec{0}\rangle && \text{(uncomputing the second register)} \\
 &= e^{iU^\dagger \mathcal{H} U t}|\vec{j}\rangle|\vec{0}\rangle && \text{(because } U^\dagger \mathcal{H} U \text{ acts on } |\vec{j}\rangle \text{ as } D_j\text{)} \\
 &= U^\dagger e^{i\mathcal{H} t} U |\vec{j}\rangle|\vec{0}\rangle.
 \end{aligned}$$

The unitary constructed above applies $U^\dagger e^{i\mathcal{H} t} U$ to any basis state $|\vec{j}\rangle$. Thus, by linearity, this operation simulates $U^\dagger e^{i\mathcal{H} t} U$ on an arbitrary state. To accomplish our goal of applying $e^{i\mathcal{H} t}$ to a given initial state $|\psi\rangle$, we simply need to compute $U(U^\dagger e^{i\mathcal{H} t} U)U^\dagger|\psi\rangle$, which is easy given our assumption that we can construct U and we have shown above how to obtain $U^\dagger e^{i\mathcal{H} t} U$. Overall, we need one application of U, U^\dagger and $(U^\dagger e^{i\mathcal{H} t} U)$.

Remark 6.13. *This simplified Hamiltonian simulation procedure only works for a diagonal Hamiltonian, and, by the preceding discussion, for Hamiltonians that we know how to diagonalize. Otherwise, it is not obvious how to identify the eigenvectors and act as $e^{i\mathcal{H} t}$ on them.*

6.2.2 Product formulas: Lie-Suzuki-Trotter decomposition

One of the most common ways of expressing a Hamiltonian is as a sum of “simple” terms. Here, “simple” can mean several different things; examples of simple terms are sparse matrices (i.e., with at most a given number of nonzero elements per row), or tensor products of Pauli matrices. In particular, for Hamiltonians arising from physical models, it is often the case that the Hamiltonian is described as a summation of several “local” terms, i.e., terms that act only on a small number of qubits (corresponding to particles) and are therefore described by small matrices tensored with identity. For this reason, Hamiltonian simulation of a sum of simple terms is particularly well studied. In other applications the Hamiltonian may be a general matrix, but there is usually an assumption of (some type of) sparsity, because Hamiltonian simulation algorithms rely on decomposing the Hamiltonian in simpler terms, and simulating these terms individually.

Let us study the case where $\mathcal{H} = \mathcal{H}_1 + \mathcal{H}_2$, and the discussion can naturally be extended to a sum of multiple terms. If the Hamiltonians \mathcal{H}_1 and \mathcal{H}_2 can be efficiently simulated, we can try to devise approaches to simulate $\mathcal{H}_1 + \mathcal{H}_2$ using simulation for \mathcal{H}_1 and \mathcal{H}_2 individually. Suppose \mathcal{H}_1 and \mathcal{H}_2 commute; then $e^{\mathcal{H}_1 + \mathcal{H}_2} = e^{\mathcal{H}_1} e^{\mathcal{H}_2}$, as can be seen from the definition of matrix exponential (Def. 6.3), therefore the simulation is trivial. Suppose now that \mathcal{H}_1 and \mathcal{H}_2 do not commute, which is the more general and difficult case. We can rely on the Lie product formula:

$$e^{i(\mathcal{H}_1 + \mathcal{H}_2)t} = \lim_{h \rightarrow \infty} \left(e^{i\mathcal{H}_1 t/h} e^{i\mathcal{H}_2 t/h} \right)^h.$$

While this is an infinite formula, it can be truncated by picking a finite h , thereby introducing some error. The error depends on the choice of h , because the error of approximating $e^{\mathcal{H}_1 + \mathcal{H}_2}$ with $e^{\mathcal{H}_1} e^{\mathcal{H}_2}$ is $\mathcal{O}(\|\mathcal{H}_1\| \|\mathcal{H}_2\|)$; this result is a consequence of the Campbell-Baker-Hausdorff theorem, see [Bhatia, 2013]. We do not prove it rigorously, but an intuitive explanation can be given by taking the first-order Taylor series approximation of the matrix exponential:

$$e^{\mathcal{H}_1} e^{\mathcal{H}_2} - e^{\mathcal{H}_1 + \mathcal{H}_2} \approx (I + \mathcal{H}_1)(I + \mathcal{H}_2) - (I + \mathcal{H}_1 + \mathcal{H}_2) = \mathcal{H}_1 \mathcal{H}_2,$$

so if $\|\mathcal{H}_1\| \|\mathcal{H}_2\|$ is small, $e^{\mathcal{H}_1} e^{\mathcal{H}_2}$ is close to $e^{\mathcal{H}_1 + \mathcal{H}_2}$. Then for any chosen integer h we have:

$$e^{i\mathcal{H} t} = (e^{i(\mathcal{H}_1/h + \mathcal{H}_2/h)t})^h = (e^{i\mathcal{H}_1 t/h} e^{i\mathcal{H}_2 t/h} + E)^h, \quad (6.5)$$

where E is the error matrix, with $\|E\| = \mathcal{O}(\|i\mathcal{H}_1 t/h\| \|i\mathcal{H}_2 t/h\|) = \mathcal{O}(\|\mathcal{H}_1\| \|\mathcal{H}_2\| t^2/h^2)$. Note that Eq. (6.5) holds as equality, because we are explicitly incorporating the error term E . Consider what happens if we replace the expression on the r.h.s. of Eq. (6.5) with $(e^{i\mathcal{H}_1 t/h} e^{i\mathcal{H}_2 t/h})^h$, which

is simply the repeated application of the unitaries $e^{i\mathcal{H}_1 t/h}$, $e^{i\mathcal{H}_2 t/h}$ a total of h times each, in an interleaved way: this is known as the Lie-Suzuki-Trotter first-order approach [Lloyd, 1996]. By Prop. 1.46, the error of approximating each unitary in a sequence is at most the sum of the errors of the individual approximations (i.e., errors in a sequence of unitaries increase at most additively, rather than multiplicatively). By neglecting the error term E a total of h times, we incur error at most:

$$h\|E\| = \mathcal{O}(h\|\mathcal{H}_1\|\|\mathcal{H}_2\|t^2/h^2) = \mathcal{O}(\|\mathcal{H}_1\|\|\mathcal{H}_2\|t^2/h). \quad (6.6)$$

Thus, for any given $\epsilon > 0$, choosing $h = \mathcal{O}\left(\|\mathcal{H}_1\|\|\mathcal{H}_2\|\frac{t^2}{\epsilon}\right)$ guarantees:

$$\left\| e^{i(\mathcal{H}_1+\mathcal{H}_2)t} - \left(e^{i\mathcal{H}_1 t/h} e^{i\mathcal{H}_2 t/h} \right)^h \right\| \leq \epsilon.$$

Remark 6.14. *It is possible to obtain an ϵ -approximation with fewer terms (i.e., fewer unitaries depending on \mathcal{H}_1 or \mathcal{H}_2 only) in the product, e.g., by using higher-order terms in the Taylor series of the matrix exponential, which leads to a more accurate approximation for the same number of product terms. The first-order approach suffices for us to get the main idea and to state the approximation results used in Ch. 9.*

Finally, we note that the product formula can be extended to a summation of several terms, using the fact that $e^{i(\sum_j \mathcal{H}_j)t} = \lim_{h \rightarrow \infty} \left(\prod_j e^{i\mathcal{H}_j t/h} \right)^h$. If the Hamiltonian is a summation of m terms, then to obtain error ϵ it is sufficient to choose $h = \mathcal{O}(m^2 t^2 / \epsilon)$. The gate complexity of a Hamiltonian simulation circuit obtained with the Lie-Suzuki-Trotter first-order approach is h times the gate complexity of each individual simulation piece $\prod_j e^{i\mathcal{H}_j t/h}$, so in the best case where each of the m terms $e^{i\mathcal{H}_j t/h}$ can be simulated with a constant number of gates, we end up with gate complexity $\mathcal{O}(m^3 t^2 / \epsilon)$; and if each term is more expensive to simulate, the total cost increases accordingly.

Remark 6.15. *The gate complexity of implementing a circuit for $e^{i\mathcal{H}_j t/h}$ depends on \mathcal{H}_j , but it is not unrealistic to think that it might be constant. For example, for many Hamiltonians arising from physical models, each term \mathcal{H}_j acts nontrivially on a constant number of qubits, and acts as the identity on the remaining ones. In that case, using properties of the tensor product, $e^{i\mathcal{H}_j t/h}$ is a constant-size matrix tensored with identity matrices, and as such, it can be implemented in a constant number of gates: we only need to act on the qubits on which \mathcal{H}_j acts nontrivially.*

Example 6.16. *Let us look at the case in which \mathcal{H} is a summation of terms, of the following form: $\mathcal{H} = \sum_{(j,k) \in E} C_{jk}$, where E is the edge set of some graph $G = (V, E)$ and C_{jk} acts on two qubits only:*

$$C_{jk} := I \otimes \cdots \otimes I \otimes \underbrace{Z}_{\text{pos. } j} \otimes I \otimes \cdots \otimes I \otimes \underbrace{Z}_{\text{pos. } k} \otimes I \otimes \cdots \otimes I.$$

In other words, C_{jk} acts as the identity on all qubits, except on qubits j and k , where it acts with the Pauli Z matrix. In the literature, such a Hamiltonian would typically be written more compactly as $\mathcal{H} = \sum_{(j,k) \in E} \sigma_j^Z \sigma_k^Z$ (see Eq. 9.4) or as $\mathcal{H} = \sum_{(j,k) \in E} Z_j Z_k$. This type of Hamiltonian appears in a certain formulation of quadratic unconstrained binary optimization problems, and it is discussed thoroughly in Ch. 9; in particular, see Sect. 9.1.1.

Suppose we want to implement $e^{i\mathcal{H}t}$ for some value of t . By our discussion above, it is sufficient to implement $e^{iC_{jk}t}$ for each term C_{jk} , because these terms commute and so the matrix exponential of the entire Hamiltonian is equal to the product of the matrix exponentials for the individual terms. Regarding the implementation of $e^{iC_{jk}t}$, note that it acts trivially (i.e., as the identity) on all qubits except j and k , by definition of the matrix exponential. We can therefore limit ourselves to understanding the effect of $e^{iC_{jk}t}$ on the two qubits j and k , which amounts to computing $e^{itZ \otimes Z}$.

This is straightforward:

$$Z \otimes Z = \begin{pmatrix} 1 & 0 & 0 & 0 \\ 0 & -1 & 0 & 0 \\ 0 & 0 & -1 & 0 \\ 0 & 0 & 0 & 1 \end{pmatrix} \quad e^{itZ \otimes Z} = \begin{pmatrix} e^{it} & 0 & 0 & 0 \\ 0 & e^{-it} & 0 & 0 \\ 0 & 0 & e^{-it} & 0 \\ 0 & 0 & 0 & e^{it} \end{pmatrix}.$$

We can decompose this unitary into basic gates like any other unitary, with CX gates and single-qubit gates: an explicit circuit for this is given in Sect. 9.2.4. The gate complexity of simulating the entire Hamiltonian in this way is $\tilde{O}(|E|)$ for error ϵ , where the errors are due to the decomposition of each term C_{jk} into basic gates (with polylogarithmic scaling in $\frac{1}{\epsilon}$).

If instead of $Z \otimes Z$ we had a more complicated (say, non-diagonal) two-qubit gate in the exponent, we can still perform Hamiltonian simulation thanks to the Lie-Suzuki-Trotter formula. For example, still assuming $\mathcal{H} = \sum_{(j,k) \in E} C_{jk}$, let us now suppose C_{jk} is a general 4×4 matrix (that we know) when restricted to the space of qubits j and k , and it acts as the identity on all other qubits. Now the terms C_{jk} no longer commute in general. However, the matrix exponential of a single C_{jk} term is still a 4×4 matrix on qubits i and j tensored with identity on the other qubits, and any such matrix can be approximated to high precision (say, error $< \epsilon'$) with $\tilde{O}(1)$ gates: we can analytically compute $e^{iC_{jk}t}$, which is unitary, and decompose it into single- and two-qubit gates, see Thm. 1.43 and the surrounding discussion. Then we apply the Lie-Suzuki-Trotter formula for a summation of multiple terms, implementing the Hamiltonian simulation with the circuit:

$$\left(\prod_{(j,k) \in E} e^{iC_{jk}t/h} \right)^h,$$

where $h = \mathcal{O}(|E|^2 t^2 / \epsilon)$ to guarantee that

$$\left\| e^{it \sum_{(j,k) \in E} C_{jk}} - \left(\prod_{(j,k) \in E} e^{iC_{jk}t/h} \right)^h \right\| \leq \epsilon.$$

The gate complexity of the resulting circuit is $\tilde{O}(|E|^3 t^2 / \epsilon)$.

6.2.3 Linear combination of unitaries

Throughout this section we assume $\|\mathcal{H}\| \leq 1$, see Rem. 6.10, and we want to give a circuit implementation for $e^{i\mathcal{H}t}$.

It is easy to apply the product of two unitary matrices, for which we have a circuit implementation, to a quantum state: we simply apply them one after the other. But how do we apply a linear combination of those unitaries? In this section we give a possible answer to this question, but before we dive into that, it is useful to discuss the connection between linear combination of unitaries and Hamiltonian simulation. The acronym LCU is often used in the literature to refer to “linear combination of unitaries.”

Connection between Hamiltonian simulation and LCU. Suppose we know a decomposition of \mathcal{H} in terms of some unitary matrices: $\mathcal{H} = \sum_{j=1}^m \beta_j U_j$, where the coefficients β_j are real numbers, which we can assume w.l.o.g. because any complex phase can be absorbed into U_j .

Remark 6.17. *A decomposition of \mathcal{H} in terms of unitaries always exist: the Pauli matrices, appropriately tensored, form a basis for the space of multi-qubit operators, and they are unitary. However, it is usually better (for computational efficiency) if one can find a simple decomposition as a linear combination of unitaries, i.e., with few terms. To consider a similar situation as in Sect. 6.2.2, if \mathcal{H} is a summation of a few terms that act only on a constant number of qubits, then each of these terms can be written as a linear combination of a constant number of unitaries:*

although this latter constant is exponential in the number of qubits involved, it is still a constant. This approach does not scale well if the number of qubits on which each term of \mathcal{H} acts is given as a (variable) input to the simulation algorithm.

By definition of matrix exponential we have:

$$e^{i\mathcal{H}t} = \sum_{k=0}^{\infty} \frac{(i\mathcal{H}t)^k}{k!} = \sum_{k=0}^{\infty} \frac{(it)^k}{k!} \left(\sum_{j=1}^m \beta_j U_j \right)^k = \sum_{k=0}^{\infty} \frac{(it)^k}{k!} \sum_{j_1, j_2, \dots, j_k \in \{1, \dots, m\}} \beta_{j_1} \beta_{j_2} \cdots \beta_{j_k} U_{j_1} U_{j_2} \cdots U_{j_k}. \quad (6.7)$$

At the r.h.s. of Eq. (6.7) we have an infinite series, but consider what happens if we truncate the Taylor series at $k = c(t + \log \frac{1}{\epsilon}) = \mathcal{O}(t + \log \frac{1}{\epsilon})$, for some constant c . Recalling that $k! \geq (k/e)^k$, we have:

$$\begin{aligned} \left\| e^{i\mathcal{H}t} - \sum_{k=0}^{c(t+\log \frac{1}{\epsilon})-1} \frac{(i\mathcal{H}t)^k}{k!} \right\| &= \left\| \sum_{k=c(t+\log \frac{1}{\epsilon})}^{\infty} \frac{(i\mathcal{H}t)^k}{k!} \right\| \leq \sum_{k=c(t+\log \frac{1}{\epsilon})}^{\infty} \left\| \frac{(i\mathcal{H}t)^k}{k!} \right\| \\ &\leq \sum_{k=c(t+\log \frac{1}{\epsilon})}^{\infty} \left\| \frac{t^k}{k!} \right\| = \sum_{k=c(t+\log \frac{1}{\epsilon})}^{\infty} \frac{t^k}{k!} \\ &\leq \sum_{k=c(t+\log \frac{1}{\epsilon})}^{\infty} \left(\frac{et}{k} \right)^k \leq \sum_{k=c(t+\log \frac{1}{\epsilon})}^{\infty} \left(\frac{et}{ct} \right)^k \\ &\leq \sum_{k=c(t+\log \frac{1}{\epsilon})}^{\infty} \left(\frac{e}{c} \right)^k \leq \frac{(e/c)^{c(t+\log(1/\epsilon))}}{1 - e/c} = \frac{(e/c)^{ct} (e/c)^{c \log(1/\epsilon)}}{1 - e/c}. \end{aligned}$$

Simple calculations show that $c = 2e$ suffices to ensure that the above expression is $\leq \epsilon$, and note that this choice is independent of t or ϵ . Thus, if we can implement the first $\mathcal{O}(t + \log \frac{1}{\epsilon})$ terms of the expression at the r.h.s. of Eq. (6.7), we obtain an ϵ -approximation of $e^{i\mathcal{H}t}$. In summary, one way to solve the Hamiltonian simulation problem is to implement:

$$\sum_{k=0}^{\mathcal{O}(t+\log \frac{1}{\epsilon})} \sum_{j_1, j_2, \dots, j_k \in \{1, \dots, m\}} \frac{(it)^k}{k!} \beta_{j_1} \beta_{j_2} \cdots \beta_{j_k} U_{j_1} U_{j_2} \cdots U_{j_k}, \quad (6.8)$$

which is a linear combination of the unitaries $(U_{j_1} U_{j_2} \cdots U_{j_k})$ with coefficients $\frac{(it)^k}{k!} \beta_{j_1} \beta_{j_2} \cdots \beta_{j_k}$. Note that if we know how to implement all the matrices U_j , then implementing $U_{j_1} U_{j_2} \cdots U_{j_k}$ is straightforward, as it is just a sequence of operations that we know how to apply. Thus, we now discuss the task of implementing a linear combination of unitaries with given coefficients in the linear combination.

Implementing a LCU. To simplify the discussion, let us rename some of the quantities involved. We can recast the problem of implementing a linear combination of unitaries as implementing $M = \sum_{j=0}^{2^q-1} \alpha_j V_j$ with α_j nonnegative and real (as before, we can absorb everything else into V_j), and where the V_j are n -qubit unitaries. M may not be unitary in general, so if we want to apply it to some state $|\psi\rangle$, we must instead aim to implement $M|\psi\rangle/\|M|\psi\rangle\|$, where the normalization ensures that we obtain a proper quantum state. Because α_j are nonnegative and real, we have $\|\alpha\|_1 = \sum_{j=0}^{2^q-1} \alpha_j$ for the ℓ^1 -norm of the vector of coefficients α . Because the coefficients α_j are known, we can construct — for example using the amplitude encoding algorithm discussed in Sect. 5.2 — a q -qubit unitary W that implements the following map:

$$W|\vec{0}\rangle_q = \frac{1}{\sqrt{\|\alpha\|_1}} \sum_{\vec{j} \in \{0,1\}^q} \sqrt{\alpha_{\vec{j}}} |\vec{j}\rangle.$$

Note that the state on the r.h.s. is a proper quantum state due to the normalization chosen. Suppose we have access to a unitary V that can implement all the V_j in a controlled manner: $V := \sum_{\vec{j} \in \{0,1\}^q} |\vec{j}\rangle\langle\vec{j}| \otimes V_j$. The effect of V is precisely that of applying V_j onto the second register if the first register contains $|\vec{j}\rangle$:

$$V|\vec{j}\rangle|\psi\rangle = |\vec{j}\rangle V_j|\psi\rangle.$$

Now consider the effect of the circuit in Fig. 6.1. After W , we are in the state $\frac{1}{\sqrt{\|\alpha\|_1}} \sum_{\vec{j} \in \{0,1\}^q} \sqrt{\alpha_j} |\vec{j}\rangle |\psi\rangle$.

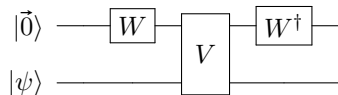


Figure 6.1: Circuit for the implementation of a linear combination of unitaries.

After V , we are in the state $\frac{1}{\sqrt{\|\alpha\|_1}} \sum_{\vec{j} \in \{0,1\}^q} \sqrt{\alpha_j} |\vec{j}\rangle V_j |\psi\rangle$. The effect of the final application of W^\dagger on the quantum state is more difficult to write down analytically, but it yields some state $|\varphi\rangle$. Let us find an expression for the part of $|\varphi\rangle$ that contains $|\vec{0}\rangle$ in the first register; formally, this can be expressed as:

$$\begin{aligned} (\langle\vec{0}| \otimes I^{\otimes n})|\varphi\rangle &= (\langle\vec{0}| \otimes I^{\otimes n})(W^\dagger \otimes I^{\otimes n})V(W \otimes I^{\otimes n})|\vec{0}\rangle|\psi\rangle = (\langle\vec{0}|W^\dagger \otimes I^{\otimes n})V(W \otimes I^{\otimes n})|\vec{0}\rangle|\psi\rangle \\ &= \left(\frac{1}{\sqrt{\|\alpha\|_1}} \sum_{\vec{j} \in \{0,1\}^q} \sqrt{\alpha_j} \langle\vec{j}| \otimes I^{\otimes n} \right) \left(\frac{1}{\sqrt{\|\alpha\|_1}} \sum_{\vec{j} \in \{0,1\}^q} \sqrt{\alpha_j} |\vec{j}\rangle V_j |\psi\rangle \right) \\ &= \frac{1}{\|\alpha\|_1} \sum_{\vec{j} \in \{0,1\}^q} \alpha_j V_j |\psi\rangle. \end{aligned}$$

Thus, the final state $|\varphi\rangle$ can be written as:

$$\frac{1}{\|\alpha\|_1} |\vec{0}\rangle M|\psi\rangle + \sqrt{1 - \frac{\|M|\psi\rangle\|^2}{\|\alpha\|_1^2}} |\phi\rangle,$$

where $|\phi\rangle$ is some quantum state that has no support on $|\vec{0}\rangle\langle\vec{0}| \otimes I^{\otimes n}$ and that we do not care about. (The coefficient under the square root is computed by noting that the entire state must have unit norm, hence the amplitude of the second part in the expression for the state must be the square root of $1 -$ (norm of the first part).) In other words, we have implemented $M|\psi\rangle$, but only if a measurement of the first register yields $|\vec{0}\rangle$: this happens with probability $\frac{\|M|\psi\rangle\|^2}{\|\alpha\|_1^2}$. We can amplify this probability of success to some value very close to 1 with $\mathcal{O}(\|\alpha\|_1/\|M|\psi\rangle\|)$ rounds of oblivious amplitude amplification (i.e., $\mathcal{O}(1/\sqrt{p})$ rounds for an algorithm with probability of success p : the usual quadratic advantage of amplitude amplification), after which we can be almost certain that we produced the state $M|\psi\rangle/\|M|\psi\rangle\|$, as desired. Note that we need oblivious amplitude amplification because $|\psi\rangle$ is given and we do not assume that we have access to a unitary to prepare it, so vanilla amplitude amplification cannot be applied directly, but fortunately we satisfy the more forgiving assumptions of oblivious amplitude amplification, see Sect. 4.2.2.

Resource analysis. We can now get back to Hamiltonian simulation and conclude our discussion on the linear combination of unitaries. We want to implement Eq. (6.8) using the algorithm outlined above, which takes $\mathcal{O}(\|\alpha\|_1/\|M|\psi\rangle\|)$ applications of W and V . We can ignore $\|M|\psi\rangle\|$, because the M that we want to implement is (an approximation of) $e^{i\mathcal{H}t}$, thus $\|M|\psi\rangle\| \approx 1$. Regarding $\|\alpha\|_1$, because the components of α are the coefficients of the linear combination in

Eq. 6.8, we have:

$$\begin{aligned} \|\alpha\|_1 &= \sum_{k=0}^{\mathcal{O}(t+\log \frac{1}{\epsilon})} \sum_{j_1, j_2, \dots, j_k \in \{1, \dots, m\}} \frac{t^k}{k!} \beta_{j_1} \beta_{j_2} \cdots \beta_{j_k} \leq \sum_{k=0}^{\infty} \sum_{j_1, j_2, \dots, j_k \in \{1, \dots, m\}} \frac{t^k}{k!} \beta_{j_1} \beta_{j_2} \cdots \beta_{j_k} \\ &= \sum_{k=0}^{\infty} \frac{(t\|\beta\|_1)^k}{k!} \leq e^{t\|\beta\|_1}, \end{aligned}$$

which is exponential in t and $\|\beta\|_1$. This would lead to $e^{t\|\beta\|_1}$ applications of V and W , but we can reduce this cost by taking advantage of the logarithmic error dependence ($\log \frac{1}{\epsilon}$) of the algorithm. Indeed, note that if t is small then the complexity of the algorithm is also small. Thus, we can divide the Hamiltonian simulation into $t\|\beta\|_1$ blocks where each block evolves the Hamiltonian for time $\tau = 1/\|\beta\|_1$ and uses precision ϵ' . The end result is the same because $(e^{i\mathcal{H}\tau})^{t\|\beta\|_1} = e^{i\mathcal{H}t}$, but the complexity of each block (in terms of the number of applications of V and W) is now $\mathcal{O}(e^{\tau\|\beta\|_1}) = \mathcal{O}(1)$. Also note that the gate complexity of W inside each block is small, because the vector of coefficients of the linear combination includes $\mathcal{O}(\tau + \log \frac{1}{\epsilon'}) = \mathcal{O}(\log \frac{1}{\epsilon'})$ nonzero terms, and similarly, V inside each block applies $\mathcal{O}(\tau + \log \frac{1}{\epsilon'}) = \mathcal{O}(\log \frac{1}{\epsilon'})$ input unitaries U_j (this is a consequence of the truncation for Eq. (6.7)). Finally, we note that it is sufficient to choose error $\epsilon' = \epsilon/(t\|\beta\|_1)$ in each block to achieve total error at most ϵ , and the total cost is $t\|\beta\|_1$ times the cost of each block. This yields an algorithm with complexity $\mathcal{O}\left(t\|\beta\|_1 \log \frac{t\|\beta\|_1}{\epsilon}\right)$, in terms of the number of applications of the unitaries U_j and additional elementary gates.

6.2.4 Hamiltonian simulation for sparse matrices with oracle access

Our goal in this section is to introduce a natural input model for matrices, and give an intuition for Hamiltonian simulation algorithms based on this model. We do not go into the details because in the rest of this set of lecture notes we only need the input model from this section, and not the algorithms.

In the preceding sections we assumed that the Hamiltonian can be expressed as a sum of local terms, i.e., operators that act only on a small number of qubits. That model is suitable for several applications originating from the study of physical systems and general abstract models, but it is not necessarily suitable for data-driven applications where the data may have little structure. In classical (i.e., non-quantum) scientific computing, data is often represented in a compact form by listing only the nonzero elements. The analog of that representation in the quantum world is the *sparse-oracle* input model. In this model, we assume that we have access to the following quantum circuits, generally called oracles in this context, that give a description of the Hamiltonian \mathcal{H} .

- The first oracle, mapping $|\vec{j}\rangle|\vec{\ell}\rangle \rightarrow |\vec{j}\rangle|\vec{c}_{j\ell}\rangle$, provides the index $c_{j\ell}$ of the ℓ -th nonzero element of column j ,
- The second oracle, mapping $|\vec{j}\rangle|\vec{k}\rangle|\vec{z}\rangle \rightarrow |\vec{j}\rangle|\vec{k}\rangle|\vec{z} \oplus \vec{\mathcal{H}}_{jk}\rangle$, provides the value of the element in position j, k of the Hamiltonian.

In other words, one map provides the indices of the nonzero elements in each column, and one map provides the values of arbitrary elements.

Remark 6.18. *The definition of the oracle providing the value for the nonzero entries of \mathcal{H} implicitly assumes that such entries are integer-valued; this is not a restrictive assumption, because as long as the entries are rational (as in any finite-precision representation), we can rescale them to integer and adjust the value of the simulation time t to compensate for any scaling.*

The sparse-oracle input model is the main subject of Sect. 7.2.2, where we discuss a circuit to construct a unitary that (in some sense, to be specified later) encodes a given matrix; that type of encoding, called block-encoding, also leads to Hamiltonian simulation algorithms, see Sect. 6.2.5. However, there are algorithms for Hamiltonian simulation tailored to the sparse-oracle input model

and that do not rely on the block-encoding framework: we give an example of such an algorithm next.

Consider the following approach: we first decompose the Hamiltonian into a sum of roughly s terms, where s is the maximum number of nonzero elements per row/column. That is, we write $\mathcal{H} = \bar{\mathcal{H}}_{\text{diag}} + \sum_j \bar{\mathcal{H}}_j$, where $\bar{\mathcal{H}}_{\text{diag}}$ is the diagonal part of the Hamiltonian, and $\bar{\mathcal{H}}_j$ are matrices containing only off-diagonal terms. To determine these matrices, we interpret the rows and columns of \mathcal{H} as nodes in a graph, with an edge between two nodes if and only if there is a nonzero element in \mathcal{H} in the corresponding position; i.e., if $\mathcal{H} \in \mathbb{C}^{2^n \times 2^n}$, we construct a graph $G = (V, E)$ with $V = \{0, 1\}^n$, $E = \{(\vec{u}, \vec{v}) : \vec{u}, \vec{v} \in \{0, 1\}^n, \mathcal{H}_{uv} \neq 0, u \neq v\}$. Then, an edge coloring of G gives a decomposition of \mathcal{H} into a sum of element-wise disjoint matrices, where each matrix contains all elements corresponding to a certain color, and by definition of edge coloring (no two edges connected to the same vertex have the same color), each matrix has at most one nonzero element per row or column. Because of this, the matrices in the decomposition are easy to diagonalize. We then simulate each matrix in the decomposition independently, e.g., using the methodology of Sect. 6.2.1, and use some approach (e.g., product formula) to compose the simulation of $\bar{\mathcal{H}}_{\text{diag}}$ and $\bar{\mathcal{H}}_j \forall j$ into a simulation for the original Hamiltonian. Note that edge colorings can be computed in polynomial time, and there always exists an edge coloring of a graph of size at most $\Delta + 1$, where Δ is the maximum degree of the graph — which, by construction, is the number s of nonzero elements per row/column of the Hamiltonian. For details of this approach, see [Childs, 2004, Chapter 2].

Although the above sketch is only a brief, high-level overview of a Hamiltonian simulation approach tailored to the sparse-oracle input model, it gives a concrete example where it is clear why we obtain an algorithm with a complexity that scales with the maximum number of nonzero elements in each column/row. In fact, this is very common for this input model, explaining why this particular model leads to algorithms with competitive performance only if the Hamiltonian is sparse (i.e., the number of nonzero terms per row or column is at most polylogarithmic in the size of Hamiltonian). Further references on Hamiltonian simulation with this input model can be found in Sect. 6.3.

6.2.5 Signal processing and the block-encoding framework

Depending on the specific situation at hand (i.e., the characteristics of the Hamiltonian and how it is specified), the fastest quantum algorithms for Hamiltonian simulation generally rely on the signal processing framework, proposed in [Low and Chuang, 2019]. The signal processing approach is best understood within the block-encoding framework. The input Hamiltonian can be specified in many possible ways in this framework. For example, it can be described in the same sparse-oracle input model as in Sect. 6.2.4, but this is not the only possibility: the only requirement is that we can construct a circuit that acts as the desired Hamiltonian on a certain subspace.

We do not have the necessary background to describe Hamiltonian simulation algorithms that rely on this input model yet, but we revisit this topic in Sect. 7.2.1, after introducing the block-encoding framework. At a very high level, it is based on the idea of implementing a polynomial transformation of the singular values of the Hamiltonian, approximating the exponential function. The polynomial approximation is constructed by acting on a quantum circuit that implements a (possibly scaled down) version of the Hamiltonian itself, so that we can implement a matrix function of it. We refer the reader to Sect. 7.2.1 and the notes in Sect. 7.3 for a more detailed discussion of the block-encoding framework, and Hamiltonian simulation within that framework; as a byproduct, the discussion also provides the main intuition of the signal processing technique.

6.3 Notes and further reading

Feynman’s groundbreaking proposal and discussion of a quantum computer to simulate the evolution of a quantum-mechanical system can be found in [Feynman, 1982, Feynman, 2018]. His work also set the foundations for showing that Hamiltonian simulation is BQP-hard, i.e., that every problem that can be efficiently solved by a quantum computer can be cast as a Hamil-

tonian simulation problem. Throughout this chapter we gave a few references to efficient (i.e., polynomial-time) quantum algorithms for Hamiltonian simulation, and several more are given below: each of these algorithms already shows that Hamiltonian simulation is in BQP, hence we conclude that it is BQP-complete. To read about additional BQP problems, [Wocjan and Zhang, 2006] is a good starting point. As it turns out, even the problem of inverting a Hermitian matrix, specified in an appropriate manner, is BQP-complete: [Harrow et al., 2009] shows that the problem of simulating an arbitrary quantum circuit can be cast as the problem of applying the inverse of a certain matrix. The matrix inversion algorithm of [Harrow et al., 2009] is discussed in Ch. 7, in the context of quantum algorithms for linear systems.

In the context of optimization, Hamiltonian simulation is used as a building block for several useful subroutines: see Ch. 7 where it is at the heart of matrix manipulation algorithms, Ch. 8 where matrix manipulation is used to build algorithms for semidefinite optimization problems, and Ch. 9, where it is used to solve minimum or maximum eigenvalue problems. In a recent line of work, initiated in [Leng et al., 2023a], the solution of the Schrödinger equation is used *directly* to solve continuous optimization problems: this is done by defining a Hamiltonian whose evolution follows a descent direction for the optimization problem. The inspiration for this work is [Wibisono et al., 2016], describing a dynamical system that follows the natural steepest descent direction. [Leng et al., 2023a] proposes a quantum Hamiltonian that closely mimics such a dynamical system, and shows that simulation of the Schrödinger equation with such a Hamiltonian converges to the global minimum for both convex and nonconvex problems — although for nonconvex problems the simulation time may need to be exponentially large, as expected (we do not expect quantum computers to solve nonconvex optimization problems in polynomial time). This algorithm for nonconvex optimization is further investigated in [Leng et al., 2023b], whereas a software package for its utilization and a numerical evaluation can be found in [Kushnir et al., 2025]. [Augustino et al., 2023a] extends this work to simulate the central path of interior point methods for linear optimization problems, yielding a provably convergent quantum algorithm for linear programs with a favorable running time compared to several classical algorithms with respect to the dimension of the problem (but $1/\epsilon$ dependence on the final optimality gap). Notably, [Leng et al., 2023a, Leng et al., 2023b, Augustino et al., 2023a] do not assume access to QRAM.

The development of an approach for Hamiltonian simulation based on a linear combination of unitaries is due to [Childs and Wiebe, 2012], and the LCU technique has found numerous applications in a variety of quantum algorithms; for further discussion, see also [Childs et al., 2017].

Several examples of efficient Hamiltonian simulation algorithms for the sparse-oracle input model are described in [Berry et al., 2007, Berry et al., 2014, Berry et al., 2015, Low, 2019].

Chapter 7

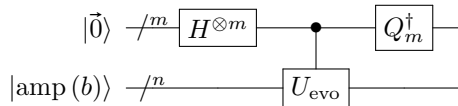
Matrix manipulation with quantum algorithms

Operations on matrices are at the heart of a vast number of optimization algorithms. Quantum computers can only apply unitary matrices directly, but there exist a vast toolbox of quantum algorithms to perform complex operations on non-unitary matrices as well. In this chapter we discuss two aspects of non-unitary matrix manipulation that have been featured prominently in existing quantum algorithms for optimization: algorithms for linear systems (i.e., matrix inversion), and the block-encoding framework. Matrix inversion can also be performed within the block-encoding framework, and it is actually more efficient in that framework than in the phase-estimation-based approach that we initially present. Because the phase estimation approach to matrix inversion is historically important, elegant, and showcases a number of powerful ideas for the design of quantum algorithm, we discuss it anyway, and in fact we begin our discussion in this chapter with it.

7.1 Quantum linear system solvers

The subject of this section is the solution of linear systems of equations, one of the most ubiquitous problems in engineering. We describe and analyze an algorithm for this task introduced by [Harrow et al., 2009]. Our description is mostly based on the original version of [Harrow et al., 2009] — typically referred to as the HHL algorithm, from the last name of the authors, Harrow, Hassidim and Lloyd — but there have been many refinements of that scheme over the years. We discuss notable improvements to the HHL algorithm in Sect. 7.1.5, yielding significantly better gate complexity bounds (even exponentially better, in some of the input parameters); see also the notes at the end of this chapter (Sect. 7.3).

We use the acronym QLSA to refer to a quantum linear system algorithm. (The abbreviation QLSA is relatively common in the literature.) The problem solved by a QLSA can be stated as follows: given a Hermitian invertible matrix $A \in \mathbb{C}^{2^n \times 2^n}$, a vector $b \in \mathbb{C}^{2^n}$, a precision parameter $\epsilon > 0$, compute an n -qubit state $|\psi\rangle$ such that $\| |\psi\rangle - |\text{amp}(A^{-1}b)\rangle \| \leq \epsilon$ (recall Def. 5.34). We assume that the input data is described by suitable quantum oracles P_A, P_b ; we discuss the exact nature of these oracles in Sect. 7.1.2. Furthermore, we assume that $\|A\| \leq 1$ and the condition number κ of A , or an upper bound on it, is known, see Sect. 7.1.4. Note that the assumption $\|A\| \leq 1$ may in general require normalizing the linear system, which in turn requires adjusting the precision. In [Harrow et al., 2009] there is also a somewhat hidden assumption that A is positive semidefinite, in which case all eigenvalues lie in $[\frac{1}{\kappa}, 1]$; this assumption shows up subtly in a few crucial points of the analysis, for example because the filter functions for the eigenvalues (described later) are defined for positive values only. This is handled carefully in several subsequent works, such as [Childs et al., 2017, Chakraborty et al., 2019, Gilyén et al., 2019b], where the assumption is that the spectrum of the matrix is in $[-1, -\frac{1}{\kappa}] \cup [\frac{1}{\kappa}, 1]$. For now we keep the more restrictive assumption.


 Figure 7.1: Determining an eigendecomposition of $|\text{amp}(b)\rangle$.

7.1.1 Algorithm description: simplified exposition

We give a simplified exposition of the algorithm that is not entirely accurate, but it conveys the main ideas without getting bogged down in details. Most of the inaccuracies of our exposition are eventually discussed in subsequent sections, in particular Sect.s 7.1.2 and 7.1.4.

The HHL algorithm for the solution of a linear system relies on quantum phase estimation and Hamiltonian simulation. The first step of this QLSA is to decompose $|\text{amp}(b)\rangle$ into an eigenbasis of A . For this, we use phase estimation. Let m be a number of qubits, to be determined later, to store the phases in quantum phase estimation; the first m qubits form the first register. We also use an n -qubit register (second register) to store the eigenstate, and an additional qubit for a certain rotation that we ignore for now and introduce only when necessary. We apply phase estimation using the circuit given in Fig. 7.1, where the controlled U_{evo} block (with the first register as control) is the unitary defined as:

$$CU_{\text{evo}} := \sum_{\vec{k} \in \{0,1\}^m} |\vec{k}\rangle\langle\vec{k}| \otimes e^{2\pi i A k}.$$

This unitary applies Hamiltonian simulation for a variable amount of time, and in particular, the length of the simulation is determined by the content of the first register, i.e., the value of the index $|\vec{k}\rangle$ in the above expression.

Let $|\psi_h\rangle, h = 0, \dots, 2^n - 1$ be an orthonormal eigenbasis of A , with corresponding real eigenvalues $\lambda_h, h = 0, \dots, 2^n - 1$; the eigenbasis exists because A is Hermitian. We make the simplifying assumption that all λ_h can be expressed exactly on m binary digits, i.e., there exists a binary string $\vec{\ell}_h$ such that $0.\vec{\ell}_h$ is an exact representation of λ_h (thus, $\lambda_h = \ell_h/2^m$).

Remark 7.1. *Because $\|A\| \leq 1$ and A is Hermitian, all eigenvalues are real numbers ≤ 1 . Although in general these eigenvalues may not be representable in finite precision, here we are (for now) assuming that they can be written as $\ell_h/2^m$, with $\ell_h \in \{0, \dots, 2^m - 1\}$, for some appropriate value of m and suitable choice of ℓ_h . Note that some values cannot ever be represented in this way, such as irrational numbers or even simply the number 1 (because $\ell_h/2^m < 1$ for any m), but the approximation error is exponentially small in m .*

Now suppose, for the sake of the analysis, that the input state for the bottom part of the circuit in Fig. 7.1 is one of the eigenstates of A , say $|\psi_h\rangle$; in other words, let us analyze what happens if we execute the circuit setting $|\text{amp}(b)\rangle = |\psi_h\rangle$. The effect of the circuit is the following. After the Hadamard gates, the state of the entire system is:

$$\frac{1}{\sqrt{2^m}} \sum_{\vec{k} \in \{0,1\}^m} |\vec{k}\rangle |\psi_h\rangle$$

This is a possibly-outdated preprint, using the author's lecture notes, of the book "Quantum algorithms for optimizers," edited by SIAM. All rights to the book's material belong to SIAM. Please refer to the SIAM version of the book.

Applying CU_{evo} on this state yields:

$$\begin{aligned} CU_{\text{evo}} \left(\frac{1}{\sqrt{2^m}} \sum_{\vec{k} \in \{0,1\}^m} |\vec{k}\rangle |\psi_h\rangle \right) &= \frac{1}{\sqrt{2^m}} \sum_{\vec{k} \in \{0,1\}^m} \left(|\vec{k}\rangle e^{2\pi i A \vec{k}} |\psi_h\rangle \right) \\ &= \frac{1}{\sqrt{2^m}} \sum_{\vec{k} \in \{0,1\}^m} \left(|\vec{k}\rangle e^{2\pi i \ell_h \vec{k} / 2^m} |\psi_h\rangle \right) \\ &= \frac{1}{\sqrt{2^m}} \sum_{\vec{k} \in \{0,1\}^m} \left(e^{2\pi i \ell_h \vec{k} / 2^m} |\vec{k}\rangle \right) |\psi_h\rangle \\ &= Q_m |\vec{\ell}_h\rangle |\psi_h\rangle. \end{aligned}$$

Thus, the first register contains the quantum Fourier transform of $|\vec{\ell}_h\rangle$. It follows that applying the inverse QFT yields:

$$Q_m^\dagger \otimes I^{\otimes n} \left(Q_m |\vec{\ell}_h\rangle |\psi_h\rangle \right) = |\vec{\ell}_h\rangle |\psi_h\rangle.$$

Because this is true for each one of the eigenstates, it also applies to a superposition of the eigenstates. Let $|\text{amp}(b)\rangle = \sum_{h=0}^{2^n-1} \beta_h |\psi_h\rangle$ be the decomposition of $|\text{amp}(b)\rangle$ in terms of the eigenbasis of A (we do not need to know the coefficients β_h , but we know that they exist). The effect of the circuit in Fig. 7.1 is therefore:

$$\begin{aligned} (Q_m^\dagger \otimes I^{\otimes n}) CU_{\text{evo}} \left(\frac{1}{\sqrt{2^m}} \sum_{\vec{k} \in \{0,1\}^m} |\vec{k}\rangle |\text{amp}(b)\rangle \right) &= (Q_m^\dagger \otimes I^{\otimes n}) CU_{\text{evo}} \left(\frac{1}{\sqrt{2^m}} \sum_{\vec{k} \in \{0,1\}^m} |\vec{k}\rangle \sum_{h=0}^{2^n-1} \beta_h |\psi_h\rangle \right) \\ &= \sum_{h=0}^{2^n-1} \beta_h (Q_m^\dagger \otimes I^{\otimes n}) CU_{\text{evo}} \left(\frac{1}{\sqrt{2^m}} \sum_{\vec{k} \in \{0,1\}^m} |\vec{k}\rangle |\psi_h\rangle \right) \\ &= \sum_{h=0}^{2^n-1} \beta_h \left(|\vec{\ell}_h\rangle |\psi_h\rangle \right). \end{aligned}$$

Next, we introduce an auxiliary qubit in state $|0\rangle$, say at the bottom of the circuit so that it becomes the last qubit, and perform the mapping:

$$\sum_{h=0}^{2^n-1} \beta_h \left(|\vec{\ell}_h\rangle |\psi_h\rangle |0\rangle \right) \xrightarrow{U_{\text{rot}}} \sum_{h=0}^{2^n-1} \beta_h \left(|\vec{\ell}_h\rangle |\psi_h\rangle \left(\sqrt{1 - \frac{C^2}{\lambda_h^2}} |0\rangle + \frac{C}{\lambda_h} |1\rangle \right) \right), \quad (7.1)$$

where C is a constant of normalization, to be discussed later. This mapping is composed of two parts: first, we map $|\vec{\ell}_h\rangle \rightarrow |\frac{1}{\pi} \sin^{-1} \frac{C}{\lambda_h}\rangle$, defining $\frac{1}{\pi} \sin^{-1} \frac{C}{\lambda_h}$ to be a binary representation of $\frac{1}{\pi} \sin^{-1} \frac{C}{\lambda_h}$ on m' qubits. Second, we make use of a unitary U_Y that implements the following operation, where $0.\vec{\theta}$ is some number in $[0, 1]$:

$$U_Y(|\vec{\theta}\rangle_{m'} |0\rangle) := |\vec{\theta}\rangle (\cos(2\pi 0.\vec{\theta}) |0\rangle + \sin(2\pi 0.\vec{\theta}) |1\rangle).$$

Remark 7.2. The operation U_Y can be implemented using one controlled- R_Y gate (Def. 4.26) for each bit of $\vec{\theta}$. Specifically, defining binary strings $\vec{u}^{(j)} \in \{0,1\}^{m'}$, $\vec{u}_h^{(j)} = 1$ if $j = h$, 0 otherwise, we can write U_Y as:

$$U_Y(|\vec{\theta}\rangle_{m'} |0\rangle) = \prod_{j=1}^{m'} \left(|\vec{u}^{(j)}\rangle \langle \vec{u}^{(j)}| \otimes R_Y(2^{2-j}\pi) \right),$$

which is a sequence of controlled rotations acting on the last qubit, where we successively halve the angle of rotation and we condition on one digit of the binary representation of $\vec{\theta}$. This expression can be easily verified by writing $0.\vec{\theta}$ as a summation of terms that depend on a single binary digit each, and recalling that the angles in consecutive rotations get summed to each other.

After taking care of normalization factors, and applying some necessary linear transformations of the domain, we are able to rotate the last qubit by $\sin \sin^{-1} \frac{C}{\lambda_h} = \frac{C}{\lambda_h}$. Here we skipped a few details for the sake of exposition, but the remaining obstacles (e.g., the value of $\frac{1}{\pi} \sin^{-1} \frac{C}{\lambda_h}$ is in $[-\frac{1}{2}, \frac{1}{2}]$ rather than $[0, 1]$) can be easily resolved using quantum circuits for binary arithmetics, similarly to what is done in classical digital computers. Putting everything together, we can see that the map in Eq. (7.1) can be implemented efficiently with the building blocks that we just described. After applying the map in Eq. (7.1), we have the following state:

$$\sum_{h=0}^{2^n-1} \beta_h \left(|\vec{\ell}_h\rangle |\psi_h\rangle \left(\sqrt{1 - \frac{C^2}{\lambda_h^2}} |0\rangle + \frac{C}{\lambda_h} |1\rangle \right) \right).$$

Remark 7.3. *The normalization constant C is necessary to ensure that what we obtain is a valid quantum state. In particular, because we need $\frac{C}{\lambda_h} \in [-1, 1]$ and we know that $\frac{1}{\kappa} \leq |\lambda_h| \leq 1$, we choose $C = \mathcal{O}(1/\kappa)$.*

We then uncompute the register containing the outcome of the phase estimation, so that we leave the working register in the initial state (and unentangled with the rest), and apply a measurement on the register corresponding to the auxiliary qubit for the rotation. This is depicted in Fig. 7.2. We claim that when the outcome of the measurement on the last qubit is $|1\rangle$,

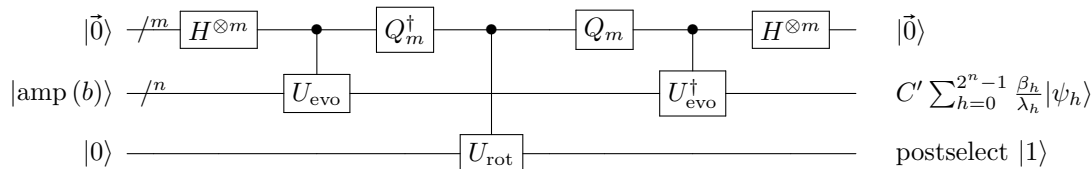


Figure 7.2: HHL algorithm for linear systems.

the register initially containing $|\text{amp}(b)\rangle$ now contains the solution $|\text{amp}(A_B^{-1}b)\rangle$. Indeed, after uncomputing the register containing the eigenvalues $|\vec{\ell}_h\rangle$, we obtain the following state:

$$\sum_{h=0}^{2^n-1} \beta_h \left(|\vec{0}\rangle |\psi_h\rangle \left(\sqrt{1 - \frac{C^2}{\lambda_h^2}} |0\rangle + \frac{C}{\lambda_h} |1\rangle \right) \right), \quad (7.2)$$

and if the outcome of the measurement in the last register is $|1\rangle$, we obtain $C' \sum_{h=0}^{2^n-1} \frac{\beta_h}{\lambda_h} |\psi_h\rangle$ in the register that initially contained $|\text{amp}(b)\rangle$, where the constant of normalization C' changes from C because we need to renormalize the state after the measurement — in particular, the state after measurement has unit norm, so $C' = 1 / \left\| \sum_{h=0}^{2^n-1} \frac{\beta_h}{\lambda_h} |\psi_h\rangle \right\|$. The only part left now is to note that $C' \sum_{h=0}^{2^n-1} \frac{\beta_h}{\lambda_h} |\psi_h\rangle$ is exactly the solution $|\text{amp}(A^{-1}b)\rangle$. Indeed:

$$A = \sum_{h=0}^{2^n-1} \lambda_h |\psi_h\rangle \langle \psi_h|, \quad A^{-1} = \sum_{h=0}^{2^n-1} \frac{1}{\lambda_h} |\psi_h\rangle \langle \psi_h|,$$

so that:

$$A^{-1}b = \sum_{h=0}^{2^n-1} \frac{1}{\lambda_h} |\psi_h\rangle \langle \psi_h| \sum_{h=0}^{2^n-1} \beta_h |\psi_h\rangle = \sum_{h=0}^{2^n-1} \frac{\beta_h}{\lambda_h} |\psi_h\rangle.$$

(This also simplifies the expression for C' to $C' = 1/\|A^{-1}b\|$.) Thus, the circuit in Fig. 7.2 constructs the state $|\text{amp}(A^{-1}b)\rangle$.

7.1.2 Complexity analysis

Let us analyze the complexity of the HHL algorithm for linear systems. We start with a discussion of the simplified version of the algorithm presented in Sect. 7.1.1. Recall that after the controlled- U_{evo} operation, we are in the state:

$$\frac{1}{\sqrt{2^m}} \sum_{h=0}^{2^n-1} \beta_h \sum_{\vec{k} \in \{0,1\}^m} \left(e^{2\pi i \ell_h k / 2^m} |\vec{k}\rangle |\psi_h\rangle \right).$$

In Sect. 7.1.1 we assumed that $\lambda_h = \ell_h / 2^m$ for some integer ℓ_h on m bits, i.e., λ_h is representable on m bits; now we drop this assumption. We need to choose the number of qubits m to represent the eigenvalues, which directly determines the time duration of Hamiltonian simulation, to ensure that we obtain a sufficiently accurate representation of the eigenvalues. First, recall from phase estimation that if we want to compute a phase to some precision ϵ' we pick $m = \mathcal{O}(\log \frac{1}{\epsilon'})$, see Thm. 3.9 and Rem. 3.13. The smallest eigenvalue of A is at least $1/\kappa$. If we want such a small eigenvalue to have error ϵ , i.e., $\log \frac{1}{\epsilon}$ digits of precision, we choose $m = \mathcal{O}(\log \frac{\kappa}{\epsilon})$: this implies that the longest time duration t for Hamiltonian simulation is $2^m = \mathcal{O}(\frac{\kappa}{\epsilon})$. (Intuitively: in the Fourier state $\frac{1}{\sqrt{2^m}} \sum_{\vec{k} \in \{0,1\}^m} e^{2\pi i \ell_h k / 2^m} |\vec{k}\rangle$ we need $k \approx \frac{\kappa}{\epsilon}$ to ensure that at least $\lceil \log \frac{1}{\epsilon} \rceil$ digits of ℓ_h are “picked up” in the state, if ℓ_h is of order $1/\kappa$; so we choose $m = \mathcal{O}(\log \frac{\kappa}{\epsilon})$ as the size of the register containing k , which is a sufficient number of bits to contain integers of the desired size.)

For the sake of accuracy, we mention that, rather than preparing the first register in the state $\frac{1}{\sqrt{2^m}} \sum_{\vec{k} \in \{0,1\}^m} |\vec{k}\rangle$ using $H^{\otimes m}$, as indicated in Sect. 7.1.1, [Harrow et al., 2009] instead suggests preparing the state:

$$|\xi\rangle := \sqrt{\frac{2}{2^m}} \sum_{\vec{r} \in \{0,1\}^m} \sin \frac{\pi(r + \frac{1}{2})}{2^m} |\vec{r}\rangle,$$

where m has to be chosen appropriately according to the discussion in this section. Although this complicated expression might appear unnecessary, it is chosen because it leads to a clean analysis of the errors in the Fourier states that we want to construct, with small errors. After applying the conditional Hamiltonian evolution CU_{evo} onto $|\xi\rangle \otimes |b\rangle$, we then obtain:

$$\begin{aligned} CU_{\text{evo}} \left(\sqrt{\frac{2}{2^m}} \sum_{h=0}^{2^n-1} \beta_h \sum_{\vec{r} \in \{0,1\}^m} \sin \frac{\pi(r + \frac{1}{2})}{2^m} |\vec{r}\rangle |\psi_h\rangle \right) = \\ \sqrt{\frac{2}{2^m}} \sum_{h=0}^{2^n-1} \beta_h \sum_{\vec{r} \in \{0,1\}^m} e^{i\lambda_h r c / 2^m} \sin \frac{\pi(r + \frac{1}{2})}{2^m} |\vec{r}\rangle |\psi_h\rangle, \end{aligned}$$

where c is a suitably chosen parameter representing the time duration parameter of the Hamiltonian evolution. Note that c determines the resolution of the estimation of the eigenvalues, because the “step” in the exponent (i.e., the difference between two exponents when t increases by one) is of size $c/2^m$. We choose $c = \mathcal{O}(\kappa/\epsilon)$ because this leads to error $\leq \epsilon$ in the final state, see [Harrow et al., 2009] as well as the intuitive explanation above regarding the choice of m for the simplified case. From the last equation, applying the inverse QFT yields:

$$\sqrt{\frac{2}{2^m}} \sum_{h=0}^{2^n-1} \beta_h \sum_{\vec{k} \in \{0,1\}^m} \sum_{\vec{r} \in \{0,1\}^m} e^{\frac{i\vec{r}}{2^m} (\lambda_h c - 2\pi k)} \sin \frac{\pi(r + \frac{1}{2})}{2^m} |\vec{k}\rangle |\psi_h\rangle.$$

At this point we need to show that the coefficients $e^{\frac{i\vec{r}}{2^m} (\lambda_h c - 2\pi k)}$ are only large when $k \approx \frac{\lambda_h c}{2\pi}$, i.e., that these coefficients are bounded above and small whenever $|k - \frac{\lambda_h c}{2\pi}| \geq 1$. The proof is long and technical, and is not discussed here, see [Harrow et al., 2009] for details; some of the calculations are similar to those in the proof of Lem. 4.28 to handle the geometric sums, see also [Nielsen and Chuang, 2002, Sect. 5.2.1]. The outcome is as desired, and allows us to focus on the basis states $|\vec{k}\rangle$ when $k \approx \frac{\lambda_h c}{2\pi}$. This lets us extract (a multiple of) the eigenvalues λ_h of A . Fortunately,

the preparation of this more complicated initial state does not increase the gate complexity by a significant amount, because the state can be prepared efficiently with the procedure of [Grover and Rudolph, 2002] (this is the same algorithm that we described at the end of Sect. 5.2, whereby instead of the precomputed binary tree of Cor. 5.37, we compute the rotation angles for each inner node of the tree on-the-fly, with a circuit exploiting the analytically-known form of the coefficients).

The complexity of the algorithm can be analyzed as follows. The input data of the algorithm is given by two oracles P_A, P_b : one that describes the entries of A , and one that prepares the state $|\text{amp}(b)\rangle$ corresponding to the r.h.s. vector b . The complexity is given in terms of the number of calls to these oracles, plus the number of additional gates. Let us assume that P_b runs in time T_b , and P_A runs in time T_A (i.e., those are their respective gate complexities). The only operation that we need to perform on the matrix A is Hamiltonian simulation (i.e., controlled U_{evo}), and the gate complexity of the algorithm depends on the complexity of performing the desired Hamiltonian simulation. Under the sparse-oracle input model (see Sect. 6.2.4), the Hamiltonian simulation algorithm employed in [Harrow et al., 2009] uses $\tilde{\mathcal{O}}(ts^2T_A)$ gates, where s is the maximum number of nonzeros in one row of A ; using better Hamiltonian simulation techniques, such as Hamiltonian simulation in the block-encoding framework starting from a sparse-access oracle (see Thm. 7.19 and Sect. 7.2.2), the complexity can be reduced to $\tilde{\mathcal{O}}(tsT_A)$. Because t is chosen as $\mathcal{O}(\kappa/\epsilon)$, this gives total complexity $\tilde{\mathcal{O}}(T_b + \frac{\kappa}{\epsilon}sT_A)$ for one execution of the circuit in Fig. 7.2: we prepare $|\text{amp}(b)\rangle$ once, and the most expensive operation in Fig. 7.2 is Hamiltonian simulation — everything else takes polylogarithmic number of gates and is therefore hidden by the $\tilde{\mathcal{O}}(\cdot)$ notation. We must, however, also consider what the probability of success is. Recall that we obtain the solution to the matrix inversion only if we obtain the state $|1\rangle$ in the register used for the final rotation (or $|11\rangle$ when we use filter functions, see Sect. 7.1.4). As it turns out, a careful analysis shows that the probability to obtain $|1\rangle$ in such register is at least $\Omega(\frac{1}{\kappa^2})$: this is a lower bound on the norm of the component of Eq. (7.2) with $|1\rangle$ in the last qubit, because we know that $C = \mathcal{O}(\frac{1}{\kappa})$, $\lambda_h \leq 1 \forall h$. Thus, to obtain the solution with some constant probability close to 1 we apply $\mathcal{O}(\kappa)$ (i.e., $1/\sqrt{p}$ where $p = 1/\kappa^2$ is the probability of success) iterations of amplitude amplification. Summarizing, the algorithm uses $\tilde{\mathcal{O}}(\kappa(T_b + \frac{\kappa}{\epsilon}sT_A))$ gates. As discussed at the beginning of this section, there have been several papers that followed up on the work of [Harrow et al., 2009] and improved its running time, sometimes significantly: we discuss some of these in Sect. 7.1.5.

7.1.3 Non-Hermitian matrices

The problem definition and the discussion in preceding sections assume that A is Hermitian, but we would like to be able to apply the QLSA also to non-Hermitian matrices. In this section we discuss how to lift this assumption, by showing a modification of the algorithm that works for non-Hermitian matrices. Suppose then that $A \in \mathbb{C}^{2^m \times 2^n}$, with $m \leq n$, not necessarily Hermitian. Let the singular value decomposition of A be:

$$A = \sum_{h=0}^{2^m-1} \sigma_h |\psi_h\rangle\langle\phi_h|,$$

where $|\psi_h\rangle$ are the left singular vectors, $|\phi_h\rangle$ the right singular vectors. Consider the matrix:

$$A' = \begin{pmatrix} 0 & A \\ A^\dagger & 0 \end{pmatrix}.$$

This matrix $A' \in \mathbb{C}^{(2^m+2^n) \times (2^m+2^n)}$ is Hermitian with 2^{m+1} nonzero eigenvalues $\pm\sigma_h$ (i.e., for each singular value, we take it with both a plus and a minus sign) and corresponding eigenvectors:

$$|w_h^\pm\rangle = \frac{1}{\sqrt{2}} (|0\rangle|\psi_h\rangle \pm |1\rangle|\phi_h\rangle).$$

(One can check that these are eigenvectors with the stated eigenvalue by performing the matrix-eigenvector multiplication.) A' also has $2^m + 2^n - 2^{m+1} = 2^n - 2^m$ zero eigenvalues. .

We then apply the QLSA using matrix A' and with the r.h.s. vector (i.e., the value of the “eigenstate” register for phase estimation) set to:

$$|0\rangle|\text{amp}(b)\rangle = |0\rangle \otimes \left(\sum_{h=0}^{2^m-1} \beta_h |\psi_h\rangle \right) = \sum_{h=0}^{2^m-1} \beta_h \frac{1}{\sqrt{2}} (|w_h^+\rangle + |w_h^-\rangle).$$

Due to the structure of the matrix A' , the QLSA produces a state proportional to:

$$\sum_{h=0}^{2^m-1} \frac{\beta_h}{\sigma_h} \frac{1}{\sqrt{2}} (|w_h^+\rangle - |w_h^-\rangle) = \sum_{h=0}^{2^m-1} \frac{\beta_h}{\sigma_h} |1\rangle |\phi_h\rangle,$$

where the sign $-$ in front of $|w_h^-\rangle$ comes from the fact that $|w_h^-\rangle$ has negative eigenvalues. This state is a solution to the linear system after dropping the first $|1\rangle$, because:

$$\underbrace{\left(\sum_{h=0}^{2^m-1} \sigma_h |\psi_h\rangle \langle \phi_h| \right)}_A \underbrace{\left(\sum_{h=0}^{2^m-1} \frac{\beta_h}{\sigma_h} |\phi_h\rangle \right)}_{\text{output state}} = \sum_{h=0}^{2^m-1} \beta_h |\psi_h\rangle = |\text{amp}(b)\rangle.$$

Thus, the QLSA applied to the modified problem A' recovers a solution to the original problem $Ax = b$ for non-Hermitian A . Note that the number of columns/rows of A' is at most double the number of columns/rows of A , so the representation of A' and its eigenvectors only requires one additional qubit compared to A . Thus, applying the QLSA to A' is not much more resource-intensive than applying it to A (of course, because A did not satisfy the Hermiticity assumption, we could not have applied the algorithm directly to A).

7.1.4 Unknown condition number

In Sect.s 7.1.1 and 7.1.2 we saw that many of the quantities involved in the QLSA depend on κ , and we need to know their value to define the quantum circuit that executes the algorithm. Thus, knowledge of κ , or an upper bound on κ , is necessary.

Remark 7.4. *An upper bound $\kappa' \geq \kappa$ is sufficient for the following reason: the assumption that eigenvalues are in the interval $[\frac{1}{\kappa}, 1]$ is clearly satisfied if we use κ' instead of κ ; κ is also used as a normalization factor to ensure that certain operations are well defined (and unitary), e.g., Eq. (7.1), and substituting κ' gives subnormalized, but valid, operations — the subnormalization can be taken care of with amplitude amplification (whose complexity would also depend on κ'). From a computational complexity point of view, we want to ensure that $\kappa' = \mathcal{O}(\kappa)$, so that, overall, the QLSA is slowed down by no more than a constant factor.*

Under the assumption that eigenvalues are in $[\frac{1}{\kappa}, 1]$, and κ is known, we may not need additional work compared to Sect. 7.1.1, as we can choose the number of qubits appropriately to represent all eigenvalues up to a small error. Suppose, however, that we do not know precisely the condition number κ ; or suppose that we only want to perform inversion of eigenvalues between certain values, because we know that the corresponding eigenspaces already span the r.h.s. vector b . In such cases we need a different approach to ensure that we are inverting the matrix correctly. There are several natural approaches to deal with an unknown condition number; we discuss them here.

Filter functions. To alleviate the issue of an unknown condition number, [Harrow et al., 2009] proposes the use of *filter functions*, a concept that is also used in numerical analysis. We remark that these are not needed with the right assumption on the spectrum of A , however it is very instructive to discuss the idea of filter functions because they show some of the techniques that can be applied to implement matrix functions on quantum computers; the block-encoding framework presented in Sect. 7.2 provides additional ways to do so.

The main complication is the fact that if some eigenvalue λ_h is very small, say $\frac{1}{\kappa}$, then a small relative error in the computation of the eigenvalue in phase estimation may lead to a very large error in the computation of the inverse $\sum_h \frac{1}{\lambda_h} |\psi_h\rangle\langle\psi_h|$ (i.e., the reciprocal of some eigenvalue is of the order of κ , which may be affected by large absolute error). In other words, the computation of the inverse matrix is not numerically stable for small eigenvalues, and small errors in the estimation of eigenvalues may yield large error in the solution of the linear system. So if we do not use the correct value for the condition number, we risk using the wrong number of bits for phase estimation, and making large errors in the matrix inversion.

The idea for filter functions is to have a pair of functions f, g that identify the eigenspaces where the inverse is well conditioned, and the eigenspaces where it is not. Intuitively, we pick a threshold value $\approx \kappa$ and essentially decide that we are performing inversion of the matrix only in the eigenspaces corresponding to eigenvalues that are approximately larger than $1/\kappa$, ignoring any smaller ones because they might be affected by too large an error. The advantages are that we no longer need to assume that the spectrum of A is contained in $[\frac{1}{\kappa}, 1]$ (the algorithm is well-defined regardless of this assumption), and that errors in the estimation of small eigenvalues are handled gracefully. The drawback is that the result of the algorithm may not be a solution to the linear system if the eigenvalues do not lie in that interval, as we discuss below — but it is relatively close to a solution if the eigenvalues violate the assumption only by a small amount.

The filter function f that identifies the well-conditioned subspace must satisfy these criteria:

- The value of the filter function must be proportional to $\frac{1}{\lambda}$ for $\lambda \geq \frac{1}{\kappa}$.
- The value of the filter function must be zero for $\lambda \leq \frac{1}{\kappa'}$, where κ' is some appropriately chosen value; say, $\kappa' = 2\kappa$.
- In the interval $[\frac{1}{\kappa'}, \frac{1}{\kappa}]$, the filter function should interpolate between the two cases above.

The other filter function g , identifying the ill-conditioned subspace, must instead satisfy:

- The value of the filter function must be 0 for $\lambda \geq \frac{1}{\kappa}$.
- The value of the filter function must be a constant for $\lambda \leq \frac{1}{\kappa'}$.
- In the interval $[\frac{1}{\kappa'}, \frac{1}{\kappa}]$, the filter function should interpolate between the two cases above.

One can notice that f and g are in some sense complementary. We additionally require that $(f(\lambda))^2 + (g(\lambda))^2 \leq 1$ for all λ , for normalization. An example of filter functions with these characteristics is:

$$f(\lambda) = \begin{cases} \frac{1}{2\kappa\lambda} & \lambda \geq \frac{1}{\kappa} \\ \frac{1}{2} \sin\left(\frac{\pi}{2} \frac{\lambda - \frac{1}{\kappa'}}{\frac{1}{\kappa} - \frac{1}{\kappa'}}\right) & \frac{1}{\kappa} > \lambda > \frac{1}{\kappa'} \\ 0 & \lambda < \frac{1}{\kappa'} \end{cases} \quad g(\lambda) = \begin{cases} 0 & \lambda \geq \frac{1}{\kappa} \\ \frac{1}{2} \cos\left(\frac{\pi}{2} \frac{\lambda - \frac{1}{\kappa'}}{\frac{1}{\kappa} - \frac{1}{\kappa'}}\right) & \frac{1}{\kappa} > \lambda > \frac{1}{\kappa'} \\ \frac{1}{2} & \lambda < \frac{1}{\kappa'} \end{cases}$$

We can apply these functions to compute the reciprocal of the eigenvalues: rather than using a single bit for the final rotation U_{rot} , we instead use a two-bit flag register, and produce the following quantum state after rotation and uncomputation:

$$\sum_{h=0}^{2^n-1} \beta_h \left(|\psi_h\rangle \left(\sqrt{1 - (f(\lambda_h))^2 - (g(\lambda_h))^2} |00\rangle + g(\lambda_h) |01\rangle + f(\lambda_h) |11\rangle \right) \right),$$

where the final two-bit register identifies the following:

- If the last register is in the state $|00\rangle$, inversion did not take place.
- If the last register is in the state $|01\rangle$, we inverted the matrix but we are in the ill-conditioned subspace, where some of the eigenvalues are very small (smaller than $\frac{1}{\kappa}$).

- If the last register is in the state $|11\rangle$, we inverted the matrix and we are in the well-conditioned subspace: this identifies the part of the quantum state where we can find the solution to the linear system, and that gets amplified by amplitude amplification.

Remark 7.5. *The use of filter functions implicitly introduces a dependence on κ , because we need to choose a threshold for the eigenvalue filters. Thus, even if we do not make the assumption that the spectrum of A is contained in $[\frac{1}{\kappa}, 1]$, we still need to choose a value of κ before we run the algorithm, and inversion of A only takes place for eigenvalues $\geq \frac{1}{\kappa}$.*

Solution verification. This approach is applicable when we have a computationally efficient procedure to verify if the correct solution to the linear system has been found. Suppose we have such a procedure, that takes as input the quantum state encoding the (potential) solution of the linear system, and outputs “yes” or “no” to indicate if the linear system has been satisfactorily solved. Then, if we do not know κ , we can start with an estimate $\tilde{\kappa} = 2$, and repeatedly execute a loop where we apply the QLSA setting $\kappa = \tilde{\kappa}$, run the verification procedure, and if the verification procedure outputs “no”, we double the current estimate $\tilde{\kappa}$. Because $\tilde{\kappa}$ increases exponentially fast, it reaches a value that is at most twice the true value of κ in a logarithmic number of iterations, and this is guaranteed to yield the correct solution.

Estimation of κ . The last approach is more involved and requires estimating κ first. This can be done using amplitude estimation (Sect. 4.3), thanks to the fact that the probability of success of the QLSA before amplitude amplification is proportional to $1/\kappa^2$: by estimating this probability with amplitude estimation, we estimate κ . Note that this requires a flag register that indicates what is the subspace whose probability (after measurement) must be estimated, and such register is available in this case: in the exposition of Sect. 7.1.1, it is the last qubit, containing $|1\rangle$ after rotation if the rotation has been successful. The complexity of executing the estimation procedure for κ is a factor $\tilde{\mathcal{O}}(1/\epsilon)$ larger than the complexity of running the QLSA, where ϵ is the precision of the estimation: intuitively, this is consistent with the fact that amplitude estimation has $\mathcal{O}(1/\epsilon)$ scaling. Such a result also holds for the improved QLSA algorithms discussed in Sect. 7.1.5. For details and a precise statement of the time complexity, see [Chakraborty et al., 2019].

7.1.5 Improvements to the running time

Two important improvements over the seminal work of [Harrow et al., 2009] have led to much faster quantum algorithms for linear systems. In this section we give an overview of the corresponding improvements. We also drop the “hidden” assumption that A is positive semidefinite, and allow A to have spectrum in $[-1, -\frac{1}{\kappa}] \cup [\frac{1}{\kappa}, 1]$.

The first improvement concerns the dependence on the precision parameter ϵ . The HHL algorithm relies on phase estimation to perform an eigendecomposition of A , but this has the inherent $\mathcal{O}(1/\epsilon)$ dependence on precision of phase estimation, and it becomes a major bottleneck for the algorithm because the factor $1/\epsilon$ then shows up directly in the running time.

Remark 7.6. *In the HHL algorithm, phase estimation is used to obtain a description of the eigenvalues, which is then used to apply the matrix function $f(x) = 1/x$ to A (i.e., apply the transformation $A = \sum_{h=0}^{2^n-1} \lambda_h |\psi_h\rangle\langle\psi_h| \rightarrow A^{-1} = \sum_{h=0}^{2^n-1} \frac{1}{\lambda_h} |\psi_h\rangle\langle\psi_h|$).*

In principle, if we could apply the matrix function $f(x) = 1/x$ without phase estimation (and therefore without an “explicit” eigendecomposition), then we could get rid of the $\mathcal{O}(1/\epsilon)$ scaling in the running time, because no other step of the algorithm has $\mathcal{O}(1/\epsilon)$ scaling. This idea is explored in [Childs et al., 2017], and subsequently in [Chakraborty et al., 2019, Gilyén et al., 2019b]. There are several algorithmic approaches to implement this idea, although all of them share the goal of approximating the matrix function $f(x) = 1/x$ in some way. One of the approaches proposed in [Childs et al., 2017], and further developed in subsequent work, is to compute a polynomial approximation of the function $1/x$, showing that a sufficiently accurate approximation can be constructed with a low-degree polynomial. Then we can directly implement the matrix function corresponding to the polynomial in place of the function $1/x$.

Remark 7.7. To construct a sufficiently accurate polynomial approximation of $1/x$, so that it can be applied as a transformation of the eigenvalues, it is important to know the domain of x , which in this case represents eigenvalues and therefore the domain is the spectrum of A . We rely on the assumptions that $\|A\| \leq 1$ and an upper bound κ on the condition number is known: this implies that we need to compute a polynomial approximation of $1/x$ only over $[-1, -\frac{1}{\kappa}] \cup [\frac{1}{\kappa}, 1]$, because all eigenvalues lie in this set.

Crucially, the complexity of implementing the desired polynomial (which directly depends on the degree of such polynomial) scales only polylogarithmically in $1/\epsilon$, improving over the $1/\epsilon$ dependence of the HHL algorithm described in the preceding sections. A more general approach is taken in the singular value transformation framework [Gilyén et al., 2019b], directly connected to block-encodings (Sect. 7.2). With singular value transformation we can implement polynomial functions to the singular values of an appropriately block-encoded matrix, and this includes a sufficiently accurate approximation of the function $f(x) = 1/x$.

The second improvement is a reduction of the dependence on κ , from quadratic to linear. To achieve this reduction we note that the κ^2 dependence in the complexity of the HHL algorithm comes from two separate sources: a factor of κ in the cost is incurred because of Hamiltonian simulation with $t = \mathcal{O}(\kappa/\epsilon)$, which appears necessary because we want to estimate the eigenvalues with error $\approx \epsilon/\kappa$ (i.e., λ_h should be affected by error at most $\epsilon\lambda_h$, and the smallest eigenvalue is of order $\approx 1/\kappa$, see Sect. 7.1.2); an additional factor κ is due to the rotation to apply the reciprocal of the eigenvalues, because of the constant C in Eq. (7.1). Indeed, before amplitude amplification the rotation is successful only with probability κ^2 : we want the last qubit on the r.h.s. of Eq. (7.1) to be $|1\rangle$ after measurement, and to boost the probability of this event to almost 1 we need $\mathcal{O}(\kappa)$ rounds of amplitude amplification. However, the worst case for these two parts of the HHL algorithm occurs in opposite situations. Suppose all the eigenvalues are small, $\lambda_h \approx 1/\kappa$: in this case estimating the eigenvalues is difficult and forces us to perform Hamiltonian simulation with $t = \mathcal{O}(\kappa/\epsilon)$, but amplitude amplification is easy, because the factor $\frac{C}{\lambda_h}$ in Eq. (7.1) is a constant (recall $C = \mathcal{O}(1/\kappa)$) so the rotation is successful with large probability. On the other hand, suppose all the eigenvalues are large, $\lambda_h \approx 1$: to estimate the eigenvalues to precision $\epsilon\lambda_h \approx \epsilon$, it would be enough to perform Hamiltonian simulation with $t = \mathcal{O}(1/\epsilon)$, but amplitude amplification requires more iterations because the factor $\frac{C}{\lambda_h}$ in Eq. (7.1) is $\mathcal{O}(1/\kappa)$. Thus, depending on λ_h , one of the steps, among eigenvalue estimation and amplification of the success probability of the rotation, is not time-consuming. The pessimistic factor κ^2 factor in the running time of HHL takes the worst case for both steps, but these worst case scenarios do not simultaneously apply to the same eigenvalue. Unfortunately, standard amplitude amplification is applied onto the entire eigenvalue estimation circuit, therefore we have to pay the cost for both accurate eigenvalue estimation, and for amplification of the large eigenvalues.

We can improve the running time with a technique known as *variable-time amplitude amplification*. We divide the eigenvalue computation into several steps. In each step we use a different value of the length t of the time horizon for the corresponding Hamiltonian simulation. We start with a short constant time, and attempt to estimate the eigenvalues. Based on t , some eigenvalues may be estimated correctly, while others may not. We use a subroutine to try to assess which ones are correct: those are no longer modified. After that we double the length of the time horizon, and repeat the procedure. The amplitude estimation part is applied differently to the different values of t . The details of this procedure are quite involved, and we do not treat them in detail. Normally, if an algorithm has success probability p , amplitude amplification would perform $1/\sqrt{p}$ iterations; thus, normally we would execute the algorithm $1/\sqrt{p}$ times for its maximum value of t . Instead, with variable-time amplitude amplification we can reduce this to $1/\sqrt{p}$ multiplied by the *average* value of t . For a detailed description of variable-time amplitude amplification we refer to [Ambainis, 2010], see also [Childs et al., 2017, Chakraborty et al., 2019] for further discussion in the context of QLSAs.

7.1.6 Extracting the solution and iterative refinement

The running time $\tilde{\mathcal{O}}(\kappa(T_b + \frac{\kappa}{\epsilon} sT_A))$ indicated in Sect. 7.1.2 refers to a QLSA in its native form: the algorithm outputs a quantum state that is close to the amplitude encoding of the solution of the linear system. (As noted in Sect.s 7.1.5 and 7.3, much faster versions of the algorithm have been developed; at the time of this writing, the fastest known QLSA runs in $\mathcal{O}(\max\{T_A, T_b\}\kappa \log 1/\epsilon)$ time.) In some applications, one may want to get a classical description of the solution to the linear system. Such a description can be obtained with a straightforward application of a quantum state tomography algorithm. For the general setting considered here, the most computationally-efficient tomography algorithm (in terms of number of calls to a unitary preparing the state of interest) is precisely the one described in Thm. 5.17; more efficient algorithms might be possible if we know some properties of the solution to the linear system. Unfortunately Thm. 5.17 introduces linear scaling in $1/\epsilon$: this means that obtaining an accurate classical description of the solution vector (e.g., $\epsilon = 10^{-10}$) would be prohibitively expensive. Thus, even if state-of-the-art QLSAs have polylogarithmic scaling in $1/\epsilon$, extracting the solution with quantum state tomography loses such favorable scaling. This fundamental issue can sometimes be circumvented with a technique known in the classical literature as *iterative refinement* [Wilkinson, 1963]. This technique has proven to be useful for the design of classical and quantum optimization algorithms, see the notes in Sect. 7.3. We describe here the main idea.

Suppose we have a linear system:

$$Ax = b. \tag{7.3}$$

Let us use x to denote the vector of unknowns, and \hat{x} to denote a candidate solution with precision δ , i.e., $\|b - A\hat{x}\| \leq \delta$. Consider the linear system obtained by subtracting $A\hat{x}$ from both sides of the equation: we obtain $A(x - \hat{x}) = b - A\hat{x}$ (the vector $b - A\hat{x}$ is often called the vector of *residuals*). Define the linear system:

$$Ay = \frac{1}{\delta}(b - A\hat{x}). \tag{7.4}$$

Suppose we solve Eq. (7.4) to precision δ , i.e., we obtain \hat{y} such that $\|\frac{1}{\delta}(b - A\hat{x}) - A\hat{y}\| \leq \delta$. Now consider $\hat{x} + \delta\hat{y}$. This vector satisfies the following:

$$\|b - A(\hat{x} + \delta\hat{y})\| = \delta \left\| \frac{1}{\delta}(b - A\hat{x}) - A\hat{y} \right\| \leq \delta^2.$$

Therefore, $\hat{x} + \delta\hat{y}$ is a δ^2 -precise solution to the linear system in Eq. (7.3), and we obtained it by solving two linear systems each with precision δ . The idea can be iterated, so that with k solves we obtain a solution with precision δ^k . We can pick any constant δ , and if we aim to obtain a solution with final precision ϵ , we can achieve this goal with $k = \mathcal{O}(\log \frac{1}{\epsilon})$ iterations, see Prop. 7.9.

Example 7.8. *Suppose we have the linear system:*

$$\begin{aligned} x_1 + x_2 &= 3 \\ 3x_1 + x_2 &= 6, \end{aligned}$$

and we use a solver for this problem that guarantees precision $\delta = 1/\sqrt{2}$. In particular, we obtain the solution $\hat{x}_1 = 1.5, \hat{x}_2 = 2$, which has residuals $(-0.5, -0.5)$. To find an adjustment to the current solution, we solve the problem:

$$\begin{aligned} y_1 + y_2 &= -\frac{1}{\sqrt{2}} \\ 3y_1 + y_2 &= -\frac{1}{\sqrt{2}}, \end{aligned}$$

again with precision $\delta = 1/\sqrt{2}$. For example, we obtain the solution $\hat{y}_1 = 0, \hat{y}_2 = -\frac{5}{4\sqrt{2}}$, with residuals $(\frac{1}{4\sqrt{2}}, \frac{1}{4\sqrt{2}})$. The vector:

$$\hat{x} + \delta\hat{y} = \begin{pmatrix} 1.5 \\ 2 \end{pmatrix} + \frac{1}{\sqrt{2}} \begin{pmatrix} 0 \\ -\frac{5}{4\sqrt{2}} \end{pmatrix} = \begin{pmatrix} 1.5 \\ 1.375 \end{pmatrix}$$

is now a solution with precision $\frac{1}{8} \leq \delta^2$, obtained with the solution of two linear systems each with precision $\delta = 1/\sqrt{2}$ (in general we can only guarantee precision δ^2 after two iterations).

We can apply the same scheme using a QLSA to solve the linear system at each iteration, followed by state tomography to extract a classical description of the solution. We use the classical description to keep track of the updated candidate solution $x^{(k)}$ at iteration k , and to compute its residual vector $b - Ax^{(k)}$ exactly (in fact, we could get away with computing the residual with some error, but it complicates the analysis slightly, so we do not discuss this case). The scheme of the algorithm is described in Alg. 5. We show below that the number of iterations performed

Algorithm 5: Iterative refinement for linear systems.

Input: Matrix A , r.h.s. b with $\|b\| = 1$, target precision ϵ , per-iteration precision δ with $0 < \epsilon < \delta < 1$.

Output: Vector x^* satisfying $\|Ax^* - b\| \leq \epsilon$.

1 **Initialize:** Set $x^{(0)} \leftarrow 0, r^{(0)} \leftarrow b, k \leftarrow 1$.

2 **while** $\|r^{(k-1)}\| > \epsilon$ **do**

3 Solve the system $Ax = \frac{1}{\|r^{(k-1)}\|} r^{(k-1)}$ and obtain solution $\hat{x}^{(k)}$ satisfying:

$$\left\| A\hat{x}^{(k)} - \frac{1}{\|r^{(k-1)}\|} r^{(k-1)} \right\| \leq \delta.$$

4 Update candidate solution: $x^{(k)} \leftarrow x^{(k-1)} + \|r^{(k-1)}\| \hat{x}^{(k)}$.

5 Update residual vector: $r^{(k)} \leftarrow b - Ax^{(k)}$.

6 Let $k \leftarrow k + 1$.

7 **end**

8 **return** $x^{(k-1)}$.

by the algorithm is polylogarithmically small.

Proposition 7.9. *The iterative refinement scheme for linear systems (Alg. 5), using constant per-iteration precision parameter δ , returns a solution x^* satisfying $\|Ax^* - b\| \leq \epsilon$ in $\mathcal{O}(\log \frac{1}{\epsilon})$ iterations.*

Proof. We show by induction that at iteration k with $k \geq 1$, we have $\|r^{(k)}\| \leq \delta^k$ (which implies $\|Ax^{(k)} - b\| \leq \delta^k$). For the base step, we know that $\|r^{(1)}\| = \|b - Ax^{(1)}\| \leq \delta$ because this is the first solution that we obtain on line 3 (recall that $\|b\| = 1$ by assumption, so on line 4 we set $x^{(1)} \leftarrow \hat{x}^{(1)}$). Then we have:

$$\begin{aligned} \|r^{(k+1)}\| &= \|Ax^{(k+1)} - b\| = \|A(x^{(k)} + \|r^{(k)}\| \hat{x}^{(k+1)}) - b\| = \|r^{(k)}\| \left\| \frac{1}{\|r^{(k)}\|} (Ax^{(k)} - b) + A\hat{x}^{(k+1)} \right\| \\ &= \|r^{(k)}\| \left\| A\hat{x}^{(k+1)} - \frac{1}{\|r^{(k)}\|} r^{(k)} \right\| \leq \delta^k \cdot \delta, \end{aligned}$$

where for the final inequality, we used $\|r^{(k)}\| \leq \delta^k$ (induction hypothesis) and $\left\| A\hat{x}^{(k+1)} - \frac{1}{\|r^{(k)}\|} r^{(k)} \right\| \leq \delta$ (by definition of $\hat{x}^{(k+1)}$ on line 3 of Alg. 5). This concludes the proof of the inductive claim. Then, to obtain final precision ϵ , i.e., $\|r^{(k)}\| \leq \epsilon$, it is sufficient to run the algorithm for $k = \lceil \log_\delta \epsilon \rceil = \mathcal{O}(\log \frac{1}{\epsilon})$ iterations. \square

Prop. 7.9 only discusses the number of iterations, not the total running time of Alg. 5. To carefully analyze the running time we would have to determine the exact cost of line 3; this involves committing to a specific QLSA, to a specific tomography algorithm, and determining their complexity

when performed with sufficient precision. Note that the complexity of state tomography (using, e.g., Cor. 5.18) scales linearly with the required inverse precision, but a precision of δ alone may not be enough to guarantee that the condition on line 3 of Alg. 5 is satisfied: other numerical parameters (such as the norm of possible solutions) may also intervene in the final expression, depending on the normalization of the problem and the guarantee provided by the QLSA. Because we do not use Alg. 5 again in the rest of this set of lecture notes, we do not pursue a detailed analysis. The interested reader can find one in [Mohammadisiahroudi, 2024].

7.2 Block-encodings

We now provide an introduction to the *block-encoding* framework, highlighting several results concerning basic operations on block-encodings, and the corresponding computational complexity. Throughout, although we skip some proofs, we try to provide intuition on why these results hold. The framework of block-encoded operators encompasses several other input models for matrices, and it is generally efficient for many forms of matrix manipulation, including Hamiltonian simulation. Results in this section are adapted from [Chakraborty et al., 2019, Gilyén, 2019, van Apeldoorn et al., 2020b, van Apeldoorn, 2020].

Let us formally define a block-encoding.

Definition 7.10 (Block-encoding). *Let $A \in \mathbb{C}^{2^q \times 2^q}$ be a q -qubit operator. Then, a $(q + a)$ -qubit unitary U is an (α, a, ξ) -block-encoding of A if $U = \begin{pmatrix} \tilde{A} & \cdot \\ \cdot & \cdot \end{pmatrix}$, where \cdot represent arbitrary entries of the matrix, with the property that*

$$\|\alpha \tilde{A} - A\| \leq \xi.$$

By definition, U is a block-encoding of A if U acts as a scaled-down version of A on some part of the vector space in which quantum states live. In particular, we can rephrase the main property in the definition as follows.

Definition 7.11 (Block-encoding (alternative-definition)). *Let $A \in \mathbb{C}^{2^q \times 2^q}$ be a q -qubit operator. Then, a $(q + a)$ -qubit unitary U is an (α, a, ξ) -block-encoding of A if*

$$\|\alpha(\tilde{0}|_a \otimes I^{\otimes q})U(\tilde{0}|_a \otimes I^{\otimes q}) - A\| \leq \xi.$$

Each block-encoding has three parameters: the subnormalization factor α , the number of auxiliary qubits a , and the error of the block-encoding ξ . It is important to keep track of these parameters when manipulating block-encodings. However, one can often simplify the exposition by reporting only the subnormalization factor, as long as the number of auxiliary qubits and error ξ scale at most polylogarithmically with all the relevant parameters of a problem instance. We try to be formal as much as possible, and keep track of the three parameters of the block-encodings; however, sometimes writing the exact expression for some of the parameters is cumbersome, and in those cases we resort to $\mathcal{O}(\cdot)$ notation to indicate only the relevant asymptotic scaling.

Def.s 7.10 and 7.11 imply that if we limit ourselves to the subspace where the first a qubits are $|0\rangle$, U implements the desired operation A , which may not be unitary and in fact does not even need to be square, because we could pad some rows or columns of A with zeroes. The price to pay for this flexibility is that we may need to scale down A , because clearly not every matrix can be embedded into a unitary without scaling, and we may need to do some work to “select” the part of the space of quantum states on which the block-encoding acts as A .

Remark 7.12. *It is important to note that the structure of a block-encoding U of A does not guarantee that it takes states of the form $|\tilde{0}\rangle|\psi\rangle$ to $|\tilde{0}\rangle\frac{A}{\alpha}|\psi\rangle$. In fact, $U|\tilde{0}\rangle|\psi\rangle$ (i.e., the image of $|\tilde{0}\rangle|\psi\rangle$ via the block-encoding) generally has nonzero support on states that do not start with $|\tilde{0}\rangle$. Thus, when we say that U acts as A “if we limit ourselves to the subspace where the first a qubits are $|0\rangle$,” not only do we need to start in some state $|\tilde{0}\rangle|\psi\rangle$, but also we have to postselect or amplify the “correct” output subspace, to ensure that the first qubits are $|\tilde{0}\rangle$.*

Example 7.13. Let $A = \begin{pmatrix} 2 & 0 \\ 0 & 0 \end{pmatrix}$. This matrix is clearly not unitary, hence there is no circuit that acts as A . The following unitary matrix U is a $(2, 1, 0)$ -block-encoding of A :

$$\begin{pmatrix} 1 & 0 & 0 & 0 \\ 0 & 0 & 1 & 0 \\ 0 & 1 & 0 & 0 \\ 0 & 0 & 0 & 1 \end{pmatrix},$$

because:

$$\alpha(\langle 0| \otimes I)U(|0\rangle \otimes I) = 2 \left((1 \ 0) \otimes \begin{pmatrix} 1 & 0 \\ 0 & 1 \end{pmatrix} \right) \begin{pmatrix} 1 & 0 & 0 & 0 \\ 0 & 0 & 1 & 0 \\ 0 & 1 & 0 & 0 \\ 0 & 0 & 0 & 1 \end{pmatrix} \left(\begin{pmatrix} 1 \\ 0 \end{pmatrix} \otimes \begin{pmatrix} 1 & 0 \\ 0 & 1 \end{pmatrix} \right) = A.$$

Note that A is a single-qubit operator, whereas U is a two-qubit operator, and we have to scale A down by a factor 2. Readers may correctly recognize that U is a SWAP gate.

Suppose we want to obtain a representation of $A|\psi\rangle$, where $|\psi\rangle = \beta|0\rangle + \gamma|1\rangle$; note that $A|\psi\rangle$ may not even be a valid quantum state. In the block-encoding framework we can obtain (some representation of) $A|\psi\rangle$ by applying U onto the state $|0\rangle|\psi\rangle$: the first qubit must be $|0\rangle$ to be in the right subspace. We have:

$$U|0\rangle|\psi\rangle = \begin{pmatrix} \beta \\ 0 \\ \gamma \\ 0 \end{pmatrix},$$

and if we look at the restriction of this state onto the basis states beginning with $|0\rangle$ (i.e., we apply $\langle 0| \otimes I$), we obtain $\beta|0\rangle$, which is precisely $\frac{A}{2}|\psi\rangle$: note once again the scaling factor 2 picked up when applying the block-encoding.

Intuitively, because we chose U to be a SWAP gate, we can see how this approach works: we apply a SWAP gate to a state of the form $|0\rangle|\psi\rangle$, so we are “zeroing out” the amplitude of $|\psi\rangle$ that corresponds to $|1\rangle$ ($|01\rangle$ in the two-qubit state). Of course this amplitude does not disappear: it simply gets “moved” to the part of the two-qubit state that has $|1\rangle$ in its first digit, i.e., to $|10\rangle$.

7.2.1 Operations on block-encodings

We now discuss several useful operations on block-encodings, starting with the product of two block-encoded matrices, which is trivial to construct.

Proposition 7.14. If U_A is an (α, a, ξ_A) -block-encoding of a q -qubit operator A , and U_B is an (β, b, ξ_B) -block-encoding of an q -qubit operator B , then $(I_b \otimes U_A)(I_a \otimes U_B)$ is an $(\alpha\beta, a + b, \alpha\xi_B + \beta\xi_A)$ -block-encoding of AB .

The proof of this result follows easily from the definition of block-encoding.

Remark 7.15. In the above proposition and in subsequent results regarding block-encodings, we abuse the tensor product notation to avoid overly complicated expressions. The expression $(I_b \otimes U_A)$ should be interpreted as “identity on the b auxiliary qubits for U_B , and U_A on all the qubits affected by U_A ,” and similarly, $(I_a \otimes U_B)$ means “identity on the a auxiliary qubits for U_A , and U_B on all the qubits affected by U_B .” Writing this accurately in tensor product notation is cumbersome: e.g., if we have three registers $|\cdot\rangle_a|\cdot\rangle_b|\cdot\rangle_q$, how do we express the matrix acting as $(I_b \otimes U_A)$ described above? It would have to act as the matrix U_A on the first and third register with a and q qubits respectively, but we have not defined a matrix that does so while tensored with identity on the second register. Hence, we use an imprecise, but considerably simpler notation, whose meaning is usually clear from the context; see also Fig. 7.3 and the surrounding discussion. Note that I_b here is a $2^b \times 2^b$ identity matrix, which we usually denote $I^{\otimes b}$: we use the subscript precisely because the meaning is different with this “improper” — but considerably simpler — tensor product

notation, where the subscript also indicates to which register the matrix should be applied. For block-encodings, sometimes we use this improper notation even when our usual notation would be sufficient.

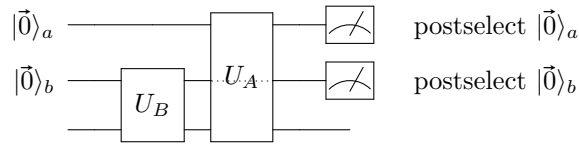


Figure 7.3: Block-encoding for the product of two matrices AB , given block-encodings of A and B . Note the dashed line through U_A : U_A does not get applied to the second register.

In circuit form, the block-encoding of AB can be implemented as depicted in Fig. 7.3. The dashed line through U_A is used to indicate that the second register (of dimension b) does not interact with U_A , which only acts on the first and third register. “Postselect $|\vec{0}\rangle$ ” indicates that the product AB is successfully applied onto the third register if the first two registers are measured and we observe $|\vec{0}\rangle$; one can of course applied amplitude amplification to amplify the probability that $|\vec{0}\rangle$ is observed in the two registers.

In addition to the product of block-encodings, linear combinations of block-encodings can also be constructed in a relatively simple manner, and the cost for doing so is merely logarithmic in the dimension: the construction is very similar to the one presented in Sect. 6.2.3. We first define a *state-preparation pair*, which encodes the coefficients to be used in the linear combination of block-encodings, then give the complexity of constructing the linear combination. A state-preparation pair is simply a pair of unitaries P_L, P_R such that the inner product of $P_L|\vec{0}\rangle$ and of $P_R|\vec{0}\rangle$ yields a vector with the desired coefficients (or something close to it). This specific form is useful for the construction of linear combinations, as shown after a formal definition and an example. In the definition below, for convenience we use zero-based indices for the vector y .

Definition 7.16 (State-preparation pair). *Let $y \in \mathbb{C}^m$ and $\|y\|_1 \leq \beta$. The pair of unitaries (P_L, P_R) is called a (β, q, ξ) -state-preparation-pair for y if $P_L|\vec{0}\rangle_q = \sum_{\vec{j} \in \{0,1\}^q} c_j |\vec{j}\rangle$ and $P_R|\vec{0}\rangle_q = \sum_{\vec{j} \in \{0,1\}^q} d_j |\vec{j}\rangle$, where the coefficients c_j, d_j satisfy the following properties: $\sum_{j=0}^{m-1} |\beta(c_j^\dagger d_j) - y_j| \leq \xi$, and $c_j^\dagger d_j = 0$ for all $j \in m, \dots, 2^q - 1$.*

Example 7.17. *Just as in Sect. 6.2.3, if we aim to construct a linear combination with nonnegative real coefficients $\alpha_0, \dots, \alpha_{m-1}$, we can define a $\lceil \log m \rceil$ -qubit unitary W such that*

$$W|\vec{0}\rangle = \frac{1}{\|\alpha\|_1} \sum_{\vec{j} \in \{0,1\}^{\lceil \log m \rceil}} \sqrt{\alpha_j} |\vec{j}\rangle.$$

Then, setting $P_L = W, P_R = W$, we see that this is a $(\|\alpha\|_1, \lceil \log m \rceil, 0)$ -state-preparation-pair for the vector of coefficients α . If $\alpha \not\geq 0$, we can adjust the signs by modifying at least one of the unitaries P_L, P_R .

Using a state-preparation pair, we can construct a linear combination of unitaries with coefficients prescribed by the state-preparation pair. To do so, we also need a controlled unitary that prepares the (unweighted) unitaries appearing in the linear combination, i.e., if we want to construct a combination of m block-encodings, we need a circuit that, given the binary string \vec{j} , implements the j -th block-encoding of the linear combination. This is once again similar to the approach discussed in Sect. 6.2.3. The circuit that applies the j -th block-encoding, controlled on some register containing $|\vec{j}\rangle$, is labeled V in the next proposition; its formal definition is somewhat convoluted because we need to specify that its action is the identity if the control register contains an index $\geq m$, but its behavior should be intuitively clear.

Proposition 7.18. *Let $A = \sum_{j=0}^{m-1} y_j A^{(j)}$ be a q -qubit operator expressed as a linear combination of matrices $A^{(j)}$ with coefficients y_j . Suppose we are given a (β, p, ξ_1) -state-preparation pair P_L, P_R*

for y , and a $(q + a + p)$ -qubit unitary:

$$V := \sum_{\substack{\vec{j} \in \{0,1\}^p \\ j \leq m-1}} |\vec{j}\rangle\langle\vec{j}| \otimes U^{(j)} + \left(I_p - \sum_{\substack{\vec{j} \in \{0,1\}^p \\ j \leq m-1}} |\vec{j}\rangle\langle\vec{j}| \right) \otimes I_a \otimes I_q,$$

with the property that $U^{(j)}$ is an (α, a, ξ_2) -block-encoding of $A^{(j)}$. Then we can implement an $(\alpha\beta, a + p, \alpha\xi_1 + \alpha\beta\xi_2)$ -block-encoding of A with a single use of V, P_R and P_L^\dagger .

Proof. The desired block-encoding is given by $(P_L^\dagger \otimes I_{q+a})V(P_R \otimes I_{q+a})$. To verify this, using the same notation as in Def. 7.16, we apply the definition of block-encoding and compute:

$$\begin{aligned} & (\langle \vec{0} |_{a+p} \otimes I_q) (P_L^\dagger \otimes I_{q+a}) V (P_R \otimes I_{q+a}) (|\vec{0}\rangle_{a+p} \otimes I_q) \\ &= \left(\sum_{\vec{j} \in \{0,1\}^p} c_j^\dagger |\vec{j}\rangle \otimes \langle \vec{0} |_a \otimes I_q \right) V \left(\sum_{\vec{j} \in \{0,1\}^p} d_j |\vec{j}\rangle \otimes |\vec{0}\rangle_a \otimes I_q \right) \\ &= \left(\sum_{\vec{j} \in \{0,1\}^p} c_j^\dagger |\vec{j}\rangle \otimes \langle \vec{0} |_a \otimes I_q \right) \left(\sum_{\substack{\vec{j} \in \{0,1\}^p \\ j \leq m-1}} d_j |\vec{j}\rangle \otimes U^{(j)} (|\vec{0}\rangle_a \otimes I_q) + \sum_{\substack{\vec{j} \in \{0,1\}^p \\ j \geq m}} d_j |\vec{j}\rangle \otimes |\vec{0}\rangle_a \otimes I_q \right) \\ &= \sum_{j=0}^{m-1} c_j^\dagger d_j \tilde{A}^{(j)}, \end{aligned}$$

where $\tilde{A}^{(j)}$ is such that $\|\alpha \tilde{A}^{(j)} - A^{(j)}\| \leq \xi_2$. For the last equality, we used the fact that the terms in the summation with $j \geq m$ disappear because of the definition of state-preparation pair (Def. 7.16), and the fact that $U^{(j)}$ is an (α, a, ξ_2) -block-encoding of $A^{(j)}$. Because we also have $\|\beta(c_j^\dagger d_j) - y_j\| \leq \xi_1$ by Def. 7.16, simple calculations show that this is indeed a $(\alpha\beta, a + p, \alpha\xi_1 + \alpha\beta\xi_2)$ -block-encoding of $A = \sum_{j=0}^{m-1} y_j A^{(j)}$. \square

At this point, we have shown how to perform products of block-encodings and linear combinations of block-encodings: this means that we can implement polynomial functions of block-encoded matrices. We can therefore implement polynomial approximations of matrix functions, which allows us to manipulate the block-encoded input matrix in a plethora of ways. For example, we can perform Hamiltonian simulation, as discussed in Sect. 6.2.5, and the corresponding complexity essentially matches the fastest known Hamiltonian simulation algorithms — for certain input models better results might be obtained without going through block-encodings, but the difference is typically small. A more precise statement of the complexity is the following.

Theorem 7.19 (Hamiltonian simulation via block-encodings). *Suppose that U is an $(\alpha, a, \xi/|2t|)$ -block-encoding of the Hamiltonian \mathcal{H} . Then, we can implement a ξ -precise Hamiltonian simulation unitary V , i.e., an $(1, a + 2, \xi)$ -block-encoding of $e^{it\mathcal{H}}$, with $\mathcal{O}(\alpha|t| + \log(1/\xi))$ uses of controlled- U and its inverse, and $\mathcal{O}(a(\alpha|t| + \log(1/\xi)))$ two-qubit gates.*

To perform Hamiltonian simulation we apply the function e^{ix} to the eigenvalues of \mathcal{H} , by adding together (via linear combination of block-encodings) an approximation of $\cos x$ and an approximation of $i \sin x$. A full proof of this result can be found in [Gilyén et al., 2019b], together with a discussion of the complexity of other matrix functions, such as the inverse (i.e., the computation of a block-encoding of A^{-1}); the complexity essentially depends on the degree of the polynomial that is necessary to obtain a sufficiently accurate approximation, and the polynomial is implemented as discussed above, using products and linear combinations of block-encodings.

We can also construct the block-encoding of a diagonal matrix that contains inner products of different quantum states on the diagonal. We show this construction because it can serve as an inspiration for other, similar building blocks. The construction involves unitaries that prepare the quantum states of which we want the inner products; in the statement of the lemma, we call these state-preparation unitaries to emphasize their role.

Lemma 7.20. *Let the matrices $U^{(j)}, V^{(j)}$ be $(a+1)$ -qubit state-preparation unitaries for some a -qubit quantum states $|\psi_j\rangle, |\phi_j\rangle, |\tilde{\psi}_j\rangle, |\tilde{\phi}_j\rangle$, i.e., matrices that implement the following maps:*

$$\begin{aligned} U^{(j)}|0\rangle|\vec{0}\rangle_a &= |0\rangle|\psi_j\rangle + |1\rangle|\tilde{\psi}_j\rangle \\ V^{(j)}|0\rangle|\vec{0}\rangle_a &= |0\rangle|\phi_j\rangle + |1\rangle|\tilde{\phi}_j\rangle, \end{aligned}$$

where the states $|\tilde{\psi}_j\rangle, |\tilde{\phi}_j\rangle$ are garbage states that we are not interested in. Let $U := \sum_{\vec{j} \in \{0,1\}^p} U^{(j)} \otimes |\vec{j}\rangle\langle\vec{j}|$ and $V := \sum_{\vec{j} \in \{0,1\}^p} V^{(j)} \otimes |\vec{j}\rangle\langle\vec{j}|$ be $(a+p+1)$ -qubit unitaries controlled by the second register. Then the unitary:

$$(I \otimes V^\dagger)(\text{SWAP} \otimes I_{a+p})(I \otimes U)$$

is an $(a+2)$ -block-encoding of the diagonal matrix $\text{diag}(\{\langle\phi_j|\psi_j\rangle\}_{j=0,\dots,2^p-1})$, where the single-qubit identity matrix I acts on the first qubit, the SWAP gate acts on the first two qubits, and the $(a+p)$ -qubit identity I_{a+p} acts on the last $a+p$ qubits.

Proof. We apply the definition of block-encoding.

$$\begin{aligned} &\langle\vec{0}\rangle_{a+2}\langle\vec{j}\rangle_p(I \otimes V^\dagger)(\text{SWAP} \otimes I_{a+p})(I \otimes U)|\vec{0}\rangle_{a+2}|\vec{k}\rangle_p \\ &= \langle 0 | \left(\langle 0 | \langle \phi_j | + \langle 1 | \langle \tilde{\phi}_j | \right) \langle \vec{j} | (\text{SWAP} \otimes I_{a+p}) | 0 \rangle \left(| 0 \rangle |\psi_k\rangle + | 1 \rangle |\tilde{\psi}_k\rangle \right) |\vec{k}\rangle \\ &= \left(\langle 00 | \langle \phi_j | + \langle 01 | \langle \tilde{\phi}_j | \right) \langle \vec{j} | (\text{SWAP} \otimes I_{a+p}) \left(| 00 \rangle |\psi_k\rangle + | 01 \rangle |\tilde{\psi}_k\rangle \right) |\vec{k}\rangle \\ &= \left(\langle 00 | \langle \phi_j | + \langle 01 | \langle \tilde{\phi}_j | \right) \langle \vec{j} | \left(| 00 \rangle |\psi_k\rangle + | 10 \rangle |\tilde{\psi}_k\rangle \right) |\vec{k}\rangle. \end{aligned}$$

This last expression is equal to $\langle\phi_j|\psi_k\rangle$ if $\vec{j} = \vec{k}$, and it is 0 otherwise. This concludes the proof. \square

For example, we can recast the gradient-based quantum state tomography algorithm of Ch. 5 in the block-encoding framework: recall that we want to obtain a phase oracle for the function $f(x)$ defined in Eq. (5.3), which is an inner product of quantum states. Given the structure of $f(x)$, we can apply Lem. 7.20 to obtain a block-encoding of a diagonal matrix containing $f(x)$ on the diagonal for all x , then use Hamiltonian simulation of the block-encoded matrix to transform them into phase factors of the form $e^{if(x)}$, thereby obtaining an implementation of the phase oracle.

7.2.2 Block-encoding from sparse matrices

The sparse-oracle access model discussed in Sect. 6.2.4 is a natural model (even in the classical world) to describe arbitrary sparse matrices. We now discuss how to implement a block-encoding of a matrix that is described in this model; in some cases, this is the first step of a quantum algorithm that uses the block-encoding framework to work on matrices, allowing us to convert a classical description of the matrix into a suitable representation on the quantum computer. The block-encoding framework therefore encompasses the sparse-oracle access model, in the sense that sparse-access oracles can be turned into a block-encoding. This conversion is computationally quite efficient, although there can be cases where working with the sparse model directly leads to computational savings, as is often the case when simulating an access model with a different one: this must be analyzed on a case-by-case basis.

A precise presentation of how to construct a block-encoding from a sparse-access oracle requires care about several details. The data of the matrix to be block-encoded is described in the usual way: we have quantum oracles (i.e., quantum circuits, so that they can be queried in superposition) that list the position of the nonzero elements of the matrix in each row/column, and an oracle that provides the corresponding values. To create certain superpositions that are crucial for the construction we need to know upper bounds on the number of nonzero elements in each row and column: we denote these upper bounds by s_r, s_c respectively. We also need a way of indicating if some rows/columns have fewer nonzero entries than the maximum allowed number s_r, s_c , because we want to construct a superposition over the indices of all the nonzero entries: such a superposition always has s_r or s_c terms, and we need a way to “mark” terms that do not

actually correspond to a nonzero entry. We do so by using some indices larger than the size of the matrix, which eventually result in some inner product being zero (see the construction in the proof), thereby correctly producing a zero in the corresponding position.

In this and subsequent sections we ignore issues related to the precision of the representation of each entry of the matrix: we simply assume that the number of bits of each register is large enough to perform sufficiently accurate calculations. This is no different from how similar operations are performed on a classical computer, and the number of (qu)bits that is sufficient to obtain a certain level of precision scales polylogarithmically with the reciprocal of the allowed error. We also assume that all entries are complex numbers with modulus at most 1, because otherwise a certain rotation in the construction is not well defined; of course, to block-encode a matrix that has entries with larger modulus, one can always rescale the entries and adjust the subnormalization factor of the final block-encoding.

Proposition 7.21. *Let $A \in \mathbb{C}^{2^q \times 2^q}$ be a matrix that has at most s_r nonzero elements per row, and at most s_c nonzero elements per column, with each element a_{ij} satisfying $|a_{ij}| \leq 1$. Suppose that we have access to the following sparse-access oracles acting on two $(q+1)$ -qubit registers:*

$$\begin{aligned} O_r &: |\vec{i}\rangle|\vec{k}\rangle \rightarrow |\vec{i}\rangle|\vec{r}_{ik}\rangle \quad \forall i = 0, \dots, 2^q - 1, k = 0, \dots, s_r - 1, \\ O_c &: |\vec{\ell}\rangle|\vec{j}\rangle \rightarrow |\vec{c}_{\ell j}\rangle|\vec{j}\rangle \quad \forall \ell = 0, \dots, s_c - 1, j = 0, \dots, 2^q - 1, \end{aligned}$$

where r_{ik} is the index of the k -th nonzero entry of the i -th row of A , or if there are less than k nonzero entries, then it is $k + 2^q$, and similarly, $c_{\ell j}$ is the index of the ℓ -th nonzero entry of the j -th column of A , or if there are less than ℓ nonzero entries, then it is $\ell + 2^q$. Additionally, assume that we have access to an oracle O_A that returns a binary description of the entries of A :

$$O_A : |\vec{i}\rangle|\vec{j}\rangle|\vec{0}\rangle_p \rightarrow |\vec{i}\rangle|\vec{j}\rangle|\vec{a}_{ij}\rangle, \quad \forall i, j = 0, \dots, 2^q - 1,$$

where \vec{a}_{ij} is a p -digit binary description of the matrix element (i, j) of A . Then, we can implement a $(\sqrt{s_r s_c}, q + 3, \xi)$ -block-encoding of A with a single use of $O_r, O_c, O_A, O_A^\dagger$, additionally using $\tilde{\mathcal{O}}(q)$ one and two-qubit gates, and $\tilde{\mathcal{O}}(p)$ auxiliary qubits.

Proof. The proof is constructive and adapted from [Gilyén et al., 2019b]. See Rem. 7.24 for remarks about the construction of the oracles O_r, O_c .

We work with three registers (plus some auxiliary space, introduced when necessary): a single-qubit register, and two $(q+1)$ -qubit registers. All indices are zero-based, as usual. Define $(q+1)$ -qubit operators W_r, W_c satisfying the following:

$$W_r|\vec{0}\rangle = \frac{1}{\sqrt{s_r}} \sum_{\substack{\vec{k} \in \{0,1\}^{q+1} \\ k \leq s_r - 1}} |\vec{k}\rangle, \quad W_c|\vec{0}\rangle = \frac{1}{\sqrt{s_c}} \sum_{\substack{\vec{\ell} \in \{0,1\}^{q+1} \\ \ell \leq s_c - 1}} |\vec{\ell}\rangle.$$

These operators construct uniform superpositions and can be implemented with $\mathcal{O}(q)$ gates, because we can always assume that s_r, s_c are powers of 2 (padding the list of nonzero entries with zeroes, if necessary) and use an appropriate number of Hadamard gates. Let SWAP_{q+1} be the operator that swaps the first $(q+1)$ -qubit register with the second $(q+1)$ -qubit register (i.e., by applying a SWAP gate to $q+1$ pairs of qubits). Define the following $2(q+1)$ -qubit operators:

$$V_L := O_r(I_{q+1} \otimes W_r)\text{SWAP}_{q+1}, \quad V_R := O_c(W_c \otimes I_{q+1}),$$

and note that their action is the following:

$$\begin{aligned} V_L|\vec{0}\rangle_{q+2}|\vec{i}\rangle_q &= \sum_{k=0}^{s_r-1} \frac{1}{\sqrt{s_r}} |\vec{i}\rangle_{q+1} |\vec{r}_{ik}\rangle_{q+1} \quad \forall i \in \{0, 1\}^q \\ V_R|\vec{0}\rangle_{q+2}|\vec{j}\rangle_q &= \sum_{\ell=0}^{s_c-1} \frac{1}{\sqrt{s_c}} |\vec{c}_{\ell j}\rangle_{q+1} |\vec{j}\rangle_{q+1} \quad \forall j \in \{0, 1\}^q. \end{aligned}$$

This is a possibly-outdated preprint, using the author's lecture notes, of the book "Quantum algorithms for optimizers," edited by SIAM. All rights to the book's material belong to SIAM. Please refer to the SIAM version of the book.

(Note that \vec{i}, \vec{j} are q -digit binary strings, but on the r.h.s., we store them in registers of length $q + 1$: this is used below because we want to take the inner product of those registers with other registers of size $q + 1$, and we need their size to match; thus, the registers are padded with a zero in front, although we do not indicate this explicitly.) Then $V_L^\dagger V_R$ block-encodes a matrix that is nonzero only in those positions where A is also nonzero; formally:

$$\begin{aligned} \langle \vec{0} |_{q+2} \langle \vec{i} | V_L^\dagger V_R | \vec{0} \rangle_{q+2} | \vec{j} \rangle &= \left(\sum_{k=0}^{s_r-1} \frac{1}{\sqrt{s_r}} \langle \vec{i} | \langle r_{ik} | \right) \left(\sum_{\ell=0}^{s_c-1} \frac{1}{\sqrt{s_c}} | c_{\ell j} \rangle | \vec{j} \rangle \right) \\ &= \frac{1}{\sqrt{s_r s_c}} \text{ if } a_{ij} \neq 0, 0 \text{ otherwise.} \end{aligned} \quad (7.5)$$

To see the last equality, note that the terms in parentheses are simply superpositions over all the nonzero elements in a row or column, and the resulting inner product is nonzero precisely if there exists an index $r_{ik} = j$ and an index $c_{\ell j} = i$, which implies that $a_{ij} \neq 0$ (when $r_{ik} \geq 2^q$ because there are not enough nonzero entries in a row, we have $\langle \vec{i} | \langle r_{ik} | \vec{j} \rangle = 0$, and similarly $\langle \vec{i} | \langle c_{\ell j} | \vec{j} \rangle = 0$ if $c_{\ell j} \geq 2^q$). Now we construct two more unitaries on $2q + 3$ qubits: $U_L := I \otimes V_L$, and the unitary U_R that satisfies the following property:

$$U_R | \vec{0} \rangle_{q+3} | \vec{j} \rangle_q = \frac{1}{\sqrt{s_c}} \sum_{\ell=0}^{s_c-1} \left(a_{c_{\ell j}} | 0 \rangle + \sqrt{1 - |a_{c_{\ell j}}|^2} | 1 \rangle \right) | c_{\ell j} \rangle_{q+1} | \vec{j} \rangle_{q+1}. \quad (7.6)$$

To construct U_R , we first apply $I \otimes V_R$ to the three registers indicated at the beginning of the proof; then we apply O_A to write a binary description of $| a_{c_{\ell j}} \rangle$ in a p -bit auxiliary register, and with this binary description we perform a rotation on the first qubit as indicated in Eq. 7.6 (see, e.g., [Berry et al., 2015] for details on how to do this, or the discussion in Rem. 7.2 regarding the final rotation of the HHL algorithm, where we describe a construction that is sufficient whenever $a_{c_{\ell j}}$ is a real number). Finally we uncompute the auxiliary register, which takes one use of O_A^\dagger . The desired block-encoding is given by $U_L^\dagger U_R$:

$$\begin{aligned} \langle \vec{0} |_{q+3} \langle \vec{i} | U_L^\dagger U_R | \vec{0} \rangle_{q+3} | \vec{j} \rangle &= \langle 0 | \left(\sum_{k=0}^{s_r-1} \frac{1}{\sqrt{s_r}} \langle \vec{i} | \langle r_{ik} | \right) \left(\sum_{\ell=0}^{s_c-1} \left(a_{c_{\ell j}} | 0 \rangle + \sqrt{1 - |a_{c_{\ell j}}|^2} | 1 \rangle \right) | c_{\ell j} \rangle | \vec{j} \rangle \right) \\ &= \frac{a_{ij}}{\sqrt{s_r s_c}}. \end{aligned}$$

□

Remark 7.22. *The error ξ in Prop. 7.21 comes from the final rotation, which is preceded by the computation of the appropriate angles to rotate $| 0 \rangle$ to $a_{c_{\ell j}} | 0 \rangle + \sqrt{1 - |a_{c_{\ell j}}|^2} | 1 \rangle$. Similarly to classical computers, this operation may not be doable exactly in finite precision (we may have to deal with complex numbers), but the error in the computation is exponentially small in the number of qubits (i.e., binary digits) of precision.*

Example 7.23. *Suppose we want to block-encode the following matrix:*

$$\begin{pmatrix} 0 & -1 & 1 & 0 \\ 1 & 1 & -1 & 0 \\ 0 & 0 & 0 & 1 \\ -1 & 0 & 0 & -1 \end{pmatrix}.$$

Then $s_r = 3, s_c = 2$, and $q = 2$ because this is a $2^q \times 2^q$ matrix with at most s_r nonzeros per row and s_c nonzeros per column. The oracles O_r, O_c are defined over two 3-qubit registers: we use integers ≥ 4 to “mark” invalid inputs because for a 4×4 matrix, the only valid indices are the numbers $\{0, 1, 2, 3\}$. For ease of exposition, throughout this example we use integer numbers rather than the corresponding binary representation on three digits; so, for example, we write $| 3 \rangle$

instead of $|011\rangle$. O_r acts as follows (writing only the output for nonzero element indices $\leq s_r - 1$):

$$\begin{array}{lll} O_r|0\rangle|0\rangle = |0\rangle|1\rangle & O_r|0\rangle|1\rangle = |0\rangle|2\rangle & O_r|0\rangle|2\rangle = |0\rangle|6\rangle \\ O_r|1\rangle|0\rangle = |1\rangle|0\rangle & O_r|1\rangle|1\rangle = |1\rangle|1\rangle & O_r|1\rangle|2\rangle = |1\rangle|2\rangle \\ O_r|2\rangle|0\rangle = |2\rangle|3\rangle & O_r|2\rangle|1\rangle = |2\rangle|5\rangle & O_r|2\rangle|2\rangle = |2\rangle|6\rangle \\ O_r|3\rangle|0\rangle = |3\rangle|0\rangle & O_r|3\rangle|1\rangle = |3\rangle|3\rangle & O_r|3\rangle|2\rangle = |3\rangle|6\rangle, \end{array}$$

and similarly, O_c acts as follows (writing only the output for nonzero element indices $\leq s_c - 1$):

$$\begin{array}{ll} O_c|0\rangle|0\rangle = |1\rangle|0\rangle & O_c|1\rangle|0\rangle = |3\rangle|0\rangle \\ O_c|0\rangle|1\rangle = |0\rangle|1\rangle & O_c|1\rangle|1\rangle = |1\rangle|1\rangle \\ O_c|0\rangle|2\rangle = |0\rangle|2\rangle & O_c|1\rangle|2\rangle = |1\rangle|2\rangle \\ O_c|0\rangle|3\rangle = |2\rangle|3\rangle & O_c|1\rangle|3\rangle = |3\rangle|3\rangle. \end{array}$$

Thus, Eq. (7.5) for position $(0, 2)$ in the matrix (i.e., the third element of the first row) reads:

$$\langle 0|\langle 0|V_L^\dagger V_R|0\rangle|2\rangle = \frac{1}{\sqrt{3}} (\langle 0|\langle 1| + \langle 0|\langle 2| + \langle 0|\langle 6|) \frac{1}{\sqrt{2}} (|0\rangle|2\rangle + |1\rangle|2\rangle) = \frac{1}{\sqrt{6}} = \frac{1}{\sqrt{s_r s_c}},$$

whereas for position $(0, 3)$ in the matrix (i.e., the last element of the first row, which is empty) it reads:

$$\langle 0|\langle 0|V_L^\dagger V_R|0\rangle|3\rangle = \frac{1}{\sqrt{3}} (\langle 0|\langle 1| + \langle 0|\langle 2| + \langle 0|\langle 6|) \frac{1}{\sqrt{2}} (|2\rangle|3\rangle + |3\rangle|3\rangle) = 0$$

Finally, the oracle O_A , when queried at a given position (i, j) , outputs a binary description of the value of the corresponding element of A .

Remark 7.24. When constructing binary oracles, in all our previous discussions we almost always acted with \oplus (binary XOR) on the register onto which we want to write, i.e., with operations of the form $|\vec{x}\rangle|\vec{y}\rangle \rightarrow |\vec{x}\rangle|\vec{y} \oplus f(\vec{x})\rangle$. In Prop. 7.21 and Ex. 7.23, however, the oracles O_r, O_c modify the value of the output register “in place”. To convince ourselves that this is implementable with a quantum circuit, observe that the action of $O_r : |\vec{i}\rangle|\vec{k}\rangle \rightarrow |\vec{i}\rangle|\vec{r}_{i\vec{k}}\rangle$ is simply a permutation of the possible basis states, as by definition it maps binary strings one-to-one (note that to have a one-to-one mapping, it is important that, when there are less than k nonzero entries in row i , we set $r_{i\vec{k}}$ to a value that depends on k — in this case, $k + 2^q$ — rather than a fixed, k -independent value). Every permutation matrix is unitary and can be implemented with Boolean logic, so a quantum circuit with only X, CX and CCX suffices. The number of gates is polynomial in the number of bits. (To see that a polynomial upper bound is possible: we can express the value of each bit of the output of the permutation as a Boolean formula of the input bits. Implementing the formula for each bit separately already gives a naive polynomial upper bound. See [Nielsen and Chuang, 2002, Sect. 4.5.2] for another construction.)

Prop. 7.21 shows that a block-encoding of a matrix in the sparse-access model can be constructed with a constant number of calls to the oracles describing the position and values of the nonzero matrix elements. However, one should carefully consider the cost of implementing those oracles. There are two natural situations that arise when evaluating the cost of the sparse-access oracles (a third situation can occur in the QRAM input model, see Sect. 7.2.3).

- Efficient algorithmic description of the matrix: for certain structured matrices, it is possible to determine the value of a matrix element with an efficient algorithm given the corresponding row and column index. In other words, given (i, j) we can determine if the element in position (i, j) is nonzero and if so, its value. In this case, the circuits for O_r, O_c, O_A implement a version of the algorithm to compute the positions and values of the nonzero elements given the input indices. Such an implementation is often extremely efficient and runs in time polynomial in the number of bits of the indices, although the details depend on the structure of the matrix that we aim to block-encode; see Ex. 7.25. This is the ideal scenario, because then all oracles of Prop. 7.21 have low or even negligible cost (such as $\tilde{O}(1)$).

- **Data-driven representation:** if an efficient algorithmic description starting from the input indices is not available, we can in general assume that the matrix is given as an unstructured list of position/value pairs for the nonzero elements. From such a list we can implement O_r, O_c, O_A using a lookup table. The drawback of this approach is that the lookup table is rather inefficient. Because the oracles can be queried in superposition, the lookup table must contain information about all the nonzero elements. This implies that the cost of each of these oracles is roughly linear in the number $\text{nnz}(A)$ of nonzero elements of the matrix A , i.e., linear in the number of entries in the lookup table, so that the gate complexity of O_r, O_c, O_A is $\tilde{O}(\text{nnz}(A))$.

Example 7.25. *Let us look at the cost for implementing sparse-access oracles for the constraint matrix of the assignment problem:*

$$\left. \begin{array}{l} \min \quad \sum_{i=1}^n \sum_{j=1}^n c_{ij} x_{ij} \\ \text{s.t.} \quad \forall i = 1, \dots, n \quad \sum_{j=1}^n x_{ij} = 1 \\ \quad \quad \quad \forall j = 1, \dots, n \quad \sum_{i=1}^n x_{ij} = 1 \\ \quad \quad \quad \forall i, j = 1, \dots, n \quad x_{ij} \geq 0. \end{array} \right\}$$

The constraint matrix of this problem has an efficient algorithmic description. Let us assume the columns (corresponding to decision variables) are ordered in the “natural” way: $x_{11}, x_{12}, \dots, x_{1n}, x_{21}, x_{22}, \dots$. It is convenient to write an example for small n to understand the structure of the constraint matrix; for $n = 3$, the matrix A is as follows:

$$\begin{pmatrix} 1 & 1 & 1 & 0 & 0 & 0 & 0 & 0 & 0 \\ 0 & 0 & 0 & 1 & 1 & 1 & 0 & 0 & 0 \\ 0 & 0 & 0 & 0 & 0 & 0 & 1 & 1 & 1 \\ 1 & 0 & 0 & 1 & 0 & 0 & 1 & 0 & 0 \\ 0 & 1 & 0 & 0 & 1 & 0 & 0 & 1 & 0 \\ 0 & 0 & 1 & 0 & 0 & 1 & 0 & 0 & 1 \end{pmatrix}.$$

Then, if we use zero-based indices for the decision variables and the constraint matrix, the matrix A has the following elements:

$$a_{ij} = \begin{cases} 1 & \text{if } i \leq n - 1 \text{ and } ni \leq j \leq n(i + 1) - 1 \\ 1 & \text{if } i \geq n \text{ and } j \equiv (i - n) \pmod n \\ 0 & \text{otherwise.} \end{cases}$$

We can therefore easily construct a circuit that computes the indices of the nonzero elements in a row, given the row index; and similarly for the columns. These circuits have cost $\tilde{O}(1)$: polynomial in the number of bits used to represent the indices. If the coefficients of the matrix were not all 1, however, and they did not follow some pattern that is easy to encode in a computer program, we would have to store them in a lookup table, increasing the cost of the sparse-access oracle that provides the element values to approximately linear in the number of nonzero elements.

Example 7.26. *Suppose we want to block-encode the adjacency matrix of a hypercube graph (i.e., the graph formed by the edges and vertices of an n -dimensional hypercube). The matrix has an efficient algorithmic description: we label the nodes with binary strings, with each bit indicating whether the corresponding coordinate is 0 or 1 (e.g., for $n = 3$, 000 is the origin, 001 is the point where the third coordinate is 1, and so on). Then, given indices (i, j) , corresponding to two vertices, based on their binary representations \vec{i}, \vec{j} we can determine if they are neighbors in the hypercube graph, by scanning the bits of the bitstrings, and checking whether they differ in exactly one position. Thus, we can efficiently output the indices of the neighbors of each node. In this case the cost of the sparse-access oracles is $\tilde{O}(n)$, which is logarithmic in the number of vertices and edges in the graph.*

Remark 7.27. *An intuitive way to recognize if a certain matrix — or, more in general, a piece of data — admits an efficient algorithmic description is to determine if it is possible to write a*

short computer code that, when queried with a certain position, outputs the corresponding element. There is nothing inherently “quantum” about this property: the computer code might as well be written in any classical language, e.g., Python. For the code to be efficient, the length of the code must be short: typically, polylogarithmic in the size of the problem whose data the code is intended to describe.

7.2.3 Block-encoding with QRAM access

We can accelerate the construction of a block-encoding of a classically-available matrix if we have access to a QRAM of an appropriate size. The sparse-access oracle model can of course be directly accelerated: the oracles O_r, O_c, O_A can be implemented with a single query to a QRAM containing the corresponding data, so the QRAM query complexity of Prop. 7.21 is exactly as stated in the proposition — similarly to the “efficient algorithmic description” case. An even more efficient strategy is described next, and it is based on the idea of constructing quantum states encoding each row of A with the QRAM-based amplitude encoding technique of Sect. 5.3.2 for vectors. Below, we denote by A_j the j -th column of A , and by p the number of bits used to represent each entry of the data structure of Sect. 5.3.2 (which, as usual, is assumed to be large enough that we can perform all calculations with negligible error — the required precision is only polylogarithmically large anyway). We recall the definition of Frobenius norm as it appears in the next proposition.

Definition 7.28 (Frobenius norm). *Given a matrix $A \in \mathbb{C}^{m \times n}$ with entries a_{ij} , its Frobenius norm is the quantity $\|A\|_F = \sqrt{\sum_{i=1}^m \sum_{j=1}^n |a_{ij}|^2}$.*

Proposition 7.29 (Adapted from [Chakraborty et al., 2019, Kerenidis and Prakash, 2017]). *Let $d = 2^q$ and $A \in \mathbb{C}^{d \times d}$. Suppose we have a classical finite-precision description of the entries of A with p bits each, and assume $p = \mathcal{O}(1)$. Then, given a QRAM of size $\mathcal{O}(d^2 p)$, we can implement a $(\|A\|_F, \tilde{\mathcal{O}}(q), \xi)$ -block-encoding of A using $\tilde{\mathcal{O}}(1)$ accesses to the QRAM and additional gates, and $\mathcal{O}(d^2)$ classical arithmetic operations to initialize the QRAM data structures.*

Proof. We use two unitaries V_L, V_R satisfying the following properties:

$$\begin{aligned} V_L |\vec{0}\rangle_q |\vec{i}\rangle_q &= |\vec{i}\rangle \sum_{\vec{\ell} \in \{0,1\}^q} \frac{\|A_{\ell}\|}{\|A\|_F} |\vec{\ell}\rangle & \forall i \in \{0,1\}^q \\ V_R |\vec{0}\rangle_q |\vec{j}\rangle_q &= \sum_{\vec{k} \in \{0,1\}^q} \frac{a_{kj}}{\|A_j\|} |\vec{k}\rangle |\vec{j}\rangle & \forall j \in \{0,1\}^q. \end{aligned}$$

The first unitary V_L can be constructed using SWAP gates and Cor. 5.45 for the vector with entries $\|A_{\ell}\|$, yielding the quantum state $\sum_{\vec{\ell} \in \{0,1\}^q} \frac{\|A_{\ell}\|}{\|A\|_F} |\vec{k}\rangle$ (because the sum of the squares of the column norms is the Frobenius norm squared). The second unitary can be constructed using Cor. 5.45 for the vectors with entries a_{kj} , conditioned on the value of the second register $|\vec{j}\rangle$ to address the correct binary tree data structure in QRAM (i.e., the one for column j), yielding the vectors $\sum_{\vec{k} \in \{0,1\}^q} \frac{a_{kj}}{\|A_j\|} |\vec{k}\rangle$. For this, auxiliary registers of size p are necessary to temporarily hold the data queried from the QRAM, before being used for some controlled operations and eventually uncomputed, as in Cor. 5.45. Note that the normalization factors once again work out, as $\sum_k |a_{kj}|^2 = \|A_j\|^2$. We now show that $V_L^\dagger V_R$ is the desired block-encoding. We have:

$$\begin{aligned} \langle \vec{0} | \langle \vec{i} | V_L^\dagger V_R | \vec{0} \rangle | \vec{j} \rangle &= \left(\langle \vec{i} | \sum_{\vec{\ell} \in \{0,1\}^q} \frac{\|A_{\ell}\|}{\|A\|_F} \langle \vec{\ell} | \right) \left(\sum_{\vec{k} \in \{0,1\}^q} \frac{a_{kj}}{\|A_j\|} |\vec{k}\rangle |\vec{j}\rangle \right) \\ &= \frac{a_{ij}}{\|A_j\|} \langle \vec{i} | \vec{i} \rangle \frac{\|A_j\|}{\|A\|_F} \langle \vec{j} | \vec{j} \rangle = \frac{a_{ij}}{\|A\|_F}. \end{aligned}$$

Regarding the complexity, we are applying Cor. 5.45 to construct the amplitude encoding of d -dimensional vectors, which can be done with $\mathcal{O}(\log d)$ QRAM calls, $\mathcal{O}(\log^2 d)$ additional gates,

and $\tilde{\mathcal{O}}(d)$ classical arithmetic operations to initialize the QRAM data structure for each vector. The quantum operations can be performed in $\tilde{\mathcal{O}}(1)$ time (we apply V_L^\dagger, V_R once, each of them calls the amplitude-encoding subroutine), and the classical initialization procedure is repeated $d + 1$ times (for the d columns plus the vector of column norms used in V_L), giving the stated complexity. Note that the target maximum error ξ determines the error ϵ with which we implement the amplitude encoding circuits in Cor. 5.45; the dependence on ϵ is polylogarithmic, so the impact of ξ on the final complexity is negligible (in $\tilde{\mathcal{O}}(\cdot)$ notation). \square

Example 7.30. Let us have a closer look at the matrices V_L, V_R of Prop. 7.29 to construct a block-encoding of the following matrix:

$$A = \begin{pmatrix} 1 & -2 \\ 0 & -2 \end{pmatrix} = \begin{pmatrix} a_{00} & a_{01} \\ a_{10} & a_{11} \end{pmatrix}.$$

By definition, V_R must have the following action:

$$\begin{aligned} V_R|00\rangle &= \left(\frac{a_{00}}{\|A_0\|}|0\rangle + \frac{a_{10}}{\|A_0\|}|1\rangle \right) |0\rangle = |00\rangle \\ V_R|01\rangle &= \left(\frac{a_{01}}{\|A_1\|}|0\rangle + \frac{a_{11}}{\|A_1\|}|1\rangle \right) |1\rangle = -\frac{1}{\sqrt{2}}|01\rangle - \frac{1}{\sqrt{2}}|11\rangle. \end{aligned} \quad (7.7)$$

This defines two columns of the matrix V_R . A unitary that implements the operation described in Eq. (7.7) is:

$$V_R = \begin{pmatrix} 1 & 0 & 0 & 0 \\ 0 & -\frac{1}{\sqrt{2}} & 0 & -\frac{1}{\sqrt{2}} \\ 0 & 0 & 1 & 0 \\ 0 & -\frac{1}{\sqrt{2}} & 0 & \frac{1}{\sqrt{2}} \end{pmatrix}.$$

By definition, V_L must have the following action:

$$\begin{aligned} V_L|00\rangle &= |0\rangle \left(\frac{\|A_0\|}{\|A\|_F}|0\rangle + \frac{\|A_1\|}{\|A\|_F}|1\rangle \right) = \frac{1}{3}|00\rangle + \frac{2\sqrt{2}}{3}|01\rangle \\ V_L|01\rangle &= |1\rangle \left(\frac{\|A_0\|}{\|A\|_F}|0\rangle + \frac{\|A_1\|}{\|A\|_F}|1\rangle \right) = \frac{1}{3}|10\rangle + \frac{2\sqrt{2}}{3}|11\rangle. \end{aligned} \quad (7.8)$$

Once again, this defines two columns of V_L , and a unitary that implements the operation is:

$$V_L = \begin{pmatrix} \frac{1}{3} & 0 & -\frac{2\sqrt{2}}{3} & 0 \\ \frac{2\sqrt{2}}{3} & 0 & \frac{1}{3} & 0 \\ 0 & \frac{1}{3} & 0 & -\frac{2\sqrt{2}}{3} \\ 0 & \frac{2\sqrt{2}}{3} & 0 & \frac{1}{3} \end{pmatrix}.$$

Finally, we can verify that these unitaries allow us to compute a $(\|A\|_F, \tilde{\mathcal{O}}(q), \xi) = (3, 1, 0)$ -block-encoding of A as $V_L^\dagger V_R$:

$$V_L^\dagger V_R = \begin{pmatrix} \frac{1}{3} & -\frac{2}{3} & 0 & -\frac{2}{3} \\ 0 & -\frac{3}{3} & \frac{1}{3} & \frac{2}{3} \\ -\frac{2\sqrt{2}}{3} & -\frac{1}{3\sqrt{2}} & 0 & -\frac{1}{3\sqrt{2}} \\ 0 & -\frac{1}{3\sqrt{2}} & -\frac{2\sqrt{2}}{3} & \frac{1}{3\sqrt{2}} \end{pmatrix}.$$

Notice the scaled-down copy of A in the top-left block of the above matrix. For this specific case the final error ξ of the block-encoding is 0, because the given matrices V_L, V_R implement the corresponding maps exactly. In general this may not be possible in actual implementations, because the coefficients in Eq.s (7.7)-(7.8) are constructed from finite-precision representations of $a_{ij}, \|A_j\|, \|A\|_F$, and therefore so are the corresponding unitaries. These finite-precision representations lead to errors that are exponentially small (but not necessarily zero) in the number of qubits used to represent each number. Furthermore, the operations used in the procedure of Cor. 5.45 may not be implemented exactly, as discussed in Sect. 5.2.

7.2.4 Sampling from Gibbs distributions and trace estimation

Before discussing the Gibbs distribution, we introduce an additional type of matrix norm that is needed in the following.

Definition 7.31 (Trace norm). *For a given matrix A , we denote its trace norm by $\|A\|_{\text{Tr}} := \text{Tr}(\sqrt{A^\dagger A})$. This is the same as the Schatten 1-norm, i.e., the sum of the singular values of A .*

Remark 7.32. *The trace distance between two density matrices ρ, ρ' , i.e., the distance measured with the trace norm $\|\rho - \rho'\|_{\text{Tr}}$, is generally used to measure the distance between mixed quantum states. One of the reasons for this choice is the fact that the trace distance is a generalization of the total variation distance for pure states, see Def. 1.47 and Prop. 1.49, because:*

$$\| |\psi\rangle\langle\psi| - |\phi\rangle\langle\phi| \|_{\text{Tr}} = 2\sqrt{1 - |\langle\psi|\phi\rangle|^2} \leq 2\| |\psi\rangle - |\phi\rangle \|,$$

for any pure states $|\psi\rangle, |\phi\rangle$ (the inequality above is due to Pythagoras' theorem). Often, the trace distance is defined with a factor $\frac{1}{2}$ in front, i.e., $\text{dist}(\rho, \rho') = \frac{1}{2}\|\rho - \rho'\|_{\text{Tr}}$, so that the correspondence with the total variation distance becomes direct when ρ, ρ' are diagonal (i.e., they encode classical probability distributions).

The Gibbs distribution plays an important role in certain classes of optimization algorithms, for example in the optimization framework discussed in Ch. 8.

Definition 7.33 (Gibbs distribution). *Given a finite set G (called ground set), a function $f : G \rightarrow \mathbb{R}$, and a parameter $\beta > 0$ (called inverse temperature), the corresponding Gibbs distribution is the discrete probability distribution over G defined by:*

$$\Pr(x) = \frac{1}{\sum_{x \in G} e^{-\beta f(x)}} e^{-\beta f(x)} \quad \forall x \in G.$$

The function f in the above definition is often called a Hamiltonian in quantum physics: Hamiltonians encode energy levels of a system (see Def. 6.1), and f associates a value with $x \in G$ (in physics, this would be an energy level). There is a natural and compact notation for a Gibbs distribution as a density matrix (i.e., a mixed quantum state). Suppose $G = \{0, 1\}^q$, and let \mathcal{H} be a diagonal matrix such that $\langle \vec{j} | \mathcal{H} | \vec{j} \rangle = -\beta f(\vec{j})$; we use \mathcal{H} to denote it due to its now obvious connection to Def. 6.1. Then $\exp(\mathcal{H})$ is a matrix that has diagonal elements equal to $e^{-\beta f(\vec{j})}$, and $\exp(\mathcal{H}) / \text{Tr}(\exp(\mathcal{H}))$ has, on its diagonal, exactly the probability values of Def. 7.33. Note that $\exp(\mathcal{H}) / \text{Tr}(\exp(\mathcal{H}))$ is also a density matrix, because it is positive definite matrix with unit trace, therefore it describes a mixed quantum state. This is called a Gibbs state; we can in fact relax the requirements that \mathcal{H} is diagonal, and obtain the following definition.

Definition 7.34 (Gibbs state). *Given a Hermitian matrix $\mathcal{H} \in \mathbb{C}^{2^q \times 2^q}$, usually called Hamiltonian, the Gibbs state corresponding to \mathcal{H} is the (possibly mixed) quantum state ρ with density matrix:*

$$\rho = \frac{\exp(\mathcal{H})}{\text{Tr}(\exp(\mathcal{H}))}.$$

Note that performing a measurement of all qubits from a quantum register in the state ρ yields a sample from the Gibbs distribution encoded by \mathcal{H} , therefore constructing a Gibbs state effectively allows us to sample from a Gibbs distribution. In this section we discuss how to construct the Gibbs state ρ given the Hamiltonian \mathcal{H} , how to block-encode a (subnormalized version of a) Gibbs state, and also how to perform certain operations on ρ . The discussion is based on [Gilyén, 2019, van Apeldoorn, 2020]: all proofs not given here can be found in one of these two references. We first need to define the concept of subnormalized density matrix, which is useful because in some situations we may not want to (or cannot) work with a density matrix, but we can work with a scaled-down version of it.

Definition 7.35 (Subnormalized density matrix). *A subnormalized density matrix ρ is a positive semidefinite matrix of trace at most 1. A purification ϱ of a subnormalized density matrix $\rho \in \mathbb{C}^{2^q \times 2^q}$ is a pure state $|\psi\rangle$ over three registers A, B, C of size, respectively, $q, 1$ and $p \leq q$ such that*

$$(I^{\otimes q} \otimes \langle 0|) \text{Tr}_C (|\psi\rangle\langle\psi|) (I^{\otimes q} \otimes |0\rangle) = \rho,$$

i.e., tracing out the third register (of size p) and projecting onto the subspace where the second register (of size 1) is $|0\rangle$ yields ρ .

Remark 7.36. *The difference between a density matrix and a subnormalized density matrix is subtle, and is worth pointing out. We have seen in Sect. 1.4, in particular Thm. 1.68, that it is possible to express every density matrix as the partial trace of a pure state, called purification (Def. 1.69). In Thm. 1.68 we only need two registers, in particular we do not need the single-qubit register used in Def. 7.35. In a subnormalized density matrix the trace does not need to be 1, whereas in a density matrix it is always 1. The second register serves the purpose of allowing a smaller trace, by defining a subspace of the entire density matrix that contains the part of interest; i.e., we have a “larger” density matrix of the form $\rho^{(00)} \otimes |0\rangle\langle 0| + \rho^{(01)} \otimes |0\rangle\langle 1| + \rho^{(10)} \otimes |1\rangle\langle 0| + \rho^{(11)} \otimes |1\rangle\langle 1|$, with $\text{Tr}(\rho^{(00)} + \rho^{(11)}) = 1$, and the subnormalized density matrix of interest is $\rho^{(00)}$. The order and size of the register that we project on are just a convention: the concept can easily be generalized, but the generalization is not necessary for the discussion in this set of lecture notes.*

Next, we give an algorithmic result that characterizes the complexity of constructing a Gibbs state from the block-encoding of some Hermitian matrix; however, for the sake of completeness we first need to define the degree of a certain polynomial that approximates the exponential function sufficiently well.

Lemma 7.37 (Lem. 4.14 in [van Apeldoorn, 2020]). *Let $\xi \in (0, 1/6]$ and $\beta \geq 1$. There exists a polynomial $P(x)$ such that:*

- For all $x \in [-1, 0]$, we have $|P(x) - \exp(2\beta x)/4| \leq \xi$.
- For all $x \in [-1, 1]$, we have $|P(x)| \leq 1/2$.
- $\text{deg}(P) = \tilde{O}(\beta)$.

The polynomial of Lem. 7.37 appears in the error requirement of the input block-encoding, because the matrix exponential (rather, the polynomial approximation of the matrix exponential) could amplify errors significantly. Lem. 7.37 simply states that we can construct the desired polynomial approximation in the eigenvalue interval $[-1, 0]$, including an amplification factor β for the block-encoding, which is used to cancel out the subnormalization factor of the input block-encoding. We are now in a position to state the complexity of constructing a Gibbs state $\exp(\mathcal{H})/\text{Tr}(\exp(\mathcal{H}))$.

Proposition 7.38 (Lem. 4.15 in [van Apeldoorn, 2020]). *Let $\mathcal{H} \in \mathbb{R}^{n \times n}$ be a Hermitian matrix. Let $\theta \in (0, 1/3]$, $\beta > 1$, and let d be the degree of the polynomial from Lemma 7.37 when we let $\xi = \frac{\theta}{128n}$. Let U be a $(\beta, a, \frac{\theta^2 \beta}{1024^2 d^2 n^2})$ -block-encoding of \mathcal{H} . Then we can create a purification of a state $\tilde{\rho}$ such that*

$$\left\| \tilde{\rho} - \frac{\exp(\mathcal{H})}{\text{Tr}(\exp(\mathcal{H}))} \right\|_{\text{Tr}} \leq \theta$$

using $\tilde{O}(\sqrt{n}\beta)$ applications of U and $\tilde{O}(\sqrt{n}\beta a)$ elementary gates.

The construction of Prop. 7.38 is based on polynomial approximations of the exponential function, which can be obtained using quantum singular value transformation techniques introduced in [Gilyén, 2019, Gilyén et al., 2019b]. The construction requires a very high precision for the block-encoding U for \mathcal{H} , but this should not be a deterrent: we already described situations where the running time of a block-encoding construction scales polylogarithmically in the desired inverse precision, e.g., Prop. 7.21, therefore obtaining a high-precision block-encoding is not necessarily a bottleneck. The result described in Prop. 7.38 is based on the following idea: assume $n = 2^q$

for simplicity, so that q is the number of qubits of the operator \mathcal{H} ; we start by constructing the state $\sum_{\vec{j} \in \{0,1\}^q} |\vec{j}\rangle |\vec{j}\rangle$, which requires only Hadamards and CNOTs, and is often called *maximally-mixed* state in the literature. If we trace out the second register, we find that the density matrix describing the first register is the rescaled identity $I^{\otimes q}/2^q$. Then if we construct and apply a block-encoding of $e^{\mathcal{H}/2}$ to the first register (keeping the auxiliary register for the block-encoding separate, as usual), the state evolves to $e^{\mathcal{H}/2} I^{\otimes q} e^{\mathcal{H}/2} = e^{\mathcal{H}}$ in the “correct” subspace, modulo normalization: this follows from the rules of evolution of a mixed state in Sect. 1.4, together with the fact that $\mathcal{H}^\dagger = \mathcal{H}$. A somewhat similar idea is described in the proof of Prop. 7.41. The construction of the block-encoding of $e^{\mathcal{H}/2}$ additionally requires shifting the spectrum of \mathcal{H} before applying the (polynomial approximation of the) exponential function, to ensure $\|\exp(\mathcal{H})\| \leq 1$. We achieve this goal by shifting the spectrum of \mathcal{H} to be negative, which is why in Lem. 7.37 we are only concerned about approximating the exponential for $x \in [-1, 0]$. The spectrum shift is not an issue, because $\exp(\mathcal{H} + \lambda I) / \text{Tr}(\exp(\mathcal{H} + \lambda I)) = \exp(\mathcal{H}) / \text{Tr}(\exp(\mathcal{H}))$ for every $\lambda \in \mathbb{R}$. After selecting the correct subspace via amplitude amplification, the resulting state is a density matrix proportional to $e^{\mathcal{H}}$, hence it is $\exp(\mathcal{H}) / \text{Tr}(\exp(\mathcal{H}))$.

We can also construct a block-encoding of a density matrix ρ from a unitary that prepares a purification of it.

Lemma 7.39 (Block-encoding of a (subnormalized) density operator; Lem. 6.4.4 in [Gilyén, 2019]). *Let U be a $(q+a)$ -qubit unitary that, given the input state $|\vec{0}\rangle_q |\vec{0}\rangle_a$, prepares a purification $|\varrho\rangle$ of the (possibly subnormalized) q -qubit density matrix ρ . Then we can implement a $(1, q+a, 0)$ -block-encoding of ρ with a single use of U and its inverse, and $q+1$ two-qubit gates.*

Finally, we can construct a trace estimator to compute quantities of the form $\text{Tr}(A\rho)$ using the block-encoding model. This result is extremely useful in the quantum algorithms for semidefinite optimization discussed in Ch. 8, because the constraints and objective function of the problems discussed in that chapter involve expressions of the form $\text{Tr}(A\rho)$: this gives us a way of estimating their value without having explicit knowledge of ρ , as long as we can construct a state with density matrix ρ . To understand some of the ideas for the construction we start with a simpler example that does not produce what we need, but it allows us to see the power of block-encoded matrices, and some of the operations that can be performed with them.

Example 7.40. *In this example we construct a block-encoding of the scalar $\text{Tr}(A\rho)$, i.e., of a 1×1 matrix, using access to a purification for ρ and a block-encoding of A . While we do not directly make use of this, it is a relatively simple construction that is instructive.*

Let U be a $(q+m)$ -qubit unitary that, given the input state $|\vec{0}\rangle_m |\vec{0}\rangle_q$, prepares a purification $|\varrho\rangle$ of the q -qubit density matrix ρ ; the m -qubit register is the purifying register. Let V be a (α, a, ξ) -block-encoding of a $2^q \times 2^q$ matrix A (where A acts on the same q -qubit register defined above for U).

Consider the circuit $(I_a \otimes U^\dagger)(V \otimes I_m)(I_a \otimes U)$; in this expression we are using the same convention whereby the subscript of the identity matrices indicates not only their size, but also which register they are applied to. This circuit first uses the unitary U to create the purification of ρ , then applies the block-encoding of A , finally applies the inverse unitary U^\dagger . The reason for the inverse unitary U^\dagger is that it allows us to “sandwich” the block encoding with $|\varrho\rangle$ on the left and $\langle\varrho|$ on the right, which results in block-encoding $\text{Tr}(A\rho/\alpha)$. To see this, let us apply the definition of block-encoding, using the $(a+m)$ auxiliary qubits as the ones that are “hit” by the all-zero basis state. We have:

$$\begin{aligned} & \langle\vec{0}\rangle_a \langle\vec{0}\rangle_m \langle\vec{0}\rangle_q (I_a \otimes U^\dagger)(V \otimes I_m)(I_a \otimes U) |\vec{0}\rangle_a |\vec{0}\rangle_m |\vec{0}\rangle_q = \langle\vec{0}\rangle_a \langle\varrho|(V \otimes I_m)|\vec{0}\rangle_a |\varrho\rangle \\ & = \langle\varrho|(A/\alpha \otimes I_m)|\varrho\rangle = \text{Tr}(\langle\varrho|(A/\alpha \otimes I_m)|\varrho\rangle) = \text{Tr}((A/\alpha \otimes I_m)|\varrho\rangle\langle\varrho|) = \text{Tr}(A/\alpha\rho). \end{aligned}$$

For the above chain of equalities, we used the fact that by definition of $|\varrho\rangle$, if we trace out the m -qubit auxiliary (purifying) register we obtain ρ , and it is easy to see that $\text{Tr}((A/\alpha \otimes I_m)|\varrho\rangle\langle\varrho|)$ corresponds to tracing out the m -qubit register (because $I_m = \sum_{\vec{j} \in \{0,1\}^m} |\vec{j}\rangle\langle\vec{j}|$). Thus, we obtained the desired block-encoding, with subnormalization factor α .

Unfortunately, it is not obvious if one can obtain an estimate of $\text{Tr}(A\rho/\alpha)$ from the block-encoding in Ex. 7.40: the block-encoding in itself ensures that $\text{Tr}(A\rho/\alpha)$ is the coefficient of $|\vec{0}\rangle$ after applying the circuit to the state $|\vec{0}\rangle$, but from there we can only recover $|\text{Tr}(A\rho/\alpha)|^2$, which is equal to the probability of observing $|\vec{0}\rangle$ when measuring; for example, we can recover it by taking repeated measurements or with amplitude estimation (Sect. 4.3). Because of the absolute value and the square, there is a sign problem and amplitude estimation would not be able to tell if $\text{Tr}(A\rho)$ is positive or negative. There is a more astute construction that leads to a much better algorithm for the estimation of $\text{Tr}(A\rho)$. Because in Ex. 7.40 we end up obtaining the square of the quantity of interest, we use the matrix square root of A . We start with the mixed state described by the density matrix ρ , then apply the matrix square root of an appropriately shifted version of A , obtaining a state corresponding to the density matrix $\sqrt{A}\rho\sqrt{A}^\dagger$ (after selecting the correct part of the space, i.e., the one with support on $|\vec{0}\rangle$ in certain registers); if the construction is applied to a Hermitian matrix, the \dagger disappears. After applying the circuit based on this idea, we show that the probability of observing $|\vec{0}\rangle$ is approximately a shifted version of $\text{Tr}(\sqrt{A}\rho\sqrt{A})$. A more precise description is given in the proof of the next result.

Proposition 7.41 (Cor. 6.4.5 in [Gilyén, 2019]). *Let ρ be the density matrix representing a given q -qubit quantum state, and U an $(\alpha, a, \theta/2)$ -block-encoding of a Hermitian matrix $A \in \mathbb{R}^{2^q \times 2^q}$ with $\|A\| \leq 1$. We can construct a quantum circuit that, after measurement, outputs a (binary-encoded) sample from a random variable Y with the property that the expected value of Y is at most $\theta/4$ away from $\text{Tr}(A\rho)$, and its standard deviation is $\sigma = \mathcal{O}(1)$. The quantum circuit uses $\tilde{\mathcal{O}}(\alpha)$ applications of U and U^\dagger , $\tilde{\mathcal{O}}(\alpha)$ two-qubit gates, and one copy of ρ .*

Proof. We provide a sketch of the proof, referring to [Gilyén, 2019] for details.

As a first step, we amplify the block-encoding U to obtain a block-encoding of $A/2$ (rather than A/α) using $\tilde{\mathcal{O}}(\alpha)$ applications of U . We do not provide a precise statement of this result, but this can be done by applying the matrix function $f(x) = \alpha x/2$ to the block-encoding (again, via a polynomial approximation). This is analogous to oblivious amplitude amplification to amplify the subspace where U acts as A/α , but amplitude amplification would only work for unitary matrices. Then, by linear combination of block-encodings (Prop. 7.18) with uniform weights, we transform it into a block-encoding of $A/4 + I/2$: this requires a single use of the block encoding of $A/2$ and of I (which is trivial). Because $\|A\| \leq 1$ the smallest eigenvalue of $A/4$ is $\geq -1/4$, so $A/4 + I/2 \geq 0$. At this point, using a polynomial approximation of the square root function, we construct a block-encoding W of $\sqrt{A/4 + I/2}/2$: this requires $\tilde{\mathcal{O}}(1)$ applications of the block-encoding for $A/4 + I/2$. Throughout these constructions we accumulate some error $\mathcal{O}(\theta)$, but as the complexity of the operations depends polylogarithmically on θ , we use $\tilde{\mathcal{O}}(\cdot)$ notation and neglect it for simplicity. In summary, W satisfies the following property:

$$\langle \vec{0} | \otimes I_q W (|\vec{0}\rangle \otimes I_q) \approx \frac{1}{2} \sqrt{\frac{A}{4} + \frac{I}{2}}.$$

Let w be the number of auxiliary qubits of the block-encoding W (w is of the same order of magnitude as a). Now we apply W to ρ , initially setting the auxiliary qubits to $|\vec{0}\rangle_w$, as usual. The state of the system is $W(|\vec{0}\rangle\langle\vec{0}| \otimes \rho)W^\dagger$, and the probability of observing $|\vec{0}\rangle_w$ when performing a measurement in the auxiliary register is:

$$\begin{aligned} \text{Tr} \left((|\vec{0}\rangle\langle\vec{0}| \otimes I_q) W (|\vec{0}\rangle\langle\vec{0}| \otimes \rho) W^\dagger \right) &= \text{Tr} \left((|\vec{0}\rangle \otimes I_q) W (|\vec{0}\rangle\langle\vec{0}| \otimes \rho) W^\dagger (|\vec{0}\rangle \otimes I_q) \right) \\ &= \text{Tr} \left(\underbrace{(|\vec{0}\rangle \otimes I_q) W^\dagger (|\vec{0}\rangle \otimes I_q)}_{\approx \sqrt{A/4 + I/2}/2} \underbrace{(|\vec{0}\rangle \otimes I_q) W (|\vec{0}\rangle \otimes I_q) \rho}_{\approx \sqrt{A/4 + I/2}/2} \right) \\ &= \frac{1}{8} + \frac{\text{Tr}(A\rho)}{16} + \mathcal{O}(\theta), \end{aligned}$$

where the term $\mathcal{O}(\theta)$ comes from the errors accumulated throughout the construction. (In the chain of equations, we used the cyclic property of the trace to bring W^\dagger to the left of ρ .) Define a

random variable Y that takes value 14 if the auxiliary register contains $|\vec{0}\rangle_w$ after measurement, and -2 otherwise. We can easily construct a circuit that looks at the first w qubits and outputs 14 or -2 depending on the value contained in the register: this is the sample from Y defined in the statement of the proposition. The expected value of Y satisfies:

$$\mathbb{E}[Y] = \frac{14}{8} + \frac{14 \operatorname{Tr}(A\rho)}{16} - 2\left(1 - \frac{1}{8} - \frac{\operatorname{Tr}(A\rho)}{16}\right) + \mathcal{O}(\theta) = \operatorname{Tr}(A\rho) + \mathcal{O}(\theta),$$

and with similar calculations, ensuring the constant in $\mathcal{O}(\theta)$ is chosen sufficiently small, we can also guarantee that the variance is $\mathcal{O}(1)$. \square

Remark 7.42. *The construction in Prop. 7.41 prepares a random variable via a quantum circuit. The general structure of an algorithm that prepares a random variable via a quantum circuit is the following: the algorithm, starting from the state $|\vec{0}\rangle$, produces a quantum state and concludes with a single measurement. From this single measurement, a (classical) computation outputs the value of the random variable. This allows us to obtain a sample.*

If we want to estimate properties of the random variable, e.g., its expected value $\mathbb{E}[Y]$ (to estimate $\operatorname{Tr}(A\rho)$), in general we need multiple copies of the state ρ : each sample of the random variable requires a measurement, and each measurement “consumes” a copy of the state ρ , which is entangled with the measured qubits. For example, if we use amplitude estimation to estimate $\mathbb{E}[Y]$ — which is possible under some conditions — then we need multiple applications of a circuit that produces ρ , and the inverse circuit; see Rem. 4.23 and Sect. 4.5 regarding controlling the bias with amplitude estimation. However, sometimes it is possible to get away with fewer copies of ρ . An example of this is discussed in Sect. 8.3.3, but the technique is rather involved and relies on the specific setting discussed in that section. Different approaches for mean estimation are possible, and depending on the properties of the specific problem at hand, one might be able to get away with more efficient algorithms. For a discussion of quantum algorithms to estimate the mean of a random variable depending on its properties, we refer to [Montanaro, 2015].

7.3 Notes and further reading

Our discussion of quantum algorithms for linear systems is mainly based on [Harrow et al., 2009], but we incorporate some subsequent developments to relax some of the strict assumptions. In addition to the massive improvements introduced in [Chakraborty et al., 2019, Childs et al., 2017, Gilyén et al., 2019b], and already discussed in Sect. 7.1.5, recent work has tightened existing bounds [Costa et al., 2022] and improved the constants [Dalzell, 2024]. The query complexity of these last two papers is $\mathcal{O}(\kappa \log \frac{1}{\epsilon})$, without hidden polylogarithmic factors, where each query is a call to an oracle block-encoding the matrix A , or preparing the state $|\operatorname{amp}(b)\rangle$. Note that this complexity is optimal, due to matching lower bounds (a lower bound of $\Omega(\kappa)$ oracle calls is proven in [Somma and Subaşı, 2021], and [Costa et al., 2022] claims that a lower bound of $\Omega(\kappa \log \frac{1}{\epsilon})$ oracle calls can also be shown, although to the best of our knowledge, such a proof has not appeared in the open literature yet).

The block-encoding framework is established in [Gilyén et al., 2019b], building on previous work on *qubitization* [Low and Chuang, 2017a, Low and Chuang, 2019] and *quantum signal processing* [Low et al., 2016, Low and Chuang, 2017b]. All the results on matrix manipulation discussed in this chapter can be found in [Gilyén et al., 2019b], or derived directly from that framework. However, the exposition in [Gilyén et al., 2019b] is very technical and building intuition on how the main results work may prove to be a difficult task. Different expositions of the fundamental concepts, which may turn out to be more accessible to some readers, are given in [Martyn et al., 2021, Tang and Tian, 2024]. The Ph.D. thesis [Gilyén, 2019] may also be a suitable starting point, as well as the excellent lecture notes [Lin, 2022]. A direct application of the block-encoding framework is discussed in Ch. 8.

Quantum linear systems algorithms and matrix manipulation via block-encoding are the main source of quantum speedup for quantum interior point methods, an algorithmic scheme that attempts to accelerate classical interior point iterations using a quantum computer for linear

algebra. This is motivated by the fact that in classical interior point methods, the most expensive step is the solution of the (large and typically dense) Newton linear system in every iteration [Roos et al., 2005, Terlaky, 2013, Wright, 1997]. The idea of using quantum computers for linear algebra in the context of interior point methods for semidefinite optimization was pioneered in [Kerenidis and Prakash, 2020] and extended in [Kerenidis et al., 2021] for second-order cone programs, although issues remained in showing convergence to a feasible solution in the usual sense. Convergence was addressed in [Augustino et al., 2023b] for semidefinite programs, using a reformulation of the Newton linear system into orthogonal bases for the primal and dual space to ensure reduction of the complementarity violation. Two major sources of slowdown of this methodology are: the reliance on quantum state tomography to extract the solution of the linear system, which incurs $1/\epsilon$ scaling in the precision; and the linear dependence of the QLSA on the condition number κ , which grows as we approach optimality. The first source of slowdown is addressed using iterative refinement, the second source is addressed with preconditioning or additional iterative refinement for certain classes of problems, see [Mohammadisiahroudi et al., 2025a, Mohammadisiahroudi et al., 2024, Mohammadisiahroudi et al., 2025b, Wu et al., 2023] as well as Sect. 7.1.6.

For a discussion on iterative refinement in the context of classical linear algebra, see [Saad, 2003, Wilkinson, 1963]. In classical optimization, iterative refinement is used in, e.g., [Gleixner et al., 2016, Weber et al., 2019]: both papers also offer accessible introductions to the topic. On the quantum side, besides the references on interior point methods cited above, a strategy based on iterative refinement is used in [Chen et al., 2024] within an algorithm to approximate the top eigenvalues of a block-encoded matrix.

Chapter 8

Quantum algorithms for SDP using mirror descent

Mirror descent is a powerful framework to solve nonlinear optimization problems by taking advantage of the geometry of the space in which the problem lives [Nemirovski and Yudin, 1983]. Mirror descent relies on the same concepts as projected (sub)gradient descent, with the significant variation that the descent takes place in a “mirror” space, which is the vector space dual to the original space. When dealing with optimization problems over the cone of positive semidefinite matrices, it is possible to apply mirror descent using the *quantum relative entropy* as the mirror map, resulting in an iterative optimization scheme for semidefinite programming that simultaneously operates in two spaces: the space of primal iterates, which are positive semidefinite matrices expressed as matrix exponentials, and the space of (vector) dual iterates (i.e., the mirror space), which are the matrix logarithms of the primal iterates. This choice of the mirror map is natural in the context of quantum algorithms that want to take advantage of the ability of quantum computers to efficiently compute Gibbs states, i.e., matrix exponentials of a certain kind, see Sect. 7.2.4 and in particular Prop. 7.38. Since the mirror descent framework has proven very fruitful for the development of quantum optimization algorithms, in this chapter we discuss its main components, with an emphasis on those that (almost) directly lead to quantum algorithms with an expectation of quantum advantage of some type.

In the following we analyze two quantum algorithms for semidefinite optimization that use the mirror descent framework. The first algorithm, to which the majority of the chapter is devoted, is in fact also an instantiation of the Multiplicative Weights Update (MWU) algorithm, a meta-algorithm that has found many applications in optimization [Arora et al., 2012]; for some references on the MWU, mostly of theoretical nature, see the notes at the end of this chapter, Sect. 8.5. The MWU algorithm is a method to find an optimal strategy in a certain game against an adversary, and can be thought of as an update rule for a probability distribution. A specific version of the MWU algorithm can solve semidefinite optimization problems (SDPs) [Arora et al., 2005, Arora and Kale, 2016], and that version is equivalent to mirror descent with a specific choice of the mirror map. The approach can be turned into a quantum algorithm for SDPs that obtains a different running time tradeoff as compared to the classical MWU algorithm. The second algorithm, based on [Brandao et al., 2022] and originally described as an instantiation of the matrix-exponentiated gradient updates approach of [Tsuda et al., 2005], applies to the SDP relaxation of MaxCut and other quadratic unconstrained binary optimization problems (as is customary, we use the acronym “SDP” to refer to both a “semidefinite optimization problem,” and “semidefinite programming,” i.e., semidefinite optimization: the context should clarify any ambiguity). This second algorithm is also a mirror descent approach with the same mirror map as the first algorithm.

Because this chapter is devoted to SDP, we formally introduce the class of optimization problems that we aim to solve. (The second algorithm discussed in this chapter solves a restricted class of SDP: we describe it in Sect. 8.4.) Given Hermitian matrices $C, A^{(1)}, \dots, A^{(m)} \in \mathbb{C}^{n \times n}$ and

reals $b_1, \dots, b_m \in \mathbb{R}$, we define the primal SDP problem as:

$$\left. \begin{array}{l} \max \quad \text{Tr}(CX) \\ \text{s.t.: } \forall j = 1, \dots, m \quad \text{Tr}(A^{(j)}X) \leq b_j \\ \quad \quad \quad X \succeq 0. \end{array} \right\} \quad (\text{P-SDP})$$

The corresponding dual is:

$$\left. \begin{array}{l} \min \quad b^\top y \\ \text{s.t.: } \sum_{j=1}^m y_j A^{(j)} - C \succeq 0 \\ \quad \quad \quad y \geq 0. \end{array} \right\} \quad (\text{D-SDP})$$

If strong duality holds, the optimal values of (P-SDP) and (D-SDP) are the same. Strong duality may not hold in general but it holds under mild conditions, for example if Slater’s condition holds (the primal and dual have strictly feasible solutions) [Boyd and Vandenberghe, 2004]. For the general-purpose SDP solver described in Sect. 8.2, we modify the problem in a suitable way so that strictly feasible solutions exist, and this ensures that strong duality holds; this is discussed in Sect. 8.2.2. Note that SDP generalizes linear programming: a linear optimization problem is simply an SDP where all the matrices $A^{(j)}, C$ are diagonal.

8.1 The mirror descent framework

Mirror descent, first introduced in [Nemirovski and Yudin, 1983], is an algorithm akin to steepest descent and its variants to solve continuous optimization problems. Here we discuss mirror descent starting from projected subgradient descent; one can think of projected subgradient descent as a natural variation of steepest descent for constrained optimization (as opposed to unconstrained optimization) of not-necessarily-differentiable functions. A reader not familiar with projected subgradient descent should still be able to follow the discussion by relying on intuition from the well-known steepest descent algorithm. The main difference between mirror descent and steepest descent is that mirror descent uses a *mirror map* with the goal of adapting steepest descent to the geometry of the space. If the mirror map is chosen appropriately, mirror descent can yield an advantage over vanilla steepest descent, for example by handling some difficult constraints in a simple way. In the next section we introduce the most important concepts of the mirror descent framework, but we do not give a fully detailed description, and we skip many of the proofs; the notes in Sect. 8.5 contain references for readers interested in the details.

8.1.1 Mirror descent as a generalization of steepest descent

We start with a discussion of the mirror descent framework as a generalization of projected subgradient descent. In this chapter we repeatedly use the concepts of subgradients and approximate subgradients, formally defined in Def. 5.24. Let us consider the problem of minimizing a convex function $f(x)$ using an iterative algorithm, with access to subgradients of the function. For now we consider the unconstrained case; at the end of this section, we discuss the case in which we want to minimize over a convex set K . Let $x^{(t)}$ be the current iterate and $g^{(t)} \in \partial f(x^{(t)})$ a subgradient of f at $x^{(t)}$. It is well known that we can construct an iterative algorithm to minimize f by using the following update rule:

$$x^{(t+1)} = x^{(t)} - \eta g^{(t)}, \quad (8.1)$$

i.e., we add to the current iterate a negative multiple of the subgradient. If the function f is differentiable, the subgradient coincides with the gradient, and the above algorithm is usually called *steepest descent*. For a comprehensive discussion of gradient-based methods, see [Bertsekas, 1999].

It is also well known that the explicit update rule in Eq. (8.1) is equivalent to the following implicit rule, where the next iterate is expressed as the solution of an optimization problem:

$$x^{(t+1)} = \arg \min_x \left\{ \frac{1}{2} \|x - x^{(t)}\|^2 + \eta \langle g^{(t)}, x - x^{(t)} \rangle \right\}. \quad (8.2)$$

The equivalence can be verified by taking the gradient with respect to x for the expression inside the min (the constant term $\eta\langle g^{(t)}, x^{(t)} \rangle$ disappears), and setting it equal to zero component-wise: this yields precisely Eq. (8.1). Readers familiar with the *proximal operator*, defined as:

$$\text{prox}_f(x^{(t)}) := \arg \min_x \left\{ \frac{1}{2} \|x - x^{(t)}\|^2 + \eta f(x) \right\}, \quad (8.3)$$

might recognize Eq. (8.2) as a linearization of $\text{prox}_f(x^{(t)})$. Comparing Eq. (8.3) to Eq. (8.2), the only difference is that the objective function term $f(x)$ in $\text{prox}_f(x^{(t)})$ is replaced with its linearization $f(x^{(t)}) + \langle g^{(t)}, x - x^{(t)} \rangle$ using $g^{(t)} \in \partial f(x^{(t)})$; the constant term $f(x^{(t)})$ does not affect the value of the minimizer of the expression, so the arg min is the same whether or not we add $\eta f(x^{(t)})$. Replacing the squared Euclidean distance term in Eq. (8.3) with more general distance functions yields generalizations of the proximal operator [Teboulle, 1992]. The main motivation for doing so is that one can sometimes fully eliminate some of the constraints of the problem simply by appropriately choosing the distance function. This statement may seem abstract at this point, so we give a quick preview of how this fact is used in the remainder of this chapter: by using a distance function called quantum relative entropy, we will automatically ensure that all the iterates are positive semidefinite matrices. This allows us to construct algorithms for optimizing over the set of density matrices without having to explicitly handle positive semidefiniteness and trace normalization. (The trace normalization is taken care of by projection onto a feasible set, still using the same distance function.)

Let us now get back to the derivation of mirror descent from projected subgradient descent. To summarize the above discussion: the implicit update in Eq. (8.2) corresponds to minimizing a weighted combination of two terms. The first term is the distance from the current iterate $x^{(t)}$. The second term is a linear approximation of the objective function obtained using a subgradient at $x^{(t)}$, $g^{(t)} \in \partial f(x^{(t)})$:

$$f(x^{(t)}) + \langle g^{(t)}, x - x^{(t)} \rangle.$$

If we were to minimize the linear approximation term only, we would move indefinitely in the direction opposite to a subgradient at $x^{(t)}$, because this is an unconstrained problem. This, however, is not a good idea: the linear approximation at $x^{(t)}$ is unlikely to be accurate once we move far away from $x^{(t)}$. For a non-differentiable function, the subgradient may not give a descent direction at all: the objective function can sometimes increase if we add a negative multiple of the subgradient to $x^{(t)}$, see Ex. 8.1.

Example 8.1. Consider the univariate function $f(x) = |x|$ and let $x^{(1)} = 0$ be our current iterate. The scalar 1 is a subgradient of $f(x)$ at $x^{(1)}$, but adding any multiple of the subgradient to $x^{(1)}$ increases the objective function value.

For a differentiable function, although the gradient gives a descent direction, we know from Taylor’s theorem that the error of the linear approximation depends on the distance from $x^{(t)}$, hence the approximation may lead us astray when we are far from $x^{(t)}$. Adding a penalty for increasing the distance from the current iterate $x^{(t)}$ ensures that we stay relatively close to it, which is a desirable feature of the descent scheme for the reason discussed above: by including the penalty term, hopefully we do not go too far along poor directions, as might occur if the linear approximation is inaccurate.

Now let us generalize Eq. 8.2. Rather than use the Euclidean distance function, we measure proximity with the *Bregman divergence*, which estimates the error between the value of a certain *mirror map*, and a linearization of the mirror map at a given point. Because the iterate is chosen by optimizing a problem involving a linear approximation of the objective function, we intuitively expect the quality of the iterates to depend on how good such an approximation is; thus, it is reasonable to use a distance function that estimates the quality of the linear approximation of a function — in this case, the mirror map. Potentially, the Bregman divergence might help us determine how far we can go from the current iterate before our model for the objective function (the linear approximation) becomes too inaccurate to be useful. The mirror map is usually chosen in such a way that the Bregman divergence is easy to compute, with the goal of achieving or maintaining computational tractability.

Definition 8.2 (Bregman divergence). *Given a continuously differentiable and strictly convex function $h : \mathbb{R}^d \rightarrow \mathbb{R}$, called mirror map, and two points $x, y \in \mathbb{R}^d$, the Bregman divergence from x to y is defined as:*

$$D_h(y||x) := h(y) - h(x) - \langle \nabla h(x), y - x \rangle.$$

Equipped with this notion, a natural generalization of Eq. (8.2) is:

$$x^{(t+1)} = \arg \min_x \left\{ D_h(x||x^{(t)}) + \eta \langle g^{(t)}, x - x^{(t)} \rangle \right\}, \quad (8.4)$$

where we are using $D_h(x||x^{(t)})$ instead of the squared Euclidean distance between $x^{(t)}$ and x . By taking the gradient of the expression inside the min and setting it equal to zero, we find:

$$\eta g^{(t)} + \nabla h(x) - \nabla h(x^{(t)}) = 0,$$

so if ∇h is invertible, the solution to Eq. 8.4 leads to the following update rule:

$$x^{(t+1)} = (\nabla h)^{-1} \left(\nabla h(x^{(t)}) - \eta g^{(t)} \right). \quad (8.5)$$

This expression can be interpreted as follows. To find the new iterate $x^{(t+1)}$, we map the current iterate $x^{(t)}$ to dual space using ∇h , and we take a descent step using the subgradient $g^{(t)}$. Then, we map back to primal space using $(\nabla h)^{-1}$: this gives us the new point. We say that $x^{(t)}$ is mapped to a dual space using ∇h because the gradient of a function lives in the dual vector space. Note that the update rule in Eq. 8.5 is derived by solving the optimization problem in Eq. 8.4 over the entire space: if we are interested in minimizing $f(x)$ over some convex set K , once we map back to primal space we must also project onto K using the same divergence D_h as the distance function. This is similarly derived starting from the projected (sub)gradient descent update rule:

$$x^{(t+1)} = \arg \min_{x \in K} \left\{ \frac{1}{2} \|x - x^{(t)}\|^2 + \eta \langle g^{(t)}, x - x^{(t)} \rangle \right\} = \arg \min_{x \in K} \left\{ \frac{1}{2} \|x - (x^{(t)} - \eta g^{(t)})\|^2 \right\} \quad (8.6)$$

(the expressions inside the two arg min are equivalent up to terms that do not depend on x , so their arg min is the same), which generalizes to:

$$x^{(t+1)} = \arg \min_{x \in K} \left\{ D_h(x||x^{(t)}) + \eta \langle g^{(t)}, x - x^{(t)} \rangle \right\} = \arg \min_{x \in K} \left\{ D_h(x||(\nabla h)^{-1}(\nabla h(x^{(t)}) - \eta g^{(t)})) \right\} \quad (8.7)$$

when replacing the squared Euclidean distance with the Bregman divergence.

8.1.2 Online mirror descent and the entropy mirror map

The mirror descent algorithm can easily be turned into an online algorithm, where the objective function is a summation of terms that are discovered one at a time. Suppose we have T convex functions f_1, \dots, f_T , and let $x^* \in \arg \min \sum_{t=1}^T f_t(x)$. We want to choose a sequence $x^{(1)}, \dots, x^{(T)}$ that minimizes the *regret* with respect to the best (single) solution in hindsight:

$$\min_{x^{(1)}, \dots, x^{(T)}} \sum_{t=1}^T f_t(x^{(t)}) - \sum_{t=1}^T f_t(x^*),$$

with the additional caveat that f_t is revealed at iteration t only after $x^{(t)}$ is determined, and therefore the choice $x^{(t)}$ can only depend on the already-seen terms f_1, \dots, f_{t-1} as well as previous iterates. Let $g^{(t)} \in \partial f_t(x^{(t)})$. We can directly use Eq. 8.6, leading to the update rule:

$$x^{(t+1)} = \arg \min_{x \in K} \left\{ \frac{1}{2} \|x - (x^{(t)} - \eta g^{(t)})\|^2 \right\} = \text{Proj}_K \left(x^{(t)} - \eta g^{(t)} \right),$$

and replacing the Euclidean distance with the Bregman divergence yields Eq. 8.7, which we restate below:

$$x^{(t+1)} = \arg \min_{x \in K} \left\{ D_h(x \| (\nabla h)^{-1}(\nabla h(x^{(t)}) - \eta g^{(t)})) \right\} = \text{Proj}_K^{D_h} \left((\nabla h)^{-1}(\nabla h(x^{(t)}) - \eta g^{(t)}) \right). \quad (8.8)$$

In the two above equations, we use Proj_K to emphasize that $x^{(t+1)}$ is simply the projection onto K of the unconstrained iterate: using the Euclidean norm for the standard projected subgradient descent approach, and using the Bregman divergence D_h , denoted $\text{Proj}_K^{D_h}$, for the more general mirror descent approach. It is immediate to verify that the value of $x^{(t+1)}$ is determined using the subgradient of f_t but not the subgradient of f_{t+1} , so this update rule can be applied to the online setting: at time t , the iterate $x^{(t)}$ is chosen by combining $x^{(t-1)}$ and a subgradient of f_{t-1} , so we are not using the yet-to-be-revealed term f_t .

Remark 8.3. *An algorithm for the online setting can be applied to the offline setting by letting $f_t = f$ for all t , and considering the average of the iterates $\frac{1}{T} \sum_{t=1}^T x^{(t)}$. If the regret is asymptotically smaller than T , the regret bound can be directly applied to get convergence to a desired error tolerance: this can be verified with straightforward algebraic manipulations.*

The convergence of mirror descent in the online setting is well known. To formally state a convergence result, we need the concept of dual norm, because the (sub)gradients of f_t live in the dual vector space.

Definition 8.4 (Dual norm). *Given a vector space V with inner product $\langle \cdot, \cdot \rangle$ and norm $\|\cdot\|$, the dual norm on V^* is defined as:*

$$\|y\|_* := \max_{x: \|x\|=1} \langle y, x \rangle,$$

for any $y \in V^*$.

Theorem 8.5 (Convergence of mirror descent; based on Thm. 4.2 in [Bansal and Gupta, 2019] and Thm. 4.1 in [Beck and Teboulle, 2003]). *Let h be α -strongly convex. The mirror descent algorithm with step size η , starting at the point $x^{(1)}$, produces a sequence x_2, \dots, x_T with subgradients $g^{(t)} \in \partial f_t(x^{(t)})$ such that:*

$$\sum_{t=1}^T f_t(x^{(t)}) - \sum_{t=1}^T f_t(x^*) \leq \frac{1}{\eta} D_h(x^* \| x^{(1)}) + \frac{\eta}{2\alpha} \sum_{t=1}^T \|g^{(t)}\|_*^2.$$

Mirror descent over the set of density matrices. We now describe a specific instantiation of the online mirror descent framework, that we use twice in the rest of this chapter and that serves as the basis for obtaining quantum algorithms. Let $\mathcal{S}_{+,1}^n$ be the set of density matrices, i.e., positive semidefinite matrices with unit trace (see Sect. 1.4), of size $n \times n$. We apply the framework to problems of this form:

$$\min_{\rho^{(1)}, \dots, \rho^{(T)} \in \mathcal{S}_{+,1}^n} \sum_{t=1}^T f_t(\rho^{(t)}),$$

where the feasible set is $K = \mathcal{S}_{+,1}^n$. Recall that f_1 is revealed only after $x^{(1)}$ is chosen; thus, $x^{(1)}$ is chosen independently of the objective function, and can be taken to be a given initial point; we set $\rho^{(1)} = I/n$. (Throughout this chapter, to shorten notation we denote by I the $n \times n$ density matrix, i.e., $I = I_{n \times n}$.) We assume we are able to compute $G^{(t)} \in \partial f_t(\rho^{(t)})$; we denote it with a capital letter because now, given that $\rho^{(t)}$ is a matrix, the subgradient is a matrix as well. We use the update rule in Eq. 8.5, where our iterate $x^{(t)}$ should now be interpreted as the vectorization of the matrix $\rho^{(t)}$, and the inner product is the trace inner product $\langle A, B \rangle := \text{Tr}(AB^\dagger)$.

Remark 8.6. *Considering how we defined the inner product in Ch. 1, it would be more consistent to define $\langle A, B \rangle = \text{Tr}(A^\dagger B)$; typically, in engineering it is common to apply the \dagger to the first argument of the inner product. However, in this chapter the definition $\langle A, B \rangle := \text{Tr}(AB^\dagger)$ makes*

the notation considerably less cumbersome, because for the cases of interest here, the matrix B is always Hermitian, so $\langle A, B \rangle = \text{Tr}(AB)$. In the literature, depending on the field, both definitions are used. It is possible to use the definition $\langle A, B \rangle = \text{Tr}(A^\dagger B)$ throughout this chapter and obtain the same results. (In fact, for the cases where we use the inner product, the matrix A is also Hermitian — even though it is not required to be so — and changing the definition would not impact the conclusions.)

We need an appropriate mirror map. The von Neumann negative entropy:

$$h(\rho) = \text{Tr}(\rho \log \rho - \rho)$$

is strictly convex and satisfies the conditions of Def. 8.2, leading to a divergence D_h that is known as the *quantum relative entropy* [Nielsen and Chuang, 2002]:

$$D_h(\rho \parallel \sigma) = \text{Tr}(\rho \log \rho - \rho \log \sigma - \rho + \sigma),$$

which simplifies to $\text{Tr}(\rho \log \rho - \rho \log \sigma)$ if ρ, σ are density matrices. Plugging h and D_h in Eq. 8.8, using the fact that $\nabla h(\rho) = \log \rho$ and $(\nabla h)^{-1}(M) = \exp(M)$, the mirror descent algorithm follows these steps at iteration t : given the current iterate $\rho^{(t)}$,

- we use ∇h to map $\rho^{(t)}$ to dual space, i.e., we compute its matrix logarithm (which yields $-\eta \sum_{\tau=1}^{t-1} G^{(\tau)}$ up to normalization, see below for a more detailed analysis);
- we add a multiple of the subgradient, specifically $-\eta G^{(t)}$, obtaining the new iterate in dual space;
- we use the inverse $(\nabla h)^{-1}$ to map back to primal space, i.e., we apply the matrix exponential;
- we project the candidate solution onto the set of density matrices, by normalizing its trace so that it has unit trace.

The steps of the algorithm are depicted in Fig. 8.1.

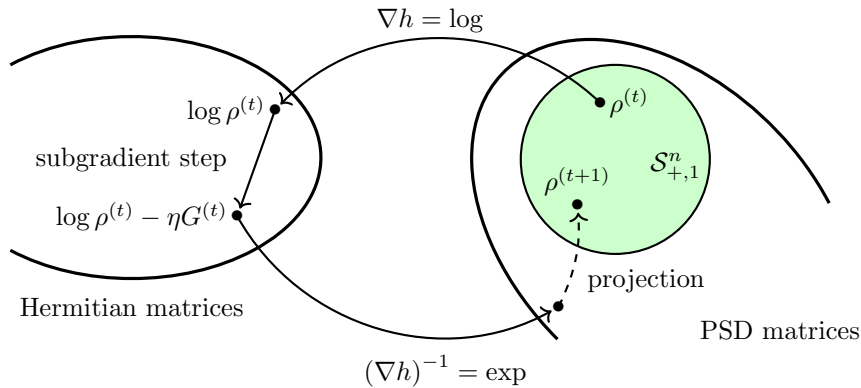


Figure 8.1: Steps of the mirror descent algorithm using the von Neumann negative entropy as the mirror map.

We can simplify the algorithm further by keeping track of the iterate in the dual space, i.e., in its matrix logarithm form, and noting that the iterates $\rho^{(t)}$ are Gibbs states (Def. 7.34). Below, $\mathbb{0}^{n \times n}$ denotes the all-zero matrix of size $n \times n$.

Proposition 8.7. For a sequence of Hermitian matrices $\mathcal{H}^{(1)}, \mathcal{H}^{(2)}, \dots$, define:

$$\rho^{(t)} := \exp(\mathcal{H}^{(t)}) / \text{Tr}(\exp(\mathcal{H}^{(t)})),$$

i.e., $\rho^{(t)}$ is the Gibbs state corresponding to the Hamiltonian $\mathcal{H}^{(t)}$. If we let:

$$\begin{aligned}\mathcal{H}^{(1)} &= \mathbb{0}^{n \times n}, \\ \mathcal{H}^{(t+1)} &= \mathcal{H}^{(t)} - \eta G^{(t)},\end{aligned}$$

then the sequence $\rho^{(1)}, \rho^{(2)}, \dots$ coincides with the iterates of the mirror descent algorithm using the von Neumann negative entropy as the mirror map, and I/n as the initial point.

Proof. By induction. For $t = 1$, $\rho^{(1)} = \exp(\mathbb{0}^{n \times n}) / \text{Tr}(\exp(\mathbb{0}^{n \times n})) = I/n$, which is the starting point of the mirror descent algorithm. Now suppose the inductive hypothesis holds for some t ; then we have:

$$\log \rho^{(t)} = \log \left(\exp(\mathcal{H}^{(t)}) / \text{Tr} \left(\exp(\mathcal{H}^{(t)}) \right) \right) = \mathcal{H}^{(t)} - \log \text{Tr} \left(\exp(\mathcal{H}^{(t)}) \right) I.$$

Exploiting the fact that ∇h is well-defined over $\mathcal{S}_{+,1}^n$, and its inverse is also well-defined for all Hermitian matrices, Eq. (8.8) has the following explicit solution, see [Tsuda et al., 2005]:

$$\rho^{(t+1)} = \frac{\exp(\log \rho^{(t)} - \eta G^{(t)})}{\text{Tr} \left(\exp(\log \rho^{(t)} - \eta G^{(t)}) \right)} \text{ where } G^{(t)} \in \partial f_t(\rho^{(t)}). \quad (8.9)$$

Intuitively, this can be verified by following the step-by-step description of the algorithm just before the proposition statement. Then:

$$\begin{aligned}\rho^{(t+1)} &= \frac{\exp(\log \rho^{(t)} - \eta G^{(t)})}{\text{Tr} \left(\exp(\log \rho^{(t)} - \eta G^{(t)}) \right)} \\ &= \frac{\exp(\mathcal{H}^{(t)} - \log \text{Tr} \left(\exp(\mathcal{H}^{(t)}) \right) I - \eta G^{(t)})}{\text{Tr} \left(\exp(\mathcal{H}^{(t)} - \log \text{Tr} \left(\exp(\mathcal{H}^{(t)}) \right) I - \eta G^{(t)}) \right)} \\ &= \frac{\exp(\mathcal{H}^{(t)} - \eta G^{(t)})}{\text{Tr} \left(\exp(\mathcal{H}^{(t)} - \eta G^{(t)}) \right)} = \frac{\exp(\mathcal{H}^{(t+1)})}{\text{Tr} \left(\exp(\mathcal{H}^{(t+1)}) \right)},\end{aligned}$$

where the third equality is due to the fact that $\exp(\mathcal{H} + \lambda I) / \text{Tr}(\exp(\mathcal{H} + \lambda I)) = \exp(\mathcal{H}) / \text{Tr}(\exp(\mathcal{H}))$ for all $\lambda \in \mathbb{R}$, so we can eliminate the term $-\log \text{Tr}(\exp(\mathcal{H}^{(t)})) I$ appearing at the numerator and denominator. \square

Using the expression for the matrices $\mathcal{H}^{(t)}$ in Prop. 8.7, in Alg. 6 we give the pseudocode for the mirror descent algorithm with the von Neumann negative entropy as the mirror map. The

Algorithm 6: Online mirror descent with the von Neumann negative entropy as the mirror map. Also known as Matrix Multiplicative Weights Update (MMWU) algorithm.

Input: Parameter $\eta \leq 1$, number of rounds T , dimension n .

Output: Sequence of density matrices $\rho^{(1)}, \dots, \rho^{(T)} \in \mathcal{S}_{+,1}^n$.

1 **Initialize:** $\mathcal{H}^{(1)} \leftarrow \mathbb{0}^{n \times n}$.

2 **for** $t = 1, \dots, T - 1$ **do**

3 Compute $\rho^{(t)} = \exp(\mathcal{H}^{(t)}) / \text{Tr}(\exp(\mathcal{H}^{(t)}))$.

4 Obtain subgradient $G^{(t)} \in \partial f_t(\rho^{(t)})$.

5 Compute $\mathcal{H}^{(t+1)} = \mathcal{H}^{(t)} - \eta G^{(t)}$, leading to the explicit update rule:

$$\rho^{(t+1)} = \exp \left(-\eta \sum_{\tau=1}^t G^{(\tau)} \right) / \text{Tr} \left(\exp \left(-\eta \sum_{\tau=1}^t G^{(\tau)} \right) \right).$$

6 **end**

7 **return** $\rho^{(1)}, \dots, \rho^{(T)}$.

convergence of Alg. 6 follows directly from Thm. 8.5. This gives a regret bound of:

$$\frac{\log n}{\eta} + \frac{\eta}{2} \sum_{t=1}^T \left\| G^{(t)} \right\|_*^2,$$

because $D_h(\rho \| I/n) = \log n - \sum_j \lambda_j(\rho) \log \frac{1}{\lambda_j(\rho)} \leq \log n$ for every ρ , where $\lambda_j(\rho)$ are the eigenvalues of ρ (see, e.g., [Tsuda et al., 2005]), and the strong convexity parameter α is 1 [Yu, 2013]. Alg. 6 is also known as the Matrix Multiplicative Weights Update (MMWU) algorithm: we discuss this interpretation in Sect. 8.2.1, where we additionally prove the convergence of the algorithm (obtaining a result akin to Thm. 8.5) from first principles.

8.2 Classical MMWU algorithm for SDP

As mentioned at the beginning of this chapter, the Multiplicative Weights Update (MWU) algorithm is a meta-algorithm; here, we are interested in its application to semidefinite optimization. Rather than describing the traditional MWU algorithm, we directly proceed with a description of the *matrix* MWU (MMWU) algorithm, which is the relevant framework for the quantum algorithms that constitute the central topic of this chapter.

8.2.1 From mirror descent to the MMWU algorithm

The MMWU algorithm can be derived from the mirror descent framework in the context of a certain two-player game; the connection to the solution of (P-SDP) is not obvious from the definition of the game, but we make it explicit in Sect. 8.2.2. The game is defined as follows. It is a two-player game; in each round t we choose a density matrix $\rho^{(t)}$, and an adversary chooses a matrix $M^{(t)}$ satisfying $\|M^{(t)}\| \leq 1$. The matrix $\rho^{(t)}$ is allowed to depend on the adversary's choices in previous rounds $M^{(1)}, \dots, M^{(t-1)}$, but not in the current round; i.e., we choose $\rho^{(t)}$ before $M^{(t)}$ is revealed. At the end of each round we pay $\text{Tr}(M^{(t)}\rho^{(t)})$, and our objective is to pay as little as possible over T rounds, i.e., minimize the total loss accumulated over T rounds.

Formally, the problem of determining an optimal strategy for this game can be formulated as follows. We want to choose $\rho^{(1)}, \dots, \rho^{(T)} \in \mathcal{S}_{+,1}^n$ so that:

$$\sum_{t=1}^T f_t(\rho^{(t)}) := \sum_{t=1}^T \text{Tr}(M^{(t)}\rho^{(t)}) \quad (8.10)$$

is minimized, with the restriction that the density matrices $\rho^{(t)}$ must be chosen sequentially and each matrix $M^{(t)}$, and therefore the function f_t , is revealed after we choose the corresponding $\rho^{(t)}$, so $\rho^{(t)}$ can only depend on $M^{(1)}, \dots, M^{(t-1)}$ and on previous iterates. This is exactly the setting for online mirror descent using the von Neumann negative entropy as the mirror map, discussed in Sect. 8.1.2. We therefore have an algorithm to attain low regret, i.e., a strategy that performs relatively well compared to the best single solution in hindsight (called x^* in Sect. 8.1.2). The best single density matrix (i.e., round-independent choice) in hindsight is the rank-1 matrix corresponding to the unit eigenvector v of $\sum_{t=1}^T M^{(t)}$ with the smallest eigenvalue: indeed,

$$\text{Tr}\left(\sum_{t=1}^T M^{(t)} v v^\top\right) = \lambda_{\min}\left(\sum_{t=1}^T M^{(t)}\right),$$

where $\lambda_{\min}\left(\sum_{t=1}^T M^{(t)}\right)$ denotes the smallest eigenvalue, and it is immediate to observe that the objective function value of any given density matrix — if the same matrix is chosen in every round — is at least as large as $\lambda_{\min}\left(\sum_{t=1}^T M^{(t)}\right)$. Of course, in general we cannot hope to construct a solution that attains value $\lambda_{\min}\left(\sum_{t=1}^T M^{(t)}\right)$, because to determine $v v^\top$ we would need to know

all the matrices $M^{(t)}$ in advance. Thus, we attempt to minimize (or at least bound) the regret, which for this problem is:

$$\sum_{t=1}^T \text{Tr} \left(M^{(t)} \rho^{(t)} \right) - \lambda_{\min} \left(\sum_{t=1}^T M^{(t)} \right).$$

This ensures that the performance attained at the task at hand is always satisfactory in some sense.

Remark 8.8. *In the game described above we are allowed to play a different $\rho^{(t)}$ in every round, so if we knew what the opponent is about to play, it would be optimal to choose $\rho^{(t)}$ such that $\text{Tr} \left(M^{(t)} \rho^{(t)} \right) = \lambda_{\min} \left(M^{(t)} \right)$ in every round: this minimizes the objective function contribution f_t for each t . However, as usual in the context of two-player games, we assume that we do not know the opponent's play in advance, and we want a strategy that performs well even if the opponent plays optimally against us.*

We apply Alg. 6, as described in Sect. 8.1.2: the feasible set is $K = \mathcal{S}_{+,1}^n$, and for the initial point we take $\rho^{(1)} = I/n$. At the end of each iteration t we are presented with the term $M^{(t)}$ that specifies f_t in the objective function, and note that $M^{(t)} \in \partial f_t(\rho^{(t)})$ because $f_t(\rho^{(t)}) = \text{Tr} \left(M^{(t)} \rho^{(t)} \right)$ is linear in $\rho^{(t)}$ with respect to the trace inner product.

Remark 8.9. *It is helpful to think of the iterates $\rho^{(t)}$ as vectors, obtained by vectorizing the corresponding matrices, i.e., taking the columns of the matrix and stacking them on top of each other to obtain a vector. With this transformation in mind, it is easy to see why $f_t(\rho^{(t)}) = \text{Tr} \left(M^{(t)} \rho^{(t)} \right) = \langle M^{(t)}, (\rho^{(t)})^\dagger \rangle$ is linear: the trace inner product is equal to the standard inner product on complex spaces (i.e., $\langle a, b \rangle = b^\dagger a = \sum_j a_j \bar{b}_j$) between the vectorizations of $M^{(t)}$ and $\rho^{(t)}$ — recall Rem. 8.6. Because the second argument of the inner product is a density matrix and therefore Hermitian, we can drop the \dagger : $\text{Tr} \left(M^{(t)} \rho^{(t)} \right) = \langle M^{(t)}, \rho^{(t)} \rangle$.*

We use the update rule in Eq. 8.9. By following Alg. 6, at every iteration t we choose a properly normalized version of $\exp \left(-\eta \sum_{\tau=1}^{t-1} M^{(\tau)} \right)$ for some parameter $0 < \eta \leq 1$; the normalization ensures that we output matrices with unit trace, which is a requirement of the game because we are only allowed to play density matrices. Alg. 6 is usually called “MMWU algorithm” in this context. Although we can derive a regret bound using Thm. 8.5, see the discussion in Sect. 8.1.2 as well as the proof in [Tsuda et al., 2005] using the quantum relative entropy as a potential function, in Thm. 8.10 we provide a tailored and self-contained proof. The main purpose of the proof is to showcase some helpful inequalities and techniques for handling similar cases.

Theorem 8.10 (Regret bound of MMWU algorithm; Thm. 3.1 in [Arora and Kale, 2016]). *For any sequence of loss matrices $M^{(1)}, \dots, M^{(T)}$ with $\|M^{(t)}\| \leq 1$, suppose we run Alg. 6 setting $f_t(\rho) = \text{Tr} \left(M^{(t)} \rho \right)$ with subgradients $M^{(t)} \in \partial f_t(\rho^{(t)})$. Then, the algorithm generates density matrices $\rho^{(1)}, \dots, \rho^{(T)}$ such that:*

$$\text{Tr} \left(\sum_{t=1}^T M^{(t)} \rho^{(t)} \right) \leq \lambda_{\min} \left(\sum_{t=1}^T M^{(t)} \right) + \eta \text{Tr} \left(\sum_{t=1}^T (M^{(t)})^2 \rho^{(t)} \right) + \frac{\ln n}{\eta}. \quad (8.11)$$

Proof. For the main chain of inequalities in the proof, we need the Golden-Thompson inequality:

$$\text{Tr} \left(\exp(A + B) \right) \leq \text{Tr} \left(\exp(A) \exp(B) \right), \quad (8.12)$$

as well as the following inequality:

$$\exp(-A) \preceq (I - A + A^2), \quad (8.13)$$

which holds for every Hermitian matrix A with $\|A\| \leq 1$ because the corresponding scalar inequality $\exp(-a) \leq 1 - a + a^2$ also holds for every $|a| \leq 1$, and diagonalizing the matrix A shows that Eq. (8.13) holds.

To simplify the calculations, it is convenient to define

$$W^{(t)} := \exp \left(-\eta \sum_{\tau=1}^{t-1} M^{(\tau)} \right),$$

and note that:

$$W^{(t)} = \text{Tr} \left(W^{(t)} \right) \rho^{(t)}. \quad (8.14)$$

Thus, $W^{(t)}$ is just a de-normalized version of the density matrices constructed by Alg. 6, where we only keep the numerator and therefore these matrices do not necessarily have unit trace.

We now proceed to the core of the proof. To prove the desired result, we define a potential function $\Phi(W^{(t)})$, and derive upper and lower bounds to its value as t increases. Combining the bounds for $t = T + 1$ yields the expression that we aim to obtain. We define the potential function as:

$$\Phi(W^{(t)}) := \text{Tr} \left(W^{(t)} \right).$$

We have:

$$\begin{aligned} \Phi(W^{(t+1)}) &= \text{Tr} \left(\exp \left(-\eta \sum_{\tau=1}^t M^{(\tau)} \right) \right) \\ &\leq \text{Tr} \left(\exp \left(-\eta \sum_{\tau=1}^{t-1} M^{(\tau)} \right) \exp(-\eta M^{(t)}) \right) && \text{(by (8.12))} \\ &= \text{Tr} \left(W^{(t)} \exp(-\eta M^{(t)}) \right) \\ &\leq \text{Tr} \left(W^{(t)} (I - \eta M^{(t)} + \eta^2 (M^{(t)})^2) \right) && \text{(by (8.13))} \\ &= \text{Tr} \left(W^{(t)} \right) (1 - \eta \text{Tr} \left(M^{(t)} \rho^{(t)} \right) + \eta^2 \text{Tr} \left((M^{(t)})^2 \rho^{(t)} \right)) && \text{(by (8.14))} \\ &\leq \Phi(W^{(t)}) \exp \left(-\eta \text{Tr} \left(M^{(t)} \rho^{(t)} \right) + \eta^2 \text{Tr} \left((M^{(t)})^2 \rho^{(t)} \right) \right). && \text{(using } e^x \geq 1 + x) \end{aligned}$$

We can now recursively apply

$$\Phi(W^{(t+1)}) \leq \Phi(W^{(t)}) \exp \left(-\eta \text{Tr} \left(M^{(t)} \rho^{(t)} \right) + \eta^2 \text{Tr} \left((M^{(t)})^2 \rho^{(t)} \right) \right),$$

expanding the r.h.s. down to $t = 1$, and use $\Phi(W^{(1)}) = \Phi(I) = n$ to obtain:

$$\Phi(W^{(T+1)}) \leq n \exp \left(-\eta \sum_{t=1}^T \text{Tr} \left(M^{(t)} \rho^{(t)} \right) + \sum_{t=1}^T \eta^2 \text{Tr} \left((M^{(t)})^2 \rho^{(t)} \right) \right).$$

We also have:

$$\Phi(W^{(T+1)}) = \text{Tr} \left(\exp \left(-\eta \sum_{\tau=1}^T M^{(\tau)} \right) \right) \geq \exp \left(\lambda_{\min} \left(-\eta \sum_{\tau=1}^T M^{(\tau)} \right) \right),$$

because the trace is the sum of the eigenvalues. Combining the lower bound and upper bound for $\Phi(W^{(T+1)})$, we obtain:

$$\exp \left(\lambda_{\min} \left(-\eta \sum_{\tau=1}^T M^{(\tau)} \right) \right) \leq n \exp \left(-\eta \sum_{t=1}^T \text{Tr} \left(M^{(t)} \rho^{(t)} \right) + \sum_{t=1}^T \eta^2 \text{Tr} \left((M^{(t)})^2 \rho^{(t)} \right) \right).$$

Taking the natural logarithm on both sides, using linearity of the trace, and rearranging the terms yields:

$$\text{Tr} \left(\sum_{t=1}^T M^{(t)} \rho^{(t)} \right) \leq \lambda_{\min} \left(\sum_{t=1}^T M^{(t)} \right) + \eta \text{Tr} \left(\sum_{t=1}^T (M^{(t)})^2 \rho^{(t)} \right) + \frac{\ln n}{\eta}.$$

□

Note that Thm. 8.10 requires $\|M^{(t)}\| \leq 1$; in Thm. 8.5, there is no bound on the norm of the subgradients, but the final regret bound depends on such norms. A tradeoff of this kind is generally inescapable in the framework of online mirror descent or MMWU: large subgradients (i.e., subgradients with large norm) typically lead to worse theoretical performance of the algorithm. Indeed, the maximum subgradient norm directly appears in the running time of the algorithm for SDP developed in Sect. 8.2.2.

8.2.2 Turning the MMWU algorithm into an SDP solver

We apply the MMWU algorithm to the primal-dual SDP pair (P-SDP)-(D-SDP), by developing a game such that a good strategy leads to (approximate) primal and dual solutions for the SDP. We make the following assumptions:

- (a) $A^{(1)} = I$ and $b_1 = R > 0$;
- (b) $\|C\| \leq 1$.

Assumption (a) ensures that any solution X satisfies $\text{Tr}(X) \leq R$. It also ensures that the dual has a strictly feasible solution, i.e., there exists a vector y satisfying $\sum_{j=1}^m y_j A^{(j)} - C \succ 0$, and this suffices to guarantee that strong duality holds. Thus, we can solve the primal or the dual and both yield the same optimal objective function value. Note that with these assumptions, the value of R is known in advance, as it is part of the input; the running time of the algorithms that we obtain depends on it.

We reduce the optimization question (“what is the optimal objective function value of P-SDP”) into a sequence of feasibility questions: for some given scalar γ , does there exist a primal feasible solution with value at least γ ? It is well known that we can approximately answer the optimization question by using binary search on γ . In particular, for the objective function the following inequality holds (recall Def. 7.31):

$$|\text{Tr}(CX)| \leq \|C\| \|X\|_{\text{Tr}} \leq R,$$

where the first inequality is known as a matrix Hölder inequality, and for the second inequality we used $\|X\|_{\text{Tr}} = \text{Tr}(X) \leq R$ (this requires $X \succeq 0$), and $\|C\| \leq 1$. Thus, we know that the optimal objective function value for the primal-dual pair lies in $[-R, R]$, and we can perform binary search to determine the optimal value:

- Set $\ell \leftarrow -R, u \leftarrow R$.
- Repeat until $u - \ell \leq \epsilon$:
 - Set $\gamma \leftarrow (\ell + u)/2$.
 - Solve a feasibility problem to determine if there exists a solution to (P-SDP)-(D-SDP) with value at least γ .
 - If “yes”, set $\ell \leftarrow (\ell + u)/2$. If “no”, set $u \leftarrow (\ell + u)/2$.

This algorithm halves the search interval $[\ell, u]$ for the optimal value γ at every iteration, and therefore takes $\mathcal{O}(\log(R/\epsilon))$ iterations to determine an interval of size ϵ that contains the optimal objective function value.

We have just seen that we can solve problem (P-SDP) if we can answer the question “does there exist a primal feasible solution with value at least γ ?” for arbitrary $\gamma \in [-R, R]$. To answer the question using the MMWU algorithm (i.e., the mirror descent scheme of Alg. 6), a sketch of the idea is as follows. We start from a candidate primal solution $\rho^{(0)} \succeq 0$. At each step t , we generate a vector $y^{(t)}$ of dual variables such that $\text{Tr}\left(\left(\sum_{j=1}^m y_j^{(t)} A^{(j)} - C\right)\rho^{(t)}\right) \geq 0$, and such that $b^\top y \leq \gamma$. We use $M^{(t)} = \sum_{j=1}^m y_j^{(t)} A^{(j)} - C$ as the adversary response. Then Eq. 8.11 from Thm. 8.10 states that:

$$\lambda_{\min}\left(\sum_{t=1}^T M^{(t)}\right) \geq \text{Tr}\left(\sum_{t=1}^T M^{(t)}\rho^{(t)}\right) - \eta \text{Tr}\left(\sum_{t=1}^T (M^{(t)})^2 \rho^{(t)}\right) - \frac{\ln n}{\eta} \geq -\eta T - \frac{\ln n}{\eta}, \quad (8.15)$$

because $\text{Tr}\left(\sum_{t=1}^T M^{(t)} \rho^{(t)}\right) \geq 0$ by construction, and $\text{Tr}\left((M^{(t)})^2 \rho^{(t)}\right) \leq 1$ by the matrix Hölder inequality. Dividing by T on both sides of Eq. 8.15, we find that $\frac{1}{T} \sum_{t=1}^T M^{(t)}$ is almost positive semidefinite: its smallest eigenvalue is only slightly negative, $\geq -\eta - \frac{\ln n}{\eta T}$. Recalling the definition of $M^{(t)}$, this implies that $\frac{1}{T} \sum_{t=1}^T \sum_{j=1}^m y_j^{(t)} A^{(j)} - C$ is almost positive semidefinite. Thus, if we define $y = \frac{1}{T} \sum_{t=1}^T y^{(t)}$ (the average of the dual vectors $y^{(t)}$ generated), we obtained an almost feasible solution y for the dual (D-SDP), and such that $b^\top y \leq \gamma$. Using the fact that $A^{(1)}$ is assumed to be the identity matrix, we can make the dual solution y feasible by increasing y_1 until $\sum_{j=1}^m y_j A^{(j)} - C \succeq 0$: the necessary shift is at most $\eta + \frac{\ln n}{\eta T}$, and with the right choice of parameters, we can ensure that the objective function deteriorates by at most ϵ , so that $b^\top y \leq \gamma + \epsilon$. This dual feasible solution y therefore certifies that there can be no primal feasible solution with value $> \gamma + \epsilon$, approximately answering the question that we posed at the beginning, and allowing us to continue in the binary search for the optimal objective function value. Otherwise, i.e., if we cannot find a vector $y^{(t)}$ with the desired properties, the primal solution $\rho^{(t)}$ can be shown to be primal feasible (after rescaling), allowing us to continue in the binary search.

Let us formalize the idea sketched in the previous paragraph. We define an oracle that is used to construct a helpful adversary matrix $M^{(t)}$ at iteration t , based on the information available up to iteration t . We call this PIC-ORACLE, for “Primal-Infeasibility-Certificate Oracle”. The purpose of the oracle is to either prove that the primal solution $X^{(t)}$ is feasible, or give some dual information regarding its infeasibility. (We use ρ for density matrices, X for general — not necessarily trace-normalized — matrices.) The dual information, in the form of a vector $y^{(t)}$, is used to construct $M^{(t)}$. The oracle makes use of a certain polytope, defined next.

Definition 8.11 (Primal-infeasibility-certificate polytope). *We define $P_\epsilon(X)$ as the following polytope, parameterized by a scalar $\epsilon > 0$ and matrix $X \succeq 0$:*

$$P_\epsilon(X) := \left\{ y \in \mathbb{R}^m : \begin{array}{l} b^\top y \leq \gamma \\ \text{Tr}\left(\left(\sum_{j=1}^m y_j A^{(j)} - C\right)X\right) \geq -\epsilon \\ y \geq 0 \end{array} \right\}. \quad (8.16)$$

The definition of the polytope should depend on γ , but in every iteration of the algorithm (using the reduction from optimality to feasibility) γ is fixed, so to ease notation we neglect this detail: γ can be considered part of the problem data (within a single iteration) just as $A^{(j)}$ and C . The oracle $\text{PIC-ORACLE}_\epsilon(X)$ is the function defined as follows:

$$\text{PIC-ORACLE}_\epsilon(X) := \begin{cases} y \in P_\epsilon(X) & \text{if } P_\epsilon(X) \neq \emptyset \\ \text{“failure”} & \text{otherwise.} \end{cases}$$

Two properties of $P_\epsilon(X)$ are important to understand why $\text{PIC-ORACLE}_\epsilon(X)$ gives information about the feasibility or infeasibility of a given primal solution X .

Lemma 8.12 (Lem. 4.2 in [Arora and Kale, 2016]). *Let $X \succeq 0$. Suppose $P_\epsilon(X)$ (Eq. 8.16) is empty. Then, up to rescaling, the matrix X is feasible for (P-SDP) with objective function value at least γ . On the contrary, suppose $P_\epsilon(X)$ is nonempty. Then X is either not feasible for (P-SDP), or it has objective function value at most $\gamma + \epsilon$.*

Proof. Suppose $P_\epsilon(X)$ is empty. Consider the following LP:

$$\min \left. \begin{array}{l} b^\top y \\ \text{Tr}\left(\sum_{j=1}^m y_j A^{(j)} X\right) \geq \text{Tr}(CX) - \epsilon \\ y \geq 0, \end{array} \right\} \quad (8.17)$$

and its dual:

$$\max \left. \begin{array}{l} (\text{Tr}(CX) - \epsilon)z \\ \forall j = 1 \dots, m \quad \text{Tr}(A^{(j)} X) z \leq b_j \\ z \geq 0. \end{array} \right\} \quad (8.18)$$

This is a possibly-outdated preprint, using the author’s lecture notes, of the book “Quantum algorithms for optimizers,” edited by SIAM. All rights to the book’s material belong to SIAM. Please refer to the SIAM version of the book.

Note that solving problem (8.17) is equivalent to determining if $P_\epsilon(X)$ is empty: indeed, if $P_\epsilon(X)$ is empty, it must be the case that the optimal value of problem (8.17) is greater than γ (at least one feasible solution for problem (8.17) exists, because $A^{(1)} = I$). So the optimum z^* of the dual, problem (8.18), has value $\geq \gamma$. Then z^*X is a feasible solution to the primal (this is directly implied by the constraints in problem (8.18)), and:

$$\text{Tr}(CXz^*) \geq \gamma + \epsilon z^* \geq \gamma,$$

showing the first half of the result.

Suppose now $P_\epsilon(X)$ is nonempty and $y \in P_\epsilon(X)$. Assume X is primal feasible — if not, the statement of the lemma already holds. Then from the constraints of problems (8.16) and (P-SDP) we have:

$$\text{Tr}(CX) \leq \text{Tr}\left(\left(\sum_{j=1}^m y_j A^{(j)}\right)X\right) + \epsilon \leq \sum_{j=1}^m y_j b_j + \epsilon = b^\top y + \epsilon \leq \gamma + \epsilon,$$

showing that the objective function value of X is at most $\gamma + \epsilon$ and concluding the proof. \square

Lem. 8.12 shows that $\text{PIC-ORACLE}_\epsilon(X)$ can provide very useful information: it either shows that we already have a primal feasible solution with value at least γ , or it gives an infeasibility certificate: the dual vector y that it returns, which we call $y^{(t)}$ at iteration t , is the infeasibility certificate. We can use the infeasibility certificate $y^{(t)}$ to construct the matrix $M^{(t)}$ for the current iteration of Alg. 6, which, from our earlier discussion, is chosen as:

$$M^{(t)} = \sum_{j=1}^m y_j^{(t)} A^{(j)} - C. \quad (8.19)$$

There remains a technical issue to resolve: in Thm. 8.10 and the surrounding discussion, we assumed $\|M^{(t)}\| \leq 1$, but there is no guarantee that the choice in Eq. 8.19 satisfies this bound. Thus, we may have to rescale $M^{(t)}$. It turns out that the magnitude of the scaling factor affects the convergence speed of the algorithm: if we must scale aggressively, the algorithm makes less progress toward feasibility, and as a result it converges more slowly. Formally, the magnitude of the scaling parameter is called the *width* of the primal-infeasibility-certificate oracle.

Definition 8.13 (Width of PIC-ORACLE). *The width of $\text{PIC-ORACLE}_\epsilon(X)$ is the smallest w^* such that $\left\|\sum_{j=1}^m y_j A^{(j)} - C\right\| \leq w^*$ for every y returned by $\text{PIC-ORACLE}_\epsilon(X)$, when $\text{PIC-ORACLE}_\epsilon(X)$ is called with $\epsilon > 0$, $X \succeq 0$ and $\gamma \in [-R, R]$.*

The unscaled choice of $M^{(t)}$ in Eq. 8.19 may not satisfy $\|M^{(t)}\| \leq 1$, but it clearly does if we divide the r.h.s. by the width w^* defined in Def. 8.13, i.e., if we choose:

$$M^{(t)} = \frac{1}{w^*} \left(\sum_{j=1}^m y_j^{(t)} A^{(j)} - C \right). \quad (8.20)$$

This is the matrix $M^{(t)}$ that defines the objective function in iteration t for Alg. 6.

Remark 8.14. *The choice of $M^{(t)}$ immediately suggests that any upper bound for w^* suffices to guarantee the desired property $\|M^{(t)}\| \leq 1$. Because the convergence speed of the algorithm depends on the magnitude of the scaling, we should still aim to find a tight bound on w^* .*

At this point we have all the necessary components to give the pseudocode of the MMWU algorithm for SDP, see Alg. 7, and show its convergence. The algorithm closely follows the informal exposition given earlier in this section.

Theorem 8.15 (Convergence of MMWU algorithm for SDP; Thm. 4.4 in [Arora and Kale, 2016], Thm. 5 in [van Apeldoorn, 2020]). *Alg. 7 returns either a feasible solution for (P-SDP) with objective function value at least γ , or a feasible solution for (D-SDP) with objective function value at most $\gamma + \epsilon$.*

Algorithm 7: Matrix Multiplicative Weights Update (MMWU) algorithm for SDP.

Input: Description of (P-SDP), trace bound $R > 0$, objective function guess γ , tolerance $\epsilon > 0$, width bound $w > 0$, oracle $\text{PIC-ORACLE}_\epsilon(X)$ with width at most w .

Output: Either a feasible solution for (P-SDP) with objective function value at least γ , or a feasible solution for (D-SDP) with objective function value at most $\gamma + \epsilon$.

1 **Initialize:** $\rho^{(1)} \leftarrow I/n$, $\eta \leftarrow \sqrt{\frac{\ln n}{T}}$, $T \leftarrow \left\lceil \frac{9w^2 R^2 \ln n}{\epsilon^2} \right\rceil$.

2 **for** $t = 1, \dots, T$ **do**

3 **if** $\text{PIC-ORACLE}_{\epsilon/3}(R\rho^{(t)})$ outputs “failure” **then**
 4 | **return** $R\rho^{(t)}$ after rescaling as described in Lem. 8.12.

5 **end**

6 Otherwise, let $y^{(t)}$ be the vector generated by $\text{PIC-ORACLE}_{\epsilon/3}(R\rho^{(t)})$.

7 Compute $M^{(t)} = \frac{1}{w} \left(\sum_{j=1}^m y_j^{(t)} A^{(j)} - C \right)$.

8 Compute $\rho^{(t+1)} = \exp \left(-\eta \sum_{\tau=1}^t M^{(\tau)} \right) / \text{Tr} \left(\exp \left(-\eta \sum_{\tau=1}^t M^{(\tau)} \right) \right)$.

9 **end**

10 **return** $\frac{1}{T} \sum_{t=1}^T y^{(t)} + \frac{\epsilon}{R} e_1$, where $e_1 = (1, 0, 0, \dots) \in \mathbb{R}^m$.

Proof. There are two possible exit points of the algorithm: either $\text{PIC-ORACLE}_{\epsilon/3}(R\rho^{(t)})$ outputs “failure” at some iteration, in which case we return a primal solution, or $\text{PIC-ORACLE}_{\epsilon/3}(R\rho^{(t)})$ never outputs “failure”, and we return a dual vector in the last line of Alg. 7.

In case $\text{PIC-ORACLE}_{\epsilon/3}(R\rho^{(t)})$ outputs “failure” at some iteration, Lem. 8.12 shows that a properly scaled version of $R\rho^{(t)}$ is primal feasible and satisfies the desired conditions.

In the other case, in every iteration we return $M^{(t)}$ according to Eq. 8.20, so the following inequality holds by definition of $\text{PIC-ORACLE}_{\epsilon/3}(R\rho^{(t)})$ (recall Def. 8.11):

$$\text{Tr} \left(\left(\sum_{j=1}^m y_j^{(t)} A^{(j)} - C \right) R\rho^{(t)} \right) \geq -\frac{\epsilon}{3},$$

so by rearranging we find:

$$\text{Tr} \left(M^{(t)} \rho^{(t)} \right) = \text{Tr} \left(\frac{1}{w} \left(\sum_{j=1}^m y_j^{(t)} A^{(j)} - C \right) \rho^{(t)} \right) \geq -\frac{\epsilon}{3wR}. \quad (8.21)$$

Following the same argument that we used to obtain Eq. 8.15, we use Eq. 8.11 from Thm. 8.10, divided by T on both sides:

$$\lambda_{\min} \left(\frac{1}{T} \sum_{t=1}^T M^{(t)} \right) \geq \text{Tr} \left(\frac{1}{T} \sum_{t=1}^T M^{(t)} \rho^{(t)} \right) - \eta \text{Tr} \left(\frac{1}{T} \sum_{t=1}^T (M^{(t)})^2 \rho^{(t)} \right) - \frac{\ln n}{\eta T} \geq -\frac{\epsilon}{3wR} - \eta - \frac{\ln n}{\eta T},$$

where we used Eq. 8.21, and $\text{Tr} \left((M^{(t)})^2 \rho^{(t)} \right) \leq 1$. Plugging in the values for η and T , as defined in Alg. 7, we finally obtain:

$$\frac{1}{w} \lambda_{\min} \left(\frac{1}{T} \sum_{t=1}^T \left(\sum_{j=1}^m y_j^{(t)} A^{(j)} - C \right) \right) \geq -\frac{\epsilon}{3wR} - \frac{\epsilon}{3wR} - \frac{\epsilon}{3wR} \geq -\frac{\epsilon}{wR},$$

hence:

$$\lambda_{\min} \left(\frac{1}{T} \sum_{t=1}^T \left(\sum_{j=1}^m y_j^{(t)} A^{(j)} - C \right) \right) \geq -\frac{\epsilon}{R}. \quad (8.22)$$

Using $A^{(1)} = I$ and the fact that Alg. 7 returns $\bar{y} = \frac{1}{T} \sum_{t=1}^T y^{(t)} + \frac{\epsilon}{R} e_1$, we have:

$$\lambda_{\min} \left(\sum_{j=1}^m \bar{y}_j^{(t)} A^{(j)} - C \right) = \lambda_{\min} \left(\frac{1}{T} \sum_{t=1}^T \left(\sum_{j=1}^m y_j^{(t)} A^{(j)} - C \right) + \frac{\epsilon}{R} I \right) \geq -\frac{\epsilon}{R} + \frac{\epsilon}{R} \geq 0,$$

where the first inequality is due to Eq. 8.22. This implies that the solution returned by Alg. 7 is dual feasible, i.e.,

$$\sum_{j=1}^m \bar{y}_j^{(t)} A^{(j)} - C \succeq 0.$$

Using the definition of PIC-ORACLE $_{\epsilon/3}(R\rho^{(t)})$ and $b_1 = R$, the objective function value of this solution satisfies:

$$b^\top \bar{y} = b^\top \left(\frac{1}{T} \sum_{t=1}^T y^{(t)} + \frac{\epsilon}{R} e_1 \right) \leq \frac{1}{T} \sum_{t=1}^T \gamma + \epsilon = \gamma + \epsilon.$$

□

Thm. 8.15 shows that the MMWU algorithm correctly determines the feasibility of (P-SDP) in $T = \left\lceil \frac{9w^2 R^2 \ln n}{\epsilon^2} \right\rceil$ iterations. In each iteration the most expensive operation is the computation of the matrix exponential, that can be carried out in $\tilde{\mathcal{O}}(n^\omega/\epsilon)$ time, where ω is the matrix multiplication exponent, by truncating the corresponding Taylor series after $\mathcal{O}(1/\epsilon)$ terms.

Remark 8.16. *The best current estimate for ω is ≈ 2.37 [Williams et al., 2024]. In practice, however, the computational complexity is $\mathcal{O}(n^3)$, i.e., the same as the “usual” complexity for LU factorization. In other words, although in theory we can multiply two $n \times n$ matrices in time $\mathcal{O}(n^{2.37\dots})$, the algorithms used in practice run in time $\mathcal{O}(n^3)$, so the running time $\tilde{\mathcal{O}}(n^\omega/\epsilon)$ for computing the matrix exponential is only aspirational.*

The binary search scheme calls Alg. 7 as a subroutine $\mathcal{O}(\log(\|C\|R/\epsilon))$ times, and by storing the primal or dual solutions returned by Alg. 7 in each iteration of binary search, we can eventually return the primal feasible solution with the largest objective function value, and the dual solution with the tightest bound.

8.3 Quantum MMWU algorithm for SDP

Looking at the classical algorithm for semidefinite optimization described in Alg. 7, one step appears as a natural candidate for quantization: the preparation of the Gibbs states $\rho^{(t)}$, that can be prepared and sampled from with a complexity that scales as \sqrt{n} on a quantum computer, depending on the input model — this is discussed in Sect. 7.2.4. This seems a clear advantage over classical algorithms: the Gibbs states are $n \times n$ matrices, and the fastest known general algorithm to construct them relies on the computation of the matrix exponential, which runs in $\mathcal{O}(n^\omega)$ time, see Rem. 8.16. But exploiting this advantage is not straightforward. In each iteration of the algorithm we must be able to output a dual vector $y^{(t)}$, computed via PIC-ORACLE: the construction of a Gibbs state by itself may not be helpful. Finding a quantum algorithm that can execute all the necessary steps requires some additional effort.

For a proper discussion of the quantum algorithm we must specify the input model. We assume the following:

- For each of the matrices $A^{(j)}$, we have access to a controlled unitary that implements a block-encoding of the matrix. That is: we have a circuit with a control register such that if the control register contains $|\vec{j}\rangle$, we apply a block-encoding of $A^{(j)}$ on a register of appropriate size.
- For the matrix C , we have access to a unitary that implements a block-encoding of it.

For simplicity, we assume that each of these block-encodings has the same subnormalization factor α , uses p auxiliary qubits, and has negligible error $\xi_a \ll \epsilon$. We do not discuss the error of the block-encodings in too much detail because we have seen in Prop.s 7.21 and 7.29 that when we construct a block-encoding from classical data, using the sparse-oracle access model or the QRAM model, we can reduce the error of a block-encoding at merely polylogarithmic cost. Thus, although in principle we have to pay attention to the error parameter, to keep our exposition simple we just assume that the error is chosen small enough, and this affects the running time only polylogarithmically. In the following, we label as “negligible” errors that have polylogarithmic scaling under these assumptions, and do not keep track of them (as usual in $\tilde{O}(\cdot)$ notation).

8.3.1 Dealing with inexact trace values

Careful examination of Alg. 7 reveals that full knowledge of the iterates $\rho^{(t)}$ is not strictly necessary: in every iteration we simply need to be able to compute an infeasibility certificate $y^{(t)}$ from the dual problem. The Gibbs state $\rho^{(t)}$ has an effect on the algorithm only insofar as it defines the feasible dual vectors $y^{(t)}$, returned by PIC-ORACLE. In the language of mirror descent, knowledge of the primal solution does not matter as long as we can compute a subgradient. Therefore we can focus on constructing PIC-ORACLE, taking advantage of a quantum computer.

The scheme that we would like to use is to exploit Prop. 7.38 to construct each Gibbs state $\rho^{(t)}$, then apply the trace estimation procedure of Prop. 7.41 to compute all the trace inner products $\text{Tr}(A^{(j)}\rho^{(t)})$, $\text{Tr}(C\rho^{(t)})$ involved in PIC-ORACLE. This immediately raises an issue: the trace estimation incurs some error, therefore we must analyze the stability of the algorithm to errors in the definition of the polytope $P_\epsilon(X)$ describing PIC-ORACLE.

Remark 8.17. *Some specialized variants of the classical algorithm of Sect. 8.2.2 (i.e., Alg. 7) described in [Kale, 2007] also rely on perturbed versions of the polytope describing PIC-ORACLE: this is not a uniquely “quantum” feature. The advantage of using a perturbed polytope lies in the fact that we can get away with imprecise trace estimation procedures, which can lead to faster classical algorithms as well.*

We need a further assumption, on top of assumptions (a) and (b) given at the beginning of Sect. 8.2.2.

- (c) There exists an optimal solution to (D-SDP) satisfying $\|y\|_1 \leq r$, and the parameter $r \geq 1$ is part of the input to the algorithm.

Assumption (c) ensures that the set of feasible dual vectors is bounded. Using this assumption we define a hierarchy of relaxations of the feasible region of (D-SDP). For this, we need a more general version of the polytope $P_\epsilon(X)$, where the entries of the defining constraints are not fixed: subsequently, we apply the general version of $P_\epsilon(X)$ using some estimates of $\text{Tr}(A^{(j)}X)$, $\text{Tr}(CX)$ (possibly affected by error) as the entries of the defining constraints.

Definition 8.18 (Generalized primal-infeasibility-certificate polytope). *We define $\hat{P}(a, c)$ as the following polytope, parameterized by a vector $a \in \mathbb{R}^m$ and a scalar $c \in \mathbb{R}$:*

$$\hat{P}(a, c) := \left\{ y \in \mathbb{R}^m : \begin{array}{l} b^\top y \leq \gamma \\ \sum_{j=1}^m y_j \leq r \\ \sum_{j=1}^m a_j y_j \geq c \\ y \geq \mathbb{0} \end{array} \right\}. \quad (8.23)$$

Note that $\hat{P}(\text{Tr}(A^{(1)}X), \dots, \text{Tr}(A^{(m)}X), \text{Tr}(CX)) = P_0(X) \cap \{y : \|y\|_1 \leq r\}$. The hierarchy of relaxations is described in the following proposition.

Proposition 8.19 ([van Apeldoorn, 2020]). *Let $X \succeq 0$ and $\rho = X/\text{Tr}(X)$, with $\text{Tr}(X) \leq R$. Let $\theta \geq 0$. Let $\tilde{a} \in \mathbb{R}^m, \tilde{c} \in \mathbb{R}$ satisfy:*

$$|\text{Tr}(C\rho) - \tilde{c}| \leq \theta, \quad \left| \text{Tr}(A^{(j)}\rho) - \tilde{a}_j \right| \leq \theta \quad \forall j = 1, \dots, m.$$

This is a possibly-outdated preprint, using the author’s lecture notes, of the book “Quantum algorithms for optimizers,” edited by SIAM. All rights to the book’s material belong to SIAM. Please refer to the SIAM version of the book.

The following chain of inclusions holds:

$$(P_0(X) \cap \{y : \|y\|_1 \leq r\}) \subseteq \hat{P}(\tilde{a}, \tilde{c} - (r+1)\theta) \subseteq (P_{4Rr\theta}(X) \cap \{y : \|y\|_1 \leq r\}).$$

Proof. Let $\bar{y} \in P_0(X) \cap \{y : \|y\|_1 \leq r\}$. We have:

$$\sum_{j=1}^m \tilde{a}_j \bar{y}_j \geq \sum_{j=1}^m \left(\text{Tr} \left(A^{(j)} \rho \right) - \theta \right) \bar{y}_j \geq \text{Tr}(C\rho) - \theta \|y\|_1 \geq \tilde{c} - (r+1)\theta,$$

where the first inequality used the definition of \tilde{a} with nonnegativity of \bar{y} , the second inequality used $\text{Tr} \left(\left(\sum_{j=1}^m y_j A^{(j)} - C \right) X \right) \geq 0$ (from the constraints of Eq. 8.16) and $\bar{y} \geq 0$, the last inequality used $\|y\|_1 \leq r$. This shows the first inclusion.

For the second inclusion, let $\bar{y} \in \hat{P}(\tilde{a}, \tilde{c} - (r+1)\theta)$. Then:

$$\begin{aligned} \text{Tr} \left(\left(\sum_{j=1}^m \bar{y}_j A^{(j)} - C \right) \rho \right) &\geq \sum_{j=1}^m (\tilde{a}_j - \theta) \bar{y}_j - \tilde{c} - \theta \geq \sum_{j=1}^m \tilde{a}_j \bar{y}_j - \tilde{c} - \theta (\|y\|_1 + 1) \\ &\geq -2(r+1)\theta \geq -4r\theta, \end{aligned}$$

where we used the definition of \tilde{a}, \tilde{c} in the first inequality, the definition of $\hat{P}(\tilde{a}, \tilde{c} - (r+1)\theta)$ in the third inequality, $r \geq 1$ in the last inequality, and $\bar{y} \geq 0$. Multiplying this inequality by $\text{Tr}(X)$, using $\rho = X / \text{Tr}(X)$ and $|\text{Tr}(X)| \leq R$, yields:

$$\text{Tr} \left(\left(\sum_{j=1}^m \bar{y}_j A^{(j)} - C \right) X \right) \geq -4 \text{Tr}(X) r\theta \geq -4Rr\theta.$$

□

Prop. 8.19 gives a precise way to deal with errors in the trace estimation: suppose we choose $\theta = \epsilon / (12Rr)$ as the maximum allowed tolerance in trace estimation. Then $\hat{P}(\tilde{a}, \tilde{c} - (r+1)\theta) \subseteq P_{\epsilon/3}(X)$, so if we can give an algorithm to compute a point in $\hat{P}(\tilde{a}, \tilde{c} - (r+1)\theta)$, we can directly implement Alg. 7. From now on, we use the following shorthand:

$$\theta = \frac{\epsilon}{12Rr}. \quad (8.24)$$

8.3.2 Computing the dual vector

Following the discussion in Sect. 8.3.1, one way to implement a quantum SDP solver is to give a quantum algorithm to compute a point in $\hat{P}(\tilde{a}, \tilde{c} - (r+1)\theta)$, after which we have all the necessary components for the MMWU framework. The simplest approach is to estimate the trace values on a quantum computer and then use a classical algorithm to find the required dual vector.

Let us do a back-of-the-envelope calculation of the running time of such an approach. Alg. 7 runs for $T = \left\lceil \frac{9w^2 R^2 \ln n}{\epsilon^2} \right\rceil$ iterations: recalling that the oracle width parameter can be chosen as $w = r$ (due to the constraint $\|y\|_1 \leq r$ in the generalized PIC polytope), we write this as $\tilde{\mathcal{O}}((Rr/\epsilon)^2)$. In each iteration the algorithm uses $M^{(t)} = \frac{1}{r} \left(\sum_{j=1}^m y_j^{(t)} A^{(j)} - C \right)$, and the Hamiltonian of the Gibbs state $\rho^{(t)}$ used at iteration t is a linear combination of the matrices $M^{(\tau)}$, $\tau = 1, \dots, t-1$; thus, at every iteration, by taking the appropriate linear combination we can compute a vector $\hat{y}^{(t)} \in \mathbb{R}^{m+1}$ such that:

$$\rho^{(t)} = \exp \left(\sum_{j=1}^m \hat{y}_j^{(t)} A^{(j)} - \hat{y}_{m+1}^{(t)} C \right) / \text{Tr} \left(\exp \left(\sum_{j=1}^m \hat{y}_j^{(t)} A^{(j)} - \hat{y}_{m+1}^{(t)} C \right) \right).$$

We can construct a state-preparation pair (Def. 7.16) for $\hat{y}^{(t)}$ with $\mathcal{O}(m)$ gates. Then, using linear combination of block-encodings (Prop. 7.18) followed by Gibbs state preparation (Prop. 7.38), we construct a purification of $\rho^{(t)}$, which we use to estimate the trace values with Prop. 7.41. We can upper bound the cost of these operations as follows:

- The state-preparation pair for \hat{y} can be constructed with negligible error, but its subnormalization factor (which then affects the subnormalization factor of the linear combination of block-encodings) is $\|\hat{y}\|_1$. We can bound the subnormalization factor as:

$$\|\hat{y}\|_1 \leq \sum_{t=1}^T \frac{\eta}{r} \|y^{(t)}\|_1 \leq \sqrt{T} \ln n = \tilde{\mathcal{O}}(Rr/\epsilon),$$

where the first inequality is due to the scaling of the vectors $y^{(t)}$ in Alg. 7, the second inequality uses $\|y\|_1 \leq r$ and $\eta = \sqrt{\ln n/T}$, and the final equality is by definition of T .

- The linear combination of block-encodings then has subnormalization factor $\tilde{\mathcal{O}}(\alpha Rr/\epsilon)$, because we need to multiply the subnormalization factor α of the input matrices $A^{(j)}, C$ with the subnormalization factor of the state-preparation pair; the additional resource consumption of this step (gates, auxiliary qubits) is negligible, and so is the error.
- We construct the purification of $\rho^{(t)}$ starting from the linear combination of block-encodings at the previous step; this gives a running time of $\tilde{\mathcal{O}}(\alpha Rr\sqrt{n}/\epsilon)$, where the running time is in terms of number of accesses to the circuit implementing controlled block-encodings of the input matrices, and a similar number of additional gates.
- Finally, we prepare a random variable with expected value very close to $\text{Tr}(A^{(j)}\rho^{(t)})$ using $\tilde{\mathcal{O}}(\alpha)$ applications of the block encoding of $A^{(j)}$, and similarly for $\text{Tr}(C\rho^{(t)})$; crucially, we can obtain one sample from one of these random variables with only a single copy of $\rho^{(t)}$, i.e., we do not need to repeat the construction of $\rho^{(t)}$ for this step. Thus, the cost for the circuit to obtain one sample is dominated by the cost for preparing $\rho^{(t)}$, which is $\tilde{\mathcal{O}}(\alpha Rr\sqrt{n}/\epsilon)$; the cost for preparing the random variable is negligible, compared to this. Note that the random variable obtained with Prop. 7.41 has a small bias, but the running time dependence on the bias is polylogarithmic, so we can make the bias very small, and the total error accumulated by the algorithm is dominated by the error in the next step.
- Each of the trace values must be estimated to error $\theta = \epsilon/(12Rr)$: we use mean estimation (see Rem. 7.42, in particular we can use the algorithm of [Montanaro, 2015]) to compute the expected values. The mean estimation algorithm applies the circuit to obtain a sample from the random variable a total of $\mathcal{O}(1/\theta)$ times. Overall, this implies that the estimation of a single value among $\text{Tr}(A^{(j)}\rho^{(t)})$ or $\text{Tr}(C\rho^{(t)})$ takes $\tilde{\mathcal{O}}(\alpha\sqrt{n}(Rr/\epsilon)^2)$ applications of the input block-encodings. Estimating all of these values, because there are $m+1$ of them, increases the total complexity to $\tilde{\mathcal{O}}(\alpha m\sqrt{n}(Rr/\epsilon)^2)$.

Multiplying the above cost by the number of iterations T , we obtain the running time:

$$\tilde{\mathcal{O}}(\alpha m\sqrt{n}(Rr/\epsilon)^4).$$

Remark 8.20. *For such an algorithm to work we have to assume that all the subroutines are successful: for example, all the trace values must be estimated within the required precision, otherwise the algorithm may not find the correct solution. This is generally not an issue as long as the complexity of all subroutines scales polylogarithmically with the inverse of the maximum failure probability: if the algorithm executes K subroutines in total, we set the maximum failure probability of each subroutine to δ/K . By the union bound, the probability that any subroutine fails is then at most δ . As long as the term $\text{polylog}(\delta/K)$ is acceptable in the running time expressions, this allows us to assume that all subroutines are successful when analyzing the algorithm. We used a similar approach in Sect. 3.3.2.*

The simple algorithm described above has linear scaling in m , because it estimates all the values $\text{Tr}(A^{(j)}\rho^{(t)})$ for $j = 1, \dots, m$. We can reduce this to \sqrt{m} based on the observation that if the generalized PIC polytope $\hat{P}(\tilde{a}, \tilde{c} - (r+1)\theta)$ is nonempty, then it contains a sparse vector. This

can be seen by reformulating the question of emptiness of $\hat{P}(\tilde{a}, \tilde{c} - (r + 1)\theta)$ as a linear program, using the definition in Eq. 8.23:

$$\min \left. \begin{array}{l} \sum_{j=1}^m y_j \\ b^\top y \leq \gamma \\ \tilde{a}^\top y \geq \tilde{c} - (r + 1)\theta \\ y \geq 0. \end{array} \right\} \quad (8.25)$$

If this problem has a solution with value $\leq r$, then $\hat{P}(\tilde{a}, \tilde{c} - (r + 1)\theta)$ is nonempty and contains the desired vector $y^{(t)}$. It is known that any feasible linear program with two constraints (besides nonnegativity) has a solution with at most two nonzero elements — a so-called *basic solution*. Thus, we can choose to solve problem 8.25 in each iteration of Alg. 7 to obtain the vector $y^{(t)}$, and we take advantage of the existence of a sparse solution to improve the performance of the algorithm.

Finding a sparse solution requires a rather sophisticated approach, and we do not discuss it in detail here. The important features of this approach that need to be highlighted are that its main idea is entirely classical (i.e., it is based on the geometry of problem 8.25, and it gives a classical algorithm as well), and it reduces the solution of problem 8.25 to the problem of searching over the points (b_j, \tilde{a}_j) . Indeed, as is shown in [van Apeldoorn et al., 2020b], calling $\|y\| = L$ and using a change of variables $z = y/L$, we can reformulate $\hat{P}(\tilde{a}, \tilde{c} - (r + 1)\theta)$, and therefore problem (8.25), as the following problem:

$$\left. \begin{array}{l} b^\top z \leq \gamma/L \\ \tilde{a}^\top z \geq (\tilde{c} - (r + 1)\theta)/L \\ \|z\| = 1 \\ z \geq 0 \\ 0 < L \leq r. \end{array} \right\}$$

Note that z defines a convex combination of the points (b_j, \tilde{a}_j) , and to satisfy the constraints, we want such a combination that lies to the upper left of the point $(\gamma/L, (\tilde{c} - (r + 1)\theta)/L)$. If such a combination exist, there is one that has nonzero coefficients for only two points (a basic solution for the linear program). We can find these two points with a procedure that we summarize as follows:

- Check if $\gamma \geq 0$ and $\tilde{c} - (r + 1)\theta \leq 0$. If so, return $z = 0$ as a feasible solution.
- Scan the points (b_j, \tilde{a}_j) to see if any of them is a solution. If so, return $z = e_j$ as a feasible solution.
- Find two points $(b_j, \tilde{a}_j), (b_k, \tilde{a}_k)$ such that the line segment connecting them intersects the feasible region. If so, return the corresponding convex combination as a feasible solution. Crucially, these two points can be found independently of each other, i.e., we do not need to search over all pairs, but rather search over the list of points at most twice: this exploits a geometric idea described in [van Apeldoorn et al., 2020b].
- If a feasible solution was not found in the steps above, return “failure”.

With this procedure we obtain the following statement.

Proposition 8.21 (Informal; see Lem. 16 in [van Apeldoorn et al., 2020b] for a precise statement). *Assume that we have access to a quantum circuit U such that:*

$$U|\vec{j}\rangle|\vec{0}\rangle|\vec{0}\rangle = |\vec{j}\rangle|\vec{a}_j\rangle|\psi_j\rangle,$$

where \tilde{a}_j is such that $|\text{Tr}(A^{(j)}\rho) - \tilde{a}_j| \leq \theta$. There is a quantum algorithm that uses $\tilde{\mathcal{O}}(\sqrt{m})$ calls to U , and a number of gates of the same order, and with high probability returns a vector in $P_{4Rr\theta}(X) \cap \{y : \|y\|_1 \leq r\}$ if $P_0(X) \cap \{y : \|y\|_1 \leq r\}$ is nonempty, and returns “failure” if $P_0(X) \cap \{y : \|y\|_1 \leq r\}$ is empty.

In fact, the above proposition also works if U outputs a superposition of possible trace values, as long as the probability of obtaining a wrong estimate is exponentially small — which is easy to achieve with Prop. 7.41. Thus, we construct U with Prop. 7.41 and a mean estimation algorithm, such as the one in [Montanaro, 2015], that has scaling $\tilde{O}(1/\theta)$ for error θ .

Summarizing, we can reduce the problem of finding a point in the generalized PIC polytope $\hat{P}(\tilde{a}, \tilde{c} - (r+1)\theta)$ to the problem of performing $\tilde{O}(\sqrt{m})$ trace estimations in quantum superposition. With this approach, the total complexity of the algorithm is:

$$\tilde{O}(\alpha\sqrt{mn}(Rr/\epsilon)^4)$$

calls to the block-encoding of the input matrices, and a similar number of additional gates.

Remark 8.22. *Although the running time reported above is attractive in its dependence on m and n , the poor scaling on Rr/ϵ is an issue. As discussed in [van Apeldoorn et al., 2020b], for the majority of known problems formulated as SDPs at least one of the parameters R, r scales linearly in the dimensions m, n . The fastest classical optimization methods for SDPs depend polylogarithmically on the size of primal/dual solutions, and the precision parameter ϵ . For example, the interior point method of [Jiang et al., 2020] has a running time of $\tilde{O}(\sqrt{n}(mn^2 + m^\omega + n^\omega))$, where ω is as discussed in Rem. 8.16. (More practical interior point methods for semidefinite optimization have running time $\tilde{O}(n^{6.5})$, see, e.g., [Monteiro, 1998, Nesterov and Todd, 1998].) Thus, the quantum MMWU algorithm for SDP discussed in this section yields an end-to-end quantum speedup only if Rr/ϵ is very small, which is not the case for most problems.*

8.3.3 Further improvements

We can reduce the complexity of the quantum MMWU algorithm even further (at least in some parameters), using techniques that we overview here because they could be useful in the design of other quantum optimization algorithms. The discussion in this section is meant to convey intuition and provide the right references, rather than giving a detailed and mathematically precise description of the corresponding ideas; thus, we do not give formal statements or proofs.

The major improvement that we aim to obtain in this section is to reduce the dependence on m and n from $\tilde{O}(\sqrt{mn})$ down to $\tilde{O}(\sqrt{m} + \sqrt{n})$. The scheme presented in Sect. 8.3.2 needs to estimate m trace values of the form $\text{Tr}(A^{(j)}\rho)$, and because the construction of the Gibbs state ρ runs in time $\tilde{O}(\alpha\sqrt{n})$, already improving over $\tilde{O}(m\sqrt{n})$ requires significant ingenuity, as we discussed. If we want to use Prop. 7.38 for the construction, an algorithm that scales as $\tilde{O}(\sqrt{m} + \sqrt{n})$ is only allowed to produce, at every iteration, a number of Gibbs states that does not scale with m .

To make progress on such a construction we separate the Gibbs state preparation from the trace estimation procedure. In the setting of the algorithm, at each iteration we construct the *same* state $\rho^{(t)}$, and we essentially want to perform a search over multiple $\text{Tr}(A^{(j)}\rho^{(t)})$: recall that the procedure of Prop. 8.21 reduces to two searches over these values. In fact, the search can be translated into a minimum finding problem: even in the most expensive part of Prop. 8.21, where we look for two points $(b_j, \tilde{a}_j), (b_k, \tilde{a}_k)$ defining a line segment with a certain property, [van Apeldoorn et al., 2020b] shows that this can be accomplished with a search over angles, and the angles can be computed easily from the trace values. For ease of exposition, we consider the problem of determining the maximum of $\text{Tr}(A^{(j)}\rho^{(t)})$ over all j ; a search over any value that can be computed easily from $\text{Tr}(A^{(j)}\rho^{(t)})$ has the same computational complexity, and this includes minimum finding (minimum finding and maximum finding are equivalent in this setting, because we can flip the sign of each value).

Classically, estimating $\text{Tr}(A^{(j)}\rho^{(t)})$ for all j only requires us to compute $\rho^{(t)}$ once: after explicitly computing the entries of the Gibbs state, we can “reuse it” in as many calculations as we want, for example estimating all $\text{Tr}(A^{(j)}\rho^{(t)})$ while paying the cost for the construction of $\rho^{(t)}$ only once. In the quantum setting this is not obvious, because a measurement after constructing the Gibbs state would generally cause the quantum state to collapse to a basis state. However, we can do something similar to “reusing” the state under certain conditions, exploiting an idea

described in the *gentle search lemma* of [Aaronson, 2018]. (To be more precise: we do not actually reuse the state; rather, we use it in a way that allows us to estimate whether m trace values are larger than a given threshold with a number of samples that does not depend on m .) Suppose we have a unitary that outputs a sample from a random variable that estimates $\text{Tr}(A^{(j)}\rho^{(t)})$ starting from a copy of $\rho^{(t)}$ (as in Prop. 7.41), and ask the question: does there exist some $j = 1, \dots, m$ such that $\text{Tr}(A^{(j)}\rho^{(t)}) \geq \mu$ for some given value μ ? If we can answer this existence question, we can perform binary search on the set $\{1, \dots, m\}$ to find the index of such a j : every time we split the current interval (initially, $\{1, \dots, m\}$) in two sets, check existence of j with $\text{Tr}(A^{(j)}\rho^{(t)}) \geq \mu$ in each of the two sets, and apply the search procedure recursively on a set that gives the positive answer. This eventually yields an index with the desired property. We are back to the existence question: does there exist $j = 1, \dots, m$ such that $\text{Tr}(A^{(j)}\rho^{(t)}) \geq \mu$? Note again that $\rho^{(t)}$ is fixed and only the $A^{(j)}$ are changing.

Recall the connection between trace values and measurement probabilities discussed in Sect. 1.4, see Rem. 1.59 and the surrounding discussion. The gentle search lemma of [Aaronson, 2018] states, informally, that if we have several two-outcome measurements $M^{(j)}$ (e.g., testing whether a qubit is $|0\rangle$ or $|1\rangle$) with the property that either $\text{Tr}(M^{(j)}\rho) \geq \beta$ for some j , or $\text{Tr}(M^{(j)}\rho) \leq \beta - \delta$ for all j , we can detect which of the two cases holds with $\tilde{O}(1/\delta^2)$ samples, and this lets us find j such that $\text{Tr}(M^{(j)}\rho) \geq \beta$ with a similar number of samples.

Remark 8.23. *Under the stated property, for fixed j , the probability of observing the first measurement outcome (“accept”) is at least β in the first case, and is at most $\beta - \delta$ in the second case. Thus, if $\text{Tr}(M^{(j)}\rho) \geq \beta$, by the Chernoff bound with very high probability at least a fraction $\approx (\beta - \delta/2)$ of the $\tilde{O}(1/\delta^2)$ samples outputs “accept”, and we can detect this by counting the number of “accept”. We now use a result from [Harrow et al., 2017]: given multiple measurements such that either (i) at least one of them is very likely to output $|1\rangle$, or (ii) all of them are very likely to output $|0\rangle$, distinguishing the two cases (i.e., determining whether there exists a measurement that outputs $|1\rangle$) is easy. Combining this with the previous construction that counts the number of “accept” in the $\tilde{O}(1/\delta^2)$ samples, and amplitude amplification, we obtain the stated result.*

The above idea gives us a blueprint to separate Gibbs state preparation and trace estimation: we prepare $\tilde{O}(1/\theta^2)$ copies (where θ is as in Eq. 8.24) in parallel. We apply the trace estimation procedure of Prop. 7.41 to each copy, controlled on the index j of the matrix $A^{(j)}$ for which we want to compute the estimate, and take the sample average of the $\tilde{O}(1/\theta^2)$ samples. By Chernoff bound, with high probability this is a trace estimate with precision $\tilde{O}(\theta)$, because the standard deviation is constant and so the sample average is unlikely to deviate much from the expected value (recall that by Prop. 7.41, the expected value is at most $\theta/4$ away from $\text{Tr}(A^{(j)}\rho^{(t)})$). Now construct a circuit that “accepts” if the sample average is larger than a given threshold value μ . If there exists j such that $\text{Tr}(A^{(j)}\rho^{(t)}) \geq \mu$, the circuit “accepts” with large probability, say at least $2/3$ — we can adjust the number of samples to ensure that the probability of acceptance is at least this much. If, on the other hand, no such j exists, the circuit “rejects” with the same large probability, and so it “accepts” with probability at most $1/3$. Using the gentle search lemma, with $\beta = 2/3, \delta = 1/3$ we can distinguish these two cases with $\tilde{O}(1/\delta^2) = \tilde{O}(1)$ samples (i.e., measurements) from these circuits: this allows us to implement a quantum search (with the usual quadratic speedup) over the values $\text{Tr}(A^{(j)}\rho^{(t)})$. The quantum search does not require the construction of additional copies of $\rho^{(t)}$, because it can be implemented following similar logic to oblivious amplitude amplification (Sect. 4.2.2), where we amplify the effect of some algorithm applied onto a given state, without constructing the given state from scratch every time. The details of this procedure are described in [van Apeldoorn and Gilyén, 2019], with one key result adapted from [Brandão et al., 2019]. Overall, this gives the following complexity of every iteration:

- We prepare $\tilde{O}((Rr/\epsilon)^2)$ copies of $\rho^{(t)}$: because each purification of $\rho^{(t)}$ uses $\tilde{O}(\alpha Rr\sqrt{n}/\epsilon)$ accesses to the block-encodings describing the input, this brings the cost to $\tilde{O}(\alpha\sqrt{n}(Rr/\epsilon)^3)$.
- We run the search procedure of Prop. 8.21. This still takes time $\tilde{O}(\alpha\sqrt{m}(Rr/\epsilon)^2)$, as in Sect. 8.3.2, because of the required precision and the subnormalization of the block-

encodings. Crucially, as we discussed above, this cost is now additive (rather than multiplicative) with the cost in the previous bullet, because we use the same $\tilde{O}((Rr/\epsilon)^2)$ copies of $\rho^{(\ell)}$.

The number of iterations is still $\tilde{O}((Rr/\epsilon)^2)$, giving a total complexity of:

$$\tilde{O}((\sqrt{m} + \sqrt{n}Rr/\epsilon)\alpha(Rr/\epsilon)^4)$$

calls to the block-encodings of the input matrices, and a similar number of additional gates, see [van Apeldoorn and Gilyén, 2019] for a formal statement and detailed proofs.

8.4 Quantum algorithm for the SDP relaxation of MaxCut

Consider the following quadratic unconstrained optimization problem with ± 1 decision variables:

$$\left. \begin{array}{l} \max \quad z^\top C z \\ \text{s.t.} \quad z \in \{-1, 1\}^n, \end{array} \right\} \quad (\pm 1\text{-QP})$$

where $C \in \mathbb{R}^{n \times n}$ is a symmetric matrix. In this section we describe a quantum algorithm for a relaxation of this problem. Problem (± 1 -QP) finds direct application in a few areas, see the notes in Sect. 8.5. Although the unconstrained formulation limits the modeling power of this problem, one could potentially incorporate constraints by penalizing their violation in the objective function.

Remark 8.24. *Exact penalization of the constraint violations in the objective function may require large penalty coefficients, severely hampering the ability to solve the problem in practice. Thus, we do not advocate constraint penalization in the objective function as a general methodology that is helpful for practical purposes. Rather, we point out that in theory it is possible, and focus on the development of a quantum algorithm for a relaxation of the problem, because it lets us discuss several interesting ideas even if the method may not be widely applicable.*

Problem (± 1 -QP) is equivalent to the combinatorial optimization problem MaxCut, whose description is as follows: given a weighted undirected graph $G = (V, E)$, partition its nodes into two sets V_1, V_2 such that the sum of the weights of edges that have one endpoint in V_1 and the other in V_2 is maximized. MaxCut is known to be NP-hard [Garey and Johnson, 1990]. Transforming an instance of MaxCut into an instance of (± 1 -QP) is easy: suppose G has vertex set $\{1, \dots, n\}$, and let w_{ij} be the weight of edge $(i, j) \in E$ with $i < j$ (the weight is 0 if the edge is not present); set the elements of the objective function matrix $C_{ij} = C_{ji} = -\frac{1}{2}w_{ij}$. This yields a symmetric matrix C , and according to the objective function, for every $(i, j) \in E$ we either gain w_{ij} if $z_i \neq z_j$ (because in this case, $z_i z_j = -1$), or we have to pay w_{ij} if $z_i = z_j$ (because in this case, $z_i z_j = 1$). Then, $\sum_{(i,j) \in E} w_{ij} + \max_{z \in \{-1, 1\}^n} z^\top C z$ equals twice the value of the MaxCut, because each edge contribution w_{ij} disappears from this expression if $z_i = z_j$, and is counted twice if $z_i \neq z_j$. The reverse equivalence (from (± 1 -QP) to MaxCut) follows from the same construction.

Remark 8.25. *The equivalence between (± 1 -QP) and MaxCut is in terms of the optimal solution vectors, not in terms of the corresponding objective function values: to translate the objective function values of the two problems we need to shift and scale, as discussed above.*

Problem (± 1 -QP) can also be reformulated into a problem with $\{0, 1\}$ binary variables, as opposed to $\{-1, +1\}$; this yields a quadratic unconstrained binary optimization problem (QUBO), see Def. 9.3 and the discussion in Sect. 9.1.1.

8.4.1 Obtaining the normalized SDP relaxation

Because (± 1 -QP) is NP-hard, its solution can be difficult, and we can consider instead a convex relaxation of the problem to obtain a bound on its optimal value. Convex relaxations of difficult discrete optimization problems are also at the heart of the branch-and-bound algorithm, so an

efficient algorithm to solve a relaxation can lead to a more effective branch-and-bound. One way to obtain a relaxation of $(\pm 1\text{-QP})$ is to define a new decision variable $X = zz^\top$. Imposing $\text{rank}(X) = 1$, $X \succeq 0$ and $X_{jj} = 1$ for all $j = 1, \dots, n$ suffices to ensure that X is of the form zz^\top for some vector $z \in \{-1, +1\}^n$. Note that if $X = zz^\top$ then $z^\top Cz = \text{Tr}(CX)$. Thus, $(\pm 1\text{-QP})$ is equivalent to:

$$\left. \begin{array}{l} \max \quad \text{Tr}(CX) \\ \text{s.t.:} \quad \forall j \quad X_{jj} = 1 \\ \quad \quad \quad X \succeq 0 \\ \quad \quad \quad \text{rank}(X) = 1. \end{array} \right\}$$

This is a nonconvex optimization problem because of the constraint $\text{Rank}(X) = 1$; dropping this constraint yields an SDP with special structure:

$$\left. \begin{array}{l} \max \quad \text{Tr}(CX) \\ \text{s.t.:} \quad \text{diag}(X) = \mathbb{1} \\ \quad \quad \quad X \succeq 0. \end{array} \right\} \quad (\text{MaxCutSDP-orig})$$

We aim to solve this problem up to some precision ϵ . In fact, we work with a normalized version where solutions are constrained to having unit trace.

Let $\hat{C} := C/\|C\|_F$ (recall Def. 7.28), and change the objective function matrix from C to \hat{C} , which can be achieved without loss of generality by rescaling C . In addition, define a new decision variable $\rho = X/n$, so that the diagonal constraints become $\text{diag}(\rho) = \frac{1}{n}\mathbb{1}$.

Remark 8.26. *These two scaling operations (of the objective function and of the decision variables) are w.l.o.g., but we should be careful about the final precision because a solution that is ϵ away from optimality in the rescaled problem might be $(n\|C\|_F\epsilon)$ away from optimality in the original problem. From now on we work with the rescaled problem, and our time and gate complexity evaluation also concerns the rescaled problem. Only at the end of our analysis, in Rem. 8.36, we discuss an ϵ -optimal solution to the original problem (MaxCutSDP-orig).*

We use ρ for the new decision variable because the (rescaled) constraints of (MaxCutSDP-orig) impose that it is a positive semidefinite matrix with unit trace; thus, it is a density matrix. We therefore obtain the following problem:

$$\left. \begin{array}{l} \max \quad \text{Tr}(\hat{C}\rho) \\ \text{s.t.:} \quad \text{diag}(\rho) = \frac{1}{n}\mathbb{1} \\ \quad \quad \quad \rho \succeq 0. \end{array} \right\} \quad (\text{MaxCutSDP})$$

The optimal objective function of the rescaled problem (MaxCutSDP) lies in the interval $[-1, 1]$, because, by the matrix Hölder inequality (see Sect. 8.2.2), we have:

$$\left| \text{Tr}(\hat{C}\rho) \right| \leq \|\hat{C}\|_F \|\rho\|_{\text{Tr}} \leq 1.$$

Similarly to our approach in Sect. 8.2.2, we reduce the solution of the optimization problem (MaxCutSDP) to a sequence of feasibility problems, each of which is solved up to precision ϵ . We perform binary search on the optimal objective function value γ in the interval $[-1, 1]$, and solve feasibility problems to determine if a feasible solution with value at least as large as the current guess γ exists. Our goal is then to solve this problem:

$$\left. \begin{array}{l} \min \\ \quad \quad \quad 0 \\ \quad \quad \quad \text{Tr}(\hat{C}\rho) \geq \gamma - \epsilon \\ \quad \quad \quad \left\| \text{diag}(\rho) - \frac{1}{n}\mathbb{1} \right\|_1 \leq \epsilon \\ \quad \quad \quad \text{Tr}(\rho) = 1 \\ \quad \quad \quad \rho \succeq 0. \end{array} \right\} \quad (\text{MaxCutSDP-F})$$

Note that the tolerance ϵ determines by how much we relax two of the constraints: the constraint that the objective function value is at least γ , and the constraint that the diagonal elements

are $1/n$. We do not relax the constraint $\rho \succeq 0$ and the (implied) constraint $\text{Tr}(\rho) = 1$. As a consequence, although solutions of problem MaxCutSDP-F satisfy the constraints of problem (MaxCutSDP) only approximately, they are still density matrices; in other words, because we keep the constraints $\text{Tr}(\rho) = 1, \rho \succeq 0$ intact, we have that $\rho \in \mathcal{S}_{+,1}^n$. We can determine the optimum of problem (MaxCutSDP) with precision ϵ by solving $\mathcal{O}(\log \frac{1}{\epsilon})$ problems of the form (MaxCutSDP-F) for different values of γ .

8.4.2 Solving the relaxation using inexact mirror descent

Define:

$$f_\gamma(\rho) := \max \left\{ \gamma - \text{Tr}(\hat{C}\rho), \sum_{j=1}^n \left| \rho_{jj} - \frac{1}{n} \right| \right\}, \quad (8.26)$$

and consider the optimization problem:

$$\begin{array}{l} \min \quad f_\gamma(\rho) \\ \text{s.t.:} \quad \rho \in \mathcal{S}_{+,1}^n. \end{array}$$

It is immediate to observe that if we find ρ such that $f_\gamma(\rho) \leq \epsilon$, ρ is a solution to (MaxCutSDP-F). Hence, our goal in this section is to minimize f_γ for a given value of γ , which is iteratively modified by the binary search scheme for the optimal objective function value.

We apply the online mirror descent scheme described in Alg. 6, see the discussion in Sect. 8.1.2, but in this case, the objective function is simply f_γ rather than the sum of T different terms f_1, \dots, f_T . Thus, we pick $f_t = f_\gamma$ for all t ; this still leads to convergence to some specified precision ϵ , see Thm. 8.30. To take advantage of a quantum computer, we employ a scheme whereby the iterate $\rho^{(t)}$, which is a density matrix, is represented by a Gibbs state constructed on the quantum computer. Classically, we keep track of the matrices $\mathcal{H}^{(t)}$ that define $\rho^{(t)}$ via matrix exponentiation. Because the (sub)gradient updates are applied to $\mathcal{H}^{(t)}$ directly, as long as we are able to compute a classical description of the subgradients $G^{(t)} \in \partial f_\gamma(\rho^{(t)})$ we can, in principle, follow Alg. 6 by updating the Hamiltonians $\mathcal{H}^{(t)}$ even without explicit classical knowledge of $\rho^{(t)}$. However, given the definition of f_γ in Eq. (8.26), it is immediate to observe that the computation of $G^{(t)} \in \partial f_\gamma(\rho^{(t)})$ requires knowledge of the terms $\text{Tr}(\hat{C}\rho^{(t)}), \rho_{jj}^{(t)}$ appearing in the objective function. Thus, some information about $\rho^{(t)}$ is necessary to proceed with Alg. 6. We show below that we can use a quantum computer, together with classical knowledge of $\mathcal{H}^{(t)}$, to determine a subgradient $G^{(t)}$.

Remark 8.27. *The crucial observation for this scheme is that we do not construct a full classical representation of $\rho^{(t)}$, and we do not need such a representation to be able to optimize: we want to avoid explicit classical computation of $\exp(\mathcal{H}^{(t)})/\text{Tr}(\exp(\mathcal{H}^{(t)}))$, and rely on the quantum computer for all calculations involving the Gibbs state. In this way, we do not have to classically compute the matrix exponential in the Gibbs state: we only compute the subgradient $G^{(t)}$.*

Because we aim to devise an algorithm that may not have access to an explicit classical description of $\rho^{(t)}$, we forego the idea of computing an exact subgradient $G^{(t)} \in \partial f_\gamma(\rho^{(t)})$. Instead, we compute an *inexact* subgradient $G^{(t)} \in \partial_\epsilon f_\gamma(\rho^{(t)})$ with the following algorithm:

- Estimate the following quantities:

$$\text{Tr}(\hat{C}\rho^{(t)}), \rho_{11}^{(t)}, \rho_{22}^{(t)}, \dots, \rho_{nn}^{(t)},$$

with sufficient precision to guarantee that:

$$\begin{aligned} \left| \text{est}\left(\text{Tr}(\hat{C}\rho^{(t)})\right) - \text{Tr}(\hat{C}\rho^{(t)}) \right| &\leq \frac{\epsilon}{4} \\ \sum_{j=1}^n \left| \text{est}(\rho_{jj}^{(t)}) - \rho_{jj}^{(t)} \right| &\leq \frac{\epsilon}{4}, \end{aligned} \quad (8.27)$$

where $\text{est}(x)$ is the computed estimate for a given quantity x .

- If $\max \left\{ \gamma - \text{est} \left(\text{Tr} \left(\hat{C} \rho^{(t)} \right) \right), \sum_{j=1}^n \left| \text{est}(\rho_{jj}^{(t)}) - \frac{1}{n} \right| \right\} \leq \frac{3\epsilon}{4}$, return $G^{(t)} = \mathbb{0}^{n \times n}$, i.e., the all-zero matrix of size $n \times n$.
- Otherwise, if $\gamma - \text{est} \left(\text{Tr} \left(\hat{C} \rho^{(t)} \right) \right)$ attains the maximum, return $G^{(t)} = -\hat{C}$.
- Otherwise, return $G^{(t)} = \mathbb{0}^{n \times n} + \sum_{j=1}^n \left(\mathbb{I} \left(\text{est}(\rho_{jj}^{(t)}) > \frac{1}{n} \right) - \mathbb{I} \left(\frac{1}{n} > \text{est}(\rho_{jj}^{(t)}) \right) \right) E_{jj}$, where E_{jj} is the $n \times n$ matrix with 1 in position jj , and 0 everywhere else (i.e., the outer product of the j -th basis vector with itself, $e_j e_j^\top$).

Proposition 8.28. *Let $G^{(t)}$ be computed according to the algorithm above. Then $G^{(t)} \in \partial_{\epsilon/2} f_\gamma(\rho^{(t)})$.*

We prove Prop. 8.28 below, but some comments are in order first. Note that we are only interested in a subgradient whenever $f_\gamma(\rho^{(t)}) > \epsilon$: if $f_\gamma(\rho^{(t)}) \leq \epsilon$, then $\rho^{(t)}$ is a solution to (MaxCutSDP-F), so the optimization algorithm can stop. Furthermore, if:

$$\max \left\{ \gamma - \text{est} \left(\text{Tr} \left(\hat{C} \rho^{(t)} \right) \right), \sum_{j=1}^n \left| \text{est}(\rho_{jj}^{(t)}) - \frac{1}{n} \right| \right\} \leq \frac{3\epsilon}{4}, \quad (8.28)$$

it must be the case that $f_\gamma(\rho^{(t)}) \leq \epsilon$, because the l.h.s. is an estimate of $f_\gamma(\rho^{(t)})$ with precision $\frac{\epsilon}{4}$ (this is easily proven with Eq. 8.27 and triangle inequalities). Thus, when Eq. (8.28) holds we can safely return $G^{(t)} = \mathbb{0}^{n \times n}$, indicating that we have a solution with the desired precision. Our proof of Prop. 8.28 relies on the following lemma.

Lemma 8.29. *Let $h_i(x)$ be 1-Lipschitz convex functions for $i = 1, \dots, m$, and $f(x) = \max_{i=1, \dots, m} h_i(x)$. For given points \bar{x}, \hat{x} such that $\|\bar{x} - \hat{x}\| \leq \frac{\epsilon}{4}$, let $j \in \arg \max_{i=1, \dots, m} h_i(\hat{x})$. Then, for $g \in \partial h_j(\hat{x})$, we have $g \in \partial_{\hat{\epsilon}} f(\bar{x})$, where $\hat{\epsilon} = \frac{\epsilon}{4}(\|g\|_* + 1)$.*

Proof. Using the fact that f is 1-Lipschitz because it is the maximum of 1-Lipschitz functions (so $f(\bar{x}) - f(\hat{x}) \leq \|\bar{x} - \hat{x}\|$), and the fact that $f(\hat{x}) \leq h_j(\hat{x})$ because index j attains the maximum in the expression $\max_{i=1, \dots, m} h_i(\hat{x})$, we have:

$$\begin{aligned} f(\bar{x}) + \langle g, \bar{x} - \hat{x} \rangle &\leq f(\hat{x}) + \underbrace{\|\bar{x} - \hat{x}\|}_{\leq \frac{\epsilon}{4}} + \langle g, \bar{x} - \hat{x} \rangle - \underbrace{\langle g, \bar{x} - \hat{x} \rangle}_{\leq \frac{\epsilon \|g\|_*}{4} \text{ in abs. val.}} \\ &\leq f(\hat{x}) + \langle g, \bar{x} - \hat{x} \rangle + \frac{\epsilon}{4}(\|g\|_* + 1) \\ &\leq \underbrace{h_j(\hat{x}) + \langle g, \bar{x} - \hat{x} \rangle}_{\leq h_j(\bar{x}) \text{ because } g \in \partial h_j(\hat{x})} + \frac{\epsilon}{4}(\|g\|_* + 1) \leq h_j(\bar{x}) + \frac{\epsilon}{4}(\|g\|_* + 1) \\ &\leq f(\bar{x}) + \frac{\epsilon}{4}(\|g\|_* + 1). \end{aligned}$$

This shows that $g \in \partial_{\hat{\epsilon}} f(\bar{x})$. □

We can now prove Prop. 8.28.

Proof. If $\max \left\{ \gamma - \text{est} \left(\text{Tr} \left(\hat{C} \rho^{(t)} \right) \right), \sum_{j=1}^n \left| \text{est}(\rho_{jj}^{(t)}) - \frac{1}{n} \right| \right\} \leq \frac{3\epsilon}{4}$, we return $G^{(t)} = \mathbb{0}^{n \times n}$. This is trivially an ϵ -subgradient: $f_\gamma(\rho^{(t)}) \leq \epsilon$ because the two terms in the max are estimated with error at most $\frac{\epsilon}{4}$ each, therefore $f_\gamma(\rho^{(t)}) + \langle \mathbb{0}^{n \times n}, \rho - \rho^{(t)} \rangle - \epsilon \leq 0 \leq f_\gamma(\rho)$ for all ρ .

Now assume at least one between $\gamma - \text{est} \left(\text{Tr} \left(\hat{C} \rho^{(t)} \right) \right)$ and $\sum_{j=1}^n \left| \text{est}(\rho_{jj}^{(t)}) - \frac{1}{n} \right|$ is $> \frac{3\epsilon}{4}$. We apply Lem. 8.29 with $h_1(\rho) = \gamma - \text{Tr} \left(\hat{C} \rho \right)$, $h_2(\rho) = \sum_{j=1}^n \left| \rho_{jj} - \frac{1}{n} \right|$ and $\bar{x} = \rho^{(t)}$. It is easy to see that h_1 and h_2 are 1-Lipschitz with respect to the trace distance (using $\|\hat{C}\| \leq 1$). Based on our estimates for $\rho^{(t)}$, satisfying the guarantees in Eq. (8.27), we are evaluating h_1, h_2 at a point $\text{est}(\rho^{(t)})$ that has trace distance at most $\frac{\epsilon}{4}$ from $\rho^{(t)}$. (Note: we may not have explicit knowledge

of the full $\text{est}(\rho^{(t)})$, because we only estimate the diagonal elements as well as $\text{Tr}(\hat{C}\rho^{(t)})$, but this is not necessary.) Then, Lem. 8.29 implies that if we take the maximum of h_1 and h_2 , and return a subgradient of the corresponding function at $\text{est}(\rho^{(t)})$, we have obtained $G^{(t)} \in \partial_{\hat{\epsilon}} f_{\gamma}(\rho^{(t)})$. Thus, we just need to show that we are correctly returning a subgradient of h_1 or h_2 at $\text{est}(\rho^{(t)})$, depending on which one attains the maximum. The function h_1 is linear in ρ and we return $-\hat{C}$ (recall Rem. 8.9) if h_1 attains the max. The second function is a sum of absolute values $|\rho_{jj} - \frac{1}{n}|$, and we return the sum of a subgradient for each term at $\text{est}(\rho^{(t)})$ (E_{jj} if $\text{est}(\rho_{jj}^{(t)}) > \frac{1}{n}$, $-E_{jj}$ if $\text{est}(\rho_{jj}^{(t)}) < \frac{1}{n}$) if h_2 attains the max. Finally, note that the norm of the returned subgradient $g = G^{(t)}$ always satisfies $\|g\|_* \leq 1$, because $\|\hat{C}\| \leq 1$ and $\max_{a_j \in \{-1, +1\}, \rho \in \mathcal{S}_{+1}^n} \langle \sum_{j=1}^n a_j E_{jj}, \rho \rangle = 1$. Thus, $\hat{\epsilon} = \frac{\epsilon}{4}(\|g\|_* + 1) = \frac{\epsilon}{2}$, and $G^{(t)} \in \partial_{\epsilon/2} f_{\gamma}(\rho^{(t)})$. \square

We can now state the main convergence result, adapted from [Brandao et al., 2022].

Theorem 8.30 (Convergence of mirror descent for MaxCut SDP). *Suppose there exists $\rho^* \in \mathcal{S}_{+1}^n$ such that $f_{\gamma}(\rho^*) = 0$, i.e., problem (MaxCutSDP-F) is feasible with $\epsilon = 0$. Then, the mirror descent algorithm Alg. 6 with step size $\eta = \frac{\epsilon}{16}$, inexact subgradients $G^{(t)} \in \partial_{\epsilon/2} f_{\gamma}(\rho^{(t)})$ computed as described above, and number of steps $T = \frac{64}{\epsilon^2} \log n$, returns density matrices $\rho^{(1)}, \dots, \rho^{(T)}$ such that:*

$$f_{\gamma} \left(\frac{1}{T} \sum_{t=1}^T \rho^{(t)} \right) \leq \epsilon.$$

Proof. We apply Thm. 8.5. Because in this case we are using $\frac{\epsilon}{2}$ -subgradients rather than exact subgradients, we need to modify the convergence result slightly: in each iteration the objective function may be worse compared to the exact case, by an amount that is at most $\frac{\epsilon}{2}$. Applying this change to Thm. 8.5, recalling that the strong convexity parameter is $\alpha = 1$ (see Sect. 8.1.2 and [Yu, 2013]), we obtain the following result:

$$\sum_{t=1}^T f_{\gamma}(\rho^{(t)}) - \sum_{t=1}^T f_{\gamma}(\rho^*) \leq \frac{1}{\eta} D_h(\rho^* \| I/n) + \frac{\eta}{2} \sum_{t=1}^T \|G^{(t)}\|_*^2 + \frac{\epsilon}{2} T. \quad (8.29)$$

(A formal proof of this inequality can be obtained by modifying the convergence proof for mirror descent and using the definition of $\frac{\epsilon}{2}$ -subgradient instead of the exact subgradient inequality; this makes the bound worse by an additive term $\frac{\epsilon}{2}$ in every iteration. See, e.g., the proof in [Bansal and Gupta, 2019, Thm. 4.2], and the analysis for inexact subgradients in [Nedic and Lee, 2014].) The function f_{γ} is convex, so we can use Jensen's inequality $f_{\gamma}(\frac{1}{T} \sum_t \rho^{(t)}) \leq \frac{1}{T} \sum_t f_{\gamma}(\rho^{(t)})$. Combining this with Eq. (8.29), after dividing by T on both sides, and remembering that $D_h(\rho^* \| I/n) \leq \log n$ (see Sect. 8.1.2), we obtain:

$$f_{\gamma} \left(\frac{1}{T} \sum_{t=1}^T \rho^{(t)} \right) \leq \frac{1}{T} \sum_{t=1}^T f_{\gamma}(\rho^{(t)}) \leq \frac{1}{T} \sum_{t=1}^T f_{\gamma}(\rho^*) + \frac{\log n}{\eta T} + \frac{\eta}{2} + \frac{\epsilon}{2} \leq \frac{\epsilon}{4} + \frac{\epsilon}{32} + \frac{\epsilon}{2} \leq \epsilon,$$

where in the second inequality we used the fact that $f_{\gamma}(\rho^*) = 0$ by assumption, and we substituted the values for η and T given in the theorem statement. \square

Remark 8.31. *Using the same choices for $\eta, T, G^{(t)}$ as indicated in Thm. 8.30, it is possible to show that the last iterate $\rho^{(T)}$ of Alg. 6 (as opposed to the average of the iterates) satisfies $f_{\gamma}(\rho^{(T)}) \leq \epsilon$, if an exactly feasible solution for (MaxCutSDP-F) exists. The proof of this result follows from [Brandao et al., 2022], in particular Theorem 2.1 and Lemma 3.1 therein, after noting that this specific instantiation of Alg. 6 follows exactly the same steps as the algorithm described in [Brandao et al., 2022]. The proof technique in [Brandao et al., 2022] uses a potential function argument, see also [Tsuda et al., 2005].*

Typically, convergence for online mirror descent is shown for the average of the iterates, rather than for the last iterate only, see, e.g., [Allen-Zhu and Orecchia, 2017]. We discuss convergence for the average iterate so that we can directly use Thm. 8.5: the bound on the quality of the

final iterate is similar to the bound on the quality of the average iterate. However, the time complexity for computing properties of the optimal solution can be worse when considering the average iterate, because to construct a mixed state corresponding to the average iterate, we have to construct a linear combination of Gibbs states rather than a single Gibbs state; we can do that with Prop. 7.18, but it may come at a cost, depending on the input model (see the discussion in Sect. 8.4.3). Overall, in theory considering the last iterate only is the better choice for this specific problem: we consider the average of the iterates for educational purposes, and because the computational complexity difference is not significant in the QRAM model.

8.4.3 Complexity of the quantum algorithm

Thm. 8.5 states that Alg. 6 runs for $T = \frac{64}{\epsilon^2} \log n$ iterations. In this section we analyze the cost (i.e., gate complexity) of each iteration, and use it to derive the overall complexity of the algorithm.

The main bottleneck of the algorithm is the computation of the subgradient $G^{(t)}$. As remarked in Rem. 8.27, we aim for a scheme where the Hamiltonians $\mathcal{H}^{(t)}$ in Alg. 6 are stored classically, but all computations involving the corresponding Gibbs state $\rho^{(t)} = \exp(\mathcal{H}^{(t)}) / \text{Tr}(\exp(\mathcal{H}^{(t)}))$ are performed on a quantum computer. In fact, it is straightforward to verify that the only thing we need to proceed with Alg. 6 is a classical description of the subgradient $G^{(t)}$. According to the procedure described in Sect. 8.4.2, we can classically construct $G^{(t)}$ after estimating $\text{Tr}(\hat{C}\rho^{(t)})$, $\rho_{11}^{(t)}$, $\rho_{22}^{(t)}$, \dots , $\rho_{nn}^{(t)}$ with sufficient precision to satisfy Eq. (8.27). Thus, our next task is to analyze the complexity of estimating these quantities. We use $\tilde{\mathcal{O}}(\cdot)$ notation in the analysis below, and for simplicity we neglect small factors that would eventually be absorbed in the $\tilde{\mathcal{O}}(\cdot)$ notation anyway.

It is obvious that the estimation of $\text{Tr}(\hat{C}\rho^{(t)})$, $\rho_{11}^{(t)}$, $\rho_{22}^{(t)}$, \dots , $\rho_{nn}^{(t)}$ requires the ability to construct $\rho^{(t)}$. Suppose we have access to a block-encoding of $\mathcal{H}^{(t)}$ with subnormalization factor α and sufficient precision (the precision is one of those parameters that can be swept under the rug in this analysis: it does not impact the final running time expression). Because $\rho^{(t)}$ is a Gibbs state, we use the Gibbs state construction procedure analyzed in Prop. 7.38. Its complexity is $\tilde{\mathcal{O}}(\sqrt{n}\alpha)$ calls to a block-encoding for $\mathcal{H}^{(t)}$, and a similar number of additional gates. Then Prop. 7.41 lets us estimate $\text{Tr}(\hat{C}\rho^{(t)})$ with one copy of $\rho^{(t)}$ and $\tilde{\mathcal{O}}(\alpha)$ applications of the block-encoding for \hat{C} and additional gates, for a high-precision estimate. The estimation of $\rho_{11}^{(t)}$, $\rho_{22}^{(t)}$, \dots , $\rho_{nn}^{(t)}$ is also quite simple, after figuring out the correct strategy.

Remark 8.32. *As we are attempting to estimate elements of the density matrix describing a mixed quantum state, this falls under the umbrella of quantum state tomography. However, Thm. 5.17 is not exactly designed for the task at hand: it assumes access to a state preparation unitary for a pure state, whereas we are now dealing with a mixed state. Furthermore, Thm. 5.17 estimates amplitudes, but the diagonal elements $\rho_{11}^{(t)}$, $\rho_{22}^{(t)}$, \dots , $\rho_{nn}^{(t)}$ are the probabilities of observing the basis states $|\vec{j}\rangle$, $\vec{j} \in \{0, 1\}^{\lceil \log n \rceil}$.*

Because our goal is to estimate the probabilities of observing $|\vec{j}\rangle$, for $\vec{j} \in \{0, 1\}^{\lceil \log n \rceil}$, when applying measurements to the mixed quantum state represented by $\rho^{(t)}$, there is no need to use the complicated tomography procedure (based on the quantum gradient algorithm) described in Thm. 5.17. It is simpler to repeatedly construct a purification of $\rho^{(t)}$ via Prop. 7.38, perform a measurement of the qubits corresponding to the state register (i.e., we ignore the purifying register), and estimate the probabilities by counting the observations. We need to satisfy Eq. (8.27), hence we require $\sum_{j=1}^n \left| \text{est}(\rho_{jj}^{(t)}) - \rho_{jj}^{(t)} \right| \leq \frac{\epsilon}{4}$. This is the same as estimating, by taking samples, an n -dimensional vector of probabilities with ℓ^1 -norm distance at most $\frac{\epsilon}{4}$ from the true vector of probabilities. It is known that this can be achieved with high probability by taking $\tilde{\mathcal{O}}\left(\frac{n}{\epsilon^2}\right)$ samples, see, e.g., [Canonne, 2020]. This brings the overall complexity of the subgradient estimation procedure to:

$$\tilde{\mathcal{O}}\left(\frac{\alpha n^{1.5}}{\epsilon^2}\right)$$

calls to a block-encoding of $\mathcal{H}^{(t)}$ with subnormalization factor α , and a similar number of additional gates; the term comes from estimating the diagonal elements, the cost for estimating $\text{Tr}(\hat{C}\rho^{(t)})$ is $\tilde{\mathcal{O}}(\alpha\sqrt{n})$, so it is asymptotically negligible in $\mathcal{O}(\cdot)$ notation.

Now we can focus on the complexity of constructing the block-encoding of $\mathcal{H}^{(t)}$, and determining its subnormalization factor α . For this, we need to analyze the structure of $\mathcal{H}^{(t)}$. According to Alg. 6, $\mathcal{H}^{(t)}$ is simply an accumulation of subgradients $G^{(t)}$ (more precisely, $\frac{\epsilon}{2}$ -subgradients in this case). The following properties hold.

Lemma 8.33. *For every iteration t of Alg. 6 applied to (MaxCutSDP-F) as described in Sect. 8.4.2, $\mathcal{H}^{(t)} = y_1\hat{C} + y_2D$ for some vector $y \in \mathbb{R}^2$, where D is a diagonal matrix. Furthermore, $\|y\|_1 \leq \frac{4}{\epsilon} \log n$.*

Proof. For each t , $G^{(t)}$ is either \hat{C} or a diagonal matrix with $-1, 0, +1$ on the diagonal. Then it is clear that in every iteration we can express $\mathcal{H}^{(t)}$ in the stated form for some coefficients y_1, y_2 . In every iteration we accumulate $G^{(t)}$ with coefficient $\eta = \frac{\epsilon}{16}$, so either y_1 or y_2 changes by at most $\frac{\epsilon}{16}$ (we can keep D normalized so that its entries are less than 1 in absolute value). Because initially $y_1 = y_2 = 0$ and we perform $T = \frac{64}{\epsilon^2} \log n$ iterations, we have $\|y\|_1 \leq \eta T = \frac{4}{\epsilon} \log n$. \square

The above result lets us utilize Prop. 7.18 to construct the block-encoding of $\mathcal{H}^{(t)}$: assuming access to a block-encoding for \hat{C} , and a block-encoding for the diagonal matrix D of Lem. 8.33, linear combination of block-encodings produces the desired quantum circuit. It is now necessary to fix the input model, so that we can analyze the cost for block-encoding \hat{C} and D . To simplify the analysis and — at the same time — obtain the fastest asymptotic running time, we assume that we have access to QRAM: in this way, we can utilize the sparse-oracle model of Prop. 7.21 or the QRAM model of Prop. 7.29, whichever is faster. To block-encode \hat{C} we rely on Prop. 7.29: because $\|\hat{C}\|_F = 1$, this gives us a $(1, \tilde{\mathcal{O}}(1), 0)$ -block-encoding with $\tilde{\mathcal{O}}(1)$ gates and accesses to QRAM. To block-encode D we rely on Prop. 7.21, because D is diagonal: this gives us a $(1, \tilde{\mathcal{O}}(1), \xi)$ -block-encoding, where ξ can be made extremely small with little extra cost and can be assumed to be zero to avoid burdensome details, see Rem. 7.22. This block-encoding uses $\tilde{\mathcal{O}}(1)$ calls to oracles describing D and additional gates, but in the QRAM model, the oracles describing D have constant cost: the sparsity of D is fixed and known (it is a diagonal matrix), its elements can be stored in QRAM and queried at unit cost. So, a $(1, \tilde{\mathcal{O}}(1), 0)$ -block-encoding of \hat{C} and D can be constructed with $\tilde{\mathcal{O}}(1)$ accesses to QRAM and additional gates. Prop. 7.18 then gives us a $(\|y\|_1, \tilde{\mathcal{O}}(1), 0)$ -block-encoding of $\mathcal{H}^{(t)}$ using a constant number of queries to block-encodings for \hat{C} , D , and to a state-preparation pair for y . Because y is 2-dimensional, the state-preparation pair has $\tilde{\mathcal{O}}(1)$ cost for any precision.

We now have all the ingredients to state the complexity of the algorithm.

Proposition 8.34. *Given access to a QRAM of size $\tilde{\mathcal{O}}(n^2)$, we can determine a solution to (MaxCutSDP) with optimality and feasibility tolerance ϵ (i.e., problem (MaxCutSDP-F)) using $\tilde{\mathcal{O}}\left(\frac{n^{1.5}}{\epsilon^5}\right)$ accesses to the QRAM and additional gates, and $\tilde{\mathcal{O}}(n^2)$ classical operations.*

Proof. The complexity of the subgradient estimation is:

$$\tilde{\mathcal{O}}\left(\frac{\alpha n^{1.5}}{\epsilon^2}\right)$$

calls to a block-encoding of $\mathcal{H}^{(t)}$ with subnormalization factor α , and a similar number of additional gates. Because $\alpha = \|y\|_1$, and $\|y\|_1 \leq \frac{4}{\epsilon} \log n$ by Lem. 8.33, substituting in the above the expression gives the asymptotic complexity bound $\tilde{\mathcal{O}}\left(\frac{n^{1.5}}{\epsilon^3}\right)$ for subgradient computation in each iteration.

The number of iterations of the algorithm is $\tilde{\mathcal{O}}\left(\frac{1}{\epsilon^2}\right)$; multiplying the per-iteration complexity by the number of iterations, we obtain the stated total complexity for the quantum part. The classical cost is inherited from Prop. 7.29, to prepare the QRAM data structures for the block-encoding of \hat{C} . \square

Remark 8.35. *Without QRAM, the main difference in the running time analysis is that the construction of block-encodings for \hat{C} and D may not be as efficient. For example, in the sparse-oracle access model, block-encoding D has gate complexity $\mathcal{O}(n)$ (because there are n diagonal elements that can be queried, potentially in superposition, so the oracle that returns their value implements a lookup table), and block-encoding \hat{C} may have gate complexity up to $\tilde{\mathcal{O}}(n^2)$ if the matrix is dense. The density of \hat{C} may also make the subnormalization factor worse due to Prop. 7.21, leading to a significant deterioration of the performance of the algorithm.*

Remark 8.36. *Prop. 8.34 analyzes the complexity of obtaining a solution to problem (MaxCutSDP), but this is not the same as the original problem (MaxCutSDP-orig). In particular, because we scaled down the objective function by a factor $\|C\|_F$, as well as the decision variable X by a factor n , to obtain a solution to problem (MaxCutSDP-orig) with additive error ϵ it is sufficient to set the error in problem (MaxCutSDP) to $n\|C\|_F\epsilon$. This yields an approximate solution to problem (MaxCutSDP-orig). [Brandão et al., 2019] shows that if ϵ is chosen small enough, an approximate solution to problem (MaxCutSDP-orig) can be turned into an exactly feasible solution (i.e., all constraints are satisfied exactly, not approximately) with a small deterioration of the objective function. Furthermore, one can use a randomized rounding procedure to turn a solution to problem (MaxCutSDP-orig) into a solution for the original discrete problem (± 1 -QP), with an approximation guarantee on the expected value of the objective function (similar in spirit to [Goemans and Williamson, 1995]).*

8.5 Notes and further reading

The mirror descent algorithm for continuous optimization was initially proposed in [Nemirovski and Yudin, 1983], and since then, it has been used extensively. For a derivation of mirror descent starting from the projected subgradient algorithm, as well as a detailed convergence analysis, we refer the reader to [Beck and Teboulle, 2003]. A clear exposition of proof techniques for convergence rates using potential functions (including for mirror descent) can be found in [Bansal and Gupta, 2019]. The relationship between MMWU and mirror descent is addressed in an appendix in [Allen-Zhu and Orecchia, 2014].

The MWU algorithm has its origin in the Fictitious Play algorithm from game theory [Brown, 1951], although it has been rediscovered multiple times under different names in several fields. An overview of the MWU algorithm and its applications to optimization is given in the excellent survey [Arora et al., 2012], see also the references mentioned therein. The classical MMWU algorithm for SDP is described in [Arora et al., 2005, Arora and Kale, 2016]. The implementation and computational evaluation of some variants of the MWU algorithm to mixed-integer nonlinear optimization is discussed in [Mencarelli et al., 2017].

The quantum MMWU was initially proposed in [Brandao and Svore, 2017, van Apeldoorn et al., 2020b]. The framework, in its first instantiation, presented several limitations, and did not yield an end-to-end speedup over classical algorithms for most problems, see [van Apeldoorn et al., 2020b] for a discussion. Nonetheless, all the basic ingredients of the framework were already present in these early works. Subsequent work has attempted to remove some of the limitations and improve the complexity of the algorithm, see [Brandão et al., 2019, van Apeldoorn and Gilyén, 2019]; these more recent works also include a primal-only algorithm, as opposed to the primal-dual framework discussed in this chapter. Despite these improvements, the running time dependence of these algorithms on the final optimality gap, as well as the size of the optimal primal and dual solution, remains poor.

The quadratic unconstrained $\{-1, +1\}$ optimization problem (± 1 -QP) finds applications in areas such as image compression [O’Leary and Peleg, 1983], correlation clustering [Mei et al., 2017], structured principal component analysis [Kueng and Tropp, 2021]. It is strongly related to the Ising model [Barahona, 1982]. The quantum algorithm discussed in Sect. 8.4.2 to solve the SDP relaxation of (± 1 -QP) was first presented in [Brandao et al., 2022], where it is called “Hamiltonian updates”; the presentation in [Brandao et al., 2022] does not rely on mirror descent, so convergence is proven from first principles, outside the mirror descent framework. Such SDP

relaxation has only diagonal constraints, i.e., constraints on the diagonal elements of the matrix, and more specifically it imposes that the diagonal elements are equal to 1. SDPs with only diagonal constraints admit specialized classical algorithms as well, see, e.g., [Lee and Padmanabhan, 2020]. Convergence of the final iterate of stochastic mirror descent, in addition to convergence of the average iterate, is discussed in [Nedic and Lee, 2014].

Chapter 9

Optimization with the adiabatic theorem

The adiabatic theorem is a powerful result concerning the evolution of quantum-mechanical systems. Intuitively, it states the following: suppose we want to study the evolution of a quantum-mechanical system governed by a given Hamiltonian \mathcal{H} (Def. 6.1), and the initial state of the system is the eigenstate of \mathcal{H} corresponding to its lowest eigenvalue. The laws of quantum physics tell us that the evolution of the system over time follows the Schrödinger equation, Eq. (6.1). Suppose now that the Hamiltonian is not fixed, but rather, it changes very slowly over time, so that the evolution of the system is described by the differential equation $i\frac{d|\psi(t)\rangle}{dt} = \mathcal{H}(t)|\psi(t)\rangle$, and $\mathcal{H}(t)$ is slowly changing. If, for any value of the time parameter t , there is always a gap between the lowest eigenvalue of $\mathcal{H}(t)$ and all other eigenvalues, then the adiabatic theorem asserts that the state of the system always remains in an eigenstate with the lowest eigenvalue throughout the evolution. One specific case of interest in this chapter occurs when the time-dependent Hamiltonian $\mathcal{H}(t)$ varies from an initial (time-independent) Hamiltonian \mathcal{H}_I to a final Hamiltonian \mathcal{H}_F . If the change happens slowly, and the initial state of the system is an eigenstate of \mathcal{H}_I with minimum eigenvalue, the adiabatic theorem asserts that the evolution eventually leads to the eigenstate with minimum eigenvalue of the final Hamiltonian \mathcal{H}_F . This result can be used for optimization: imagine that the initial Hamiltonian encodes an easy problem for which we can construct the eigenstate with minimum eigenvalue, and the final Hamiltonian encodes a difficult optimization problem whose solution is given by the eigenstate with minimum eigenvalue. By the adiabatic theorem, evolving the eigenstate of the initial Hamiltonian while slowly changing the Hamiltonian into the final one leads to the solution of the difficult optimization problem. Of course we need to know how slowly \mathcal{H}_I should be changed into \mathcal{H}_F . The adiabatic theorem is at the heart of the quantum approximate optimization algorithm (QAOA), a framework that has been widely used to implement optimization algorithms on existing quantum hardware, because it has low requirements of quantum resources — although it does not guarantee improvements over classical algorithms in general. In this chapter we first discuss the adiabatic theorem, and then give an overview of QAOA.

Remark 9.1. *The term adiabatic refers to a process that occurs without heat or mass transfer between a thermodynamic system and its environment. For the purposes of this chapter (and quantum algorithms more in general), it should be intended as a process where the evolution of the system is slow enough that the system has time to adapt, i.e., remain in some instantaneous eigenstate evolving through time, typically the one corresponding to the smallest eigenvalue. Conversely, in a diabatic process the system evolves too rapidly, and it may not remain in an instantaneous eigenstate of the system.*

9.1 The adiabatic theorem

Before diving into a formal statement of the adiabatic theorem, it may be helpful to make its connection with optimization apparent. In this chapter, optimization refers to the NP-hard problem of optimizing a quadratic function over binary variables.

9.1.1 Combinatorial optimization as an eigenvalue problem

Suppose we have the following optimization problem:

$$\min f(\vec{x}) \quad \vec{x} \in \{0, 1\}^n. \quad (9.1)$$

We put no restriction on $f : \{0, 1\}^n \rightarrow \mathbb{R}$ for now, therefore we can encode any combinatorial optimization problem in this way (e.g., by assigning value ∞ to infeasible binary strings, if there are any, or some large finite value that effectively amounts to ∞). We encode this problem in a diagonal Hamiltonian $\mathcal{H} \in \mathbb{R}^{2^n \times 2^n}$ defined as follows:

$$\mathcal{H} := \sum_{\vec{j} \in \{0, 1\}^n} f(\vec{j}) |\vec{j}\rangle \langle \vec{j}|.$$

Note that \mathcal{H} contains all the possible objective function values on its diagonal, each one in the position associated with the corresponding binary string ($\langle \vec{j} | \mathcal{H} | \vec{j} \rangle = f(\vec{j}) \quad \forall \vec{j} \in \{0, 1\}^n$), and zeroes everywhere else ($\langle \vec{j} | \mathcal{H} | \vec{k} \rangle = 0 \quad \forall \vec{j} \neq \vec{k}$). Then problem (9.1) can be trivially reformulated as follows:

$$\min_{\vec{j} \in \{0, 1\}^n} \langle \vec{j} | \mathcal{H} | \vec{j} \rangle,$$

and this problem has the same optimal solution as:

$$\min_{|\psi\rangle} \langle \psi | \mathcal{H} | \psi \rangle. \quad (9.2)$$

To see the equivalence, simply note that $|\vec{j}\rangle, \vec{j} \in \{0, 1\}^n$ is an eigenbasis for \mathcal{H} (because \mathcal{H} is diagonal), so we can express every state $|\psi\rangle$ in terms of the eigenbasis, and the problem becomes:

$$\min_{\substack{\alpha \in \mathbb{C}^{2^n} \\ \|\alpha\|=1}} \left(\sum_{\vec{j} \in \{0, 1\}^n} \alpha_j^\dagger \langle \vec{j} | \right) \mathcal{H} \left(\sum_{\vec{j} \in \{0, 1\}^n} \alpha_j | \vec{j} \rangle \right) = \min_{\substack{\alpha \in \mathbb{C}^{2^n} \\ \|\alpha\|=1}} \sum_{\vec{j} \in \{0, 1\}^n} |\alpha_j|^2 \mathcal{H}_{jj} = \min_{\vec{j} \in \{0, 1\}^n} f(\vec{j}).$$

The same argument also works to show that for every Hamiltonian \mathcal{H} — including those that are not necessarily diagonal — problem (9.2) is a minimum eigenvalue problem, i.e., it is equivalent to determining $\lambda_{\min}(\mathcal{H})$, the minimum eigenvalue of \mathcal{H} . Recall that Hamiltonians are Hermitian. Let $|\psi_0\rangle, \dots, |\psi_{2^n-1}\rangle$ be a basis of orthonormal eigenstates of \mathcal{H} , and V a matrix with those vectors as its columns. Then $\mathcal{H} = V \Lambda V^\dagger$, and

$$\begin{aligned} \min_{|\psi\rangle \in (\mathbb{C}^2)^{\otimes n}} \langle \psi | \mathcal{H} | \psi \rangle &= \min_{\substack{\alpha \in \mathbb{C}^{2^n} \\ \|\alpha\|=1}} \left(\sum_{\vec{j} \in \{0, 1\}^n} \alpha_j^\dagger \langle \psi_j | \right) \mathcal{H} \left(\sum_{\vec{j} \in \{0, 1\}^n} \alpha_j | \psi_j \rangle \right) \\ &= \min_{\substack{\alpha \in \mathbb{C}^{2^n} \\ \|\alpha\|=1}} \left(\sum_{\vec{j} \in \{0, 1\}^n} \alpha_j^\dagger \langle \psi_j | \right) V \Lambda V^\dagger \left(\sum_{\vec{j} \in \{0, 1\}^n} \alpha_j | \psi_j \rangle \right) \\ &= \min_{\substack{\alpha \in \mathbb{C}^{2^n} \\ \|\alpha\|=1}} \left(\sum_{\vec{j} \in \{0, 1\}^n} \alpha_j^\dagger \langle \vec{j} | \right) \Lambda \left(\sum_{\vec{j} \in \{0, 1\}^n} \alpha_j | \vec{j} \rangle \right) \\ &= \min_{\substack{\alpha \in \mathbb{C}^{2^n} \\ \|\alpha\|=1}} \sum_{\vec{j} \in \{0, 1\}^n} |\alpha_j|^2 \Lambda_{jj} = \lambda_{\min}(\mathcal{H}). \end{aligned}$$

Thus, the general combinatorial optimization problem in Eq. (9.1) can be solved as the problem of determining the minimum eigenvalue of a certain Hamiltonian, written compactly as problem (9.2).

One may wonder how to construct the Hamiltonian $\mathcal{H} = \sum_{\vec{j} \in \{0,1\}^n} f(\vec{j}) |\vec{j}\rangle\langle\vec{j}|$ starting from a “reasonable” description of f : usually listing all values of $f(\vec{j})$ is not efficient, because there are 2^n of them. Thus, we are looking for some implicit, more compact representation, for example by means of an analytical description of the objective function, and that representation should allow for efficient construction of \mathcal{H} . An especially straightforward way to construct \mathcal{H} is applicable whenever we start from a problem stated as a quadratic unconstrained binary optimization problem (QUBO), see Def. 9.3, because there is a simple transformation from a QUBO to the desired Hamiltonian. Also note that, because QUBOs are NP-complete [Barahona, 1982], any problem in NP can be formulated as a QUBO with an appropriate polynomial transformation.

Remark 9.2. *The fact that it is possible to formulate every problem in NP as a QUBO does not mean that it is wise to do so. For example, it is well known that polynomial transformations (intended here as polynomial-time reductions, or Karp reductions) map an instance of a problem to an instance of a different problem with polynomial overhead [Garey and Johnson, 1990]. However, the overhead for such a mapping can be very large, and applying a solution algorithm to the transformed problem could be considerably less efficient, in practice, than applying a solution algorithm to the original problem. Thus, formulating a combinatorial optimization problem as a QUBO, and solving it as such, may end up being much slower than solving the problem in a different form.*

Definition 9.3 (Quadratic Unconstrained Binary Optimization (QUBO) problem). *The following problem is called a Quadratic Unconstrained Binary Optimization (QUBO) problem with n decision variables:*

$$\min_{\vec{x} \in \{0,1\}^n} \vec{x}^\top Q \vec{x}, \tag{QUBO}$$

where $Q \in \mathbb{R}^{n \times n}$ is a symmetric matrix.

(In certain algebraic expressions, such as the above, we use binary strings also as “regular” 0-1 column vectors, allowing them to appear in operations such as matrix-vector multiplication. The meaning of these expressions should be clear from the context.)

The mapping from (QUBO) to a Hamiltonian is via Pauli Z matrices. First, transform the $\{0,1\}$ -variables \vec{x}_j into $\{-1,+1\}$ -variables z_j , using the linear transformation $\vec{x}_j = (1 - z_j)/2$. With this transformation, $z = 1 - 2\vec{x}$ so $z \in \{-1,+1\}^n$. Problem (QUBO) becomes:

$$\min_{z \in \{-1,+1\}^n} z^\top A z + c^\top z + b \tag{9.3}$$

where $A \in \mathbb{R}^{n \times n}, c \in \mathbb{R}^n, b \in \mathbb{R}$ are easily computed from (QUBO):

$$A = \frac{Q}{4} \quad c^\top = -\frac{\mathbb{1}^\top Q}{2} \quad b = \frac{\mathbb{1}^\top Q \mathbb{1}}{4}.$$

The sought Hamiltonian can be obtained from these quantities using matrices σ_j^Z :

$$\sigma_j^Z := \underbrace{I \otimes \cdots \otimes I}_{n \text{ times}} \otimes \overset{\text{position } j}{\downarrow} Z \otimes I \cdots \otimes I, \tag{9.4}$$

where Z is the Pauli Z matrix as given in Def. 1.36.

Proposition 9.4. *The Hamiltonian:*

$$\mathcal{H} := \sum_{j,k=1}^n A_{jk} \sigma_j^Z \sigma_k^Z + \sum_{j=1}^n c_j \sigma_j^Z$$

satisfies the properties:

$$\langle \vec{x} | \mathcal{H} | \vec{x} \rangle = z^\top A z + c^\top z \quad \forall \vec{x} \in \{0, 1\}^n, \quad \langle \vec{j} | \mathcal{H} | \vec{k} \rangle = 0 \quad \forall \vec{j} \neq \vec{k},$$

where $z = 1 - 2\vec{x} \in \{-1, +1\}^n$.

Proof. Both properties can be verified with simple algebraic manipulations. It is immediate to see that the matrices σ_j^Z, σ_k^Z commute when $j \neq k$. By definition we have:

$$\langle \vec{x} | \mathcal{H} | \vec{x} \rangle = \langle \vec{x} | \left(\sum_{j,k=1}^n A_{jk} \sigma_j^Z \sigma_k^Z + \sum_{j=1}^n c_j \sigma_j^Z \right) | \vec{x} \rangle. \quad (9.5)$$

Note that for every $h = 1, \dots, n$,

$$\langle \vec{j} | \sigma_h^Z | \vec{k} \rangle = \langle \vec{j}_1 | \vec{k}_1 \rangle \otimes \dots \otimes \langle \vec{j}_{h-1} | \vec{k}_{h-1} \rangle \otimes \langle \vec{j}_h | Z | \vec{k}_h \rangle \otimes \langle \vec{j}_{h+1} | \vec{k}_{h+1} \rangle \otimes \dots \otimes \langle \vec{j}_n | \vec{k}_n \rangle,$$

so each such term is zero if $\vec{j} \neq \vec{k}$, and it is equal to $\langle \vec{j}_h | Z | \vec{j}_h \rangle = (-1)^{\vec{j}_h}$ if $\vec{j} = \vec{k}$. Similarly, for every $h, \ell = 1, \dots, n$:

$$\langle \vec{j} | \sigma_h^Z \sigma_\ell^Z | \vec{k} \rangle = \langle \vec{j}_1 | \vec{k}_1 \rangle \otimes \dots \otimes \underbrace{\langle \vec{j}_h | Z | \vec{k}_h \rangle}_{\text{position } h} \otimes \dots \otimes \underbrace{\langle \vec{j}_\ell | Z | \vec{k}_\ell \rangle}_{\text{position } \ell} \otimes \dots \otimes \langle \vec{j}_n | \vec{k}_n \rangle,$$

which is zero if $\vec{j} \neq \vec{k}$, and it is equal to $\langle \vec{j}_h | Z | \vec{j}_h \rangle \langle \vec{j}_\ell | Z | \vec{j}_\ell \rangle = (-1)^{\vec{j}_h} (-1)^{\vec{j}_\ell}$ if $\vec{j} = \vec{k}$. (The latter expression also works if $h = \ell$, in which case $\langle \vec{j} | \sigma_h^Z \sigma_h^Z | \vec{j} \rangle = 1$.) So:

$$\langle \vec{x} | \sigma_j^Z | \vec{x} \rangle = (-1)^{\vec{x}_j} = z_j, \quad \langle \vec{x} | \sigma_j^Z \sigma_k^Z | \vec{x} \rangle = (-1)^{\vec{x}_j + \vec{x}_k} = z_j z_k,$$

and using linearity in Eq. (9.5), we finally obtain $\langle \vec{x} | \mathcal{H} | \vec{x} \rangle = \sum_{j,k=1}^n A_{jk} z_j z_k + \sum_{j=1}^n c_j z_j = z^\top A z + c^\top z$ with $z = 1 - 2\vec{x} \in \{-1, +1\}^n$. \square

Prop. 9.4 gives an explicit construction of a Hamiltonian that has the possible objective function values of Eq. (9.3) on the diagonal, minus the scalar shift b that is not influential for optimization anyway. After establishing that we can cast problem (QUBO) as the problem of finding the minimum eigenvalue of a certain Hamiltonian, explicitly constructed using a linear combination of tensor products of Z and identity matrices, we now discuss the adiabatic theorem, which gives a sufficient condition to find the minimum eigenvalue via time-dependent Hamiltonian simulation.

9.1.2 Theorem statement

Properly introducing the context of the adiabatic theorem requires several pieces of notation. Our exposition in the next few sections is based on [Ambainis and Regev, 2004]. Although the result proven in [Ambainis and Regev, 2004] is not as strong as it could be, it provides the key elements, and the proof relies on linear algebra only. Tighter and more precise bounds can be found in, e.g., [Jansen et al., 2007, Childs, 2017], see also Sect. 9.1.5.

From now on, for brevity we write *minimum eigenpair* to indicate the lowest eigenvalue and its corresponding eigenvector of a Hamiltonian, and *minimum eigenvector* to indicate the eigenvector corresponding to the lowest eigenvalue. (Although we often write “eigenstate” for “eigenvector”, in this chapter we also use the more generic term eigenvector because we sometimes deal with vectors that are not normalized quantum states.)

Let $\mathcal{H}(s)$ be a time-dependent Hamiltonian, with $0 \leq s \leq 1$. For now we use s to denote time because we reserve t to denote “unnormalized” time outside the interval $[0, 1]$: this aspect is clarified subsequently in this section. We assume that the entries of $\mathcal{H}(s)$ are twice differentiable. We denote the first and second derivatives of \mathcal{H} at time s as $\mathcal{H}'(s), \mathcal{H}''(s)$, respectively: these are intended to be the matrices of element-wise derivatives.

The adiabatic theorem concerns the situation where we know the minimum eigenstate of $\mathcal{H}(0)$, and we want to determine the minimum eigenstate of $\mathcal{H}(1)$.

Remark 9.5. *This setup is helpful for combinatorial optimization in the following sense. As discussed in Sect. 9.1.1, we know how to construct a Hamiltonian \mathcal{H}_F that encodes a combinatorial optimization problem of the form (QUBO), and this is already a form that encompasses all optimization problems in the complexity class NP (although it is important to keep Rem 9.2 in mind). In the notation \mathcal{H}_F , we use the subscript “F” for “final”. Pick a simple Hamiltonian \mathcal{H}_I (the subscript “I” stands for “initial”) for which we know the minimum eigenpair; for example, we could define $|\phi\rangle := \frac{1}{\sqrt{2^n}} \sum_{\vec{j} \in \{0,1\}^n} |\vec{j}\rangle$ and pick:*

$$\mathcal{H}_I = I^{\otimes n} - |\phi\rangle\langle\phi|,$$

that has minimum eigenvalue 0 achieved by the state $|\phi\rangle$ (we do not claim that this is a good choice for the initial Hamiltonian, but it is a valid choice). We can then define the time-dependent Hamiltonian:

$$\mathcal{H}(s) = (1-s)\mathcal{H}_I + s\mathcal{H}_F. \quad (9.6)$$

By construction, this Hamiltonian is such that we know the minimum eigenstate of $\mathcal{H}(0) = \mathcal{H}_I$, and we want to determine the minimum eigenstate of $\mathcal{H}(1) = \mathcal{H}_F$, as that corresponds to the solution of (QUBO) and therefore problem (9.1). The Hamiltonian in Eq. 9.6 is a linear interpolation between the initial and final Hamiltonian, but some of the results that we prove in this chapter hold for more general types of interpolation. In fact, the discussion in Sect. 9.1.5 shows that other forms of interpolation may be advantageous in certain situations.

Definition 9.6 (Norm of time-dependent quantities). *We denote $\|\mathcal{H}\| := \max_{s \in [0,1]} \|\mathcal{H}(s)\|$, i.e., the norm of a time-dependent quantity, when written without the time variable, is intended to be the maximum norm over the time horizon. We extend this notation to all time-dependent quantities.*

We also need the concept of *spectral gap* of a Hamiltonian, as the statement of the adiabatic theorem depends on it. The concept of spectral gap relies on properties of the spectrum of \mathcal{H} . It is known that, when the entries of \mathcal{H} vary continuously over time, the eigenvalues of \mathcal{H} are also continuous functions of time. In other words, one can pick continuous functions $\lambda_1(s), \lambda_2(s), \dots$ that describe the eigenvalues of \mathcal{H} as s varies. Intuitively, this is a consequence of the fact that the eigenvalues are the roots of the characteristic polynomial of \mathcal{H} , and the coefficients of the characteristic polynomial are continuous functions of the entries of \mathcal{H} . For a formal proof, see [Kato, 1995, Thm. 5.2].

Remark 9.7. *As stated earlier, in this chapter all Hamiltonians are assumed to have twice-differentiable entries, therefore their eigenvalues vary continuously as functions of time. We do not repeat this assumption in the statement of subsequent results: when we mention a time-dependent Hamiltonian, it has twice-differentiable entries. We emphasize this fact because without the assumption, some of the statements would not make sense, so it is important to keep it in mind.*

Definition 9.8 (Instantaneous spectral gap). *Let $\mathcal{H}(s)$ be a time-dependent Hamiltonian, and $\lambda(s)$ an eigenvalue of $\mathcal{H}(s)$, for $s \in [0,1]$. Let $\gamma(s), s \in [0,1]$ be the quantity defined in the following way:*

- *if $\lambda(s)$ has algebraic multiplicity > 1 , $\gamma(s) := 0$;*
- *otherwise, let $\lambda_{<}(s)$ be the largest eigenvalue strictly smaller than $\lambda(s)$, $\lambda_{>}(s)$ the smallest eigenvalue strictly larger than $\lambda(s)$, and $\gamma(s) := \min\{\lambda(s) - \lambda_{<}(s), \lambda_{>}(s) - \lambda(s)\}$.*

We say that $\mathcal{H}(s)$ has instantaneous spectral gap $\gamma(s)$ around $\lambda(s)$.

In other words, the instantaneous spectral gap around an eigenvalue is a “buffer zone” in the spectrum of the Hamiltonian that contains no other eigenvalue, at a specific time.

Definition 9.9 (Spectral gap). *Let $\mathcal{H}(s)$, $\lambda(s)$ and $\gamma(s)$ be as in Def. 9.8. We say that $\mathcal{H}(s)$ has a spectral gap γ around $\lambda(s)$ if $\gamma = \min_s \gamma(s)$. The spectral gap of $\mathcal{H}(s)$ is the spectral gap around its minimum eigenvalue.*

Note that the spectral gap could be zero, if the eigenvalues are not distinct. Note also that if $\mathcal{H}(s)$ has spectral gap γ around $\lambda(s)$, then all other eigenvalues of $\mathcal{H}(s)$ are $\leq \lambda(s) - \gamma$ or $\geq \lambda(s) + \gamma$ for all s . In the literature, the term “spectral gap” is sometimes used to implicitly refer to a *nonzero* spectral gap (sometimes one also reads “gapped Hamiltonian”, to refer to a Hamiltonian that has nonzero spectral gap); we use the more general definition above, and explicitly require $\gamma > 0$ for the main result.

In the adiabatic theorem we consider a slow time evolution according to the Hamiltonian $\mathcal{H}(s)$. Recall that the time-independent Schrödinger equation, Eq. (6.1), is:

$$i \frac{d|\psi(t)\rangle}{dt} = \mathcal{H}|\psi(t)\rangle,$$

and it has solution $|\psi(t)\rangle = e^{-i\mathcal{H}t}|\psi(0)\rangle$. Thus, if $|\psi(0)\rangle$ is an eigenstate of \mathcal{H} , the system remains in an eigenstate as time evolves (see Def. 6.3 and the surrounding discussion: the eigenvectors of $e^{-i\mathcal{H}t}$ are the same as the eigenvectors of \mathcal{H} , only the eigenvalues change; this can be seen by diagonalizing \mathcal{H} and applying the definition of matrix exponential). This applies to time-independent Hamiltonians. When the Hamiltonian is time-dependent this property is not true in general, but intuitively it is conceivable that if the Hamiltonian changes slowly enough, the evolution of the system under a time-dependent Hamiltonian is similar to the evolution for time-independent Hamiltonians; thus, the system remains in the instantaneous eigenstate for each time instant. This is the essence of the adiabatic theorem; of course, we need to prove that such a result holds.

For some large value $T \in \mathbb{R}$, we consider the following slow evolution, modified from Eq. (6.1) by absorbing a multiplicative factor -1 into the Hamiltonian for ease of subsequent calculations, and by introducing a time-dependent Hamiltonian that slowly changes between $\mathcal{H}(0)$ and $\mathcal{H}(1)$ (note that the larger the value of T , the slower the change):

$$\frac{d|\varphi(t)\rangle}{dt} = i\mathcal{H}(t/T)|\varphi(t)\rangle, \quad t \in [0, T], \tag{9.7}$$

where time t progresses from 0 to T . With a change of variable $s = t/T$, we have $Tds = dt$, and therefore Eq. (9.7) can be rewritten as:

$$\frac{d|\varphi(sT)\rangle}{Tds} = i\mathcal{H}(s)|\varphi(sT)\rangle, \quad s \in [0, 1].$$

Defining $|\psi(s)\rangle := |\varphi(sT)\rangle$, we finally obtain:

$$\frac{d|\psi(s)\rangle}{ds} = iT\mathcal{H}(s)|\psi(s)\rangle, \quad s \in [0, 1]. \tag{9.8}$$

From now on we always refer to Eq. (9.8) rather than Eq. (9.7), using s as our time variable; to build intuition, it is useful to remember that $s = t/T$, and so as $T \rightarrow \infty$, time evolves very slowly.

We want to determine a value of T with the following property: if the initial state $|\psi(0)\rangle$ in Eq. (9.8) is the minimum eigenvector of $\mathcal{H}(0)$, then the final state $|\psi(1)\rangle$ is the minimum eigenvector of $\mathcal{H}(1)$.

Remark 9.10. *At this point it is not clear that such a value of T exists. The main reason to believe that such a property may hold is the intuition given earlier in this section: if $T \rightarrow \infty$, the system should behave similarly to the case of a time-independent Hamiltonian, thus it should remain in an (instantaneous) eigenstate of the Hamiltonian.*

The adiabatic theorem provides sufficient conditions so that the value of T with the desired property not only exists, but can also be lower bounded, so that picking any T larger than a threshold suffices to guarantee that the final state $|\psi(1)\rangle$ is (approximately) the minimum eigenvector of $\mathcal{H}(1)$.

Theorem 9.11 (Adiabatic theorem). *Let $\mathcal{H}(s)$ be a time-dependent Hamiltonian, let $\lambda(s)$ be an eigenvalue of $\mathcal{H}(s)$, and let $|\varphi(s)\rangle$ be an eigenstate of $\mathcal{H}(s)$ with eigenvalue $\lambda(s)$. Assume that*

there is a spectral gap $\gamma > 0$ around $\lambda(s)$. Assume further that, from the initial state $|\varphi(0)\rangle$, we apply the following time evolution:

$$\frac{d|\psi(s)\rangle}{ds} = iT\mathcal{H}(s)|\psi(s)\rangle, \quad s \in [0, 1], \quad |\psi(0)\rangle = |\varphi(0)\rangle,$$

and for some $\delta > 0$, T satisfies:

$$T \geq \frac{10^4}{\delta^2} \left(\frac{\|\mathcal{H}'\|^3}{\gamma^4} + \frac{\|\mathcal{H}'\|\|\mathcal{H}''\|}{\gamma^3} \right).$$

Then the system approximately remains in the instantaneous eigenstate $|\varphi(s)\rangle$ with eigenvalue $\lambda(s)$ for all s , and in particular, the final state $|\psi(1)\rangle$ has Euclidean distance at most δ from $|\varphi(1)\rangle$, up to global phase:

$$\|e^{i\theta}|\psi(1)\rangle - |\varphi(1)\rangle\| \leq \delta \quad \text{for some } \theta.$$

Remark 9.12. It is intuitive to see that the nonzero spectral gap condition is necessary even just to have the concept of an adiabatic theorem. Suppose there is no spectral gap, i.e., the eigenvalue $\lambda(s)$ corresponding to the initial eigenstate “crosses” another eigenvalue $\lambda'(s)$ as s goes from 0 to 1. In that case, the corresponding instantaneous eigenstate $|\varphi(s)\rangle$ would not be well-defined, due to the degenerate eigenvalue. When there are two eigenvalues $\lambda(s) = \lambda'(s)$ that are identical at time s , the eigenstate $|\varphi(s)\rangle$ corresponding to $\lambda(s)$ is no longer unique, and we cannot properly define how the state of the system is supposed to approximately follow $|\varphi(s)\rangle$. With nonzero spectral gap these issues do not arise: the eigenvalue of interest is nondegenerate, and there is always a unique eigenstate corresponding to $\lambda(s)$.

A proof of Thm. 9.11 is given in Sect.s 9.1.3 and 9.1.4. In the first section we give a shorter, more intuitive but less precise version of the argument of the proof. Several gaps are filled in in the second section, although we do not give all the details, and refer to [Ambainis and Regev, 2004] for the (very few) missing pieces.

9.1.3 High-level proof

Simulating Eq. (9.8) directly is difficult because it is a continuous-time dynamical system where the evolution operator (the Hamiltonian) also changes with time. The approach that we take, as one generally takes on all digital computers, is to discretize time into very small steps, and perform time evolution in each of those time steps with a fixed Hamiltonian. As the size of those steps goes down to zero, the discrete-time evolution approaches the continuous-time evolution, so we can analyze properties of the discrete-time evolution instead of Eq. (9.8). More specifically, we divide the time interval $[0, 1]$ (for the normalized time variable s) into N equally-spaced subintervals with breakpoints $\frac{0}{N}, \frac{1}{N}, \dots, \frac{N-1}{N}, \frac{N}{N}$. In each interval we apply the time-independent Hamiltonian $\mathcal{H}(j/N)$ for $\frac{1}{N}$ units of time. It is easy to verify that the solution to the differential equation with time-independent Hamiltonian:

$$\frac{d|\psi(s)\rangle}{ds} = iT\mathcal{H}(j/N)|\psi(s)\rangle$$

is:

$$|\psi(s)\rangle = e^{iT\mathcal{H}(j/N)s}|\psi(0)\rangle.$$

Thus, applying the time-independent Hamiltonian $\mathcal{H}(j/N)$ for $\frac{1}{N}$ units of time is equivalent to applying $e^{iT/N\mathcal{H}(j/N)}$ to the initial state (we obtain this by setting $s = \frac{1}{N}$ in the last equation). As a consequence, defining

$$U_j := e^{iT/N\mathcal{H}(j/N)}, \tag{9.9}$$

the original continuous-time evolution in Eq. (9.8) can be approximated by applying to the initial state a sequence of N unitaries:

$$|\psi(1)\rangle \approx U_{N-1}U_{N-2}\cdots U_1U_0|\psi(0)\rangle, \quad |\psi(0)\rangle = |\varphi(0)\rangle.$$

As $N \rightarrow \infty$, this approximation gets better and the error goes to zero [van Dam et al., 2001]. For brevity and for notational similarity to other vectors that appear in the rest of the analysis, it is convenient to denote by $g_j = |\varphi(j/N)\rangle$ a unit eigenvector of $\mathcal{H}(j/N)$ (and, consequently, U_j) corresponding to $\lambda(j/N)$, see Rem. 9.12:

$$g_j = |\varphi(j/N)\rangle \in \{x : \mathcal{H}(j/N)x = \lambda(j/N)x, \|x\| = 1\}. \quad (9.10)$$

The vector g_j is normalized, whereas other vectors for which we do not use the bra-ket notation are typically not normalized. It is important to note that due to the gap assumption $\gamma > 0$ in Thm. 9.11, $\lambda(j/N)$ is an eigenvalue with algebraic multiplicity 1, therefore there is a single eigenspace associated with it.

Remark 9.13. *Eigenvectors can only be defined up to a global phase: if g_j is an eigenvector, then $e^{i\theta}g_j$ is also an eigenvector with the same eigenvalue and the same magnitude, i.e., $\|g_j\| = \|e^{i\theta}g_j\|$. These eigenvectors are equivalent for the purposes of defining the final state of the adiabatic evolution, but we need to choose the phases appropriately to be able to compute Euclidean distances between eigenvectors: we could have eigenvectors g_j, g_{j+1} of $\mathcal{H}(j/N), \mathcal{H}((j+1)/N)$ that are close to each other for some choice of their global phases, but far from each other for different global phases. In the high-level exposition given in this section we simply ignore the issue of choosing the global phases of the eigenvectors, so the results should be interpreted as “there exists a choice of the global phases such that these results hold.” A more precise discussion is given in Sect. 9.1.4.*

Note that in the limit $N \rightarrow \infty$, and assuming that the adiabatic theorem (Thm. 9.11) holds, the state $|\psi(j/N)\rangle$ of the system is essentially the same as $g_j = |\varphi(j/N)\rangle$. Thus, we want to show that, as $N \rightarrow \infty$:

$$g_N \approx U_{N-1}g_{N-1} \approx U_{N-1}U_{N-2}g_{N-2} \approx U_{N-1}U_{N-2} \cdots U_1U_0g_0.$$

Remark 9.14. *Because $N \rightarrow \infty$, in $\mathcal{O}(\cdot)$ expressions containing N we only write the terms that depend on N , which is always the leading term. This means that, for example, instead of $\mathcal{O}(\|\mathcal{H}\|/N)$ we write $\mathcal{O}(1/N)$.*

For simplicity, from now on we consider the case in which $\lambda(s) = 0$ for all s , i.e., we are tracking the eigenvector corresponding to the zero eigenvalue for the entire time evolution.

Remark 9.15. *This is without loss of generality because, given a general Hamiltonian $\mathcal{H}(s)$ and eigenvalue of interest $\lambda(s)$, we can always consider a new Hamiltonian defined as $\hat{\mathcal{H}}(s) := \mathcal{H}(s) - \lambda(s)I$, while keeping the initial state fixed. These Hamiltonians define the same adiabatic evolution up to a time-dependent global phase, and by construction, for the new Hamiltonian $\hat{\mathcal{H}}(s)$ the system always remains in the eigenvector with eigenvalue 0. To ensure correctness of this argument we also need to show that the value of T in Thm. 9.11 applies to both $\mathcal{H}(s)$ and $\hat{\mathcal{H}}(s)$, i.e., that this transformation does not require us to choose a significantly larger T ; we do this subsequently in Cor. 9.21.*

Consider a decomposition of g_j in terms of g_{j+1} and its orthogonal complement, the subspace G_{j+1}^\perp . Define:

$$p_{j+1} := \text{Proj}_{G_{j+1}^\perp}(g_j - g_{j+1}) \quad (9.11)$$

as the projection of $g_j - g_{j+1}$ onto G_{j+1}^\perp , i.e., onto the space perpendicular to g_{j+1} , see Fig. 9.1 for a graphical representation of these vectors. Clearly $g_j = g_{j+1} + (g_j - g_{j+1})$. It turns out that $g_j - g_{j+1}$ is almost orthogonal to g_{j+1} , i.e., p_{j+1} almost coincides with $g_j - g_{j+1}$:

$$\|p_{j+1} - (g_j - g_{j+1})\| = \mathcal{O}\left(\frac{1}{N^2}\right). \quad (9.12)$$

Thus, using the fact that $U_j g_j = g_j$, because g_j is an eigenvector with eigenvalue $e^{iT/N\lambda(j/N)} = 1$, we can write:

$$U_j g_j - (g_{j+1} + p_{j+1}) = g_j - (g_{j+1} + p_{j+1}) = (g_j - g_{j+1}) - p_{j+1} = v_{j+1} \text{ with } \|v_{j+1}\| = \mathcal{O}\left(\frac{1}{N^2}\right).$$

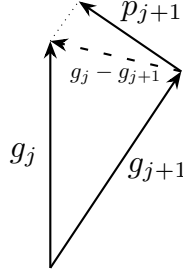


Figure 9.1: Representation of the eigenvectors g_j, g_{j+1} , and the projection p_j of $g_j - g_{j+1}$ onto the space orthogonal to g_{j+1} .

Rearranging the terms in the last equality yields $U_j g_j = g_{j+1} + p_{j+1} + v_{j+1}$. As a consequence, if we apply all the unitaries U_0, \dots, U_{N-1} in sequence, we obtain:

$$\begin{aligned} U_{N-1} \cdots U_1 U_0 g_0 &= U_{N-1} \cdots U_2 U_1 (g_1 + p_1 + v_1) = U_{N-1} \cdots U_2 U_1 g_1 + U_{N-1} \cdots U_2 U_1 (p_1 + v_1) \\ &= U_{N-1} \cdots U_3 U_2 (g_2 + p_2 + v_2) + U_{N-1} \cdots U_2 U_1 (p_1 + v_1) \\ &= U_{N-1} \cdots U_3 U_2 g_2 + U_{N-1} \cdots U_3 U_2 (p_2 + v_2) + U_{N-1} \cdots U_2 U_1 (p_1 + v_1) = \dots \\ &= g_N + \sum_{j=1}^N U_{N-1} \cdots U_j p_j + \underbrace{\sum_{j=1}^N U_{N-1} \cdots U_j v_j}_{\text{error term}}, \end{aligned}$$

and the norm of the error term can be upper bounded as:

$$\left\| \sum_{j=1}^N U_{N-1} \cdots U_j v_j \right\| \leq \sum_{j=1}^N \|v_j\| = \mathcal{O}\left(\frac{1}{N}\right).$$

Remark 9.16. The summation $\sum_{j=1}^N U_{N-1} \cdots U_j p_j$ is written with upper limit N , even though the sequence of matrices stops at U_{N-1} , as a shorthand for the inclusion of the term p_N . In other words, $\sum_{j=1}^N U_{N-1} \cdots U_j p_j = p_N + \sum_{j=1}^{N-1} U_{N-1} \cdots U_j p_j$. We use the same convention for $\sum_{j=1}^N U_{N-1} \cdots U_j v_j$, although the latter sum stops being important in the following.

If we can show that $\left\| \sum_{j=1}^N U_{N-1} \cdots U_j p_j \right\|$ is small, then $U_{N-1} \cdots U_0 g_0 \approx g_N$, proving the desired result. More precisely, to show Thm. 9.11 we in fact need to show that $\left\| \sum_{j=1}^N U_{N-1} \cdots U_j p_j \right\| \leq \delta$: because $N \rightarrow \infty$, the norm of the error term goes to zero, implying that the distance between the final state produced by the evolution and $g_N = |\varphi(1)\rangle$ is at most δ , as desired. Thus, our last task is to prove:

$$\left\| \sum_{j=1}^N U_{N-1} \cdots U_j p_j \right\| \leq \delta. \quad (9.13)$$

To this end, we split $\sum_{j=1}^N U_{N-1} \cdots U_j p_j$ into groups with M terms each, where we choose an appropriate $M = \mathcal{O}(N)$, i.e., we partition the expression into N/M sums:

$$\sum_{j=1}^M U_{N-1} \cdots U_j p_j, \quad \sum_{j=M+1}^{2M} U_{N-1} \cdots U_j p_j, \quad \sum_{j=2M+1}^{3M} U_{N-1} \cdots U_j p_j, \quad \dots \quad (9.14)$$

The precise value of M is important and is specified later, but for now we can just take it to be some small fraction of N . We then show that each group has a small norm. The reason for

performing this split is not readily apparent, and it may be useful to give some intuition. The expression $\sum_{j=1}^N U_{N-1} \cdots U_j p_j$ is not easy to analyze; however, if we could replace each p_j with p_1 , and each U_j with U_1 , then we would obtain the much simpler expression $\sum_{j=1}^{N-1} U_1^j p_1$, which is relatively easy to analyze by expressing p_1 in terms of eigenvectors of U_1 . The issue is, of course, that replacing each p_j with p_1 , and each U_j with U_1 , incurs a large total error, so this strategy would fail. However, a more nuanced version of this strategy can be made to work. By triangle inequality, partitioning the “large” sum into M/N terms, we obtain:

$$\left\| \sum_{j=1}^N U_{N-1} \cdots U_j p_j \right\| \leq \sum_{k=0}^{N/M-1} \left\| \sum_{j=kM+1}^{(k+1)M} U_{N-1} \cdots U_j p_j \right\|,$$

so if we can show that:

$$\left\| \sum_{j=kM+1}^{(k+1)M} U_{N-1} \cdots U_j p_j \right\| \leq \frac{\delta M}{N},$$

this immediately implies Eq. (9.13). We look at the case $k = 0$ to understand the main idea, as the other cases are very similar. Thus, we are looking for an upper bound to $\left\| \sum_{j=1}^M U_{N-1} \cdots U_j p_j \right\|$. The terms $U_{N-1} \cdots U_M$ appear in every term of the summation on the l.h.s., and because they are unitary, they do not affect the norm and can be suppressed. In Sect. 9.1.4 we show that:

$$\left\| \sum_{j=1}^M U_{M-1} \cdots U_j p_j \right\| \approx \left\| \sum_{j=0}^{M-1} U_1^j p_1 \right\|,$$

with some error that is discussed below. This lets us work with an approximation that is much easier to analyze. To generalize this idea for all $k = 0, \dots, N/M - 1$, we exploit the fact that $N \rightarrow \infty$, so, recalling the definitions of U_j, g_j, p_j in Eqs (9.9), (9.10), (9.11), we see that U_j and p_j change relatively slowly, i.e., the differences $\|U_{j+1} - U_j\|, \|p_{j+1} - p_j\|$ are small. Then we perform the following substitution in Eq. (9.14):

$$\text{for } k = 0, \dots, \frac{N}{M} - 1 \quad \sum_{j=kM+1}^{(k+1)M} U_{(k+1)M-1} \cdots U_j p_j \longrightarrow \sum_{j=0}^{M-1} U_{kM+1}^j p_{kM+1}. \quad (9.15)$$

Note that for each k , we suppressed unitaries $U_{N-1} \cdots U_{(k+1)M}$ from the l.h.s., because in the corresponding group in Eq. (9.14) those unitaries appear in all terms of the summation and are uninfluential for the norm. The proposed substitution incurs smaller total error (when summing over all groups of terms, and taking the norm) than approximating the entire summation $\sum_{j=1}^N U_{N-1} \cdots U_j p_j$ with $\sum_{j=0}^{N-1} U_1^j p_1$. This is intuitive, because the substitution with N/M groups of terms uses U_{kM+1}, p_{kM+1} for multiple values of k , rather than just for $k = 0$, and follows the original summation more closely. Further, it can be shown (see Sect. 9.1.4) that the substitution indicated in Eq. (9.15) introduces an error of $\frac{\delta M}{2N}$, which is half of the target upper bound for the norm of $\left\| \sum_{j=1}^M U_{N-1} \cdots U_j p_j \right\|$. The choice for the value of T in Thm. 9.11 comes up in this step of the proof, because we need a T large enough to cancel out some other terms and eventually upper bound the error of Eq. (9.15) by $\frac{\delta M}{2N}$. So now, restricting ourselves to the case $k = 0$ because the same argument works for all k , we aim to show that $\left\| \sum_{j=0}^{M-1} U_{kM+1}^j p_{kM+1} \right\| = \left\| \sum_{j=0}^{M-1} U_1^j p_1 \right\| \leq \frac{\delta M}{2N}$. We can express p_1 in an eigenbasis of U_1 , and because by assumption p_1 is orthogonal to g_1 , we know that p_1 is a combination of the eigenvectors of U_1 (hence, $\mathcal{H}(1/N)$) that are not g_1 . Calling these unit eigenvectors v_2, \dots, v_d (for simplicity and without loss of generality, we assume $v_1 = g_1$) with eigenvalues $\sigma_2, \dots, \sigma_d$, and

calling a_2, \dots, a_d the coefficients such that $\sum_{h=2}^d a_h v_h = p_1$, we have:

$$\begin{aligned} \left\| \sum_{j=0}^{M-1} U_1^j p_1 \right\| &= \left\| \sum_{j=0}^{M-1} U_1^j \sum_{h=2}^d a_h v_h \right\| = \left\| \sum_{h=2}^d a_h \sum_{j=0}^{M-1} U_1^j v_h \right\| = \left\| \sum_{h=2}^d a_h \sum_{j=0}^{M-1} e^{iT/N\sigma_h^j} v_h \right\| \\ &\leq \left\| \sum_{h=2}^d a_h v_h \left| \sum_{j=0}^{M-1} e^{iT/N\sigma_h^j} \right| \right\| \leq \left\| \sum_{h=2}^d a_h \right\| \max_h \left| \sum_{j=0}^{M-1} e^{iT/N\sigma_h^j} \right| \\ &\leq \|p_1\| \max_h \left| \sum_{j=0}^{M-1} e^{iT/N\sigma_h^j} \right|, \end{aligned} \quad (9.16)$$

where the third equality uses the fact that v_h is an eigenvector of U_1^j with eigenvalue σ_h^j , and the second inequality uses the fact that the vectors v_h have unit norm. It is possible to show that

$$\|p_1\| \leq \|\mathcal{H}'\|/(\gamma N), \quad (9.17)$$

see Sect. 9.1.4: the quantities involved in this bound are rather intuitive, because by Eq. (9.11), we expect that the speed by which \mathcal{H} changes affects the difference between the consecutive (in time) eigenvectors g_1 and g_2 . Let us now focus on the remaining term $\max_h \left| \sum_{j=0}^{M-1} e^{iT/N\sigma_h^j} \right|$. This is simply a geometric sum, thus:

$$\left| \sum_{j=0}^{M-1} e^{iT/N\sigma_h^j} \right| = \frac{|1 - e^{iMT/N\sigma_h}|}{|1 - e^{iT/N\sigma_h}|} \leq \frac{2}{|1 - e^{iT/N\sigma_h}|} \leq \frac{4N}{T\sigma_h} \leq \frac{4N}{T\gamma}, \quad (9.18)$$

where for the first equality we use the formula for the geometric sum and the fact that $|a/b| = |a|/|b|$ for $a, b \in \mathbb{C}$, for the second inequality we use the fact that $|e^{i\theta} - 1| \geq |\theta|/2$ for small θ , and for the last inequality we used the fact that $|\sigma_h| > \gamma$ for all h (recall Def. 9.9 and the assumptions of Thm. 9.11: there is a spectral gap γ around the eigenvalue 0 that is being “tracked” by the adiabatic evolution). Using Eq.s (9.17) and (9.18):

$$\|p_1\| \max_h \left| \sum_{j=0}^{M-1} e^{iT/N\sigma_h^j} \right| \leq \frac{4\|\mathcal{H}'\|}{\gamma^2 T} \leq \underbrace{\frac{8\|\mathcal{H}'\|N}{\gamma^2 T \delta}}_{\text{this is how we choose } M} \frac{\delta}{N} \leq \frac{\delta M}{N}. \quad (9.19)$$

In the above expression, we had to pick M appropriately to ensure that we obtain the desired upper bound $\frac{\delta M}{N}$, thereby proving Eq. (9.13) and Thm. 9.11. (The choice $M = \lceil 8\|\mathcal{H}'\|N/(\delta\gamma^2 T) \rceil = \mathcal{O}(N)$ is discussed in Sect. 9.1.4.)

The discussion above gives the essence of a possible proof of the adiabatic theorem. In short, starting from an eigenvector of $\mathcal{H}(j/N)$ whose eigenvalue evolves through time without crossing any other eigenvalue, we would like to show that the eigenvector evolves into the corresponding eigenvector in $\mathcal{H}((j+1)/N)$. There is a small component of the former eigenvector that is orthogonal to the latter eigenvector. However, up to some small error, successive powers of $e^{iT/N\mathcal{H}((j+1)/N)}$ act on this orthogonal component, leading to a geometric series that ends up mostly canceling out. Because the component orthogonal to the evolution of the initial eigenvector cancels out in these geometric sums, the only meaningful part of the state of the system that “survives” through the evolution is precisely the desired sequence of eigenvectors of $\mathcal{H}(j/N)$. This eventually brings us to the final eigenvector, i.e., the state $|\psi(1)\rangle$ is almost equal to $|\varphi(1)\rangle$.

9.1.4 Filling the gaps

We now describe in more detail several components that were omitted from the proof in Sect. 9.1.3. We begin by stating a version of Thm. 9.11 for the case where the eigenvalue $\lambda(s)$ is identically zero, which is the special case discussed in Sect. 9.1.3. For this special case we can get somewhat tighter bounds on T . At the end of this section we show that the assumption is not restrictive, and use the Hamiltonian transformation of Rem. 9.15 to prove the bound on T given in Thm. 9.11.

Theorem 9.17 (Special case of the adiabatic theorem). *Let $\mathcal{H}(s)$ be a time-dependent Hamiltonian, and let $|\varphi(s)\rangle$ be an eigenstate of $\mathcal{H}(s)$ with eigenvalue $\lambda(s) = 0$ for all $s \in [0, 1]$. Assume that there is a spectral gap $\gamma > 0$ around $\lambda(s) = 0$, i.e., all other eigenvalues are at least γ in absolute value. Assume further that, from the initial state $|\varphi(0)\rangle$, we apply the following time evolution:*

$$\frac{d|\psi(s)\rangle}{ds} = iT\mathcal{H}(s)|\psi(s)\rangle, \quad s \in [0, 1], \quad |\psi(0)\rangle = |\varphi(0)\rangle,$$

and for some $\delta > 0$, T satisfies:

$$T \geq \frac{10^3}{\delta^2} \max \left\{ \frac{\|\mathcal{H}'\|^3}{\gamma^4}, \frac{\|\mathcal{H}'\|\|\mathcal{H}''\|}{\gamma^3} \right\}.$$

Then the system approximately remains in the instantaneous eigenstate $|\varphi(s)\rangle$ with eigenvalue 0 for all s , and in particular, the final state $|\psi(1)\rangle$ has Euclidean distance at most δ from $|\varphi(1)\rangle$, up to global phase:

$$\|e^{i\theta}|\psi(1)\rangle - |\varphi(1)\rangle\| \leq \delta \quad \text{for some } \theta.$$

To show Thm. 9.17 we need the following lemma, which we state without proof.

Lemma 9.18 (Lem. 3.2 in [Ambainis and Regev, 2004]). *In the context of Thm. 9.17, assume the phase of $|\varphi(s)\rangle$ is chosen so that $\langle\varphi'(s)|\varphi(s)\rangle = 0$. Then the following holds:*

$$\|\varphi'\| \leq \frac{\|\mathcal{H}'\|}{\gamma} \quad \|\varphi''\| \leq \frac{\|\mathcal{H}''\|}{\gamma} + \frac{3\|\mathcal{H}'\|^2}{\gamma^2}.$$

Remark 9.19. $|\varphi'(s)\rangle, |\varphi''(s)\rangle$ are not normalized quantum states: they are the column vectors with the component-wise first-order and second-order derivatives of $|\varphi(s)\rangle$. We (exceptionally) write these vectors using the bra-ket notation because we frequently take their inner product with normalized quantum states, and this avoids the need for further notation.

We can now proceed with the proof of Thm. 9.17.

Proof. Fix $M = \lceil 8\|\mathcal{H}'\|N/(\delta\gamma^2T) \rceil$. The proof follows exactly the same structure given in Sect. 9.1.3. There are a few intermediate results that are used without proof in Sect. 9.1.3, and need to be proven here.

- (i) The choice of the phases of the eigenvectors g_j of Eq. (9.10), see Rem. 9.13. An alternative approach would be to measure distances using a metric that is insensitive to phase, but we stick with the familiar Euclidean norm.
- (ii) Eq. (9.12), stating that $g_j - g_{j+1}$ is approximated well by p_{j+1} .
- (iii) Eq. (9.15), i.e., the approximation whereby we substitute:

$$\sum_{j=kM+1}^{(k+1)M} U_{(k+1)M-1} \cdots U_j p_j \longrightarrow \sum_{j=0}^{M-1} U_{kM+1}^j p_{kM+1}.$$

We discuss a proof for $k = 0$, as the argument works in the same way for all k .

- (iv) The bound on $\|p_j\|$ given in Eq. (9.17). We discuss the case $j = 1$, the proof can be easily generalized to any j .

(i). The speed by which the phase of a (generic) time-dependent, differentiable complex unit vector $|\psi(s)\rangle$ changes is measured by the quantity $\langle\psi'(s)|\psi(s)\rangle$. To see this, note first that $\langle\psi'(s)|\psi(s)\rangle$ is an imaginary number, therefore it is zero for real vectors. Indeed, $\langle\psi(s)|\psi(s)\rangle = 1$, and if we take the derivative with respect to s on both sides of this equation we obtain:

$$\frac{d}{ds} \langle\psi(s)|\psi(s)\rangle = \langle\psi(s)'|\psi(s)\rangle + \langle\psi(s)|\psi'(s)\rangle = 0,$$

so $\langle \psi(s)' | \psi(s) \rangle$ has no real part. This is geometrically clear: a real unit vector lies on the unit sphere, and if it moves around the sphere, its derivative is orthogonal to the vector itself because it needs to remain on the sphere. Not so for complex vectors, where a rotation can also pick up a phase, hence the possibility of a nonzero (but imaginary) $\langle \psi'(s) | \psi(s) \rangle$. We fix the evolution of the eigenvectors by requiring that:

$$\langle \varphi'(s) | \varphi(s) \rangle = 0 \quad \text{for all } s \in [0, 1]. \quad (9.20)$$

This is always possible. Consider $|\phi(s)\rangle = e^{i\beta(s)}|\varphi(s)\rangle$, where $\beta(s) = \int_0^s i\langle \varphi'(x) | \varphi(x) \rangle dx$. Then $|\phi(s)\rangle$ is equal to $|\varphi(s)\rangle$ up to global phase, and it satisfies the condition in Eq. (9.20):

$$\begin{aligned} \langle \phi'(s) | \phi(s) \rangle &= \left(i e^{i\beta(s)} \beta'(s) \langle \varphi(s) | + e^{i\beta(s)} \langle \varphi'(s) | \right) e^{i\beta(s)} |\varphi(s)\rangle \\ &= \left(-e^{i\beta(s)} \langle \varphi'(s) | \varphi(s) \rangle \langle \varphi(s) | + e^{i\beta(s)} \langle \varphi'(s) | \right) e^{i\beta(s)} |\varphi(s)\rangle = 0. \end{aligned}$$

The evolution of $|\phi(s)\rangle$ is equivalent to the evolution of $|\varphi(s)\rangle$ because they are eigenvectors with the same eigenvalue, so we can choose to study $|\phi(s)\rangle$ instead of $|\varphi(s)\rangle$. This fixes our choice of phases. In the following, we still denote by $|\varphi(s)\rangle$ the eigenvector of $\mathcal{H}(s)$ corresponding to $\lambda(s) = 0$, but we can now assume that Eq. (9.20) holds without loss of generality.

(ii). We want to show

$$\|p_{j+1} - (g_j - g_{j+1})\| = \mathcal{O}\left(\frac{1}{N^2}\right).$$

We take the Taylor expansion of $|\varphi(s)\rangle$ as a function of s , centered at $s = (j+1)/N$, and we evaluate it at $s = j/N$:

$$|\varphi(j/N)\rangle = |\varphi((j+1)/N)\rangle - \frac{1}{N}|\varphi'((j+1)/N)\rangle + \mathcal{O}\left(\left\|\frac{j+1}{N} - \frac{j}{N}\right\|^2\right).$$

(Here and in the following, we employ the usual convention of indicating error terms in a Taylor series approximation as additive $\mathcal{O}(\cdot)$ terms, to be interpreted as: there is an error term whose norm is $\mathcal{O}(\cdot)$.) Remembering that g_j is the eigenvector $|\varphi(j/N)\rangle$ with eigenvalue $\lambda(s) = 0$ of $\mathcal{H}(j/N)$, we can rewrite this as:

$$g_j - g_{j+1} = -\frac{1}{N}|\varphi'((j+1)/N)\rangle + \mathcal{O}\left(\frac{1}{N^2}\right).$$

Project both sides of the equation onto G_{j+1}^\perp , the orthogonal complement of the space spanned by g_{j+1} , by applying the corresponding projector. Using the definition of p_{j+1} in Eq. (9.11), we obtain:

$$\begin{aligned} p_{j+1} &= \text{Proj}_{G_{j+1}^\perp}(g_j - g_{j+1}) = \text{Proj}_{G_{j+1}^\perp}\left(-\frac{1}{N}|\varphi'((j+1)/N)\rangle\right) + \mathcal{O}\left(\frac{1}{N^2}\right) \\ &= -\frac{1}{N}|\varphi'((j+1)/N)\rangle + \mathcal{O}\left(\frac{1}{N^2}\right), \end{aligned} \quad (9.21)$$

because $\langle \varphi'((j+1)/N) | \varphi((j+1)/N) \rangle = 0$ (recall Eq. (9.20)), implying that $|\varphi'((j+1)/N)\rangle$ fully lies in the orthogonal complement of $|\varphi((j+1)/N)\rangle = g_{j+1}$. Subtracting this equation from the previous one, and taking the norm, yields:

$$\|p_{j+1} - (g_j - g_{j+1})\| = \mathcal{O}\left(\frac{1}{N^2}\right).$$

(iii). We want to show (recall that we are looking at the case $k = 0$ in Eq. 9.15):

$$\left\| \sum_{j=1}^M U_{M-1} \cdots U_j p_j - \sum_{j=0}^{M-1} U_1^j p_1 \right\| \leq \frac{\delta M}{2N}. \quad (9.22)$$

The proof of Eq. (9.22) is rather long and tedious, but it is important to sketch it because it is where the particular choice of T comes into play. We first study the effect of replacing all p_j with p_1 . Using Eq. (9.21), we can write:

$$p_{j+h} - p_j = -\frac{1}{N} (|\varphi'((j+h)/N)\rangle - |\varphi'(j/N)\rangle) + \mathcal{O}\left(\frac{1}{N^2}\right).$$

Applying the mean value theorem to the difference within parentheses at the r.h.s., the following equation holds at some point $y \in [j/N, (j+h)/N]$:

$$\frac{|\varphi'((j+h)/N)\rangle - |\varphi'(j/N)\rangle}{h/N} = |\varphi''(y)\rangle.$$

Therefore, taking a worst-case upper bound on the norm of $|\varphi''(y)\rangle$ and then using Lem. 9.18, we obtain:

$$\begin{aligned} \|p_{j+h} - p_j\| &\leq \frac{h}{N^2} \|\varphi''(y)\| + \mathcal{O}\left(\frac{1}{N^2}\right) \leq \frac{h}{N^2} \|\varphi''\| + \mathcal{O}\left(\frac{1}{N^2}\right) \\ &\leq \frac{h}{N^2} \left(\frac{\|\mathcal{H}''\|}{\gamma} + \frac{3\|\mathcal{H}'\|^2}{\gamma^2} \right) + \mathcal{O}\left(\frac{1}{N^2}\right). \end{aligned} \quad (9.23)$$

Analyzing the very first summation appearing in Eq. (9.22), using the triangle inequality and Eq. (9.23), we have:

$$\begin{aligned} \left\| \sum_{j=1}^M U_{M-1} \cdots U_j p_j - \sum_{j=1}^M U_{M-1} \cdots U_j p_1 \right\| &\leq \sum_{j=1}^M \|U_{M-1} \cdots U_j p_j - U_{M-1} \cdots U_j p_1\| = \sum_{j=1}^M \|p_j - p_1\| \\ &\leq \sum_{j=1}^M \left(\frac{j}{N^2} \left(\frac{\|\mathcal{H}''\|}{\gamma} + \frac{3\|\mathcal{H}'\|^2}{\gamma^2} \right) + \mathcal{O}\left(\frac{1}{N^2}\right) \right) \\ &\leq \frac{M^2}{N^2} \left(\frac{\|\mathcal{H}''\|}{\gamma} + \frac{3\|\mathcal{H}'\|^2}{\gamma^2} \right) + \mathcal{O}\left(\frac{1}{N}\right). \end{aligned}$$

Recall our definition of $M = \lceil 8\|\mathcal{H}'\|N/(\delta\gamma^2T) \rceil$, and substitute into the last equation (but, for ease of subsequent calculations, keep one ‘‘copy’’ of M ; i.e., write $M^2 = M \lceil 8\|\mathcal{H}'\|N/(\delta\gamma^2T) \rceil$). We get:

$$\frac{M^2}{N^2} \left(\frac{\|\mathcal{H}''\|}{\gamma} + \frac{3\|\mathcal{H}'\|^2}{\gamma^2} \right) = \frac{8M\|\mathcal{H}'\|}{N\delta\gamma^2T} \left(\frac{\|\mathcal{H}''\|}{\gamma} + \frac{3\|\mathcal{H}'\|^2}{\gamma^2} \right) = \frac{\delta M}{4N} \left(\frac{32\|\mathcal{H}'\|\|\mathcal{H}''\|}{\delta^2\gamma^3T} + \frac{96\|\mathcal{H}'\|^3}{\delta^2\gamma^4T} \right). \quad (9.24)$$

Because, by assumption,

$$T \geq \frac{10^3 \|\mathcal{H}'\|^3}{\delta^2 \gamma^4}, \quad T \geq \frac{10^3 \|\mathcal{H}'\|\|\mathcal{H}''\|}{\delta^2 \gamma^3}, \quad (9.25)$$

the term in parentheses at the r.h.s. in Eq. (9.24) is upper bounded by 1. Thus, thanks to our choice of M and T , we obtain:

$$\left\| \sum_{j=1}^M U_{M-1} \cdots U_j p_j - \sum_{j=1}^M U_{M-1} \cdots U_j p_1 \right\| \leq \frac{\delta M}{4N} + \mathcal{O}\left(\frac{1}{N}\right). \quad (9.26)$$

This bounds the approximation error incurred by substituting p_1 to replace each p_j . Finally, we

analyze the effect of replacing each U_j with U_1 ; in particular, we want to show:

$$\begin{aligned} \left\| \sum_{j=1}^M U_{M-1} \cdots U_j p_1 - \sum_{j=0}^{M-1} U_1^j p_1 \right\| &= \left\| \sum_{j=1}^M U_{M-1} \cdots U_j p_1 - \sum_{j=1}^M U_1^{M-j} p_1 \right\| \\ &= \left\| \sum_{j=1}^{M-1} U_{M-1} \cdots U_j p_1 - \sum_{j=1}^{M-1} U_1^{M-j} p_1 \right\| \\ &\leq \frac{\delta M}{4N} + \mathcal{O}\left(\frac{1}{N^2}\right). \end{aligned} \quad (9.27)$$

In Eq. 9.27, the second equality is due to the fact that one term in each summation is equal to p_1 (recall Rem. 9.16), so it cancels out. We prove Eq. 9.27 by induction. Note that in the first summation, i.e., $\sum_{j=1}^M U_{M-1} \cdots U_j p_1$, U_1 appears once, U_2 appears twice, U_3 appears three times, and so on. In this summation we replace each unitary up to U_h with U_1 , and proceed by induction on h . The inductive statement is:

$$\left\| \sum_{j=1}^h U_h U_{h-1} \cdots U_j p_1 - \sum_{j=1}^h U_1^{h+1-j} p_1 \right\| \leq \frac{2(h+1)h \|\mathcal{H}'\|^2}{\gamma^2 N^2} + \mathcal{O}(h/N^3). \quad (9.28)$$

We prove the statement in Lem. 9.20. Applying it for $h = M - 1$ yields:

$$\left\| \sum_{j=1}^{M-1} U_{M-1} U_{M-2} \cdots U_j p_1 - \sum_{j=1}^{M-1} U_1^{M-j} p_1 \right\| \leq \frac{2M^2 \|\mathcal{H}'\|^2}{\gamma^2 N^2} + \mathcal{O}\left(\frac{1}{N^2}\right).$$

By definition of $M = \lceil 8\|\mathcal{H}'\|N/(\delta\gamma^2 T) \rceil$, and by our choice of T (see Eq. (9.25)), we finally upper bound the r.h.s. of the above equation as follows:

$$\frac{2M^2 \|\mathcal{H}'\|^2}{\gamma^2 N^2} = \frac{16M \|\mathcal{H}'\|^3}{\delta \gamma^4 N T} = \frac{\delta M}{4N} \left(\frac{64 \|\mathcal{H}'\|^3}{\delta^2 \gamma^4 T} \right) \leq \frac{\delta M}{4N}.$$

This proves Eq. 9.27. Putting together Eq.s 9.26 and 9.27 with a final triangle inequality completes the proof of (iii): up to error terms that go to zero as $N \rightarrow \infty$, replacing all p_j with p_1 introduces an error of $\frac{\delta M}{4N}$, and replacing all U_j with U_1 introduces an error of $\frac{\delta M}{4N}$, yielding (9.22).

(iv). The inequality $\|p_1\| \leq \|\mathcal{H}'\|/(\gamma N)$ in Eq. (9.17) follows immediately by applying Lem. 9.18 to Eq. 9.21. \square

The lemma below is used in the proof of Thm. 9.17.

Lemma 9.20. *Let p_j, U_j for $j = 1, \dots, N$ be defined as in Thm. 9.17. Then:*

$$\left\| \sum_{j=1}^k U_k U_{k-1} \cdots U_j p_1 - \sum_{j=1}^k U_1^{k+1-j} p_1 \right\| \leq \frac{2(k+1)k \|\mathcal{H}'\|^2}{\gamma^2 N^2} + \mathcal{O}(k/N^3).$$

Proof. We proceed by induction on k . For $k = 1$, the statement is trivial: the two summations inside the norm are equal to $U_1 p_1$, hence the l.h.s. is zero. To inductively go from $k - 1$ to k , we

use the triangle inequality as follows:

$$\begin{aligned}
 & \left\| \sum_{j=1}^k U_k U_{k-1} \dots U_j p_1 - \sum_{j=1}^k U_1^{k+1-j} p_1 \right\| \\
 = & \left\| \sum_{j=1}^k U_k U_{k-1} \dots U_j p_1 - \sum_{j=1}^k U_k U_1^{k-j} p_1 + \sum_{j=1}^k U_k U_1^{k-j} p_1 - \sum_{j=1}^k U_1^{k+1-j} p_1 \right\| \\
 \leq & \underbrace{\left\| \sum_{j=1}^k U_k U_{k-1} \dots U_j p_1 - \sum_{j=1}^k U_k U_1^{k-j} p_1 \right\|}_{\text{term (a)}} + \underbrace{\left\| \sum_{j=1}^k U_k U_1^{k-j} p_1 - \sum_{j=1}^k U_1^{k+1-j} p_1 \right\|}_{\text{term (b)}}.
 \end{aligned} \tag{9.29}$$

For term (a), note that the terms of the two summations for $j = k$ are both equal to $U_k p_1$, so they cancel out. Thus, we can write:

$$\begin{aligned}
 & \left\| \sum_{j=1}^k U_k U_{k-1} \dots U_j p_1 - \sum_{j=1}^k U_k U_1^{k-j} p_1 \right\| = \left\| U_k \left(\sum_{j=1}^{k-1} U_{k-1} \dots U_j p_1 - \sum_{j=1}^{k-1} U_1^{k-j} p_1 \right) \right\| = \\
 & \left\| \sum_{j=1}^{k-1} U_{k-1} \dots U_j p_1 - \sum_{j=1}^{k-1} U_1^{k-j} p_1 \right\| \leq \frac{2k(k-1)\|\mathcal{H}'\|^2}{\gamma^2 N^2} + \mathcal{O}(k/N^3).
 \end{aligned}$$

where for the second equality we used the fact that U_k is unitary, and the final inequality applies the inductive hypothesis. For term (b) we have:

$$\left\| \sum_{j=1}^k U_k U_1^{k-j} p_1 - \sum_{j=1}^k U_1^{k+1-j} p_1 \right\| = \left\| (U_k - U_1) \sum_{j=1}^k U_1^{k-j} p_1 \right\| \leq \|U_k - U_1\| \left\| \sum_{j=1}^k U_1^{k-j} p_1 \right\|. \tag{9.30}$$

We bound $\|U_k - U_1\|$ using a telescopic sum:

$$\|U_k - U_1\| = \left\| \sum_{j=1}^{k-1} U_{j+1} - U_j \right\| \leq \sum_{j=1}^{k-1} \|U_{j+1} - U_j\|. \tag{9.31}$$

Recall that $U_{j+1} = e^{i\frac{T}{N}\mathcal{H}((j+1)/N)}$ (Eq. 9.9). Using a Trotter formula (Sect. 6.2.2), we have:

$$U_{j+1} = e^{i\frac{T}{N}(\mathcal{H}((j+1)/N) - \mathcal{H}(j/N) + \mathcal{H}(j/N))} \approx e^{i\frac{T}{N}(\mathcal{H}((j+1)/N) - \mathcal{H}(j/N))} e^{i\frac{T}{N}\mathcal{H}(j/N)},$$

with error:

$$\begin{aligned}
 \mathcal{O} \left(\left\| \frac{T}{N} (\mathcal{H}((j+1)/N) - \mathcal{H}(j/N)) \right\| \left\| \frac{T}{N} \mathcal{H}(j/N) \right\| \right) &= \mathcal{O} \left(\frac{T^2}{N^2} \|(\mathcal{H}((j+1)/N) - \mathcal{H}(j/N))\| \|\mathcal{H}(j/N)\| \right) \\
 &= \mathcal{O} \left(\frac{T^2}{N^2} \left\| \frac{1}{N} \mathcal{H}'(j/N) \right\| \|\mathcal{H}(j/N)\| \right) \\
 &= \mathcal{O} \left(\frac{T^2 \|\mathcal{H}\| \|\mathcal{H}'\|}{N^3} \right) = \mathcal{O} \left(\frac{1}{N^3} \right),
 \end{aligned}$$

where for the second equality we used the fact that $\lim_{N \rightarrow \infty} \frac{\mathcal{H}((j+1)/N) - \mathcal{H}(j/N)}{1/N} = \mathcal{H}'(j/N)$, and for the final equality we neglected all terms except the ones that depend on N , see Rem. 9.14. Thus:

$$\begin{aligned}
 \|U_{j+1} - U_j\| &= \left\| e^{i\frac{T}{N}\mathcal{H}((j+1)/N)} - e^{i\frac{T}{N}\mathcal{H}(j/N)} \right\| \\
 &= \left\| e^{i\frac{T}{N}\mathcal{H}(j/N)} \left(e^{i\frac{T}{N}(\mathcal{H}((j+1)/N) - \mathcal{H}(j/N))} - I \right) \right\| + \mathcal{O} \left(\frac{1}{N^3} \right) \\
 &= \left\| \frac{T}{N} (\mathcal{H}((j+1)/N) - \mathcal{H}(j/N)) \right\| + \mathcal{O} \left(\frac{1}{N^3} \right) \leq \frac{T\|\mathcal{H}'\|}{N^2} + \mathcal{O} \left(\frac{1}{N^3} \right).
 \end{aligned} \tag{9.32}$$

In the chain above, for the third equality we used the fact that $e^{i\frac{T}{N}\mathcal{H}(j/N)}$ is unitary plus the fact that $e^{i\frac{T}{N}(\mathcal{H}((j+1)/N)-\mathcal{H}(j/N))} - I = i\frac{T}{N}(\mathcal{H}((j+1)/N) - \mathcal{H}(j/N)) + \mathcal{O}\left(\frac{T^2}{N^2}\frac{\|\mathcal{H}'\|^2}{N^2}\right)$ by definition of matrix exponential and because $\lim_{N \rightarrow \infty} \frac{\mathcal{H}((j+1)/N) - \mathcal{H}(j/N)}{1/N} = \mathcal{H}'(j/N)$, and for the inequality we again used the limit defining $\mathcal{H}'(j/N)$. Using Eq. (9.32) in Eq. (9.31), we finally obtain:

$$\|U_k - U_1\| \leq \frac{kT\|\mathcal{H}'\|}{N^2} + \mathcal{O}\left(\frac{k}{N^3}\right).$$

We plug this into Eq. (9.30). For the remaining term in Eq. (9.30), i.e., $\left\|\sum_{j=1}^k U_1^{k-j} p_1\right\|$, we apply exactly the same argument used in Eq.s (9.16)-(9.19) to show that:

$$\left\|\sum_{j=1}^k U_1^{k-j} p_1\right\| = \left\|\sum_{j=0}^{k-1} U_1^j p_1\right\| \leq \frac{4\|\mathcal{H}'\|}{T\gamma^2},$$

see in particular the first inequality in Eq. (9.19). Eq. (9.30) then yields:

$$\left\|\sum_{j=1}^k U_k U_1^{k-j} p_1 - \sum_{j=1}^k U_1^{k+1-j} p_1\right\| \leq \left(\frac{kT\|\mathcal{H}'\|}{N^2} + \mathcal{O}\left(\frac{k}{N^3}\right)\right) \frac{4\|\mathcal{H}'\|}{T\gamma^2} = \frac{4k\|\mathcal{H}'\|^2}{\gamma^2 N^2} + \mathcal{O}\left(\frac{k}{N^3}\right).$$

We can now continue the chain of inequalities in Eq. (9.29), using the upper bounds for terms (a) and (b) that we derived:

$$\begin{aligned} \left\|\sum_{j=1}^k U_k U_{k-1} \dots U_j p_1 - \sum_{j=1}^k U_1^{k+1-j} p_1\right\| &\leq \frac{2k(k-1)\|\mathcal{H}'\|^2}{\gamma^2 N^2} + \frac{4k\|\mathcal{H}'\|^2}{\gamma^2 N^2} + \mathcal{O}\left(\frac{k}{N^3}\right) \\ &= \frac{2(k+1)k\|\mathcal{H}'\|^2}{\gamma^2 N^2} + \mathcal{O}\left(\frac{k}{N^3}\right). \end{aligned}$$

This concludes the proof. \square

We end the section by formally proving the general version of the adiabatic theorem, Thm. 9.11, using the special case proven in this section. Specifically, in Thm. 9.17 we assume $\lambda(s) = 0$ for all s , but Thm. 9.11 applies to any eigenpair. We show that the assumption $\lambda(s) = 0$ is not restrictive by using the Hamiltonian transformation sketched in Rem. 9.15: for any given Hamiltonian \mathcal{H} and eigenpair $(|\varphi(s)\rangle, \lambda(s))$ for the adiabatic evolution, we transform \mathcal{H} into a new Hamiltonian $\hat{\mathcal{H}}$ with eigenpair $(|\varphi(s)\rangle, 0)$, apply Thm. 9.17, and the value of T required by Thm. 9.17 for $\hat{\mathcal{H}}$ corresponds to the value of T stated in Thm. 9.11.

Corollary 9.21. *The lower bound for T stated in Thm. 9.11 suffices to ensure adiabatic evolution, i.e., a final state such that:*

$$\|e^{i\theta}|\psi(1)\rangle - |\varphi(1)\rangle\| \leq \delta \quad \text{for some } \theta.$$

Proof. Consider the Hamiltonian $\hat{\mathcal{H}}(s) = \mathcal{H}(s) - \lambda(s)I$. Because $|\varphi(s)\rangle$ is an eigenvector of $\mathcal{H}(s)$ with eigenvalue $\lambda(s)$, we have, for all s :

$$\hat{\mathcal{H}}(s)|\varphi(s)\rangle = \mathcal{H}(s)|\varphi(s)\rangle - \lambda(s)|\varphi(s)\rangle = 0,$$

thus $|\varphi(s)\rangle$ is an eigenvector of $\hat{\mathcal{H}}(s)$ with eigenvalue 0. [Ambainis and Regev, 2004][Lem. 4.1] shows that for any s :

$$\lambda'(s) \leq \|\mathcal{H}'\|, \quad \lambda''(s) \leq \|\mathcal{H}''\| + 4\|\mathcal{H}'\|^2/\gamma. \quad (9.33)$$

Using Eq. (9.33), we therefore have:

$$\|\hat{\mathcal{H}}'\| = \max_{s \in [0,1]} \left\| \frac{d(\mathcal{H}(s) - \lambda(s)I)}{ds} \right\| \leq \|\mathcal{H}'\| + \|\lambda'\| \leq 2\|\mathcal{H}'\|,$$

and:

$$\|\hat{\mathcal{H}}''\| = \max_{s \in [0,1]} \left\| \frac{d^2(\mathcal{H}(s) - \lambda(s)I)}{ds^2} \right\| \leq \|\mathcal{H}''\| + \|\lambda''\| \leq 2\|\mathcal{H}''\| + 4\|\mathcal{H}''\|^2/\gamma.$$

Applying Thm. 9.17 to the Hamiltonian $\hat{\mathcal{H}}$, and using the above bounds for the norm of the derivatives of $\hat{\mathcal{H}}$, we see that it is sufficient to choose $T \geq \frac{1000}{\delta^2} \max \left\{ \frac{\|\hat{\mathcal{H}}'\|^3}{\gamma^4}, \frac{\|\hat{\mathcal{H}}'\|\|\hat{\mathcal{H}}''\|}{\gamma^3} \right\}$. We upper bound the r.h.s. of this inequality as follows:

$$\begin{aligned} \frac{1000}{\delta^2} \max \left\{ \frac{\|\hat{\mathcal{H}}'\|^3}{\gamma^4}, \frac{\|\hat{\mathcal{H}}'\|\|\hat{\mathcal{H}}''\|}{\gamma^3} \right\} &\leq \frac{1000}{\delta^2} \max \left\{ \frac{8\|\mathcal{H}'\|^3}{\gamma^4}, \frac{2\|\mathcal{H}'\|(2\|\mathcal{H}''\| + 4\|\mathcal{H}'\|^2/\gamma)}{\gamma^3} \right\} \\ &= \frac{1000}{\delta^2} \left(\frac{8\|\mathcal{H}'\|^3}{\gamma^4} + \frac{4\|\mathcal{H}'\|\|\mathcal{H}''\|}{\gamma^3} \right) \\ &\leq \frac{10^4}{\delta^2} \left(\frac{\|\mathcal{H}'\|^3}{\gamma^4} + \frac{\|\mathcal{H}'\|\|\mathcal{H}''\|}{\gamma^3} \right). \end{aligned}$$

This is the lower bound for T stated in Thm. 9.11, and it completes its proof. \square

9.1.5 Spectral gap dependence and estimation

To understand if the adiabatic theorem can lead to an effective optimization algorithm in theory, we must analyze its running time relative to the problem instance parameters. Recall how optimization with the adiabatic theorem works: we start in the ground state of a known, “easy” Hamiltonian (i.e., one for which the ground state is known and can be easily prepared), then we transform this initial Hamiltonian into a target Hamiltonian that encodes the desired optimization problem; see the discussion in Rem. 9.5. When applying the adiabatic theorem to solve an optimization problem in the above manner, the value of T (i.e., the length of the simulation of the Schrödinger equation) determines the running time: as we have seen in Ch. 6, the time complexity of efficient Hamiltonian simulation algorithms is linear in the length of the time horizon — the parameter that we called “ t ” in Ch. 6.

Remark 9.22. *In fact, no quantum algorithm can solve the Hamiltonian simulation problem with fewer than $\Omega(t)$ operations, due to existing lower bounds [Berry et al., 2007, Berry et al., 2015]. So in general we do not expect that it is possible to perform optimization using the adiabatic theorem with fewer than T operations on a quantum computer.*

In turn, the spectral gap γ is often the crucial parameter that determines the value of T .

According to Thm. 9.11, to ensure that the slow time evolution in Eq. (9.8) always leaves the system in an instantaneous eigenstate of the Hamiltonian (with at most a small error), the choice of T satisfies $T \geq \|\mathcal{H}'\|^3/\gamma^4 + \|\mathcal{H}'\|\|\mathcal{H}''\|/\gamma^3$. Thus, our proof of the adiabatic theorem yields a dependence on the spectral gap parameter γ that is in the order of $1/\gamma^4$. As stated in Sect. 9.1.3, this is not tight. The folklore result is that for the main statement of Thm. 9.11 to hold, it is sufficient to choose:

$$T \gg \int_0^1 \frac{\|\mathcal{H}'(s)\|}{\gamma^2} ds,$$

see, e.g., [van Dam et al., 2001, Reichardt, 2004]. It should be noted that in the open literature, occasionally doubt has been cast on the sufficiency of the above condition on T for the general case. This is likely due to the paucity of rigorous proofs and the appearance of counterexamples under specific conditions; see, e.g., the discussion in [Ambainis and Regev, 2004], as well as [Jansen et al., 2007, Sect. 5]. A more precise characterization of a sufficient value of T , taken from [Childs, 2017] which is itself based on [Teufel, 2003], is the following (recall Def.s 9.8 and 9.9):

Theorem 9.23 (Adiabatic theorem with tighter spectral bound; Thm. 28.1 in [Childs, 2017]). *There exists some constant c such that the statement of Thm. 9.11 holds if we choose T satisfying:*

$$T \geq \frac{c}{\delta} \left(\frac{\|\mathcal{H}'(0)\|}{\gamma(0)^2} + \frac{\|\mathcal{H}'(1)\|}{\gamma(1)^2} + \int_0^1 \left(\frac{\|\mathcal{H}'(s)\|^2}{\gamma(s)^3} + \frac{\|\mathcal{H}''(s)\|}{\gamma(s)^2} \right) ds \right).$$

An essentially identical result is also proven in [Jansen et al., 2007]. This result tightens the dependence on the spectral gap parameter to the order of $1/\gamma^3$. The expression in Thm. 9.23 depends on some instantaneous quantities, in particular the instantaneous spectral gap $\gamma(s)$ as well as $\|\mathcal{H}'(s)\|$ evaluated at specific points. We can simplify it in the case of linear interpolation between the initial and final Hamiltonian: from Eq. (9.6) we compute \mathcal{H}' and \mathcal{H}'' , and taking some pessimistic bounds to eliminate s from the expression, we obtaining the following.

Corollary 9.24 (Adiabatic theorem for linear interpolation). *There exists some constant c such that, when the Hamiltonian $\mathcal{H}(s)$ performs linear interpolation between an initial and a final Hamiltonian, as in Eq. (9.6), the statement of Thm. 9.11 holds if we choose T satisfying:*

$$T \geq \frac{c}{\delta} \left(\frac{\|\mathcal{H}_F - \mathcal{H}_I\|}{\gamma^2} + \frac{\|\mathcal{H}_F - \mathcal{H}_I\|^2}{\gamma^3} \right).$$

Unfortunately estimating γ is often very difficult. Even when using the linear interpolation strategy of Eq. (9.6), gap estimation requires the analysis of the spectrum of a time-dependent matrix that is the sum of two terms, i.e., the initial and final Hamiltonian. This is notoriously difficult, because there is no precise relationship between the spectrum of each term and the spectrum of their sum: although several results to bound the eigenvalues of a sum of two Hermitian matrices are known (e.g., Weyl’s inequality, see also [Bhatia, 2013]), they generally do not provide useful characterizations of the spectral gap. Note that we are interested in *lower bounds* to the spectral gap, because γ appears at the denominator of the expression for the simulation running time T .

The spectral gap for just a few time-dependent Hamiltonians that solve combinatorial optimization problems is known. Typically, a lot of structure is required and ad-hoc procedures are necessary. We provide two illustrative examples below: in one case, Ex. 9.25, the gap is polynomially small, leading to a polynomial-time algorithm to solve a trivial optimization problem; in the other case, Ex. 9.26, the gap is exponentially small, and leads to an algorithm that is slower than Grover’s algorithm for black-box search, unless we modify the time-dependent Hamiltonian and do something more sophisticated than the linear interpolation of Rem. 9.5.

Example 9.25. *Let us apply adiabatic optimization to the problem of minimizing the Hamming weight (i.e., the number of “1”s) of a binary string. This problem has the all-zero binary string $\vec{0}$ as the obvious solution, therefore it is not a difficult problem to solve — we can determine the solution analytically. Nonetheless, the application of adiabatic optimization is instructive, and gives us an opportunity to showcase the choices involved in the application of the approach, and the type of analysis that is necessary.*

For $\vec{j} \in \{0, 1\}^n$, let $w(\vec{j}) := \sum_{k=1}^n j_k$ be its Hamming weight. We aim to solve the following optimization problem:

$$\min_{\vec{j} \in \{0, 1\}^n} w(\vec{j}). \tag{9.34}$$

We choose the final Hamiltonian, for which we want to find the minimum eigenvector, as:

$$\mathcal{H}_F = \sum_{\vec{j} \in \{0, 1\}^n} w(\vec{j}) |\vec{j}\rangle\langle\vec{j}|.$$

It is straightforward to observe that $\mathcal{H}_F |\vec{j}\rangle = w(\vec{j}) |\vec{j}\rangle$, therefore the eigenvector with minimum eigenvalue encodes the global optimum of problem (9.34).

To optimize via the adiabatic algorithm we also need to choose an initial Hamiltonian. We choose:

$$\mathcal{H}_I = \sum_{\vec{j} \in \{0, 1\}^n} w(\vec{j}) H^{\otimes n} |\vec{j}\rangle\langle\vec{j}| H^{\otimes n},$$

where $H^{\otimes n}$ denotes the tensor of n Hadamard gates. (Recall: \mathcal{H} denotes a Hamiltonian, H a Hadamard gate.) The minimum eigenpair of \mathcal{H}_I is the eigenstate $H^{\otimes n}|\vec{0}\rangle$ with eigenvalue $w(\vec{0}) = 0$.

We want to analyze the spectrum of the time-dependent Hamiltonian:

$$\mathcal{H}(s) = (1 - s)\mathcal{H}_I + s\mathcal{H}_F,$$

so that we have an expression for the spectral gap γ to plug into Cor. 9.24. We can do so by decomposing \mathcal{H}_I and \mathcal{H}_F into sums of single-qubit Hamiltonians. By definition, $w(\vec{j})$ is a sum of terms that depend on a single digit of the string \vec{j} . We can then write \mathcal{H}_I as sums of n Hamiltonians dependent on a single digit:

$$\begin{aligned} \mathcal{H}_I &= \sum_{\vec{j} \in \{0,1\}^n} w(\vec{j}) H^{\otimes n} |\vec{j}\rangle \langle \vec{j}| H^{\otimes n} = \sum_{\vec{j} \in \{0,1\}^n} \left(\sum_{k=1}^n \vec{j}_k \right) H^{\otimes n} |\vec{j}\rangle \langle \vec{j}| H^{\otimes n} \\ &= \underbrace{\sum_{k=1}^n I \otimes \cdots \otimes I \otimes \left(\sum_{x \in \{0,1\}} x H |x\rangle \langle x| H \right)}_{\substack{\text{position } k \\ n \text{ terms}}} \otimes I \otimes \cdots \otimes I, \\ \mathcal{H}_F &= \sum_{\vec{j} \in \{0,1\}^n} w(\vec{j}) |\vec{j}\rangle \langle \vec{j}| = \sum_{\vec{j} \in \{0,1\}^n} \left(\sum_{k=1}^n \vec{j}_k \right) |\vec{j}\rangle \langle \vec{j}| \\ &= \underbrace{\sum_{k=1}^n I \otimes \cdots \otimes I \otimes \left(\sum_{x \in \{0,1\}} x |x\rangle \langle x| \right)}_{\substack{\text{position } k \\ n \text{ terms}}} \otimes I \otimes \cdots \otimes I, \end{aligned}$$

where we used the facts that $\sum_{x \in \{0,1\}} |x\rangle \langle x| = I$ and $\sum_{x \in \{0,1\}} H |x\rangle \langle x| H = H \left(\sum_{x \in \{0,1\}} |x\rangle \langle x| \right) H = I$. Thus:

$$\mathcal{H}(s) = \sum_{k=1}^n I \otimes \cdots \otimes I \otimes \underbrace{\left(\sum_{x \in \{0,1\}} x ((1-s)H|x\rangle \langle x|H + s|x\rangle \langle x|) \right)}_{\text{position } k} \otimes I \otimes \cdots \otimes I. \quad (9.35)$$

Let us analyze a single term of the summation, i.e., a term for fixed k — the other Hamiltonians are similar. For each k the only nontrivial action is on the k -th qubit. The corresponding single-qubit Hamiltonian on the k -th digit is:

$$\sum_{x \in \{0,1\}} x ((1-s)H|x\rangle \langle x|H + s|x\rangle \langle x|) = \frac{1}{2} \begin{pmatrix} 1-s & s-1 \\ s-1 & 1+s \end{pmatrix}.$$

The eigendecomposition of this matrix is straightforward to calculate, yielding eigenvalues:

$$\lambda_0(s) = \frac{1}{2} \left(1 - \sqrt{2s^2 - 2s + 1} \right) \quad \lambda_1(s) = \frac{1}{2} \left(1 + \sqrt{2s^2 - 2s + 1} \right),$$

with corresponding eigenstates that we label $|\psi_0(s)\rangle, |\psi_1(s)\rangle$ respectively. Having established the eigenvalues of a single term in Eq. (9.35), we can easily establish the eigenvalues of $\mathcal{H}(s)$. Indeed, for every $\vec{x} \in \{0,1\}^n$, the state:

$$|\psi_{\vec{x}}(s)\rangle := |\psi_{\vec{x}_1}(s)\rangle \otimes |\psi_{\vec{x}_2}(s)\rangle \otimes \cdots \otimes |\psi_{\vec{x}_n}(s)\rangle,$$

i.e., a tensor product of the eigenstate $|\psi_0(s)\rangle$ or $|\psi_1(s)\rangle$ for each qubit, is an eigenstate of $\mathcal{H}(s)$ with eigenvalue $(n - w(\vec{x}))\lambda_0(s) + w(\vec{x})\lambda_1(s)$. This follows from the fact that the k -th term in $\mathcal{H}(s)$

has $|\psi_{\vec{x}}(s)\rangle$ as an eigenstate, with eigenvalue $\lambda_0(s)$ or $\lambda_1(s)$ depending on \vec{x}_k . The vectors of the form $|\psi\rangle_{\vec{x}}$ are 2^n linearly independent eigenstates, therefore we have characterized the full set of eigenvectors for $\mathcal{H}(s)$. It follows that the instantaneous spectral gap is:

$$\gamma(s) = ((n-1)\lambda_0(s) + \lambda_1(s)) - n\lambda_0(s) = \sqrt{2s^2 - 2s + 1}.$$

Solving $\min_{s \in [0,1]} \gamma(s)$ yields $\gamma = \min_{s \in [0,1]} \gamma(s) = 1/\sqrt{2}$, attained at $s = 1/2$: the spectral gap γ is constant. Using Cor. 9.24, we see that we must choose $T = \mathcal{O}\left(\|\mathcal{H}_F - \mathcal{H}_I\|^2\right) = \mathcal{O}(n^2)$. With this choice of the initial and final Hamiltonians, problem (9.34) is solved in polynomial time via adiabatic optimization. As remarked at the beginning of this example, the problem is trivial so this discussion is simply meant to illustrate a problem with constant spectral gap. In [van Dam et al., 2001], which was the inspiration for this example, the reader can find a proof that a perturbed version of problem (9.34) requires exponential time.

Example 9.26. We now study the application of adiabatic optimization to the black-box search problem solved with Grover's algorithm in Sect. 4.1. Let $\vec{\ell} \in \{0,1\}^n$ be the marked element, which we assume to be unique for simplicity, and define:

$$f(\vec{j}) := \begin{cases} 0 & \text{if } \vec{j} = \vec{\ell} \\ 1 & \text{if } \vec{j} \neq \vec{\ell}. \end{cases} \quad (9.36)$$

Our goal is to determine $\vec{\ell}$, which we can do by solving the following optimization problem and finding its global optimum:

$$\min_{\vec{j} \in \{0,1\}^n} f(\vec{j}).$$

We want to solve this problem using the adiabatic theorem. As a Hamiltonian, the problem can be encoded by:

$$\mathcal{H}_F = I^{\otimes n} - |\vec{\ell}\rangle\langle\vec{\ell}|.$$

This is the projector onto states orthogonal to $|\vec{\ell}\rangle$. The state $|\vec{\ell}\rangle$ is an eigenstate of \mathcal{H}_F with eigenvalue 0, whereas every state orthogonal to $|\vec{\ell}\rangle$ is an eigenstate with eigenvalue 1. This corresponds precisely to the objective function in Eq. (9.36). Thus, \mathcal{H}_F is our final Hamiltonian for which we want to determine the eigenstate with the smallest eigenvalue. Note that $\vec{\ell}$ is supposed to be unknown, so we assume that we have the ability to apply and operate on the Hamiltonian \mathcal{H}_F , but we do not know its analytical description — otherwise, we would know the value of $\vec{\ell}$.

As in the previous example, we need to choose an initial Hamiltonian. Define $|\phi\rangle := (H|0\rangle)^{\otimes n} = \frac{1}{\sqrt{2^n}} \sum_{\vec{j} \in \{0,1\}^n} |\vec{j}\rangle$, i.e., the uniform superposition state. We choose the initial Hamiltonian as:

$$\mathcal{H}_I = I^{\otimes n} - |\phi\rangle\langle\phi|.$$

This is the projector onto states orthogonal to $|\phi\rangle$; the state $|\phi\rangle$ is an eigenvector of \mathcal{H}_I with eigenvalue 0. Linear interpolation between \mathcal{H}_I and \mathcal{H}_F yields the time-dependent Hamiltonian:

$$\mathcal{H}(s) = (1-s)\mathcal{H}_I + s\mathcal{H}_F = I^{\otimes n} + (s-1)|\phi\rangle\langle\phi| - s|\vec{\ell}\rangle\langle\vec{\ell}|.$$

The spectrum of $\mathcal{H}(s)$ is easy to analyze. \mathcal{H}_I acts as the identity on every state orthogonal to $|\phi\rangle$, whereas \mathcal{H}_F acts as the identity on every state orthogonal to $|\vec{\ell}\rangle$. Thus, if a state is orthogonal to both $|\phi\rangle$ and $|\vec{\ell}\rangle$, $\mathcal{H}(s)$ acts as the identity. It follows that the only nontrivial action of $\mathcal{H}(s)$ takes place in the subspace spanned by $|\phi\rangle$ and $|\vec{\ell}\rangle$, which is two-dimensional. An orthonormal basis for this two-dimensional space is given by $\{|\vec{\ell}\rangle, |\vec{\ell}^\perp\rangle\}$, where:

$$|\vec{\ell}^\perp\rangle := \frac{1}{\sqrt{1 - |\langle\phi|\vec{\ell}\rangle|^2}} \left(|\phi\rangle - \langle\phi|\vec{\ell}\rangle|\vec{\ell}\rangle \right) = \frac{\sqrt{2^n}}{\sqrt{2^n - 1}} \left(|\phi\rangle - \frac{1}{\sqrt{2^n}}|\vec{\ell}\rangle \right)$$

is the (normalized) projection of $|\phi\rangle$ onto the space orthogonal to $|\vec{\ell}\rangle$. We can then express $\mathcal{H}(s)$ in the basis $\{|\vec{\ell}\rangle, |\vec{\ell}^\perp\rangle\}$:

$$\mathcal{H}_F = \begin{pmatrix} 0 & 0 \\ 0 & 1 \end{pmatrix}, \quad \mathcal{H}_I = \begin{pmatrix} 1 - \frac{1}{2^n} & -\frac{\sqrt{2^n-1}}{2^n} \\ -\frac{\sqrt{2^n-1}}{2^n} & \frac{1}{2^n} \end{pmatrix},$$

therefore:

$$\mathcal{H}(s) = (1-s)\mathcal{H}_I + s\mathcal{H}_F = \begin{pmatrix} (1-s)(1 - \frac{1}{2^n}) & -(1-s)\frac{\sqrt{2^n-1}}{2^n} \\ -(1-s)\frac{\sqrt{2^n-1}}{2^n} & (1-s)\frac{1}{2^n} + s \end{pmatrix}. \quad (9.37)$$

The eigenvalues of this matrix can be obtained with straightforward calculations, yielding:

$$\lambda_0(s) = \frac{1}{2} \left(1 - \sqrt{1 - 4s(1-s) \left(1 - \frac{1}{2^n} \right)} \right) \quad \lambda_1(s) = \frac{1}{2} \left(1 + \sqrt{1 - 4s(1-s) \left(1 - \frac{1}{2^n} \right)} \right).$$

The instantaneous spectral gap is the difference between $\lambda_1(s)$ and $\lambda_0(s)$:

$$\gamma(s) = \lambda_1(s) - \lambda_0(s) = \sqrt{1 - 4s(1-s) \left(1 - \frac{1}{2^n} \right)},$$

and $\gamma(s)$ is minimized at $s = 1/2$, where $\gamma(1/2) = \frac{1}{\sqrt{2^n}}$. Thus, the spectral gap is exponentially small. Applying Cor. 9.24 with $\gamma = \frac{1}{\sqrt{2^n}}$ gives a running time of $\mathcal{O}(2^{3n/2})$, worse than Grover's algorithm and worse than evaluating $f(\vec{j})$ for all values of $\vec{j} \in \{0, 1\}^n$. To get a tighter bound, we apply Thm. 9.23 directly (remember that Cor. 9.24 intentionally loosened some bounds to get a simpler expression). Using the fact that $\mathcal{H}' = \mathcal{H}_F - \mathcal{H}_I$, $\mathcal{H}'' = 0$, we obtain:

$$\begin{aligned} T &\geq \frac{c}{\delta} \left(\frac{\|\mathcal{H}'(0)\|}{\gamma(0)^2} + \frac{\|\mathcal{H}'(1)\|}{\gamma(1)^2} + \int_0^1 \left(\frac{\|\mathcal{H}'(s)\|^2}{\gamma(s)^3} + \frac{\|\mathcal{H}''(s)\|}{\gamma(s)^2} \right) ds \right) \\ &= \frac{c}{\delta} \left(\|\mathcal{H}_F - \mathcal{H}_I\| + \int_0^1 \frac{\|\mathcal{H}_F - \mathcal{H}_I\|^2}{(1 - 4s(1-s) \left(1 - \frac{1}{2^n} \right))^{3/2}} ds \right) = \mathcal{O}(2^n). \end{aligned}$$

(The last equality is not obvious, but the computation of the integral is tedious and not particularly insightful, so we skip it.) This is still no better than evaluating $f(\vec{j})$ for all values of $\vec{j} \in \{0, 1\}^n$, therefore giving no quantum speedup.

We can do better, while still relying on the adiabatic theorem, but we need to adjust our strategy. One approach would be to change the initial Hamiltonian \mathcal{H}_I , and try to come up with an \mathcal{H}_I that yields a better running time. There is another possibility: we can change the time-dependent Hamiltonian $\mathcal{H}(s)$, while keeping \mathcal{H}_I and \mathcal{H}_F fixed. Our current definition of $\mathcal{H}(s)$ performs linear interpolation between \mathcal{H}_I and \mathcal{H}_F , see Eq. (9.6); however, the adiabatic theorem as stated (Thm.s 9.11 and 9.23) allows for a general time-varying Hamiltonian, provided that it is twice differentiable and we can bound the norm of its derivatives. Thus, we are allowed to perform nonlinear interpolation, and that can change the running time because it can affect the spectral gap and the derivatives of $\mathcal{H}(s)$. In Eq. (9.37) we replace the linear interpolation terms $(1-s), s$ with more general functions $1-h(s), h(s)$, yielding $\gamma(s) = \sqrt{1 - 4h(s)(1-h(s)) \left(1 - \frac{1}{2^n} \right)}$. With an appropriate choice of $h(s)$, the value of T for adiabatic optimization to work in this context goes down to $\mathcal{O}(\sqrt{2^n})$, matching the query and gate complexity of Grover's algorithm: this can be achieved by choosing $h(s)$ so that the Hamiltonian changes more slowly when the instantaneous spectral gap is small, i.e., around $s = 1/2$, and to compensate for the slowdown, the pace of the interpolation is increased around the two endpoints, $s = 0$ and $s = 1$. (Recall: a smaller spectral gap requires a larger evolution time to ensure that the system remains in the correct eigenspace; increasing the time horizon is equivalent to decreasing the rate of change of the Hamiltonian.) The function should of course also satisfy $h(0) = 0, h(1) = 1$. For example, one can choose h so that $h'(s) \propto \gamma(s)^{3/2}$, which ensures that the interpolation proceeds very slowly when the gap is close to zero, and faster when the gap is close to 1. More details on this can be found in, e.g., [Childs, 2017].

In both examples we could characterize the spectral gap because we managed to reduce the time-dependent Hamiltonian $\mathcal{H}(s)$ to one or more two-dimensional time-dependent Hamiltonians, allowing us to analyze the spectrum with simple linear algebra. Many interesting problems do not have sufficient amount of structure to give tight bounds on the gap, and as a result, they are difficult to study in the context of adiabatic optimization.

9.2 The quantum approximate optimization algorithm

The Quantum Approximate Optimization Algorithm (QAOA), initially proposed in [Farhi et al., 2014a], is designed as a low-resource approximation of adiabatic evolution, with the goal of being implementable even on quantum computers that can only successfully execute a relatively small number of gates — or in any case, fewer gates than would be necessary for an accurate simulation of the Schrödinger equation involved in adiabatic optimization. The QAOA is characterized by an algorithmic parameter p that determines the number of layers of its circuit implementation, and essentially trades quantum resources for quality of the approximation. However, we note that, in practice, larger p , while better in theory, does not always mean that a better solution to an optimization problem is obtained; this is discussed later in this section, after the necessary concepts have been introduced.

9.2.1 Derivation from the adiabatic theorem

QAOA is traditionally discussed in the setting of solving a binary optimization problem in maximization form:

$$\max f(\vec{x}) \quad \vec{x} \in \{0, 1\}^n. \quad (9.38)$$

Remark 9.27. *All of the discussion in this section can be converted to minimization with the usual transformation $\max f(x) = -\min -f(x)$, but for reasons that come up subsequently in our presentation, QAOA is more naturally discussed for maximization.*

Problem (9.38) is encoded by the following Hamiltonian:

$$\mathcal{H}_F = \sum_{\vec{j} \in \{0,1\}^n} f(\vec{j}) |\vec{j}\rangle\langle\vec{j}|. \quad (9.39)$$

The maximum eigenpair of \mathcal{H}_F is a solution of problem (9.38). We can determine such eigenpair by using adiabatic optimization. It should be clear from the statement of Thm. 9.11 that the derivation of adiabatic optimization in Sect. 9.1 is perfectly symmetric with respect to minimization or maximization: if we start in a minimum eigenstate of the initial Hamiltonian, adiabatic evolution eventually converges to a minimum eigenstate of the final Hamiltonian, whereas if we start in a maximum eigenstate of the initial Hamiltonian, we find a maximum eigenstate of the final Hamiltonian. For adiabatic optimization we need an initial Hamiltonian \mathcal{H}_I ; defining matrices σ_j^X :

$$\sigma_j^X := \underbrace{I \otimes \cdots \otimes I \otimes X \otimes I \cdots \otimes I}_{n \text{ times}},$$

position j
 \downarrow
 X

where X is the Pauli X matrix as given in Def. 1.36, we choose the Hamiltonian:

$$\mathcal{H}_I = \sum_{j=1}^n \sigma_j^X, \quad (9.40)$$

for which an eigenstate with maximum eigenvalue is given by the product state:

$$|\varphi(0)\rangle = (H|0\rangle)^{\otimes n}.$$

This is easy to prove: each term σ_j^X has eigenvalues with absolute value at most 1 because it is a real unitary matrix, and the vector that has $H|0\rangle$ on the j -th qubit is an eigenvector with eigenvalue 1, which is therefore the maximum. Thus:

$$\sum_{j=1}^n \sigma_j^X (H|0\rangle)^{\otimes n} = n (H|0\rangle)^{\otimes n}.$$

Now we apply the adiabatic theorem, and obtain the following result.

Proposition 9.28. *Consider the time-dependent Hamiltonian:*

$$\mathcal{H}(s) = (1 - s)\mathcal{H}_I + s\mathcal{H}_F, \tag{9.41}$$

where $\mathcal{H}_F, \mathcal{H}_I$ are defined as in Eq.s (9.39), (9.40) respectively. For $p \in \mathbb{N}, p > 0$, let $\beta, \theta \in [0, 2\pi]^p$ be p -dimensional vectors, and define the following unitary parameterized by p, β and θ :

$$U_{QAOA}(p, \beta, \theta) := e^{-i\beta_p \mathcal{H}_I} e^{-i\theta_p \mathcal{H}_F} e^{-i\beta_{p-1} \mathcal{H}_I} e^{-i\theta_{p-1} \mathcal{H}_F} \dots e^{-i\beta_1 \mathcal{H}_I} e^{-i\theta_1 \mathcal{H}_F}. \tag{9.42}$$

Then, for any $\delta > 0$ and for $p \rightarrow \infty$, there exists a choice β^*, θ^* of β, θ such that $U_{QAOA}(p, \beta^*, \theta^*)$ approximates an adiabatic evolution of $\mathcal{H}(s)$, and in particular, the following holds:

$$\left\| \lim_{p \rightarrow \infty} U_{QAOA}(p, \beta^*, \theta^*) (H|0\rangle)^{\otimes n} - |\varphi(1)\rangle \right\| \leq \delta,$$

where $|\varphi(1)\rangle$ is an eigenstate of $\mathcal{H}(1) = \mathcal{H}_F$ with maximum eigenvalue, encoding a solution to problem (9.38).

In the proof of Prop. 9.28 we use the following definition; the definition can be skipped if the reader is not interested in the details of the proof.

Definition 9.29 (Irreducible matrix). *Given a matrix $M \in \mathbb{R}^{n \times n}$ with nonnegative entries, the matrix graph associated with M is the directed graph $G_M = (V, A)$ with $V := \{1, \dots, n\}$ and $A = \{(i, j) : M_{ij} \neq 0\}$, i.e., there is an arc between i and j if and only if the element M_{ij} is nonzero. The matrix M is said to be irreducible if its matrix graph G_M is strongly connected.*

We can now proceed with the proof of Prop. 9.28.

Proof. Thm. 9.11 states that if we start in the state $(H|0\rangle)^{\otimes n}$, which is an eigenstate of \mathcal{H}_I with maximum eigenvalue, and simulate the time-dependent Schrödinger equation in Eq. (9.8), we remain in a maximum eigenvalue of the time-dependent Hamiltonian $\mathcal{H}(s)$, provided that there is a nonzero spectral gap and T is chosen large enough.

First, let us address the spectral gap γ . Here it is sufficient to show that the spectral gap around the maximum eigenvalue is nonzero: we eventually choose a very large T , going to infinity, therefore we do not have to worry about the gap dependence even if γ is very small — we only need to make sure that the lower bound on T given in Thm. 9.11 is finite for this problem. To show that $\gamma > 0$ we use the Perron-Frobenius theorem. One version of the Perron-Frobenius theorem states that if a nonnegative matrix is irreducible, then its largest eigenvalue is positive and simple, i.e., it has algebraic multiplicity 1 [Horn and Johnson, 2012]. Note that if such properties hold, then $\gamma > 0$, because the largest eigenvalue is strictly larger than the second largest. We can w.l.o.g. assume that \mathcal{H}_F is nonnegative: shifting the objective function value by a constant does not change the optimum and only translates the spectrum of the Hamiltonian. \mathcal{H}_I is also nonnegative by construction, hence $\mathcal{H}(s)$ is nonnegative. Proving irreducibility of $\mathcal{H}(s)$ is relatively straightforward: \mathcal{H}_F is a diagonal matrix, and does not affect the rest of the analysis; \mathcal{H}_I has a special structure and its graph is strongly connected, as we show next. Recall that $\mathcal{H}_I \in \mathbb{R}^{2^n \times 2^n}$ and its rows and columns can be indexed by n -digit binary strings, so the nodes of the matrix graph of \mathcal{H}_I also correspond to n -digit binary strings. From Eq. (9.40), \mathcal{H}_I is a sum of terms, each of which corresponds to the unitary matrix σ_j^X that applies an X gate on a single qubit. It is clear that σ_j^X connects nodes in the matrix graph such that the corresponding labels differ by



Figure 9.2: Matrix graph of σ_2^X (on the left) and σ_1^X (on the right) over two qubits.

one bit-flip in the j -th bit, see Fig. 9.2. Because \mathcal{H}_I is the sum of σ_j^X for all j and this yields no cancellations in the matrix terms, the matrix graph of \mathcal{H}_I is the union of the matrix graphs of all σ_j^X (all of these graphs have the same vertex set, we just take the union of the sets of arcs). Then, proving that \mathcal{H}_I is strongly connected is equivalent to proving that from any given starting bitstring, we can reach another arbitrary bitstring using a sequence of bit-flips on any bit, which is obviously true. Therefore $\mathcal{H}(s)$ is irreducible for every $s \in [0, 1)$, and by the Perron-Frobenius theorem it has nonzero spectral gap $\gamma > 0$. (The spectral gap could be zero for $s = 1$ if \mathcal{H}_F has a degenerate largest eigenvalue, i.e., if there are multiple optimal solutions for the optimization problem, but there are many ways to deal with this issue; for example, we can assume that the optimal solution is unique after adding a small random perturbation to the objective function values.) Because $\gamma > 0$, there exists a possibly very large but finite T that satisfies the conditions in Thm. 9.11 (or Thm. 9.23), and whose value depends only on the problem instance. We fix such value of T .

We now consider the simulation of the dynamics of the Schrödinger equation (Eq. (9.8)) with the given value of T , which guarantees finding the maximum eigenstate of \mathcal{H}_F because we start in a maximum eigenstate of \mathcal{H}_I . Just as in Sect. 9.1.3, we discretize time in an infinitely-large number of time steps N , and simulate $\mathcal{H}(s)$ for an infinitesimally-small time $1/N$, where in each time step $\mathcal{H}(s)$ is fixed. Recalling Eq. (9.9), in the j -th time step the system evolves by applying:

$$e^{iT/N\mathcal{H}(j/N)} = \exp\left(i\frac{T}{N}\left(\frac{N-j}{N}\mathcal{H}_I + \frac{j}{N}\mathcal{H}_F\right)\right). \quad (9.43)$$

We now apply a product formula (Sect. 6.2.2) to compute an approximation of Eq. (9.43). By Eq. (6.6), the error of the approximation:

$$\exp\left(i\frac{T}{N}\left(\frac{N-j}{N}\mathcal{H}_I + \frac{j}{N}\mathcal{H}_F\right)\right) \approx \left(\exp\left(i\frac{T}{hN}\frac{N-j}{N}\mathcal{H}_I\right)\exp\left(i\frac{T}{hN}\frac{j}{N}\mathcal{H}_F\right)\right)^h \quad (9.44)$$

decreases as N and h grow, and in particular, with $N \rightarrow \infty, h \rightarrow \infty$, the error of the entire adiabatic evolution goes to zero. Comparing Eq.s (9.42) and (9.44), we see that the angles β, θ in Eq. (9.42) can be chosen to obtain Eq. (9.44): pick N and h large enough so that applying Eq. (9.44) with $j = 0, \dots, N-1$ guarantees sufficiently small error (the error is arbitrarily small), fix $p = Nh$, finally choose $\beta_1, \dots, \beta_p, \theta_1, \dots, \theta_p$ to match Eq. (9.44). This proves that there is a choice β^*, θ^* such that $\lim_{p \rightarrow \infty} U_{\text{QAOA}}(p, \beta^*, \theta^*)(H|0\rangle)^{\otimes n}$ follows the trajectory for adiabatic optimization according to Thm. 9.11, and therefore, the final state can be made to have arbitrarily small distance from a maximum eigenstate $|\varphi(1)\rangle$ of $\mathcal{H}(1) = \mathcal{H}_F$. \square

The unitary $U_{\text{QAOA}}(p, \beta, \theta)$ is the main operator of the QAOA, as we discuss in the next section.

9.2.2 Algorithm description and properties

Prop. 9.28 states that the unitary operator $U_{\text{QAOA}}(p, \beta, \theta)$ can approximate adiabatic evolution, for some choice of the angles β, θ , in the limit $p \rightarrow \infty$, i.e., when it includes an infinite sequence of matrix exponentials of \mathcal{H}_F and \mathcal{H}_I . To derive an implementable algorithm we need to work with finite p . The QAOA is a general framework that leaves many important decisions open, allowing the details to be specified based on the properties of the optimization problem at hand. The basic scheme followed by QAOA is: pick a finite value of p ; determine values of the angles $\beta, \theta \in [0, 2\pi]^p$; construct $U_{\text{QAOA}}(p, \beta, \theta)(H|0\rangle)^{\otimes n}$, and sample from the corresponding quantum states a few times. We summarize this scheme in Alg. 8. This general description leaves open several crucial

Algorithm 8: Quantum approximate optimization algorithm (QAOA).

Input: Hamiltonian \mathcal{H}_F encoding problem (9.38), parameter p , number of samples r .

Output: Best solution found.

- 1 Determine angles $\beta, \theta \in [0, 2\pi]^p$.
 - 2 Construct the state $U_{\text{QAOA}}(p, \beta, \theta) (H|0\rangle)^{\otimes n}$, and perform r measurements on it. Let M be the set of observed measurement outcomes.
 - 3 **return** $\vec{j} \in \arg \max_{\vec{j} \in M} \{f(\vec{j})\}$.
-

choices that have tremendous impact on the performance of the algorithm: the choice of p , the choice of the angles β, θ , and, to a lesser extent, the number of samples. These choices can be made based on theoretical or practical considerations. We discuss the three components separately. We begin with choosing the angles because the corresponding considerations make the discussion on choosing p clearer.

Choosing the angles β, θ . For this discussion assume that p is fixed and given. We need to choose $\beta, \theta \in [0, 2\pi]^p$ so as to maximize the objective function value of the solution that is returned in the final step of Alg. 8, after taking r samples from the quantum state constructed with $U_{\text{QAOA}}(p, \beta, \theta)$. To do so, we must fix the criterion that is used to compare different values of β, θ : how do we measure the quality of a certain choice? A natural approach, proposed in the seminal QAOA paper [Farhi et al., 2014a], is to compare the expected value of the measurement outcomes from the final state $U_{\text{QAOA}}(p, \beta, \theta) (H|0\rangle)^{\otimes n}$. Recall from Eq. (9.39) that \mathcal{H}_F is a diagonal matrix with the objective function values $f(\vec{j})$ on the diagonal. Given a quantum state $|\psi\rangle = \sum_{\vec{j} \in \{0,1\}^n} \alpha_j |\vec{j}\rangle$ (in this case $|\psi\rangle$ is the state produced by QAOA, but the property stated next holds for any state), it is easy to see that $\langle \psi | \mathcal{H}_F | \psi \rangle$ is precisely the expected value of the objective function f with respect to the probability distribution over the measurement outcomes:

$$\langle \psi | \mathcal{H}_F | \psi \rangle = \left(\sum_{\vec{j} \in \{0,1\}^n} \alpha_j^\dagger \langle \vec{j} | \right) \mathcal{H}_F \left(\sum_{\vec{j} \in \{0,1\}^n} \alpha_j |\vec{j}\rangle \right) = \sum_{\vec{j} \in \{0,1\}^n} |\alpha_j|^2 f(\vec{j}) = \mathbb{E}[f(X)], \quad (9.45)$$

where X is the random variable over measurement outcomes with probability distribution $\Pr(X = \vec{j}) = |\alpha_j|^2$. The quantity $\langle \psi | \mathcal{H}_F | \psi \rangle$ can be computed in multiple ways. For example, we can measure $|\psi\rangle$ multiple times, say m times, and compute the sample average $\frac{1}{m} \sum_{k=1}^m f(\vec{j}^{(k)})$ where $\vec{j}^{(k)}$ is the k -th observed sample; if \mathcal{H}_F is a weighted summation of tensor products of σ_j^Z terms, as in Prop. 9.4, we can estimate each term of the summation by checking the corresponding bits of the measurement outcomes across samples (i.e., computing the sample average for each single σ_j^Z or $\sigma_j^Z \otimes \sigma_k^Z$ term, then calculating their weighted combination). The angles can then be chosen as the solution to the following optimization problem for fixed p :

$$\max_{\beta, \theta} \left(\langle (|0\rangle H)^{\otimes n} U_{\text{QAOA}}^\dagger(p, \beta, \theta) \mathcal{H}_F \left(U_{\text{QAOA}}(p, \beta, \theta) (H|0\rangle)^{\otimes n} \right) \right). \quad (9.46)$$

This is equivalent to:

$$\max_{\beta, \theta} \mathbb{E}[f(X)], \quad (9.47)$$

where the relationship between β, θ and the random variable X is via the probabilities $|\alpha_j|^2$: in other words, we aim to maximize the expected objective function value of the binary strings (i.e., solutions) sampled from the quantum state. Problem (9.46) is a continuous optimization problem that can be solved (usually in a heuristic manner, see Rem. 9.30) with many possible classical algorithms; in the literature it is often solved with derivative-free optimization techniques, using the quantum computer only to evaluate the objective function, but derivatives can be computed, and no clearly dominant solution strategy has emerged so far. We discuss some of the issues related to the solution of problem (9.46) in Sect. 9.2.4.

Remark 9.30. *Problem (9.46) is continuous but nonconvex in general, and can be very difficult to solve to the global optimum. In very special cases, the Hamiltonian \mathcal{H}_F may have sufficient structure that problem (9.46) can be solved efficiently — at least in practice, if not in theory — but in general we can only hope for a local minimum that may be of poor quality. Thus, the solution of problem (9.46) can be a significant obstacle. In fact, it may be as difficult as solving the original combinatorial optimization problem (9.38): we are replacing the solution of a difficult problem (problem (9.38)) with the solution of another difficult problem (problem (9.46)), and may not gain any quantum advantage in the process.*

Although using problems (9.46)-(9.47) to guide the choice of the angles is natural and well-motivated, it is not the only possibility. In light of the fact that the ultimate goal is to obtain a sample from $U_{\text{QAOA}}(p, \beta, \theta) (H|0\rangle)^{\otimes n}$ with maximum objective function value in problem (9.38), it may be reasonable to utilize a metric different from the expected value. For example, [Barkoutsos et al., 2020] proposes focusing on the lower tail of the distribution (for a minimization problem) rather than the expected value, using the Conditional Value-at-Risk (CVaR) of $f(X)$ at a given level as the objective function in problem (9.47).

Choice of p . The set of quantum states that can be obtained as $U_{\text{QAOA}}(p, \beta, \theta) (H|0\rangle)^{\otimes n}$ gets larger as p increases. This is easy to see: any unitary $U_{\text{QAOA}}(p, \beta, \theta)$ can also be obtained as $U_{\text{QAOA}}(p', \beta, \theta)$ for $p' > p$, simply by setting to zero $\beta_j, \theta_j : j > p$. Thus, the following relationship holds for $p' > p$:

$$\begin{aligned} \max_{\beta, \theta} \left(\langle \langle 0|H \rangle^{\otimes n} U_{\text{QAOA}}^\dagger(p, \beta, \theta) \right) \mathcal{H}_F \left(U_{\text{QAOA}}(p, \beta, \theta) (H|0\rangle)^{\otimes n} \right) &\leq \\ \max_{\beta, \theta} \left(\langle \langle 0|H \rangle^{\otimes n} U_{\text{QAOA}}^\dagger(p', \beta, \theta) \right) \mathcal{H}_F \left(U_{\text{QAOA}}(p', \beta, \theta) (H|0\rangle)^{\otimes n} \right). & \end{aligned}$$

As a consequence, at least in theory it is reasonable to choose p as large as possible. However, a large p has at least two important practical drawbacks: (i) it leads to circuits that require more gates; (ii) it may lead to worse solutions, because heuristic algorithms to solve the nonconvex problem (9.46) may struggle if there are additional parameters β, θ to optimize.

From a theoretical point of view, a few results are known showing that, for small p , QAOA achieves an expected approximation ratio with respect to the optimal solution. Here, approximation ratio is meant in the usual optimization sense, as for approximation algorithms.

Definition 9.31 (Approximation algorithm). *An approximation algorithm with approximation ratio $r \leq 1$ is an algorithm that, given a maximization problem with optimal objective function value f^* , returns a solution with objective function value at least rf^* .*

There are two main approximation results that sparked the interest in QAOA, as the first quantum algorithm with an approximation guarantee for some optimization problem. We report them below.

Theorem 9.32 (QAOA for MaxCut on 3-regular graphs; [Farhi et al., 2014a]). *Given a 3-regular graph G (i.e., a graph where each node has exactly three incident edges), for $p = 1$ there is a choice of the angles β, θ such that QAOA (Alg. 8) returns a solution to the MaxCut problem on G achieving approximation ratio 0.6924, in expectation.*

For the second result we first define the optimization problem, called Max E3LIN2, as it is not as well known as MaxCut. We are given a set of linear equations modulo 2 over n binary variables. Each equation contains exactly three variables. Thus, each equation is of the form:

$$x_j + x_k + x_h \equiv b \pmod{2},$$

where $b \in \{0, 1\}$. Our goal is to find an assignment of the binary decision variables that maximizes the number of satisfied equations.

Theorem 9.33 (QAOA for Max E3LIN2; [Farhi et al., 2014b]). *Given an instance of Max E3LIN2 such that each variable appears in no more than $D + 1$ equations, for $p = 1$ there is a choice of the angles β, θ such that QAOA (Alg. 8) returns a solution achieving approximation ratio $\frac{1}{2} + \frac{1}{101\sqrt{D} \ln D}$, in expectation.*

Remark 9.34. *The approximation ratios in Thm.s 9.32 and 9.33 are lower than (i.e., not as good as) the best approximation ratios that can be obtained by classical algorithms. Thus, QAOA with $p = 1$ does not lead to provable quantum advantage for these problems, at least based on existing results.*

Although we do not give a full proof of how these approximation ratios are obtained, it may be useful to provide a high-level overview, which has the added benefit of illustrating the difficulties faced when trying to extend these results to higher values of p or other types of combinatorial optimization problems. In Sect. 9.2.3 we sketch the main ideas of the analysis behind Thm. 9.32.

Number of samples. The main consideration to determine the number of samples is the variance of the random variable whose value is the objective function value of the sample. As before, let X be the random variable characterizing the measurement outcomes, and consider the distribution of $f(X)$, i.e., the objective function values of the samples. Applying the formula $\text{Var}(X) = \mathbb{E}[X^2] - (\mathbb{E}[X])^2$, recalling problems (9.46)-(9.47), we see that the variance can be expressed as:

$$\begin{aligned} & \left(\langle (0|H)^{\otimes n} U_{\text{QAOA}}^\dagger(p, \beta, \theta) \right) \mathcal{H}_{\mathbb{F}}^2 \left(U_{\text{QAOA}}(p, \beta, \theta) (H|0)^{\otimes n} \right) - \\ & \left(\langle (0|H)^{\otimes n} U_{\text{QAOA}}^\dagger(p, \beta, \theta) \right) \mathcal{H}_{\mathbb{F}} \left(U_{\text{QAOA}}(p, \beta, \theta) (H|0)^{\otimes n} \right)^2. \end{aligned}$$

Although such an expression is typically difficult to analyze, for special cases it may have sufficient structure. [Farhi et al., 2014a] shows that for the MaxCut problem on graphs with bounded degree and $|E|$ edges, if p is fixed, the variance is $\mathcal{O}(|E|)$ and the standard deviation is $\sigma = \mathcal{O}(\sqrt{|E|})$. By central limit theorem, the sample mean of $\mathcal{O}(|E|^{2k})$ samples, $k > 1$, is normally distributed with mean $\mu = \mathbb{E}[f(X)]$ and standard deviation $\sigma/\sqrt{|E|^{2k}} = \mathcal{O}(1/|E|^{k-1/2})$. Applying Chebyshev's inequality (i.e., $\Pr(|X - \mu| \geq h\sigma) \leq 1/h^2$) and choosing the constants appropriately, we then obtain:

$$\Pr(|f(X) - \mu| \geq 1) \leq \frac{1}{|E|^{2k-1}}.$$

So, for example, setting $k = 1$ we find that with probability at least $1 - 1/|E|$, the sample mean of $\mathcal{O}(|E|^2)$ samples estimates the expected value with error at most 1.

Remark 9.35. *The concentration around the mean has the benefit that we can expect to quickly (i.e., with few samples) obtain binary strings corresponding to solutions with objective function value close to $\mathbb{E}[f(X)]$, but it also has the drawback that we cannot expect to sample solutions with objective function value much better than $\mathbb{E}[f(X)]$.*

9.2.3 QAOA for MaxCut with fixed p

We present a high-level overview of the argument that leads to Thm. 9.32. We fix $p = 1$ for now. Define:

$$C_{jk} := \frac{1}{2} (I^{\otimes n} - \sigma_j^Z \sigma_k^Z). \quad (9.48)$$

By definition, σ_j^Z acts as the identity on every qubit except j , see Eq. (9.4). Restricted to the space of qubits j and k (i.e., the j -th and k -th digit of the n -digit basis states that we are considering), C_{jk} acts as the following matrix:

$$\begin{pmatrix} 0 & 0 & 0 & 0 \\ 0 & 1 & 0 & 0 \\ 0 & 0 & 1 & 0 \\ 0 & 0 & 0 & 0 \end{pmatrix}.$$

This is a possibly-outdated preprint, using the author's lecture notes, of the book "Quantum algorithms for optimizers," edited by SIAM. All rights to the book's material belong to SIAM. Please refer to the SIAM version of the book.

Thus, each basis state is an eigenstate of C_{jk} , with eigenvalue 1 if qubits j and k take different values, and with eigenvalue 0 otherwise. This is exactly the objective function contribution of edge (j, k) in the MaxCut problem: we gain 1 if the endpoints of an edge have different labels (e.g., $|0\rangle$ and $|1\rangle$), we gain nothing if they have the same label. It follows that, for the (unweighted) MaxCut problem on a graph $G = (V, E)$, where the vertex set is $V = \{1, \dots, n\}$, the final Hamiltonian \mathcal{H}_F on n qubits can be written as:

$$\mathcal{H}_F = \sum_{(j,k) \in E} C_{jk}.$$

Now let us analyze the expected objective function value in Eq. (9.45) for the state produced by QAOA with $p = 1$. By definition of \mathcal{H}_F , we have:

$$\begin{aligned} & \left(\langle 0|H \rangle^{\otimes n} U_{\text{QAOA}}^\dagger(p, \beta, \theta) \right) \mathcal{H}_F \left(U_{\text{QAOA}}(p, \beta, \theta) (H|0) \rangle^{\otimes n} \right) = \\ & \sum_{(j,k) \in E} \left(\langle 0|H \rangle^{\otimes n} U_{\text{QAOA}}^\dagger(p, \beta, \theta) \right) C_{jk} \left(U_{\text{QAOA}}(p, \beta, \theta) (H|0) \rangle^{\otimes n} \right). \end{aligned}$$

A single term C_{jk} in the above expression is of the following form — using brackets to more easily identify the constituents:

$$\langle 0|H \rangle^{\otimes n} \left[e^{i\theta \sum_{(h,\ell) \in E} C_{h\ell}} \right] \left[e^{i\beta \sum_{h=1}^n \sigma_h^X} \right] C_{jk} \left[e^{-i\beta \sum_{h=1}^n \sigma_h^X} \right] \left[e^{-i\theta \sum_{(h,\ell) \in E} C_{h\ell}} \right] (H|0) \rangle^{\otimes n}.$$

(Recall that $p = 1$ so β, θ are scalars, not vectors.) By definition of C_{jk} , this is equal to:

$$\langle 0|H \rangle^{\otimes n} \left[e^{i\theta \sum_{(h,\ell) \in E} C_{h\ell}} \right] \left[e^{i\beta \sum_{h=1}^n \sigma_h^X} \right] \frac{1}{2} (I^{\otimes n} - \sigma_j^Z \sigma_k^Z) \left[e^{-i\beta \sum_{h=1}^n \sigma_h^X} \right] \left[e^{-i\theta \sum_{(h,\ell) \in E} C_{h\ell}} \right] (H|0) \rangle^{\otimes n}.$$

To better understand the structure of this expression, we drop the rescaling factor $\frac{1}{2}$, and we can drop the identity matrix too: distributing the multiplication and looking at the term with the identity matrix, we see that it yields a constant shift to the entire value of the above expression (each term that multiplies the identity from the right simplifies with a term that multiplies the identity from the left), which does not depend on β or θ . Such a constant term can be dropped. Thus, we are left with:

$$\langle 0|H \rangle^{\otimes n} \left[e^{i\theta \sum_{(h,\ell) \in E} C_{h\ell}} \right] \left[e^{i\beta \sum_{h=1}^n \sigma_h^X} \right] (-\sigma_j^Z \sigma_k^Z) \left[e^{-i\beta \sum_{h=1}^n \sigma_h^X} \right] \left[e^{-i\theta \sum_{(h,\ell) \in E} C_{h\ell}} \right] (H|0) \rangle^{\otimes n}.$$

The central term $-\sigma_j^Z \sigma_k^Z$ acts as the identity on every qubit except the j -th and k -th, and the matrix exponential $e^{-i\beta \sum_{h=1}^n \sigma_h^X}$ can be written as the product $\prod_{h=1}^n e^{-i\beta \sigma_h^X}$ because the matrices σ_h^X commute; similarly for $e^{i\beta \sum_{h=1}^n \sigma_h^X}$. Thus, all terms $e^{-i\beta \sigma_h^X}$ except for $h = j, k$ commute through $-\sigma_j^Z \sigma_k^Z$, and cancel out with the respective terms in $e^{i\beta \sum_{h=1}^n \sigma_h^X}$. This leads to the following simplification:

$$\langle 0|H \rangle^{\otimes n} \left[e^{i\theta \sum_{(h,\ell) \in E} C_{h\ell}} \right] \left[e^{i\beta(\sigma_j^X + \sigma_k^X)} \right] (-\sigma_j^Z \sigma_k^Z) \left[e^{-i\beta(\sigma_j^X + \sigma_k^X)} \right] \left[e^{-i\theta \sum_{(h,\ell) \in E} C_{h\ell}} \right] (H|0) \rangle^{\otimes n}.$$

Now we analyze $e^{-i\theta \sum_{(h,\ell) \in E} C_{h\ell}}$. Each term of the summation in the exponent is diagonal, hence everything commutes. Then, all terms in $e^{-i\theta \sum_{(h,\ell) \in E} C_{h\ell}}$ that do not involve qubit j or k commute through $\left[e^{i\beta(\sigma_j^X + \sigma_k^X)} \right] (-\sigma_j^Z \sigma_k^Z) \left[e^{-i\beta(\sigma_j^X + \sigma_k^X)} \right]$, and cancel out the corresponding term in $e^{i\theta \sum_{(h,\ell) \in E} C_{h\ell}}$. We are left with the following simplified expression:

$$\begin{aligned} & \langle 0|H \rangle^{\otimes n} \left[\exp \left(i\theta \sum_{\substack{(h,\ell) \in E \\ \{h,\ell\} \cap \{j,k\} \neq \emptyset}} C_{h\ell} \right) \right] \left[e^{i\beta(\sigma_j^X + \sigma_k^X)} \right] (-\sigma_j^Z \sigma_k^Z) \\ & \left[e^{-i\beta(\sigma_j^X + \sigma_k^X)} \right] \left[\exp \left(-i\theta \sum_{\substack{(h,\ell) \in E \\ \{h,\ell\} \cap \{j,k\} \neq \emptyset}} C_{h\ell} \right) \right] (H|0) \rangle^{\otimes n}. \quad (9.49) \end{aligned}$$

This expression depends only on qubits j, k , and qubits that are adjacent to j or k in the graph G . In other words, to compute the value of the objective function contribution for edge (j, k) we only need to consider the subgraph containing edge (j, k) and all edges adjacent to it.

Remark 9.36. *This argument can be extended beyond $p = 1$: for $p = 1$, we need to consider the subgraph including edges at distance 1 from node j or node k ; if we apply exactly the same line of reasoning, we obtain that in general we need to consider the subgraph including edges at distance p from node j or node k .*

The above discussion helps us characterize the performance of QAOA with $p = 1$ for MaxCut on a 3-regular graph. Because the graph is 3-regular, for every term C_{jk} in the expected objective function value, and therefore for every edge (j, k) in the graph, there are only three possible subgraphs with distance 1 from (j, k) , illustrated in Fig. 9.3. Specifically, each of the three

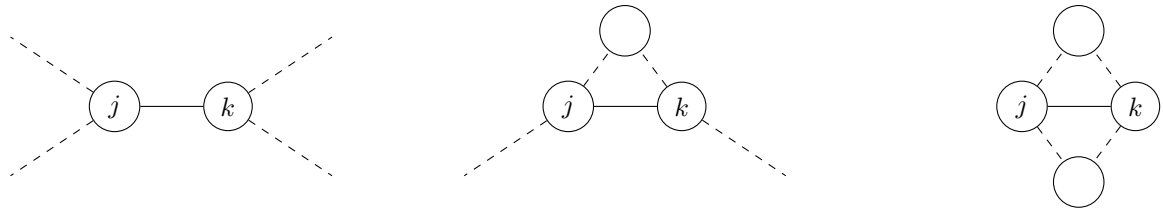


Figure 9.3: Possible subgraphs at distance 1 from (j, k) in a 3-regular graph.

subgraphs occurs when nodes j and k have, respectively, zero, one or two neighbors in common. For fixed β, θ , we can compute the value of Eq. (9.49) for the three subgraph types. Using the fact that the graph is 3-regular and combinatorial arguments, we can derive a formula for the number of subgraphs of each type in Fig. 9.3 that can possibly appear in the graph, in relation to each other. Then it is a simple exercise to numerically determine the optimal angles β, θ and the worst-case value (i.e., minimum value) for the expected objective function value:

$$\min_{\substack{\text{all possible} \\ \text{3-regular graphs}}} \max_{\beta, \theta} \left(\langle 0|H\rangle^{\otimes n} U_{\text{QAOA}}^\dagger(1, \beta, \theta) \right) \mathcal{H}_F \left(U_{\text{QAOA}}(1, \beta, \theta) (H|0\rangle)^{\otimes n} \right).$$

This is how the approximation ratio 0.6924 of Thm. 9.32 is shown in [Farhi et al., 2014a].

9.2.4 Implementation

The circuit $U_{\text{QAOA}}(p, \beta, \theta)$ is simple to implement, consisting of a small number of gates relative to most of the algorithms discussed before. Assuming a QUBO objective function (Def. 9.3), yielding the Hamiltonian of Prop. 9.4 as in the MaxCut discussion of Sect. 9.2.3, the unitary $e^{-i\theta\mathcal{H}_F}$ can be decomposed into two-qubit blocks $e^{-i\theta\sigma_j^Z\sigma_k^Z}$, and single-qubit gates. The unitary $e^{-i\theta\sigma_j^Z\sigma_k^Z}$ can be implemented with two CX gates and the single qubit rotation $R_Z(2\theta) = e^{-i\theta Z}$ that implements the matrix exponential of the Pauli matrix Z , using the circuit represented in Fig. 9.4.

Definition 9.37 (Z rotation gate). *The gate $R_Z(\theta)$ is defined as the matrix:*

$$R_Z(\theta) := \begin{pmatrix} e^{-i\theta/2} & 0 \\ 0 & e^{i\theta/2} \end{pmatrix}.$$

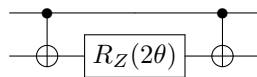


Figure 9.4: Circuit implementing $e^{-i\theta\sigma_1^Z\sigma_2^Z}$.

Remark 9.38. *The $R_Z(\theta)$ gate is equivalent, up to a global phase factor, to the phase shift gate $P(\theta)$ of Def. 3.5; in particular we can obtain $e^{-i\theta\sigma_1^Z\sigma_2^Z}$ up to global phase substituting $P(2\theta)$ for $R_Z(2\theta)$ in Fig. 9.4. However, controlled versions of R_Z are not equivalent to controlled versions of P , and vice-versa, because of relative phases: controlled- $R_Z(\theta)$ acts as $|0\rangle\langle 0| \otimes I + |1\rangle\langle 1| \otimes R_Z(\theta)$, and controlled- $P(\theta)$ acts as $|0\rangle\langle 0| \otimes I + |1\rangle\langle 1| \otimes P(\theta)$, so even if $P(\theta) = e^{i\theta/2}R_Z(\theta)$, the controlled unitaries are not equal up to a global phase. This remark acts as a reminder to be careful about equivalence up to global phase, when controlled operations are involved.*

The unitary $e^{-i\beta\mathcal{H}_1}$, by its equivalence with the product of single-qubit operators $\prod_{j=1}^n e^{-i\beta\sigma_j^X}$, can be decomposed into single-qubit gates $R_X(2\beta) = e^{-i\beta X}$ that implement the matrix exponential of the Pauli matrix X , applied to each qubit.

Definition 9.39 (X rotation gate). *The gate $R_X(\theta)$ is defined as the matrix:*

$$R_X(\theta) := \begin{pmatrix} \cos \theta/2 & -i \sin \theta/2 \\ -i \sin \theta/2 & \cos \theta/2 \end{pmatrix}.$$

Thus, the number of basic gates of $U_{\text{QAOA}}(p, \beta, \theta)$ is directly proportional to p , the number of qubits, and the number of terms $\sigma_j^Z \sigma_k^Z$ in \mathcal{H}_F (which depends on the sparsity of the QUBO matrix).

For the solution of problem (9.46), there is no known theoretically-elegant solution, except for very few special cases where the angles can be determined analytically. The use of classical derivative-free algorithms is common in the literature. The derivatives of the objective function in problem (9.46) can be computed analytically, and evaluated using circuits with similar building blocks as $U_{\text{QAOA}}(p, \beta, \theta)$. The widespread use of derivative-free algorithms for a continuous optimization problem with a differentiable objective function is likely due to practical and numerical considerations: the execution of quantum circuits to compute derivatives can represent a significant time investment, from a practical point of view, and the presence of noise because of hardware limitations may reduce the impact of (imperfectly-estimated) partial derivatives. Because of the nonconvexity of problem (9.46), the problem is typically solved without optimality guarantees. This makes it difficult to show rigorous approximation guarantees similarly to Thm.s 9.32 and 9.33. Overall, limited to the analysis reported in this chapter, QAOA does not yield a provable advantage over classical algorithms, and can be considered a heuristic with an approximation guarantee for some structured problems.

9.3 Notes and further reading

The adiabatic theorem is a foundational result dating back to the early days of quantum mechanics [Born and Fock, 1928]. Its use in the theory of quantum computing is often associated with the minimization of diagonal Hamiltonians for combinatorial optimization problems (the same type of problems discussed in Sect. 9.2.1), but it has further and much broader implications. Throughout this set of lecture notes we employed the circuit model for quantum computers. Alternatively, it is possible to model quantum computers purely using an adiabatic evolution. Intuitively, this may not be surprising: if a quantum computer can exist in the physical world, its evolution must admit a description in terms of some quantum-mechanical system, so in theory we can describe that system and simulate its evolution using the Schrödinger equation. Perhaps more surprisingly, it is possible to give an explicit construction for an initial Hamiltonian, an initial eigenstate of the initial Hamiltonian, and a final Hamiltonian such that the adiabatic evolution of the system in the sense of Thm. 9.11 simulates any given quantum circuit, in time that is polynomial in the size of the circuit. Because we have already shown in Sect. 9.1 that quantum circuits can simulate the adiabatic evolution, this implies that the adiabatic model and the circuit model are equivalent. This fundamental result is shown in [Aharonov et al., 2008].

There is vast literature on the subject of combinatorial optimization with the adiabatic theorem, e.g., [Farhi et al., 2001, Finnila et al., 1994, Santoro et al., 2002]. An area of particular

interest for computational optimization is that of quantum annealers [Johnson et al., 2011], a physical implementation of the adiabatic model of computation that, due to hardware restrictions, is not fully general, and cannot simulate an arbitrary quantum circuit. It can, however, attempt to simulate the adiabatic evolution of QUBO Hamiltonians as those in Prop. 9.4. Although it does not guarantee finding the global optimum due to hardware restrictions and evolution time, it may heuristically find a solution with optimal or near-optimal objective function value; see [McGeoch, 2020] for a general introduction and [Crosson and Lidar, 2021] for a discussion on the prospects of proving speedups for some type of problems. The comparison between the computational performance of quantum annealers and classical algorithms on meaningful combinatorial optimization problems is the subject of many works in the past ten years, and we refer to [Albash and Lidar, 2018, Jünger et al., 2021, Rehfeldt et al., 2023, Tasseff et al., 2022] as entry points to survey the state of the field.

For readers interested in QAOA, in addition to the seminal articles [Farhi et al., 2014a, Farhi et al., 2014b], a good starting point may be the PhD thesis [Hadfield, 2018]. The performance of QAOA is the subject of numerous papers. One of the reasons for this interest is the fact that QAOA circuits can produce samples from probability distributions that are hard to construct classically; this is shown in [Farhi and Harrow, 2016], by first proving that it is $\#P$ -hard to compute matrix elements of a quantum circuit, and then showing that QAOA with $p = 1$ already produces distributions that are hard to sample classically. Thus, QAOA as a framework exhibits a form of likely quantum advantage. We emphasize that the computation of the expected value in Eq. (9.45) for the QAOA circuit (i.e., the objective function of problem (9.46)) sometimes admits an efficient classical algorithm; see, e.g., [Bravyi et al., 2020, Ozaeta et al., 2022] for analytic formulas for $p = 1$, and [Boulebnane and Montanaro, 2024] for a characterization of the success probability of QAOA on random k -SAT instances. While the expected values can sometimes be efficiently computed without a quantum computer, sampling from the distribution created by the QAOA circuit is believed to be difficult, as discussed above. The fact that QAOA produces a hard-to-sample probability distribution does not necessarily translate into good theoretical or practical performance for combinatorial optimization. Some papers suggest that QAOA may yield advantage over classical optimization algorithms for some problems, e.g., [Lykov et al., 2023, Montanaro and Zhou, 2024, Shaydulin et al., 2024], while others bring arguments in favor of the opposite conclusion, e.g., [Hastings, 2019, Bravyi et al., 2020]. [Bravyi et al., 2020] additionally proposes the idea of employing the QAOA framework to recursively identify pairs of binary variables that can be fixed to either have the same value, or different value. (This is equivalent to imposing constraints $x_j = x_k$ or $x_j = 1 - x_k$ for a binary integer program.) Each of these fixings reduces the size of the problem. Assume p is given and fixed. Using the MaxCut problem as an example, and the same notation as in Sect. 9.2.3, a fixing can be identified by first choosing β, θ to solve problem (9.46), then scanning the edges and picking the edge (j, k) that maximizes the expression:

$$\left(\langle 0|H \rangle^{\otimes n} U_{\text{QAOA}}^\dagger(p, \beta, \theta) \sigma_j^Z \sigma_k^Z \left(U_{\text{QAOA}}(p, \beta, \theta) |H|0 \rangle^{\otimes n} \right) \right),$$

i.e., finding the pair of variables that is maximally correlated or anticorrelated in the QAOA solution. This idea has been shown to outperform the traditional QAOA both numerically and theoretically on several problems [Bae and Lee, 2024, Kondo et al., 2024].

List of Definitions

1.1	Definition (Tensor product)	8
1.2	Definition (Kronecker product)	8
1.5	Definition (Binary string)	9
1.6	Definition (Bra-ket)	10
1.7	Definition (Standard basis in bra-ket notation)	10
1.11	Definition (Big- \mathcal{O} notation)	11
1.16	Definition (Superposition)	13
1.21	Definition (Entangled state)	15
1.33	Definition (Bitwise XOR)	24
1.34	Definition (Bitwise dot product)	24
1.35	Definition (Matrix norm)	24
1.36	Definition (Pauli gates)	24
1.42	Definition (Universal set of gates)	28
1.47	Definition (Total variation distance)	31
1.52	Definition (Uncomputation)	33
1.54	Definition (Pure state)	34
1.55	Definition (Mixed state)	35
1.62	Definition (Partial trace)	37
1.64	Definition (Reduced density matrix)	38
1.69	Definition (Purification)	40
2.3	Definition (Eigenstate)	44
3.1	Definition (Quantum Fourier transform)	55
3.3	Definition (Binary fraction)	57
3.5	Definition (Phase shift gate)	58
3.10	Definition (Normalized sinc function)	62
4.26	Definition (Y rotation gate)	90
5.1	Definition (Addition modulo the largest representable integer)	106
5.8	Definition (Central difference approximation)	112
5.9	Definition (Probability oracle)	112
5.10	Definition (Phase oracle)	112
5.20	Definition (Ball in ℓ^p -norm)	119
5.21	Definition (Neighborhood and interior of a convex set)	119
5.22	Definition (Membership, separation and optimization oracles)	119
5.24	Definition (Subgradient and ϵ -subgradient)	120
5.26	Definition (Finite-difference gradient approximation)	121
5.27	Definition (Finite-difference Laplace approximation)	121
5.34	Definition (Amplitude encoding)	124
5.39	Definition (QRAM)	128

6.1	Definition (Hamiltonian)	133
6.3	Definition (Matrix exponential)	134
6.4	Definition (Hamiltonian simulation)	134
6.7	Definition (Bounded-error Quantum Polynomial time (BQP) class)	134
7.10	Definition (Block-encoding)	159
7.11	Definition (Block-encoding (alternative-definition))	159
7.16	Definition (State-preparation pair)	161
7.28	Definition (Frobenius norm)	168
7.31	Definition (Trace norm)	170
7.33	Definition (Gibbs distribution)	170
7.34	Definition (Gibbs state)	170
7.35	Definition (Subnormalized density matrix)	171
8.2	Definition (Bregman divergence)	180
8.4	Definition (Dual norm)	181
8.11	Definition (Primal-infeasibility-certificate polytope)	188
8.13	Definition (Width of PIC-ORACLE)	189
8.18	Definition (Generalized primal-infeasibility-certificate polytope)	192
9.3	Definition (Quadratic Unconstrained Binary Optimization (QUBO) problem)	209
9.6	Definition (Norm of time-dependent quantities)	211
9.8	Definition (Instantaneous spectral gap)	211
9.9	Definition (Spectral gap)	211
9.29	Definition (Irreducible matrix)	230
9.31	Definition (Approximation algorithm)	233
9.37	Definition (Z rotation gate)	236
9.39	Definition (X rotation gate)	237

Bibliography

- [Aaronson, 2018] Aaronson, S. (2018). Shadow tomography of quantum states. In *Proceedings of the 50th annual ACM SIGACT symposium on theory of computing*, pages 325–338.
- [Aharonov et al., 2017] Aharonov, D., Ben-Or, M., Eban, E., and Mahadev, U. (2017). Interactive proofs for quantum computations. *arXiv preprint arXiv:1704.04487*.
- [Aharonov et al., 2008] Aharonov, D., van Dam, W., Kempe, J., Landau, Z., Lloyd, S., and Regev, O. (2008). Adiabatic quantum computation is equivalent to standard quantum computation. *SIAM review*, 50(4):755–787.
- [Albash and Lidar, 2018] Albash, T. and Lidar, D. A. (2018). Demonstration of a scaling advantage for a quantum annealer over simulated annealing. *Physical Review X*, 8(3):031016.
- [Allen-Zhu and Orecchia, 2014] Allen-Zhu, Z. and Orecchia, L. (2014). Linear coupling: An ultimate unification of gradient and mirror descent. *arXiv preprint arXiv:1407.1537*.
- [Allen-Zhu and Orecchia, 2017] Allen-Zhu, Z. and Orecchia, L. (2017). Linear coupling: An ultimate unification of gradient and mirror descent. In Papadimitriou, C. H., editor, *8th Innovations in Theoretical Computer Science Conference (ITCS 2017)*. Schloss Dagstuhl-Leibniz-Zentrum fuer Informatik.
- [Ambainis, 2010] Ambainis, A. (2010). Variable time amplitude amplification and a faster quantum algorithm for solving systems of linear equations. *arXiv preprint arXiv:1010.4458*.
- [Ambainis et al., 2019] Ambainis, A., Balodis, K., Iraids, J., Kokainis, M., Prūsis, K., and Vihrovs, J. (2019). Quantum speedups for exponential-time dynamic programming algorithms. In *Proceedings of the Thirtieth Annual ACM-SIAM Symposium on Discrete Algorithms*, pages 1783–1793. SIAM.
- [Ambainis and Regev, 2004] Ambainis, A. and Regev, O. (2004). An elementary proof of the quantum adiabatic theorem. *arXiv preprint quant-ph/0411152*.
- [van Apeldoorn, 2020] van Apeldoorn, J. (2020). *A quantum view on convex optimization*. PhD thesis, Centrum Wiskunde & Informatika, University of Amsterdam.
- [van Apeldoorn and Gilyén, 2019] van Apeldoorn, J. and Gilyén, A. (2019). Improvements in Quantum SDP-Solving with Applications. In Baier, C., Chatzigiannakis, I., Flocchini, P., and Leonardi, S., editors, *46th International Colloquium on Automata, Languages, and Programming (ICALP 2019)*, volume 132 of *Leibniz International Proceedings in Informatics (LIPIcs)*, pages 99:1–99:15, Dagstuhl, Germany. Schloss Dagstuhl–Leibniz-Zentrum fuer Informatik.
- [van Apeldoorn et al., 2020a] van Apeldoorn, J., Gilyén, A., Gribling, S., and de Wolf, R. (2020a). Convex optimization using quantum oracles. *Quantum*, 4:220.
- [van Apeldoorn et al., 2020b] van Apeldoorn, J., Gilyén, A., Gribling, S., and de Wolf, R. (2020b). Quantum sdp-solvers: Better upper and lower bounds. *Quantum*, 4:230.

- [Arora et al., 2005] Arora, S., Hazan, E., and Kale, S. (2005). Fast algorithms for approximate semidefinite programming using the multiplicative weights update method. In *46th Annual IEEE Symposium on Foundations of Computer Science (FOCS'05)*, pages 339–348. IEEE.
- [Arora et al., 2012] Arora, S., Hazan, E., and Kale, S. (2012). The multiplicative weights update method: a meta-algorithm and applications. *Theory of computing*, 8(1):121–164.
- [Arora and Kale, 2016] Arora, S. and Kale, S. (2016). A combinatorial, primal-dual approach to semidefinite programs. *Journal of the ACM (JACM)*, 63(2):12.
- [Arunachalam et al., 2015] Arunachalam, S., Gheorghiu, V., Jochym-O’Connor, T., Mosca, M., and Srinivasan, P. V. (2015). On the robustness of bucket brigade quantum ram. *New Journal of Physics*, 17(12):123010.
- [Augustino et al., 2023a] Augustino, B., Leng, J., Nannicini, G., Terlaky, T., and Wu, X. (2023a). A quantum central path algorithm for linear optimization. *arXiv preprint arXiv:2311.03977*.
- [Augustino et al., 2023b] Augustino, B., Nannicini, G., Terlaky, T., and Zuluaga, L. (2023b). Quantum interior point methods for semidefinite optimization. *Quantum*, 7:1110.
- [Bae and Lee, 2024] Bae, E. and Lee, S. (2024). Recursive qaoa outperforms the original qaoa for the max-cut problem on complete graphs. *Quantum Information Processing*, 23(3):78.
- [Bansal and Gupta, 2019] Bansal, N. and Gupta, A. (2019). Potential-function proofs for gradient methods. *Theory of Computing*, 15(1):1–32.
- [Barahona, 1982] Barahona, F. (1982). On the computational complexity of ising spin glass models. *Journal of Physics A: Mathematical and General*, 15(10):3241.
- [Barenco et al., 1995] Barenco, A., Bennett, C. H., Cleve, R., DiVincenzo, D. P., Margolus, N., Shor, P., Sleator, T., Smolin, J. A., and Weinfurter, H. (1995). Elementary gates for quantum computation. *Physical review A*, 52(5):3457.
- [Barkoutsos et al., 2020] Barkoutsos, P. K., Nannicini, G., Robert, A., Tavernelli, I., and Woerner, S. (2020). Improving variational quantum optimization using cvar. *Quantum*, 4:256.
- [Beck and Teboulle, 2003] Beck, A. and Teboulle, M. (2003). Mirror descent and nonlinear projected subgradient methods for convex optimization. *Operations Research Letters*, 31(3):167–175.
- [Bennett, 1973] Bennett, C. H. (1973). Logical reversibility of computation. *IBM journal of Research and Development*, 17(6):525–532.
- [Bennett et al., 1997] Bennett, C. H., Bernstein, E., Brassard, G., and Vazirani, U. (1997). Strengths and weaknesses of quantum computing. *SIAM Journal on Computing*, 26(5):1510–1523.
- [Bernstein and Vazirani, 1997] Bernstein, E. and Vazirani, U. (1997). Quantum complexity theory. *SIAM Journal on Computing*, 26(5):1411–1473.
- [Berry et al., 2007] Berry, D. W., Ahokas, G., Cleve, R., and Sanders, B. C. (2007). Efficient quantum algorithms for simulating sparse hamiltonians. *Communications in Mathematical Physics*, 270:359–371.
- [Berry et al., 2014] Berry, D. W., Childs, A. M., Cleve, R., Kothari, R., and Somma, R. D. (2014). Exponential improvement in precision for simulating sparse hamiltonians. In *Proceedings of the forty-sixth annual ACM symposium on Theory of computing*, pages 283–292.
- [Berry et al., 2015] Berry, D. W., Childs, A. M., and Kothari, R. (2015). Hamiltonian simulation with nearly optimal dependence on all parameters. In *2015 IEEE 56th Annual Symposium on Foundations of Computer Science*, pages 792–809. IEEE.

- [Bertsekas, 1999] Bertsekas, D. P. (1999). *Nonlinear Programming, 2nd Edition*. Athena Scientific, Belmont, MA.
- [Bhatia, 2013] Bhatia, R. (2013). *Matrix analysis*, volume 169. Springer Science & Business Media.
- [Blencowe, 2010] Blencowe, M. (2010). Quantum ram. *Nature*, 468(7320):44–45.
- [Born and Fock, 1928] Born, M. and Fock, V. (1928). Beweis des adiabatenatzes. *Zeitschrift für Physik*, 51(3):165–180.
- [Boulebnane and Montanaro, 2024] Boulebnane, S. and Montanaro, A. (2024). Solving boolean satisfiability problems with the quantum approximate optimization algorithm. *PRX Quantum*, 5(3):030348.
- [Boyd and Vandenberghe, 2004] Boyd, S. and Vandenberghe, L. (2004). *Convex Optimization*. Cambridge University Press, Cambridge.
- [Boyer et al., 1998] Boyer, M., Brassard, G., Høyer, P., and Tapp, A. (1998). Tight bounds on quantum searching. *Fortschritte der Physik: Progress of Physics*, 46(4-5):493–505.
- [Brandão et al., 2019] Brandão, F. G., Kalev, A., Li, T., Lin, C. Y.-Y., Svore, K. M., and Wu, X. (2019). Quantum sdp solvers: Large speed-ups, optimality, and applications to quantum learning. In *46th International Colloquium on Automata, Languages, and Programming (ICALP 2019)*. Schloss-Dagstuhl-Leibniz Zentrum für Informatik.
- [Brandao and Svore, 2017] Brandao, F. G. and Svore, K. M. (2017). Quantum speed-ups for solving semidefinite programs. In *2017 IEEE 58th Annual Symposium on Foundations of Computer Science (FOCS)*, pages 415–426. IEEE.
- [Brandao et al., 2022] Brandao, F. G. L., Kueng, R., and França, D. S. (2022). Faster quantum and classical sdp approximations for quadratic binary optimization. *Quantum*, 6:625.
- [Brassard et al., 2002] Brassard, G., Hoyer, P., Mosca, M., and Tapp, A. (2002). Quantum amplitude amplification and estimation. *Contemporary Mathematics*, 305:53–74.
- [Bravyi et al., 2020] Bravyi, S., Kliesch, A., Koenig, R., and Tang, E. (2020). Obstacles to variational quantum optimization from symmetry protection. *Physical review letters*, 125(26):260505.
- [Broadbent et al., 2009] Broadbent, A., Fitzsimons, J., and Kashefi, E. (2009). Universal blind quantum computation. In *Foundations of Computer Science, 2009. FOCS'09. 50th Annual IEEE Symposium on*, pages 517–526. IEEE.
- [Brown, 1951] Brown, G. W. (1951). Iterative solution of games by fictitious play. *Activity Analysis of Production and Allocation*, 13(1):374.
- [Canonne, 2020] Canonne, C. L. (2020). A short note on learning discrete distributions. *arXiv preprint arXiv:2002.11457*.
- [Castelvecchi, 2017] Castelvecchi, D. (2017). Quantum computers ready to leap out of the lab in 2017. *Nature News*, 541(7635):9.
- [Chakrabarti et al., 2020] Chakrabarti, S., Childs, A. M., Li, T., and Wu, X. (2020). Quantum algorithms and lower bounds for convex optimization. *Quantum*, 4:221.
- [Chakraborty et al., 2019] Chakraborty, S., Gilyén, A., and Jeffery, S. (2019). The Power of Block-Encoded Matrix Powers: Improved Regression Techniques via Faster Hamiltonian Simulation. In Baier, C., Chatzigiannakis, I., Flocchini, P., and Leonardi, S., editors, *46th International Colloquium on Automata, Languages, and Programming (ICALP 2019)*, volume 132 of *Leibniz International Proceedings in Informatics (LIPIcs)*, pages 33:1–33:14, Dagstuhl, Germany. Schloss Dagstuhl–Leibniz-Zentrum fuer Informatik.

- [Chen et al., 2024] Chen, Y., Gilyén, A., and de Wolf, R. (2024). A quantum speed-up for approximating the top eigenvectors of a matrix. *arXiv preprint arXiv:2405.14765*.
- [Childs, 2004] Childs, A. M. (2004). *Quantum information processing in continuous time*. PhD thesis, Massachusetts Institute of Technology.
- [Childs, 2017] Childs, A. M. (2017). Lecture notes on quantum algorithms. *Lecture notes at University of Maryland*.
- [Childs et al., 2017] Childs, A. M., Kothari, R., and Somma, R. D. (2017). Quantum algorithm for systems of linear equations with exponentially improved dependence on precision. *SIAM Journal on Computing*, 46(6):1920–1950.
- [Childs and Wiebe, 2012] Childs, A. M. and Wiebe, N. (2012). Hamiltonian simulation using linear combinations of unitary operations. *arXiv preprint arXiv:1202.5822*.
- [Cleve and Watrous, 2000] Cleve, R. and Watrous, J. (2000). Fast parallel circuits for the quantum fourier transform. In *Proceedings 41st Annual Symposium on Foundations of Computer Science*, pages 526–536. IEEE.
- [Coffman et al., 2000] Coffman, V., Kundu, J., and Wootters, W. K. (2000). Distributed entanglement. *Physical Review A*, 61(5):052306.
- [Cornelissen and Hamoudi, 2023] Cornelissen, A. and Hamoudi, Y. (2023). A sublinear-time quantum algorithm for approximating partition functions. In *Proceedings of the 2023 Annual ACM-SIAM Symposium on Discrete Algorithms (SODA)*, pages 1245–1264. SIAM.
- [Costa et al., 2022] Costa, P. C., An, D., Sanders, Y. R., Su, Y., Babbush, R., and Berry, D. W. (2022). Optimal scaling quantum linear-systems solver via discrete adiabatic theorem. *PRX quantum*, 3(4):040303.
- [Crosson and Lidar, 2021] Crosson, E. and Lidar, D. (2021). Prospects for quantum enhancement with diabatic quantum annealing. *Nature Reviews Physics*, 3(7):466–489.
- [Dalzell, 2024] Dalzell, A. M. (2024). A shortcut to an optimal quantum linear system solver. *arXiv preprint arXiv:2406.12086*.
- [Dalzell et al., 2025] Dalzell, A. M., Gilyén, A., Hann, C. T., McArdle, S., Salton, G., Nguyen, Q. T., Kubica, A., and Brandão, F. G. (2025). A distillation-teleportation protocol for fault-tolerant qram. *arXiv preprint arXiv:2505.20265*.
- [van Dam et al., 2006] van Dam, W., Hallgren, S., and Ip, L. (2006). Quantum algorithms for some hidden shift problems. *SIAM Journal on Computing*, 36(3):763–778.
- [van Dam et al., 2001] van Dam, W., Mosca, M., and Vazirani, U. (2001). How powerful is adiabatic quantum computation? In *Proceedings 42nd IEEE symposium on foundations of computer science*, pages 279–287. IEEE.
- [Dawson and Nielsen, 2005] Dawson, C. M. and Nielsen, M. A. (2005). The Solovay-Kitaev algorithm. *arXiv preprint quant-ph/0505030*.
- [Deutsch, 1985] Deutsch, D. (1985). Quantum theory, the Church-Turing principle and the universal quantum computer. In *Proceedings of the Royal Society of London A: Mathematical, Physical and Engineering Sciences*, volume 400, pages 97–117. The Royal Society.
- [Deutsch and Jozsa, 1992] Deutsch, D. and Jozsa, R. (1992). Rapid solution of problems by quantum computation. *Proceedings of the Royal Society of London A*, 439(1907):553–558.
- [Devoret and Schoelkopf, 2013] Devoret, M. H. and Schoelkopf, R. J. (2013). Superconducting circuits for quantum information: an outlook. *Science*, 339(6124):1169–1174.

- [Durr and Hoyer, 1996] Durr, C. and Hoyer, P. (1996). A quantum algorithm for finding the minimum. *arXiv preprint quant-ph/9607014*.
- [Farhi et al., 2014a] Farhi, E., Goldstone, J., and Gutmann, S. (2014a). A quantum approximate optimization algorithm. *arXiv preprint arXiv:1411.4028*.
- [Farhi et al., 2014b] Farhi, E., Goldstone, J., and Gutmann, S. (2014b). A quantum approximate optimization algorithm applied to a bounded occurrence constraint problem. *arXiv preprint arXiv:1412.6062*.
- [Farhi et al., 2001] Farhi, E., Goldstone, J., Gutmann, S., Lapan, J., Lundgren, A., and Preda, D. (2001). A quantum adiabatic evolution algorithm applied to random instances of an np-complete problem. *Science*, 292(5516):472–475.
- [Farhi and Harrow, 2016] Farhi, E. and Harrow, A. W. (2016). Quantum supremacy through the quantum approximate optimization algorithm. *arXiv preprint arXiv:1602.07674*.
- [Feynman, 1982] Feynman, R. P. (1982). Simulating physics with computers. *International journal of theoretical physics*, 21(6):467–488.
- [Feynman, 2018] Feynman, R. P. (2018). *Feynman lectures on computation*. CRC Press.
- [Finnila et al., 1994] Finnila, A. B., Gomez, M. A., Sebenik, C., Stenson, C., and Doll, J. D. (1994). Quantum annealing: A new method for minimizing multidimensional functions. *Chemical physics letters*, 219(5-6):343–348.
- [Garey and Johnson, 1990] Garey, M. R. and Johnson, D. S. (1990). *Computers and Intractability; A Guide to the Theory of NP-Completeness*. W. H. Freeman & Co., USA.
- [Gilyén, 2019] Gilyén, A. (2019). *Quantum singular value transformation & its algorithmic applications*. PhD thesis, University of Amsterdam.
- [Gilyén et al., 2019a] Gilyén, A., Arunachalam, S., and Wiebe, N. (2019a). Optimizing quantum optimization algorithms via faster quantum gradient computation. In *Proceedings of the Thirtieth Annual ACM-SIAM Symposium on Discrete Algorithms*, pages 1425–1444. SIAM.
- [Gilyén et al., 2019b] Gilyén, A., Su, Y., Low, G. H., and Wiebe, N. (2019b). Quantum singular value transformation and beyond: exponential improvements for quantum matrix arithmetics. In *Proceedings of the 51st Annual ACM SIGACT Symposium on Theory of Computing*, pages 193–204.
- [Giovannetti et al., 2008] Giovannetti, V., Lloyd, S., and Maccone, L. (2008). Quantum random access memory. *Physical review letters*, 100(16):160501.
- [Gleixner et al., 2016] Gleixner, A. M., Steffy, D. E., and Wolter, K. (2016). Iterative refinement for linear programming. *INFORMS Journal on Computing*, 28(3):449–464.
- [Goemans and Williamson, 1995] Goemans, M. X. and Williamson, D. P. (1995). Improved approximation algorithms for maximum cut and satisfiability problems using semidefinite programming. *Journal of the ACM (JACM)*, 42(6):1115–1145.
- [Grange et al., 2023] Grange, C., Bourreau, E., Poss, M., and t’Kindt, V. (2023). Quantum speed-ups for single-machine scheduling problems. In *Proceedings of the Companion Conference on Genetic and Evolutionary Computation*, pages 2224–2231.
- [Grigni et al., 2001] Grigni, M., Schulman, L., Vazirani, M., and Vazirani, U. (2001). Quantum mechanical algorithms for the nonabelian hidden subgroup problem. In *Proceedings of the thirty-third annual ACM symposium on Theory of computing*, pages 68–74.
- [Gross et al., 2010] Gross, D., Liu, Y.-K., Flammia, S. T., Becker, S., and Eisert, J. (2010). Quantum state tomography via compressed sensing. *Physical review letters*, 105(15):150401.

- [Grötschel et al., 1988] Grötschel, M., Lovász, L., and Schrijver, A. (1988). *Geometric algorithms and combinatorial optimization*. Springer, Berlin.
- [Grover and Rudolph, 2002] Grover, L. and Rudolph, T. (2002). Creating superpositions that correspond to efficiently integrable probability distributions. *arXiv preprint quant-ph/0208112*.
- [Grover, 1996] Grover, L. K. (1996). A fast quantum mechanical algorithm for database search. In *Proceedings of the twenty-eighth annual ACM Symposium on Theory of Computing*, pages 212–219. ACM.
- [Haah et al., 2017] Haah, J., Harrow, A. W., Ji, Z., Wu, X., and Yu, N. (2017). Sample-optimal tomography of quantum states. *IEEE Transactions on Information Theory*, 63(9):5628–5641.
- [Hadfield, 2018] Hadfield, S. A. (2018). *Quantum algorithms for scientific computing and approximate optimization*. Columbia University.
- [Harrow et al., 2009] Harrow, A. W., Hassidim, A., and Lloyd, S. (2009). Quantum Algorithm for Linear Systems of Equations. *Physical Review Letters*, 103(15):150502.
- [Harrow et al., 2017] Harrow, A. W., Lin, C. Y.-Y., and Montanaro, A. (2017). Sequential measurements, disturbance and property testing. In *Proceedings of the Twenty-Eighth Annual ACM-SIAM Symposium on Discrete Algorithms*, pages 1598–1611. SIAM.
- [Harrow and Wei, 2020] Harrow, A. W. and Wei, A. Y. (2020). Adaptive quantum simulated annealing for bayesian inference and estimating partition functions. In *Proceedings of the Fourteenth Annual ACM-SIAM Symposium on Discrete Algorithms*, pages 193–212. SIAM.
- [Hastings, 2019] Hastings, M. B. (2019). Classical and quantum bounded depth approximation algorithms. *arXiv preprint arXiv:1905.07047*.
- [Holevo, 1973] Holevo, A. S. (1973). Bounds for the quantity of information transmitted by a quantum communication channel. *Problems of Information Transmission*, 9:177–183.
- [Horn and Johnson, 2012] Horn, R. A. and Johnson, C. R. (2012). *Matrix analysis*. Cambridge university press.
- [Høyer et al., 2003] Høyer, P., Mosca, M., and de Wolf, R. (2003). Quantum search on bounded-error inputs. In *International Colloquium on Automata, Languages, and Programming*, pages 291–299. Springer.
- [Jansen et al., 2007] Jansen, S., Ruskai, M.-B., and Seiler, R. (2007). Bounds for the adiabatic approximation with applications to quantum computation. *Journal of Mathematical Physics*, 48(10).
- [Jaques and Rattew, 2023] Jaques, S. and Rattew, A. G. (2023). QRAM: A survey and critique. *arXiv preprint arXiv:2305.10310*.
- [Jiang et al., 2020] Jiang, H., Kathuria, T., Lee, Y. T., Padmanabhan, S., and Song, Z. (2020). A faster interior point method for semidefinite programming. In *2020 IEEE 61st annual symposium on foundations of computer science (FOCS)*, pages 910–918. IEEE.
- [Johnson et al., 2011] Johnson, M. W., Amin, M. H., Gildert, S., Lanting, T., Hamze, F., Dickson, N., Harris, R., Berkley, A. J., Johansson, J., Bunyk, P., et al. (2011). Quantum annealing with manufactured spins. *Nature*, 473(7346):194–198.
- [Jordan, 2005] Jordan, S. P. (2005). Fast quantum algorithm for numerical gradient estimation. *Physical review letters*, 95(5):050501.
- [Jozsa, 2001] Jozsa, R. (2001). Quantum factoring, discrete logarithms, and the hidden subgroup problem. *Computing in science & engineering*, 3(2):34–43.

- [Jünger et al., 2021] Jünger, M., Lobe, E., Mutzel, P., Reinelt, G., Rendl, F., Rinaldi, G., and Stollenwerk, T. (2021). Quantum annealing versus digital computing: An experimental comparison. *Journal of Experimental Algorithmics (JEA)*, 26:1–30.
- [Kale, 2007] Kale, S. (2007). *Efficient algorithms using the multiplicative weights update method*. PhD thesis, Princeton University.
- [Kato, 1995] Kato, T. (1995). *Perturbation theory for linear operators*. Springer. first edition in 1966.
- [Kay, 2010] Kay, A. (2010). A review of perfect, efficient, state transfer and its application as a constructive tool. *International Journal of Quantum Information*, 8(04):641–676.
- [Kaye et al., 2007] Kaye, P., Laflamme, R., and Mosca, M. (2007). *An introduction to quantum computing*. Oxford University Press.
- [Kerenidis and Prakash, 2017] Kerenidis, I. and Prakash, A. (2017). Quantum Recommendation Systems. In Papadimitriou, C. H., editor, *8th Innovations in Theoretical Computer Science Conference (ITCS 2017)*, volume 67 of *Leibniz International Proceedings in Informatics (LIPIcs)*, pages 49:1–49:21, Dagstuhl, Germany. Schloss Dagstuhl – Leibniz-Zentrum für Informatik.
- [Kerenidis and Prakash, 2020] Kerenidis, I. and Prakash, A. (2020). A quantum interior point method for LPs and SDPs. *ACM Transactions on Quantum Computing*, 1(1):1–32.
- [Kerenidis et al., 2021] Kerenidis, I., Prakash, A., and Szilágyi, D. (2021). Quantum algorithms for second-order cone programming and support vector machines. *Quantum*, 5:427.
- [Kitaev, 1997] Kitaev, A. Y. (1997). Quantum computations: algorithms and error correction. *Russian Mathematical Surveys*, 52(6):1191–1249.
- [Kitaev et al., 2002] Kitaev, A. Y., Shen, A., Vyalıy, M. N., and Vyalıy, M. N. (2002). *Classical and quantum computation*. Number 47. American Mathematical Soc.
- [Kliuchnikov et al., 2016] Kliuchnikov, V., Maslov, D., and Mosca, M. (2016). Practical approximation of single-qubit unitaries by single-qubit quantum clifford and t circuits. *IEEE Transactions on Computers*, 65(1):161–172.
- [Kondo et al., 2024] Kondo, R., Sato, Y., Raymond, R., and Yamamoto, N. (2024). Recursive quantum relaxation for combinatorial optimization problems. *arXiv preprint arXiv:2403.02045*.
- [Kueng and Tropp, 2021] Kueng, R. and Tropp, J. A. (2021). Binary component decomposition part i: the positive-semidefinite case. *SIAM Journal on Mathematics of Data Science*, 3(2):544–572.
- [Kuperberg, 2005] Kuperberg, G. (2005). A subexponential-time quantum algorithm for the dihedral hidden subgroup problem. *SIAM Journal on Computing*, 35(1):170–188.
- [Kuperberg, 2011] Kuperberg, G. (2011). Another subexponential-time quantum algorithm for the dihedral hidden subgroup problem. *arXiv preprint arXiv:1112.3333*.
- [Kuperberg, 2023] Kuperberg, G. (2023). Breaking the cubic barrier in the solovay-kitaev algorithm. *arXiv preprint arXiv:2306.13158*.
- [Kushnir et al., 2025] Kushnir, S., Leng, J., Peng, Y., Fan, L., and Wu, X. (2025). Qhdopt: A software for nonlinear optimization with quantum hamiltonian descent. *INFORMS Journal on Computing*, 37(1):107–124.
- [Lee and Padmanabhan, 2020] Lee, Y. T. and Padmanabhan, S. (2020). An $\tilde{\gamma}(m/\epsilon^{3.5})$ -cost algorithm for semidefinite programs with diagonal constraints. In *Conference on Learning Theory (COLT), Proceedings of Machine Learning Research*. PMLR.

- [Lee et al., 2018] Lee, Y. T., Sidford, A., and Vempala, S. S. (2018). Efficient convex optimization with membership oracles. In *Conference On Learning Theory*, pages 1292–1294. PMLR.
- [Lee et al., 2015] Lee, Y. T., Sidford, A., and Wong, S. C.-w. (2015). A faster cutting plane method and its implications for combinatorial and convex optimization. In *2015 IEEE 56th Annual Symposium on Foundations of Computer Science*, pages 1049–1065. IEEE.
- [Leng et al., 2023a] Leng, J., Hickman, E., Li, J., and Wu, X. (2023a). Quantum hamiltonian descent. *arXiv preprint arXiv:2303.01471*.
- [Leng et al., 2023b] Leng, J., Zheng, Y., and Wu, X. (2023b). A quantum-classical performance separation in nonconvex optimization. *arXiv preprint arXiv:2311.00811*.
- [Li, 2005] Li, J. (2005). General explicit difference formulas for numerical differentiation. *Journal of Computational and Applied Mathematics*, 183(1):29–52.
- [Lin, 2022] Lin, L. (2022). Lecture notes on quantum algorithms for scientific computation. *arXiv preprint arXiv:2201.08309*.
- [Linden and de Wolf, 2022] Linden, N. and de Wolf, R. (2022). Average-case verification of the quantum fourier transform enables worst-case phase estimation. *Quantum*, 6:872.
- [Lloyd, 1996] Lloyd, S. (1996). Universal quantum simulators. *Science*, 273(5278):1073–1078.
- [Low, 2019] Low, G. H. (2019). Hamiltonian simulation with nearly optimal dependence on spectral norm. In *Proceedings of the 51st Annual ACM SIGACT Symposium on Theory of Computing*, pages 491–502.
- [Low and Chuang, 2017a] Low, G. H. and Chuang, I. L. (2017a). Hamiltonian simulation by uniform spectral amplification. *arXiv preprint arXiv:1707.05391*.
- [Low and Chuang, 2017b] Low, G. H. and Chuang, I. L. (2017b). Optimal hamiltonian simulation by quantum signal processing. *Physical review letters*, 118(1):010501.
- [Low and Chuang, 2019] Low, G. H. and Chuang, I. L. (2019). Hamiltonian simulation by qubitization. *Quantum*, 3:163.
- [Low et al., 2016] Low, G. H., Yoder, T. J., and Chuang, I. L. (2016). Methodology of resonant equiangular composite quantum gates. *Physical Review X*, 6(4):041067.
- [Lu and Lin, 2022] Lu, X. and Lin, H. (2022). Unbiased quantum phase estimation. *arXiv preprint arXiv:2210.00231*.
- [Lykov et al., 2023] Lykov, D., Wurtz, J., Poole, C., Saffman, M., Noel, T., and Alexeev, Y. (2023). Sampling frequency thresholds for the quantum advantage of the quantum approximate optimization algorithm. *npj Quantum Information*, 9(1):73.
- [Mahadev, 2018] Mahadev, U. (2018). Classical verification of quantum computations. In *Foundations of Computer Science, 2018. FOCS’18. 59th Annual IEEE Symposium on*, pages 259–267. IEEE.
- [Markov et al., 2018] Markov, I. L., Fatima, A., Isakov, S. V., and Boixo, S. (2018). Quantum supremacy is both closer and farther than it appears. *arXiv preprint arXiv:1807.10749*.
- [Martyn et al., 2021] Martyn, J. M., Rossi, Z. M., Tan, A. K., and Chuang, I. L. (2021). Grand unification of quantum algorithms. *PRX quantum*, 2(4):040203.
- [McGeoch, 2020] McGeoch, C. C. (2020). Theory versus practice in annealing-based quantum computing. *Theoretical Computer Science*, 816:169–183.

- [Mei et al., 2017] Mei, S., Misiakiewicz, T., Montanari, A., and Oliveira, R. I. (2017). Solving sdps for synchronization and maxcut problems via the grothendieck inequality. In *Conference on learning theory*, pages 1476–1515. PMLR.
- [Mencarelli et al., 2017] Mencarelli, L., Sahraoui, Y., and Liberti, L. (2017). A multiplicative weights update algorithm for minlp. *EURO Journal on Computational Optimization*, 5(1-2):31–86.
- [Mermin, 2007] Mermin, N. D. (2007). *Quantum computer science: an introduction*. Cambridge University Press.
- [Mohammadisiahroudi, 2024] Mohammadisiahroudi, M. (2024). *Quantum Computing and Optimization Methods*. PhD thesis, Lehigh University.
- [Mohammadisiahroudi et al., 2025a] Mohammadisiahroudi, M., Augustino, B., Sampourmahani, P., and Terlaky, T. (2025a). Quantum computing inspired iterative refinement for semidefinite optimization. *Mathematical Programming*, pages 1–40.
- [Mohammadisiahroudi et al., 2024] Mohammadisiahroudi, M., Fakhimi, R., and Terlaky, T. (2024). Efficient use of quantum linear system algorithms in inexact infeasible ipms for linear optimization. *Journal of Optimization Theory and Applications*, pages 1–38.
- [Mohammadisiahroudi et al., 2025b] Mohammadisiahroudi, M., Wu, Z., Augustino, B., Carr, A., and Terlaky, T. (2025b). Improvements to quantum interior point method for linear optimization. *ACM Transactions on Quantum Computing*, 6(1):1–24.
- [Montanaro, 2015] Montanaro, A. (2015). Quantum speedup of monte carlo methods. *Proceedings of the Royal Society A: Mathematical, Physical and Engineering Sciences*, 471(2181):20150301.
- [Montanaro and Zhou, 2024] Montanaro, A. and Zhou, L. (2024). Quantum speedups in solving near-symmetric optimization problems by low-depth qaoa. *arXiv preprint arXiv:2411.04979*.
- [Monteiro, 1998] Monteiro, R. D. (1998). Polynomial convergence of primal-dual algorithms for semidefinite programming based on the monteiro and zhang family of directions. *SIAM Journal on Optimization*, 8(3):797–812.
- [Nam et al., 2020] Nam, Y., Su, Y., and Maslov, D. (2020). Approximate quantum fourier transform with $o(n \log(n))$ t gates. *npj Quantum Information*, 6(1):26.
- [Nedic and Lee, 2014] Nedic, A. and Lee, S. (2014). On stochastic subgradient mirror-descent algorithm with weighted averaging. *SIAM Journal on Optimization*, 24(1):84–107.
- [Nemirovski and Yudin, 1983] Nemirovski, A. S. and Yudin, D. B. (1983). Problem complexity and method efficiency in optimization.
- [Nesterov and Todd, 1998] Nesterov, Y. E. and Todd, M. J. (1998). Primal-dual interior-point methods for self-scaled cones. *SIAM Journal on optimization*, 8(2):324–364.
- [Nielsen and Chuang, 2002] Nielsen, M. A. and Chuang, I. (2002). *Quantum computation and quantum information*. Cambridge University Press, Cambridge.
- [O’Donnell and Wright, 2016] O’Donnell, R. and Wright, J. (2016). Efficient quantum tomography. In *Proceedings of the forty-eighth annual ACM symposium on Theory of Computing*, pages 899–912.
- [O’Leary and Peleg, 1983] O’Leary, D. and Peleg, S. (1983). Digital image compression by outer product expansion. *IEEE Transactions on Communications*, 31(3):441–444.
- [Ozaeta et al., 2022] Ozaeta, A., Van Dam, W., and McMahon, P. L. (2022). Expectation values from the single-layer quantum approximate optimization algorithm on ising problems. *Quantum Science and Technology*, 7(4):045036.

- [Pednault et al., 2019] Pednault, E., Gunnels, J. A., Nannicini, G., Horesh, L., Magerlein, T., Solomonik, E., Draeger, E. W., Holland, E. T., and Wisnieff, R. (2019). Pareto-efficient quantum circuit simulation using tensor contraction deferral. *arXiv preprint arXiv:1710.05867*.
- [Rall and Fuller, 2023] Rall, P. and Fuller, B. (2023). Amplitude estimation from quantum signal processing. *Quantum*, 7:937.
- [Regev and Schiff, 2008] Regev, O. and Schiff, L. (2008). Impossibility of a quantum speed-up with a faulty oracle. In *International Colloquium on Automata, Languages, and Programming*, pages 773–781. Springer.
- [Rehfeldt et al., 2023] Rehfeldt, D., Koch, T., and Shinano, Y. (2023). Faster exact solution of sparse maxcut and qubo problems. *Mathematical Programming Computation*, pages 1–26.
- [Reichardt, 2004] Reichardt, B. W. (2004). The quantum adiabatic optimization algorithm and local minima. In *Proceedings of the thirty-sixth annual ACM symposium on Theory of computing*, pages 502–510.
- [Reichardt et al., 2013] Reichardt, B. W., Unger, F., and Vazirani, U. (2013). Classical command of quantum systems. *Nature*, 496(7446):456.
- [Rieffel and Polak, 2011] Rieffel, E. G. and Polak, W. H. (2011). *Quantum computing: A gentle introduction*. MIT Press.
- [Roos et al., 2005] Roos, C., Terlaky, T., and Vial, J.-P. (2005). *Interior point methods for linear optimization*. Springer Science & Business Media.
- [Rosmanis, 2023] Rosmanis, A. (2023). Quantum search with noisy oracle. *arXiv preprint arXiv:2309.14944*.
- [Saad, 2003] Saad, Y. (2003). *Iterative methods for sparse linear systems*. SIAM.
- [Santoro et al., 2002] Santoro, G. E., Martonák, R., Tosatti, E., and Car, R. (2002). Theory of quantum annealing of an ising spin glass. *Science*, 295(5564):2427–2430.
- [Selinger, 2012] Selinger, P. (2012). Efficient Clifford+T approximation of single-qubit operators. *arXiv preprint arXiv:1212.6253*.
- [Shaydulin et al., 2024] Shaydulin, R., Li, C., Chakrabarti, S., DeCross, M., Herman, D., Kumar, N., Larson, J., Lykov, D., Minssen, P., Sun, Y., et al. (2024). Evidence of scaling advantage for the quantum approximate optimization algorithm on a classically intractable problem. *Science Advances*, 10(22):eadm6761.
- [Shor, 1997] Shor, P. W. (1997). Polynomial-time algorithms for prime factorization and discrete logarithms on a quantum computer. *SIAM Journal on Computing*, 26(5):1484–1509.
- [Simon, 1997] Simon, D. R. (1997). On the power of quantum computation. *SIAM Journal on Computing*, 26(5):1474–1483.
- [Somma and Subaşı, 2021] Somma, R. D. and Subaşı, Y. (2021). Complexity of quantum state verification in the quantum linear systems problem. *PRX Quantum*, 2(1):010315.
- [Stamatopoulos et al., 2022] Stamatopoulos, N., Mazzola, G., Woerner, S., and Zeng, W. J. (2022). Towards quantum advantage in financial market risk using quantum gradient algorithms. *Quantum*, 6:770.
- [Suzuki et al., 2020] Suzuki, Y., Uno, S., Raymond, R., Tanaka, T., Onodera, T., and Yamamoto, N. (2020). Amplitude estimation without phase estimation. *Quantum Information Processing*, 19:1–17.

- [Tang and Tian, 2024] Tang, E. and Tian, K. (2024). A cs guide to the quantum singular value transformation. In *2024 Symposium on Simplicity in Algorithms (SOSA)*, pages 121–143. SIAM.
- [Tasseff et al., 2022] Tasseff, B., Albash, T., Morrell, Z., Vuffray, M., Lokhov, A. Y., Misra, S., and Coffrin, C. (2022). On the emerging potential of quantum annealing hardware for combinatorial optimization. *arXiv preprint arXiv:2210.04291*.
- [Teboulle, 1992] Teboulle, M. (1992). Entropic proximal mappings with applications to nonlinear programming. *Mathematics of Operations Research*, 17(3):670–690.
- [Temme, 2014] Temme, K. (2014). Runtime of unstructured search with a faulty hamiltonian oracle. *Physical Review A*, 90(2):022310.
- [Terlaky, 2013] Terlaky, T. (2013). *Interior point methods of mathematical programming*, volume 5. Springer Science & Business Media.
- [Teufel, 2003] Teufel, S. (2003). *Adiabatic perturbation theory in quantum dynamics*. Springer Science & Business Media.
- [Tsuda et al., 2005] Tsuda, K., Rätsch, G., and Warmuth, M. K. (2005). Matrix exponentiated gradient updates for on-line learning and bregman projection. *Journal of Machine Learning Research*, 6(Jun):995–1018.
- [van Apeldoorn et al., 2023] van Apeldoorn, J., Cornelissen, A., Gilyén, A., and Nannicini, G. (2023). Quantum tomography using state-preparation unitaries. In *Proceedings of the 2023 Annual ACM-SIAM Symposium on Discrete Algorithms (SODA)*, pages 1265–1318. SIAM.
- [van den Berg, 2020] van den Berg, E. (2020). Iterative quantum phase estimation with optimized sample complexity. In *2020 IEEE International Conference on Quantum Computing and Engineering (QCE)*, pages 1–10.
- [Vrana et al., 2014] Vrana, P., Reeb, D., Reitzner, D., and Wolf, M. M. (2014). Fault-ignorant quantum search. *New Journal of Physics*, 16(7):073033.
- [Weber et al., 2019] Weber, T., Sager, S., and Gleixner, A. (2019). Solving quadratic programs to high precision using scaled iterative refinement. *Mathematical Programming Computation*, 11(3):421–455.
- [Wibisono et al., 2016] Wibisono, A., Wilson, A. C., and Jordan, M. I. (2016). A variational perspective on accelerated methods in optimization. *Proceedings of the National Academy of Sciences*, 113(47):E7351–E7358.
- [Wilkinson, 1963] Wilkinson, J. H. (1963). *Rounding errors in algebraic processes*. Prentice-Hall, Englewood Cliffs, NJ.
- [Williams et al., 2024] Williams, V. V., Xu, Y., Xu, Z., and Zhou, R. (2024). New bounds for matrix multiplication: from alpha to omega. In *Proceedings of the 2024 Annual ACM-SIAM Symposium on Discrete Algorithms (SODA)*, pages 3792–3835. SIAM.
- [Wocjan and Zhang, 2006] Wocjan, P. and Zhang, S. (2006). Several natural bqp-complete problems. *arXiv preprint quant-ph/0606179*.
- [Woerner and Egger, 2019] Woerner, S. and Egger, D. J. (2019). Quantum risk analysis. *npj Quantum Information*, 5(1):15.
- [de Wolf, 2019] de Wolf, R. (2019). Quantum computing: Lecture notes. *arXiv preprint arXiv:1907.09415*.
- [Wright, 1997] Wright, S. J. (1997). *Primal-dual interior-point methods*. SIAM.

- [Wu et al., 2023] Wu, Z., Mohammadisiahroudi, M., Augustino, B., Yang, X., and Terlaky, T. (2023). An inexact feasible quantum interior point method for linearly constrained quadratic optimization. *Entropy*, 25(2):330.
- [Yao, 1993] Yao, A. C.-C. (1993). Quantum circuit complexity. In *Foundations of Computer Science, 1993. FOCS'93. 34th Annual IEEE Symposium on*, pages 352–361. IEEE.
- [Yoder et al., 2014] Yoder, T. J., Low, G. H., and Chuang, I. L. (2014). Fixed-point quantum search with an optimal number of queries. *Physical review letters*, 113(21):210501.
- [Yu, 2013] Yu, Y.-L. (2013). The strong convexity of von Neumann’s entropy. *Unpublished note*, page 15.